

Dynamic Loading	93
Nonlinear Behavior	101
Problems	108

131

Introduction	131
Torsion of Circular Bars	131
Nonuniform Torsion	138
Shear	141
Relationship Between Moduli of Elasticity E and G	146
Transmission of Power by Circular Shafts	148
statically Indeterminate Torsional Members	151
Strain Energy in Pure Shear and Torsion	155
Thin-Walled Tubes	160
Nonlinear Torsion of Circular Bars	167
Problems	170

Bending Moment 181

Types of Beams	181
Shear Force and Bending Moment	184
Relationships Between Load, Shear Force, and Bending Moment	188
Shear-Force and Bending-Moment Diagrams	192
Problems	199

205

Introduction	205
Normal Strains in Beams	207
Normal Stresses in Beams	212
Cross-Sectional Shapes of Beams	220
Shear Stresses in Rectangular Beams	226
Shear Stresses in the Webs of Beams with Flanges	232
Shear Stresses in Circular Beams	236
Split-Up Beams	238

Contents i

*5.9 Stresses in Nonprismatic Beams	2
*5.10 Composite Beams	2
5.11 Beams with Axial Loads	2
Problems	2

CHAPTER 6

Analysis of Stress and Strain 2

6.1 Introduction	2
6.2 Plane Stress	2
6.3 Principal Stresses and Maximum Shear Stresses	2
6.4 Mohr's Circle for Plane Stress	2
6.5 Hooke's Law for Plane Stress	3
6.6 Spherical and Cylindrical Pressure Vessels (Biaxial Stress)	3
6.7 Combined Loadings (Plane Stress)	3
6.8 Principal Stresses in Beams	3
6.9 Triaxial Stress	3
*6.10 Three-Dimensional Stress	3
6.11 Plane Strain	3
Problems	3

CHAPTER 7

Deflections of Beams

7.1 Introduction	
7.2 Differential Equations of the Deflection Curve	
7.3 Deflections by Integration of the Bending-Moment Equation	
7.4 Deflections by Integration of the Shear-Force and Load Equations	
7.5 Moment-Area Method	
7.6 Method of Superposition	
7.7 Nonprismatic Beams	
7.8 Strain Energy of Bending	
*7.9 Discontinuity Functions	
*7.10 Use of Discontinuity Functions to Obtain Beam Deflections	
*7.11 Temperature Effects	
*7.12 Effects of Shear Deformations	
*7.13 Large Deflections of Beams	
Problems	

ite Beams	429
Statically Indeterminate Beams	429
Analysis by the Differential Equations of the Deflection Curve	431
Moment-Area Method	434
Method of Superposition (Flexibility Method)	439
Continuous Beams	447
Temperature Effects	455
Horizontal Displacements at the Ends of a Beam	457
Problems	459

g	469
Introduction	469
Doubly Symmetric Beams with Skew Loads	470
Pure Bending of Unsymmetric Beams	474
Generalized Theory of Pure Bending	481
Bending of Beams by Lateral Loads; Shear Center	486
Shear Stresses in Beams of Thin-Walled Open Cross Sections	490
Shear Centers of Thin-Walled Open Sections	496
General Theory for Shear Stresses	501
Problems	507

	515
Introduction	515
Equations of Inelastic Bending	516
Plastic Bending	517
Plastic Hinges	522
Plastic Analysis of Beams	524
Deflections	532
Inelastic Bending	535
Residual Stresses	541
Problems	542

Moments of Inertia of Plane Areas	700
Centroids of Areas	700
Centroids of Composite Areas	702
Moments of Inertia of Areas	704
Parallel-Axis Theorem for Moments of Inertia	707
Polar Moments of Inertia	710
Products of Inertia	712
Rotation of Axes	715
Principal Axes	716
Problems	720

lance Areas	724
lected Structural-Steel Shapes	729
l Slopes of Beams	736
roperties of Materials	742

s to Selected Problems	748
ndex	763
Index	764

CHAPTER 11

Columns

11.1	Buckling and Stability
11.2	Columns with Pinned Ends
11.3	Columns with Other Support Conditions
11.4	Columns with Eccentric Axial Loads
11.5	Secant Formula
*11.6	Imperfections in Columns
11.7	Elastic and Inelastic Column Behavior
*11.8	Inelastic Buckling
11.9	Column Design Formulas
	Problems

CHAPTER 12

Energy Methods

12.1	Introduction
12.2	Principle of Virtual Work
12.3	Unit-Load Method for Calculating Displacements
12.4	Reciprocal Theorems
12.5	Strain-Energy and Complementary Energy
12.6	Strain-Energy Methods
12.7	Complementary-Energy Methods
12.8	Castigliano's Second Theorem
*12.9	Shear Deflections of Beams
	Problems

References and Historical Notes

APPENDIX A Systems of Units

A.1	Introduction
A.2	SI Units
A.3	U.S. Customary Units
A.4	Conversions

APPENDIX B Significant Digits

B.1	Significant Digits
B.2	Rounding off Numbers

List of Symbol

A	area, action (force or couple), constant
a, b, c	dimensions, distances, constants
C	centroid, constant of integration, compressive force
c	distance from neutral axis to outer surface of a beam
D	displacement (translation or rotation)
d	diameter, dimension, distance
E	modulus of elasticity, elliptic integral of the second kind
E_r	reduced modulus of elasticity
E_t	tangent modulus of elasticity
e	eccentricity, dimension, distance, unit volume change (dilatation, volumetric strain)
F	force, discontinuity function, elliptic integral of the first kind, flexibi
f	shear flow, shape factor for plastic bending, flexibility, frequency (
f_s	form factor for shear
G	modulus of elasticity in shear
g	acceleration of gravity
H	distance, force, reaction, horsepower
h	height, dimension
I	moment of inertia (or second moment) of a plane area
I_x, I_y, I_z	moments of inertia with respect to x , y , and z axes
I_{xy}	product of inertia with respect to the x and y axes
I_p	polar moment of inertia
I_1, I_2	principal moments of inertia
J	torsion constant
K	bulk modulus of elasticity, effective length factor for a column
k	spring constant, stiffness, symbol for $\sqrt{P/EI}$
L	length, distance, span length
L_e	effective length of a column
M	bending moment, couple, mass
M_p	plastic moment for a beam
M_y	yield moment for a beam
m	moment per unit length, mass per unit length

Tension, Compression, and Shear

tress (or working stress) in shear
 ess in shear
 in shear
 e of twist
 onal ratio
 ocity, angular frequency ($\omega = 2\pi f$)

denotes a difficult or advanced section, example, or

Greek Alphabet

ha	N	v	Nu
a	Ξ	ξ	Xi
mma	O	o	Omicron
ta	Π	π	Pi
ilon	P	ρ	Rho
a	Σ	σ	Sigma
	T	τ	Tau
ta	Υ	υ	Upsilon
a	Φ	ϕ	Phi
ppa	X	χ	Chi
nbda	Ψ	ψ	Psi
i	Ω	ω	Omega

1.1 INTRODUCTION

Mechanics of materials is a branch of applied mechanics that deals with the behaviour of solid bodies subjected to various types of loading. This field of study is known by several names, including "strength of materials" and "mechanics of deformable bodies." The solid bodies considered in this book include axially loaded members, shafts in torsion, thin shells, beams, and columns, as well as structures that are assemblies of these components. Usually the objectives of our analysis will be the determination of the stresses, strains, and deflections produced by the loads. If these quantities can be found for all values of load up to the failure load, then we will have a complete picture of the mechanical behaviour of the body.

A thorough understanding of mechanical behaviour is essential for the safe design of all structures, whether buildings and bridges, machines and motors, submarines and ships, or aeroplanes and antennas. Hence, mechanics of materials is a basic subject in many engineering fields. Of course, statics and dynamics are also essential, but they deal primarily with the forces and motions associated with particles and rigid bodies. In mechanics of materials, we go one step further by examining the stresses and strains that occur inside real bodies that deform under loads. We use the physical properties of the materials (obtained from experiments) as well as numerous theoretical laws and concepts, which are explained in succeeding sections of this book.

Theoretical analyses and experimental results have equally important roles in the study of mechanics of materials. On many occasions, we will make logical derivations to obtain formulas and equations for predicting mechanical behaviour, but we must recognize that these formulas cannot be used in a realistic way unless certain properties of the mate-

ssion, and Shear

experiments have been carried out in the laboratory. Also, because many practical problems of great importance in engineering cannot be handled efficiently by theoretical means, experimental measurements become a necessity.

The historical development of mechanics of materials is a fascinating blend of both theory and experiment; experiments have pointed the way to useful results in some instances, and theory has done so in others. Such famous men as Leonardo da Vinci (1452–1519) and Galileo Galilei (1564–1642) performed experiments to determine the strength of wires, bars, and beams, although they did not develop any adequate theories (by today's standards) to explain their test results. Such theories came much later. By contrast, the famous mathematician Leonhard Euler (1707–1783) developed the mathematical theory of columns and calculated the theoretical critical load of a column in 1744, long before any experimental evidence existed to show the significance of his results. Thus, for want of appropriate tests, Euler's results remained unused for many years, although today they form the basis of column theory.*

When studying mechanics of materials from this book, you will find that your efforts are divided naturally into two parts: first, understanding the logical development of the concepts, and second, applying those concepts to practical situations. The former is accomplished by studying the derivations, discussions, and examples, and the latter by solving problems. Some of the examples and problems are numerical in character, and others are algebraic (or symbolic). An advantage of numerical problems is that the magnitudes of all quantities are evident at every stage of the calculations. Sometimes these values are needed to ensure that practical limits (such as allowable stresses) are not exceeded. Algebraic solutions have certain advantages, too. Because they lead to formulas, algebraic solutions make clear the variables that affect the final result. For instance, a certain quantity may actually cancel out of the solution, a fact that would not be evident from a numerical problem. Also apparent in algebraic solutions is the manner in which variables affect the results, such as the appearance of one variable in the numerator and another in the denominator. Furthermore, a symbolic solution provides the opportunity to check the dimensions at any stage of the work. Finally, the most important reason for obtaining an algebraic solution is to obtain a general formula that can be programmed on a computer and used for many different problems. In contrast, a numerical solution applies to only one set of circumstances. Of course, you must be adept at both kinds of solutions, hence you will find a mixture of numerical and algebraic problems throughout the book.

Numerical problems require that you work with specific units of measurements. This book utilizes the International System of Units (SI). A discussion of this system and the U.S. Customary System (USCS)

* The history of mechanics of materials, beginning with Leonardo and Galileo, is given in Refs. 1-1, 1-2, and 1-3.

1.2 Normal Stress and Str

or Imperial System appears in Appendix A, which also provides useful tables and conversion factors. The matter of significant digits, which is very important in engineering, is discussed in Appendix B. As explained there, examples in this book are usually solved to a final accuracy of three significant digits.

1.2 NORMAL STRESS AND STRAIN

The fundamental concepts of stress and strain can be illustrated by considering a prismatic bar that is loaded by axial forces P at the ends, as shown in Fig. 1-1. A **prismatic bar** is a straight structural member having constant cross section throughout its length. In this illustration, the axial forces produce a uniform stretching of the bar; hence, the bar is said to be in **tension**.

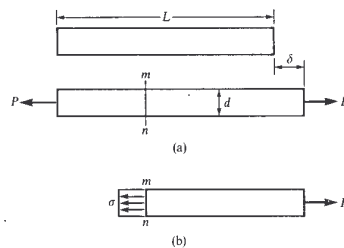


Fig. 1-1 Prismatic bar in tension

To investigate the internal stresses produced in the bar by the axial forces, we make an imaginary cut at section mn (Fig. 1-1a). This section is taken perpendicular to the longitudinal axis of the bar; hence, it is known as a **cross section**. We now isolate the part of the bar to the right of the cut as a free body (Fig. 1-1b). The tensile load P acts at the right-hand end of the free body; at the other end are forces representing the action of the removed part of the bar upon the part that remains. These forces are continuously distributed over the cross section, analogous to the continuous distribution of hydrostatic pressure over a submerged horizontal surface. The intensity of force (that is, the force per unit area) is called the **stress** and is commonly denoted by the Greek letter σ (sigma). Assuming that the stress has a uniform distribution over the cross section (see Fig. 1-1b), we can readily see that its resultant is equal to the intensity σ times the cross-sectional area A of the bar. Furthermore, from the equilibrium of the body shown in Fig. 1-1b, it is also

evident that this resultant must be equal in magnitude and opposite in direction to the applied load P . Hence, we obtain

$$\sigma = \frac{P}{A} \quad (1-1)$$

as the equation for the uniform stress in an axially loaded, prismatic bar of arbitrary cross-sectional shape. When the bar is stretched by the forces P , as shown in the figure, the resulting stresses are **tensile stresses**; if the forces are reversed in direction, causing the bar to be compressed, we obtain **compressive stresses**. Inasmuch as the stress σ acts in a direction perpendicular to the cut surface, it is referred to as a **normal stress**. Thus, normal stresses may be either tensile or compressive stresses. Later, we will encounter another type of stress, called a **shear stress**, that acts parallel to the surface.

When a **sign convention** for normal stresses is required, it is customary to define tensile stresses as positive and compressive stresses as negative.

Because the normal stress σ is obtained by dividing the axial force by the cross-sectional area, it has units of force per unit of area. When SI units are used, force is expressed in newtons (N) and area in square metres (m^2). Hence, stress has units of newtons per square metre (N/m^2), or pascals (Pa). However, the pascal is such a small unit of stress that it is necessary to work with large multiples. To illustrate this point, we have only to note that it takes almost 7000 pascals to make 1 psi.* As an example, a typical tensile stress in a steel bar might have a magnitude of 140 megapascals (140 MPa), which is 140×10^6 pascals. Other units that may be convenient to use are the kilopascal (kPa) and gigapascal (GPa); the former equals 10^3 pascals and the latter equals 10^9 pascals. Although it is not recommended in SI, you will sometimes find stress given in newtons per square millimetre (N/mm^2), which is a unit identical to the megapascal (MPa).

When using USCS units, stress is customarily expressed in pounds per square inch (psi) or kips per square inch (ksi).** For instance, a typical stress in a steel bar might be 20,000 psi or 20 ksi.

In order for the equation $\sigma = P/A$ to be valid, the stress σ must be uniformly distributed over the cross section of the bar. This condition is realized if the axial force P acts through the centroid of the cross-sectional area, as demonstrated in Example 1. When the load P does not act at the centroid, bending of the bar will result, and a more complicated analysis is necessary (see Section 5.11). However, we will assume throughout this book that all axial forces are applied at the centroid of the cross section unless specifically stated otherwise.

The uniform stress condition pictured in Fig. 1-1b exists throughout

* See Table A-3 in Appendix A for conversion factors between USCS and SI units.

the length of the member except near the ends. The stress distribution at the ends of the bar depends upon the details of how the axial load P is actually applied. If the load itself is distributed uniformly over the end, then the stress pattern at the end will be the same as elsewhere. However, the load is usually concentrated over a small area, resulting in high localized stresses and nonuniform stress distributions over cross sections in the vicinity of the load. As we move away from the ends, the stress distribution gradually approaches the uniform distribution shown in Fig. 1-1b. It is usually safe to assume that the formula $\sigma = P/A$ may be used with good accuracy at any point within the bar that is at least a distance d away from the ends, where d is the largest transverse dimension of the bar (see Fig. 1-1a). Of course, even when the stress is not uniform, the equation $\sigma = P/A$ will give the **average normal stress**.

An axially loaded bar undergoes a change in length, becoming longer when in tension and shorter when in compression. The total change in length is denoted by the Greek letter δ (delta) and is pictured in Fig. 1-1a for a bar in tension. This elongation is the cumulative result of the stretching of the material throughout the length L of the bar. Let us now assume that the material is the same everywhere in the bar. Then, if we consider half of the bar, it will have an elongation equal to $\delta/2$; similarly, if we consider a unit length of the bar, it will have an elongation equal to $1/L$ times the total elongation δ . In this manner, we arrive at the concept of elongation per unit length, or **strain**, denoted by the Greek letter ϵ (epsilon) and given by the equation

$$\epsilon = \frac{\delta}{L} \quad (1-2)$$

If the bar is in tension, the strain is called a **tensile strain**, representing an elongation or stretching of the material. If the bar is in compression, the strain is a **compressive strain** and the bar shortens. Tensile strain is taken as positive, and compressive strain as negative. The strain ϵ is called a **normal strain** because it is associated with normal stresses.

Because normal strain ϵ is the ratio of two lengths, it is a **dimensionless quantity**; that is, it has no units. Thus, strain is expressed as a pure number, independent of any system of units. Numerical values of strain are usually very small, especially for structural materials, which ordinarily undergo only small changes in dimensions. As an example, consider a steel bar having length L of 2.0 m. When loaded in tension, the bar might elongate by an amount δ equal to 1.4 mm. The corresponding strain is

$$\epsilon = \frac{\delta}{L} = \frac{1.4 \times 10^{-3} \text{ m}}{2.0 \text{ m}} = 0.0007 = 700 \times 10^{-6}$$

In practice, the original units of δ and L are sometimes attached to the

$\mu\text{m/m}$, and in./in. For instance, the strain ϵ in the preceding illustration could be given as $700 \mu\text{m/m}$ or $700 \times 10^{-6} \text{ in./in.}$

The definitions of normal stress and strain are based upon purely statical and geometrical considerations, hence Eqs. (1-1) and (1-2) can be used for loads of any magnitude and for any material. The principal requirement is that the deformation of the bar be uniform, which in turn requires that the bar be prismatic, the loads act through the centroids of the cross sections, and the material be **homogeneous** (that is, the same throughout all parts of the bar). The resulting state of stress and strain is called **uniaxial stress and strain**. Further discussions of uniaxial stress, including stresses and strains in other than the longitudinal direction of the bar, are given in later sections. We will also encounter more complicated stress states, such as biaxial stress and plane stress, in later chapters.

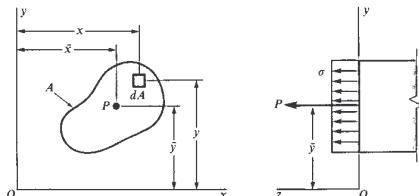
Example 1

Show that the axial forces P producing uniform tension or compression in a prismatic member (see Fig. 1-1) must act through the centroid of the cross section.

Let us assume that the cross section has the arbitrary shape shown in Fig. 1-2a, and for reference let us take any set of xy axes in the plane of the cross section. Then the z axis is parallel to the long direction of the bar (Fig. 1-2b). The stress distribution over the cross section is assumed to be a uniform tensile stress $\sigma = P/A$, as shown in Fig. 1-2b. The resultant of this stress distribution is the axial force P .

The x and y coordinates of the line of action of the force P are denoted by \bar{x} and \bar{y} in the figure. To determine these coordinates, we observe that the moments M_x and M_y of the force P about the x and y axes, respectively, must be equal to the corresponding moments of the uniformly distributed stresses. The moments of the force P are

$$M_x = P\bar{y} \quad M_y = -P\bar{x} \quad (a)$$



in which a moment is considered positive when its vector (using the right-hand rule) acts in the positive direction of the axis. To obtain the moments of the distributed stresses, we consider an element of area dA in the cross section (Fig. 1-2a) and note that the differential force acting on this element is σdA . The moments of this elemental force about the x and y axes are $\sigma y dA$ and $-\sigma x dA$, respectively, in which x and y denote the coordinates of the element dA . The total moments can be obtained by integrating over the entire cross-sectional area A ; thus, the moments about the x and y axes are

$$M_x = \int \sigma y dA \quad M_y = -\int \sigma x dA \quad (b)$$

Next, we equate the moments given by expressions (a) and (b):

$$P\bar{y} = \int \sigma y dA \quad P\bar{x} = \int \sigma x dA$$

Noting that the force P equals σA and that the stress σ is a constant, we obtain from the preceding equations the following formulas for the coordinates \bar{y} and \bar{x} :

$$\bar{y} = \frac{\int y dA}{A} \quad \bar{x} = \frac{\int x dA}{A}$$

These equations show that the coordinates of the line of action of the resultant force P are equal to the first moments of the cross-sectional area divided by the area itself. Thus, these equations are identical to the equations defining the coordinates of the centroid of the area.*

We have arrived, therefore, at an important general conclusion. In order to have uniform tension or compression in a prismatic bar, the axial force must act through the centroid of the cross-sectional area.

Example 2

A prismatic bar with rectangular cross section ($20 \times 40 \text{ mm}$) and length $L = 2.8 \text{ m}$ is subjected to an axial tensile force of 70 kN (Fig. 1-3). The measured elongation of the bar is $\delta = 1.2 \text{ mm}$. Calculate the tensile stress and strain in the bar.

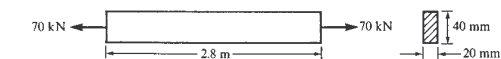


Fig. 1-3 Example 2. Prismatic bar of rectangular cross section

Assuming that the axial forces act at the centroids of the end cross sections, we can use Eq. (1-1) to calculate the stress:

$$\sigma = \frac{P}{A} = \frac{70 \text{ kN}}{(20 \text{ mm})(40 \text{ mm})} = 87.5 \text{ MPa}$$

* Centroids of an area are explained in Section C.1 of Appendix C.

1.3 and Shear

Also, the strain (from Eq. 1-2) is

$$\epsilon = \frac{\delta}{L} = \frac{1.2 \text{ mm}}{2.8 \text{ m}} = 429 \times 10^{-6}$$

The quantities σ and ϵ represent the tensile stress and strain, respectively, in the longitudinal direction of the bar.

Example 3

A deep-well pump is operated by a crank that moves a piston up and down (Fig. 1-4). The pump rod has a diameter $d = 15 \text{ mm}$ and a length $L = 97.5 \text{ m}$. It is made of steel having specific weight $\gamma = 7.85 \text{ t/m}^3$. The resistance encountered by the piston during the downstroke is 890 N and during the upstroke it creates a tensile force $T = 8.9 \text{ kN}$. Determine the maximum tension and compression stresses in the pump rod considering only the resistance forces and the weight of the rod.

During the downstroke, the resistance of the piston creates a compressive force $C = 890 \text{ N}$ throughout the length of the rod, and during the upstroke it creates a tensile force $T = 8.9 \text{ kN}$. The weight of the rod produces a tensile force that varies from zero at the lower end to a maximum at the upper end. The maximum weight force equals the weight of the entire rod, given by the expression

$$W = \gamma LA$$

where γ is the specific weight of the material, L is the length of the rod, and A is the cross-sectional area. Substituting into this equation, we get

$$W = (7.85 \text{ t/m}^3 \times 9.81 \times 10^3 \text{ N/t})(97.5 \text{ m})\left(\frac{\pi}{4}\right)(0.015 \text{ m})^2 = 1327 \text{ N}$$

as the tensile force at the upper end due to the weight.

The maximum tensile force occurs during the upstroke at the upper end of the pump rod and is equal to $T + W$, or $10,227 \text{ kN}$. The corresponding maximum tensile stress is

$$\sigma_t = \frac{P}{A} = \frac{10,227 \text{ kN} \times 10^3}{\pi(15 \text{ mm})^2/4} = 57.9 \text{ MPa}$$

In a similar manner, we can calculate the maximum compressive stress, which occurs at the lower end during the downstroke:

$$\sigma_c = \frac{P}{A} = \frac{890 \text{ N}}{\pi(15 \text{ mm})^2/4} = 5.0 \text{ MPa}$$

These calculations give the axial stresses in the pump rod due only to the specified loads under idealized conditions. Other considerations, such as bending of the pump rod and dynamic effects, have not been taken into account.

Compression, and Shear

so that failure will occur in the central uniform region, where the stress is easy to calculate, rather than near the ends, where the stress distribution is complicated. The figure shows a steel specimen that has just fractured under load. The device at the left, which is attached by two arms to the specimen, is an **extensometer** that measures the elongation during loading.

The ASTM standard tension specimen has a diameter of 12.7 mm and a **gauge length** of 50.8 mm between the gauge marks, which are the points where the extensometer arms are attached to the specimen, as shown in Fig. 1-6. As the specimen is pulled, the load P is measured and recorded, either automatically or by reading from a dial. The elongation over the gauge length is measured simultaneously with the load, usually by mechanical gauges of the kind shown in Fig. 1-6, although electric-resistance strain gauges are also used. In a **static test**, the load is applied very slowly; however, in a **dynamic test**, the rate of loading may be very high and also must be measured because it affects the properties of the materials.

The axial stress σ in the test specimen is calculated by dividing the load P by the cross-sectional area A (see Eq. 1-1). When the initial area of the bar is used in this calculation, the resulting stress is called the **nominal stress** (other names are *conventional stress* and *engineering stress*). A more exact value of the axial stress, known as the **true stress**, can be calculated by using the actual area of the bar, which can become significantly less than the initial area (as shown in Fig. 1-6) for some materials. True stress is discussed later in this section.

The average axial strain in the bar is found from the measured elongation δ between the gauge marks by dividing δ by the gauge length L (see Eq. 1-2). If the initial gauge length is used (for instance, 50 mm), then the **nominal strain** is obtained. Of course, the distance between the gauge marks increases as the tensile load is applied. If the actual distance is used in calculating the strain, we obtain the **true strain**, or **natural strain**.

Compression tests of metals are customarily made on small specimens in the shape of cubes or circular cylinders. Cubes are often 50 mm on a side, and cylinders usually have diameters of about 25 mm with lengths of 25 to 300 mm . Both the load applied by the machine and the shortening of the specimen may be measured. The shortening should be measured over a gauge length that is less than the total length of the specimen in order to eliminate end effects. Concrete is tested in compression on every important construction project to ensure that the required strengths have been obtained. The standard ASTM concrete test specimen is 152 mm in diameter, 305 mm long, and 28 days old (the age of concrete is important because concrete gains strength as it cures).

After performing a tension or compression test and determining the stress and strain at various magnitudes of the load, we can plot a diagram of stress versus strain. Such a **stress-strain diagram** is charac-

1.3 STRESS-STRAIN DIAGRAMS

The mechanical properties of materials used in engineering are determined by tests performed on small specimens of the material. The tests are conducted in materials-testing laboratories equipped with testing machines capable of loading the specimens in a variety of ways, including static and dynamic loading in tension and compression. One such machine is shown in Fig. 1-5. A test specimen is in place in the middle of the loading assembly, and the control console is the separate unit on the left.

In order that test results may be compared easily, the dimensions of test specimens and the methods of applying loads have been standardized. One of the major standards organizations is the *American Society for Testing and Materials (ASTM)*, a national technical society that publishes specifications and standards for materials and testing. Other standardizing organizations are the *American Standards Association (ASA)*, the *National Bureau of Standards (NBS)*, and the *British Standards Institution (BSI)*.

The most common materials test is the **tension test**, in which tensile loads are applied to a cylindrical specimen like the one shown in Fig. 1-6. The ends of the specimen are enlarged where they fit in the grips

Fig. 1-5 General-purpose testing machine. (Courtesy of MTS Systems Corporation)

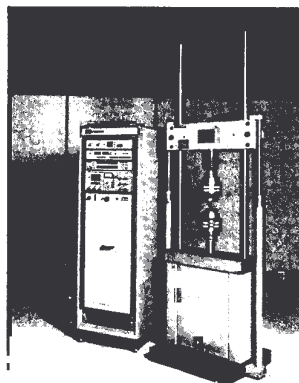
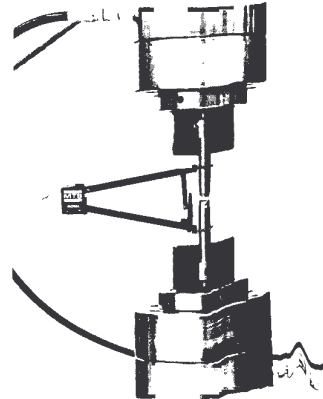


Fig. 1-6 Typical tensile-test specimen with extensometer attached; the specimen has just fractured in tension. (Courtesy of MTS Systems Corporation)



1.3 Stress-Strain Diagrams

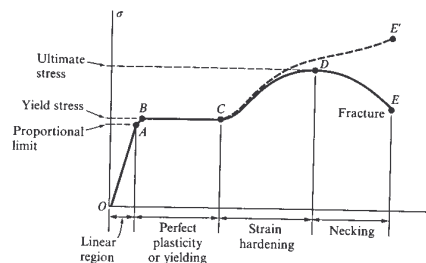


Fig. 1-7 Stress-strain diagram for typical structural steel (not to scale)

teristic of the material and conveys important information about the mechanical properties and type of behaviour.* The first material we will discuss is **structural steel**, also known as mild steel or low-carbon steel. Structural steel is one of the most widely used metals, being the principal steel used in buildings, bridges, towers, and many other types of construction. A stress-strain diagram for a typical structural steel in tension is shown in Fig. 1-7 (not to scale). Strains are plotted on the horizontal axis and stresses on the vertical axis. The diagram begins with a straight line from O to A . In this region, the stress and strain are directly proportional, and the behaviour of the material is said to be **linear**. Beyond point A , the linear relationship between stress and strain no longer exists; hence, the stress at A is called the **proportional limit**. For low-carbon steels, this limit is in the range 200 to 280 MPa , but high-strength steels (with higher carbon content plus other alloys) can have proportional limits of 550 MPa and more.

With an increase in the load beyond the proportional limit, the strain begins to increase more rapidly for each increment in stress. The stress-strain curve then has a smaller and smaller slope, until, at point B , the curve becomes horizontal. Beginning at this point, considerable elongation occurs, with no noticeable increase in the tensile force (from B to C on the diagram). This phenomenon is known as **yielding** of the material, and the stress at point B is called the **yield stress**, or **yield point**. In the region from B to C , the material becomes **perfectly plastic**, which means that it can deform without an increase in the applied load. The elongation of a mild-steel specimen in the perfectly plastic region is typically 10 to 15 times the elongation that occurs between the onset of loading and the proportional limit.

After undergoing the large strains that occur during yielding in the region BC , the steel begins to **strain harden**. During strain hardening,

* Stress-strain diagrams were originated by Jacob Bernoulli (1654–1705) and J. V. Poncelet (1788–1867); see Ref. 1-4.

the material undergoes changes in its atomic and crystalline structure, resulting in increased resistance of the material to further deformation. Thus, additional elongation requires an increase in the tensile load, and the stress-strain diagram has a positive slope from C to D. The load eventually reaches its maximum value, (at point D) is called the **ultimate stress**. Further stretching of the bar is actually accompanied by a reduction in the load, and **fracture** finally occurs at a point such as E on the diagram.

Lateral contraction of the specimen occurs when it is stretched, resulting in a decrease in the cross-sectional area, as previously mentioned. The reduction in area is too small to have a noticeable effect on the calculated value of stress up to about point C, but beyond that point the reduction begins to alter the shape of the diagram. Of course, the true stress is larger than the nominal stress because it is calculated with a smaller area. In the vicinity of the ultimate stress, the reduction in area of the bar becomes clearly visible and a pronounced **necking** of the bar occurs (see Figs. 1-6 and 1-8). If the actual cross-sectional area at the narrow part of the neck is used to calculate the stress, the **true stress-strain curve** will follow the dashed line CE' in Fig. 1-7. The total load the bar can carry does indeed diminish after the ultimate stress is reached (curve DE), but this reduction is due to the decrease in area of the bar and not to a loss in strength of the material itself. In reality, the material withstands an increase in stress up to failure (point E). For most practical purposes, however, the conventional stress-strain curve OABCDE, which is based upon the original cross-sectional area of the specimen and hence is easy to calculate, provides satisfactory information for use in design.

The diagram in Fig. 1-7 shows the general characteristics of the stress-strain curve for mild steel, but its proportions are not realistic because, as already mentioned, the strain that occurs from B to C may be 15 times the strain occurring from O to A. Furthermore, the strains from C to E are many times greater than those from B to C. Figure 1-9 shows a stress-strain diagram for mild steel drawn to scale. In this figure, the strains from O to A are so small in comparison to the strains from A to E that they cannot be seen, and the linear part of the diagram appears to be a vertical line.

The presence of a pronounced yield point followed by large plastic strains is an important characteristic of mild steel that is sometimes utilized in practical design (see, for instance, the discussion of plastic bending in Chapter 10). Materials that undergo large strains before failure are classified as **ductile**. An advantage of ductility is that visible distortions may occur if the loads become too large, thus providing an opportunity to take remedial action before an actual fracture occurs. Also, ductile materials are capable of absorbing large amounts of energy prior to fracture, as explained in Sections 2.8 and 2.9. Ductile materials include mild steel, aluminium and some of its alloys, copper, magnesium,

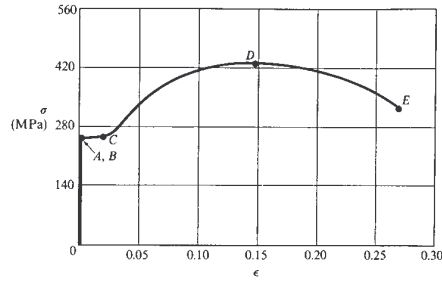


Fig. 1-9 Stress-strain diagram for typical structural steel in tension (drawn to scale)

lead, molybdenum, nickel, brass, bronze, monel metal, nylon, teflon, and many others.

Structural steel contains about 0.2% carbon as an alloy and is classified as a low-carbon steel. With increasing carbon content, steel becomes less ductile but has a higher yield stress and higher ultimate stress. The physical properties of steel are also affected by heat treating, the presence of other alloys, and manufacturing processes such as rolling.

Many **aluminium alloys** possess considerable ductility, although they do not have a clearly definable yield point. Instead, they exhibit a gradual transition from the linear to the nonlinear region, as shown by the stress-strain diagram in Fig. 1-10. Aluminium alloys suitable for structural purposes are available with proportional limits in the range 70 to 420 MPa and ultimate stresses in the range 140 to 560 MPa.

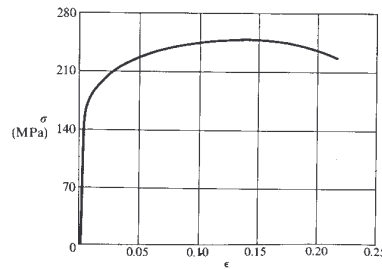


Fig. 1-10 Typical stress-strain diagram for an aluminium alloy

When a material such as aluminium does not have an obvious yield point and yet undergoes large strains after the proportional limit is exceeded, an arbitrary yield stress may be determined by the **offset method**. A line is drawn on the stress-strain diagram parallel to the initial linear part of the curve (see Fig. 1-11) but is offset by some standard amount of strain, such as 0.002 (or 0.2%). The intersection of the offset line and the stress-strain curve (point A in the figure) defines the yield stress. Since this stress is determined by an arbitrary rule and is not an inherent physical property of the material, it should be referred to as the **offset yield stress**. For a material such as aluminium, the offset yield stress is slightly above the proportional limit. In the case of structural steel, with its abrupt transition from the linear region to the region of plastic stretching, the offset stress is essentially the same as both the yield stress and the proportional limit.

Rubber maintains a linear relationship between stress and strain up to very large strains in the vicinity of 0.1 or 0.2. The behaviour after the proportional limit is exceeded depends upon the type of rubber (see Fig. 1-12). Some kinds of soft rubber continue to stretch enormously without failure. The material eventually offers increasing resistance to the load, and the stress-strain curve turns markedly upward prior to failure. You can easily sense this characteristic behaviour by stretching a rubber band.

The ductility of a material in tension can be characterized by its elongation and by the reduction in area at the cross section where fracture occurs. The **percent elongation** is defined as follows:

$$\text{Percent elongation} = \frac{L_f - L_o}{L_o} (100) \quad (1-3)$$

in which L_o is the original gauge length and L_f is the distance between the gauge marks at fracture. Because the elongation is not uniform over the length of the specimen but is concentrated in the region of the necking, the present elongation depends upon the gauge length. Therefore, when

stating the percent elongation, the gauge length should also be given. For a 50 mm gauge length, steel may have an elongation in the range of 10% to 40%, depending upon composition; for structural steel, values of 25% or 30% are common. In the case of aluminium alloys, the elongation varies from 1% to 45%, depending upon composition and treatment.

The **percent reduction in area** measures the amount of necking that occurs and is defined as follows:

$$\text{Percent reduction in area} = \frac{A_o - A_f}{A_o} (100) \quad (1-4)$$

in which A_o is the original cross-sectional area and A_f is the final area at the fracture section. For ductile steels, the reduction is about 50%.

Materials that fail in tension at relatively low values of strain are classified as **brittle** materials. Examples are concrete, stone, cast iron, glass, ceramic materials, and many common metallic alloys. These materials fail with only little elongation after the proportional limit (point A in Fig. 1-13) is exceeded, and the fracture stress (point B) is the same as the ultimate stress. High-carbon steels behave in a brittle manner; they may have a very high yield stress (over 700 MPa in some cases), but fracture occurs at an elongation of only a few percent.

Ordinary glass is a nearly ideal brittle material, because it exhibits almost no ductility whatsoever. The stress-strain curve for glass in tension is essentially a straight line, with failure occurring before any yielding takes place. The ultimate stress is about 70 MPa for certain kinds of plate glass, but great variation exists, depending upon the type of glass, size of specimen, and the presence of microscopic defects. Glass fibers can develop enormous strengths, and ultimate stresses over 7 GPa have been attained.

Stress-strain diagrams for **compression** have different shapes from those for tension. Ductile metals such as steel, aluminium, and copper have proportional limits in compression very close to those in tension, hence the initial regions of their compression stress-strain diagrams are very similar to the tension diagrams. However, when yielding begins, the behaviour is quite different. In a tension test, the specimen is being stretched, necking may occur, and ultimately fracture takes place. When a small specimen of ductile material is compressed, it begins to bulge outward on the sides and become barrel shaped. With increasing load, the specimen is flattened out, thus offering increased resistance to further shortening (which means the stress-strain curve goes upward). These characteristics are illustrated in Fig. 1-14, which shows a compression stress-strain diagram for copper.

Brittle materials in compression typically have an initial linear region followed by a region in which the shortening increases at a higher rate than does the load. Thus, the compression stress-strain diagram has a shape that is similar to the shape of the tensile diagram. However,

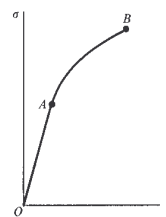
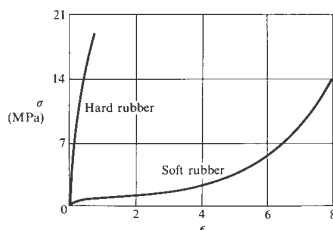
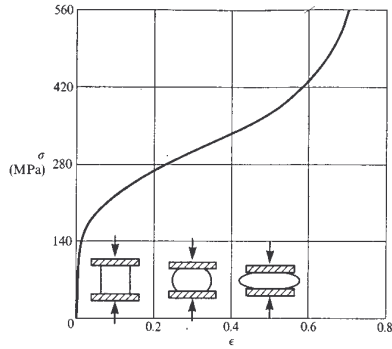


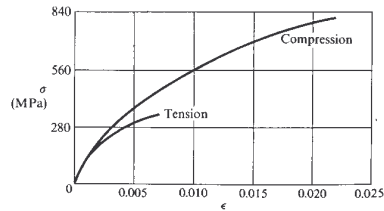
Fig. 1-13 Typical stress-strain diagram for a brittle material





brittle materials usually reach much higher ultimate stresses in compression than in tension. Also, unlike ductile materials in compression (see Fig. 1-14), brittle materials actually fracture or break at the maximum load. The tension and compression stress-strain diagrams for a particular type of cast iron are given in Fig. 1-15. Curves for other brittle materials, such as concrete and stone, have similar shapes but quite different numerical values.

A table of important **mechanical properties** for various materials is given in Appendix H. However, properties and stress-strain curves vary greatly, even for the same material, because of different manufacturing processes, chemical composition, internal defects, temperature, and many other factors. Hence, any data obtained from general tables should



Diagrams for compression

set (that is, if the elongation of the bar returns to zero) then the material is elastic up to the stress represented by the selected value of the load. This process of loading and unloading can be repeated for successively higher values of load. Eventually, a stress will be reached such that not all the strain is recovered during unloading. By this procedure, it is possible to determine the stress at the upper limit of the elastic region; for instance, it could be the stress at point *E* in Figs. 1-16a and b. This stress is known as the **elastic limit** of the material.

Many materials, including most metals, have linear regions at the beginning of their stress-strain curves (see Figs. 1-7 and 1-10). As explained in Section 1.3, the upper limit of this linear region is defined by the proportional limit. Usually the elastic limit is slightly above, or nearly the same as, the proportional limit. Hence, for many materials the two limits are assigned the same numerical value. In the case of mild steel, the yield stress is also very close to the proportional limit, so that for practical purposes the yield stress, the elastic limit, and the proportional limit are assumed to be equal. Of course, this situation does not hold for all materials. Rubber provides the outstanding example of a material that is elastic far beyond the proportional limit.

The characteristic of a material by which it undergoes inelastic strains beyond those at the elastic limit is known as **plasticity**. Thus, on the stress-strain curve in Fig. 1-16a, we have an elastic region followed by a plastic region. When large deformations occur in a ductile material loaded into the plastic region, the material is said to undergo **plastic flow**.

If the material remains within the elastic range, it can be loaded, unloaded, and loaded again without significantly changing the behaviour. However, when loaded into the plastic range, the internal structure of the material is altered and its properties change. For instance, we have already observed that a permanent strain exists in the specimen after unloading from the plastic region (Fig. 1-16b). Now suppose that the material is reloaded after such an unloading (Fig. 1-17). The new loading begins at point *C* on the diagram and continues upward to *B*, the point at which unloading began during the first loading cycle. The material then follows the original stress-strain diagram toward point *F*. During the second loading, the material behaves in a linear manner from *C* to *B*, hence the material has a higher proportional limit and a higher yield stress than before. Thus, by stretching a material, it is possible to raise the yield point, although the ductility is reduced because the amount of yielding from *B* to *F* is less than from *E* to *F*.*

Creep. The stress-strain diagrams previously described are obtained from tension tests involving only static loading of the specimens; hence, the passage of time did not enter into our discussions. However,

* The study of material behaviour under various environmental and loading conditions is an important branch of applied mechanics. For more detailed engineering information about materials, consult the books and documents listed in this appendix.

be considered as typical, but not necessarily suitable for a specific application.

1.4 ELASTICITY AND PLASTICITY

The stress-strain diagrams described in the preceding section illustrate the behavior of various materials as they are loaded statically in tension or compression. Now let us consider what happens when the load is slowly removed, and the material is **unloaded**. Assume, for instance, that we apply a load to a tensile specimen so that the stress and strain go from *O* to *A* on the stress-strain curve in Fig. 1-16a. Suppose further that, when the load is removed, the material follows exactly the same curve back to the origin *O*. This property of a material, by which it returns to its original dimensions during unloading, is called **elasticity**, and the material itself is said to be **elastic**. Note that the stress-strain curve from *O* to *A* need not be linear in order for the material to be elastic.

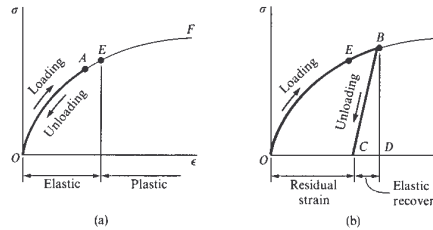


Fig. 1-16 (a) Elastic behavior (b) Partially elastic behavior

Now let us suppose that we load this same material to a much higher level, so that point *B* is reached on the stress-strain diagram (Fig. 1-16b). In this case, when unloading occurs, the material follows line *BC* on the diagram. This unloading line typically is parallel to the initial portion of the loading curve; that is, line *BC* is parallel to a tangent to the stress-strain curve at *O*. When point *C* is reached, the load has been entirely removed, but a **residual strain**, or **permanent strain**, *OC* remains in the material. The corresponding residual elongation of the bar is called the **permanent set**. Of the total strain *OD* developed during loading from *O* to *B*, the strain *CD* has been recovered elastically and the strain *OC* remains as a permanent strain. Thus, during unloading the bar returns partially to its original shape; hence, the material is said to be **partially elastic**.

When a bar is being tested, the load can be increased from zero to some small selected value and then removed. If there is no permanent

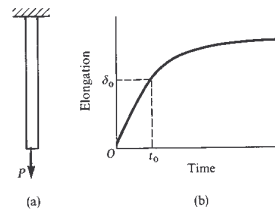


Fig. 1-18 Creep in a bar under constant load

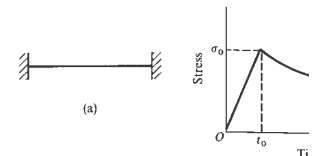


Fig. 1-19 Relaxation of stress in a wire under constant strain

some materials develop additional strains over long periods of time and are said to **creep**. This phenomenon can manifest itself in a variety of ways. For instance, let us suppose that a vertical bar (Fig. 1-18a) is loaded by a constant force *P*. When the load is applied initially, the bar elongates by an amount δ_0 . Let us assume that this loading and the corresponding elongation take place during a time interval of duration t_0 (Fig. 1-18b). Subsequent to time t_0 , the load remains constant. However, due to creep, the bar may gradually lengthen, as shown in Fig. 1-18b, even though the load does not change. This behaviour occurs with many materials, although sometimes the change is too small to be of concern.

As a second example of creep, consider a wire that is stretched between two immovable supports so that it has an initial tension stress σ_0 (Fig. 1-19a). Again, we will denote the time during which the wire is loaded initially as t_0 (Fig. 1-19b). With the elapse of time, the stress in the wire gradually diminishes, eventually reaching a constant value, even though the supports at the ends of the wire do not move. This process, which is a manifestation of creep, is called **relaxation** of the material.

Creep is usually more important at high temperatures than at ordinary temperatures; hence, it must be considered in the design of engines, furnaces, and other structures that operate at elevated temperatures for long periods of time. However, materials such as steel, concrete, and wood creep slightly even at atmospheric temperatures. Therefore, it is sometimes necessary to compensate for creep effects in ordinary structures. For example, creep of concrete can create "waves" in bridge decks because of sagging between the supports. One remedy is to construct the deck with an upward **camber**, which is an initial deflection above the horizontal, so that, when creep occurs, the spans lower to the level position.

1.5 LINEAR ELASTICITY AND HOOKE'S LAW

Most structural materials have an initial region on the stress-strain diagram in which the material behaves both elastically and linearly. An

example is the region from the origin O up to the proportional limit at point A on the stress-strain curve for structural steel (see Fig. 1-7). Other examples are the regions below *both* the proportional limits and the elastic limits on the diagrams of Figs. 1-10 through 1-15. When a material behaves elastically and also exhibits a linear relationship between stress and strain, it is said to be **linearly elastic**. This type of behaviour is extremely important in engineering because many structures and machines are designed to function at low levels of stress in order to avoid permanent deformations from yielding or plastic flow. Linear elasticity is a property of many solid materials, including metals, wood, concrete, plastics, and ceramics.

The linear relationship between stress and strain for a bar in simple tension or compression can be expressed by the equation

$$\sigma = E\epsilon \tag{1-5}$$

in which E is a constant of proportionality known as the **modulus of elasticity** for the material. The modulus of elasticity is the slope of the stress-strain diagram in the linearly elastic region, and its value depends upon the particular material being used. The units of E are the same as the units of stress, inasmuch as strain is dimensionless. Hence, the units of E are pascals (or multiples thereof) in SI units.

The equation $\sigma = E\epsilon$ is commonly known as **Hooke's law**, named for the famous English scientist Robert Hooke (1635–1703). Hooke was the first person to investigate the elastic properties of materials, and he tested such diverse materials as metal, wood, stone, bones, and sinews. He measured the stretching of long wires supporting weights and observed that the elongations “always bear the same proportions one to the other that the weights do that make them” (Refs. 1-5 and 1-6). Thus, Hooke established the linear relationship between the applied load and the resulting elongation.

Equation (1-5) applies only to ordinary tension and compression; for more complicated states of stress, a generalized Hooke's law is required (see Chapter 6). In calculations, tensile stress and strain are usually considered as positive, and compressive stress and strain as negative.

The modulus of elasticity E has relatively large values for materials that are very stiff, such as structural metals. Steel has a modulus of approximately 200 GPa; for aluminium, E equals approximately 70 GPa. More flexible materials have a lower modulus; a typical value for wood is 11 GPa. Some representative values of E are listed in Table H-2, Appendix H. For most materials, the value of E in compression is the same as in tension.

The modulus of elasticity is often called **Young's modulus**, after

another English scientist, Thomas Young (1773–1829). In connection with an investigation of tension and compression of prismatic bars, Young introduced the idea of a “modulus of the elasticity.” However, his modulus was not the same as the one in use today, because it involved properties of the bar as well as of the material (Refs. 1-7 and 1-8).

Poisson's ratio. When a prismatic bar is loaded in tension, the axial elongation is accompanied by **lateral contraction** (normal to the direction of the applied load). This change in shape is pictured in Fig. 1-20, in which the dashed lines represent the shape before loading and the solid lines give the shape after loading. Lateral contraction is readily seen in a stretched rubber band, but in metals the changes in lateral dimensions are usually too small to be visible. However, they can easily be detected with measuring devices.

The **lateral strain** is proportional to the axial strain in the linear elastic range, provided the material is both homogeneous and isotropic. A material is **homogeneous** if it has the same composition throughout the body; hence, the elastic properties are the same at every point in the body. Note, however, that the properties need not be the same in all directions for the material to be homogeneous. For instance, the modulus of elasticity could be different in the axial and transverse directions. **Isotropic** materials have the same elastic properties in all directions. Therefore, the material must be both homogeneous and isotropic in order for the lateral strains in a bar in tension (Fig. 1-20) to be the same at every point. Many structural materials meet these requirements.

The ratio of the strain in the lateral direction to the strain in the axial direction is known as **Poisson's ratio** and is denoted by the Greek letter ν (nu); thus,

$$\nu = - \frac{\text{lateral strain}}{\text{axial strain}} \tag{1-6}$$

For a bar in tension, the lateral strain represents a decrease in width (negative strain) and the axial strain represents elongation (positive strain). For compression we have the opposite situation, with the bar becoming shorter (negative axial strain) and wider (positive lateral strain). Therefore, Poisson's ratio has a positive value for most materials.

Poisson's ratio is named for the famous French mathematician Siméon Denis Poisson (1781–1840), who attempted to calculate this ratio by a molecular theory of materials (Ref. 1-9). For isotropic materials, Poisson found $\nu = \frac{1}{2}$. However, more recent calculations based upon a model of atomic structure give $\nu = \frac{1}{3}$. Both of these values are close to actual measured values, which are in the range of 0.25 to

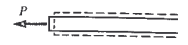
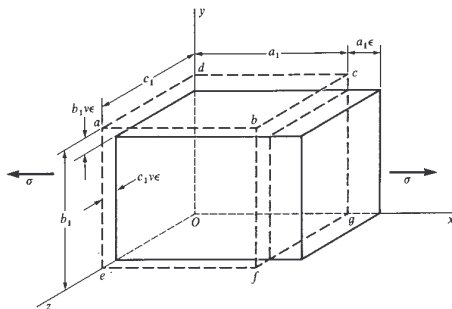


Fig. 1-20 Axial elongation lateral contraction of a bar in



shape of an

0.35 for many metals and other materials. Materials with an extremely low value of Poisson's ratio include cork, for which ν is practically zero,* and concrete, for which ν is about 0.1 or 0.2. A theoretical upper limit for Poisson's ratio is 0.5, as explained in the following subsection on volume changes. Rubber comes close to this limiting value. A table of values of Poisson's ratio for various materials in the elastic range is given in Appendix H (see Table H-2). For most practical purposes, the value of ν can be taken as the same in both tension and compression.

The lateral contraction of a bar in tension, or the expansion of a bar in compression, is an illustration of strain without a corresponding stress. There is no normal stress in the transverse direction of an axially loaded bar, yet there is strain because of the Poisson effect. Another common instance of strain without stress is thermal strain, which is produced by a change in temperature (see Section 2.6).

Volume change. Because the dimensions of a bar in tension or compression are changed when the load is applied (see Fig. 1-20), the volume of the bar changes too. The change in volume can be calculated from the axial and lateral strains. Let us take a small element of material cut out from an isotropic bar in tension (Fig. 1-21). The original shape of the element is shown by the rectangular parallelepiped $abcdefgO$ having sides of lengths a_1 , b_1 , and c_1 in the x , y , and z directions, respectively.** The x axis is taken in the longitudinal direction of the bar, which is also indicated in the figure by showing the directions of the normal stresses σ produced by the axial forces. The final shape of the element is shown by

solid lines. The elongation of the element in the direction of loading is $a_1\epsilon$, where ϵ is the axial strain. Because the lateral strains are $-\nu\epsilon$ (see Eq. 1-6), the lateral dimensions decrease by $b_1\nu\epsilon$ and $c_1\nu\epsilon$ in the y and z directions, respectively. Thus, the final dimensions of the element are $a_1(1 + \epsilon)$, $b_1(1 - \nu\epsilon)$, and $c_1(1 - \nu\epsilon)$, and the final volume is

$$V_f = a_1 b_1 c_1 (1 + \epsilon)(1 - \nu\epsilon)(1 - \nu\epsilon)$$

When this expression is expanded, we obtain terms involving the square and cube of ϵ . Because ϵ is very small compared to unity, its square and cube are negligible in comparison to ϵ itself and may be dropped from the expression. Therefore, the final volume of the element is

$$V_f = a_1 b_1 c_1 (1 + \epsilon - 2\nu\epsilon)$$

and the change in volume is

$$\Delta V = V_f - V_o = a_1 b_1 c_1 \epsilon (1 - 2\nu)$$

where V_o is the original volume $a_1 b_1 c_1$. The **unit volume change** e is defined as the change in volume divided by the original volume, or

$$e = \frac{\Delta V}{V_o} = \epsilon(1 - 2\nu) = \frac{\sigma}{E}(1 - 2\nu) \tag{1-7}$$

The quantity e is also known as the **dilatation**. Equation (1-7) can be used to calculate the increase in volume of a bar in tension provided the axial strain ϵ (or stress σ) and Poisson's ratio ν are known. This equation may also be used for compression, in which case ϵ is a negative strain and the volume of the bar decreases.

From Eq. (1-7) we see that the maximum possible value of ν for ordinary materials is 0.5, because any larger value means that the volume decreases when the material is stretched, which seems physically unlikely. As already pointed out, for most materials ν is about $\frac{1}{3}$ or $\frac{1}{2}$ in the linear elastic region, which means that the unit volume change is in the range 0.3ϵ to 0.5ϵ . In the plastic region of behaviour, no volume changes occur, so Poisson's ratio may be taken as 0.5.

Example

A prismatic bar of circular cross section is loaded by tensile forces $P = 85$ kN (see Fig. 1-20). The bar has length $L = 3.0$ m and diameter $d = 30$ mm. It is made of aluminium with modulus of elasticity $E = 70$ GPa and Poisson's ratio $\nu = \frac{1}{3}$. Calculate the elongation δ , the decrease in diameter Δd , and the increase in volume ΔV of the bar.

The longitudinal stress σ in the bar can be obtained from the equation

$$\sigma = \frac{P}{A} = \frac{85 \text{ kN}}{\pi(30 \text{ mm})^2/4} = 120 \text{ MPa}$$

* Hence its suitability for a bottle stopper.
** A parallelepiped is a prism whose bases are parallelograms; thus, a parallelepiped has six faces, each of which is a parallelogram. Opposite faces are parallel and identical parallelograms. A rectangular parallelepiped has all faces in the form of rectangles.

This stress is probably below the proportional limit (see Table H-3, Appendix H), hence we will assume that the material behaves linearly elastically. Then the axial strain is found from Hooke's law:

$$\epsilon = \frac{\sigma}{E} = \frac{120 \text{ MPa}}{70 \text{ GPa}} = 0.00171$$

The total elongation is

$$\delta = \epsilon L = (0.00171)(3.0 \text{ m}) = 5.14 \text{ mm}$$

The lateral strain is obtained from Poisson's ratio:

$$\epsilon_{\text{lateral}} = -\nu\epsilon = -\frac{1}{3}(0.00171) = -0.000570$$

The decrease in diameter equals numerically the lateral strain times the diameter:

$$\Delta d = \epsilon_{\text{lateral}} d = (0.000570)(30 \text{ mm}) = 0.0171 \text{ mm}$$

Finally, the change in volume is calculated from Eq. (1-7):

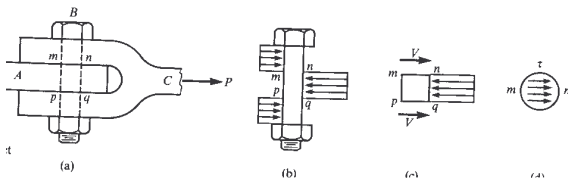
$$\begin{aligned} \Delta V &= V_0\epsilon(1 - 2\nu) \\ &= \left(\frac{\pi}{4}\right)(30 \text{ mm})^2(3.0 \text{ m})(0.00171)\left(1 - \frac{2}{3}\right) = 1210 \text{ mm}^3 \end{aligned}$$

Because the bar is in tension, ΔV represents an increase in volume.

1.6 SHEAR STRESS AND STRAIN

In the preceding sections, we dealt primarily with the effects of normal stresses produced by axial forces. We shall now consider a different kind of stress, known as a **shear stress**, that acts **parallel** or **tangential** to the surface.

As an example of a practical situation in which shear stresses are present, consider the bolted connection shown in Fig. 1-22a. This connection consists of a flat bar *A*, a clevis *C*, and a bolt *B* that passes through holes in the bar and clevis. Under the action of the tensile loads



P, the bar and clevis will press against the bolt in **bearing**; and contact stresses, called **bearing stresses**, will be developed against the bolt. A free-body diagram of the bolt (Fig. 1-22b) shows these bearing stresses. The actual distribution of the bearing stresses against the bolt is difficult to determine, so for simplicity the stresses are shown as though they were uniformly distributed. Based upon the assumption of uniform distribution, we can calculate an average bearing stress by dividing the total force by the bearing area. This area is taken as the projected area of the curved bearing surface, which in this case is a rectangle.

The free-body diagram of Fig. 1-22b shows that there is a tendency to shear the bolt along cross sections *mn* and *pq*. From a free-body diagram of the portion *mnpq* of the bolt (see Fig. 1-22c), we see that **shear forces** *V* must act over the cut surfaces of the bolt. In this particular example, each shear force *V* is equal to *P*/2. These shear forces are actually the resultants of the shear stresses distributed over the cross-sectional areas of the bolt. The shear stresses on cross section *mn* are shown by small arrows in Fig. 1-22d. The exact distribution of these stresses is not known, but they are highest near the middle and become zero at certain locations on the edges. Shear stresses are customarily denoted by the Greek letter τ (tau).

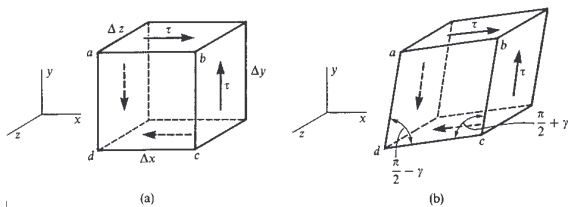
The average shear stress on the cross section of the bolt is obtained by dividing the total shear force *V* by the area *A* over which it acts:

$$\tau_{\text{aver}} = \frac{V}{A} \tag{1-8}$$

In the example shown in Fig. 1-22, the shear force is *P*/2 and the area *A* is the cross-sectional area of the bolt. From Eq. (1-8) we see that shear stresses, like normal stresses, represent intensity of force, or force per unit of area. Thus, the units of shear stress are the same as those for normal stress, namely pascals in SI units.

The loading arrangement shown in Fig. 1-22a is an example of **direct shear**, or **simple shear**, in which the shear stresses are created by a direct action of the forces in trying to cut through the material. Direct shear arises in the design of bolts, pins, rivets, keys, welds, and glued joints. Shear stresses also arise in an indirect manner when members are subjected to tension, torsion, and bending, as discussed in later chapters.

To obtain a more complete picture of the action of shear stresses, let us consider a small element of material in the form of a rectangular parallelepiped having sides of length Δx , Δy , and Δz (Fig. 1-23a). The front and rear faces of the element are assumed to be free of any stresses. Now suppose that a shear stress τ is distributed uniformly over the top face of the element. Then, in order for the element to be in equilibrium in the *x* direction, an equal but oppositely directed shear stress must also act on the bottom face. Note that the total shear force on the top



face is $\tau\Delta x\Delta z$ and that this force is balanced by the equal and oppositely directed force on the bottom face. These two forces form a couple having a moment about the *z* axis of magnitude $\tau\Delta x\Delta y\Delta z$, clockwise in the figure. Equilibrium of the element requires that this moment be balanced by an equal and opposite moment resulting from shear stresses acting on the side faces of the element. Denoting the stresses on the side faces as τ_1 , we see that the vertical shear forces are $\tau_1\Delta y\Delta z$ and that they form a counterclockwise couple of moment $\tau_1\Delta x\Delta y\Delta z$. It follows from moment equilibrium that $\tau_1 = \tau$, and hence the magnitudes of the shear stresses on the four faces of the element are equal, as shown in Fig. 1-23a. Thus, we have reached the following conclusions:

1. Shear stresses on opposite faces of an element are equal in magnitude and opposite in direction.
2. Shear stresses on perpendicular faces of an element are equal in magnitude and have directions such that both stresses point toward, or both point away from, the line of intersection of the faces.

These conclusions concerning the shear stresses hold even when normal stresses also act on the faces of the element.

An element subjected to shear stresses only, as pictured in Fig. 1-23a, is said to be in **pure shear**.^{*} Under the action of these shear stresses, the material is deformed, resulting in **shear strains**. In order to visualize these strains, we note first that the shear stresses have no tendency to elongate or shorten the element in the *x*, *y*, and *z* directions; in other words, the lengths of the sides of the element do not change. Instead, the shear stresses produce a change in the shape of the element, as shown in Fig. 1-23b. The original element is deformed into an oblique parallelepiped,^{**} and the front face *abcd* of the element becomes a rhomboid.[†] The angles between the faces at points *b* and *d*, which were

^{*} Pure shear is discussed in greater detail in Section 3.4.

^{**} An **oblique angle** can be either acute or obtuse, but it is *not* a right angle.

[†] A **rhomboid** is a parallelogram with oblique angles and all four sides *not* equal. (If the sides Δx and Δy of the element are equal, then face *abcd* is a rhombus, which is a

$\pi/2$ before deformation, are reduced by a small angle γ to $\pi/2 - \gamma$ (see Fig. 1-23b). At the same time, the angles at *a* and *c* are increased to $\pi/2 + \gamma$. The angle γ is a measure of the distortion, or change in shape, of the element and is called the **shear strain**. The units of shear strain are radians.

Shear stresses and strains having the directions shown in Fig. 1-23 are assumed to be positive. To make this sign convention clear, we will refer to the faces oriented toward the positive directions of the axes as the positive faces of the element. In other words, a positive face has its outward normal directed in the positive direction of a coordinate axis. The opposite faces are negative faces. Thus, in Fig. 1-23a, the right-hand, top, and front faces are the positive *x*, *y*, and *z* faces, respectively, and the opposite faces are the negative *x*, *y*, and *z* faces. Using this terminology, we may state the **sign convention for shear stresses** as follows: A shear stress acting on a positive face of an element is positive if it acts in the positive direction of one of the coordinate axes and negative if it acts in the negative direction of the axis. A shear stress acting on a negative face of an element is positive if it acts in the negative direction of an axis and negative if it acts in the positive direction. Thus, all shear stresses shown in Fig. 1-23a are positive.

The **sign convention for shear strains** is related to that for stresses. Shear strain in an element is positive when the angle between two positive (or two negative) faces is reduced. The strain is negative when the angle between two positive (or two negative) faces is increased. Thus, the strains shown in Fig. 1-23b are positive, and we see that positive shear stresses produce positive shear strains.

The properties of a material in shear can be determined experimentally from direct-shear tests or torsion tests. The latter tests are performed by twisting hollow, circular tubes, thereby producing a state of pure shear stress, as explained in Chapter 3. From the results of these tests, **stress-strain diagrams in shear** may be plotted. These diagrams of τ versus γ are similar in shape to the tension-test diagrams (σ versus ϵ) for the same materials. From the shear diagrams, we can obtain shear properties such as the proportional limit, the yield stress, and the ultimate stress. These properties in shear are usually about half as large as those in tension. For instance, the yield stress for structural steel in shear is 0.5 to 0.6 times the yield stress in tension.

The initial part of the shear stress-strain diagram is a straight line, just as in tension. For this linear elastic region, the shear stress and shear strain are directly proportional, and we have the following equation for **Hooke's law in shear**:

$$\tau = G\gamma \tag{1-9}$$

in which *G* is the **shear modulus of elasticity** (also called the **modulus of rigidity** or **shear modulus**), which is defined as the ratio of shear stress to shear strain.

Compression, and Shear

ulus E , namely, psi or ksi in USCS units and pascals in SI units. For mild steel, typical values of G are 75 GPa; for aluminium, typical values are 28 GPa. Additional values are listed in Table H-2, Appendix H.

The moduli of elasticity in tension and shear (E and G) are related by the following equation:

$$G = \frac{E}{2(1 + \nu)} \quad (1-10)$$

in which ν is Poisson's ratio. This relationship, which is derived in Section 3.5, shows that E , G , and ν are not independent elastic properties of the material. Because the value of Poisson's ratio for ordinary materials is between zero and one-half, we see from Eq. (1-10) that G must be from one-third to one-half of E .

Example 1

A punch with a diameter of 19 mm is used to punch a hole in a 6 mm steel plate (Fig. 1-24). A force $P = 116$ kN is required. What is the average shear stress in the plate and the average compressive stress in the punch?

The average shear stress is obtained by dividing the force P by the area being sheared by the punch. This area is equal to the circumference of the hole times the thickness of the plate:

$$A_s = \pi(19 \text{ mm})(6 \text{ mm}) = 358 \text{ mm}^2$$

Therefore, the average shear stress is

$$\tau_{\text{aver}} = \frac{P}{A_s} = \frac{116 \text{ kN} \times 10^3}{358 \text{ mm}^2} = 324 \text{ MPa}$$

Also, the average compressive stress in the punch is

$$\sigma_c = \frac{P}{A_c} = \frac{116 \text{ kN} \times 10^3}{\pi(19 \text{ mm})^2/4} = 409 \text{ MPa}$$

in which A_c is the cross-sectional area of the punch.

Example 2

A bearing pad consisting of a flexible material of thickness h capped by a thin steel plate of dimensions $a \times b$ (Fig. 1-25a) is subjected to a horizontal shear force V (Fig. 1-25b). Determine the average shear stress and strain in the pad

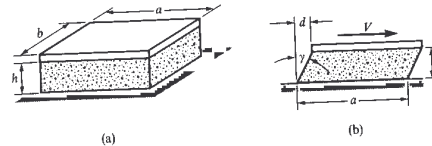


Fig. 1-25 Example 2

The average shear stress equals the force V divided by the area over which it acts:

$$\tau_{\text{aver}} = \frac{V}{ab}$$

The corresponding shear strain (assumed to be uniform throughout the pad) is

$$\gamma_{\text{aver}} = \frac{\tau_{\text{aver}}}{G} = \frac{V}{abG}$$

in which G is the shear modulus of the material. Finally, the displacement d is equal to $h \tan \gamma$ (see Fig. 1-25b). However, if γ is a very small angle, we may replace $\tan \gamma$ by γ itself and obtain

$$d = h\gamma = \frac{hV}{abG}$$

as the horizontal displacement of the plate.

1.7 ALLOWABLE STRESSES AND ALLOWABLE LOADS

An important consideration in engineering design is the capacity of the object being designed to support or transmit loads. Objects that must sustain loads include building structures, machines, aircraft, vehicles, ships, and a seemingly endless list of other man-made things. For simplicity, we will refer to all such objects as **structures**; thus, a structure is any object that must support or transmit loads.

If structural failure is to be avoided, the loads that a structure actually can support must be greater than the loads it will be required to sustain when in service. The ability of a structure to resist loads is called **strength**, hence the preceding criterion can be restated as follows: The actual strength of a structure must exceed the required strength. The ratio of the actual strength to the required strength is called the **factor of safety** n :

$$\text{Factor of safety } n = \frac{\text{actual strength}}{\text{required strength}} \quad (1-11)$$

1.7 Allowable Stresses and Allowable Loads

Compression, and Shear

Of course, the factor of safety must be greater than 1.0 if failure is to be avoided. Depending upon the circumstances, factors of safety from slightly above 1.0 to as much as 10 are used.

The incorporation of factors of safety into design is not a simple matter, because both strength and failure have many different meanings. **Failure** can mean the fracture or complete collapse of a structure, or it can mean that the deformations have exceeded some limiting value so that the structure is no longer able to perform its intended functions. The latter kind of failure may occur at loads much smaller than those that cause actual collapse. The determination of a factor of safety must also take into account such matters as the following: the probability of accidental overloading of the structure; the types of loads (static, dynamic, or repeated) and how accurately they are known; the possibility of fatigue failure; inaccuracies in construction; quality of workmanship; variations in properties of materials; deterioration due to corrosion or other environmental effects; accuracy of the methods of analysis; whether failure is gradual (ample warning) or sudden (no warning); consequences of failure (minor damage or major catastrophe); and other such considerations. If the factor of safety is too low, the likelihood of failure will be high and hence the structure will be unacceptable; if the factor is too large, the structure will be wasteful of materials and perhaps unsuitable for its function (for instance, it may be too heavy). Because of these complexities, good engineering judgment is required when establishing factors of safety. They are usually determined by groups of experienced engineers who write the codes and specifications used by other designers.

In actual practice, there are several ways in which factors of safety are defined and implemented. For many structures, it is important that the material remain within the linear elastic range in order to avoid permanent deformations when the loads are removed. Hence, a common method of design is to use a factor of safety with respect to yielding of the structure. The structure begins to yield when the yield stress is reached at any point within the structure. By applying a factor of safety with respect to the yield stress, we obtain an **allowable stress**, or **working stress**, that must not be exceeded anywhere in the structure. Thus,

$$\text{Allowable stress} = \frac{\text{yield stress}}{\text{factor of safety}}$$

or

$$\sigma_{\text{allow}} = \frac{\sigma_y}{n} \quad (1-12)$$

in which we have introduced the notations σ_{allow} and σ_y for the allowable and yield stresses, respectively. In building design, a typical factor of safety n with respect to yielding is 1.67; thus, a mild steel having a yield stress σ_y of 250 MPa has an allowable stress σ_{allow} in tension of 150 MPa.

Another method of design is to establish the allowable stress by

applying a factor of safety with respect to the **ultimate stress** instead of the yield stress. This method is suitable for brittle materials, such as concrete, and it also is used for wood. The allowable stress is obtained from the equation

$$\sigma_{\text{allow}} = \frac{\sigma_u}{n} \quad (1-13)$$

in which σ_u is the ultimate stress. The factor of safety is normally much greater with respect to the ultimate stress than with respect to the yield stress. In the case of mild steel, a factor of safety of 1.67 with respect to yielding corresponds to a factor of approximately 2.8 with respect to the ultimate stress.

The last method we will describe involves the application of factors of safety to loads rather than to stresses. We will use the term **ultimate loads** to mean the loads that produce failure or collapse of the structure. The loads that the structure must support in service are called **service loads** or **working loads**. The factor of safety is the ratio of the former to the latter:

$$\text{Factor of safety } n = \frac{\text{ultimate load}}{\text{service load}} \quad (1-14)$$

Inasmuch as the service loads are known quantities, the usual design procedure is to multiply them by the factor of safety to obtain the ultimate loads. Then the structure is designed so that it can just sustain the ultimate loads at failure. This method of design is known as **strength design**, or **ultimate-load design**, and the factor of safety is called the **load factor** because it is a multiplier of the service loads:

$$\text{Ultimate load} = (\text{service load})(\text{load factor}) \quad (1-15)$$

Typical load factors used in the design of reinforced concrete structures are 1.4 for **dead load**, which is the weight of the structure itself, and 1.7 for **live loads**, which are loads applied to the structure. The strength-design method is used regularly for reinforced concrete structures and occasionally for steel structures. Methods for determining ultimate loads of some simple structures are given in Section 2.10 and in Chapter 10.

In aircraft design, it is customary to speak of the margin of safety rather than the factor of safety. The **margin of safety** is defined as the factor of safety minus one:

$$\text{Margin of safety} = n - 1 \quad (1-16)$$

Thus, a structure having an ultimate strength that is twice the required strength has a factor of safety of 2.0 and a margin of safety of 1.0. When the margin of safety is reduced to zero or less, the structure (presumably) will fail.

Example 1

A short, hollow, circular, cast-iron cylinder (Fig. 1-26) is to support an axial compressive load $P = 580$ kN. The ultimate stress in compression for the material is $\sigma_u = 240$ MPa. It is decided to design the cylinder with a wall thickness t of 25 mm and a factor of safety of 3.0 with respect to the ultimate strength. Compute the minimum required outside diameter d of the cylinder.

The allowable compressive stress is equal to the ultimate stress divided by the factor of safety (Eq. 1-13):

$$\sigma_{\text{allow}} = \frac{\sigma_u}{n} = \frac{240 \text{ MPa}}{3} = 80 \text{ MPa}$$

The required cross-sectional area can now be found:

$$A = \frac{P}{\sigma_{\text{allow}}} = \frac{580 \text{ kN} \times 10^3}{80 \text{ MPa}} = 7250 \text{ mm}^2$$

The actual cross-sectional area is

$$A = \frac{\pi d^2}{4} - \frac{\pi(d-2t)^2}{4} = \pi t(d-t)$$

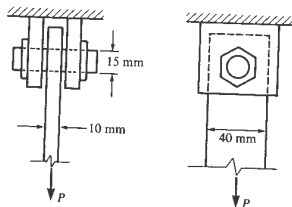
in which d is the outside diameter and $d - 2t$ is the inside diameter. Solving for d and then substituting $t = 25$ mm and $A = 7250 \text{ mm}^2$, we get

$$d = t + \frac{A}{\pi t} = 117 \text{ mm}$$

The outside diameter must be at least this large in order to have the desired factor of safety.

Example 2

A steel bar of rectangular cross section (10×40 mm) carries a tensile load P and is attached to a support by means of a round pin of diameter 15 mm (Fig. 1-27). The allowable stresses for the bar in tension and the pin in shear are



At the top of the pillar, the required cross-sectional area A_0 and corresponding radius r_0 (Fig. 1-28b) are

$$A_0 = \frac{P}{\sigma_c} \quad r_0 = \left(\frac{A_0}{\pi}\right)^{1/2} = \left(\frac{P}{\pi\sigma_c}\right)^{1/2} \quad (1-17)$$

At a lower elevation, the required area is larger because the weight of the pillar above that elevation also must be supported. To aid in evaluating this weight, let us use xy axes as shown in Fig. 1-28b. Then, at distance ξ from the top of the pillar, the required area A_ξ is

$$A_\xi = \frac{P + W_\xi}{\sigma_c}$$

where W_ξ is the weight of the pillar between cross sections at $x = 0$ and $x = \xi$. The required area at distance $\xi + d\xi$ is equal to the area A_ξ plus an additional area dA_ξ due to the weight of the small element shown shaded in Fig. 1-28b:

$$A_{\xi+d\xi} = A_\xi + dA_\xi = \frac{P + W_\xi}{\sigma_c} + \frac{\gamma A_\xi d\xi}{\sigma_c}$$

Thus, the increment dA_ξ in the area is

$$dA_\xi = \frac{\gamma A_\xi d\xi}{\sigma_c}$$

or

$$\frac{dA_\xi}{A_\xi} = \frac{\gamma d\xi}{\sigma_c}$$

This last expression can be integrated between the cross sections at $\xi = 0$ and $\xi = x$. Therefore, the limits on ξ are 0 and x , and the corresponding limits on A_ξ are A_0 and A_x . Thus, we obtain

$$\int_{A_0}^{A_x} \frac{dA_\xi}{A_\xi} = \frac{\gamma}{\sigma_c} \int_0^x d\xi$$

After carrying out these integrations and substituting the limits, we obtain*

$$\ln \frac{A_x}{A_0} = \frac{\gamma x}{\sigma_c}$$

or

$$A_x = A_0 \exp(\gamma x / \sigma_c) \quad (1-18)$$

This equation gives the required area A_x as a function of the distance x from the top of the pillar. Note that, if $x = 0$, A_x is equal to A_0 . At the bottom of the pillar, the required area is

$$A_1 = A_0 \exp(\gamma h / \sigma_c) \quad (1-19)$$

* The symbol \ln stands for natural logarithm, and the notation $\exp(z)$ denotes e^z , where e is the base of the natural logarithm.

$\sigma_{\text{allow}} = 120$ MPa and $\tau_{\text{allow}} = 60$ MPa, respectively. What is the maximum permissible value of the load P ?

The tensile stress in the rectangular bar must be calculated using the net area at the cross section containing the hole for the pin. This area is

$$A_{\text{net}} = (40 \text{ mm} - 15 \text{ mm})(10 \text{ mm}) = 250 \text{ mm}^2$$

Hence, the allowable load P_1 based upon tension in the bar is

$$P_1 = \sigma_{\text{allow}} A_{\text{net}} = (120 \text{ MPa})(250 \text{ mm}^2) = 30 \text{ kN}$$

This calculation disregards any localized stresses due to the presence of the hole.

Next, we calculate the allowable load based upon shear in the pin. The pin tends to shear on two cross sections, hence the total force that can be carried is

$$P_2 = \tau_{\text{allow}} (2A)$$

in which A is the cross-sectional area of the pin. Substitution of numerical values gives

$$P_2 = (60 \text{ MPa})(2)\left(\frac{\pi}{4}\right)(15 \text{ mm})^2 = 21.2 \text{ kN}$$

Comparing the two preceding values for P , we see that shear in the pin governs and that

$$P_{\text{allow}} = 21.2 \text{ kN}$$

is the maximum permissible value of the load.

***Example 3**

Determine the radius r of a pillar of circular cross section and height h in order that the volume of the pillar will be a minimum if the pillar supports a compressive load P at the top as well as its own weight (Fig. 1-28a). Let σ_c denote the allowable stress in compression and γ the specific weight of the material.

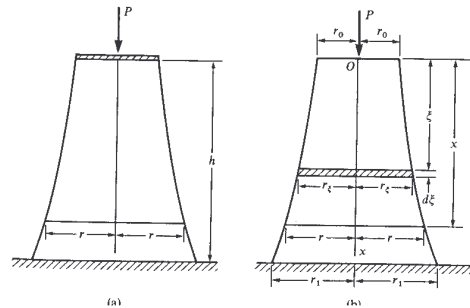


Fig. 1-28 Example 3. Pillar of

The corresponding radii are

$$r = \left(\frac{A_x}{\pi}\right)^{1/2} \quad r_1 = \left(\frac{A_1}{\pi}\right)^{1/2} \quad (1-20)$$

These equations give the dimensions of an optimum pillar having minimum volume (and, hence, also minimum weight), because at every cross section the area of the pillar is just sufficient to support the superimposed load.

The volume of the optimum pillar can also be calculated if desired:

$$V = \int_0^h A_x dx = \int_0^h A_0 \exp(\gamma x / \sigma_c) dx = \frac{A_0 \sigma_c}{\gamma} [\exp(\gamma h / \sigma_c) - 1] = \frac{P}{\gamma} [\exp(\gamma h / \sigma_c) - 1] \quad (1-21)$$

Another form of this equation is

$$V = \frac{\sigma_c}{\gamma} (A_1 - A_0) \quad (1-22)$$

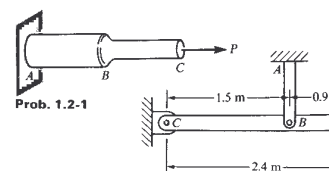
which gives the volume in terms of the areas at the ends.

This example illustrates the concept of an optimum structure, which is a hypothetical structure that meets a certain criterion, such as minimum volume or minimum weight. In practice, it usually is not feasible to build a structure that has the properties of the "ideal" optimum structure. Nevertheless, knowledge of the properties of an optimum structure can serve an important role in design, because the properties of a realistic structure can be compared with those of the ideal structure in order to determine the degree of efficiency of the actual structure. For instance, the formulas derived in this example show that the optimum structure differs very little from a prismatic structure. In a typical case, the required area A_1 at the base is only a few percent larger than the area A_0 at the top. (Thus, the pillar pictured in Fig. 1-28 is drawn with its variation in radius from top to bottom greatly exaggerated.) We learn from this example that a prismatic structure is very nearly an optimum structure for this particular loading, and it is not worthwhile to improve upon it by varying the cross section (see Problem 1.7-16).

PROBLEMS/CHAPTER 1

1.2-1 A bar ABC having two different cross-sectional areas is loaded by an axial force $P = 425$ kN (see figure). Both parts of the bar have circular cross sections. The diameters of parts AB and BC are 100 mm and 65 mm respectively. Calculate the normal stresses σ_{ab} and σ_{bc} in each part of the bar.

1.2-2 A horizontal bar CBD having a length of 2.4 m is supported and loaded as shown in the figure. The vertical member AB has a cross-sectional area of 550 mm². Determine the magnitude of the load P so that it produces a normal stress of 100 MPa in the bar.



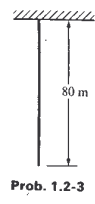
Compression, and Shear

of length 80 m hangs freely (see figure). Determine the maximum stress in the cable, assuming that aluminium has a specific weight of 26.6 kN/m^3 .

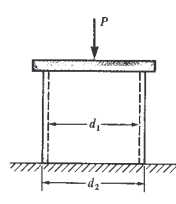
A round bar of diameter $d_1 = 100 \text{ mm}$ and length $L = 2 \text{ m}$ is compressed by an axial load P . Calculate the average compressive stress σ_c .

A rectangular cross section of a concrete column is shown in the figure. The column is subjected to a concentrated load P at the top. Determine the average compressive stress σ_c in the concrete.

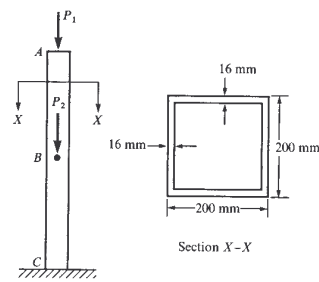
A cross section of a concrete column is shown in the figure. The column is subjected to a concentrated load P at the top. Determine the average compressive stress σ_c in the concrete.



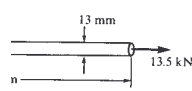
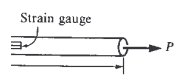
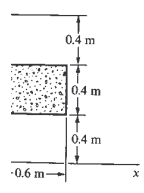
Prob. 1.2-3



Prob. 1.2-4



Prob. 1.2-5

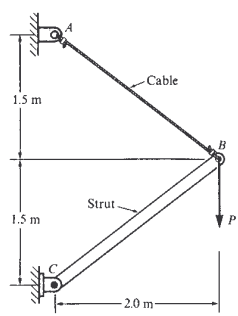


1.2-7 A high-strength steel wire to be used for prestressing a concrete beam has a length of 24 m and is stretched by 75 mm. What is the tensile strain in the wire?

1.2-8 A round bar of length $L = 1.5 \text{ m}$ is loaded in tension as shown in the figure. A normal strain $\epsilon = 2 \times 10^{-3}$ is measured by a strain gauge placed on the bar. What elongation δ of the entire bar can be expected at this load?

1.2-9 A steel rod 1 m long and 13 mm in diameter carries a tensile load of 13.5 kN (see figure). The bar increases in length by 0.5 mm when the load is applied. Determine the

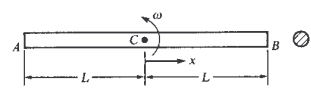
1.2-10 A strut and cable assembly ABC (see figure) supports a vertical load $P = 15 \text{ kN}$. The cable has an effective cross-sectional area of 120 mm^2 , and the strut has an area of 250 mm^2 . (a) Calculate the normal stresses σ_{ab} and σ_{bc} in the cable and strut, and indicate whether they are tension or compression. (b) If the cable elongates 1.3 mm, what is the strain? (c) If the strut shortens 0.62 mm, what is the strain?



Prob. 1.2-10

1.2-11 A long wire of specific weight γ hangs freely under its own weight. Derive a formula for the tensile stress σ_x in the wire as a function of the distance y from the lower end (see figure).

1.2-12 A round bar ACB of total length $2L$ rotates about an axis through the midpoint C with constant angular speed ω (radians per second). The material of the bar has specific weight γ . Derive a formula for the tensile stress σ_x in the bar as a function of the distance x from point C . What is the maximum tensile stress?



Prob. 1.2-12

1.3-1 A long wire hangs vertically under its own weight. What is the greatest length it can have without yielding if it is made of: (a) steel having a yield stress of 248 MPa and (b) aluminium having a yield stress of 124 MPa? (Note: The specific weight of steel is 7.85 t/m^3 and of aluminium is 2.75 t/m^3 .)

1.3-2 Three different materials A , B , and C are tested in tension using standard test specimens having diameters of 13 mm and gauge lengths of 50 mm. After the specimens are fractured, the distances between the gauge marks are found to be 54, 63, and 71 mm, respectively. Also, the diameters are 12.3, 10.1, and 16.4 mm, respectively, at the failure cross sections. Determine the percent elongation and percent reduction in area of each specimen. Also, classify the materials as brittle or ductile.

1.3-3 The data shown in the table were obtained from a tensile test of high-strength steel. The test specimen had a diameter of 13 mm, and a gauge length of 50 mm was used. The total elongation between the gauge marks at fracture was 10.7 mm, and the minimum diameter was 9.4 mm. Plot the nominal stress-strain diagram for the steel and determine the proportional limit, yield stress at 0.1% offset, ultimate stress, percent elongation in 50 mm,

Tensile-test data for Problem 1.3-3

Load (kN)	Elongation (mm)
5	0.005
10	0.015
30	0.048
50	0.084
60	0.102
64.5	0.109
67	0.119
68	0.137
69	0.160
70	0.229
72	0.300
76	0.424
84	0.668
92	0.965
100	1.288
112	2.814
127	fracture

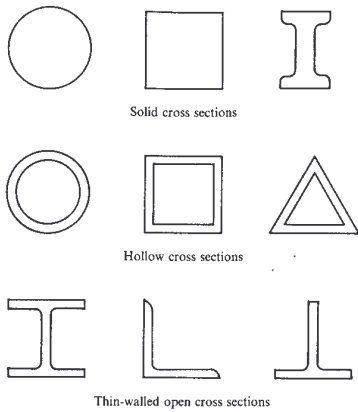
CHAPTER

Axially Loaded Members

2.1 INTRODUCTION

This chapter is devoted to the behavior of axially loaded members, which are structural elements having straight longitudinal axes and carrying only axial forces (tensile or compressive). Members of this type appear in such diverse forms as diagonals in trusses, connecting rods in engines, cables in bridges, columns in buildings, and struts in aircraft engine mounts. Their cross sections may be solid, hollow, or thin-walled and open (Fig. 2-1). Whether you are designing a member for a proposed structure or analyzing an existing structure, it often is necessary to find not only the maximum stresses in the member (as discussed in Chapter 1) but also the deflections. For instance, the deflections may have to be kept within limits in order to maintain certain clearances. Deflections are also needed in the analysis of statically indeterminate structures, a vast subject that we will introduce in Section 2.4. Other topics of this chapter include temperature effects, stresses on inclined sections, strain energy, dynamic loading, and nonlinear behavior. Although in this chapter we consider only members with axial loads, we will see later that these same topics are important for all types of structural elements. In treating these subjects, we will make use of the material on tension, compression, and shear that we discussed in Chapter 1.

Throughout the remainder of this book, the words *analysis* and *design* appear many times. The term *analysis* is customarily used in mechanics to mean the calculation of such quantities as stresses, strains, deflections, and load-carrying capacity. When analyzing a structure, or part of a structure, we assume that the dimensions of the structure and the material of which it is composed are known. Hence, we may speak of analyzing a structure in order to determine its behavior under known loads. A more difficult task is that of *design*, which is the determination of the geometric configuration of a structure in order that it will fulfill



sections of

a prescribed function. For instance, we may speak of designing a structure to support certain given loads. Designing a structure invariably requires that analyses be performed on that structure, often more than once. Still another common term is **optimization**, which is part of the design process. Optimization is the task of designing the "best" structure to meet a particular goal, such as designing a structure with the least weight. Of course, the goal must be achieved within certain restrictions; for instance, the goal might be to design a structure having the least weight but with the deflection not to exceed a specified amount. Thus, analysis, design, and optimization are closely linked, as illustrated in the examples and problems that appear in this and later chapters.

2.2 DEFLECTIONS OF AXIALLY LOADED MEMBERS

A prismatic bar of length L loaded in tension by axial forces P is shown in Fig. 2-2. If the forces P act at the centroid of the cross section, the uniform stress in the bar at sections away from the ends is given by the formula $\sigma = P/A$, where A is the cross-sectional area (see Eq. 1-1). Also, if the bar is made of a homogeneous material, the axial strain is $\epsilon = \delta/L$, where δ is the total elongation produced by the axial forces (see Eq. 1-2). Let us now assume that the material is linearly elastic so that Hooke's law ($\sigma = E\epsilon$) applies. Then the preceding expressions for σ and

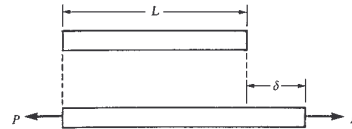


Fig. 2-2 Elongation of a bar in tension

ϵ can be combined to give the following equation for the elongation of the bar:

$$\delta = \frac{PL}{EA} \tag{2-1}$$

This equation shows that the elongation of a homogeneous bar made of linearly elastic material is directly proportional to the load P and the length L and is inversely proportional to the modulus of elasticity E and the cross-sectional area A . The product EA is known as the **axial rigidity** of the bar. Of course, Eq. (2-1) also can be used for a member in compression, in which case δ represents the shortening of the bar. When a **sign convention** is needed, elongation is taken as positive and shortening as negative.

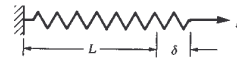


Fig. 2-3 Linear elastic spring in tension

From Eq. (2-1) we see that a bar in tension is analogous to an axially loaded spring (Fig. 2-3). Under the action of the force P , the spring elongates an amount δ , so that its total length becomes $L + \delta$, where L is the original length. The **spring constant** k is defined as the force required to produce a unit elongation of the spring, that is, $k = P/\delta$. The **compliance** of the spring is the reciprocal of the spring constant, or the deflection produced by a load of unit value. In the case of a bar in tension (Fig. 2-2) or any other structural element, such as a beam, it is customary to speak of stiffnesses and flexibilities rather than spring constants and compliances.

The **stiffness** k of an axially loaded bar is defined as the force required to produce a unit deflection; hence, we see from Eq. (2-1) that the stiffness of the bar in Fig. 2-2 is

$$k = \frac{EA}{L} \tag{2-2}$$

In an analogous manner, the **flexibility** f is defined as the deflection due to a unit load. Thus, the flexibility of an axially loaded bar is

$$f = \frac{L}{EA} \tag{2-3}$$

which is the reciprocal of the stiffness. Stiffnesses and flexibilities have an important role in the analysis of many types of structures. Note that an increase in the length of the bar means a reduction in stiffness and an increase in flexibility.

The change in length of a prismatic bar loaded only at the ends can be found without difficulty by using Eq. (2-1). However, the equation can be readily adapted to handle more general situations. Suppose, for instance, that a bar is loaded by one or more intermediate axial forces (Fig. 2-4). Then we can determine the axial force in each part of the bar (that is, in parts AB , BC , and CD) and calculate the elongation or shortening of each part separately. Finally, these changes in lengths can be added algebraically to obtain the total change in length of the entire bar. The same method can be used when the bar consists of prismatic parts having different cross-sectional areas (Fig. 2-5).

In general, the total elongation δ of a bar consisting of several parts having different axial forces and cross-sectional areas may be obtained from the equation

$$\delta = \sum_{i=1}^n \frac{P_i L_i}{E_i A_i} \tag{2-4}$$

in which the subscript i is a numbering index for the various parts of the bar and n is the total number of parts. The use of this equation is illustrated in Example 1 at the end of this section.

When either the axial force or the cross-sectional area varies continuously along the axis of the bar, then Eq. (2-4) is no longer suitable. Instead, the elongation can be found by considering a differential element of the bar, obtaining an expression for its elongation, and then integrating over the entire length of the bar. This idea is illustrated in Fig. 2-6, which shows a tapered bar subjected to a continuously distributed axial load (such as the weight of a bar hanging vertically), thus producing a varying axial force in the bar. An element of length dx can be cut from the bar at distance x from the left-hand end. Both the axial force P_x acting at the cut section (Fig. 2-6b) and the cross-sectional area A_x of the element must be expressed as functions of x . Then the equation for the elongation $d\delta$ of the element becomes

$$d\delta = \frac{P_x dx}{EA_x}$$

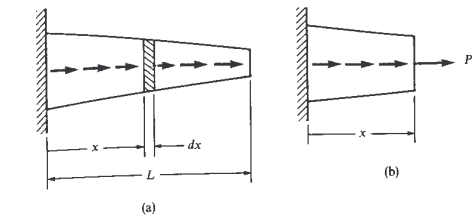


Fig. 2-6 Bar with varying sectional area and varying axial force

and the total elongation of the bar is

$$\delta = \int_0^L d\delta = \int_0^L \frac{P_x dx}{EA_x} \tag{2-5}$$

If the expressions for P_x and A_x are not too complicated, the integral can be evaluated analytically and a formula for δ can be obtained (see Example 2). However, if the integration is difficult or impossible, then a numerical method for evaluating the integral can be used.

Because Eq. (2-5) was derived from the formula $\sigma = P/A$ for prismatic bars, it will give accurate results for tapered bars only if the angle between the sides of the bar is small. For instance, if the angle between the sides is 20° , the maximum error in the normal stress calculated from the expression $\sigma = P/A$ is 3% as compared to the exact stress. For smaller angles, the error is less. If the taper of the bar is large, more accurate methods of analysis may be needed (see Ref. 2-1).

Example 1

A vertical steel bar ABC has length L_1 and cross-sectional area A_1 from A to B and length L_2 and area A_2 from B to C (Fig. 2-7a). A load P_1 acts at point C . A horizontal arm BD is pinned to the vertical bar at B and carries a load P_2 at D . Calculate the vertical deflection δ at point C if $P_1 = 10$ kN, $P_2 = 26$ kN, $a = b$, $L_1 = 0.5$ m, $A_1 = 160$ mm², $L_2 = 0.8$ m, $A_2 = 100$ mm², and $E = 200$ GPa for steel. (Disregard the weight of the bar.)

From the moment equilibrium of arm BD , we see that a vertical force $P_3 = P_2 b/a$ is transmitted through the pin at B . This force acts upward on the vertical bar ABC (Fig. 2-7b). In this example, we have $a = b$, hence $P_3 = P_2 = 26$ kN. Part AB of the vertical bar is subjected to an axial force $P_3 - P_1$, or 16 kN com-

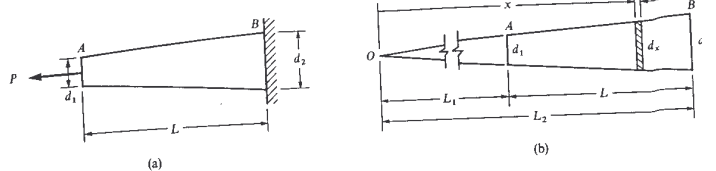
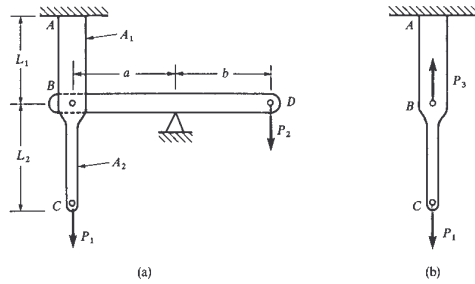


Fig. 2-8 Example 2. Tapered bar of circular cross section

7 Example 1

pression. Part BC carries a tensile force equal to P_1 , or 10 kN tension. Therefore, with tension considered positive, Eq. (2-4) yields

$$\delta = \sum \frac{P_i L_i}{E_i A_i} = \frac{(10 \text{ kN})(0.8 \text{ m})}{(200 \text{ GPa})(100 \text{ mm}^2)} - \frac{(16 \text{ kN})(0.5 \text{ m})}{(200 \text{ GPa})(160 \text{ mm}^2)}$$

$$= 0.400 - 0.250 = 0.150 \text{ mm}$$

Since δ is positive, representing an elongation, the deflection of point C is downward.

Example 2

A slightly tapered bar AB of circular cross section and length L is supported at end B and subjected to a load P at the free end (Fig. 2-8a). The diameters of the bar at ends A and B are d_1 and d_2 , respectively. Derive a formula for the elongation δ of the bar due to the load P.

In this example, the bar has constant axial force P throughout its length, but the cross-sectional area varies. Thus, the first step in the solution is to obtain an expression for the area A_x at any cross section. To simplify the integration that must be performed, let us extend the sides of the tapered bar until they meet at point O (Fig. 2-8b). Then we will use this point as the origin for the distance x. The distances L_1 and L_2 from the origin to ends A and B, respectively, are in the ratio

$$\frac{L_1}{L_2} = \frac{d_1}{d_2} \tag{a}$$

as obtained by considering the similar triangles in Fig. 2-8b. The diameter d_x of the bar at distance x from the origin (Fig. 2-8b) is

$$d_x = \frac{d_1 x}{L_1}$$

and the corresponding cross-sectional area is

$$\pi d_x^2 = \pi d_1^2 \frac{x^2}{L_1^2}$$

Now we substitute into Eq. (2-5) for δ and obtain

$$\delta = \int \frac{P_x dx}{E A_x} = \int_{L_1}^{L_1+L} \frac{P dx (4L_1^2)}{E (\pi d_1^2 \frac{x^2}{L_1^2})} = \frac{4PL_1^3}{\pi E d_1^2} \int_{L_1}^{L_1+L} \frac{dx}{x^2}$$

By performing the integration and substituting the limits, we get

$$\delta = \frac{4PL_1^3}{\pi E d_1^2} \left[-\frac{1}{x} \right]_{L_1}^{L_1+L} = \frac{4PL_1^3}{\pi E d_1^2} \left(\frac{1}{L_1} - \frac{1}{L_1+L} \right)$$

This expression for δ can be simplified by noting that

$$\frac{1}{L_1} - \frac{1}{L_1+L} = \frac{L_1+L - L_1}{L_1(L_1+L)} = \frac{L}{L_1 L_2}$$

Thus, the equation for δ becomes

$$\delta = \frac{4PL}{\pi E d_1^2} \left(\frac{L_1}{L_2} \right)$$

Finally, we substitute $L_1/L_2 = d_1/d_2$ (see Eq. a) and obtain

$$\delta = \frac{4PL}{\pi E d_1 d_2} \tag{2-6}$$

This equation gives the required formula for the elongation of the tapered bar. As a special case, note that, if the bar is prismatic with $d_1 = d_2 = d$, Eq. (2-6) simplifies to

$$\delta = \frac{4PL}{\pi E d^2} = \frac{PL}{EA}$$

in which $A = \pi d^2/4$.

A common mistake is to assume that the elongation of a tapered bar is equal to the elongation of a prismatic bar having the same cross-sectional area as the middle cross section of the tapered bar. (The middle cross section is located halfway between the ends A and B.) Examination of Eq. (2-6) shows that such is not the case for the tapered bar in this example, nor is it generally the case.

2.3 DISPLACEMENT DIAGRAMS

Procedures for finding changes in lengths of axially loaded members were described and illustrated in the preceding section. The displacement of any point in such a member can be found easily after the changes in lengths of the parts of the member have been determined. For instance, the displacement of the free end of the bar pictured in Fig. 2-4 can be found by summing algebraically the changes in lengths of the three parts of the bar. However, the determination of displacements is much more complicated when the structure consists of more than one member.

In this section, we will describe a geometric method for determining displacements when the structure contains two axially loaded members having pinned connections at their ends. Such a structure is actually the simplest form of a truss. The diagrams used to obtain the displacements (or deflections) of the truss are called **displacement diagrams**. These diagrams are constructed geometrically after the changes in lengths of the individual members have been calculated.

To illustrate the geometric method for finding displacements, let us consider Fig. 2-9a, which shows a truss consisting of a horizontal bar AB and an inclined bar BC. Our objective is to obtain the deflection of joint B due to the vertical load P. The procedure is to calculate the forces in the bars, then the changes in lengths, and finally the displacement of B.

The axial forces F_{ab} and F_{bc} in members AB and BC, respectively, are obtained from the equilibrium of forces acting at joint B:

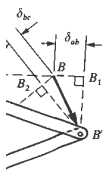
$$F_{ab} = P \cot \theta \quad F_{bc} = P \csc \theta$$

where F_{ab} is a tensile force, F_{bc} is a compressive force, and θ is the angle between the bars. The resulting changes in lengths of the members are

$$\delta_{ab} = \frac{P L_{ab} \cot \theta}{E_{ab} A_{ab}} \quad \delta_{bc} = \frac{P L_{bc} \csc \theta}{E_{bc} A_{bc}} \tag{2-7a, b}$$

In these equations, the subscripts indicate the member to which the properties L , E , and A are applicable. In practical situations, the changes in lengths are usually found numerically, rather than as formulas.

To determine the displacement of joint B, we begin by assuming that the members are separated from each other at B. Then we assume that member AB is elongated by the amount δ_{ab} , so that its end moves from B to B_1 (Fig. 2-9b). Next, member BC is shortened by the amount δ_{bc} , so we draw an arc with center at A and radius equal to the distance AB_1 . Because the actual displacement of joint B is very small, the arc can be replaced by a straight line through B_1 perpendicular to the axis of member AB. The final location of joint B must be somewhere along this perpendicular line (line $B_1 B'$ in Fig. 2-9b).



In a similar manner, member BC shortens by the amount δ_{bc} , which moves its end from B to B_2 . Then member BC rotates about C; so we draw another arc, with its center at C and radius equal to distance CB_2 . This arc is replaced by a straight line through B_2 perpendicular to CB_2 . The intersection of the two perpendicular lines (or the intersection $B_2 B'$) is the final location of joint B. This point is labeled B' in the figure. Thus, the vector from B to B' represents the displacement δ_b of joint B of the truss.

The displacement δ_b can be calculated from the geometry of Fig. 2-9b. However, the task is made easier if we construct a separate diagram, showing only the displacements. Such a displacement diagram is shown in Fig. 2-9c. Line BB_1 represents the elongation δ_{ab} , and BB_2 represents the shortening δ_{bc} . The perpendicular lines are $B_1 B'$ and $B_2 B'$, intersecting at B' . Since these lines are perpendicular to AB and BC, respectively, the angle between them is equal to θ . Thus, the displacement diagram of Fig. 2-9c is identical (except for scale) to the part of Fig. 2-9b that shows the displacements. From the displacement diagram, we can calculate (or measure, if the diagram is drawn to scale) the resultant displacement δ_b of joint B and the horizontal and vertical components of that displacement. In this illustration, the horizontal component δ_h is the same as δ_{ab} and is directed toward the right:

$$\delta_h = \frac{P L_{ab} \cot \theta}{E_{ab} A_{ab}} \tag{2-8}$$

The vertical component δ_v is downward and consists of two parts in the figure ($B_1 B_3$ and $B_3 B'$). The distance $B_1 B_3$, which is the same as distance BB_4 , is equal to $\delta_{bc} \sin \theta$. The distance $B_3 B'$ can be found from triangle $B_2 B_3 B'$, which has side $B_2 B_3$ equal to $\delta_{bc} \cos \theta + \delta_{ab}$. Therefore, the vertical component of δ_b is

$$\delta_v = B_1 B' = \delta_{bc} \sin \theta + (\delta_{bc} \cos \theta + \delta_{ab}) \cot \theta$$

$$= \delta_{bc} \csc \theta + \delta_{ab} \cot \theta \tag{2-9}$$

Having found the horizontal and vertical components of the displacement of joint B, we now can find the resultant displacement δ_b by taking the square root of the sum of the squares of the components.

The method just described can be used for two-bar trusses having any geometric arrangement. In each case, a different displacement diagram must be drawn, based upon the particular truss that is being analyzed. Such diagrams are also called **Williot diagrams** because they were proposed by the French engineer J. V. Williot in 1877 (Ref. 2-2). They are useful only for very simple structures such as the one discussed in Fig. 2-9; for larger trusses it is necessary to use more general analytical methods such as the method of virtual work (Chapter 12).

Example

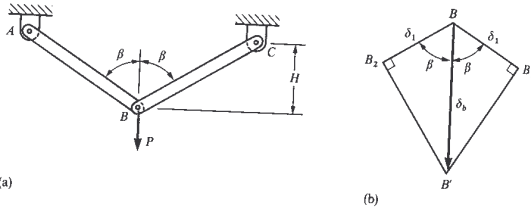
Obtain a formula for the deflection δ_b of joint B of the symmetric truss shown in Fig. 2-10a. Assume that both bars have cross-sectional area A and modulus of elasticity E .

We begin the analysis by determining the tensile forces F in the members:

$$F = \frac{P}{2 \cos \beta}$$

as found from the equilibrium of forces at joint B . Noting that the length L_1 of each member is $L_1 = H/\cos \beta$, we next obtain the elongation δ_1 of either bar:

$$\delta_1 = \frac{FL_1}{EA} = \frac{PH}{2EA \cos^2 \beta}$$



Example (a)

Finally, the displacement diagram is drawn (Fig. 2-10b). Starting with point B , which represents the original position of the joint, we note that member AB would elongate from B to B_1 if the two bars were separated. A line through B_1 perpendicular to BB_1 must pass through the final position of joint B . Because the truss and loading are symmetric, there can be no horizontal displacement of B . Hence, B must displace from B to B' , which is the point at which the perpendicular line from B_1 intersects a vertical line through B . A similar construction on the left-hand side of the diagram is obtained by considering the elongation of member BC . In this case, B moves to B_2 as BC elongates by the amount δ_1 ; a line perpendicular to BB_2 then determines the final position of joint B at B' .

The vertical deflection δ_b of joint B is

$$\delta_b = \frac{\delta_1}{\cos \beta} = \frac{PH}{2EA \cos^3 \beta} \quad (2-10)$$

as obtained by trigonometry from the displacement diagram.

2.4 STATICALLY INDETERMINATE STRUCTURES (FLEXIBILITY METHOD)

In the preceding discussions, we dealt with axially loaded bars and other simple structures that could be analyzed by static equilibrium. In all of the examples, it was possible to determine axial forces in the members and reactions at the supports by drawing free-body diagrams and solving equilibrium equations. Such structures are classified as **statically determinate**. For many structures, however, the equations of static equilibrium are not sufficient for the calculation of axial forces and reactions; these structures are called **statically indeterminate**. Structures of this type can be analyzed by supplementing the equilibrium equations with additional equations pertaining to the displacements of the structure.

The two general methods for analyzing statically indeterminate structures are the **flexibility method** and the **stiffness method**, described in this section and the one that follows. These methods are complementary to each other, and each has its advantages. They are suitable for many different kinds of structures, provided the material remains within the linearly elastic range.

To explain the flexibility method, let us consider the analysis of the statically indeterminate bar shown in Fig. 2-11. The prismatic bar AB is attached at both ends to rigid supports and is axially loaded by the force P at an intermediate point C . As a consequence, reactions R_a and R_b will develop at the ends of the bar.* These reactions cannot be found

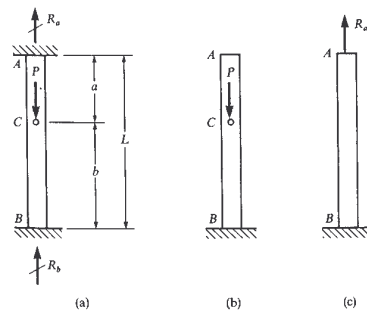


Fig. 2-11 Statically indeterminate bar (flexibility method of analysis)

* To distinguish between reactions and loads, reactive forces will usually be indicated by drawing a slash, or slanted line, across the arrows, as illustrated in Fig. 2-11a.

by statics alone, because only one independent equation of static equilibrium exists for this bar, as follows:

$$R_a + R_b = P \quad (a)$$

Because this equation contains both unknown reactions, it is not sufficient for their calculation. A second equation must be obtained from the deflections of the bar.

To begin the analysis, we designate one of the unknown reactions as the **statical redundant**, or the force that is in excess of those that can be obtained by statics alone. Let us choose R_a as the redundant reaction in this example. If R_a can be found, then the other reaction R_b can be obtained by static equilibrium from Eq. (a). When the unknown reaction R_a is removed from the structure, the effect is to release the support at end A , thereby producing the statically determinate and stable structure shown in Fig. 2-11b. Thus, from the standpoint of having a structure that is capable of supporting loads, the reaction at end A is not needed; that is, it is redundant. The structure that remains after releasing the redundant is called the **released structure**, or the **primary structure**.

Now let us consider the effect of the load P on the displacement of point A in the released structure (Fig. 2-11b). This displacement is

$$\delta_p = \frac{Pb}{EA}$$

and is downward. Next, let us consider the effect of the redundant R_a on the displacement of point A (Fig. 2-11c). Note that, although it is an unknown quantity, R_a is now visualized as a load acting on the released structure. The upward displacement of point A due to R_a is

$$\delta_R = \frac{R_a L}{EA}$$

The final displacement δ of point A due to both P and R_a acting simultaneously is found by combining δ_p and δ_R . Thus, taking downward displacements as positive, we obtain

$$\delta = \delta_p - \delta_R$$

Because the actual displacement δ of point A is equal to zero (Fig. 2-11a), the preceding equation becomes

$$\delta_R = \delta_p \quad (b)$$

or

$$\frac{R_a L}{EA} = \frac{Pb}{EA} \quad (c)$$

from which

$$R_a = \frac{Pb}{L} \quad (2-11)$$

Thus, the redundant reaction has been calculated from an equation related to the displacements of the bar (Eq. b). Now that the redundant has been determined, we can find R_b from equilibrium by using Eq. (a):

$$R_b = P - R_a = \frac{Pa}{L} \quad (2-12)$$

Thus, both reactions for the bar have been found.

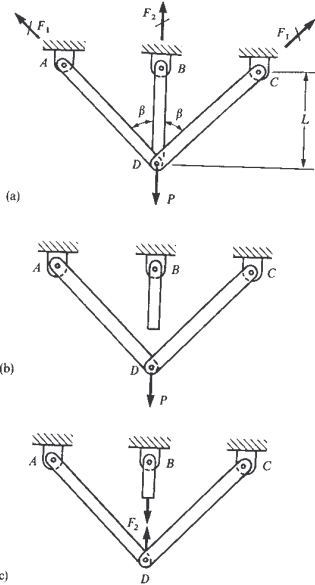
The foregoing method for analyzing the statically indeterminate bar of Fig. 2-11a may be summarized as follows. First, one of the unknown reactions is selected as the redundant and then released from the structure by cutting through the bar and removing the support. The released structure, which is statically determinate and stable, is then loaded separately by the actual load P and by the redundant itself. The displacements caused by these two quantities are calculated and then combined into an equation of **compatibility of displacements** (Eq. b). This equation of compatibility expresses a condition pertaining to the deflection of the original structure, namely, that the deflection δ at end A is zero. When the expressions for the displacements are substituted, the equation of compatibility takes the form of Eq. (c), which then can be solved for the redundant force R_a (Eq. 2-11). Finally, the remaining unknown force is found by statics.

This method of analysis is called the **flexibility method** because flexibilities appear in the equation of compatibility. In this example, the equation of compatibility (Eq. c) contains the flexibility L/EA (see Eq. 2-3) as the coefficient of the unknown redundant R_a . Another name is the **force method**, because forces are the unknown quantities. The method can be used for different types of structures and for structures having many redundant forces. However, in this section, only elementary indeterminate structures with one redundant force will be considered. Because the method requires adding the deflections caused by different forces, it is valid only when the material behaves in a linear elastic manner.

To further illustrate the flexibility method, let us analyze the plane truss shown in Fig. 2-12a. This truss consists of three members attached to pin supports at A , B , and C and pinned together at joint D , where a load P acts in the vertical direction. All bars are assumed to have the same axial rigidity EA . The truss is statically indeterminate because there are three unknown member forces but only two equations of static equilibrium. By summing forces in the horizontal direction, or merely by observing that the layout of the truss is symmetric, we recognize that the tensile forces in the two outer bars are the same. Then, from equilibrium of forces in the vertical direction, we obtain

$$2F_1 \cos \beta + F_2 = P \quad (d)$$

in which β is the angle between the vertical and inclined bars. This equation contains two unknown forces (F_1 and F_2); hence, one addi-



minate
analysis)

tional equation is needed. We will obtain this equation from compatibility of the displacements at joint D.

The axial force F_2 in member BD is selected arbitrarily as the redundant in this example; therefore, member BD is cut at its lower end in order to release this force (Fig. 2-12b). The bar could be cut at some other cross section if desired, and the calculations would be similar to those given here. When the load P acts on the released structure (Fig. 2-12b), the downward displacement of joint D (found from Eq. 2-10 in the preceding section) is

$$\delta_p = \frac{PL}{2EA \cos^3 \beta} \quad (e)$$

in which L is the length of the vertical bar. When the redundant force F_2 acts on the released structure (Fig. 2-12c), the cut bar BD will be placed in tension by the force F_2 pulling downward while joint D is

pulled upward by an equal and opposite force. The latter force causes joint D to displace upward by the amount

$$\delta_F = \frac{F_2 L}{2EA \cos^3 \beta} \quad (f)$$

(compare with Eq. e). The total downward displacement of joint D due to P and F_2 acting simultaneously is $\delta_p - \delta_F$. We must also observe that bar BD elongates by an amount $F_2 L / EA$. The condition of compatibility of displacements at joint D expresses the fact that the downward displacement of joint D is equal to the elongation of bar BD ; thus,

$$\delta_p - \delta_F = \frac{F_2 L}{EA}$$

Substituting Eqs. (e) and (f) into this equation and solving for F_2 , we obtain

$$F_2 = \frac{P}{1 + 2 \cos^3 \beta} \quad (2-13)$$

Finally, from the equation of equilibrium (Eq. d), we obtain

$$F_1 = \frac{P \cos^2 \beta}{1 + 2 \cos^3 \beta} \quad (2-14)$$

In this example, the axial force in the middle bar is greater than the forces in the outer bars. Also, as a limiting case, we can set $\beta = 0$ and obtain $F_1 = F_2 = P/3$, as expected.

This example illustrates the general method of solution described previously for the flexibility method. The unknown force F_2 is taken as the redundant, giving the released structure shown in Fig. 2-12b. Then the released structure is subjected first to the load P and next to the redundant itself. The displacements of joint D caused by these forces are determined and combined into an equation of compatibility. The displacement due to P is known, whereas the redundant and the displacement it produces are unknown. However, solving the equation of compatibility yields the value of the redundant. After that, the other unknown bar force can be obtained by statics.

As an additional step in the analysis of the truss of Fig. 2-12, we can now find the vertical deflection δ_d of joint D . We merely note that this deflection is equal to the elongation of bar BD :

$$\delta_d = \frac{F_2 L}{EA} = \frac{PL}{EA(1 + 2 \cos^3 \beta)} \quad (2-15)$$

Of course, the horizontal deflection of joint D is zero because the truss and its loading are symmetrical.

In the preceding two examples of the flexibility method, we found it helpful to identify a redundant force and then to find deflections in the released structure (obtained by removing the redundant). In some

Axially Loaded Members

kinds of problems, this step is unnecessary. Instead, it may be sufficient to cut through the structure, thereby exposing the unknown forces, and then obtain an equation of compatibility simply by inspection of the deflection conditions. The following two examples illustrate this procedure.

Example 1

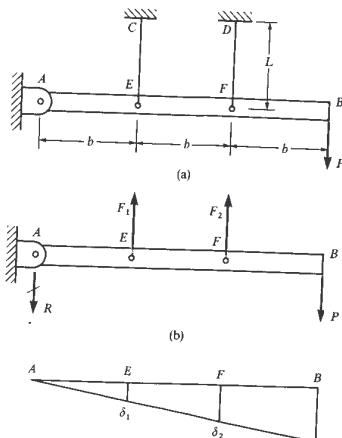
A horizontal bar AB , assumed to be rigid, is supported by two identical wires CE and DF (Fig. 2-13a). If each wire has cross-sectional area A , determine the tensile stresses σ_1 and σ_2 in wires CE and DF , respectively.

This structure is statically indeterminate because it is impossible to find the forces in the wires by statics. For instance, a free-body diagram of the rigid bar (Fig. 2-13b) yields the following equation of moment equilibrium about point A :

$$F_1 b + 2F_2 b - 3Pb = 0 \quad \text{or} \quad F_1 + 2F_2 = 3P \quad (g)$$

In this equation, F_1 and F_2 are the unknown forces in the wires. The equation of vertical equilibrium introduces the reaction R as a new unknown; hence, this equation is of no benefit in finding F_1 and F_2 . An equation involving the deformations of the wires is needed.

When the load P is applied, bar AB rotates about the support, and the two



e 1. Statically
ire (flexibility

2.4 Statically Indeterminate Structures (Flexibility Meth

wires lengthen. The resulting displacement diagram is shown in Fig. 2-13c, in which δ_1 and δ_2 represent the elongations of wires CE and DF , respectively. The condition of compatibility is

$$\delta_2 = 2\delta_1$$

as obtained from the geometry of the displacement diagram. The elongations of the wires can be expressed in terms of the unknown forces:

$$\delta_1 = \frac{F_1 L}{EA} \quad \delta_2 = \frac{F_2 L}{EA}$$

which L represents the length and EA the axial rigidity of the wires. Now substituting these expressions for δ_1 and δ_2 into the equation of compatibility, we get

$$F_2 = 2F_1 \quad (h)$$

Finally, Eqs. (g) and (h) are combined to give the forces in the wires:

$$F_1 = \frac{3P}{5} \quad F_2 = \frac{6P}{5}$$

The corresponding tensile stresses are

$$\sigma_1 = \frac{F_1}{A} = \frac{3P}{5A} \quad \sigma_2 = \frac{F_2}{A} = \frac{6P}{5A}$$

Knowing the forces F_1 and F_2 , we can find the actual elongations of the wires, if desired.

Example 2

A circular steel cylinder and hollow copper tube (labeled S and C in Fig. 2-14a) are compressed between the heads of a testing machine. Determine the average stresses in the steel and the copper and the average compressive strain in the vertical direction due to the axial force P .

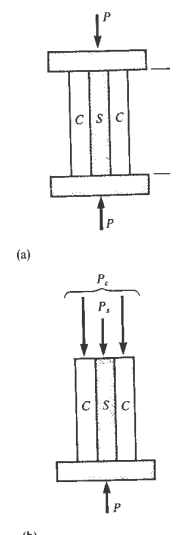
When using the flexibility method, we remove the upper plate and obtain the structure shown in Fig. 2-14b. The unknown forces P_s and P_c , representing the axial forces in the steel and the copper, respectively, are related by the following equation of equilibrium:

$$P_s + P_c = P \quad (i)$$

The shortening of the steel cylinder is given by the expression $P_s L / E_s A_s$, in which $L/E_s A_s$ is the flexibility of the steel cylinder. Also, the shortening of the copper tube is equal to $P_c L / E_c A_c$, in which $L/E_c A_c$ is the flexibility of the tube. The equation of compatibility is obtained from the fact that the steel cylinder and the copper tube shorten the same amount; thus:

$$\frac{P_s L}{E_s A_s} = \frac{P_c L}{E_c A_c} \quad (j)$$

Fig. 2-14 Example 2. Stat indeterminate system (flexibility method of analysis)



Solving simultaneously the two equations (i) and (j), we obtain the two unknown forces:

$$P_s = \frac{E_s A_s}{E_s A_s + E_c A_c} P \quad P_c = \frac{E_c A_c}{E_s A_s + E_c A_c} P \quad (2-16a, b)$$

These equations show that the forces in the steel and the copper are in proportion to their axial rigidities.

The compressive stress σ_s in the steel can be obtained by dividing P_s by A_s , and the stress σ_c can be found in a similar manner. The compressive strain ϵ , which must be the same for both materials, can then be found from Hooke's law; the result is

$$\epsilon = \frac{P}{E_s A_s + E_c A_c} \quad (2-17)$$

This equation shows that the strain is equal to the total load divided by the sum of the axial rigidities of the steel and copper parts.

force R_a in the upper part, and the compressive force R_b in the lower part. From static equilibrium, we then obtain

$$R_a + R_b = P \quad (b)$$

or, upon substituting from Eqs. (a),

$$\frac{EA}{a} \delta_c + \frac{EA}{b} \delta_c = P \quad (c)$$

which yields

$$\delta_c = \frac{Pab}{EAL} \quad (d)$$

(since $a + b = L$). Knowing the displacement δ_c , we now can find R_a and R_b from Eqs. (a):

$$R_a = \frac{Pb}{L} \quad R_b = \frac{Pa}{L} \quad (e)$$

These results are, of course, the same as those obtained in Section 2.4 (see Eqs. 2-11 and 2-12).

Let us now summarize the procedure for the stiffness method of analysis. The first step is to select a suitable displacement as the unknown quantity. A displacement will be suitable if the forces in the individual parts of the structure can be expressed in terms of that displacement (see Eqs. a). Then the forces are related by an equation of equilibrium, such as Eq. (b) in the preceding example. Next, the expressions giving the forces in terms of the unknown displacement are substituted into the equation of equilibrium, thereby producing an equation with only the selected displacement as an unknown (Eq. c). Note that the coefficients of δ_c in this equation are stiffnesses. This equation is solved for the unknown displacement (Eq. d), and, finally, the forces are found from the displacement (Eqs. e). Thus, the stiffness method produces all of the desired results.

As a second illustration of the stiffness method, consider the analysis of the plane truss shown in Fig. 2-16a (this same truss was discussed in the preceding section). The vertical bar has length L , the inclined bars have length $L/\cos \beta$, and all three bars have the same axial rigidity EA . A vertical load P acts at joint D . Thus, the truss and its loading are symmetric, and there will be no horizontal displacement of joint D . The vertical displacement δ of joint D is the distance DD' in the figure. The dashed lines AD' and CD' show the deflected configuration of the truss.

The displacement diagram for joint D is sketched in Fig. 2-16b (see Section 2.3 for a discussion of displacement diagrams). Lines DD_1 and DD_2 represent the elongations of bars CD and AD , respectively, and line DD' represents the vertical displacement δ of joint D . From the diagram, we see that the elongations of the inclined bars are

2.5 STATICALLY INDETERMINATE STRUCTURES (STIFFNESS METHOD)

The **stiffness method** for analyzing statically indeterminate structures differs from the flexibility method in that displacements (rather than forces) are taken as the unknown quantities. Hence, the method is also called the **displacement method**. The unknown displacements are obtained by solving equations of equilibrium (rather than equations of compatibility) that contain coefficients in the form of stiffnesses (see Eq. 2-2). The stiffness method is quite general and can be used for a wide variety of structures. However, like the flexibility method, it is limited to structures that behave in a linear elastic manner.

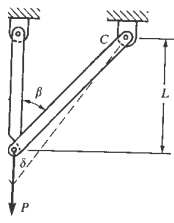
In order to explain the stiffness method, let us again analyze a prismatic bar AB held between rigid supports (Fig. 2-15a). The reactions at the supports are denoted R_a and R_b , as before. In this new solution, the vertical displacement δ_c of point C , which is the junction of the two parts of the bar, is taken as the unknown quantity. The axial forces R_a and R_b in the upper and lower parts of the bar can be expressed in terms of δ_c , as follows:

$$R_a = \frac{EA}{a} \delta_c \quad R_b = \frac{EA}{b} \delta_c \quad (a)$$

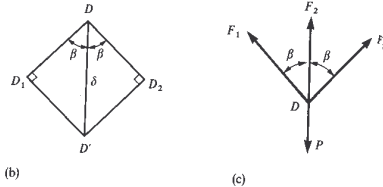
In writing these equations, we have assumed that δ_c is positive downward, thereby producing tension in the upper part of the bar and compression in the lower part.

The next step is to isolate point C in the bar as a free body (Fig. 2-15b). Acting on the free body are the downward load P , the tensile

Axially Loaded Members



indeterminate of analysis)



Example

A reinforced concrete pedestal of height h and square cross section ($b = 0.5$ m on each side) is constructed with 12 steel reinforcing bars (Figs. 2-17a and b). Each bar has diameter $d = 25$ mm. The pedestal supports a compressive load P applied through a rigid bearing plate. Assuming linear elastic behavior, calculate the maximum permissible value of the load P if the allowable stresses in the steel and concrete are 70 MPa and 8 MPa, respectively. Disregard the weight of the pedestal itself. (Assume that the modulus of elasticity for steel is $E_s = 200$ GPa and for concrete is $E_c = 25$ GPa.)

To analyze this structure by the stiffness method, we remove the rigid plate and replace its action on the pedestal by two forces P_s and P_c , representing the loads carried by the steel and concrete, respectively (Fig. 2-17c). The pedestal is statically indeterminate, because we cannot calculate these forces from static equilibrium alone (see the free-body diagram of the rigid plate in Fig. 2-17d). Therefore, we select the vertical deflection δ at the upper end of the pedestal as the unknown displacement. Since this deflection is the same as the shortening of the pedestal, we can express the forces P_s and P_c in terms of δ as follows:

$$P_s = \frac{E_s A_s \delta}{h} \quad P_c = \frac{E_c A_c \delta}{h} \quad (i)$$

in which A_s and A_c represent the cross-sectional areas of the steel and concrete, respectively. The equation of equilibrium (from Fig. 2-17d) is

$$P_s + P_c = P \quad (m)$$

or, when Eqs. (i) are substituted,

$$\frac{E_s A_s \delta}{h} + \frac{E_c A_c \delta}{h} = P \quad (n)$$

Therefore, the force F_1 in either of the inclined bars is

$$F_1 = \frac{EA \delta \cos \beta}{L/\cos \beta} = \frac{EA \delta \cos^2 \beta}{L} \quad (f)$$

and the force F_2 in the vertical bar is

$$F_2 = \frac{EA \delta}{L} \quad (g)$$

Equations (f) and (g) express the bar forces in terms of a single unknown, namely, the deflection δ .

The next step in the analysis is to obtain the equation of equilibrium. From a free-body diagram of joint D (Fig. 2-16c), we see that

$$2F_1 \cos \beta + F_2 = P \quad (h)$$

Substituting the expressions for F_1 and F_2 (see Eqs. f and g) into this equation, we obtain

$$\frac{2EA \delta \cos^3 \beta}{L} + \frac{EA \delta}{L} = P \quad (i)$$

This equation contains only the deflection δ as an unknown, hence we can now solve for δ :

$$\delta = \frac{PL}{EA} \frac{1}{1 + 2 \cos^3 \beta} \quad (j)$$

The final step in the analysis is to determine the bar forces F_1 and F_2 by substituting this expression for δ into Eqs. (f) and (g); thus, we obtain

$$F_1 = \frac{P \cos^2 \beta}{1 + 2 \cos^3 \beta} \quad F_2 = \frac{P}{1 + 2 \cos^3 \beta} \quad (k)$$

These results are the same as those obtained previously by the flexibility method (see Eqs. 2-13, 2-14, and 2-15).

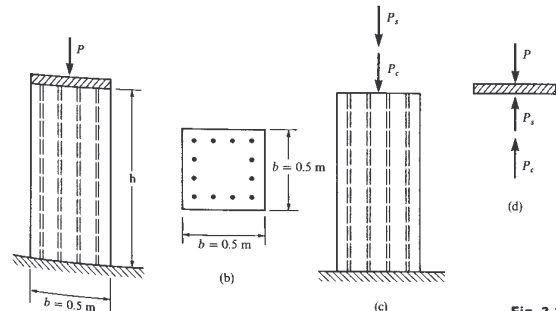


Fig. 2-17 Example. Reinforced concrete pedestal (stiffness method)

from which we find

$$\delta = \frac{Ph}{E_s A_s + E_c A_c} \quad (2-18)$$

Substituting this expression for δ into Eqs. (1) gives the following formulas for the axial forces:

$$P_s = \frac{E_s A_s}{E_s A_s + E_c A_c} P \quad P_c = \frac{E_c A_c}{E_s A_s + E_c A_c} P \quad (2-19a, b)$$

Thus, the forces and displacement are found, and the analysis by the stiffness method is completed.

However, in this particular example, we also need to obtain the stresses σ_s and σ_c in the steel and concrete (in order to determine the allowable load).

$$\sigma_s = \frac{P_s}{A_s} = \frac{E_s P}{E_s A_s + E_c A_c} \quad \sigma_c = \frac{P_c}{A_c} = \frac{E_c P}{E_s A_s + E_c A_c} \quad (c)$$

Each of these equations can be solved for the load P in terms of the stress in the material:

$$P = \left(A_s + \frac{E_c}{E_s} A_c \right) \sigma_s \quad P = \left(A_c + \frac{E_s}{E_c} A_s \right) \sigma_c \quad (2-20a, b)$$

From these equations, the permissible values of the load P can be found based upon the allowable stresses in the steel and concrete. The lower of the two loads is the allowable load P on the pedestal. Thus, the calculations for the load P proceed as follows. The areas of the steel (12 bars) and concrete are

$$A_s = 12 \left(\frac{\pi d^2}{4} \right) = 3\pi(25 \text{ mm})^2 = 5,890 \text{ mm}^2$$

$$A_c = b^2 - A_s = (0.5 \text{ m})^2(1,000)^2 - 5,890 = 244,100 \text{ mm}^2$$

Also, the ratio of the moduli is

$$\frac{E_s}{E_c} = 8$$

Substituting these values, as well as the allowable stresses, into Eqs. (2-20a and b) yields two values of the load P :

$$P = \left(A_s + \frac{E_c}{E_s} A_c \right) \sigma_s = \left(5,890 \text{ mm}^2 + \frac{244,100}{8} \text{ mm}^2 \right) (70 \text{ MPa}) = 2.55 \text{ MN}$$

$$P = \left(A_c + \frac{E_s}{E_c} A_s \right) \sigma_c = (244,100 \text{ mm}^2 + 8 \times 5,890 \text{ mm}^2) (8 \text{ MPa}) = 2.33 \text{ MN}$$

The first result is based upon the allowable stress in the steel, and the second is based upon the allowable stress in the concrete. The allowable load P is the lower of the two values:

At this load, the stress in the concrete is 8 MPa (the allowable stress), and the stress in the steel, which is below its allowable stress because the stress in the concrete governs, is $(2.33/2.55)(70 \text{ MPa}) = 64.0 \text{ MPa}$.

In the case of elementary statically indeterminate structures of the type analyzed in this chapter, the choice between the displacement and flexibility methods is somewhat arbitrary because little difference exists between the two methods in terms of calculating effort. (Of course, fundamental differences between the methods exist in terms of procedures and point of view.) In more complicated structures, however, one method may require significantly fewer calculations than the other. As an example, suppose that the symmetric truss shown in Figs. 2-12 and 2-16 is made more complex (but still symmetric) by the addition of several bars (Fig. 2-18). The solution by the stiffness method proceeds in the manner just described and is quite simple, whereas a solution by the flexibility method becomes much more complex and requires the solution of three simultaneous equations. In still other instances, the situation is reversed, and the flexibility method provides the easier solution.*

From a historical viewpoint, it appears that Euler in 1774 was the first to analyze a statically indeterminate system; he considered the problem of a rigid table with four legs supported on an elastic foundation (Refs. 2-4 and 2-5). The next work was done by the French mathematician and engineer L. M. H. Navier, who in 1825 pointed out that statically indeterminate reactions could be found only by taking into account the elasticity of the structure (Ref. 2-6). Navier solved a truss similar to the one shown in Fig. 2-16a.

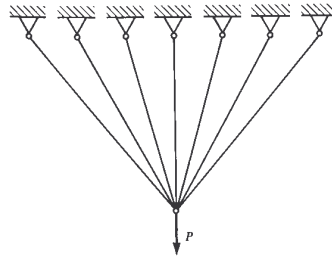
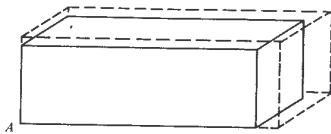


Fig. 2-18 Statically indeterminate truss

*When writing computer programs for structural analysis, the stiffness method is

2.6 TEMPERATURE AND PRESTRAIN EFFECTS

A change in the temperature of an object tends to produce a change in its dimensions. A simple illustration of this effect is given in Fig. 2-19, which shows a block of homogeneous and isotropic material that is free to expand in all directions. If the material is heated uniformly, the sides of the block will increase in length. Thus, with corner A taken as a



lock with uniform temperature

reference point, the block will adopt the shape shown by the dashed lines. The material undergoes a **uniform thermal strain** ϵ_t , given by the expression

$$\epsilon_t = \alpha(\Delta T) \quad (2-21)$$

in which α is the **coefficient of thermal expansion** and ΔT is the increase in temperature. The coefficient α is a property of the material* and has units equal to the reciprocal of temperature change. Thus, in SI units, α has dimensions of either $1/\text{K}$ (the reciprocal of kelvins) or $1/^\circ\text{C}$ (the reciprocal of degrees Celsius), because a change in temperature is numerically the same in both kelvins and degrees Celsius. In USCS units, the dimensions of α are $1/^\circ\text{F}$ (the reciprocal of degrees Fahrenheit).** Thermal strain ϵ_t is a dimensionless quantity that is considered positive when it represents expansion and negative when it represents contraction.

Ordinary materials expand when heated and contract when cooled; hence, an increase in temperature produces a positive thermal strain. Thermal strains usually are reversible, in the sense that the member returns to its original shape when the temperature returns to its original value. However, some special metals have been developed recently that do not behave in the customary manner. Instead, over certain temperature ranges, their dimensions decrease when the metals are heated and increase when they are cooled. These metals also differ from ordinary materials in that the strains are related nonlinearly to the temperature and sometimes are irreversible, because the internal structure of the

*Typical values of the coefficient of thermal expansion α are listed in Appendix H, Table H-4.

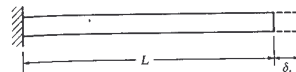


Fig. 2-20 Increase in length bar due to a uniform increase in temperature (Eq. 2-22)

material is altered. (Another unusual material is water, which expands when heated at temperatures above 4°C but also expands when cooled at temperatures below 4°C . Hence, water has its maximum density at 4°C .)

The changes in the dimensions of the block of material shown in Fig. 2-19 can be calculated by multiplying the original dimensions by the thermal strain. If, for instance, one of the dimensions is L , then that dimension will increase by the amount

$$\delta_t = \epsilon_t L = \alpha(\Delta T)L \quad (2-22)$$

in which δ_t represents the elongation due to the temperature increase ΔT . Equation (2-22) is used to calculate changes in lengths of structural members, such as the bar shown in Fig. 2-20, which is supported at the left end and is free to displace at the other end. The transverse dimensions of the bar also change, but, since such changes usually have no effect on the forces being transmitted by the member, they are not shown in the figure.

In general, changes in lengths due to thermal strains may be calculated from Eq. (2-22) provided that the members are able to expand or contract freely, a situation that exists in statically determinate structures. As a consequence, no stresses are produced in a statically determinate structure when one or more members undergo a uniform temperature change. On the other hand, a temperature change in a statically indeterminate structure will usually produce stresses in the members, called **thermal stresses**. Such stresses also may occur when a member is heated in a nonuniform manner, irrespective of whether the structure is determinate or indeterminate.

To illustrate some of these ideas about thermal effects, consider the symmetric two-bar truss ABC of Fig. 2-21a and assume that the tem-

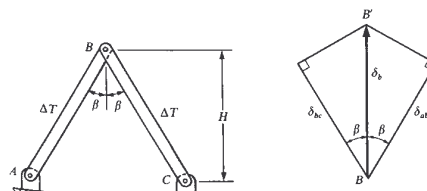


Fig. 2-21 Truss with uniform

perature is raised by ΔT . Because the truss is statically determinate, bars are free to lengthen, thus producing a vertical deflection of joint B . (If the truss were not symmetric, or if the temperature changes were not the same for both bars, then joint B would displace horizontally, as well as vertically.) The elongations of the bars are obtained from (2-22):

$$\delta_{ab} = \delta_{bc} = \frac{\alpha(\Delta T)H}{\cos \beta}$$

in which $H/\cos \beta$ is the length of a bar. To find the deflection of joint B , we can treat the changes in lengths due to temperature changes in the same manner as if they were caused by axial forces in the bars (see Section 2.3). The resulting displacement diagram for joint B is shown in Fig. 2-21b. The vertical deflection δ_b can be measured from a diagram drawn to scale, or it can be calculated directly from the figure:

$$\delta_b = \frac{\delta_{ab}}{\cos \beta} = \frac{\alpha(\Delta T)H}{\cos^2 \beta} \quad (2-23)$$

This deflection is upward if ΔT is positive (heating), and downward if it is negative (cooling). Although joint B undergoes a displacement, there are no stresses in either bar and no reactions at the supports. Thus we note that temperature changes can produce strains in a statically determinate structure without creating any corresponding stresses. If a structure is statically indeterminate, free expansion or contraction is no longer possible. An example is a bar AB held between immovable supports, as shown in Fig. 2-22a. If the temperature increases uniformly by ΔT , a compressive axial force R will be developed in the bar. This force can be calculated by either of the methods described in Sections 2.4 and 2.5. Using the flexibility method, we cut through the bar at its upper end and release the support (Fig. 2-22b). The temperature

change ΔT produces an elongation of this released structure, resulting in an upward displacement δ_T at point A equal to $\alpha(\Delta T)L$. The force R acting on the released structure (Fig. 2-22c) produces a downward displacement δ_R equal to RL/EA . Inasmuch as the actual displacement of the end of the bar is zero (Fig. 2-22a), we obtain the following equation of compatibility:

$$\delta_T - \delta_R = \alpha(\Delta T)L - \frac{RL}{EA} = 0 \quad (a)$$

From this equation, we obtain the reaction R :

$$R = EA\alpha(\Delta T) \quad (2-24)$$

Note that R does not depend upon the length of the bar. Next, we obtain the compressive stress in the bar:

$$\sigma = \frac{R}{A} = E\alpha(\Delta T) \quad (2-25)$$

which does not depend upon the cross-sectional area.

The preceding example shows how temperature changes can produce stresses in a statically indeterminate system even when there are no loads. Furthermore, the bar in this example has zero longitudinal displacement, not only at the fixed ends but also at every cross section. Thus, there are no axial strains in this bar, and we have a situation involving stresses without strains. In a more general case, such as a bar consisting of two parts having different cross-sectional areas, there will be both axial strains and stresses due to a temperature change (see Problems 2.6-12 and 2.6-13).

Example 1

Consider a symmetric three-bar truss, as shown in Fig. 2-23a, and assume that the temperature is increased uniformly by ΔT . Assume also that E , A , and α are the same for all three bars.

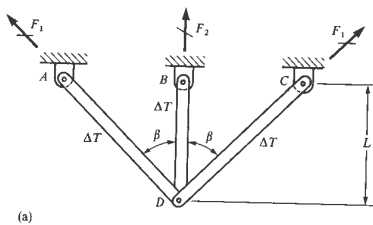
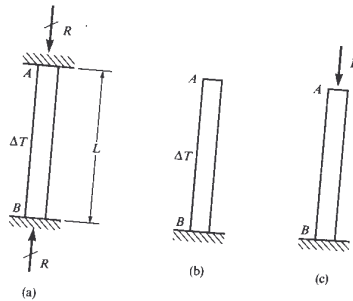
To find the forces F_1 and F_2 in the members of this statically indeterminate truss, we will use the flexibility method. The vertical bar BD is cut at its lower end, giving the statically determinate released structure shown in Fig. 2-23b. This released structure is free to deform when the temperature change ΔT occurs. The downward displacement of joint D , which is caused by the change in temperature of the two outer bars, is

$$\delta_1 = \frac{\alpha(\Delta T)L}{\cos^2 \beta}$$

(see Eq. 2-23). The elongation of the vertical bar is

$$\delta_2 = \alpha(\Delta T)L$$

statically determinate
temperature increase



tion of bar BD is $\delta_2 + \delta_4$. Equating these deflections expresses the condition of compatibility of displacements at joint D :

$$\delta_1 - \delta_3 = \delta_2 + \delta_4$$

or

$$\frac{\alpha(\Delta T)L}{\cos^2 \beta} - \frac{F_2 L}{2EA \cos^3 \beta} = \alpha(\Delta T)L + \frac{F_2 L}{EA} \quad (b)$$

This equation is easily solved for the force F_2 in the vertical bar:

$$F_2 = \frac{2EA\alpha(\Delta T) \sin^2 \beta \cos \beta}{1 + 2 \cos^3 \beta} \quad (2-26)$$

This force is tension if ΔT is positive (that is, if the temperature increases).

The force F_1 in the inclined bars is determined from equilibrium of the forces acting on the truss (Fig. 2-23a):

$$2F_1 \cos \beta + F_2 = 0 \quad (c)$$

or

$$F_1 = -\frac{EA\alpha(\Delta T) \sin^2 \beta}{1 + 2 \cos^3 \beta} \quad (2-27)$$

The minus sign shows that F_1 is a compressive force when the temperature increases.

The downward displacement δ_d of joint D is obtained by substituting the expression for F_2 from Eq. (2-26) into either side of the compatibility equation (Eq. b); thus,

$$\delta_d = \delta_1 - \delta_3 = \delta_2 + \delta_4 = \frac{\alpha(\Delta T)L(1 + 2 \cos \beta)}{1 + 2 \cos^3 \beta} \quad (2-28)$$

This expression shows that δ_d is downward (positive) whenever ΔT is positive.

1. Statically indeterminate
with uniform

F_2 acting at the cut section of bar BD (Fig. 2-23c). This force produces an upward displacement of joint D equal to

$$\delta_3 = \frac{F_2 L}{2EA \cos^3 \beta}$$

(see Eq. 2-10) and an elongation of BD equal to

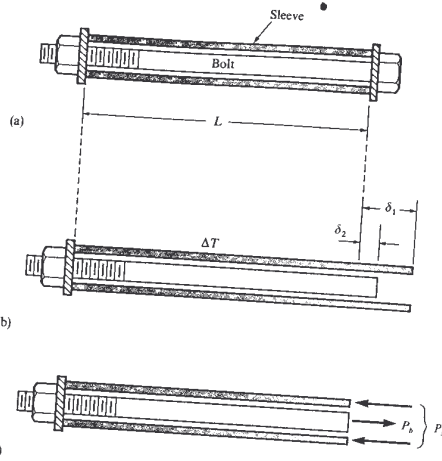
$$\delta_4 = \frac{F_2 L}{EA}$$

Example 2

A sleeve in the form of a tube of length L is placed around a bolt and held in position by a nut that is turned until it is just snug (Fig. 2-24a). The sleeve and bolt are made of different materials. If the temperature of the entire assembly is raised by an amount ΔT , what forces are developed in the sleeve and bolt?

Because the sleeve and bolt are of different materials, they would elongate by different amounts if they were free to expand. However, they are held together by the assembly, hence thermal stresses are developed. The system is statically indeterminate because the stresses cannot be determined by static equilibrium alone. For illustration, we will obtain the stresses by both the flexibility and stiffness methods.

In the flexibility method, we begin by cutting the assembly apart so that a statically determinate released structure is obtained. A simple way to accomplish this result is to remove the head of the bolt, as shown in Fig. 2-24b.



Then the temperature change ΔT is assumed to occur, producing elongations δ_1 and δ_2 of the sleeve and bolt, respectively:

$$\delta_1 = \alpha_s(\Delta T)L \quad \delta_2 = \alpha_b(\Delta T)L$$

in which α_s and α_b are the coefficients of thermal expansion. In drawing the figure, it has been arbitrarily assumed that δ_1 is greater than δ_2 (that is, $\alpha_s > \alpha_b$).

The forces existing in the sleeve and bolt in the original assembly must be such that they shorten the sleeve and stretch the bolt until the final elongations of the sleeve and bolt are the same. These forces are shown in Fig. 2-24c, where P_s denotes the compressive force in the sleeve and P_b denotes the tensile force in the bolt. The corresponding shortening δ_3 of the sleeve and elongation δ_4 of the bolt are

$$\delta_3 = \frac{P_s L}{E_s A_s} \quad \delta_4 = \frac{P_b L}{E_b A_b}$$

in which $E_s A_s$ and $E_b A_b$ are the respective axial rigidities.

Now we can write an equation of compatibility expressing the fact that the final elongation δ is the same for both bars. The elongation of the sleeve is $\delta_1 - \delta_3$ and of the bolt is $\delta_2 + \delta_4$; therefore,

$$\delta = \delta_1 - \delta_3 = \delta_2 + \delta_4 \quad (d)$$

or

$$\delta = \alpha_s(\Delta T)L - \frac{P_s L}{E_s A_s} = \alpha_b(\Delta T)L + \frac{P_b L}{E_b A_b} \quad (e)$$

A second equation for the axial forces is obtained from static equilibrium (see Fig. 2-24c):

$$P_s = P_b \quad (f)$$

That is, the compressive force in the sleeve is equal to the tensile force in the bolt. Combining Eqs. (e) and (f), we obtain the forces in the original assembly (Fig. 2-24a) subjected to the temperature change:

$$P_s = P_b = \frac{(\alpha_s - \alpha_b)\Delta T L}{\frac{1}{E_s A_s} + \frac{1}{E_b A_b}} \quad (2-29)$$

If α_s is greater than α_b , the force P_s is compression and P_b is tension. Note also that the forces are independent of the length L .

The final elongation of the system is found by substituting from Eq. (2-29) into Eq. (e), yielding

$$\delta = \frac{(\alpha_s E_s A_s + \alpha_b E_b A_b)(\Delta T)L}{E_s A_s + E_b A_b} \quad (2-30)$$

A special case occurs when both bars are of the same material and $\alpha_s = \alpha_b$; then $P_s = P_b = 0$ and $\delta = \alpha_b(\Delta T)L$, as expected.

Now consider the analysis of this assembly by the stiffness method. In this case, we take the displacement δ of the bolt head as the unknown quantity, and we express the forces in the two parts in terms of that displacement. Then we write an equation of equilibrium for the forces and solve for the displacement δ .

Since the bars elongate by an amount equal to the final displacement δ , part of which is produced by the temperature change and part by the force in the bar, we can write the following equations relating the forces to the displacement:

$$P_s = -\frac{E_s A_s}{L} [\delta - \alpha_s(\Delta T)L] \quad P_b = \frac{E_b A_b}{L} [\delta - \alpha_b(\Delta T)L] \quad (g)$$

In these equations, the terms in brackets represent the changes in lengths produced by the forces P_s and P_b alone. The minus sign is placed in the first equation because P_s is assumed to be positive in compression. These expressions for P_s and P_b are substituted into the equation of equilibrium, $P_s = P_b$, to give

$$-\frac{E_s A_s}{L} [\delta - \alpha_s(\Delta T)L] = \frac{E_b A_b}{L} [\delta - \alpha_b(\Delta T)L]$$

from which we get the displacement:

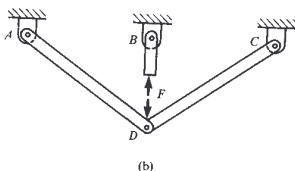
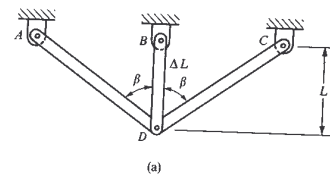
$$\delta = \frac{(\alpha_s E_s A_s + \alpha_b E_b A_b)(\Delta T)L}{E_s A_s + E_b A_b}$$

This result is the same as that obtained by the flexibility method (Eq. 2-30). Substituting this expression for δ into Eqs. (g) gives the forces P_s and P_b ; again, the results are the same as those obtained by the flexibility method (Eq. 2-29).

Prestrains. Suppose that a member of a structure is accidentally fabricated with a length that is different from its theoretical length. The effect is similar to that of a temperature change, although the cause of the change in length is different. Therefore, the effect on a statically determinate structure will be deviations from the theoretical configuration, although no strains or stresses will be created. However, a statically indeterminate structure, which is not free to adjust to the change in length of a member, will develop internal strains. These strains exist at the time the structure is built and before any loads are applied, hence they are called **prestrains**. Such strains result in a **prestressed** condition in the structure. Sometimes structures are deliberately prestressed in order to obtain more favorable stress conditions under loads. Common examples of this type are prestressed concrete beams, shrink-fitted machine parts, and prestressed spokes in bicycle wheels (which would collapse if not prestressed).

The analysis of a statically indeterminate structure with prestrains proceeds in the same manner as for temperature changes. To illustrate this point, consider again a three-bar truss, as shown in Fig. 2-25a, and assume that the unstressed length of the vertical bar is $L + \Delta L$ instead of L . Then the bars can be assembled into the truss only after compressing the vertical bar and stretching the inclined bars. Let F denote the compressive force in the vertical bar (Fig. 2-25b). This force produces a downward displacement δ_1 of joint D (see Eq. 2-10):

$$\delta_1 = \frac{FL}{2EA \cos^3 \beta}$$



assuming that L is the length of the vertical member and that all bars have the same axial rigidity EA . The shortening of the vertical member due to the force F is

$$\delta_2 = \frac{FL}{EA}$$

The condition of compatibility at joint D states that the downward displacement of joint D is equal to the initial increase in length ΔL of the vertical bar minus its shortening due to F . Therefore, the equation of compatibility is

$$\delta_1 = \Delta L - \delta_2$$

or

$$\frac{FL}{2EA \cos^3 \beta} = \Delta L - \frac{FL}{EA} \quad (h)$$

Solving this equation for the force F yields

$$F = \frac{2EA(\Delta L) \cos^3 \beta}{L(1 + 2 \cos^3 \beta)} \quad (2-31)$$

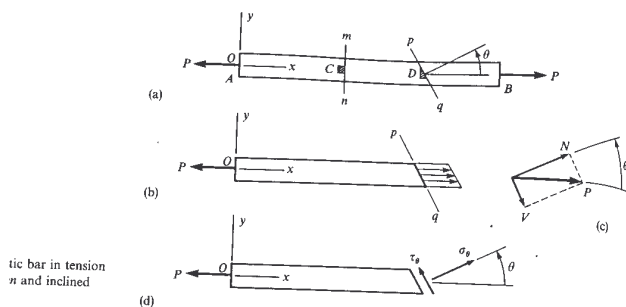
This force is compression when ΔL is positive (that is, when ΔL represents an increase in length). Knowing the force F in the vertical bar, we can easily obtain the forces in the inclined bars from static equilibrium.

This example illustrates that the analysis of a statically indeterminate structure due to prestrains is essentially the same as for temperature changes. The results of such analyses can easily be converted from one case to the other. For instance, suppose that the truss of Fig. 2-25a is subjected to a temperature change ΔT in the vertical bar, but the inclined bars remain at constant temperature. The resulting effect on the forces in the bars is the same as though the vertical bar had an excess length of ΔL , provided that we make ΔL equal to the thermal elongation that would occur if the bar were free to expand. Therefore, in Eq. (2-31) we replace ΔL by $\alpha(\Delta T)L$ in order to obtain the force F in the vertical bar due to the temperature change.

2.7 STRESSES ON INCLINED SECTIONS

In the preceding discussions of tension and compression in a bar, the only stresses we considered were the normal stresses acting on cross sections, such as cross section mn of bar AB shown in Fig. 2-26a. Let us now investigate the stresses acting on sections such as pq (Fig. 2-26a) that are inclined to the axis.

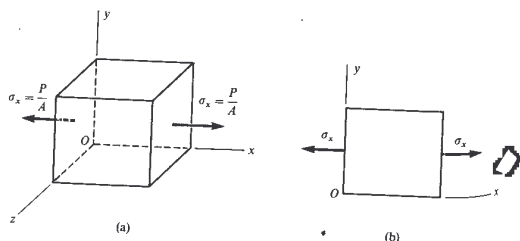
To begin the discussion, we recall that the normal stresses acting on cross section mn may be calculated from the formula $\sigma = P/A$, pro-



tic bar in tension n and inclined

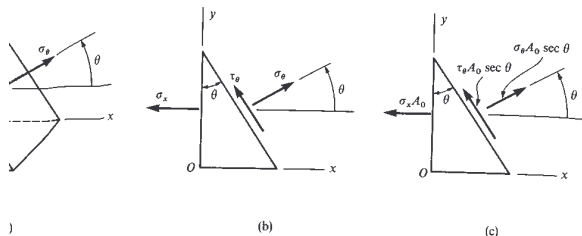
vided that the stress distribution is uniform over the entire cross-sectional area. As explained previously, this condition exists if the bar is prismatic, the material is homogeneous, the axial force P acts at the centroid of the cross-sectional area, and the cross section is away from the ends of the bar where high localized stresses may exist. Let us assume that the bar of Fig. 2-26a meets all of these conditions, so that the distribution of normal stresses on cross section mn is uniform. Of course, there are no shear stresses acting on this section, because it is cut at right angles to the longitudinal axis.

A convenient way to represent the stresses in the bar is to isolate a small element of material, such as the element labeled C in Fig. 2-26a, and then to show the stresses acting on all sides of this element. We shall refer to such an element as a **stress element**. The stress element at point C has the shape of a rectangular parallelepiped, and its right-hand face (or positive x face) is in cross section mn . Of course, the dimensions of a stress element are assumed to be infinitesimally small, but for clarity we can draw the element to a larger scale, as in Fig. 2-27a.



at point C 26a: of element, presentation

ially Loaded Members



nt at point D of 26a

(Fig. 2-28c). The force $\sigma_x A_0$ on the left-hand face can be resolved into components that are perpendicular and parallel to the inclined face; the perpendicular component is $\sigma_x A_0 \cos \theta$, and the parallel component is $\sigma_x A_0 \sin \theta$. Now we can write two equations of static equilibrium for the element, one in each of the directions mentioned. The first equation is obtained by summing forces perpendicular to the inclined face (that is, in the direction of σ_θ):

$$\sigma_\theta A_0 \sec \theta - \sigma_x A_0 \cos \theta = 0$$

or

$$\sigma_\theta = \sigma_x \cos^2 \theta$$

which is the same as Eq. (2-33a). The second equation is obtained by summing forces in the direction of τ_θ :

$$\tau_\theta A_0 \sec \theta + \sigma_x A_0 \sin \theta = 0$$

or

$$\tau_\theta = -\sigma_x \sin \theta \cos \theta$$

which is the same as Eq. (2-33b). This method for finding stresses on inclined planes, which is based upon the equilibrium of a stress element, will be used in discussions of pure shear (Section 3.4) and more general states of stress (Chapter 6).

Equations (2-33a and b) give the normal and shear stresses acting on any inclined section. Figure 2-29 shows the manner in which the stresses vary as the section is cut at angles varying from $\theta = -90^\circ$ to $\theta = +90^\circ$. Note that a positive angle θ is measured counterclockwise from the x axis and a negative angle is measured clockwise (Figs. 2-26 and 2-28). When $\theta = 0$, plane pq becomes a cross section and the graph gives $\sigma_\theta = \sigma_x$, as expected. As θ increases or decreases, the stress σ_θ diminishes until at $\theta = \pm 90^\circ$ it becomes zero, indicating that there are no normal stresses on a plane cut parallel to the longitudinal axis (as

The edges of the element are parallel to the x , y , and z axes, and the only stresses acting on the element are the normal stresses on the x faces, denoted as σ_x . For convenience, we often will use only a two-dimensional sketch of the element as shown in Fig. 2-27b.

The inclined section pq is cut through the bar at an angle θ between the x axis and the normal to the plane (Fig. 2-26a). Thus, cross section mn has an angle θ equal to zero, and a longitudinal section would have an angle θ equal to 90° or $\pi/2$ radians. Because all parts of the bar have the same axial strains, the stresses acting over section pq must be uniformly distributed (Fig. 2-26b). The resultant of these stresses must be a force that is equal in magnitude to the axial force P , in order to maintain equilibrium of the left-hand part of the bar. This resultant may be resolved into two components, a normal force N and a shear force V (Fig. 2-26c), that are normal and tangential, respectively, to the inclined plane pq . These components are

$$N = P \cos \theta \quad V = P \sin \theta \quad (2-32a, b)$$

Associated with the forces N and V are normal stresses σ_θ and shear stresses τ_θ , respectively (see Fig. 2-26d), that are uniformly distributed over the inclined section. These stresses are shown acting in their positive directions; that is, σ_θ is positive in tension, and τ_θ is positive when it tends to produce counterclockwise rotation of the material. Because the area A_1 of the inclined section is $A/\cos \theta$, in which A is the cross-sectional area, we see that the stresses σ_θ and τ_θ are given by the following equations:

$$\sigma_\theta = \frac{N}{A_1} = \frac{P}{A} \cos^2 \theta = \sigma_x \cos^2 \theta \quad (2-33a)$$

$$\tau_\theta = \frac{V}{A_1} = \frac{P}{A} \sin \theta \cos \theta = -\sigma_x \sin \theta \cos \theta \quad (2-33b)$$

in which $\sigma_x = P/A$ is the normal stress on a cross section.

The preceding equations for σ_θ and τ_θ also can be obtained by considering the equilibrium of a stress element at point D in the bar in Fig. 2-26a. In this instance, the element is wedge shaped and has one face along the inclined section pq . The element is shown again in Fig. 2-28a, with the stresses σ_θ and τ_θ acting on the inclined face and the stress σ_x acting on the left-hand face. There are no stresses on the other faces of the element. Again, a two-dimensional sketch of the element is useful for many purposes (Fig. 2-28b). To obtain σ_θ and τ_θ , we consider the equilibrium of the element. The forces acting on the faces are obtained by multiplying the stresses by the areas over which they act (that is, by the areas of the faces). For instance, the force on the left-hand face is equal to $\sigma_x A_0$ (Fig. 2-28c), where A_0 is the area of the face. This force acts in the negative x direction. Because the thickness of the element is constant, the area of the inclined face is $A_0 \sec \theta$. Therefore, the normal and shear forces on this face are $\sigma_\theta A_0 \sec \theta$ and $\tau_\theta A_0 \sec \theta$, respectively

2.7 Stresses on Inclined Section

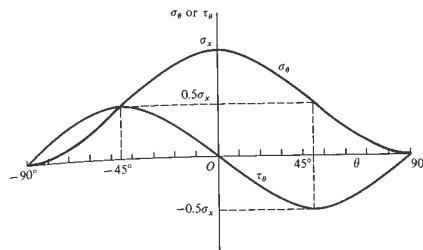


Fig. 2-29 Graph of normal stress and shear stress τ_θ versus angle θ of the inclined section pq (see Fig. 2-26

expected). The maximum normal stress occurs at $\theta = 0$ and is

$$\sigma_{\max} = \sigma_x \quad (2-34)$$

At $\theta = \pm 45^\circ$, the normal stress is one-half the maximum value.

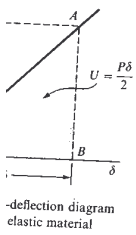
The shear stress τ_θ is zero on cross sections ($\theta = 0$) and longitudinal sections ($\theta = \pm 90^\circ$). Between these extremes, the stress varies as shown in Fig. 2-29, reaching the largest positive value when $\theta = -45^\circ$ and the largest negative value when $\theta = 45^\circ$. These maximum shear stresses have the same magnitude, but of course they tend to rotate the element in opposite directions. Thus, we can summarize by saying that the numerically largest shear stresses are

$$\tau_{\max} = \frac{\sigma_x}{2} \quad (2-35)$$

and they occur on planes at 45° to the axis.

The complete state of stress on sections cut at 45° to the axis is represented by the stress element shown in Fig. 2-30. On face ab ($\theta = 45^\circ$), the normal and shear stresses (from Eqs. 2-33a and b) are $\sigma_x/2$ and $-\sigma_x/2$, respectively. Hence, the normal stress is tension, and the shear stress acts clockwise against the element, as shown in the figure. The stresses on the remaining faces bc , cd , and ad can be obtained in a similar manner by substituting $\theta = -45^\circ$, -135° and 135° , respectively, into Eqs. (2-33a and b). Note that the normal stresses in this special case are the same on all four faces and that the shear stresses have the maximum value. Also, the shear stresses acting on perpendicular planes are equal in magnitude and have directions either toward or away from the line of intersection of the planes, as discussed in Section 1.6.

If a bar is loaded in compression instead of tension, the stress σ_x will have a negative value and the stresses acting on an element will have directions opposite to those for a bar in tension. Of course, Eqs. (2-33a and b) can still be used for numerical calculations by substituting σ_x as a negative quantity.



below the elastic limit load (that is, below the load at which the stress in the material reaches the elastic limit). This load is represented by the ordinate at point A in the diagram of Fig. 2-36. As long as the load is below this value, all of the strain energy is recovered during unloading and no permanent set remains in the bar. Hence, the bar acts as an elastic spring that stores and releases energy as the load is applied and removed.

If the material of the bar is elastic and if it follows Hooke's law, then the load-deflection diagram is a straight line (Fig. 2-37). In this case, the strain energy U stored in the bar (equal to the total work W done by the load P) is

$$U = W = \frac{P\delta}{2} \quad (2-38)$$

which is the area of the shaded triangle OAB in the figure.* Because we know that $\delta = PL/EA$ for a prismatic bar, we can substitute into Eq. (2-38) and express the strain energy in either of the following forms:

$$U = \frac{P^2L}{2EA} \quad U = \frac{EA\delta^2}{2L} \quad (2-39a, b)$$

The first of these equations expresses the strain energy of the bar as a function of the load P , and the second expresses it as a function of the elongation δ . The same equations apply to a linear elastic spring if the stiffness EA/L for a prismatic bar is replaced by the spring stiffness k (see Eq. 2-2).

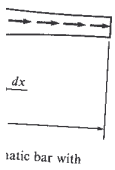
The strain energy of a nonprismatic bar or a bar with varying axial force (Fig. 2-38) can be obtained by applying Eq. (2-39a) to the differential element (shown shaded) and then integrating:

$$U = \int_0^L \frac{P_x^2 dx}{2EA_x} \quad (2-40)$$

In this expression P_x and A_x are the axial force and cross-sectional area at distance x from the end of the bar.

It is often convenient to use a quantity known as the **strain energy density** u , which is the strain energy per unit volume of the material. Expressions for u in the linear elastic case can be obtained by dividing the total strain energy U (see Eqs. 2-39a and b) by the volume AL of

* The principle that the work of the external loads is equal to the strain energy (for the case of linear elastic behavior) was first stated by the French engineer B. P. E. Clapeyron (1799–1864) and is known as *Clapeyron's theorem* (Dof 2.11).



lastic bar with

the bar, because the strain energy density is uniform throughout the volume in this example; thus,

$$u = \frac{\sigma^2}{2E} \quad u = \frac{E\epsilon^2}{2} \quad (2-41a, b)$$

in which $\sigma = P/A$ and $\epsilon = \delta/L$ are the normal stress and strain, respectively. The strain energy density is equal to the area under the stress-strain curve from the origin to the point on the curve representing the stress σ and the strain ϵ .

Strain energy density has units of energy divided by volume. Thus, the SI units for u are joules per cubic meter (J/m^3), and the USCS units are foot-pounds per cubic foot, inch-pounds per cubic inch, or other similar units. All of these units are the same as the units of stress; hence, we can also use pascals or psi as the units for u (see Eqs. 2-41a and b).

The strain energy density when the material is stressed to the proportional limit is called the **modulus of resilience** u_r . It is found by substituting the proportional limit stress σ_{pl} into Eq. (2-41a):

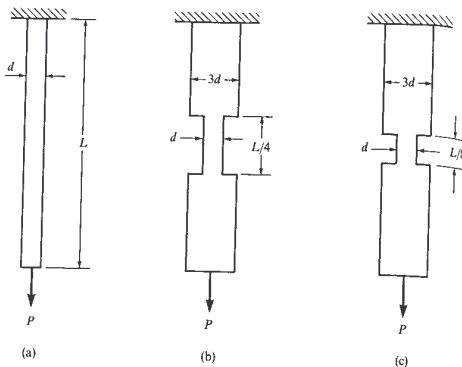
$$u_r = \frac{\sigma_{pl}^2}{2E} \quad (2-42)$$

As an example, a mild steel having $\sigma_{pl} = 30,000$ psi and $E = 30 \times 10^6$ psi has a modulus of resilience $u_r = 15$ psi (or 103 kPa). Note that the modulus of resilience is equal to the area under the stress-strain curve up to the proportional limit. **Resilience** represents the ability of the material to absorb energy within the elastic range. Another quantity, called **toughness**, refers to the ability of the material to absorb energy without fracturing. Hence, the **modulus of toughness** u_t is the strain energy density when the material is stressed to the point of failure. It is equal to the area under the entire stress-strain curve.

The preceding discussions of strain energy for a member in tension apply also for a member in compression. Since the work done by the axial force is positive regardless of whether the force causes tension or compression, it follows that the strain energy is always a positive quantity. This conclusion is also apparent from the expressions for strain energy (Eqs. 2-39 through 2-41), all of which are positive because the algebraic terms are squared.

Example 1

Three round bars having the same length L but different shapes are shown in Fig. 2-39. The first bar has diameter d over its entire length, the second has diameter over one-fourth of its length, and the third has this diameter over one-eighth of its length. All three bars are subjected to the same load P . Compare the amounts of strain energy stored in the bars, assuming linear elastic behavior.



3 Example 1

The strain energy of the first bar (from Eq. 2-39a) is

$$U_1 = \frac{P^2L}{2EA}$$

where $A = \pi d^2/4$. Assuming that the stress distribution is uniform over every cross section, we find the strain energy of the second bar to be

$$U_2 = \frac{P^2(L/4)}{2EA} + \frac{P^2(3L/4)}{2E(9A)} = \frac{P^2L}{6EA} = \frac{U_1}{3}$$

For the third bar we find

$$U_3 = \frac{P^2(L/8)}{2EA} + \frac{P^2(7L/8)}{2E(9A)} = \frac{P^2L}{9EA} = \frac{2U_1}{9}$$

Comparison of these results shows that the strain energy decreases as the volume of the bar increases, although all three bars have the same maximum stress. Thus, the third bar has less energy-absorbing capacity than the other two. Therefore, it takes only a small amount of work to bring the tensile stress to a high value in a bar with a groove, and the narrower the groove, the more severe the condition. When the loads are dynamic in character and the ability to absorb energy is important, the presence of grooves is very damaging. Of course, for static loads the maximum stresses, rather than the ability to absorb energy, are important in design.

Example 2

Determine the strain energy stored in a prismatic bar suspended from one end (Fig. 2-40) due to its own weight, assuming linear elastic behavior.

in the figure). The axial force P_x acting on this element is equal to the weight of the bar below the element:

$$P_x = \gamma A(L - x) \quad (a)$$

in which γ is the specific weight of the material and A is the cross-sectional area of the bar. Substituting into Eq. (2-40) and integrating gives the total strain energy:

$$U = \int_0^L \frac{[\gamma A(L - x)]^2 dx}{2EA} = \frac{\gamma^2 AL^3}{6E} \quad (2-43)$$

This same result can be obtained by integrating the strain energy density. At any distance x from the support, the stress is

$$\sigma = \frac{P_x}{A} = \gamma(L - x)$$

and, therefore, the strain energy density (see Eq. 2-41a) is

$$u = \frac{\sigma^2}{2E} = \frac{\gamma^2(L - x)^2}{2E}$$

The total strain energy is now found by integrating u throughout the volume of the bar:

$$U = \int u dV = \int_0^L u(A dx) = \int_0^L \frac{\gamma^2 A(L - x)^2 dx}{2E} = \frac{\gamma^2 AL^3}{6E}$$

This result agrees with Eq. (2-43).

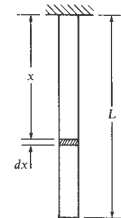


Fig. 2-40 Example 2. Bar hangs under its own weight

Example 3

Determine the strain energy in a prismatic bar suspended from one end if, in addition to its own weight, it supports a load P at the lower end (Fig. 2-41).

In this case, the axial force P_x acting on the element shown shaded in the figure is

$$P_x = \gamma A(L - x) + P$$

(see Eq. a). From Eq. (2-40) we now obtain

$$U = \int_0^L \frac{[\gamma A(L - x) + P]^2 dx}{2EA} = \frac{\gamma^2 AL^3}{6E} + \frac{\gamma PL^2}{2E} + \frac{P^2L}{2EA} \quad (2-44)$$

Upon examining this result, we see that the first term is the same as that given in Eq. (2-43) for the strain energy of a bar hanging under its own weight. Also, the last term is the same as the strain energy of a bar subjected only to an axial force P (Eq. 2-39a). The middle term contains both γ and P , showing that it depends upon both the weight of the bar and the magnitude of the applied load.

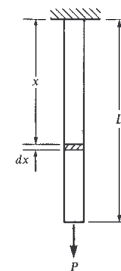


Fig. 2-41 Example 3. Bar hangs under its own weight and supports a load P

The important conclusion from the preceding example is that we cannot

merely by adding the strain energies obtained from the individual loads acting separately. The reason is that strain energy is a quadratic function of the loads (see Eq. 2-40), not a linear function.

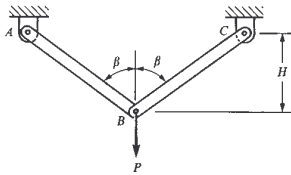
Deflections caused by a single load. Consider a linear elastic structure that is subjected to a single concentrated load P . Then the work W done by this load, equal to the strain energy U stored in the structure, is given by Eq. (2-38):

$$U = W = \frac{P\delta}{2}$$

where δ is the deflection through which the force P moves. This equation provides a simple method for finding the deflection δ if the strain energy can be determined. However, the limitations of the method must be kept in mind: (1) only one load may act on the structure, and (2) the only deflection that can be determined by this method is the deflection at the load itself. The following example illustrates the procedure.

Example 4

Determine the vertical deflection δ_b of joint B for the truss of Fig. 2-42. Note that the only load acting on the truss is a vertical load P at joint B . Assume that both members have the same axial rigidity EA .



Example 4

In this example, the deflection will be found by equating the work of the load to the strain energy stored in the members. The force F in either bar is

$$F = \frac{P}{2 \cos \beta}$$

as found from equilibrium of joint B . Also, the length of each bar is $L_1 = H/\cos \beta$. Then, using Eq. (2-39a), we get the strain energy of the two bars:

$$U = \frac{F^2 L_1}{2EA} (2) = \frac{P^2 H}{4EA \cos^3 \beta}$$

The work of the load P is

$$W = \frac{P\delta_b}{2}$$

Equating U and W , we obtain the deflection of joint B :

$$\delta_b = \frac{PH}{2EA \cos^3 \beta}$$

This result is the same as that obtained previously from a displacement diagram (see Eq. 2-10).

***2.9 DYNAMIC LOADING**

Dynamic loads differ from static loads in that they vary with time. A static load is slowly applied, gradually increasing from zero to its maximum value; thereafter, the load remains constant. However, dynamic loads may be applied very suddenly, thus causing vibrations of the structure, or they may change in magnitude as time elapses. Examples are impact loads, such as when two objects collide or when a falling object strikes a structure, and cyclical loads caused by rotating machinery. Other examples are the loads caused by traffic, wind gusts, water, waves, earthquakes, and manufacturing processes, all of which are dynamic in character. To aid in understanding the nature of such loads, we will consider in this section the most basic type of dynamic load, namely, an **impact load**.

As an example of an impact load, consider the simple arrangement shown in Fig. 2-43. A collar of mass M , initially at rest, falls from a height h onto a flange at the lower end of bar AB . When the collar strikes the flange, the bar begins to elongate, creating axial stresses and strains within the bar. In a very short interval of time, the flange will have moved downward to its position of maximum deflection. Then the

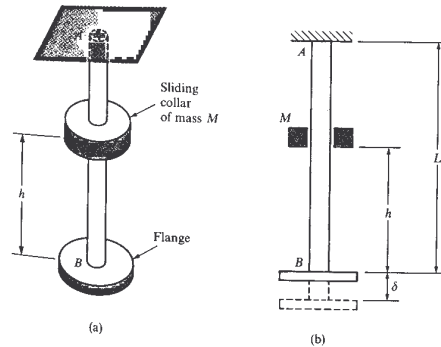


Fig. 2-43 Impact load on a prismatic bar due to a falling mass

Axially Loaded Members

bar immediately begins to shorten, and longitudinal vibrations of the bar occur. The situation is analogous to jumping onto a pogo stick or dropping a mass onto a spring. Soon the vibrations cease because of damping effects, and the bar is at rest with the mass M supported on the flange. The behavior of this system under the action of the falling collar is obviously very complicated, and a complete analysis requires the use of advanced mathematical techniques. However, we can make an approximate analysis by using the concept of strain energy and making some simplifying assumptions.

The potential energy of the mass M with respect to the elevation of the flange is Mgh , where g is the acceleration of gravity.* This potential energy is converted into kinetic energy as the mass falls. At the instant the mass strikes the flange, its potential energy (with respect to the elevation of the flange) has become zero and its kinetic energy is $Mv^2/2$, where $v = \sqrt{2gh}$ is the velocity of the mass. The kinetic energy of the falling mass then is transformed to other forms of energy. Part of it is transformed into strain energy of the stretched bar. Some of it is dissipated in the form of heat, some is dissipated in causing localized plastic strains in the bar and flange, and some may remain as kinetic energy of the mass (which either continues to move downward with the flange or bounces upward). Let us assume that the mass M "sticks" to the flange and moves downward with it. This assumption is valid only if the mass of the falling object is very large compared to the mass of the bar and flange. Also, we will disregard energy losses and assume that all of the kinetic energy of the falling mass is transformed into strain energy of the bar. This second assumption is conservative in the sense that it results in larger stresses in the bar than would result otherwise. In addition, we disregard any change in the potential energy of the bar itself. Finally, we will assume that the stresses in the bar remain within the linear elastic range and that the stress distribution is the same as for static loading. On the basis of these assumptions, we can calculate the maximum tensile stress and maximum elongation of the bar due to the impact load.

The maximum elongation δ of the bar (Fig. 2-43b) can be obtained by equating the potential energy lost by the falling mass to the strain energy acquired by the bar. The potential energy lost is $W(h + \delta)$, where $W = Mg$ is the weight of the collar and $h + \delta$ is the distance through which it moves. The strain energy of the bar is $EA\delta^2/2L$, where EA is the axial rigidity and L is the length of the bar (see Eq. 2-39b). Thus, we obtain the following equation from the principle of conservation of energy:

$$W(h + \delta) = \frac{EA\delta^2}{2L} \tag{2-45}$$

This equation is quadratic in δ and can be solved for its positive root; the result is

$$\delta = \frac{WL}{EA} + \left[\left(\frac{WL}{EA} \right)^2 + \frac{2WLh}{EA} \right]^{1/2} \tag{2-46}$$

Note that the elongation of the bar increases if either the mass or the height of fall is increased and diminishes if the stiffness EA/L is increased. The preceding equation can be written in simpler form by introducing the notation

$$\delta_{st} = \frac{WL}{EA} \tag{2-47}$$

for the static deflection of the bar due to the weight W . Then Eq. (2-46) becomes

$$\delta = \delta_{st} + (\delta_{st}^2 + 2h\delta_{st})^{1/2} \tag{2-48}$$

If the static deflection is very small compared to the height h , we can further simplify the preceding equation to the following:

$$\delta \approx \sqrt{2h\delta_{st}} \tag{2-49}$$

This approximate equation gives deflections that are always less than those obtained from Eq. (2-48). For instance, if $h = 40\delta_{st}$, the approximate equation gives $\delta = 8.9\delta_{st}$, which is 0.89 times the deflection of $10\delta_{st}$ obtained from Eq. (2-48).

The maximum stress in the bar can be calculated from the maximum elongation if we assume that the stress distribution is uniform throughout the length. Of course, this condition is only an approximation because, in reality, longitudinal stress waves exist in the bar (see Refs. 2-12 and 2-13). Nevertheless, based on the assumption of a uniform stress distribution, we obtain the following equations for the maximum tensile stress (see Eq. 2-46):

$$\sigma = \frac{E\delta}{L} = \frac{W}{A} + \left[\left(\frac{W}{A} \right)^2 + \frac{2WhE}{AL} \right]^{1/2} \tag{2-50}$$

or

$$\sigma = \sigma_{st} + \left(\sigma_{st}^2 + \frac{2hE}{L} \sigma_{st} \right)^{1/2} \tag{2-51}$$

in which $\sigma_{st} = W/A$ is the stress when the load acts statically. Again considering the case where the height h is large compared to the elongation (see Eq. 2-49), and also noting that $\sigma_{st} = W/A$ and $M = W/g$, we obtain

$$\sigma \approx \sqrt{\frac{2hE}{L} \sigma_{st}} = \sqrt{\left(\frac{Mv^2}{2} \right) \left(\frac{2E}{AL} \right)} \tag{2-52}$$

in which $v = \sqrt{2gh}$ is the velocity of the mass M when it strikes the bar.

* In SI units, $g = 9.81 \text{ m/s}^2$; in USCS units, $g = 32.2 \text{ ft/s}^2$. For more precise values of g , as well as for a discussion of mass and weight, see Appendix A.

Next, the value of k is substituted into Eq. (2-47) in place of EA/L in order to obtain the static deflection caused by the mass M :

$$\delta_{st} = \frac{W}{k} = \frac{Mg}{k} = \frac{(20 \text{ kg})(9.81 \text{ m/s}^2)}{31.8 \text{ MN/m}} = 0.00617 \text{ mm}$$

Then we use Eq. (2-48) to obtain the dynamic deflection:

$$\begin{aligned} \delta &= \delta_{st} + (\delta_{st}^2 + 2h\delta_{st})^{1/2} \\ &= 0.00617 \text{ mm} + [(0.00617 \text{ mm})^2 + 2(50 \text{ mm})(0.00617 \text{ mm})]^{1/2} \\ &= 0.792 \text{ mm} \end{aligned}$$

Note that this deflection is less than for the prismatic bar of Example 1. However, the impact factor is $0.792/0.00617 = 128$, which is greater than the impact factor for the prismatic bar.

The static load P that would produce the same deflection δ is

$$P = k\delta = (31.8 \text{ MN/m})(0.792 \text{ mm}) = 25.2 \text{ kN}$$

Therefore, the maximum stress σ is

$$\sigma = \frac{P}{A} = \frac{25.2 \text{ kN}}{(\pi/4)(15 \text{ mm})^2} = 143 \text{ MPa}$$

and it occurs in the lower half of the bar. Comparing this stress with the maximum stress of 106 MPa calculated in Example 1, we see that the stress in the nonprismatic bar is 35% greater than the stress in the prismatic bar. We conclude that enlarging the bar over part of its length is detrimental from the standpoint of the bar's resistance to an impact load, because the energy-absorbing capacity of the bar is reduced, as pointed out previously in Example 1 of Section 2.8. In general, bars that must resist dynamic loads should be prismatic so that the stress distribution is uniform throughout their lengths.

***Example 3**

An elevator car of weight W is supported by a cable that is moving downward with constant velocity v (Fig. 2-48). What maximum stress is produced in the cable when the drum suddenly is locked?

This example differs significantly from the previous ones. In the earlier examples, the bars being struck were unstressed prior to impact, hence they had no strain energy before impact. However, the cable in this example supports the weight W , hence strain energy is stored in the cable even before the drum is locked. Therefore, we cannot use the previously derived equations; we must write a new equation of conservation of energy.

Let us assume that there are no energy losses when the drum is locked, hence the total energy of the system (kinetic plus potential energy) just prior to stoppage is equal to the total energy at the instant the cable has its maximum elongation δ . Prior to stoppage, the kinetic energy of the moving elevator is $Wv^2/2g$. We will disregard the kinetic energy of the cable in this example, on the basis that it is relatively small compared to the kinetic energy of the elevator. The potential energy of the weight W with respect to its lowest position is $W\delta_1$, where δ_1 is the distance that the weight moves downward after the drum locks.

This distance is equal to $\delta - \delta_{st}$, where δ is the total elongation of the cable and δ_{st} is the elongation of the cable under the load W . Of course, the cable is elongated by the amount δ_{st} prior to locking of the drum; hence, the strain energy of the cable before stoppage is $EA\delta_{st}^2/2L$ (see Eq. 2-39b), where EA/L is the stiffness of the cable. After stoppage, and at the instant the cable has its maximum elongation, its strain energy is $EA\delta^2/2L$. No kinetic energy exists at this instant because the velocity is zero.

Using the principle of conservation of energy and equating the energies before and after locking of the drum, we obtain

$$\frac{Wv^2}{2g} + W(\delta - \delta_{st}) + \frac{EA\delta_{st}^2}{2L} = \frac{EA\delta^2}{2L} \quad (a)$$

This equation can be solved for the maximum elongation δ of the cable in the following manner. First, we note that the static deflection is

$$\delta_{st} = \frac{WL}{EA} \quad (b)$$

from which $W = EA\delta_{st}/L$. Next, we substitute this expression for W into the second term of Eq. (a), thereby obtaining

$$\frac{Wv^2}{2g} + \frac{EA\delta_{st}}{L}(\delta - \delta_{st}) = \frac{EA}{2L}(\delta^2 - \delta_{st}^2)$$

or, upon rearranging terms,

$$\frac{Wv^2}{2g} = \frac{EA}{2L}(\delta - \delta_{st})^2$$

Now we solve this equation for the maximum elongation of the cable:

$$\delta = \delta_{st} + \sqrt{\frac{Wv^2 L}{gEA}} \quad (c)$$

Finally, we obtain the maximum stress in the cable:

$$\sigma = \frac{E\delta}{L} = \frac{W}{A} \left(1 + \sqrt{\frac{v^2 EA}{gWL}} \right) \quad (d)$$

The term in parentheses, which is the impact factor, may be many times greater than unity. Hence, the dynamic stress in the cable may be much greater than the static stress W/A . Note that, if $v = 0$, Eq. (d) gives the static stress, as expected.

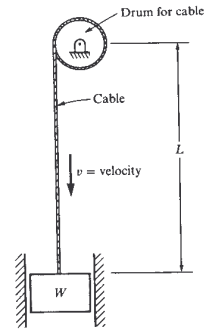


Fig. 2-48 Example 3

***2.10 NONLINEAR BEHAVIOR**

In the preceding sections, we analyzed both statically determinate and statically indeterminate structures using the assumption that the materials followed Hooke's law. Let us now consider the behavior of axially loaded structures when the stresses exceed the proportional limit. In such cases, it is necessary to make use of the stress-strain diagram for the material. Occasionally the diagram is available from an actual test

axially Loaded Members

linear

elastic

plastic

strain hardening

elastic

idealized diagrams:

graph; m; and

of the material, but more often an idealized stress-strain diagram is used. Hooke's law is one example of such an idealized diagram. Figure 2-49 illustrates other examples.

Figure 2-49a shows a diagram consisting of an initial region in which Hooke's law holds, followed by a nonlinear region defined by some appropriate mathematical function. Aluminum is one material that has a diagram of this shape (see Fig. 1-10). For purposes of mathematical analysis, a single mathematical function is sometimes used for the entire diagram.

Figure 2-49b portrays a diagram that is widely used for structural steel. This material has a linear elastic region followed by a region of considerable yielding (see Fig. 1-7); hence, it can be idealized with good accuracy by two straight lines, as shown in the figure. The material is assumed to follow Hooke's law up to the yield stress, after which it yields under constant stress; the latter behavior is known as perfect plasticity. The yield stress and yield strain are denoted by σ_y and ϵ_y , respectively. The perfectly plastic region continues until the strains are many times larger than the yield strain. A material having a diagram of this kind is called an elastic-plastic material. As the strain becomes very large, the stress-strain curve rises above the yield stress due to strain hardening as explained in Section 1.3. But, by the time strain hardening begins, the deflections are so large that the structure probably has lost its usefulness. Hence, it has become common practice to analyze steel structures on the basis of the elastic-plastic diagram shown in Fig. 2-49b. For steel, the same diagram may be used for both tension and compression. An analysis made with these assumptions is usually called a plastic analysis, although the term elastic-plastic analysis is more accurate.

Figure 2-49c shows a diagram made up of two lines having different slopes called a bilinear diagram. This diagram is sometimes used to represent a material with strain hardening, or it can be used as an approximation to a diagram of the general shape shown in Fig. 2-49a.

Now let us consider the analysis of a statically determinate system loaded into the nonlinear range. Suppose, for instance, that we wish to find the deflection of joint C of the truss shown in Fig. 2-50a, assuming that the material has the stress-strain diagram of Fig. 2-50b. Because the

truss is statically determinate, we can find the axial forces in the members from equilibrium without considering the material properties, provided that the elongations of the members remain small. We can then obtain the stresses by dividing the axial forces by the cross-sectional areas. Next, we determine the strains from the stress-strain diagram, and from the strains we find the elongations of both bars. Finally, we determine the deflection of joint C from the changes in lengths of the members. This procedure must be modified if the changes in lengths are large enough to alter the configuration of the truss. In such a case, the analysis must be performed in a step-by-step, or incremental, manner, utilizing the new dimensions of the truss at each step.

Plastic analysis of statically indeterminate systems.

If a structure is statically indeterminate, the analysis becomes much more complicated than for a determinate system. In an indeterminate system, the forces cannot be found without first finding the displacements, but the displacements depend upon both the forces and the stress-strain diagram. Hence, a complete analysis usually requires a trial-and-error method or a method of successive approximations (described at the end of this section). However, for a material such as mild steel having an elastic-plastic diagram (Fig. 2-49b), the behavior of the structure is greatly simplified and a plastic analysis can usually be performed without difficulty.

To illustrate the techniques of plastic analysis, let us consider again a symmetric three-bar truss, as shown in Fig. 2-51a. Assume that the bars are made of structural steel having an elastic-plastic stress-strain diagram (Fig. 2-51b). When the load P is small, the stresses in all three bars will be less than the yield stress σ_y ; hence, the bar forces can be determined by an elastic analysis using either the flexibility or the stiffness method (Sections 2.4 and 2.5). As the load P is gradually increased, the stresses in the bars increase until eventually the yield stress σ_y is reached in one or more of the bars. If we assume that the bars have

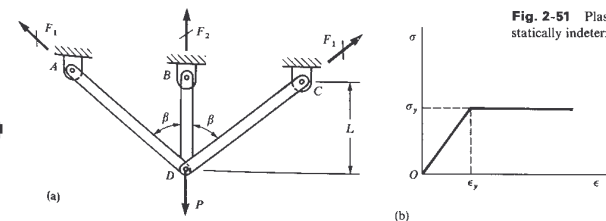
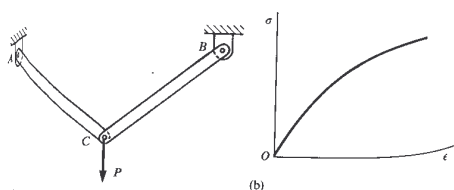


Fig. 2-51 Plastic analysis of a statically indeterminate truss

determinate truss
rain diagram

equal cross-sectional areas A , then the forces F_1 and F_2 in the bars under elastic conditions are obtained from Eqs. (2-14) and (2-13):

$$F_1 = \frac{P \cos^2 \beta}{1 + 2 \cos^3 \beta} \quad F_2 = \frac{P}{1 + 2 \cos^3 \beta} \quad (a)$$

Because the force F_2 is larger than F_1 , the axial stress in the middle bar will reach σ_y first, which occurs when the force F_2 is equal to $\sigma_y A$. The corresponding value of the load P is called the yield load P_y . We can obtain P_y by setting F_2 (see Eqs. a) equal to $\sigma_y A$ and solving for the load:

$$P_y = \sigma_y A (1 + 2 \cos^3 \beta) \quad (b)$$

Thus, as long as P is less than P_y , the structure behaves elastically and the forces in the bars are calculated from Eqs. (a). The deflection δ_y of joint D at the yield load is obtained by noting that this deflection is equal to the elongation of member BD :

$$\delta_y = \frac{F_2 L}{EA} = \frac{\sigma_y L}{E} \quad (c)$$

load-deflection diagram 2-51

The behavior of the truss up to the yield load is represented by line OA on the load-deflection diagram of Fig. 2-52.

With a further increase in the load P , the forces F_1 in the inclined bars also increase, but the force F_2 remains constant and equal to $\sigma_y A$ because the middle bar has become perfectly plastic (see Fig. 2-51b). Eventually the forces F_1 reach the value $\sigma_y A$, and the inclined bars also become plastic. Then the structure can carry no additional load. Instead, all three bars continue to elongate under this constant (and maximum) value of the load, which is called the ultimate load P_u . This load is represented by point B on the load-deflection diagram; the horizontal line BC represents the region of continuous plastic deformation of the structure.

The ultimate load P_u can be calculated from equilibrium of forces at joint D . The bar forces at the ultimate load are

$$F_1 = F_2 = \sigma_y A \quad (d)$$

Hence, from equilibrium we obtain

$$P_u = \sigma_y A (1 + 2 \cos \beta) \quad (e)$$

The corresponding deflection δ_u is found by observing that the inclined bars have elongated by an amount $\delta_1 = \epsilon_y L_1$, where $L_1 = L/\cos \beta$ is the length of an inclined bar. Since $\epsilon_y = \sigma_y/E$, the elongation of each inclined bar is $\delta_1 = \sigma_y L/E \cos \beta$. From this elongation, we can find the vertical deflection of the joint by means of a displacement diagram (see Fig. 2-10b); the result is

$$\delta_u = \frac{\delta_1}{\cos \beta} = \frac{\sigma_y L}{E \cos^2 \beta} \quad (f)$$

Comparing δ_u with δ_y , we see that their ratio is

$$\frac{\delta_u}{\delta_y} = \frac{1}{\cos^2 \beta} \quad (g)$$

Also, the ratio of the loads is

$$\frac{P_u}{P_y} = \frac{1 + 2 \cos \beta}{1 + 2 \cos^3 \beta} \quad (h)$$

For example, if $\beta = 45^\circ$, we obtain $\delta_u/\delta_y = 2$ and $P_u/P_y = \sqrt{2}$.

When the load is between the values P_y and P_u (region AB on the load-deflection diagram), the force F_2 remains constant and equal to $\sigma_y A$. Hence, the forces F_1 in the inclined bars can be obtained from static equilibrium at joint D :

$$F_1 = \frac{P - \sigma_y A}{2 \cos \beta} \quad (i)$$

The deflection of the truss in the region AB of the diagram varies linearly because the force F_2 is constant and the force F_1 is a linear function of P , as shown by Eq. (i). However, the slope of the load-deflection diagram is less in region AB than in the elastic region (line OA), because only the inclined bars remain elastic and are effective in resisting an increased load P .

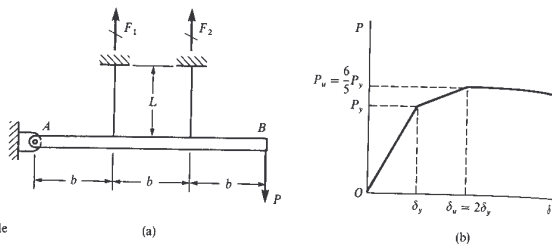
From this example, we see that the calculation of the ultimate load P_u of a statically indeterminate structure requires only the use of statics, because all members have yielded and, hence, their axial forces are known to be $\sigma_y A$. In contrast, the calculation of P_y requires an indeterminate analysis, which requires that both static equilibrium and compatibility of deflections be satisfied.

After the ultimate load is reached, the structure continues to deform. Strain hardening eventually occurs, and then the structure is able to support an additional load. However, the presence of very large deflections means that the structure has failed in a utilitarian sense. Hence, the load P_u is indeed the ultimate load for most purposes, and its determination is of considerable interest to design engineers.

This discussion has dealt with the behavior of structures as the load is applied for the first time. If the load is removed before the yield load P_y is reached, the structure will behave elastically and will return to its original unstressed condition. However, if the load P_y is exceeded, some part of the structure will retain a permanent set when the load is removed. Consequently, a statically indeterminate structure will have residual stresses remaining in it, even though no external load exists. Under a second application of the load, the structure will behave in a different manner.

Example

Determine the yield load P_y and the ultimate load P_u for the structure shown in Fig. 2-53a if the horizontal bar AB is rigid and the two vertical wires are made of an elastic-plastic material. Also, find the allowable load P_{allow} for the structure using a load factor of 1.85. (Assume that both wires have the same cross-sectional area A .)



53 Example

An equation relating the forces F_1 and F_2 in the wires to the load P can be obtained from equilibrium by taking moments about end A of the bar:

$$3P = F_1 + 2F_2 \quad (j)$$

Because this equation is based only upon statics, it is valid for any value of the load P from zero up to the ultimate load. Also, it can be seen from the figure that the elongation of the right-hand wire is always twice that of the left-hand wire. Therefore, under elastic conditions we have $F_2 = 2F_1$, and we see that the force F_2 will be the first to reach the yield value $\sigma_y A$. At that instant, the force F_1 will be equal to $\sigma_y A/2$. Therefore, the yield load P_y , found from Eq. (j), is

$$P_y = \frac{5\sigma_y A}{6} \quad (k)$$

The corresponding elongation of the right-hand wire is $\delta_2 = \sigma_y L/E$, where L is the length of the wires. The deflection at point B is

$$\delta_y = \frac{3\delta_2}{2} = \frac{3\sigma_y L}{2E} \quad (l)$$

Both P_y and δ_y are indicated on the load-deflection diagram (Fig. 2-53b).

When the ultimate load P_u is reached, both F_1 and F_2 will be equal to $\sigma_y A$. Thus, from Eq. (j) we find

$$P_u = \sigma_y A \quad (m)$$

At this load, the left-hand wire has just reached the yield stress; therefore, its elongation is $\delta_1 = \sigma_y L/E$, and the deflection of B is

$$\delta_u = 3\delta_1 = \frac{3\sigma_y L}{E} \quad (n)$$

Note that the ratios δ_u/δ_y and P_u/P_y are 2 and 6/5, respectively, as shown on the load-deflection diagram.

The allowable load P_{allow} is found by dividing the ultimate load by the load factor, as explained in Section 1.7; thus,

$$P_{allow} = \frac{P_u}{\text{load factor}} = \frac{\sigma_y A}{1.85}$$

At this value of the load, both wires are stressed within the elastic range.

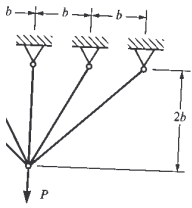
Nonlinear analysis of statically indeterminate systems.

If the material of the structure behaves nonlinearly but cannot be represented as an elastic-plastic material, then the analysis is more difficult to make. In the general case, a trial-and-error procedure is needed. To illustrate the method, let us refer again to the symmetric truss of Fig. 2-51a, but now we will assume that the material has a general stress-strain diagram such as the one shown in Fig. 2-49a. We may begin the analysis by assuming a trial value for the vertical deflection δ at joint D . Then, from a displacement diagram at joint D , we can obtain the corresponding elongations of the bars, thus ensuring that the condition of compatibility at the joint is satisfied. Equilibrium of forces at the joint must be checked next. The strains in the bars can be found from the elongations, and then the stresses can be found from the stress-strain diagram. Knowing the stresses in the bars, we can calculate the forces in the bars and check equilibrium at joint D . If the true value of δ was assumed initially, we will find that equilibrium of forces at joint D will be satisfied. Otherwise, we will find that the forces are not in equilibrium, and, therefore, a new trial value of δ must be selected and the process repeated. Eventually, we will arrive at a value of δ such that both compatibility and equilibrium are satisfied at joint D . The corresponding forces in the bars, as well as the deflection δ , will have their true values.

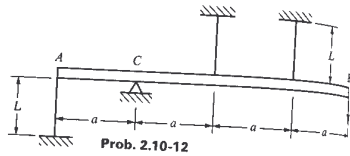
An alternate trial-and-error procedure begins by our assuming a value for one of the bar forces, say, the force F_2 in the vertical bar. Then, using equilibrium of forces at joint D , we can calculate the forces in the other bars. Next, we can determine the stresses (from the forces), then the strains (from the stress-strain diagram), and then the elongations (from the strains). Finally, from the displacement diagram at joint D , we can determine whether the elongations of all three bars was compatible with one another. If they are, then the trial value of F_2 was the correct one, and the analysis is completed. Otherwise, a new trial value for F_2 must be selected and the process repeated until both equilibrium and compatibility are satisfied.

er 2 Axially Loaded Members

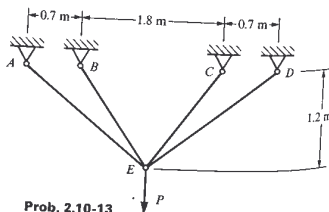
wires, each having a diameter of 10 mm, P as shown in the figure. Determine the P_u if the material is elastic-plastic with yield M_p .



***2.10-12** A rigid bar AB is supported on a fulcrum C and loaded by a force P at end B (see figure). The bar is supported by four wires made of an elastic-plastic material. Each wire has cross-sectional area A and length L . Determine the yield load P_y , the corresponding yield deflection δ_y at point B , the ultimate load P_u , and the deflection δ of point B when the load just reaches the value P_u . Also draw the load-deflection diagram showing the force P versus the deflection δ of point B .



***2.10-13** The symmetric truss $ABCDE$ shown in the figure is constructed of four bars and supports a load P at joint E . Each of the two outer bars has a cross-sectional area of 200 mm^2 , and each of the two inner bars has an area of 400 mm^2 . The material is elastic-plastic with yield stress $\sigma_y = 240 \text{ MPa}$ and modulus of elasticity $E = 200 \text{ GPa}$. Determine the yield load P_y , the corresponding deflection δ_y of joint E , the ultimate load P_u , and the corresponding deflection δ_u . Then construct a load-deflection diagram.

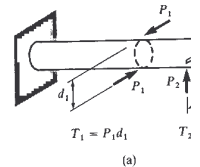


P is carried by a horizontal beam that is supported by rods arranged symmetrically as shown. Each rod has cross-sectional area A and is made of elastic-plastic material having yield stress σ_y . Determine the ultimate load P_u .

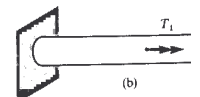


3.1 INTRODUCTION

Torsion refers to the twisting of a structural member when it is loaded by couples that produce rotation about its longitudinal axis. This type of loading is pictured in Fig. 3-1a, which shows a straight bar that is supported at one end and loaded by two pairs of forces. Each pair of forces forms a couple that tends to twist the bar about its longitudinal axis. The moment of a couple is equal to the product of one of the forces and the distance between the lines of action of the forces; thus, the first couple has a moment $T_1 = P_1 d_1$ and the second has a moment $T_2 = P_2 d_2$.



For convenience in representing couples, we will show the moment of a couple by means of a vector in the form of a double-headed arrow (Fig. 3-1b). The arrow is perpendicular to the plane containing the couple, and the direction, or sense, of the couple is indicated by the right-hand rule for moment vectors. An alternate representation is the use of a curved arrow acting in the direction of twist (Fig. 3-1c). Couples that produce twisting of a bar, such as couples T_1 and T_2 in Fig. 3-1, are called **torques, twisting couples, or twisting moments**.



In this chapter, we will develop formulas for the stresses and deformations produced in circular bars subjected to torsion. Examples of such bars are axles and drive shafts in machinery. We will also consider thin-walled tubular members of the kind found in aerospace structures and elsewhere. However, the analysis of more complicated shapes requires the use of methods more advanced than those presented here.

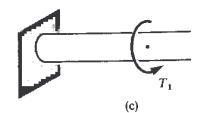


Fig. 3-1 Bar in torsion loaded by couples T_1 and T_2

3.2 TORSION OF CIRCULAR BARS

Let us consider a bar or shaft of circular cross section twisted by couples T acting at the ends (Fig. 3-2a). A bar loaded in this manner is

Torsion



said to be in **pure torsion**. From considerations of symmetry we can show that cross sections of the circular bar rotate as rigid bodies about a longitudinal axis, with radii remaining straight and the cross section remaining plane and circular. Also, if the total angle of twist of the bar is small, neither the length of the bar nor its radius will change.

During twisting, there will be a rotation about the longitudinal axis of one end of the bar with respect to the other. For instance, if the left-hand end of the bar is fixed, then the right-hand end will rotate through a small angle ϕ with respect to the left-hand end (Fig. 3-2b). The angle ϕ is known as the **angle of twist**. In addition, a longitudinal line on the surface of the bar, such as line mn , will rotate through a small angle to the position $m'n'$. Because of this rotation, an infinitesimal rectangular element on the surface of the bar, such as the element of length dx shown in the figure, is distorted into a rhomboid. This element is shown again in Fig. 3-2b, where the disk-like portion of the bar is isolated from the remainder of the bar. The original configuration of the element is labeled $abcd$. During torsion, the right-hand cross section rotates with respect to the opposite face, and points b and c move to b' and c' , respectively. The lengths of the sides of the element do not change during this rotation, but the angles at the corners are no longer equal to 90° . Thus, we see that the element is in a state of **pure shear** (see Section 1.6), and the magnitude of the shear strain γ is equal to the decrease in the right angle at a . This decrease in angle is

$$\gamma = \frac{bb'}{ab}$$

The distance bb' is the length of a small arc of radius r subtended by the angle $d\phi$, which is the angle of rotation of one cross section with respect to the other. Thus, we find $bb' = r d\phi$. Also, the distance ab is equal to dx , the length of the element. Substituting these quantities into the preceding equation, we get

$$\gamma = \frac{r d\phi}{dx}$$

as the expression for the shear strain.

The quantity $d\phi/dx$ represents the rate of change of the angle of twist ϕ . In general, both ϕ and $d\phi/dx$ are functions of x . We will denote the quantity $d\phi/dx$ by the symbol θ and refer to it as the **angle of twist per unit length**. Thus,

$$\gamma = \frac{r d\phi}{dx} = r\theta$$

In the special case of pure torsion, the rate of change $d\phi/dx$ is constant along the length of the bar, because every cross section is subjected to

the same torque. Therefore, we obtain $\theta = \phi/L$, where L is the length of the shaft, and Eq. (3-1) becomes

$$\gamma = r\theta = \frac{r\phi}{L} \quad (3-2)$$

for pure torsion. Note that the preceding equations are based only upon geometric concepts and are valid for a circular bar of any material, whether elastic or inelastic, linear or nonlinear.

The shear stresses τ in the circular bar have the directions shown in Fig. 3-2a. For a linear elastic material, these shear stresses are related to the shear strains by Hooke's law in shear (Eq. 1-9); therefore, from Eq. (3-1) we get

$$\tau = G\gamma = Gr\theta \quad (3-3)$$

in which G is the shear modulus of elasticity. Equations (3-1) and (3-3) relate the strains and stresses for an element at the surface of the shaft to the angle of twist per unit length.

The strains and stresses within the interior of the shaft can be determined in a manner similar to that used for an element at the surface of the shaft. Because radii in the cross sections of the bar remain straight and undistorted during twisting, we see that the preceding discussion for an element $abcd$ at the outer surface will also hold for a similar element situated at the surface of an interior cylinder of radius ρ (Fig. 3-2c). Therefore, such an interior element is also in pure shear with the corresponding shear strain and shear stress being given by the following equations:

$$\gamma = \rho\theta \quad \tau = G\rho\theta \quad (3-4a, b)$$

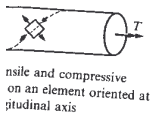
These equations show that the shear strain and stress in a circular bar vary linearly with the radial distance ρ from the center, and they have their maximum values on an element at the outer surface. The stress distribution over the cross section of the bar is pictured in Fig. 3-2c by the triangular stress diagram.

The shear stresses acting on the plane of the cross section are accompanied by shear stresses of the same magnitude acting on longitudinal planes of the bar (see Fig. 3-3). This result follows from the fact that equal shear stresses always exist on mutually perpendicular planes, as explained in Section 1.6. If a material is weaker in shear on longitudinal planes than on cross-sectional planes, as in the case of a circular bar made of wood, the first cracks due to twisting will appear on the surface in the longitudinal direction.

The state of pure shear stress at the surface of the shaft (Fig. 3-2a) is equivalent to equal tensile and compressive stresses on an element



Fig. 3-3 Longitudinal shear stress in a circular bar



rotated through an angle of 45°, as explained in Section 3.4. The rectangular element with sides at 45° to the axis of the shaft submitted to the tensile and compressive stresses shown in Fig. 3-4a twisted bar is made of a material that is weaker in tension than in shear, failure will occur in tension along a helix inclined at 45° to the axis. This type of failure is easy to demonstrate by twisting a piece of ordinary chalk.

The relationship between the applied torque T and the angle of twist ϕ (Fig. 3-2a) may now be determined from the condition that the resultant couple of the shear stresses acting over the cross section (Fig. 3-2c) must be statically equivalent to the applied torque T . The shear force acting on an element of area dA (shown shaded in the figure) is τdA , and the moment of this force about the axis of the bar is $\tau \rho dA$. Using Eq. (3-4b), we find that this moment is also equal to $G\theta\rho^2 dA$. The total torque T is the summation over the entire cross-sectional area of such elemental moments; thus,

$$T = \int G\theta\rho^2 dA = G\theta \int \rho^2 dA = G\theta I_p$$

in which

$$I_p = \int \rho^2 dA \tag{3-3}$$

is the **polar moment of inertia** of the circular cross section. For a circle of radius r and diameter d , the polar moment of inertia (see Appendix D, Case 9) is

$$I_p = \frac{\pi r^4}{2} = \frac{\pi d^4}{32} \tag{3-6}$$

Next, from Eq. (a) we obtain

$$\theta = \frac{T}{GI_p} \tag{3-7}$$

which shows that θ , the angle of twist per unit length, is directly proportional to the torque T and inversely proportional to the product GI_p known as the **torsional rigidity** of the shaft. The total angle of twist ϕ equal to θL , is

$$\phi = \frac{TL}{GI_p} \tag{3-8}$$

The angle of twist ϕ is measured in radians. If SI units are used, the torque T may be expressed in newton meters (N·m), the length L in meters (m), the shear modulus G in pascals (Pa), and the polar moment

of inertia I_p in metres to the fourth power (m⁴). Similarly, if USCS units are used, T may be expressed in inch-pounds (in.-lb), L in inches (in.), G in pounds per square inch (psi), and I_p in inches to the fourth power (in.⁴).

The quantity GI_p/L is the **torsional stiffness** of a circular bar, and it represents the torque required to produce a unit angle of rotation of one end with respect to the other. Also, the **torsional flexibility** is defined as the reciprocal of the stiffness, or L/GI_p , and it is equal to the rotation produced by a unit torque. The preceding expressions are analogous to those for axial stiffness EA/L and axial flexibility L/EA (see Eqs. 2-2 and 2-3).

Equation (3-8) is used for determining the shear modulus of elasticity G for various materials. By conducting a torsion test on a circular specimen, the angle of twist ϕ produced by a known torque T can be determined. Then the magnitude of G can be calculated from Eq. (3-8).

The **maximum shear stress** τ_{max} in a circular bar subjected to torsion may be found by substituting the expression for θ (Eq. 3-7) into the expression for τ (Eq. 3-3); thus,

$$\tau_{max} = \frac{Tr}{I_p} \tag{3-9}$$

This equation, which is known as the **torsion formula**, shows that the maximum shear stress is proportional to the applied torque T and the radius r and inversely proportional to the polar moment of inertia of the cross section. Substituting $r = d/2$ and $I_p = \pi d^4/32$, we get

$$\tau_{max} = \frac{16T}{\pi d^3} \tag{3-10}$$

as the formula for the maximum shear stress in a solid bar. The shear stress at distance ρ from the centre is

$$\tau = \frac{T\rho}{I_p} \tag{3-11}$$

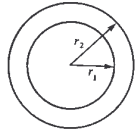
which is obtained from Eq. (3-4b). The units of shear stress are pascals (Pa) if SI units are used.*

Hollow circular bars. Hollow bars are much more efficient in resisting torsional loads than are solid bars. As explained in the preceding paragraphs, the shear stresses in a solid circular bar are maxi-

* The torsion theory for circular bars originated with the work of the famous French scientist C. A. de Coulomb (1736–1806); further developments were due to Thomas Young and A. Duleau (see Ref. 3-1). The general theory of torsion (for bars of any shape) is due to the most famous elastician of all time, Barré de Saint-Venant (1797–1886); see Ref. 3-2.

imum at the outer boundary of the cross section and zero at the centre. Therefore, most of the material in a solid shaft is stressed significantly below the allowable shear stress. If weight reduction and savings in material are important, it is advisable to use hollow shafts.

The analysis of the torsion of a hollow circular bar is almost identical to that for a solid bar. The derivations already presented for solid bars are essentially unchanged if the bar is hollow. Thus, the same basic expressions for shear strain γ and shear stress τ may still be used



Hollow circular bar

(see Eqs. 3-4a and b). Of course, the radial distance ρ appearing in those expressions is limited to the range of r_1 to r_2 , where r_1 is the inside radius and r_2 is the outside radius of the circular bar (Fig. 3-5).

The relationship between the applied torque T and the angle of twist θ per unit length is given by Eq. (a), except that the limits on the integral for the polar moment of inertia I_p (see Eq. 3-5) are $\rho = r_1$ and $\rho = r_2$. Thus I_p , which is the polar moment of inertia of the ring-shaped area shown in Fig. 3-5, is

$$I_p = \frac{\pi}{2} (r_2^4 - r_1^4) = \frac{\pi}{32} (d_2^4 - d_1^4) \tag{3-12}$$

If the hollow tube is very thin (that is, if its thickness t is small compared to its radius), then the following approximate formulas (see Case 10 in Appendix D) may be used:

$$I_p \approx 2\pi r^3 t = \frac{\pi d^3 t}{4} \tag{3-13}$$

in which r and d are the average radius and diameter, respectively. The equations for θ , ϕ , and τ derived for a circular bar (see Eqs. 3-7 through 3-9) may be used for a hollow bar provided I_p is evaluated according to Eq. (3-12) or, if appropriate, Eq. (3-13). Of course, the wall thickness of a hollow shaft must be large enough to avoid the possibility of wrinkling or buckling of the wall.

Example 1

A solid steel shaft of diameter 60 mm is to be designed using an allowable shear stress $\tau_{allow} = 40$ MPa and an allowable angle of twist per unit length θ_{allow}

1° per meter. Determine the maximum permissible torque T that may be applied to the shaft, assuming $G = 80$ GPa.

The permissible torque T_1 based upon the allowable shear stress is obtained from the torsion formula $\tau_{max} = 16T/\pi d^3$ (see Eq. 3-10). Thus, we get

$$T_1 = \frac{\pi d^3 \tau_{allow}}{16} = \frac{\pi (0.060 \text{ m})^3 (40 \text{ MPa})}{16} = 1700 \text{ N}\cdot\text{m}$$

Based upon the allowable angle of twist per unit length, we obtain the permissible torque T_2 from Eq. (3-7):

$$T_2 = GI_p \theta = (80 \text{ GPa}) \left(\frac{\pi}{32} \right) (0.060 \text{ m})^4 \left(1 \times \frac{\pi}{180} \text{ rad} \right) \left(\frac{1}{1.0 \text{ m}} \right) = 1780 \text{ N}\cdot\text{m}$$

The smaller of these two values is the maximum permissible torque; thus, $T = 1700$ N·m.

Example 2

A hollow shaft and a solid shaft constructed of the same material have the same length and the same outside radius r (Fig. 3-6). The inside radius of the hollow shaft is $0.6r$. Assuming that both shafts are subjected to the same torque, compare the maximum shear stresses developed in the shafts. Also, compare the weights of the two shafts and their angles of rotation.

The maximum shear stresses are proportional to $1/I_p$ (see Eq. 3-9), inasmuch as the torques T and radii r are the same. For the solid shaft, we have

$$I_p = \frac{\pi r^4}{2} = 0.5\pi r^4$$

and for the hollow shaft

$$I_p = \frac{\pi r^4}{2} - \frac{\pi (0.6r)^4}{2} = 0.4352\pi r^4$$

Therefore, the ratio of the maximum shear stress in the hollow shaft to that in the solid shaft is $0.5/0.4352$, or 1.15. The angles of rotation are in the same proportion as the stresses (see Eq. 3-3).

The weights of the shafts are proportional to the cross-sectional areas; hence, the weight of the solid shaft is proportional to πr^2 and the weight of the hollow shaft is proportional to

$$\pi r^2 - \pi (0.6r)^2 = 0.64\pi r^2$$

Therefore, the weight of the hollow shaft is 64% of the weight of the solid shaft. These results show the inherent advantage of hollow shafts. In this example, the hollow bar has 15% greater stress and angle of rotation, but 36% less weight. Of course, these proportions will be different for other ratios of the inner and outer radii.

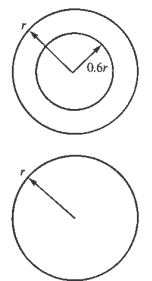
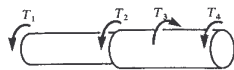


Fig. 3-6 Example 2

3.3 NONUNIFORM TORSION

As explained in the preceding section, *pure torsion* refers to torque of a prismatic bar subjected to torques acting only at the ends. *Nonuniform torsion* differs from pure torsion in that the bar need not be prismatic and the applied torques may vary along the length. In such cases, we usually can analyze the bar by applying the formulas of pure torsion in specialized ways, as illustrated in the following discussion.

An example of nonuniform torsion is pictured in Fig. 3-7, which



7 Bar in nonuniform torsion

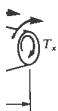
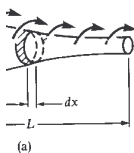
shows a bar made of two segments of different diameters and having torques applied at several cross sections. Each region of the bar between applied loads or between changes in cross section is in pure torsion, hence the formulas derived in the preceding section may be applied to each part separately. In so doing, it is necessary to determine the magnitude and direction of the internal torque in each region. Then, from the internal torque, the maximum stress and angle of rotation for each region can be calculated from Eqs. (3-9) and (3-8), respectively. The total angle of twist of one end of the bar with respect to the other is obtained by summation, using the general formula

$$\phi = \sum_{i=1}^n \frac{T_i L_i}{G J_{pi}} \quad (3-14)$$

In this equation, the subscript i is a numbering index for the various regions of the bar, and n is the total number of parts. High localized stresses occur at the sections where the diameter changes abruptly; however, these stresses have relatively little effect on the total angle of twist ϕ , and Eq. (3-14) can be used with good accuracy.

If either the torque or the cross section changes continuously along the axis of the bar, then the summation formula must be replaced by an integration formula. This situation is pictured in Fig. 3-8a, where the tapered bar is subjected to a torque of intensity q per unit distance along the axis of the bar. The torque T_x at a cross section located at distance x from the end of the bar may be found by statics (Fig. 3-8b). Then, assuming that the taper is gradual, we can calculate the maximum shear stress at that cross section from the torsion formula (Eq. 3-8). The differential angle of rotation for an element of length dx (Fig. 3-8c)

$$d\phi = \frac{T_x dx}{G J_{px}}$$



varying cross torque

orsion

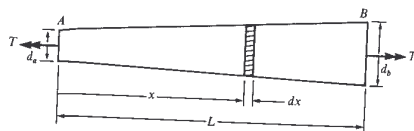
The angle of twist ϕ at end D (with respect to end A) is determined from Eq. (3-14), as follows:

$$\begin{aligned} \phi &= \sum_{i=1}^n \frac{T_i L_i}{G J_{pi}} = \frac{1}{G J_p} (T_{ab} L_1 + T_{bc} L_2 + T_{cd} L_3) \\ &= \frac{1}{(75 \text{ GPa})(\pi/32)(75 \text{ mm})^4} [(3.65 \text{ kN}\cdot\text{m})(0.5 \text{ m}) + (1.4 \text{ kN})(0.75 \text{ m}) + 0] \\ &= 0.0123 \text{ rad} = 0.707^\circ \end{aligned}$$

The procedures illustrated in this example can also be used for shafts having parts of different diameters or even of different materials.

Example 2

A tapered bar AB of solid circular cross section is twisted by torques T applied at the ends (Fig. 3-10). The diameter of the bar varies uniformly from d_a at the left end to d_b at the right end. Derive a formula for the angle of twist ϕ of the bar.



Example 2

Because the polar moment of inertia of the cross section varies continuously with the distance x from end A , we may use Eq. (3-15) to determine ϕ . We note first that the diameter d_x at distance x from end A is

$$d_x = d_a + \frac{d_b - d_a}{L} x \quad (a)$$

Hence, the polar moment of inertia is

$$J_{px} = \frac{\pi d_x^4}{32} = \frac{\pi}{32} \left(d_a + \frac{d_b - d_a}{L} x \right)^4 \quad (b)$$

Also, the torque T_x is constant and equal to the torque T applied at the ends. Therefore, the expression for the angle of twist (Eq. 3-15) becomes

$$\phi = \int_0^L \frac{T dx}{G J_{px}} \quad (c)$$

in which L is the length of the bar, G is the shear modulus of the material and J_{px} is given by Eq. (b). This integral is of the form

$$\int \frac{a dx}{(b + cx)^4}$$

where J_{px} is the polar moment of inertia of the cross section at distance x from the end. The total angle of twist between the ends of the bar is

$$\phi = \int_0^L d\phi = \int_0^L \frac{T_x dx}{G J_{px}} \quad (3-15)$$

This integral can be evaluated in analytical form in some cases, but otherwise it must be evaluated by numerical methods. Equations (3-14) and (3-15) can be used for either solid or hollow bars of circular cross section.

Example 1

A solid steel shaft $ABCD$ (Fig. 3-9) having diameter $d = 75$ mm turns freely in a bearing at D and is loaded at B and C by torques $T_1 = 2.25$ kN·m and $T_2 = 1.4$ kN·m. The shaft is connected in the gear box at A to gears that are temporarily locked in position. Determine the maximum shear stress in each part of the shaft and the angle of twist ϕ at end D . (Assume $L_1 = 0.5$ m, $L_2 = 0.75$ m, $L_3 = 0.5$ m, and $G = 75$ GPa).

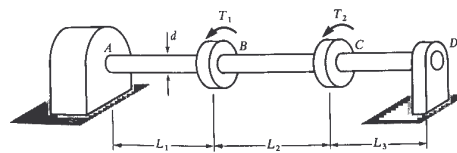


Fig. 3-9 Example 1

The maximum shear stresses are found from the torsion formula $\tau_{max} = 16T/\pi d^3$ (Eq. 3-10), in which T represents the internal torque in each part of the shaft. The torque is zero between C and D because no load is applied at D . From B to C the torque is equal to T_2 , and from A to B the torque is the sum of T_1 and T_2 . Thus, we obtain

$$T_{ab} = T_1 + T_2 = 3.65 \text{ kN}\cdot\text{m} \quad T_{bc} = T_2 = 1.4 \text{ kN}\cdot\text{m} \quad T_{cd} = 0$$

The corresponding maximum stresses are calculated as follows:

$$\begin{aligned} \tau_{ab} &= \frac{16T_{ab}}{\pi d^3} = \frac{16(3.65 \times 10^6 \text{ N}\cdot\text{mm})}{\pi(75 \text{ mm})^3} = 44.1 \text{ MPa} \\ \tau_{bc} &= \frac{16T_{bc}}{\pi d^3} = \frac{16(1.4 \times 10^6 \text{ N}\cdot\text{mm})}{\pi(75 \text{ mm})^3} = 16.9 \text{ MPa} \\ \tau_{cd} &= 0 \end{aligned}$$

in which

$$a = \frac{32T}{\pi G} \quad b = d_a \quad c = \frac{d_b - d_a}{L} \quad (d)$$

With the aid of a table of integrals, we find

$$\int \frac{a dx}{(b + cx)^4} = -\frac{a}{3c(b + cx)^3}$$

Now we can complete the evaluation of the integral by substituting for x the limits 0 and L and also substituting the expressions in Eq. (d) for a , b , and c . The final result is

$$\phi = \frac{32TL}{3\pi G(d_b - d_a)} \left(\frac{1}{d_a^3} - \frac{1}{d_b^3} \right) \quad (3-16)$$

The preceding analysis could have been performed in a slightly different mathematical way by taking the origin of the distance x at the apex of the cone formed by extending the surface of the bar to the left in Fig. 3-10, as was done in the solution to Example 2 of Section 2.2.

A convenient form in which to write the solution for ϕ is

$$\phi = \frac{TL}{G J_{pa}} \left(\frac{\beta^2 + \beta + 1}{3\beta^3} \right) \quad (3-17)$$

in which $\beta = d_b/d_a$, and $J_{pa} = \pi d_a^4/32$ is the polar moment of inertia at end A . For example, if $\beta = 1$, we get $\phi = TL/G J_{pa}$, which is the angle of rotation of a prismatic bar of diameter d_a . If $\beta = 2$, we get $\phi = (7/24)(TL/G J_{pa})$, which is less than for the case of $\beta = 1$ because of the increased stiffness due to the larger diameter at end B .

3.4 PURE SHEAR

When a circular bar, either solid or hollow, is subjected to torsion, shear stresses τ act over the cross sections and on longitudinal planes, as explained in Section 3.2. Thus, a small, thin stress element $abcd$ cut out between two cross sections and between two longitudinal planes (Fig. 3-11) is in a state of *pure shear*, because the only stresses acting on this element are the shear stresses on the four side faces. The directions of these stresses depend upon the directions of the applied torques T . In this discussion, we shall assume that the torques rotate the right-hand end of the bar clockwise when viewed from the right (Fig. 3-11a),

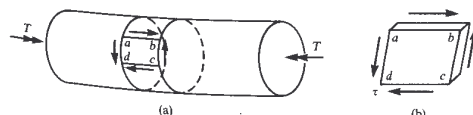
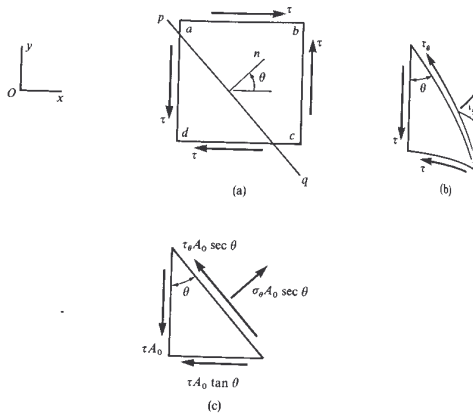


Fig. 3-11 Stresses acting on an element for a bar in torsion



of stresses on element in pure

of the left-hand face denoted as A_0 and because the thickness of the element in the z direction is constant, it follows that the area of the bottom face is $A_0 \tan \theta$ and the area of the inclined face is $A_0 \sec \theta$. Thus, multiplying the stresses by the areas over which they act gives the forces acting on all faces of the element (Fig. 3-12c). The forces acting on the left-hand and bottom faces can easily be resolved into components acting perpendicular and parallel to the inclined face (that is, in the directions of σ_θ and τ_θ , respectively). Then we can write two equations of static equilibrium for the element, one in each of these directions. The first equation, obtained by summing forces in the direction of σ_θ , is

$$\sigma_\theta A_0 \sec \theta = \tau A_0 \sin \theta + \tau A_0 \tan \theta \cos \theta$$

$$\text{or} \quad \sigma_\theta = 2\tau \sin \theta \cos \theta \quad (3-18a)$$

The second equation is obtained by summing forces in the direction of τ_θ :

$$\tau_\theta A_0 \sec \theta = \tau A_0 \cos \theta - \tau A_0 \tan \theta \sin \theta$$

$$\text{or} \quad \tau_\theta = \tau(\cos^2 \theta - \sin^2 \theta) \quad (3-18b)$$

These equations can be expressed in an alternate form by introducing the following trigonometric identities:

$$2 \sin \theta \cos \theta = \sin 2\theta$$

$$\cos^2 \theta - \sin^2 \theta = \cos 2\theta$$

Then the equations for σ_θ and τ_θ become

$$\sigma_\theta = \tau \sin 2\theta \quad \tau_\theta = \tau \cos 2\theta \quad (3-19a, b)$$

Equations (3-18) and (3-19) give the normal and shear stresses acting on any inclined plane in terms of the shear stresses τ acting on the x and y planes (Fig. 3-12a) and in terms of the angle θ defining the orientation of the inclined plane (Fig. 3-12b).

The manner in which the stresses σ_θ and τ_θ vary with the orientation of the inclined plane is shown by the graph in Fig. 3-13. We see that for $\theta = 0^\circ$, which is the right-hand, or x , face of the stress element in Fig. 3-12a, the graph gives $\sigma_\theta = 0$ and $\tau_\theta = \tau$, as expected. Also, for the top, or y , face of the element ($\theta = 90^\circ$), we obtain $\sigma_\theta = 0$ and $\tau_\theta = -\tau$. The minus sign means that the shear stress acts in the negative τ_θ direction. These are the numerically largest shear stresses τ_θ acting on any planes.

The normal stress σ_θ reaches a maximum value at $\theta = 45^\circ$, where the stress is tension and is numerically equal to the shear stress τ . Similarly, σ_θ has its numerically largest negative value (that is, compression) at $\theta = -45^\circ$. At these same angles, the shear stress τ_θ is equal to zero.

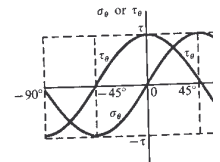
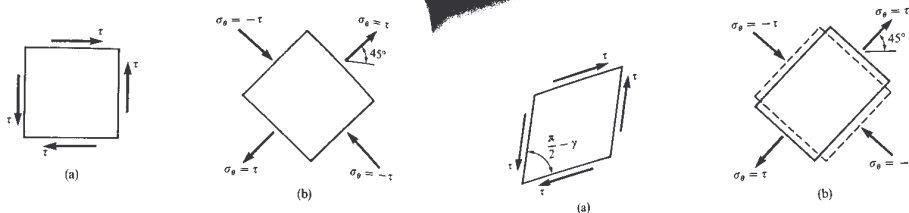


Fig. 3-13 Graph of normal stress and shear stress τ_θ versus angle θ of inclined plane

hence the shear stresses acting on an element have the directions shown in Fig. 3-11b. The same state of stress exists for an element of similar shape cut out from the interior of the bar, except that the magnitude of the shear stresses will be smaller because the radius of the element is smaller.

The stresses acting on planes inclined to the axis of the bar can be determined by considering the stress element $abcd$, which is shown again in Fig. 3-12a. The figure shows the front face of the element, which is free of any stresses, and the shear stresses τ that act on the side faces. For reference purposes, the figure also shows a set of xy axes. To obtain the stresses on an inclined plane, we make a cut through the element along the plane pq , which is perpendicular to the plane of the figure and which has its normal n at an angle θ to the x axis (Fig. 3-12a). We then isolate as a free body the resulting triangular, or wedge-shaped, element (Fig. 3-12b). Acting on the left-hand and bottom faces of this element are the shear stresses τ . On the inclined face, there may be both normal stresses σ_θ and shear stresses τ_θ , shown acting in their positive directions in the figure.

The stresses on the inclined plane may be determined from the equilibrium of the triangular element (Fig. 3-12b), which is acted upon by forces on all three of its side faces. These forces can be obtained by multiplying the stresses by the areas of the faces on which they act. For instance, the force on the left-hand face is equal to τA_0 , where A_0 is the area of the face; this force acts in the negative y direction. With the area



lements at $\theta = 0^\circ$: shear

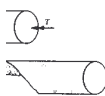
Fig. 3-16 Strains in pure shear: (a) element at $\theta = 0^\circ$, and (b) element at $\theta = 45^\circ$

Thus, a stress element rotated through an angle of 45° is acted upon by equal tensile and compressive stresses in perpendicular directions, but no shear stresses are present (Fig. 3-14b). The directions of the normal stresses shown in Fig. 3-14b are for an element subjected to shear stresses acting in the directions shown in Fig. 3-14a. If the shear stresses acting on the element of Fig. 3-14a have their directions reversed, the normal stresses acting on the 45° planes also will change directions.

If a stress element is rotated through an angle other than 45° , both normal and shear stresses will act on the side faces, as given by Eqs. (3-18) and (3-19). These more general stress conditions are discussed in Chapter 6.

The equations derived in this section hold for a stress element in pure shear regardless of whether the element is cut from a bar in torsion or from some other structural element. Also, since Eqs. (3-18) and (3-19) were derived only from equilibrium, they are valid for any material, whether it is linearly elastic or not.

The presence of maximum tensile stresses on planes at 45° to the x axis accounts for the fact that brittle materials that are weak in tension fail in torsion by cracking along a 45° helical surface (Fig. 3-15). As mentioned in Section 3.2, this type of failure is readily demonstrated by twisting a piece of classroom chalk.



failure of a brittle material cracking along a

Let us now consider the strains that occur when a material is subjected to pure shear. The stress element pictured in Fig. 3-14a will undergo shear strains γ , resulting in a deformation of the element, as shown in Fig. 3-16a and discussed previously in Section 1.6. The shear strain γ is measured as the change in angle between two planes that were originally perpendicular to each other. Thus, in Fig. 3-16a, the decrease in the right angle at the lower left-hand corner of the element is the shear strain γ , measured in radians. This same change in angle occurs at the upper right-hand corner, where the angle decreases, and at the other two corners, where the angles increase by γ . However, the lengths of the sides of the element, including the thickness perpendicular to the plane of the paper, do not change. Thus, the element changes its shape from a rectangular parallelepiped to an oblique parallelepiped; this change in shape is referred to as **shear distortion**.

Now let us consider the strains that occur in a stress element oriented at 45° (see Fig. 3-14b). The tensile stresses acting at 45° tend to elongate the element in that direction and, because of the Poisson effect, tend to shorten it in the perpendicular direction (the direction where $\theta = 135^\circ$ or -45°). Similarly, the compressive stresses acting at 135° tend to shorten the element in the 135° direction and elongate it in the 45° direction. Thus, the element undergoes changes in dimensions as shown in Fig. 3-16b. Note, however, that the element remains a rectangular parallelepiped, and there is no shear distortion.

If the material is linearly elastic, the shear strain for the element at $\theta = 0^\circ$ (Fig. 3-16a) is related to the shear stress by Hooke's law in shear:

$$\gamma = \frac{\tau}{G} \quad (3-20)$$

For the element at $\theta = 45^\circ$ (Fig. 3-16b), we may use Poisson's ratio and Hooke's law for uniaxial stress to obtain the normal strains. The tensile stress $\sigma_\theta = \tau$ (at $\theta = 45^\circ$) produces a positive strain equal to τ/E . It also produces a negative strain in the perpendicular direction, equal to $-\nu\tau/E$, where ν is Poisson's ratio. Similarly, the stress $\sigma_\theta = -\tau$ (at $\theta = 135^\circ$) produces a negative strain equal to $-\tau/E$ and a positive strain in the perpendicular direction equal to $\nu\tau/E$. Therefore, the resultant normal strain ϵ in the 45° direction (that is, in the direction of the positive normal stress $\sigma_\theta = \tau$) is

$$\epsilon = \frac{\tau}{E} + \frac{\nu\tau}{E} = \frac{\tau}{E}(1 + \nu) \quad (3-21)$$

which is positive, representing an elongation. The strain in the perpendicular direction is a negative strain of the same amount. Thus, we see that pure shear produces an elongation in the 45° direction and a shortening in the 135° direction, which is consistent with the shape of the deformed element of Fig. 3-16a.

We have already mentioned that the thickness of an element in pure shear (Fig. 3-16a) does not change. Of course, the thickness of the rotated element (Fig. 3-16b) does not change either, because it repre-

sents the same state of stress. This observation is consistent with discussion in the preceding paragraph, which pointed out that the stress $\sigma_\theta = \tau$ acting at 45° produces a lateral strain equal to $-\nu\tau/E$ and the stress $\sigma_\theta = -\tau$ acting at 135° produces a lateral strain equal to $\nu\tau/E$. Therefore, the decrease in thickness of the element due to the stress at 45° is exactly matched by the increase in thickness due to compressive stress at 135° .

In the next section, we will use the geometry of the deformed element pictured in Fig. 3-16a to relate the strains γ and ϵ (Eqs. 3-20 and 3-21). We will then be able to derive the relationship between the moduli of elasticity E and G .

Example

A hollow circular shaft has outside diameter of 100 mm and inside diameter 80 mm (Fig. 3-17). If the shaft is subjected to a torque $T = 12 \text{ kN}\cdot\text{m}$, what are the maximum tensile, compressive, and shear stresses?

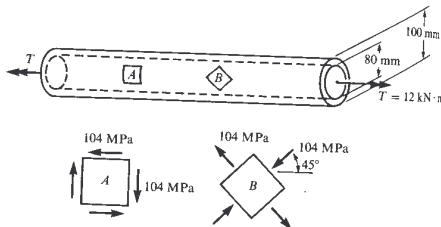


Fig. 3-17 Example

The maximum values of all three stresses are equal numerically, although they act on different planes. The maximum values are found from the torsion formula:

$$\tau_{\max} = \frac{T r}{I_p} = \frac{(12,000 \text{ N}\cdot\text{m})(0.050 \text{ m})}{(\pi/32)[(0.100 \text{ m})^4 - (0.080 \text{ m})^4]} = 104 \text{ MPa}$$

The maximum shear stresses act on cross-sectional and longitudinal planes, as shown for element A in Fig. 3-17, and the maximum normal stresses act on planes at 45° to the axis (element B).

3.5 RELATIONSHIP BETWEEN MODULI OF ELASTICITY E AND G

Let us now use the equations derived in the preceding section to obtain an important relationship between the moduli of elasticity E and G .

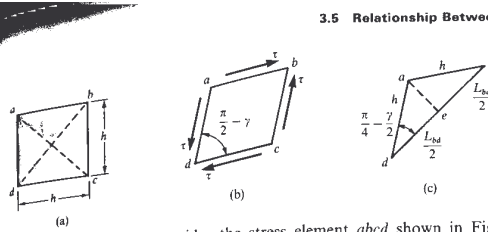


Fig. 3-18 Geometry of deformed element in pure shear

For this purpose, consider the stress element $abcd$ shown in Fig. 3-18a. The front face of the element is assumed to be square, with the side length of each side denoted as h . When this element is subjected to pure shear by stresses τ , the front face distorts into a rhombus (Fig. 3-18b) with sides of length h and with the shear strain $\gamma = \tau/G$, as explained in Section 3.4. Because of the distortion, diagonal bd is lengthened and diagonal ac is shortened. The increase Δ_{bd} in the length of diagonal bd can be obtained by multiplying its initial length $\sqrt{2}h$ by the normal strain ϵ in the 45° direction; thus,

$$\Delta_{bd} = \sqrt{2} h \epsilon \tag{a}$$

or, using Eq. (3-21), from the preceding section,

$$\Delta_{bd} = \frac{\sqrt{2} h \tau}{E} (1 + \nu) \tag{b}$$

in which ν is Poisson's ratio. These equations relate the increase in length to the normal strain ϵ and the shear stress τ .

The increase in length Δ_{bd} can also be related to the shear strain γ by using the geometry of the distorted element (Fig. 3-18b). Consider triangle abd (Fig. 3-18c), which is obtained from one-half of the rhombus pictured in Fig. 3-18b. Angle adb of the triangle is equal to one-half of angle adc of the rhombus, or $\pi/4 - \gamma/2$, and sides ad and ab of the triangle have length h . The length of the remaining side bd of the triangle is denoted L_{bd} . This length is equal to the initial diagonal length $\sqrt{2}h$ plus the elongation Δ_{bd} ; thus,

$$L_{bd} = \sqrt{2} h + \Delta_{bd} \tag{c}$$

A line ae perpendicular to the diagonal is drawn from a , thus dividing the diagonal into two equal parts. From the new triangle ade , we obtain

$$\cos\left(\frac{\pi}{4} - \frac{\gamma}{2}\right) = \frac{L_{bd}}{2h}$$

or, using Eq. (c),

$$\cos\left(\frac{\pi}{4} - \frac{\gamma}{2}\right) = \frac{\sqrt{2} h + \Delta_{bd}}{2h} = \frac{1}{\sqrt{2}} + \frac{\Delta_{bd}}{2h} \tag{d}$$

Using the trigonometric identity

$$\cos(\alpha - \beta) = \cos \alpha \cos \beta + \sin \alpha \sin \beta$$

Torsion

we get

$$\cos\left(\frac{\pi}{4} - \frac{\gamma}{2}\right) = \cos \frac{\pi}{4} \cos \frac{\gamma}{2} + \sin \frac{\pi}{4} \sin \frac{\gamma}{2} = \frac{1}{\sqrt{2}} \left(\cos \frac{\gamma}{2} + \sin \frac{\gamma}{2} \right)$$

Comparing Eqs. (d) and (e), and also noting that γ is a small angle (hence, $\cos \gamma/2 \approx 1$ and $\sin \gamma/2 \approx \gamma/2$), we obtain

$$\Delta_{bd} = \frac{\sqrt{2} h \gamma}{2} \tag{f}$$

In addition, since $\gamma = \tau/G$, we obtain

$$\Delta_{bd} = \frac{\sqrt{2} h \tau}{2G} \tag{g}$$

These equations relate the increase in length to the shear strain γ and the shear stress τ .

Comparing Eqs. (a) and (f), we see that

$$\epsilon = \frac{\gamma}{2} \tag{3-22}$$

for an element in pure shear. Also, comparing Eqs. (b) and (g), we get

$$G = \frac{E}{2(1 + \nu)} \tag{3-23}$$

Thus, it is apparent that E , G , and ν are not independent properties of a linear elastic material. Instead, if two of them are known, the third can be calculated from the preceding equation. Some typical values of E , G , and ν are listed in Table H-2, Appendix H. (Equation 3-23 was derived by Poisson using the value $\frac{1}{3}$ for ν ; see Ref. 3-3.)

3.6 TRANSMISSION OF POWER BY CIRCULAR SHAFTS

The most important use of circular shafts is to transmit mechanical power from one device or machine to another, as in the drive shaft of an automobile, the propeller shaft of a ship, or the axle of a bicycle. The power is transmitted through the rotary motion of the shaft, and the amount of power transmitted depends upon the magnitude of the torque and the speed of revolution. A common design problem is the determination of the required size of a shaft so that it will transmit a specified amount of power at a specified speed of revolution without exceeding the allowable stresses for the material.

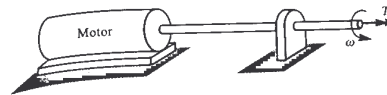


Fig. 3-19 Shaft transmitting a torque T at an angular velocity ω

Let us suppose that a motor-driven shaft (Fig. 3-19) is rotating at an angular speed ω , measured in radians per second (rad/s). The shaft is transmitting a torque T . In general, the work W done by any torque of constant magnitude T is equal to the product of the torque and the angle through which it rotates; that is,

$$W = T \phi$$

where ϕ is the angular rotation in radians. Power is the time rate at which work is done, or

$$P = \frac{dW}{dt} = T \frac{d\phi}{dt}$$

in which P is the symbol for power and t represents time. The rate of change $d\phi/dt$ of the angular displacement ϕ is the angular speed ω ; hence,

$$P = T \omega \quad (\omega = \text{rad/s}) \tag{3-24}$$

This formula, which is familiar from elementary physics, gives the power transmitted by a rotating shaft. If T is expressed in newton meters, then the power is expressed in watts (W). One watt is equal to one newton meter per second (or one joule per second). If T is expressed in foot-pounds, then power is expressed in foot-pounds per second.*

Angular speed is also expressed as the frequency f of revolution, or the number of revolutions per unit of time. The unit of frequency is the hertz (Hz), which is one revolution per second (s^{-1}). Therefore,

$$\omega = 2\pi f$$

inasmuch as one revolution equals 2π radians. The expression for power then becomes

$$P = 2\pi f T \quad (f = \text{Hz} = \text{s}^{-1}) \tag{3-25}$$

Another commonly used unit is the number of revolutions per minute (rpm), denoted by the letter n . Hence,

$$n = 60f$$

and

$$P = \frac{2\pi n T}{60} \quad (n = \text{rpm}) \tag{3-26}$$

In Eqs. (3-25) and (3-26), P and T have the same units as in Eq. (3-24);

* See Appendix A for units of power and conversion factors.

that is, P has units of watts if T has units of newton metres, and P has units of foot-pounds per second if T has units of foot-pounds.

In U.S. engineering practice, power is often expressed in horsepower (hp), a unit equal to 550 ft-lb/s. Thus, the horsepower H being transmitted is

$$H = \frac{2\pi nT}{60(550)} = \frac{2\pi nT}{33,000} \quad (n = \text{rpm}, T = \text{ft-lb}, H = \text{hp}) \quad (3-27)$$

One horsepower is approximately equal to 746 watts.

The preceding equations relate transmitted power to the torque T in the shaft. Of course, the torque is related to the shear stresses, shear strains, and angles of twist by the formulas discussed in Sections 3.2 through 3.5.

Example 1

What is the minimum required diameter d for a solid circular shaft if it is to transmit 30 kW at 600 rpm without exceeding an allowable shear stress of 28 MPa?

The relationship between power P and torque T is given by Eq. (3-26). Using that equation, we obtain

$$T = \frac{60P}{2\pi n} = \frac{60(30 \times 10^3 \text{ W})}{2\pi(600 \text{ rpm})} = 477.5 \text{ N}\cdot\text{m}$$

as the torque that must be transmitted by the shaft.

The maximum shear stress produced by the torque T can be obtained from the torsion formula (Eq. 3-10). Solving that equation for the diameter of the shaft and substituting τ_{allow} for τ_{max} , we get

$$d^3 = \frac{16T}{\pi\tau_{\text{allow}}} = \frac{16(477.5 \times 10^3 \text{ N}\cdot\text{m})}{\pi(28 \text{ MPa})} = 86,853 \text{ mm}^3$$

from which

$$d = 44.3 \text{ mm}$$

The diameter of the shaft must be at least this large if the allowable shear stress is not to be exceeded.

Example 2

A steel shaft ABC (Fig. 3-20a) of 50 mm diameter is driven at A by a motor that transmits 50 kW to the shaft at 10 Hz. The gears at B and C remove 30 kW and 20 kW, respectively. Compute the maximum shear stress τ in the shaft and the angle of twist ϕ between the ends A and C .

The power transmitted between A and B is 50 kW, hence the torque T (from Eq. 3-25) is

$$T = \frac{P}{2\pi f} = \frac{50 \text{ kW}}{2\pi(10 \text{ Hz})} = 796 \text{ N}\cdot\text{m}$$

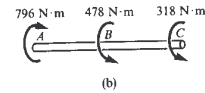
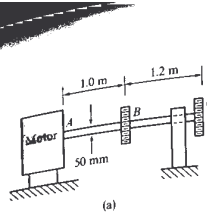


Fig. 3-20 Example 2

This torque is assumed to have the direction shown in Fig. 3-20b. The shear stress and angle of twist for part AB of the shaft are

$$\tau_{ab} = \frac{16T}{\pi d^3} = \frac{16(796 \text{ N}\cdot\text{m})}{\pi(50 \text{ mm})^3} = 32.4 \text{ MPa}$$

$$\phi_{ab} = \frac{TL}{GI_p} = \frac{(796 \text{ N}\cdot\text{m})(1.0 \text{ m})}{(80 \text{ GPa})(\pi/32)(50 \text{ mm})^4} = 0.0162 \text{ rad}$$

in which we have assumed that $G = 80 \text{ GPa}$.

For the other part BC of the shaft, the power transmitted is 20 kW, hence,

$$T = \frac{P}{2\pi f} = \frac{20 \text{ kW}}{2\pi(10 \text{ Hz})} = 318 \text{ N}\cdot\text{m}$$

The corresponding shear stress and angle of twist are

$$\tau_{bc} = \frac{16T}{\pi d^3} = \frac{16(318 \text{ N}\cdot\text{m})}{\pi(50 \text{ mm})^3} = 13.0 \text{ MPa}$$

$$\phi_{bc} = \frac{TL}{GI_p} = \frac{(318 \text{ N}\cdot\text{m})(1.2 \text{ m})}{(80 \text{ GPa})(\pi/32)(50 \text{ mm})^4} = 0.0078 \text{ rad}$$

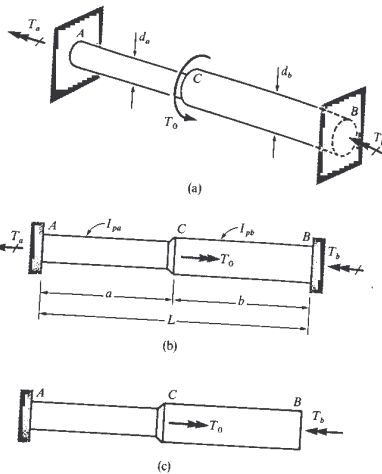
Thus, the maximum shear stress is $\tau = 32.4 \text{ MPa}$, which occurs in part AB . Also, the total angle of twist is

$$\phi = \phi_{ab} + \phi_{bc} = 0.0240 \text{ rad}$$

inasmuch as both parts of the shaft twist in the same direction (Fig. 3-20b).

3.7 STATICALLY INDETERMINATE TORSIONAL MEMBERS

Because of the nature of the torsion examples discussed in preceding sections, the torques acting at all cross sections of the members could be obtained by static equilibrium. Hence, those examples dealt only with statically determinate members. Of course, torsion members may be statically indeterminate if they are constrained by more supports than are required to hold them in static equilibrium. Torsion members of this kind can be analyzed by supplementing the equilibrium equations with equations pertaining to the displacements (that is, by compatibility equations). The flexibility and stiffness methods, described



T_a act as loads on this released structure. They produce an angle of twist ϕ_b at end B that is equal to the algebraic sum of the angle of twist of the two parts AC and CB . Thus, we get

$$\phi_b = \frac{T_0 a}{GI_{pa}} - \frac{T_b a}{GI_{pb}} - \frac{T_b b}{GI_{pb}}$$

in which I_{pa} and I_{pb} are the polar moments of inertia of the left-hand and right-hand parts of the bar, respectively. Because the angle of rotation at end B in the original bar is equal to zero, the equation of compatibility is $\phi_b = 0$, or

$$\frac{T_0 a}{I_{pa}} - \frac{T_b a}{I_{pb}} - \frac{T_b b}{I_{pb}} = 0 \quad (b)$$

This equation can be solved for the redundant torque T_b , which then can be substituted into Eq. (a) in order to obtain T_a . The results are

$$T_a = T_0 \left(\frac{bI_{pa}}{aI_{pb} + bI_{pa}} \right) \quad T_b = T_0 \left(\frac{aI_{pb}}{aI_{pb} + bI_{pa}} \right) \quad (3-28a, b)$$

If the bar has a constant cross section, so that $I_{pa} = I_{pb} = I_p$, then these equations simplify as follows:

$$T_a = \frac{T_0 b}{L} \quad T_b = \frac{T_0 a}{L} \quad (3-29a, b)$$

These equations are analogous to those for an axially loaded bar with fixed ends (see Eqs. 2-11 and 2-12).

The maximum shear stresses in each part of the bar are obtained directly from the torsion formula; thus,

$$\tau_{ac} = \frac{T_0 a}{2I_{pa} d_a} \quad \tau_{cb} = \frac{T_b d_b}{2I_{pb}}$$

Substituting from Eqs. (3-28a and b) gives

$$\tau_{ac} = \frac{T_0 b d_a}{2(aI_{pb} + bI_{pa})} \quad \tau_{cb} = \frac{T_0 a d_b}{2(aI_{pb} + bI_{pa})} \quad (3-30a, b)$$

By comparing the product $b d_a$ with the product $a d_b$, we can immediately determine which region of the bar has the larger stress.

Having already found the torques T_a and T_b acting in the two parts of the bar, we can now obtain the angle of rotation ϕ_c at section C where the load is applied (Fig. 3-21b). This angle is equal to the angle of rotation of either part of the bar, since both parts must rotate through the same angle in order to have compatibility of rotations at C . Thus, we obtain

$$\phi_c = \frac{T_a a}{GI_{pa}} = \frac{T_b b}{GI_{pb}} = \frac{abT_0}{G(aI_{pb} + bI_{pa})} \quad (3-31)$$

in Section 2.4 for axially loaded members, may also be used for torsional members. However, for the types of torsion problems ordinarily encountered, only the flexibility method is needed, hence we will limit our discussion to that method.

To illustrate the flexibility method as applied to bars in torsion, we will consider the torsion member AB shown in Figs. 3-21a and b. This bar is fixed at both ends; therefore, it is statically indeterminate. The member has different diameters d_a and d_b in parts AC and CB , respectively, and it is loaded by a torque T_0 at C . The material of the bar is the same throughout both parts. The objectives of our analysis are to determine the reactive torques T_a and T_b at the ends, the maximum shear stresses, and the angle of rotation ϕ_c at the section where T_0 is applied.

From static equilibrium, we obtain the following equation relating the torques (see Fig. 3-21b):

$$T_a + T_b = T_0 \quad (a)$$

In order to obtain a second equation between T_a and T_b , we must select a redundant torque and then analyze the corresponding released structure. Let us select T_b as the redundant, so that the released structure is obtained by removing support B (Fig. 3-21c). The two torques T_0 and

We note that, if $a = b = L/2$ and $I_{pa} = I_{pb} = I_p$, the angle is

$$\phi_c = \frac{T_0 L}{4GI_p}$$

as anticipated from the symmetry of the bar and loading.

The preceding example illustrates the procedure that must be followed when analyzing a statically indeterminate torsional system by the flexibility method. The method is quite general and can be used in a great variety of situations, another of which is presented in the following discussion.

Composite bars. A composite bar is made of concentric circular torsional bars that are firmly bonded together to act as a single member. An example is shown in Fig. 3-22, where a hollow tube *B* and a core *A* are securely bonded to act as a solid bar. If the two parts of the bar are constructed of the same material, then the bar behaves in the same manner as if it were made of one piece, and all of the formulas derived in preceding sections may be used directly. However, if the tube and core have different properties, the bar is statically indeterminate and a more detailed analysis is required.

For the purpose of making such an analysis, let us use the following notation:

G_a, G_b = shear moduli of elasticity for inner and outer parts, respectively

d_a, d_b = diameters of inner and outer parts, respectively

I_{pa}, I_{pb} = polar moments of inertia of inner and outer parts, respectively

Also, we will assume that the composite bar is acted upon by a total torque T , which is resisted by torques T_a and T_b developed in the core and tube, respectively.

The first equation is obtained from static equilibrium, as follows:

$$T = T_a + T_b \quad (d)$$

Furthermore, the angles of twist ϕ must be the same for both parts inasmuch as they are held together and must rotate the same amount. Therefore, from compatibility of rotations, we find the second equation:

$$\phi = \frac{T_a L}{G_a I_{pa}} = \frac{T_b L}{G_b I_{pb}} \quad (e)$$

in which L is the length of the bar. Solving Eqs. (d) and (e) gives the torques in the two parts of the bar:

$$T_a = T \left(\frac{G_a I_{pa}}{G_a I_{pa} + G_b I_{pb}} \right) \quad T_b = T \left(\frac{G_b I_{pb}}{G_a I_{pa} + G_b I_{pb}} \right) \quad (3-32a, b)$$

The angle of rotation ϕ now becomes

$$\phi = \frac{TL}{G_a I_{pa} + G_b I_{pb}} \quad (3-33)$$

which is obtained by substituting from Eqs. (3-32a and b) into Eq. (e).

The shear stresses in the bar can be obtained by applying the torsion formula to each part. For instance, the maximum shear stresses τ_a and τ_b in the core and tube, respectively, are

$$\tau_a = \frac{T_a(d_a/2)}{I_{pa}} \quad \tau_b = \frac{T_b(d_b/2)}{I_{pb}} \quad (3-34a, b)$$

Thus, the ratio of the stress τ_b at the outer boundary of the tube to the stress τ_a at the outer boundary of the core is

$$\frac{\tau_b}{\tau_a} = \frac{G_b d_b}{G_a d_a} \quad (3-35)$$

Note that it is possible for this ratio to be less than unity.

The shear stress in the tube at its inner boundary is not the same as the stress τ_a at the outer boundary of the core. Although the shear strains in the two parts must be the same where they come in contact, the stresses are different because the materials have different moduli.

3.8 STRAIN ENERGY IN PURE SHEAR AND TORSION

When an object is subjected to a statically applied load, work is done by the load and strain energy is absorbed by the object. The evaluation of this strain energy is important in dynamic analyses and in many aspects of theory of structures (see Chapter 12). If no energy is lost in the form of heat, the work W will be equal to the strain energy U , as discussed in Section 2.8 for the case of a bar in tension. This equality between work and energy may also be used to obtain expressions for the strain energy stored in an element in pure shear. For this purpose, let us consider again a small element of material subjected to shear stresses τ on its side faces (Fig. 3-23a). For convenience, we will assume that the front face of the element is square, with each side having length h . The thickness of the element (perpendicular to the paper) is denoted by t . Under the action of the shear stresses τ , the element is distorted so that the front face becomes the rhombus shown in Fig. 3-23b, in which the shear strain is denoted as γ .

The shear forces V acting on the side faces of the element (Fig. 3-23c) are found by multiplying the stresses by the areas on which they act:

$$V = \tau ht \quad (a)$$

Because the volume of the element is $h^2 t$, the strain energy density (that is, the strain energy per unit volume) is

$$u = \frac{\tau \gamma}{2} \quad (3-36)$$

Finally, we introduce Hooke's law in shear ($\tau = G\gamma$) and obtain the following equations for the strain energy density:

$$u = \frac{\tau^2}{2G} \quad u = \frac{G\gamma^2}{2} \quad (3-37a, b)$$

These equations are similar in form to those for uniaxial stress (Eqs. 2-41a and b). The strain energy density in pure shear may be visualized as the area under the shear stress-strain curve. The SI units for u are joules per cubic meter (J/m^3), and the USCS units are inch-pounds per cubic inch (or other similar units). Since these units are the same as those for stress, we may also express u in pascals or psi.

Now that we have obtained expressions for the strain energy density in pure shear, we can easily determine the amount of strain energy stored in a circular bar (either solid or hollow) subjected to pure torsion (Fig. 3-25a). Consider an elemental circular tube of material that extends for the length of the bar and has radius ρ and thickness $d\rho$. A small element from this tube is shown in Fig. 3-25b. It is subjected on its side faces to shear stresses τ given by the torsion formula $\tau = T\rho/I_p$. Hence, the strain energy density at radius ρ is

$$u = \frac{\tau^2}{2G} = \frac{T^2 \rho^2}{2GI_p^2}$$

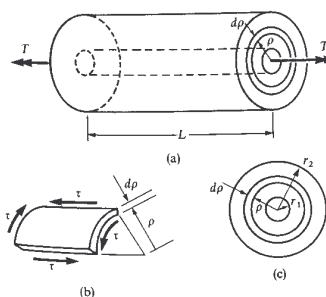


Fig. 3-25 Bar in pure torsion

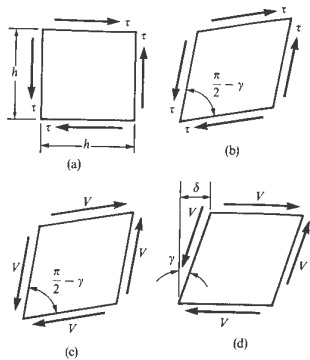


bar of two

Torsion

work in pure shear

on diagram



These forces produce work as the element deforms from its initial shape (Fig. 3-23a) to its distorted shape (Fig. 3-23b). To calculate this work, we need to determine the relative distances through which the shear forces move. This task is made easier if the element is rotated as a rigid body until two of its faces are horizontal, as in Fig. 3-23d. During the rigid-body rotation, the net work done by the forces V is zero because the forces occur in pairs that form two equal and opposite couples. As can be seen in Fig. 3-23d, the top face of the element is displaced horizontally through the distance δ (relative to the bottom face) as the shear force is gradually increased from zero to its final value V . The displacement δ is equal to the shear strain γ (which is a small angle) times the vertical dimension of the element:

$$\delta = \gamma h \quad (b)$$

If we assume that the material is linearly elastic and that it follows Hooke's law, then the load-deflection diagram is linear (Fig. 3-24). The strain energy U stored in the element is equal to the work W done by the shear force, which is equal to the area under the load-deflection curve:

$$U = W = \frac{V\delta}{2} \quad (c)$$

The forces on the side faces of the element do not move along their lines of action, hence they do no work. Substituting from Eqs. (a) and (b) into Eq. (c), we get the total strain energy of the element:

$$U = \frac{\tau \gamma h^2 t}{2}$$

The strain energy dU in the elemental tube is found by multiplying density u by the volume of the tube:

$$dU = uL dA = \frac{T^2 L \rho^2 dA}{2GI_p^2}$$

in which $dA = 2\pi\rho d\rho$ is the ring-shaped area of the end face of the elemental tube. Next, the total strain energy of the bar may be obtained by integrating the preceding expression for dU between the limits $\rho = r_1$ and $\rho = r_2$ (Fig. 3-25c):

$$U = \int dU = \frac{T^2 L}{2GI_p^2} \int_{\rho=r_1}^{\rho=r_2} \rho^2 dA$$

Of course, the integral in this equation is the polar moment of inertia I_p . Hence, the elastic strain energy of a circular bar in pure torsion is

$$U = \frac{T^2 L}{2GI_p} \quad (3-38a)$$

This formula gives U in terms of the applied torque T . An alternate equation can be obtained by substituting from the formula for the angle of twist ($\phi = TL/GI_p$); thus,

$$U = \frac{GI_p \phi^2}{2L} \quad (3-38b)$$

which gives U in terms of ϕ . The units for U are joules (J) in SI and inch-pounds (or other similar units) in USCS. Note the analogy between Eqs. (3-38a and b) for torsion and Eqs. (2-39a and b) for uniaxial loading.

A more direct way to obtain the preceding formulas for strain energy in pure torsion is to make use of a **torque-rotation diagram** for the bar (Fig. 3-26). This diagram is linear if the material follows Hooke's law and if the strains are small. During twisting of the bar, the torque T does work equal to the area under the line on the diagram, hence the corresponding elastic strain energy of the bar is

$$U = \frac{T\phi}{2} \quad (3-39)$$

Combining this equation with the equation $\phi = TL/GI_p$ gives the same expressions for strain energy (Eqs. 3-38a and b).

Nonuniform torsion. If the bar has a circular cross section of varying radius or if the torque changes along the axis of the bar (see Figs. 3-7 and 3-8), then we must develop more general formulas for strain energy in torsion. To accomplish this result, consider an elemental

disk of length dx at distance x from one end of the bar (Fig. 3-8). Assuming that the torque acting on this element is T_x and that the polar moment of inertia of its cross section is I_{px} , we obtain from Eq. (3-38a) the following expression for the strain energy of the element:

$$dU = \frac{T_x^2 dx}{2GI_{px}}$$

Therefore, the total strain energy of the bar is

$$U = \int_0^L \frac{T_x^2 dx}{2GI_{px}} \quad (3-40a)$$

An alternate expression for U is obtained by applying Eq. (3-38b) to the element of length dx :

$$dU = \frac{GI_{px}(d\phi)^2}{2dx} = \frac{GI_{px}}{2} \left(\frac{d\phi}{dx}\right)^2 dx$$

in which $d\phi$ is the angle of twist of the element and $d\phi/dx$ is the angle of twist ϕ per unit length. The total energy now becomes

$$U = \int_0^L \frac{GI_{px}}{2} \left(\frac{d\phi}{dx}\right)^2 dx \quad (3-40b)$$

Either of Eqs. (3-40a and b) can be used to find the strain energy in non-uniform torsion, depending upon whether the torque or the angle of twist is known as a function of x .

Example 1

A circular bar AB of length L is fixed at end A and free at B (Fig. 3-27). Three different loading conditions are to be considered: (a) torque T_1 acting at end B ; (b) torque T_1 acting at the midpoint C ; and (c) torques T_1 acting simultaneously at B and C . For each case of loading, determine the strain energy U stored in the bar.

(a) For torque T_1 acting at end B , the strain energy is obtained directly from Eq. (3-38a):

$$U_a = \frac{T_1^2 L}{2GI_p}$$

(b) For torque T_1 acting at the midpoint C , we apply Eq. (3-38a) to part AC of the bar:

$$U_b = \frac{T_1^2 (L/2)}{2GI_p} = \frac{T_1^2 L}{4GI_p}$$

(c) When both loads are acting, the torque in part CB is T_1 and in part AC is $2T_1$; hence,

$$U = \frac{T_1^2 (L/2)}{2GI_p} + \frac{(2T_1)^2 (L/2)}{2GI_p} = \frac{5T_1^2 L}{4GI_p}$$

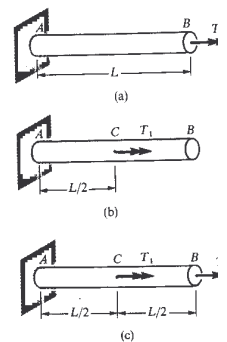


Fig. 3-27 Example 1

3 Torsion

It is important to observe that the strain energy produced by the two loads acting simultaneously is not equal to the sum of the strain energies due to the loads acting separately. As pointed out in Section 2.8, the explanation lies in the fact that strain energy is a quadratic function of the loads, not a linear function.

Example 2

A circular bar AB , fixed at one end and free at the other, is loaded by a distributed torque of constant intensity q per unit distance along the axis of the bar (Fig. 3-28). Derive a formula for the amount of strain energy stored in the bar when the load is applied. Then evaluate the strain energy for the following numerical values: $L = 8$ m, $I_p = 120 \times 10^{-6}$ m⁴, $q = 5$ kN/m, and $G = 78$ GPa. The torque T_x acting at distance x from the free end of the bar is obtained by statics:

$$T_x = qx$$

Substituting into Eq. (3-40a), we obtain

$$U = \int_0^L \frac{T_x^2 dx}{2GI_p} = \frac{1}{2GI_p} \int_0^L (qx)^2 dx = \frac{q^2 L^3}{6GI_p} \quad (3-41)$$

as the formula for the strain energy stored in the bar.

The strain energy can be evaluated numerically from Eq. (3-41) by substituting the given data:

$$U = \frac{(5 \text{ kN}\cdot\text{m/m})^2 (8 \text{ m})^3}{6(78 \text{ GPa})(120 \times 10^{-6} \text{ m}^4)} = 228 \text{ J}$$

Remember that one joule is equal to one newton meter ($1 \text{ J} = 1 \text{ N}\cdot\text{m}$).

3.9 THIN-WALLED TUBES

The torsion theory described in the preceding sections is applicable to bars of circular cross sections, either solid or hollow. Such shapes are commonly used for torsional members, especially in machinery. However, in lightweight structures, such as aircraft and spacecraft, thin-walled tubular members of noncircular shapes are often required to resist torsion. In this section, we describe the analysis of structural members of this type.

To obtain formulas that are applicable to a variety of shapes, let us consider a thin-walled tube of arbitrary cross-sectional shape (Fig. 3-29a). The tube is cylindrical (that is, all cross-sections have the same dimensions), and it is subjected to pure torsion by torques T acting at the ends. The thickness t of the wall of the tube may vary around the cross section, but it is assumed to be small in comparison with the total width of the tube. The shear stresses τ acting on the cross sections are pictured in Fig. 3-29b, which shows an element of the tube cut out be-

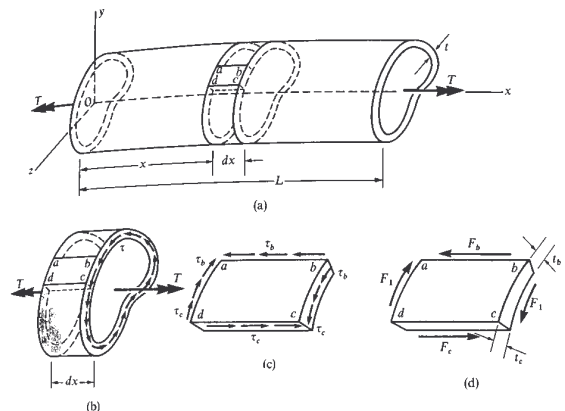


Fig. 3-29 Thin-walled tube of arbitrary cross-sectional shape

tween two cross sections a distance dx apart. The shear stresses are directed parallel to the edges of the cross section, and they "flow" around the tube. The intensity of the shear stresses varies so slightly across the thickness of the tube (because the tube is assumed to be thin) that for many purposes we may assume τ to be constant across the thickness. However, the manner in which τ varies around the cross section must be determined from equilibrium considerations.

To determine the magnitude of the shear stresses, consider a rectangular element obtained by making two longitudinal cuts ab and cd (Figs. 3-29a and b). This element is isolated as a free body in Fig. 3-29c. Acting on the cross-sectional face bc are the shear stresses τ shown in Fig. 3-29b. It is assumed that these stresses may vary in intensity as we move along the cross section from b to c . Thus, at b the shear stress is denoted τ_b , and at c it is denoted τ_c . As we know from equilibrium, identical shear stresses act in the opposite direction on the other cross-sectional face ad . On the longitudinal faces ab and cd , there will act shear stresses of the same magnitude as those on the cross sections, inasmuch as shear stresses on perpendicular planes are equal in magnitude (see Section 1.6). Thus, the constant shear stresses on faces ab and cd are equal to τ_b and τ_c , respectively.

The shear stresses acting on the longitudinal faces produce forces F_b and F_c (Fig. 3-29d) that can be obtained by multiplying the stresses by the areas on which they act; thus,

$$F_b = \tau_b t dx \quad F_c = \tau_c t dx$$

3.9 Thin-Walled Tubes

in which t_b and t_c represent the thicknesses of the tube at b and c , respectively. In addition, forces F_1 are produced by the stresses acting on faces bc and ad , but these forces do not enter into our discussion. From the equilibrium of the element in the x direction, we see that $F_b = F_c$ or

$$\tau_b t_b = \tau_c t_c$$

Because the locations of the longitudinal cuts ab and cd were selected arbitrarily, it follows from the preceding equation that the product of the shear stress τ and the thickness t of the tube is the same at every point in the cross section. This product is known as the **shear flow** and is denoted by the letter f :

$$f = \tau t = \text{constant} \tag{3-43}$$

Thus, the largest shear stress occurs where the thickness of the tube is smallest, and vice versa. Of course, in regions where the thickness is constant, the shear stress also is constant.

The next step in the analysis is to relate the shear flow f (and, hence, the stress τ) to the torque T acting on the tube. Consider an element of area of length ds in the cross section (Fig. 3-30). The distance s is measured along the **median line** of the cross section (shown as a dashed line in the figure). The total shear force acting on the element of area is $f ds$ and the moment of this force about any point O is

$$dT = r f ds$$

in which r is the perpendicular distance from O to the line of action of the force. The latter is tangent to the median line of the cross section at the element ds . The total torque T produced by the shear stresses is obtained by integrating along the full length L_m of the median line of the cross section:

$$T = f \int_0^{L_m} r ds$$

The integral in this expression has a simple geometric interpretation. The quantity $r ds$ represents twice the area of the shaded triangle shown in Fig. 3-30; note that the triangle has a base length ds and a height equal to r . Therefore, the integral represents double the area A_m enclosed by the median line of the cross section; thus,

$$T = 2fA_m$$

From this equation, we get

$$f = \tau t = \frac{T}{2A_m} \quad \tau = \frac{T}{2tA_m} \tag{3-43a, b}$$

having constant thickness t , the expression for J (Eq. 3-45) simplifies to

$$J = \frac{4tA_m^2}{L_m}$$

Note that J has units of length to the fourth power.

For each shape of cross section, we can evaluate J from one of the preceding equations (Eqs. 3-45 or 3-47). For example, consider a thin-walled circular tube (Fig. 3-31) of thickness t and radius r to the median line. The length of the median line and the area enclosed by it are

$$L_m = 2\pi r \quad A_m = \pi r^2$$

Hence, the torsion constant is

$$J = 2\pi r^3 t \tag{3-46}$$

as obtained from Eq. (3-47). Figure 3-32 shows another example, a thin-walled rectangular tube. The tube has thickness t_1 on the sides and t_2 on the top and bottom; the height and width (to the median line of the cross section) are h and b , respectively. For this cross section, we have

$$L_m = 2(b + h) \quad A_m = bh$$

and

$$\int_0^{L_m} \frac{ds}{t} = 2 \int_0^h \frac{ds}{t_1} + 2 \int_0^b \frac{ds}{t_2} = 2 \left(\frac{h}{t_1} + \frac{b}{t_2} \right)$$

Thus, the torsion constant is

$$J = \frac{2b^2 h^2 t_1 t_2}{bt_1 + ht_2} \tag{3-48}$$

as obtained from Eq. (3-45).

The angle of twist ϕ for a thin-walled tube may be determined by equating the work done by the applied torques T to the strain energy of the bar:

$$\frac{T\phi}{2} = \frac{T^2 L}{2GJ}$$

from which

$$\phi = \frac{TL}{GJ} \tag{3-50}$$

Again we observe that the equation is of the same form as that for a circular bar (Eq. 3-8). If the angle of twist θ per unit length is needed, it can be obtained by dividing ϕ by L ; thus, $\theta = T/GJ$ (compare with Eq. 3-7).*

* The torsion theory for thin-walled tubes is due to the German engineer R. Bredt who presented it in 1896 (Ref. 3-4).

From these equations, the shear flow f and the shear stresses τ can be calculated for any thin-walled tube.

The angle of twist ϕ can be calculated by considering the strain energy of the tube. Because elements of the tube are in pure shear, the strain energy density is $\tau^2/2G$, as given by Eq. (3-37a). Hence, the strain energy of a small element of the tube having cross-sectional area $t ds$ (Fig. 3-30) and length dx (Fig. 3-29) is

$$dU = \frac{\tau^2}{2G} t ds dx = \frac{\tau^2 t^2 ds}{2G t} dx = \frac{f^2 ds}{2G t} dx$$

Therefore, the total strain energy of the tube is

$$U = \int dU = \frac{f^2}{2G} \int_0^{L_m} \left[\int_0^L dx \right] \frac{ds}{t}$$

in which we have utilized the fact that the shear flow f is a constant and may be placed outside the integral signs. Also, we note that t may vary with position around the median line, hence it must remain under the integral sign with ds . The inner integral is equal to the length L of the tube, hence the equation for U becomes

$$U = \frac{f^2 L}{2G} \int_0^{L_m} \frac{ds}{t}$$

Substituting for the shear flow from Eq. (3-43a), we obtain

$$U = \frac{T^2 L}{8GA_m^2} \int_0^{L_m} \frac{ds}{t} \tag{3-44}$$

as the equation for the strain energy of the tube in terms of the torque T .

The expression for strain energy can be written in simpler form by introducing a new property of the cross section that is known in general as the **torsion constant** J . For a thin-walled tube, the torsion constant is

$$J = \frac{4A_m^2}{\int_0^{L_m} \frac{ds}{t}} \tag{3-45}$$

With this notation, the equation for strain energy (Eq. 3-44) becomes

$$U = \frac{T^2 L}{2GJ} \tag{3-46}$$

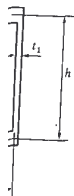
This equation has the same form as the one for strain energy in a circular bar (see Eq. 3-38a) except that the torsion constant J has replaced the polar moment of inertia I_p . In the special case of a cross section



on of a thin-



n-walled circular tube



walled rectangular

3.9 Thin-Walled Tubes

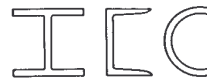


Fig. 3-33 Thin-walled open section



Fig. 3-34 Solid noncircular section

The quantity GJ is known in general as the **torsional rigidity** of a bar. In the case of a circular bar, the torsion constant J is the polar moment of inertia; in the case of a thin-walled tube, J is given by Eq. (3-45). For other shapes of cross sections, different formulas for J are required. For instance, formulas for J for thin-walled open sections (Fig. 3-33) and solid noncircular sections (Fig. 3-34) can be obtained by more advanced methods of analysis.

Thin-walled, circular tubes. Let us again consider the circular tube illustrated in Fig. 3-31. The shear flow and shear stresses in this tube are given by the formulas

$$f = \frac{T}{2\pi r^2} \quad \tau = \frac{T}{2\pi r^2 t} \tag{3-51a, b}$$

which are obtained from Eqs. (3-43a and b) by substituting $A_m = \pi r^2$. Also, the angle of twist (see Eqs. 3-50 and 3-48) is

$$\phi = \frac{TL}{2\pi G r^3 t} \tag{3-52}$$

These results agree with those obtained from the previously derived equations for a hollow circular bar (Section 3.2). If the hollow bar is thin walled, the polar moment of inertia (see Eq. 3-13) is approximately

$$I_p = 2\pi r^3 t$$

which agrees with Eq. (3-48) for J . Using this expression for I_p in the torsion formula (Eq. 3-9) leads to Eq. (3-51b) for τ .

If a tube subjected to torsion has very thin walls, the possibility of buckling of the walls must be taken into account. For example, a long circular tube constructed of mild steel will buckle at normal working stresses when the ratio r/t (see Fig. 3-31) is about 60 (see Ref. 3-5). Thus, we assume in this section that the wall thickness is great enough to prevent buckling by torsion.

Example 1

Compare the maximum shear stress in a circular tube (Fig. 3-31) as calculated from Eq. (3-51b) for a thin-walled tube with the stress calculated from the torsion formula (Eq. 3-9).

The formula for the shear stress in a thin-walled tube gives

$$\tau_1 = \frac{T}{2\pi r^2 t} = \frac{T}{2\pi r^3 \beta^2} \tag{a}$$

in which the notation $\beta = r/t$ is introduced. The exact maximum shear stress in the tube is given by the torsion formula:

$$\tau_2 = \frac{T(r + t/2)}{I_p} \tag{b}$$

where

$$I_p = \frac{\pi}{2} \left[\left(r + \frac{t}{2} \right)^4 - \left(r - \frac{t}{2} \right)^4 \right]$$

as obtained from Eq. (3-12). After expansion, this expression for I_p simplifies

$$I_p \approx \frac{\pi r t}{2} (4r^2 + t^2)$$

so that the expression for τ_2 (Eq. b) becomes

$$\tau_2 = \frac{T(2r+t)}{\pi r t (4r^2 + t^2)} = \frac{T(2\beta + 1)}{\pi t^3 \beta (4\beta^2 + 1)}$$

The ratio τ_1/τ_2 is

$$\frac{\tau_1}{\tau_2} = \frac{4\beta^2 + 1}{2\beta(2\beta + 1)} \quad (3-5)$$

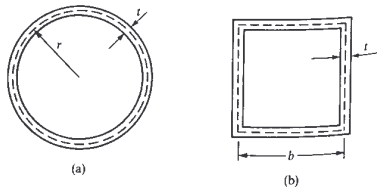
which depends only on the quantity β (that is, on the ratio r/t). For values of β equal to 5, 10, and 20, we obtain from Eq. (3-5) the ratios $\tau_1/\tau_2 = 0.92, 0.95,$ and 0.98 , respectively. Thus, Eq. (3-5) shows that the approximate formula for the shear stresses gives results that are only slightly less than those obtained from the exact formula and that the accuracy of the approximate formula increases as the tube becomes relatively thinner.

Example 2

A circular tube and a square tube (Fig. 3-35) are constructed of the same material. Both tubes have the same length, thickness, and cross-sectional area and both are subjected to the same torque. What are the ratios of the shear stresses and of the angles of twist for the tubes? (Disregard the effects of stress concentrations at the corners of the square tube.)

For the circular tube, the area A_{m1} enclosed by the median line of the cross section is $A_{m1} = \pi r^2$, where r is the radius to the median line. Also, the cross-sectional area of the circular tube is $A_1 = 2\pi r t$, and its torsion constant is $J_1 = 2\pi r^3 t$ (Eq. 3-48).

For the square tube, the cross-sectional area is $A_2 = 4bt$, where b is the



3-35 Example 2

length of one side, measured along the median line. Inasmuch as the areas of both tubes are the same, we obtain $b = \pi r/2$. Also, the area enclosed by the median line of the cross section is $A_{m2} = b^2$, and its torsion constant $J_2 = \pi^2 r^3 t/8$ (obtained from Eq. 3-49).

The ratio τ_1/τ_2 of the shear stress in the circular tube to the shear stress in the square tube (see Eq. 3-43b) is

$$\frac{\tau_1}{\tau_2} = \frac{A_{m2}}{A_{m1}} = \frac{b^2}{\pi r^2} = \frac{\pi}{4} = 0.785 \quad (d)$$

The ratio of the angles of twist (see Eq. 3-50) is

$$\frac{\phi_1}{\phi_2} = \frac{J_2}{J_1} = \frac{\pi^2}{16} = 0.617 \quad (e)$$

These results show that the circular tube has not only a lower shear stress than does the square tube but also greater stiffness against rotation.

***3.10 NONLINEAR TORSION OF CIRCULAR BARS**

The equations derived in the preceding sections for the torsion of circular bars apply only if the material follows Hooke's law. Let us now consider the behavior of bars when the shear stresses exceed the proportional limit. For such bars, we may still assume from considerations of symmetry that the circular cross sections remain plane and that their radii remain straight. Therefore, the shear strain γ at a distance ρ from the axis of the bar (see Fig. 3-2c) is given by the same formula as in the case of elastic torsion, namely,

$$\gamma = \rho\theta \quad (3-54)$$

Also, the maximum shear strain, which occurs at the outer edge of the cross section, is

$$\gamma_{max} = r\theta \quad (3-55)$$

in which r is the radius of the bar.

For any assumed value of θ , the shear stress τ at any point in the bar can be determined if the shear stress-strain diagram for the material is known (Fig. 3-36a). At the outer edge of the cross section, the strain

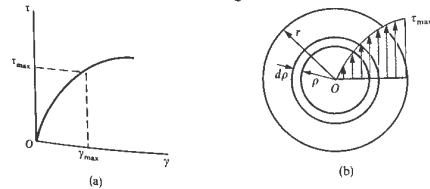


Fig. 3-36 Nonlinear torsion of circular bar: (a) shear stress-strain diagram, and (b) distribution of stresses acting on the cross section

is γ_{max} , and the corresponding stress τ_{max} can be obtained from the strain diagram. At intermediate points in the cross section, the same procedure can be used. As a result, the distribution of shear stresses in the cross section (Fig. 3-36b) will have the same shape as the strain diagram itself.

The torque T that must act on the bar in order to produce an assumed angle of twist θ per unit length may be obtained from an equation of statics (see Fig. 3-36b):

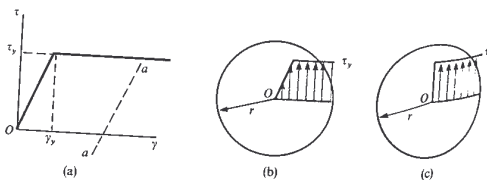
$$T = \int_0^r 2\pi\rho^2\tau d\rho \quad (3-56)$$

From Eq. (3-54), we obtain $\rho = \gamma/\theta$ and $d\rho = d\gamma/\theta$. Substituting these relations into Eq. (3-56), and also changing the upper limit of integration to γ_{max} , we obtain

$$T = \frac{2\pi}{\theta^3} \int_0^{\gamma_{max}} \tau\gamma^2 d\gamma \quad (3-57)$$

The integral on the right-hand side of this equation has a simple geometric interpretation. It is the moment of inertia with respect to the vertical axis (that is, the τ axis) of the area under the stress-strain curve (Fig. 3-36a) between the origin O and the maximum strain γ_{max} . Thus for any assumed value of θ , we can calculate γ_{max} and the corresponding moment of inertia. Then from Eq. (3-57) we can obtain the value of the torque T . By repeating this procedure for various values of θ , we obtain a curve representing the relationship between T and θ . Having such a curve, we can determine both θ and τ_{max} for any given value of T .

If the material of the bar has a pronounced yield stress τ_y , the stress-strain diagram can be idealized as shown in Fig. 3-37a. The diagram consists of two straight lines, the first representing linear elastic behavior and the second representing perfectly plastic behavior. As long as the maximum strain in the bar is less than the yield strain γ_y , the bar behaves elastically and the formulas derived in Section 3.2 can be used. When the strain at the outer edge of the cross section exceeds γ_y , the stress distribution on the cross section will have the form shown in Fig. 3-37b. Yielding begins at the outer edges of the bar and moves progressively inward as the strains increase. If the strains become very large, the region



circular bar of

of yielding will approach the middle of the bar and the stress distribution will approach the uniform distribution shown in Fig. 3-37c. The corresponding torque T_u is the ultimate torque for the bar, and its value (from Eq. 3-56) is

$$T_u = \int_0^r 2\pi\rho^2\tau_y d\rho = \frac{2\pi r^3\tau_y}{3} \quad (3-58)$$

When this value of torque is reached, further twisting of the shaft will occur without an increase in torque. Eventually, the effects of strain hardening will become noticeable, and then stresses greater than τ_y will occur.

The torque T_y at which yielding first begins in the bar is found from the torsion formula (Eq. 3-9) by substituting τ_y for τ_{max} :

$$T_y = \frac{\tau_y J_p}{r} = \frac{\pi r^3\tau_y}{2} \quad (3-59)$$

Comparing Eqs. (3-58) and (3-59), we see that the ratio of the ultimate torque to the yield torque is

$$\frac{T_u}{T_y} = \frac{4}{3} \quad (3-60)$$

From this result we observe that, after yielding begins in the bar, only a one-third increase in the torque will bring the bar to its ultimate load-carrying capacity.

Residual stresses. If a bar in torsion is loaded beyond the elastic limit and then the load is removed, some stresses will remain in the bar. Such stresses are known as residual stresses. To illustrate their calculation, let us assume that a solid circular bar is loaded to the ultimate torque T_u , thereby producing the stress distribution shown in Fig. 3-37c, and that this torque is then removed completely. During the unloading process, the material follows a straight line on the stress-strain diagram (line $a-a$ in Fig. 3-37a), parallel to the initial straight line representing Hooke's law. Thus, the stresses produced during unloading can be obtained from the equations for linear elastic behavior (Eqs. 3-9 through 3-11).

The superposition of the stresses produced during loading and unloading is shown in Fig. 3-38. The stresses reached during loading are shown in the first part of the figure; the corresponding torque is $T_u = 2\pi r^3\tau_y/3$. This same torque is represented by the unloading stress diagram in Fig. 3-38b, except that now the torque acts in the opposite direction and the behavior is linearly elastic. The maximum stress is $\tau_{max} = T_u/J$, or $\tau_{max} = 4\tau_y/3$. The residual stresses in the bar, obtained by superimposing the stresses due to loading and unloading, are shown in Fig. 3-38c. At the center of the bar, the residual stress is

$$\tau_1 = \tau_y \quad (3-61)$$

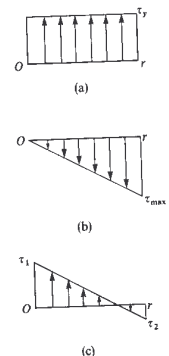
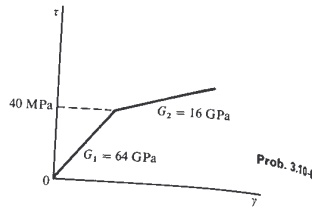


Fig. 3-38 Residual stresses in

the residual stresses in a bar subjected to torsion are zero after the load is removed. This can be verified by statics (see Eq. 3-56) that the torque by the residual stresses in a bar of elastic material is zero (see Fig. 3-38c).

A solid circular bar of radius $r = 35$ mm is constructed of a material having the bilinear stress-strain curve shown in the figure. Calculate the maximum shear stress τ_{max} in the bar when the torque T is 5 kN·m.



Shear Force and Bending Moment

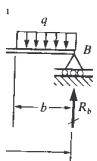
4.1 TYPES OF BEAMS

A structural member that is designed to resist forces acting transverse to its axis is called a **beam**. Thus, beams differ from bars in tension and bars in torsion primarily because of the directions of the loads that act upon them. A bar in tension is subjected to loads directed along the axis, and a bar in torsion is subjected to torques having their vectors along the axis. By contrast, the loads on a beam are directed normal to the axis, as illustrated by the force P_1 acting on beam AB of Fig. 4-1a.

In this chapter we will consider only the simplest types of beams, such as those illustrated in Fig. 4-1. These beams are planar structures because all of the loads act in the plane of the figure and all deflections occur in that same plane, which is called the **plane of bending**. The beam of Fig. 4-1a, which has a pin support at one end and a roller support at the other, is called a **simply supported beam** or a **simple beam**. The essential feature of a pin support is that it restrains the beam from translating both horizontally and vertically, but it does not prevent rotation. Thus, end A of the beam does not translate, but the longitudinal axis of the beam may rotate in the plane of the figure. Therefore, a pin support is capable of developing a reactive force with both horizontal and vertical components, but there will be no moment reaction. At the roller support B , translation is prevented in the vertical direction but not in the horizontal direction; hence, the support can resist a vertical force but not a horizontal force. Of course, the beam axis is free to rotate at B in the same manner as at A . The vertical reactions at the supports of a simple beam may act either upward or downward, as required for equilibrium.

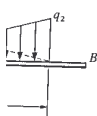
When making a sketch of a beam, we show the type of support by a conventional diagram that indicates the manner in which the beam is restrained; hence, the diagram also indicates the nature of the reactive

4.1 Shear Force and Bending Moment



forces. However, these conventional diagrams are not intended to represent the actual physical construction. For instance, the end of a beam resting on a wall and bolted down against uplift is represented in the sketch as a pin connection, but in reality there is no pin at the end of the beam.

The beam shown in Fig. 4-1b, which is built-in or fixed at one end and free at the other, is called a **cantilever beam**. At the fixed (or clamped) support, the beam can neither translate nor rotate, whereas at the free end it may do both. Consequently, both force and moment reactions may exist at the fixed support.



The third example in the figure is a beam with an **overhang** (Fig. 4-1c). This beam is simply supported at A and B , but it also projects beyond the support to point C , which is a free end. Many other arrangements of supports for beams are possible, depending upon the particular applications. However, the examples given here are sufficient to illustrate the basic concepts.

Loads acting on beams may be of several kinds, as illustrated in Fig. 4-1. **Concentrated loads** are forces such as P_1 and P_2 . **Distributed loads** act over a distance, as shown by the load q in Fig. 4-1a. Such loads are measured by their **intensity**, which is expressed in units of force per unit distance along the axis of the beam (for example, newtons per meter or pounds per foot). A uniformly distributed load, or **uniform load**, has constant intensity q per unit distance. A varying load has an intensity that changes with distance along the axis; for instance, the **linearly varying load** of Fig. 4-1b has an intensity that varies from q_1 to q_2 . Another kind of load is a **couple**, illustrated by the couple of moment M_1 acting on the overhanging beam (Fig. 4-1c).

As mentioned previously, we assume in this discussion that the loads on the beams act in the plane of the figure. This assumption requires that all forces have their vectors in the plane of the figure and that all couples have their moment vectors perpendicular to that plane. Furthermore, the beams must be symmetric about that plane; that is, the plane of bending must be a plane of symmetry of the beam itself. Thus, the cross section of each beam must have a vertical axis of symmetry. Under these conditions, the beam will deflect only in the plane of bending. However, if these conditions are not met, the beam will bend out of its plane and a more general bending analysis is required (see Chapter 9).

The beams shown in Fig. 4-1 are **statically determinate**; hence, their reactions can be determined from equilibrium equations. For instance, in the case of the simple beam AB of Fig. 4-1a, we note first that the only reactions are the vertical forces R_a and R_b at the ends. (If a horizontal load were to act on the beam, a horizontal reaction would also be induced at support A .) By summing moments about point B , we can calculate the reaction at A , and vice versa. The results are

$$R_a = \frac{P_1(L-a)}{L} + \frac{qb^2}{2L}, \quad R_b = \frac{P_1a}{L} + \frac{qb(2L-b)}{2L}$$

An equation of equilibrium of forces in the vertical direction provides a check on these results.

The cantilever beam of Fig. 4-1b is subjected to a linearly varying distributed load, hence the diagram of load intensity is trapezoidal. This load is equilibrated by a vertical force R_a and a couple M_a acting at the fixed support. From the equilibrium of forces in the vertical direction, we get

$$R_a = \frac{(q_1 + q_2)b}{2}$$

in which we have utilized the fact that the resultant of the distributed load is equal to the area of the load-intensity diagram. The moment about A is found from equilibrium of moments. It is convenient in this example to sum moments about point A in order to eliminate R_a from the moment equation. For the purpose of obtaining the moment about A of the distributed load, we divide the trapezoidal diagram into two triangles, as shown by the dashed line in Fig. 4-1b. Then the moment about A of the lower triangular part of the load is

$$\frac{1}{2}(q_1b)\left(a + \frac{b}{3}\right)$$

in which $q_1b/2$ is the resultant force (equal to the area of the lower triangular load diagram) and $a + b/3$ is the moment arm of the resultant. A similar procedure may be used to obtain the moment of the upper triangular portion of the load, and the final result is

$$M_a = \frac{q_1b}{2}\left(a + \frac{b}{3}\right) + \frac{q_2b}{2}\left(a + \frac{2b}{3}\right)$$

This reactive moment acts counterclockwise, as shown in the figure.

The beam with an overhang (Fig. 4-1c) is subjected to a vertical force P_2 and a couple of moment M_1 . Taking moments about points B and A gives the following equations of static equilibrium (counterclockwise moments are positive):

$$-R_aL + P_2(L-a) + M_1 = 0 \quad \text{or} \quad R_a = \frac{P_2(L-a)}{L} + \frac{M_1}{L}$$

$$-P_2a + R_bL + M_1 = 0 \quad \text{or} \quad R_b = \frac{P_2a}{L} - \frac{M_1}{L}$$

Again, summation of forces in the vertical direction provides a check on these results.

The preceding examples illustrate how the reactions (forces and couples) of statically determinate beams are calculated from equilibrium equations. Of course, the reactions of statically indeterminate beams cannot be found from equilibrium alone; their calculation requires consideration of the deflections caused by bending. This subject is discussed in later chapters.

ms: (a) simple beam, and (b) cantilever beam

The support conditions shown in Fig. 4-1 are idealizations of actual conditions encountered in practice. Due to lack of perfect rigidity in the supporting structures or foundations, there may be a small amount of translation at a pin support or a small rotation at a fixed support. Also it is rare to find complete lack of restraint against horizontal translation to friction and other effects. Under most conditions, especially for statically determinate beams, these minor deviations from idealized conditions have little effect on the action of the beam and therefore can be disregarded.

4.2 SHEAR FORCE AND BENDING MOMENT

When a beam is loaded by forces or couples, internal stresses and strains are created. To determine these stresses and strains, we first must find the **internal forces** and **internal couples** that act on cross sections of the beam. As an illustration, consider a cantilever beam acted upon by a vertical force P at its free end (Fig. 4-2a). Now imagine that we cut through the beam at a cross section mn located at distance x from the free end and isolate the left-hand part of the beam as a free body (Fig. 4-2b). The free body is held in equilibrium by the force P and by the stresses that act over the cut cross section mn . These stresses represent the action of the right-hand part of the beam on the left-hand part. Of course, at this stage of our discussion, we do not know the distribution of the stresses acting over the cross section; all we know is that the resultant of these stresses must be such as to maintain equilibrium of the free body we selected.

It is convenient to reduce the resultant to a **shear force** V acting parallel to the cross section and a **bending couple** of moment M . Because the load P is transverse to the axis of the beam, no axial force exists at the cross section. Both the shear force and the bending couple act in the plane of the beam, which means that the moment vector for the couple is perpendicular to the plane of the figure. The moment of the bending couple is called the **bending moment** M . Because shear forces and bending moments, like axial forces in bars and twisting couples in shafts, are the resultants of stresses distributed over the cross section, they are known collectively as **stress resultants**.

The stress resultants in statically determinate beams can be calculated from equations of static equilibrium. As an example, consider again the cantilever beam of Fig. 4-2a. From the free-body diagram of Fig. 4-2b, we obtain

$$V = P \quad M = Px$$

where x is the distance from the free end to section mn . Thus, through the use of a free-body diagram and equations of equilibrium, we are able to calculate the stress resultants without difficulty. In the next

chapter, we will see how to determine the internal stresses associated with V and M .

The shear force and bending moment are assumed to be positive when they act on the left-hand part of the beam in the directions shown in Fig. 4-2c. If we consider the right-hand part of the beam (Fig. 4-2c), then the directions of these same stress resultants are reversed. Therefore, the directions of the algebraic sign of a stress resultant does not depend upon its direction in space, such as upward or downward, or clockwise or counterclockwise, but rather the sign depends upon the direction of the stress resultant with respect to the material against which it acts. To make this point clear, the **sign conventions** for shear forces and bending moments are repeated in Fig. 4-3, where V and M are shown acting on an element of the beam cut out between two cross sections that are a small distance apart.

The deformations of an element caused by both positive and negative shear forces and bending moments are sketched in Fig. 4-4. We see that a positive shear force tends to deform the element by causing the right-hand face to move downward with respect to the left-hand face, and a positive bending moment elongates the lower part of the beam and compresses the upper part. Because the signs for V and M are related to the deformations of the material, these sign conventions are called **deformation sign conventions**. We previously used a deformation sign convention for axial forces (tension is positive, compression is negative). A different kind of sign convention, called a **static sign convention**, is used in equations of static equilibrium. When using a static sign convention, forces are taken as positive when they act in the positive direction of a coordinate axis.

To illustrate the two types of sign conventions, let us write equations of equilibrium for the two parts of the beam shown in Fig. 4-2. Note that V and M are positive according to the deformation sign convention for stress resultants. However, if the y axis is positive upward, then the shear force V in Fig. 4-2b is given a negative sign in the equilibrium equation, which is written according to a static sign convention:

$$\sum F_y = 0 \quad \text{or} \quad P - V = 0$$

Of course, V would be given a positive sign in an equation of equilibrium for the right-hand part of the beam. Thus, a positive shear force may appear in a force equilibrium equation with either a positive or a negative sign, depending upon the free-body diagram that is considered. An analogous situation exists for bending moments when moment equilibrium equations are used. Difficulties with signs can be avoided by keeping in mind that two types of sign conventions are used in mechanics; deformation sign conventions for stress resultants and static sign conventions for equations of equilibrium. The former are based upon how the material is deformed, and the latter are based upon directions in space.



Fig. 4-3 Sign conventions for force V and bending moment M

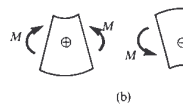
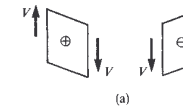


Fig. 4-4 Deformations (highly exaggerated) of an element cut (a) shear forces and (b) bending moments

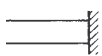
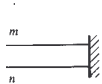


Fig. 4-2 Internal forces and bending moments

Example 1

A simple beam AB supports two loads, a force P and a couple M_0 , acting as shown in Fig. 4-5a. Find the shear force V and bending moment M in the beam at cross sections located as follows: (a) a small distance to the left of the middle of the beam and (b) a small distance to the right of the middle of the beam.

The first step in the analysis of this beam is to find the reactions R_a and R_b . Taking moments about ends A and B gives two equations of equilibrium from which we find

$$R_a = \frac{3P}{4} - \frac{M_0}{L} \quad R_b = \frac{P}{4} + \frac{M_0}{L}$$

Next, the beam is cut at a cross section just to the left of the middle, and a free-body diagram is drawn of either half of the beam. In this example, we choose the left-hand half of the beam, and the corresponding diagram is shown in Fig. 4-5b. The force P and the reaction R_a appear in this diagram, along with the unknown shear force V and bending moment M , both of which are shown in their positive directions. The couple M_0 does not appear in the figure because the beam is cut to the left of the point of application of M_0 . A summation of forces in the vertical direction gives

$$R_a - P - V = 0 \quad \text{or} \quad V = \frac{P}{4} - \frac{M_0}{L}$$

This result shows that when P and M_0 act in the directions shown in Fig. 4-5a, the shear force is negative and acts in the direction opposite to that assumed in Fig. 4-5b. Taking moments about an axis through the cross section where the beam is cut (Fig. 4-5b) gives

$$-R_a\left(\frac{L}{2}\right) + P\left(\frac{L}{4}\right) + M = 0 \quad \text{or} \quad M = \frac{PL}{8} - \frac{M_0}{2}$$

The bending moment M may be either positive or negative, depending upon the relative magnitudes of the terms in this equation.

To obtain the stress resultants at a cross section just to the right of the middle, we cut the beam at that section and again draw a free-body diagram (Fig. 4-5c). The difference between this diagram and the former one is that the couple M_0 now acts on the part of the beam to the left of the cut section. Again summing forces in the vertical direction, and also taking moments about an axis through the cut section, we obtain

$$V = -\frac{P}{4} - \frac{M_0}{L} \quad M = \frac{PL}{8} + \frac{M_0}{2}$$

We see from these results that, when the cut section is shifted from left to right of the couple M_0 , the shear force does not change but the bending moment increases algebraically by an amount equal to M_0 .

Example 2

A cantilever beam that is free at end A and fixed at end B is subjected to a distributed load of linearly varying intensity q (see Fig. 4-6a). The maximum distributed load occurs at the fixed support and is denoted by q_0 . Find the intensity of the shear force V and bending moment M at distance x from the free end.

We begin by cutting through the beam at distance x from the left-hand end and isolating part of the beam as a free body (Fig. 4-6b). As in the preceding example, the unknown shear force V and bending moment M are assumed to be positive. The intensity of the distributed load is $q = q_0x/L$; therefore, the total downward load on the free body of Fig. 4-6b is equal to $q_0x^2/2L$. Hence, we downward load on the free body in the vertical direction that

$$V = -\frac{q_0x^2}{2L} \tag{a}$$

From this equation, we note that at the free end A ($x = 0$) the shear force is $V = 0$ and at the fixed end B ($x = L$) the shear force is $V = -q_0L/2$.

To find the bending moment in the beam, we write an equation of moment equilibrium about an axis through the cut section and solve for M :

$$M = -\frac{q_0x^3}{6L} \tag{b}$$

Again considering the two ends of the beam, we see that the bending moment is equal to zero when $x = 0$ and equal to $-q_0L^2/6$ when $x = L$. Equations (a) and (b) can be used to obtain V and M at any point in the beam, and we see from these equations that both the shear force and the bending moment reach their numerically largest values at the fixed end of the beam.

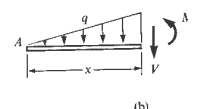
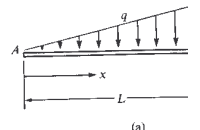


Fig. 4-6 Example 2

Example 3

A beam ABC with an overhang supports a uniform load of intensity $q = 6 \text{ kN/m}$ and a concentrated load $P = 28 \text{ kN}$ (Fig. 4-7a, page 188). Calculate the shear force V and bending moment M at a cross section D located 5 m from the left-hand support.

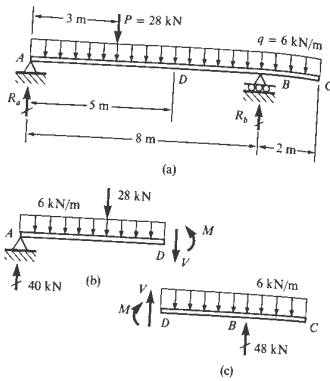
We begin by calculating the reactions from equations of equilibrium for the entire beam. Thus, taking moments about the support at B , we get

$$-R_a(8 \text{ m}) + (28 \text{ kN})(5 \text{ m}) + (6 \text{ kN/m})(10 \text{ m})(3 \text{ m}) = 0$$

from which $R_a = 40 \text{ kN}$. In a similar manner, equilibrium of moments about support A yields $R_b = 48 \text{ kN}$. (We also observe that equilibrium of forces in the vertical direction is satisfied.)

Next, we make a cut at section D and construct a free-body diagram of the left-hand part of the beam (Fig. 4-7b). When drawing this diagram, we assume that the unknown stress resultants V and M are positive. The equations of equilibrium for the free body are as follows:

$$\begin{aligned} \sum F_y = 0 & \quad 40 \text{ kN} - 28 \text{ kN} - (6 \text{ kN/m})(5 \text{ m}) - V = 0 \\ \sum M = 0 & \quad -(40 \text{ kN})(5 \text{ m}) + (28 \text{ kN})(2 \text{ m}) \\ & \quad + (6 \text{ kN/m})(5 \text{ m})(2.5 \text{ m}) + M = 0 \end{aligned}$$



Example 3

from which

$$V = -18 \text{ kN} \quad M = 69 \text{ kN}\cdot\text{m}$$

The minus sign in the result for V means that the shear force acts in the negative direction (opposite to the direction shown in Fig. 4-7b).

An alternate method of solution is to obtain V and M from a free-body diagram of the right-hand part of the beam (Fig. 4-7c). When drawing this diagram, we again assume that the unknown shear force and unknown bending moment are positive. Then the two equations of equilibrium are

$$\begin{aligned} \sum F_y = 0 & \quad V - (6 \text{ kN/m})(5 \text{ m}) + 48 \text{ kN} = 0 \\ \sum M = 0 & \quad -M - (6 \text{ kN/m})(5 \text{ m})(2.5 \text{ m}) + (48 \text{ kN})(3 \text{ m}) = 0 \end{aligned}$$

from which

$$V = -18 \text{ kN} \quad M = 69 \text{ kN}\cdot\text{m}$$

as before.

4.3 RELATIONSHIPS BETWEEN LOAD, SHEAR FORCE, AND BENDING MOMENT

We will now obtain some important relationships between the loads on a beam, the shear force V , and the bending moment M . These relationships are quite useful when investigating the shear force and bending moment throughout the entire length of a beam, and they are especially helpful when constructing shear-force and bending-moment diagrams (see Section 4.4). As a means of obtaining the relationships, let us con-

sider an element of a beam cut out between two cross sections that are distance dx apart (Fig. 4-8a). On the left-hand face of the element are shown the shear force V and bending moment M , acting in their positive directions. In general, V and M are functions of the distance x measured along the axis of the beam; hence, on the right-hand face of the element, both the shear force and the bending moment will have values that are slightly different from their values on the left-hand face. If we denote the increments in V and M by dV and dM , respectively, then the corresponding stress resultants on the right-hand face are $V + dV$ and $M + dM$.

The load acting on the top surface of the element may be a distributed load, a concentrated load, or a couple. Let us assume first that the load is distributed and of intensity q , as shown in Fig. 4-8a. Then, from equilibrium of forces in the vertical direction, we get

$$V - (V + dV) - q dx = 0$$

or

$$\frac{dV}{dx} = -q \tag{4-1}$$

Thus, as the shear force V varies with the distance x , its rate of change with respect to x is equal to $-q$. As a special case, note that the shear force is constant if the beam has no load ($q = 0$). In deriving Eq. (4-1), we assumed that the load shown in Fig. 4-8a is a positive load; thus, we have adopted the sign convention that *distributed loads are positive when acting downward and negative when acting upward*.

As an illustration of the use of Eq. (4-1), consider the cantilever beam with a linearly varying load that we discussed in Example 2 of the preceding section (see Fig. 4-6). The load on the beam is

$$q = \frac{q_0 x}{L}$$

which we assume is positive when downward, as explained in the preceding paragraph. The shear force is

$$V = -\frac{q_0 x^2}{2L}$$

(see Eq. a, Section 4.2). Taking the derivative dV/dx gives

$$\frac{dV}{dx} = -\frac{q_0 x}{L} = -q$$

which is in accord with Eq. (4-1).

Equation (4-1) can be integrated along the axis of the beam to obtain a useful equation pertaining to the shear forces acting at two different cross sections. To obtain this relationship, we multiply both sides of

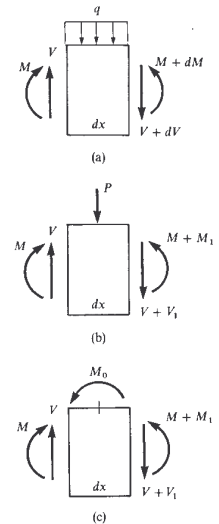


Fig. 4-8 Element of a beam used in deriving relationships between loads, shear forces, and bending moments

Eq. (4-1) by dx and then integrate between two points A and B on the axis of the beam. The result is

$$\int_A^B dV = -\int_A^B q dx$$

The left-hand side of this equation equals the difference $V_b - V_a$ of the shear forces at sections B and A . The integral on the right-hand side represents the area of the load-intensity diagram between A and B , which is also equal to the resultant of the distributed load between A and B . Thus,

$$V_b - V_a = -\int_A^B q dx = -(\text{Area of load-intensity diagram between } A \text{ and } B) \tag{4-2}$$

Because Eq. (4-1) was derived for an element of the beam subjected only to a continuously distributed load (or to no load), we cannot use Eq. (4-1) at a point where a concentrated load is applied. In a similar manner, we cannot use Eq. (4-2) if a concentrated load P acts on the beam between points A and B , because the intensity of load q is undefined for a concentrated load. Note that the area of the load-intensity diagram may be positive or negative.

Returning to the beam element shown in Fig. 4-8a, let us now consider equilibrium by summing moments about an axis through the left-hand face of the element and perpendicular to the plane of the figure. Taking moments as positive when counterclockwise, we obtain

$$-M - q dx \left(\frac{dx}{2}\right) - (V + dV) dx + M + dM = 0$$

Discarding products of differentials because they are negligible compared to the other terms, we obtain the following relationship:

$$\frac{dM}{dx} = V \tag{4-3}$$

This equation shows that the rate of change of M with respect to x is equal to the shear force. If the shear force is zero, then the bending moment is constant. Equation (4-3) applies only in regions where distributed loads act on the beam. At a point where a concentrated load acts, a sudden change (or discontinuity) in the shear force results and the derivative dM/dx is undefined.

Again using the cantilever beam in Fig. 4-8a as an example, we recall that the bending moment (see Eq. b, Section 4.2) is

$$M = -\frac{q_0 x^3}{6L}$$

The derivative dM/dx is

$$\frac{dM}{dx} = -\frac{q_0 x^2}{2L}$$

which is the same as the shear force V in the beam; thus, Eq. (4-3) is satisfied.

Integrating Eq. (4-3) between two points A and B on the beam axis gives

$$\int_A^B dM = \int_A^B V dx \tag{4-4}$$

The integral on the left-hand side of this equation is equal to the difference $M_b - M_a$ of the bending moments at points A and B . To interpret the integral on the right-hand side, we need to consider V as a function of x and to visualize a diagram showing the manner in which V varies with x . Then we see that the integral on the right represents the area under the curve between A and B . Therefore, we can express Eq. (4-4) in the following manner:

$$M_b - M_a = \int_A^B V dx = \text{Area of shear-force diagram between } A \text{ and } B \tag{4-4}$$

This equation can be used even when concentrated loads are acting on the beam between points A and B . However, it is not valid if a couple acts between A and B , because a couple produces a sudden change in the bending moment and the left-hand side of Eq. (4-4) cannot be integrated across such a discontinuity.

Now let us consider a concentrated load P acting on the beam element (Fig. 4-8b). In order to have a sign convention for concentrated loads, we assume that a *downward load is positive*. As before, the stress resultants on the left-hand face are denoted by V and M . On the right-hand face, they are denoted by $V + V_1$ and $M + M_1$, where V_1 and M_1 represent the possible increments in the shear force and bending moment. From equilibrium of forces in the vertical direction, we get

$$V_1 = -P \tag{4-5}$$

Thus, an abrupt change occurs in the shear force at a point where a concentrated load acts. As we pass from left to right through the point of load application, the shear force decreases by an amount equal to the magnitude of the downward load. From equilibrium of moments (Fig. 4-8b), we get

$$-M - P \left(\frac{dx}{2}\right) - (V + V_1) dx + M + M_1 = 0$$

or

$$M_1 = P \left(\frac{dx}{2}\right) + V dx + V_1 dx$$

Since the length dx of the element is infinitesimally small, we see from this equation that the increment M_1 in the bending moment is also infinitesimally small. Thus, we conclude that the bending moment does

not change as we pass through the point of application of a concentrated load.

Even though the bending moment M does not change at a concentrated load, its rate of change (derivative) dM/dx undergoes an abrupt change. At the left-hand side of the element (Fig. 4-8b), the rate of change of the bending moment (see Eq. 4-3) is $dM/dx = V$. At the right-hand side, the rate of change is $dM/dx = V + V_1$. Therefore, the rate of change dM/dx decreases abruptly by an amount equal to P .

The last case is a load in the form of a couple M_0 , assumed to be positive when counterclockwise (Fig. 4-8c). From equilibrium of the element in the vertical direction, we obtain $V_1 = 0$, which shows that the shear force does not change at the point of application of a couple. Equilibrium of moments for the element gives

$$-M + M_0 - (V + dV)dx + M + M_1 = 0$$

or, disregarding terms that contain differentials,

$$M_1 = -M_0 \quad (4-5)$$

This equation shows that there is an abrupt decrease in the bending moment in the beam due to the applied couple M_0 as we move from left to right through the point of load application.

Equations (4-1) through (4-6) are useful when making a complete investigation of the shear forces and bending moments in a beam, as illustrated in the next section.

we construct a free-body diagram of the left-hand part of the beam, and we find from equilibrium that

$$V = R_a = \frac{Pb}{L} \quad M = R_a x = \frac{Pbx}{L} \quad (b)$$

These equations show that the shear force is constant from support A to the point of application of the load P and that the bending moment varies linearly with x . The expressions for V and M are plotted directly beneath the sketch of the beam (Fig. 4-9). In the case of the shear-force diagram, we begin at the end of the beam with an abrupt jump in the diagram, we begin at the reaction R_a . Then the shear force remains constant up to $x = a$. In this same region, the bending-moment diagram is a straight line increasing from $M = 0$ at the support to $M = Pab/L$ at $x = a$.

Next we cut through the beam to the right of the load P (that is, in the region $a < x < L$), and, from equilibrium of the left-hand part of the beam, we obtain the following expressions:

$$V = \frac{Pb}{L} - P = -\frac{Pa}{L} \quad (c)$$

$$M = \frac{Pbx}{L} - P(x - a) = Pa\left(1 - \frac{x}{L}\right) \quad (d)$$

Again we see that the shear force is constant and that the bending moment is a linear function of x . At $x = a$, the bending moment is equal to Pab/L ; at $x = L$, it is zero. Equations (c) and (d) for V and M are also plotted on the diagrams in Fig. 4-9.

In deriving Eqs. (c) and (d) for the shear force and bending moment to the right of the load P , we considered the equilibrium of the left-hand part of the beam, which is acted upon by the two forces R_a and P . It would have been slightly simpler in this example to consider the right-hand portion of the beam as a free body. From equilibrium of the right-hand part, we obtain the equations

$$V = -R_b = -\frac{Pa}{L} \quad M = R_b(L - x) = \frac{Pa}{L}(L - x)$$

which are the same results as obtained from Eqs. (c) and (d).

Let us now observe certain characteristics of the diagrams in Fig. 4-9. We note first that the slope dV/dx of the shear-force diagram is zero in the regions $0 < x < a$ and $a < x < L$, which is in accord with the equation $dV/dx = -q$ (Eq. 4-1). Also, in these same regions, the slope dM/dx of the bending moment is equal to V (Eq. 4-3). At the point of application of the load P , there is an abrupt change in the slope of the shear-force diagram (equal to P) and a corresponding change in the slope of the bending-moment diagram. To the left of the load P , the slope of the shear-force diagram is positive and equal to Pb/L ; to the right, it is negative and equal to $-Pa/L$.

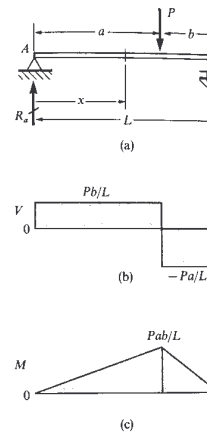


Fig. 4-9 Shear-force and bending-moment diagrams for a simple beam with a concentrated load

4.4 SHEAR-FORCE AND BENDING-MOMENT DIAGRAMS

The shear forces V and bending moments M in a beam are functions of the distance x measured along the longitudinal axis. When designing a beam, it is desirable to know the values of V and M at all cross sections. A convenient way to provide this information is to draw a graph showing how V and M vary with x . To plot such a graph, we take the abscissa as the position of the cross section (that is, the distance x), and we take the ordinate as the corresponding value of either the shear force or the bending moment. These graphs are called **shear-force and bending-moment diagrams**.

To illustrate the construction of the diagrams, let us consider a simple beam AB carrying a concentrated load P (Fig. 4-9a). The reactions for this beam are

$$R_a = \frac{Pb}{L} \quad R_b = \frac{Pa}{L} \quad (e)$$

as found from equilibrium of the entire beam. Next, we cut through the beam to the left of the load P and at distance x from support A . Then

Shear Force and Bending Moment



nd bending-moment diagrams for a simple beam

Consider next the area of the shear-force diagram (see Eq. 4-4). As we move from $x = 0$ to $x = a$, the area of the shear-force diagram is $(Pb/L)a$, or Pab/L . This quantity represents the increase in bending moment between these same two points. From $x = a$ to $x = L$, the area of the shear-force diagram is $-Pab/L$, which means that in this region the bending moment decreases by that amount. Thus, the bending moment is zero at end B of the beam, as expected. If we consider the entire shear-force diagram, and if we note that $M = 0$ at both ends of the beam, then Eq. (4-4) requires that the area of the diagram between the ends of the beam be zero. This conclusion would not apply if the beam were subjected to a load in the form of a couple.

The maximum or minimum values of shear forces and bending moments are needed when designing beams. For a simple beam with a single concentrated load, the maximum shear force occurs at the end of the beam nearest to the concentrated load, and the maximum bending moment occurs under the load itself.

To further illustrate the construction of shear-force and bending-moment diagrams, let us consider a simple beam with a uniformly distributed load (Fig. 4-10a). In this case, each of the reactions R_a and R_b is equal to $qL/2$; hence, at a cross section at distance x from the left-hand end A , we obtain

$$V = \frac{qL}{2} - qx \quad M = \frac{qLx}{2} - \frac{qx^2}{2} \quad (f)$$

The first of these equations shows that the shear-force diagram consists of an inclined straight line having ordinates $qL/2$ and $-qL/2$ at $x = 0$ and $x = L$, respectively (Fig. 4-10b). The slope of this line is $-q$, as expected from the equation $dV/dx = -q$ (Eq. 4-1). The bending-moment diagram is a parabolic curve that is symmetric about the middle of the beam (Fig. 4-10c). At each cross section, the slope of the bending-moment diagram is equal to the shear force (see Eq. 4-3):

$$\frac{dM}{dx} = \frac{d}{dx} \left(\frac{qLx}{2} - \frac{qx^2}{2} \right) = \frac{qL}{2} - qx = V$$

The maximum value of the bending moment occurs at the point where $dM/dx = 0$ (that is, at the cross section where the shear force is zero). This section is at the middle of the beam in our example; hence, we substitute $x = L/2$ into the expression for M to obtain

$$M_{\max} = \frac{qL^2}{8} \quad (i)$$

as shown in the bending-moment diagram.

The diagram of load intensity (Fig. 4-10a) has area qL . In accord with Eq. (4-2), the shear force V decreases by this amount as we move along the beam from A to B . The area of the shear-force diagram between $x = 0$ and $x = L/2$ is $qL^2/8$, and this area represents the increase

in the bending moment between those same two points. In a similar manner, the bending moment decreases by $qL^2/8$ as we proceed from $x = L/2$ to $x = L$.

If several concentrated loads act on a simple beam (Fig. 4-11a), expressions for V and M may be determined for each region of the beam between the points of load application. Again measuring distance x from end A of the beam, we obtain for the first region of the beam ($0 < x < a_1$) the following equations:

$$V = R_a \quad M = R_a x \quad (g)$$

For the second region ($a_1 < x < a_2$), we obtain

$$V = R_a - P_1 \quad M = R_a x - P_1(x - a_1) \quad (h)$$

For the third region of the beam ($a_2 < x < a_3$), it is advantageous to consider the right-hand part of the beam rather than the left, because fewer loads act on the corresponding free body. Hence, we obtain

$$V = -R_b + P_3 \quad (i)$$

and

$$M = R_b(L - x) - P_3(L - b_3 - x) \quad (j)$$

Finally, for the fourth portion of the beam, we obtain

$$V = -R_b \quad M = R_b(L - x) \quad (k)$$

From Eqs. (g) through (k) we see that in each region of the beam the shear force remains constant; hence, the shear-force diagram has the shape shown in Fig. 4-11b. Also, the bending moment in each part of the beam is a linear function of x ; therefore, the corresponding diagram is represented by an inclined straight line. To assist in drawing these lines, we obtain the bending moments under the concentrated loads by substituting $x = a_1$, $x = a_2$, and $x = a_3$ into Eqs. (g), (h), and (k), respectively. In this manner we obtain for the bending moments the values

$$M_1 = R_a a_1 \quad M_2 = R_a a_2 - P_1(a_2 - a_1) \quad M_3 = R_b b_3 \quad (l)$$

From these values, we can readily construct the bending-moment diagram (Fig. 4-11c) because the diagram consists of straight lines between points of loading.

Note that, at each point where a concentrated load acts, the shear-force diagram changes abruptly by an amount equal to the load. Furthermore, at each such discontinuity in shear force, there is a corresponding change in the slope dM/dx of the bending-moment diagram. Also, the change in bending moment between two load points equals the area of the shear-force diagram between those same two points (see Eq. 4-4). For example, the change in bending moment between loads P_1 and P_2 is $M_2 - M_1$. Substituting from Eqs. (l), we get

$$M_2 - M_1 = (R_a - P_1)(a_2 - a_1)$$

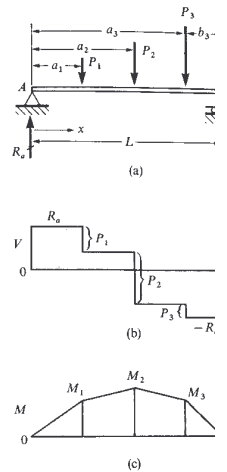


Fig. 4-11 Shear-force and bending-moment diagrams for a simple beam with several concentrated loads

which is the area of the rectangular shear-force diagram between a_1 and $x = a_2$.

The maximum bending moment in a beam with only concentrated loads must occur under one of the loads or at a reaction. From the equation $dM/dx = V$, we know that the slope of the bending-moment diagram is equal to the shear force. Hence, the bending moment is maximum or minimum value at cross sections where the shear force changes sign, which occurs only under a load. If, as we proceed along the x axis, the shear force changes from a positive to a negative value (as in Fig. 4-11b), then the slope in the bending-moment diagram changes from positive to negative. Therefore, we must have a maximum bending moment at this cross section. Conversely, a change in the shear force from a negative to a positive value indicates a minimum bending moment. The shear-force diagram can (but usually does not) intersect the horizontal axis at several points. Corresponding to each such intersection point, there is a local maximum or minimum in the bending-moment diagram. The values of all local maximums and minimums must be calculated in order to find the absolute maximum positive and negative bending moments in the beam for use in design.

In general, the maximum positive or negative bending moment in a beam may occur at a concentrated load (provided the shear force changes sign at the load), at a reaction, at a cross section where the shear force equals zero (see Fig. 4-10), or at a section where a couple is applied. The discussions and examples in this section illustrate all of these possibilities.

When several loads act on a beam, the shear-force and bending-moment diagrams can be obtained by superposition (or summation) of the diagrams obtained from each of the loads acting separately. For instance, the shear-force diagram of Fig. 4-9b is actually the sum of three separate diagrams, each of the type shown in Fig. 4-9b for a single concentrated load. We can make an analogous comment for the bending-moment diagram of Fig. 4-11c. These conclusions concerning superposition of shear-force and bending-moment diagrams follow from the fact that shear forces and bending moments are linear functions of the applied loads.

Example 1

Determine the shear-force and bending-moment diagrams for a simple beam with a uniform load of constant intensity q acting over a part of the span (Fig. 4-12a).

We begin the analysis by determining the reactions for the beam:

$$R_a = \frac{qb}{L} \left(c + \frac{b}{2} \right) \quad R_b = \frac{qb}{L} \left(a + \frac{b}{2} \right)$$

To obtain the shear forces and bending moments, we consider separately the three regions of the beam. For the left-hand part of the beam ($0 < x < a$), we

$$V = R_a \quad M = R_a x \quad (n)$$

For a cross section within the loaded portion of the beam, the shear force is obtained by subtracting from the reaction R_a the load $q(x-a)$ acting on the beam to the left of the cross section. The bending moment in this same region is obtained by subtracting the moment of the load to the left of the cross section from the moment of the reaction R_a . In this manner, we find

$$V = R_a - q(x-a) \quad (o)$$

$$M = R_a x - \frac{q(x-a)^2}{2} \quad (p)$$

For the unloaded portion of the beam at the right-hand end, we get

$$V = -R_b \quad M = R_b(L-x) \quad (q)$$

Using Eqs. (n) through (q), we can readily construct the shear-force and bending-moment diagrams.

The shear-force diagram (Fig. 4-12b) consists of horizontal straight lines in the unloaded regions of the beam and an inclined straight line in the loaded region, as expected from the equation $dV/dx = -q$. The bending-moment diagram (Fig. 4-12c) consists of two inclined straight lines in the unloaded portions of the beam and a parabolic curve in the loaded portion. The inclined lines have slopes equal to R_a and $-R_b$, respectively (see Eq. 4-3). Each of these lines is tangent to the parabolic curve at the point where it meets the curve. This tangency follows from the fact that there are no abrupt changes in the magnitude of the shear force at these points. Hence, from Eq. (4-3), we see that the slope of the bending-moment diagram cannot change abruptly. The maximum bending moment occurs where the shear force equals zero. Its value can be found by setting the shear force V (from Eq. o) equal to zero, solving for x , and then substituting this value of x into the expression for the bending moment (Eq. p).

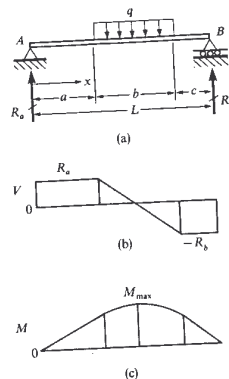


Fig. 4-12 Example 1

Example 2

Construct the shear-force and bending-moment diagrams for the cantilever beam shown in Fig. 4-13a.

Again measuring distance x from the left-hand end of the beam, and considering first the region $0 < x < a$, we obtain

$$V = -P_1 \quad M = -P_1 x$$

For the right-hand portion of the beam ($a < x < L$), we obtain

$$V = -P_1 - P_2 \quad M = -P_1 x - P_2(x-a)$$

The corresponding shear-force and bending-moment diagrams are shown in Figs. 4-13b and c. The shear force is constant between the loads, and it reaches its maximum numerical value at the support. The bending-moment diagram consists of two inclined straight lines, the slopes of which are equal to the shear forces in the corresponding portions of the cantilever beam. The maximum bending moment occurs at the support ($x = L$), and it is equal to the area of the shear-force diagram, as expected from Eq. (4-4).

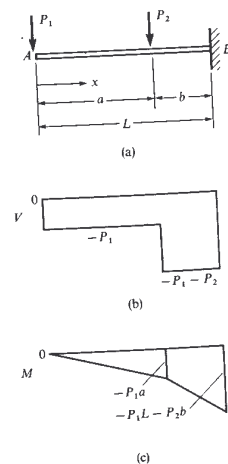
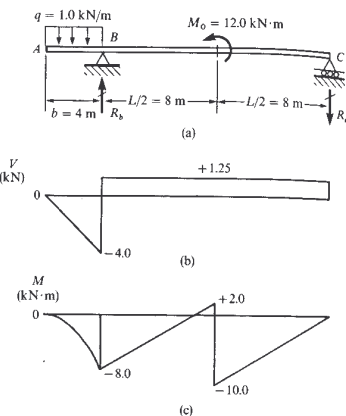


Fig. 4-13 Example 2

Example 3

Construct shear-force and bending-moment diagrams for the beam with an overhang shown in Fig. 4-14a. The beam is subjected to a uniform load of constant intensity $q = 1.0$ kN/m on the overhang and a counterclockwise couple $M_0 = 12.0$ kN·m acting midway between the supports.



We can readily calculate the reactions R_b and R_c , and we find that R_b is upward and R_c is downward, as shown in the figure. Their numerical values are as follows:

$$R_b = 5.25 \text{ kN} \quad R_c = 1.25 \text{ kN}$$

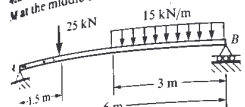
Utilizing the techniques already described, we now draw the shear-force diagram (Fig. 4-14b). Note that the shear force does not change at the point of application of the couple M_0 . The bending-moment diagram has the shape shown in Fig. 4-14c. At B , the moment is

$$M_b = \frac{qb^2}{2} = -\frac{1}{2}(1.0 \text{ kN/m})(4 \text{ m})^2 = -8.0 \text{ kN}\cdot\text{m}$$

which is also equal to the area of the shear-force diagram between A and B . The slope of the bending-moment diagram from B to C is 1.25 kN (that is, the slope equals the shear force), but the bending moment changes abruptly due to the couple M_0 . Note that this change is equal to M_0 (see Eq. 4-6). Maximum minimum values of the bending moment occur where the shear force changes sign and where the couple is applied.

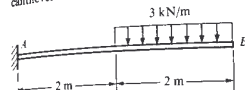
PROBLEMS/CHAPTER 4

4.2-1 Determine the shear force V and bending moment M at the middle of the simple beam AB shown in the figure.



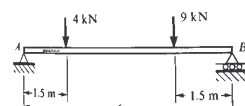
Prob. 4.2-1

4.2-2 Calculate the shear force V and bending moment M at a section located 1.0 m from the fixed support A of the cantilever beam shown in the figure.



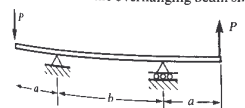
Prob. 4.2-2

4.2-3 Find the shear force V and bending moment M at a section just to the left of the 9 kN load acting on the simple beam AB shown in the figure.



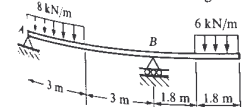
Prob. 4.2-3

4.2-4 What are the shear force V and bending moment M at the middle of the overhanging beam shown in the figure?



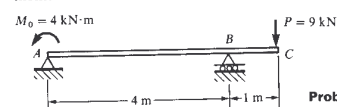
Prob. 4.2-4

4.2-5 Find the shear force V and bending moment M at a section located 4.5 m from the left-hand end A of the beam with an overhang shown in the figure.



Prob. 4.2-5

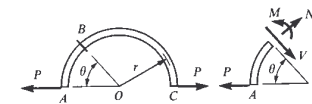
4.2-6 The beam shown in the figure is simply supported at A and B and is subjected to a couple $M_0 = 4$ kN·m at A and a concentrated load $P = 9$ kN at the end of the overhang. Determine the shear force V and bending moment M at a section 3 m from the left-hand support.



Prob. 4.2-6

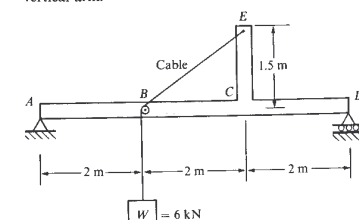
4.2-7 A lumberjack weighing 102 kg stands at the midpoint of a floating log that is 4 m long. What is the maximum bending moment in the log?

4.2-8 A curved bar ABC is subjected to loads in the form of two equal and opposite forces P , as shown in the figure. The axis of the bar forms a semicircle of radius r . Determine the axial force N , shear force V , and bending moment M acting at a cross section defined by the angle θ (see figure).



Prob. 4.2-8

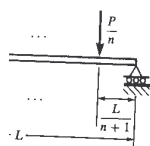
4.2-9 The beam $ABCD$ is loaded by a force $W = 6$ kN by the arrangement shown in the figure. The cable passes over a small frictionless pulley at B and is attached at E to the vertical arm. Calculate the shear force V and bending moment M at section C , which is just to the left of the vertical arm.



Prob. 4.2-9

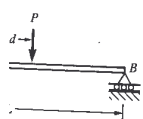
4.4 Shear Force and Bending Moment

loads on a simple beam consist of n equally spaced loads (see figure). The total applied load is P ; therefore each load is P/n . The length of the beam is L , and the distance between loads is $L/(n+1)$. (a) Derive a formula for the maximum bending moment in the beam. (b) For each of these formulas, determine the maximum bending moment for several successive values of n . (c) Compare these results with the maximum bending moment in the beam due to a uniformly distributed load of intensity q such that $qL = P$.



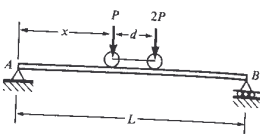
Prob. 4.4-37

all loads P are separated by a fixed distance d . This load combination may be considered as a uniformly distributed load of intensity $q = P/d$. For what distance x will the shear force be zero? Also, derive a formula for the maximum bending moment in the beam. (b) Derive a formula for the maximum bending moment in the beam. (c) Compare these results with the maximum bending moment in the beam due to a uniformly distributed load of intensity q such that $qL = P$.



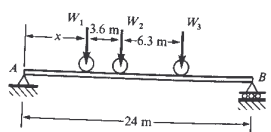
Prob. 4.4-38

4.4-39 A simple beam AB carries two connected wheel loads P and $2P$ that are distance d apart (see figure). The support of the beam may be placed at any distance x from the left-hand support of the beam. Determine the distance x for which the maximum shear force in the beam and (b) the maximum bending moment in the beam if $P = 6$ kN, $d = 1.6$ m, and $L = 8$ m. Also, determine the maximum shear force V_{max} and maximum bending moment M_{max} .



Prob. 4.4-39

4.4-40 Three wheel loads W_1 , W_2 , and W_3 move across a simply supported beam as shown in the figure. Determine the position of the wheels, as defined by the distance x from end A , so as to produce the maximum bending moment in the beam, assuming that $W_1 = 20$ kN and $W_2 = W_3 = 80$ kN. Also, determine the maximum bending moment M_{max} .



Prob. 4.4-40

5.1 INTRODUCTION

A beam is a structural member that is subjected to loads acting transversely to the longitudinal axis, as explained in the preceding chapter. The loads create internal actions, or stress resultants, in the form of shear forces and bending moments. In this chapter, we discuss the stresses and strains associated with the shear forces and bending moments, and we also examine several topics of practical importance in the design of beams. We will consider only beams having initially straight longitudinal axes.

Lateral loads acting on a beam cause the beam to bend, or flex, thereby deforming the axis of the beam into a curved line. An illustration is given in Fig. 5-1, which shows a cantilever beam AB subjected to a load P at the free end. Before the load is applied, the longitudinal axis of the beam is a straight line. After loading, the axis is bent into a curve (Fig. 5-1b) that is known as the **deflection curve** of the beam.

For reference purposes, we construct a system of coordinate axes with its origin at the support. The positive x axis is directed to the right along the longitudinal axis of the beam, and the y axis is positive downward. The z axis, which is not shown in this figure, is directed inward (that is, away from the viewer), so that the axes form a right-handed coordinate system.

The beams considered in this chapter are assumed to be symmetric about the xy plane, which means that the y axis is an axis of symmetry of the cross sections. In addition, all loads are assumed to act in the xy plane, as a consequence, the bending deflections occur in this same plane, which is known as the **plane of bending**. Thus, the deflection plane AB of the beam shown in Fig. 5-1b is a plane curve lying in the plane of bending. We will denote the deflection in the y direction by the letter v .

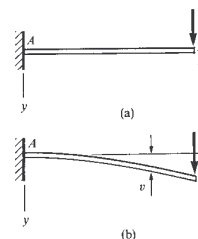
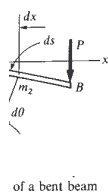


Fig. 5-1 Bending of a cantilever beam

Stresses in Beams



Now consider two points m_1 and m_2 on the deflection curve (Fig. 5-2); point m_1 is located at distance x from the y axis, and point m_2 is situated a small distance ds further along the curve. At each of these points, we draw a line normal to the tangent to the deflection curve. These normals intersect at point O' , which is the **center of curvature** for the deflection curve at distance x from the support. The length of a normal (that is, the distance from the center of curvature to the curve itself) is called the **radius of curvature** ρ (Greek letter rho). As defined in calculus and analytic geometry, the **curvature** κ (Greek letter kappa) is the reciprocal of the radius of curvature:

$$\kappa = \frac{1}{\rho} \quad (5-1)$$

Also, from the geometry of the figure, we obtain

$$\rho d\theta = ds \quad (5-2)$$

in which $d\theta$ is the small angle between the normals and ds is the distance along the curve between the normals. If the deflections of the beam are small, which is the most common situation, then the deflection curve is very flat and the distance ds along the curve may be set equal to its horizontal projection dx (Fig. 5-2). We then obtain

$$\kappa = \frac{1}{\rho} = \frac{d\theta}{dx} \quad (5-1)$$

In general, the curvature varies along the axis of the beam; that is, κ is a function of x .

The **sign convention for curvature** is related to the orientation of the coordinate axes. If the x axis is positive to the right and the y axis is positive downward, as shown in Fig. 5-2, then the curvature of the beam axis is positive when the beam is bent concave downward and negative when it is bent concave upward. This sign convention is portrayed in Fig. 5-3. We have not adopted this sign convention by choice; rather, it is established mathematically from the directions of the coordinate axes, as explained in Section 6.1.

Equation (5-1) will be used in the next section for obtaining the strains in a bent beam and in Chapter 6 for determining the equation of the deflection curve. However, before beginning a discussion of flexural strains and stresses, we need to point out the distinction between pure bending and nonuniform bending. **Pure bending** refers to flexure of a beam under a constant bending moment, which means that the shear force is zero (because $V = dM/dx$; see Eq. 4-3). In contrast, **nonuniform bending** refers to flexure in the presence of shear forces, which means that the bending moment changes as we move along the axis of the beam. To illustrate these definitions, consider a simple beam loaded symmetrically by two point loads P (see Fig. 5-4). The shear force and

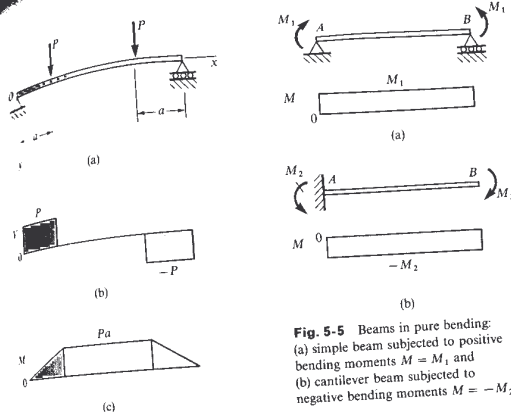


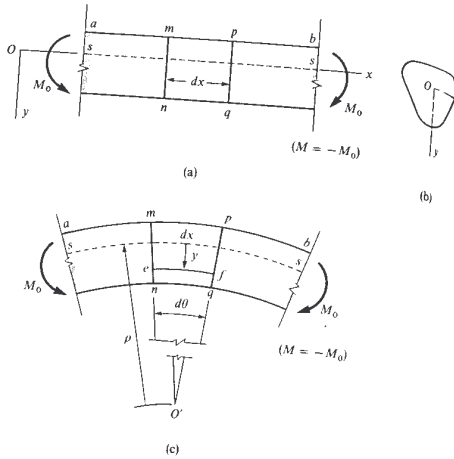
Fig. 5-4 Beam with central region in pure bending

bending-moment diagrams are shown in Figs. 5-4b and c. The region between the loads P has no shear force and is subjected only to a constant bending moment equal to Pa ; hence, the central region of this beam is in pure bending. The regions of length a near the ends of the beam are in nonuniform bending because the bending moment M is not constant and shear forces are present. Other examples of pure bending are shown in Fig. 5-5. In each of these latter cases, the beam is loaded only by couples that produce constant bending moments and no shear forces. In the next two sections, we will determine the normal strains and stresses in pure bending, and then in later sections we will investigate the shear stresses in nonuniform bending.

5.2 NORMAL STRAINS IN BEAMS

To find the internal strains in a beam, we must consider the curvature of the beam and the associated deformations. For this purpose, Fig. 5-6a shows a portion ab of a beam in pure bending produced by couples M_0 . The directions of the couples M_0 are selected so as to produce positive curvature of the bent beam (see Fig. 5-3a), although they produce negative bending moments M (see Figs. 4-3 and 4-4). Hence, the bending moment M equals $-M_0$, as indicated in Fig. 5-6. The beam initially has a straight longitudinal axis (the x axis), and the cross-section may be of any shape provided it is symmetric about the y axis (Fig.

Fig. 5-5 Beams in pure bending: (a) simple beam subjected to positive bending moments $M = M_1$ and (b) cantilever beam subjected to negative bending moments $M = -M_2$



Deformations of a beam in bending produced by couples M_0 . The bending moment M equals M_0 .

the cross section; for instance, the z axis is the neutral axis for the cross section shown in Fig. 5-6b.

The planes of cross sections mn and pq of the deformed beam intersect in a line through the center of curvature O' (Fig. 5-6c). The angle between these planes is denoted $d\theta$, and the distance from O' to the neutral surface is the radius of curvature ρ . The initial distance dx between the two planes (Fig. 5-6a) is unchanged at the neutral surface (Fig. 5-6c), hence $\rho d\theta = dx$. However, all other longitudinal fibers either lengthen or shorten, thereby creating longitudinal strains ϵ_x . To evaluate these strains, consider a typical longitudinal fiber ef located within the beam at a distance y from the neutral surface (Fig. 5-6c). The length L_1 of this fiber is

$$L_1 = (\rho - y)d\theta = dx - \frac{y}{\rho} dx$$

Inasmuch as the original length of ef is dx , it follows that its elongation is $L_1 - dx$, or $-y dx/\rho$. The corresponding strain is equal to the elongation divided by the initial length dx ; hence,

$$\epsilon_x = -\frac{y}{\rho} = -\kappa y \tag{5-2}$$

where κ is the curvature. This equation shows that the longitudinal strains in the beam are proportional to the curvature and that they vary linearly with the distance y from the neutral surface. When a fiber is below the neutral surface, the distance y is positive; if the curvature also is positive (as in Fig. 5-6c), then ϵ_x will be a negative strain, representing a shortening. When a fiber is above the neutral surface, the distance y is negative; then, for positive curvature, ϵ_x will be positive, which represents an elongation. Note that the sign convention for ϵ_x in Eq. (5-2) is the same as that used for normal strains in earlier chapters.

We derived Eq. (5-2) solely from the geometry of the deformed beam; the properties of the material did not enter into the discussion. Therefore, the equation is valid irrespective of the shape of the stress-strain diagram of the material.

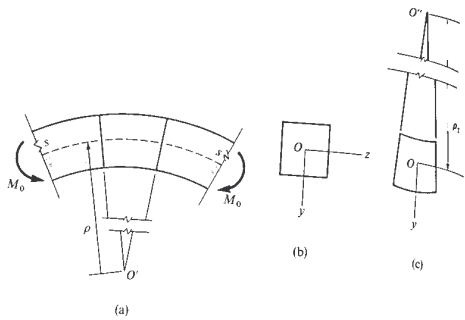
Transverse strains. The axial strains ϵ_x given by Eq. (5-2) are accompanied by lateral or transverse strains ϵ_z due to the effects of Poisson's ratio, as discussed in Section 1.5. Positive strains ϵ_x above the neutral surface (Fig. 5-7a) are accompanied by negative transverse strains, whereas below the neutral axis the transverse strains are positive. Thus, the transverse strains are given by the equation

$$\epsilon_z = -\nu \epsilon_x = \nu \kappa y \tag{5-3}$$

in which ν is Poisson's ratio. As a result of these strains, the shape of

5-6b). Under the action of the couples M_0 , the beam deflects in the xy plane and its axis is bent into a circular curve (Fig. 5-6c). Cross sections of the beam, such as mn and pq , remain plane and normal to longitudinal lines, or fibers, of the beam. The fact that cross sections of a beam in pure bending remain plane can be established experimentally by making precise strain measurements, or it can be proven theoretically using arguments of symmetry. The symmetry of the beam and its loading (Fig. 5-6a) requires that all elements of the beam (such as element $mnop$) deform in an identical manner, which is possible only if the deflection curve is circular (Fig. 5-6c) and if cross sections remain plane during loading (Ref. 5-1). These conclusions are valid for a beam of any material (elastic or inelastic, linear or nonlinear); of course, the material properties must be symmetric about the y axis (Fig. 5-6b).

As a result of the bending deformations shown in Fig. 5-6c, cross sections mn and pq rotate with respect to each other about axes perpendicular to the xy plane. The longitudinal fibers on the convex side of the beam are elongated, whereas those on the concave side are shortened. Thus, the fibers in the upper part of the beam are in tension, whereas those in the lower part are in compression. Somewhere between the top and bottom of the beam is a surface in which the longitudinal fibers do not change in length. This surface, indicated by the dashed line ss in Figs. 5-6a and c, is called the **neutral surface** of the beam. Its intersection with any cross-sectional plane is called the **neutral axis** of



Deformations of a beam in bending.

the cross section changes. For instance, consider a beam of rectangular cross section (Fig. 5-7b). The strains ϵ_x cause the width of the cross section to increase below the z axis and decrease above. Since these changes in width are directly proportional to y (Eq. 5-3), the sides of the rectangular cross section become inclined to each other (Fig. 5-7c). Also, all straight lines in the cross section that were originally parallel to the z axis become slightly curved so as to remain normal to the sides of the section. The center of curvature O'' of these lines is above the beam, and the corresponding transverse radius of curvature ρ_1 is larger than the longitudinal radius of curvature ρ in the same proportion that ϵ_z is numerically larger than ϵ_x (see Eq. 5-3); hence, we obtain

$$\rho_1 = \frac{\rho}{\nu} \quad \kappa_1 = \nu \kappa \tag{5-4a, b}$$

in which $\kappa_1 = 1/\rho_1$ is the transverse curvature.

The deformed shape of a rectangular beam in pure bending by couples M_0 is shown highly exaggerated in Fig. 5-8. The longitudinal curvature in the xy plane is positive, whereas the transverse curvature in the yz plane is negative. As a result, the top surface of the beam becomes saddle shaped. When a surface has curvatures of opposite signs in two perpendicular planes, as in the case of a saddle, it is said to have **anticlastic curvature**. By contrast, if the curvatures are of the same sign, as when the surface has the shape of a dome, the curvature is **synclastic**. We see from Fig. 5-8 that all planes of the beam that were initially parallel to the neutral surface (the xz plane) develop anticlastic curva-

Example

A simply supported steel beam AB (Fig. 5-9) of length $L = 4$ m is bent by couples M_0 that produce a strain at the top surface of the beam equal to the yield strain of the steel. The distance from the top surface of the beam to the neutral surface is 150 mm. Calculate the radius of curvature ρ , the curvature κ , and the vertical deflection δ at the middle of the beam, assuming that the yield strain is 0.0014. Equation (5-2) relates ρ and κ to the normal strain ϵ_x . Substituting into that equation, and using only absolute values, we obtain

$$\rho = \frac{y}{\epsilon_x} = \frac{150 \text{ mm}}{0.0014} = 107.14 \text{ m}$$

$$\kappa = \frac{1}{\rho} = 0.0093/\text{m}$$

These results show that, even at relatively large strains in the material, the radius of curvature is extremely large and, hence, the deflection curve of the beam is very flat.

To further emphasize this point, let us now calculate the deflection δ at the middle of the beam. Because the deflection curve is a circular arc, we see that the deflection δ is

$$\delta = \rho(1 - \cos \theta) \tag{a}$$

where θ is the angle shown in the figure; that is,

$$\sin \theta = \frac{L}{2\rho} \tag{b}$$

Substitution of numerical values produces the following results:

$$\frac{L}{2\rho} = 0.0187 \quad \theta = \arcsin \frac{L}{2\rho} = 0.0187 \text{ rad}$$

$$\delta = \rho(1 - \cos \theta) = (107.14 \text{ m})(1 - 0.9998252) = 0.0187 \text{ m} = 18.7 \text{ mm}$$

Thus, the ratio of the span length of the beam to the deflection at the middle is

$$\frac{L}{\delta} = \frac{4 \text{ m}}{0.0187 \text{ m}} = 214$$

which confirms that the deflection curve is extremely flat. Of course, the deflection δ shown in the figure is highly exaggerated for clarity.

Inasmuch as $L/2\rho$ is a small quantity and θ is a small angle, we may use the following approximate relationships:

$$\sin \theta \approx \theta \quad \cos \theta \approx 1 - \frac{\theta^2}{2} \tag{c}$$

Then Eqs. (b) and (a) become

$$\theta \approx \frac{L}{2\rho} \quad \delta \approx \frac{\rho \theta^2}{2} = \frac{L^2}{8\rho} \tag{d}$$

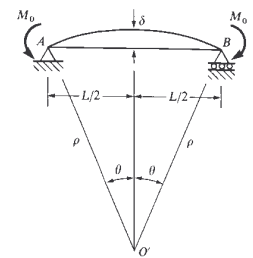


Fig. 5-9 Example

Again substituting numerical values, we find

$$\theta = 0.0187 \quad \delta = 18.7 \text{ mm}$$

which are the same results as obtained before. To detect the differences in results between the exact formulas (Eqs. a and b) and the approximate formulas (Eq. d), we must calculate to a larger number of significant digits.

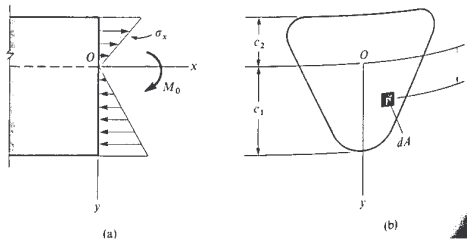
5.3 NORMAL STRESSES IN BEAMS

We can obtain the stresses σ_x acting normal to the cross section of a beam from the normal strains ϵ_x . Each longitudinal fiber of the beam is subjected only to tension or compression (that is, the fibers are in uniaxial stress); hence, the stress-strain diagram for the material will provide the relationship between σ_x and ϵ_x . If the material is elastic with a linear stress-strain diagram, we can use Hooke's law for uniaxial stress ($\sigma = E\epsilon$) and obtain

$$\sigma_x = E\epsilon_x = -E\kappa y \quad (5-5)$$

(see Eq. 5-2). Thus, the normal stresses acting on the cross section vary linearly with distance y from the neutral surface. This type of stress distribution is pictured in Fig. 5-10a, where the stresses are negative (compression) below the neutral surface and positive (tension) above the surface when the applied couple M_0 acts in the direction shown. As explained in the preceding section, this couple produces a positive curvature κ in the beam, although it represents a negative bending moment M .

Let us now consider the resultant of the normal stresses σ_x acting over the cross section. In general, this resultant may consist of a horizontal force in the x direction and a couple acting about the z axis. However, because no axial force acts on the cross section, the only resultant is the couple M_0 . Thus, we obtain two equations of statics



Distribution of normal stress in a beam of linear elastic material

the first states that the resultant force in the x direction is zero, and the second states that the resultant moment is equal to M_0 . To evaluate these resultants, consider an element of area dA in the cross section at distance y from the neutral axis (Fig. 5-10b). The force acting on this element is normal to the cross section and has a magnitude $\sigma_x dA$. Because no resultant normal force acts on the cross section, the integral of $\sigma_x dA$ over the entire area of the cross section must vanish; thus,

$$\int \sigma_x dA = - \int E\kappa y dA = 0$$

Because the curvature κ and modulus of elasticity E are constants at the cross section, we conclude that

$$\int y dA = 0 \quad (5-6)$$

for a beam in pure bending. This equation shows that the first moment of the area of the cross section with respect to the z axis is zero; hence, we see that the z axis must pass through the centroid of the cross section. Since the z axis is also the neutral axis, we conclude that the neutral axis passes through the centroid of the cross section when the material of the beam follows Hooke's law. This property can be used to determine the position of the neutral axis for a beam of any cross-sectional shape. Of course, our discussion is limited to beams for which the y axis is an axis of symmetry, as explained previously. As a consequence, the y axis also must pass through the centroid; hence, the origin of coordinates O is located at the centroid of the cross section. In addition, the symmetry of the cross section about the y axis means that the y axis is a principal axis (see Section C.8, Appendix C, for a discussion of principal axes). The z axis is also a principal axis since it is perpendicular to the y axis. Therefore, when a beam of linear elastic material is subjected to pure bending, the y and z axes are principal centroidal axes.

Let us consider next the moment resultant of the stresses σ_x acting over the cross section (Fig. 5-10a). The element of force $\sigma_x dA$ on the element dA acts in the positive direction of the x axis when σ_x is positive and in the negative direction when σ_x is negative. Hence, its moment about the z axis, which represents the infinitesimal contribution of $\sigma_x dA$ to the moment M_0 , is

$$dM_0 = -\sigma_x y dA$$

The integral of all such elemental moments over the entire cross-sectional area must result in the total moment M_0 ; thus,

$$M_0 = - \int \sigma_x y dA$$

Noting again that the bending moment M is equal to $-M_0$, and also substituting for σ_x from Eq. (5-5), we get

$$M = \int \sigma_x y dA = -\kappa E \int y^2 dA$$

This equation can be expressed in the simpler form

$$M = -\kappa EI$$

in which

$$I = \int y^2 dA$$

is the moment of inertia of the cross-sectional area with respect to the z axis (that is, with respect to the neutral axis). Moments of inertia have dimensions of length to the fourth power, and typical units are in⁴, ft⁴, and mm⁴ for beam calculations.* Equation (5-7) can be rearranged as follows:

$$\kappa = \frac{1}{\rho} = -\frac{M}{EI} \quad (5-8)$$

This equation shows that the curvature of the longitudinal axis of a beam is proportional to the bending moment M and inversely proportional to the quantity EI , which is known as the **flexural rigidity** of the beam.

The minus sign in the moment-curvature equation (Eq. 5-9) is a consequence of the sign convention we have adopted for bending moments. Comparing the sign convention for moments (Fig. 4-3) with that for curvatures (Fig. 5-3), we see that a positive bending moment produces negative curvature and a negative moment produces positive curvature, as shown in Fig. 5-11. (If the opposite sign convention for bending moments is used, or if the y axis is positive upward, then the minus sign is omitted in Eq. 5-9.)

The normal stresses in the beam are related to the bending moment by substituting the expression for curvature (Eq. 5-9) into the expression for σ_x (Eq. 5-5), yielding

$$\sigma_x = \frac{My}{I} \quad (5-10)$$

This equation shows that the stresses are proportional to the bending moment M and inversely proportional to the moment of inertia I of the cross section. Also, the stresses vary linearly with the distance y from the neutral axis. If a positive bending moment acts on the beam, the stresses are positive (tension) over the part of the cross section where y is positive. If a negative moment acts, negative stresses (compression) are produced where y is positive. These relationships are shown in Fig. 5-12. Equation (5-10) for the normal stresses is usually called the **flexure formula**. (Note that, if the sign convention for M is reversed, or if the

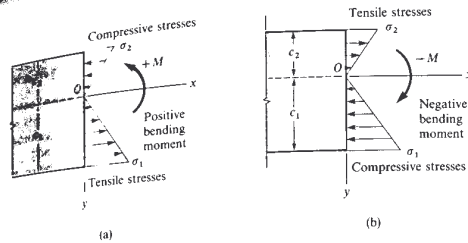


Fig. 5-12 Relationships between signs of bending moments and signs of normal stresses (Eq. 5-10)

y axis is taken positive upward, a minus sign is required in the flexure formula.)

The maximum tensile and compressive stresses in the beam occur at points located farthest from the neutral axis. Let us denote by c_1 and c_2 the distances from the neutral axis to the extreme fibers in the positive and negative y directions, respectively (see Figs. 5-10 and 5-12). Then the maximum normal stresses (from Eq. 5-10) are as follows:

$$\sigma_1 = \frac{Mc_1}{I} = \frac{M}{S_1} \quad \sigma_2 = -\frac{Mc_2}{I} = -\frac{M}{S_2} \quad (5-11a, b)$$

in which

$$S_1 = \frac{I}{c_1} \quad S_2 = \frac{I}{c_2} \quad (5-12a, b)$$

The quantities S_1 and S_2 are known as the **section moduli** of the cross-sectional area, and they have dimensions of length to the third power (for example, in³, m³, and mm³). If the bending moment M is positive, the stress σ_1 is tension and σ_2 is compression; if M is negative, the stresses are reversed (see Fig. 5-12).

If the cross section is symmetric with respect to the z axis (doubly symmetric cross section), then $c_1 = c_2 = c$, and the maximum tensile and compressive stresses are equal numerically:

$$\sigma_1 = -\sigma_2 = \frac{Mc}{I} = \frac{M}{S} \quad (5-13)$$

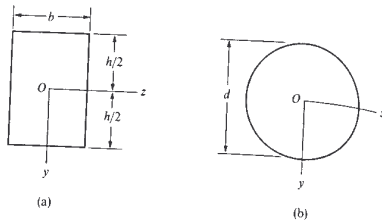
in which

$$S = \frac{I}{c} \quad (5-14)$$

is the section modulus. For a beam of rectangular cross section with width b and height h (Fig. 5-13a), the moment of inertia and the section modulus are

$$I = \frac{bh^3}{12} \quad S = \frac{bh^2}{6} \quad (5-15a, b)$$

* Moments of inertia of areas are discussed in Appendix C.



Doubly symmetric cross-sections

For a circular cross section of diameter d (Fig. 5-13b), these properties are

$$I = \frac{\pi d^4}{64} \quad S = \frac{\pi d^3}{32} \quad (5-16a, b)$$

Properties of many plane figures are listed in Appendix D. For cross-sectional shapes not listed, we must obtain the location of the neutral axis, the moment of inertia, and the section moduli by direct calculation, using the techniques described in Appendix C. The dimensions and properties of beams that are available commercially are listed in various handbooks and in Appendices E and F, as explained in more detail in the next section.

The preceding analysis of normal stresses in beams concerned pure bending, which means that no shear forces act on the cross sections. In the case of nonuniform bending, the presence of shear forces produces warping, or out-of-plane distortion, of the cross sections; thus, a section that is plane before bending is no longer plane after bending. Warping due to shear greatly complicates the behavior of the beam, but more elaborate analyses show that the normal stresses σ_x calculated from the flexure formula are not significantly altered by the presence of the shear stresses and the associated warping (Ref. 5-2). Thus, we may justifiably use the theory of pure bending for calculating normal stresses even when we have nonuniform bending. The calculation of the shear stresses is considered in Section 5.5.*

The flexure formula gives results that are accurate only in the regions of the beam where the stress distribution is not disrupted by irregularities in the shape of the beam or by discontinuities in loading. Such irregularities may produce localized stresses, called *stress concentrations*, that are much greater than the stresses obtained from the flexure formula.

* Beam theory began with Galileo Galilei (1564–1642), who investigated the behavior of various types of beams. His work in mechanics of materials is described in his famous book *Two New Sciences*, first published in 1638 (Ref. 5-3). Although Galileo made many important discoveries regarding beams, he did not obtain correctly the distribution of stresses in a beam. Further progress was made by Mariotte, Jacob Bernoulli, Euler, Parent, Saint-Venant, and others (Ref. 5-4).

Example 1

A steel wire of diameter d is bent over a drum of radius r (Fig. 5-14). Calculate the maximum bending stress σ_{\max} and the bending moment M in the wire, assuming $E = 200$ GPa, $d = 4$ mm, and $r = 0.5$ m.

The radius of curvature of the bent wire, measured to the neutral axis of the cross section, is

$$\rho = r + \frac{d}{2} \quad (a)$$

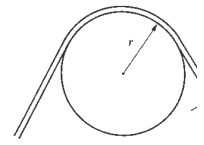


Fig. 5-14 Example 1

Next, the maximum tensile and compressive stresses, which are numerically equal, are obtained from Eq. (5-5) by substituting $\kappa = 1/\rho$ and $y = d/2$:

$$\sigma_{\max} = \frac{Ed}{2r + d} \quad (5-17)$$

If the radius of the drum is large compared to the diameter of the wire, the second term in the denominator may be disregarded.

To calculate the maximum stress, we now substitute numerical values for E , d , and r :

$$\sigma_{\max} = \frac{(200 \text{ GPa})(4 \text{ mm})}{2(500 \text{ mm}) + 4 \text{ mm}} = 797 \text{ MPa}$$

If d is disregarded in the denominator, the result is $\sigma_{\max} = 800$ MPa, which differs from the preceding result by less than 1%.

The maximum bending moment in the wire may be found from the equation $M = \sigma S$ (see Eq. 5-13), in which σ is obtained from Eq. (5-17) and $S = \pi d^3/32$; thus,

$$M_{\max} = \sigma_{\max} S = \frac{\pi E d^4}{32(2r + d)} \quad (5-18)$$

Again substituting numerical values, we obtain $M_{\max} = 5.01$ N·m.

Example 2

A simple beam AB of span length $L = 6$ m (Fig. 5-15) supports a uniform load of intensity $q = 20$ kN/m and a concentrated load $P = 50$ kN. The beam is constructed of glued laminated wood with width $b = 220$ mm and depth $d = 700$ mm. Determine the maximum tensile and compressive stresses in the beam due to bending.

The maximum bending stresses occur at the cross section of maximum bending moment. To aid in locating this cross section, we construct the shear-force diagram shown in the figure. We see that the shear force changes sign under the concentrated load; hence, the maximum bending moment occurs at this location. The moment diagram is also sketched in the figure, and the maximum moment is found to be

$$M = 160.4 \text{ N}\cdot\text{m}$$

Stresses in Beams

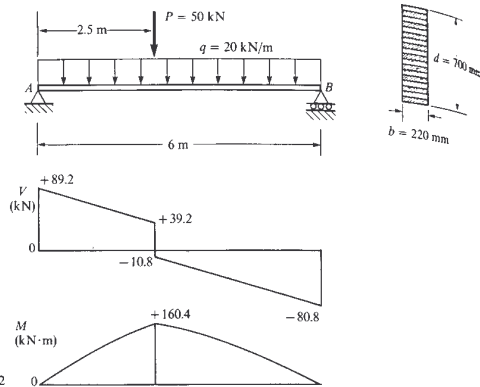


Fig. 5-15 Example 2

Next, we calculate the section modulus of the cross-sectional area (Eq. 5-15b):

$$S = \frac{bh^2}{6} = \frac{1}{6}(0.22 \text{ m})(0.7 \text{ m})^2 = 0.018 \text{ m}^3$$

Finally, we determine the maximum tensile and compressive stresses σ_t and σ_c from Eq. (5-13):

$$\sigma_t = \sigma_1 = \frac{M}{S} = \frac{160.4 \text{ kN}\cdot\text{m}}{0.018 \text{ m}^3} = 8.9 \text{ MPa}$$

$$\sigma_c = \sigma_2 = -\frac{M}{S} = -8.9 \text{ MPa}$$

In this example, the bending moment is positive; therefore, the maximum tensile stress occurs at the bottom of the beam (σ_1), and the maximum compressive stress occurs at the top (σ_2).

Example 3

The beam ABC shown in Fig. 5-16 has simple supports at A and B and an overhang from B to C . A uniform load of intensity $q = 3.0$ kN/m acts throughout the length of the beam. The beam is constructed of 12 mm thick steel plates welded to form a channel section, the dimensions of which are shown in Fig. 5-17a. Calculate the maximum tensile and compressive stresses in the beam.

The bending-moment diagram for this beam can be obtained by the methods described in Chapter 4. The resulting diagram is shown in Fig. 5-16, and we see that the maximum positive and negative bending moments are 1.898 kN·m

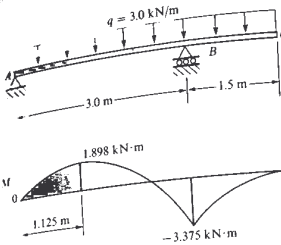


Fig. 5-16 Example 3

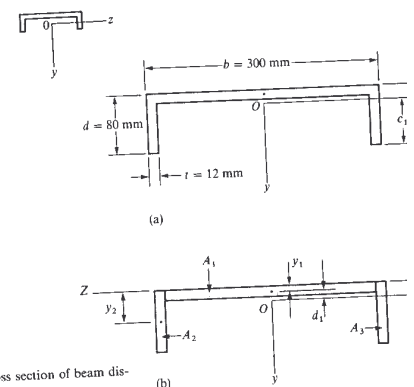


Fig. 5-17 Cross section of beam discussed in Example 3

The position of the neutral axis is found by locating the centroid of the cross-sectional area shown in Fig. 5-17a. Using the techniques described in Appendix C, Section C.2, we divide the area into three parts, as shown in Fig. 5-17b, and then take axis $Z-Z$ at the top of the section as a reference axis. The resulting calculations are as follows:

$$y_1 = 6 \text{ mm} \quad A_1 = (276 \text{ mm})(12 \text{ mm}) = 3312 \text{ mm}^2$$

$$y_2 = 40 \text{ mm} \quad A_2 = (12 \text{ mm})(80 \text{ mm}) = 960 \text{ mm}^2$$

$$y_3 = y_2 \quad A_3 = A_2$$

$$c_2 = \frac{\sum y_i A_i}{\sum A_i} = 18.48 \text{ mm}$$

$$c_1 = 80 \text{ mm} - c_2 = 61.52 \text{ mm}$$

Thus, the position of the neutral axis is determined.

To calculate the moment of inertia of the cross-sectional area about the neutral axis, we make use of the parallel-axis theorem (see Section C.5). Beginning with area A_1 , we obtain its moment of inertia about the z axis from the equation

$$I_{z_1} = I_{z_c} + A_1 d_1^2 \quad (b)$$

(see Appendix C). The quantity I_{z_c} represents the moment of inertia of area A_1 about its own centroidal axis; thus,

$$I_{z_c} = \frac{1}{12}(276 \text{ mm})(12 \text{ mm})^3 = 39,744 \text{ mm}^4$$

The distance d_1 extends from the centroidal axis of area A_1 to the z axis; hence,

$$d_1 = c_1 - 6 \text{ mm} = 12.48 \text{ mm}$$

Therefore, the moment of inertia of area A_1 about the z axis (from Eq. b)
 $I_{z_1} = 39,744 \text{ mm}^4 + (3,312 \text{ mm}^2)(12.48 \text{ mm})^2 = 555,600 \text{ mm}^4$
 Proceeding in the same manner for areas A_2 and A_3 , we get
 $I_{z_2} = I_{z_3} = 956,600 \text{ mm}^4$

and, hence, the centroidal moment of inertia of the entire cross-sectional area
 $I = I_{z_1} + I_{z_2} + I_{z_3} = 2.469 \times 10^6 \text{ mm}^4$
 The section moduli for the bottom and top of the beam (see Eqs. 5-12a and b) are

$$S_1 = \frac{I}{c_1} = 40,100 \text{ mm}^3 \quad S_2 = \frac{I}{c_2} = 133,600 \text{ mm}^3$$

With these properties determined, we can now proceed to calculate the stresses from Eqs. (5-11a and b).

At the section of maximum positive bending moment, the largest tensile stress occurs at the bottom of the beam (σ_1) and the largest compressive stress occurs at the top (σ_2); hence,

$$\sigma_1 = \sigma_1 = \frac{M}{S_1} = \frac{1.898 \text{ kN}\cdot\text{m}}{40,100 \text{ mm}^3} = 47.3 \text{ MPa}$$

$$\sigma_2 = \sigma_2 = \frac{M}{S_2} = \frac{1.898 \text{ kN}\cdot\text{m}}{133,600 \text{ mm}^3} = -14.2 \text{ MPa}$$

Similarly, the largest stresses at the section of maximum negative moment are

$$\sigma_1 = \sigma_2 = \frac{M}{S_2} = \frac{-3.375 \text{ kN}\cdot\text{m}}{133,600 \text{ mm}^3} = -25.3 \text{ MPa}$$

$$\sigma_2 = \sigma_1 = \frac{M}{S_1} = \frac{-3.375 \text{ kN}\cdot\text{m}}{40,100 \text{ mm}^3} = -84.2 \text{ MPa}$$

A comparison of the preceding four stresses shows that the maximum tensile stress in the beam is 47.3 MPa and the maximum compressive stress is -84.2 MPa.

For the purpose of selecting a beam, it is convenient to determine the required section modulus S by dividing the maximum bending moment by the allowable stress in the material (see Eq. 5-13):

$$S = \frac{M_{\max}}{\sigma_{\text{allow}}} \quad (5-19)$$

In this equation, σ_{allow} is the maximum permissible normal stress, which is based upon the properties of the material and the magnitude of the desired factor of safety. To ensure that the allowable stresses are not exceeded, the selected beam must have a cross-sectional area that provides a section modulus at least as large as that obtained from Eq. (5-19). If the allowable stresses are the same for both tension and compression, then (for a particular bending moment M) it is logical to choose a cross-sectional shape that is doubly symmetric and that has its centroid (and, hence, also the neutral axis) at the midheight of the beam. If the allowable stresses are different for tension and compression, it may be desirable to use an unsymmetric cross section such that the distances to the extreme fibers in tension and compression are in nearly the same ratio as the respective allowable stresses. Of course, to minimize the weight of a beam, and thereby save material, it is common practice to select a beam that has not only the required section modulus but also the smallest cross-sectional area.

Beams of steel, aluminium, and wood are manufactured in standard sizes. The dimensions and properties of steel and aluminium beams are listed in engineering handbooks such as those published by Constrado and the American Aluminium Association (see Refs. 5-5 through 5-9). However, for use in solving problems in this book, some abridged tables of structural steel sections are given in Appendix E. These tables give the dimensions of the cross section and important properties such as area, moment of inertia, and section modulus.

Structural steel sections are given a designation such as UB 610 \times 305 \times 138 kg, which means that the section is of I-section (and is called a Universal Beam) with a nominal depth of 610 mm and a weight of 138 kg per metre of length. Analogous designations are used for Universal Columns, Joists and channel sections, as shown in the tables in Appendix E. Angle sections, or L shapes, are designated by giving the lengths of the two legs and the thickness; for example, L 200 \times 100 \times 10 denotes an angle of thickness 10 mm and with unequal legs, one of length 200 mm and the other of length 100 mm. All of these sections are manufactured by the rolling process. In this process, a hot billet of steel is passed back and forth between rolls until it is formed into the desired shape.

Aluminium structural sections are made by the extrusion process, in which a hot billet is pushed, or extruded, through a shaped die.

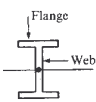
5.4 CROSS-SECTIONAL SHAPES OF BEAMS

The overall process of designing a beam requires consideration of numerous factors, such as the type of construction, materials, loads, and environmental conditions. However, in many cases, this task eventually is reduced to the selection of a particular beam shape and size such that the actual stresses in the beam do not exceed the allowable stresses. In this discussion, we will consider only the bending stresses (that is, the stresses obtained from the flexure formula, Eq. 5-10). A complete design also requires that the shear stresses be kept below their allowable values (see Section 5.5) and that the effects of buckling and stress concentrations be considered.

Stresses in Beams



(b)



(d)

I-section

Since dies are relatively easy to make, aluminium beams can be extruded in almost any desired shape. The Aluminum Construction Manual (Ref. 5-7) lists many standard shapes of wide-flange beams, I-beams, channels, angles, and other sections, but custom-made shapes also can be ordered.

Wood beams have rectangular cross sections that are denoted by nominal dimensions, such as 4 \times 8 (inches). These dimensions represent the rough-cut size of the timber. The net dimensions of a beam are smaller if the surfaces of the rough timber are planed, or surfaced, to make them smooth. Thus, a 4 \times 8 section is actually 3.5 \times 7.25 in. in size after it is surfaced. The net dimensions should be used in all computations for surfaced timber.

Let us now compare various cross-sectional shapes with respect to their efficiency in bending. Consider first a rectangle of width b and depth h (Fig. 5-18a). The section modulus (Eq. 5-15b) is

$$S = \frac{bh^2}{6} = \frac{Ah}{6} = 0.167Ah \quad (a)$$

where A denotes the cross-sectional area. This equation shows that a rectangular cross section of given area becomes more efficient as the depth h is increased. However, there is a limit to this increase, because the beam becomes laterally unstable when the ratio of height to width becomes too large. Thus, a beam of very narrow rectangular section may fail because of lateral (sideways) buckling rather than insufficient strength of the material (Ref. 5-10).

For a circular cross section of diameter d (Fig. 5-18b), we have

$$S = \frac{\pi d^3}{32} = \frac{Ad}{8} = 0.125Ad \quad (b)$$

Comparing a circular cross section and a square cross section of the same area, we find that the side h of the square will be $h = d\sqrt{\pi}/2$, for which Eq. (a) gives

$$S = 0.148Ad$$

Comparison of this result with Eq. (b) shows that a beam of square cross section is more efficient than a circular one of the same area.

Consideration of the stress distribution over the depth of the cross section (Fig. 5-10a) leads to the conclusion that, for economical design, the material of the beam should be located as far as possible from the neutral axis. The most favorable case for a given cross-sectional area A and depth h would be to distribute each half of the area at a distance $h/2$ from the neutral axis, as shown in Fig. 5-18c. Then

$$I = 2\left(\frac{A}{2}\right)\left(\frac{h}{2}\right)^2 = \frac{Ah^2}{4} \quad S = 0.5Ah \quad (c)$$

This ideal limit may be approximated in practice by the use of a wide-flange section or an I-section with most of the material in the flanges (Fig. 5-19d). Because of the concentration of section part of the material in

the web of the beam, the limiting condition (Eq. c) can never be realized. For standard wide-flange beams, the section modulus is approximately

$$S \approx 0.35Ah \quad (d)$$

Comparison of Eq. (d) with Eq. (a) shows that a wide-flange section is more efficient than a rectangular section of the same area and depth. The reason is that much of the material in a rectangular beam is located near the neutral axis where it is understressed. By contrast, in a wide-flange beam, most of the material is located in the flanges, at the greatest distance from the neutral axis. In addition, a wide-flange beam is wider and therefore more stable with respect to sideways buckling than a beam of rectangular section of the same depth and section modulus. Of course, if the web of a wide-flange beam is made too thin, it will be susceptible to buckling or it may be overstressed in shear, as discussed in the next section.

Example 1

A temporary wooden dam is constructed of horizontal planks A supported by vertical posts B that are built into the ground so that they act as cantilever beams (Figs. 5-19a and b). The posts are of square cross section (dimensions $b \times b$) and spaced at distance s = 0.8 m. The water level is at the full height h = 2 m of the dam. Determine the minimum required dimension b of the posts if the allowable bending stress in the wood is σ_{allow} = 8 MPa.

The loading diagram for one of the posts is triangular in shape (Fig. 5-19c), and the maximum intensity of the load is

$$q_0 = \gamma h s$$

where γ is the specific weight of water. Therefore, the maximum bending moment in a post is

$$M_{\max} = \frac{q_0 h}{2} \left(\frac{h}{3}\right) = \frac{\gamma h^3 s}{6}$$

and the required section modulus is

$$S = \frac{M_{\max}}{\sigma_{\text{allow}}} = \frac{\gamma h^3 s}{6\sigma_{\text{allow}}} \quad (e)$$

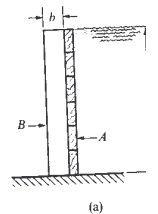
For a beam of square cross section, the section modulus is $S = b^3/6$. Substituting this expression for S into Eq. (e) yields

$$b^3 = \frac{\gamma h^3 s}{\sigma_{\text{allow}}}$$

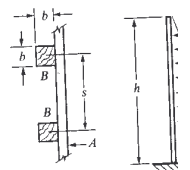
Then, substituting numerical values, we obtain

$$b^3 = \frac{(9.81 \text{ kN/m}^3)(2 \text{ m})^3(0.8 \text{ m})}{8 \text{ MPa}} = 0.007848 \text{ m}^3 \quad b = 199 \text{ mm}$$

Hence, the minimum required dimension b of the square posts is 199 mm. Any larger dimension, such as 200 mm, will ensure that the actual bending stress is less than the allowable stress.



(a)



(b)

(c)

Fig. 5-19 Example 1

Example 2

A simple beam *AB* of span length 7 m must support a uniform load $q = 60 \text{ kN/m}$ distributed as shown in Fig. 5-20. Determine the required section modulus S if the allowable bending stress is $\sigma_{\text{allow}} = 110 \text{ MPa}$. Then select a Universal Beam from Table E-1 in Appendix E, and recalculate S taking into account the weight of the beam itself. Select a new beam size if necessary.

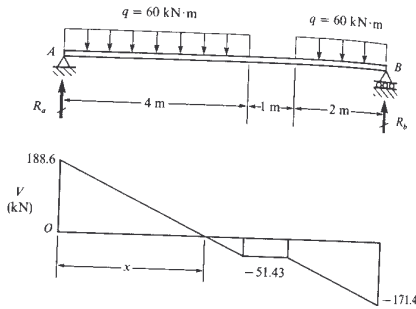


Fig. 5-20 Example 2

To locate the section of maximum bending moment, it is helpful to construct the shear-force diagram, as shown in the figure. The reactions at the supports are

$$R_a = 188.6 \text{ kN} \quad R_b = 171.4 \text{ kN}$$

The distance x to the section of zero shear is obtained from the equation

$$R_a - qx = 0$$

Solving this equation, we obtain $x = R_a/q = 3.143 \text{ m}$. The maximum bending moment occurs at this same section and is

$$M_{\text{max}} = R_a x - \frac{qx^2}{2} = 296.3 \text{ kN}\cdot\text{m}$$

The required section modulus (disregarding the weight of the beam) is

$$S = \frac{M_{\text{max}}}{\sigma_{\text{allow}}} = \frac{296.3 \times 10^6 \text{ N}\cdot\text{mm}}{110 \text{ N/mm}^2} = 2.694 \times 10^6 \text{ mm}^3$$

We may now enter Table E-1 and select a Universal Beam that has a section modulus greater than 2694 cm^3 , because we know that a slightly larger value of S will be required when the weight of the beam is considered. The lightest beam that provides the required section modulus is $762 \times 267 \text{ kg UB}$. Of course, the table in Appendix E is abridged; hence, lighter sections may be available commercially.

When the weight of the beam (147 kg/m) is taken into account, the reaction R_a becomes 193.6 kN , the distance x to the cross section of zero shear increases to 1.51 m , and the maximum bending moment becomes $305.2 \text{ kN}\cdot\text{m}$. Hence, the required section modulus becomes

$$S = \frac{M_{\text{max}}}{\sigma_{\text{allow}}} = \frac{305.2 \times 10^6 \text{ N}\cdot\text{mm}}{110 \text{ N/mm}^2} = 2.774 \times 10^6 \text{ mm}^3 = 2774 \text{ cm}^3$$

and the $762 \times 267 \text{ Universal Beam}$ is still satisfactory. If it were not, a new beam would be selected and the process repeated.

Example 3

A beam of square cross section is bent in the plane of a diagonal (Fig. 5-21). Show that the maximum stresses in the beam may be reduced by removing a small amount of material at the top and bottom corners, as shown by the shaded areas in the figure.

The moment of inertia and the section modulus of the entire square area about the z axis are, respectively,

$$I_1 = \frac{a^4}{12} \quad S_1 = \frac{I_1}{a/\sqrt{2}} = \frac{a^3\sqrt{2}}{12}$$

where a is the length of each side of the square. Let us now cut off the corners so that each side is shortened by βa , where β is a number between zero and unity. The new cross section consists of a square $mnpq$, with sides $a(1 - \beta)$, and two parallelograms mm_1n_1n and nn_1p_1p . The moment of inertia of the square is obtained from the formula for I_1 by replacing a with $a(1 - \beta)$:

$$I_2 = \frac{a^4(1 - \beta)^4}{12}$$

The moment of inertia of one parallelogram about the z axis is given by the formula $bh^3/3$, where b is the base width and h is the height; thus,

$$I_3 = \frac{1}{3}(\beta a\sqrt{2})\left[\frac{a(1 - \beta)}{\sqrt{2}}\right]^3 = \frac{a^4\beta(1 - \beta)^3}{6}$$

Thus, the moment of inertia of the total remaining cross section is

$$I = I_2 + 2I_3 = \frac{a^4}{12}(1 + 3\beta)(1 - \beta)^3$$

The section modulus of this area is

$$S = \frac{I}{a(1 - \beta)/\sqrt{2}} = \frac{a^3(1 + 3\beta)(1 - \beta)^2\sqrt{2}}{12}$$

The value of β that makes the section modulus a maximum is obtained by setting $dS/d\beta$ equal to zero and solving for β ; the result is

$$\beta = \frac{1}{9}$$

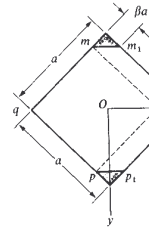


Fig. 5-21 Example 3

Substituting this value of β into the expression for S gives the maximum section modulus:

$$S_{\text{max}} = \frac{64a^3\sqrt{2}}{729} = \frac{256}{243} S_1 \approx 1.053 S_1$$

This result shows that cutting off the corners by the calculated amount increases the section modulus by about 5%, thereby also reducing the maximum bending stresses by about 5%.

This observation is easily explained when we consider that the section modulus is equal to the moment of inertia divided by half the depth of the cross section. By cutting off the corners, the moment of inertia of the cross section is diminished by a relatively smaller amount than the depth is diminished. Thus, the section modulus is increased and the beam is made stronger, even though the area of the cross section is reduced.

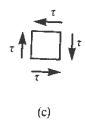
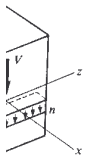
5.5 SHEAR STRESSES IN RECTANGULAR BEAMS

When a beam is subjected to nonuniform bending, both bending moments M and shear forces V act on the cross sections. The normal stresses σ_x associated with the bending moments are obtained from the flexure formula, as described in Section 5.3. In this and the following sections, we will investigate the distribution of shear stresses τ associated with the shear force V .

Let us begin with the simplest case of a beam of rectangular cross section having width b and height h (Fig. 5-22a). We can reasonably assume that the shear stresses τ act parallel to the shear force V (that is, parallel to the vertical sides of the cross section). Let us also assume that the distribution of shear stresses is uniform across the width of the beam. The use of these two assumptions will enable us to determine completely the distribution of the shear stresses acting on the cross section.

A small element of the beam may be cut out between two adjacent cross sections and between two planes that are parallel to the neutral surface, as shown by element m_n in Fig. 5-22a. In accord with the foregoing assumptions, the vertical shear stresses τ are uniformly distributed on the vertical faces of this element. We also know from the discussions on shear stresses in Section 1.6 that shear stresses on one side of an element are accompanied by shear stresses of equal magnitude acting on perpendicular faces of the element (Figs. 5-22b and c). Thus, there will be horizontal shear stresses between horizontal layers of the beam as well as transverse shear stresses on the vertical cross sections. At any point within the beam, these complementary shear stresses are equal in magnitude.

This observation about the equality of the horizontal and vertical shear stresses leads to an interesting conclusion regarding the shear stresses at the top and bottom of the beam. If we consider the element



(c) in a beam of

shown in Fig. 5-22 to be at either the top or the bottom, it is apparent that the horizontal shear stresses must vanish because there are no normal stresses on the outer surfaces of the beam. Therefore, the vertical shear stresses τ also must vanish at the top and bottom of the beam (that is, $\tau = 0$ where $y = \pm h/2$).

The existence of horizontal shear stresses in a beam can be demonstrated by a simple experiment. Take two equal rectangular bars of height h and place them on simple supports, as shown in Fig. 5-23a, and then load them by a force P . If no friction exists between the bars, and the two bars will occur independently. Each bar will be in bending of the two bars will occur independently. Each bar will be in compression above its neutral axis and in tension below its neutral axis, and each will deform as indicated in Fig. 5-23b. The lower longitudinal fibers of the upper bar will slide with respect to the upper fibers of the lower bar. If, instead of two bars, we have a solid bar of depth $2h$, shear stresses must exist along the neutral plane of such magnitude as to prevent the sliding shown in Fig. 5-23b. Because of the presence of shear stresses that prevent sliding, the single bar of depth $2h$ is much stiffer and stronger than two separate bars each of depth h .

In order to evaluate the shear stresses, let us consider the equilibrium of an element pp_1n_1n (Fig. 5-24a) cut out from a beam between two adjacent cross sections mn and m_1n_1 separated by a distance dx . The bottom face of this element is the lower surface of the beam and is free from stress; its top face is parallel to the neutral surface and at an arbitrary distance y_1 from that surface. The top face is acted upon by the horizontal shear stresses τ existing at this level in the beam. The end faces of the element are acted upon by the normal bending stresses σ_x produced by the bending moments. In addition, there are vertical shear stresses on the end faces, but these stresses will not enter into the equation of equilibrium of the element in the horizontal direction (the x direction); hence, they are not shown in Fig. 5-24a.

If the bending moments at cross sections mn and m_1n_1 are equal (that is, if the beam is in pure bending), the normal stresses σ_x acting over the sides np and n_1p_1 also will be equal. Hence, the element will be in equilibrium under the action of these stresses alone; therefore, the

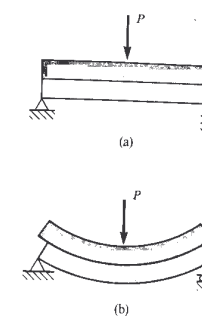
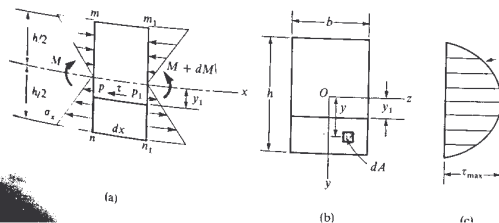


Fig. 5-23 Bending of two sep. bars

Fig. 5-24 Shear stresses in a beam

shear stress τ must be equal to zero. This conclusion is obvious as much as no shear force V exists if the beam is in pure bending. In the more general case of a varying bending moment (nonuniform bending), let us denote by M and $M + dM$ the bending moments acting at cross sections mn and m_1n_1 , respectively. Considering an element of area dA at distance y from the neutral axis (Fig. 5-24b), we see that the normal force acting on this element is $\sigma_x dA$, in which σ_x is the normal stress obtained from the flexure formula (Eq. 5-10). If the element of area is located on the left-hand face pn of the element, the normal force is

$$\sigma_x dA = \frac{My}{I} dA$$

Summing these elemental forces over the area of the face pn of the solid element gives the total horizontal force F_1 acting on that face:

$$F_1 = \int \frac{My}{I} dA$$

in which the integration is performed over the shaded area of the cross section (that is, over the area of the cross section from $y = y_1$ to $y = h/2$). In the same manner, we find that the total force F_2 acting on the right-hand face p_1n_1 of the solid element is

$$F_2 = \int \frac{(M + dM)y}{I} dA$$

Finally, the horizontal force F_3 acting on the top face pp_1 of the element is

$$F_3 = \tau b dx \tag{a}$$

in which $b dx$ is the area of the top face. The forces F_1 , F_2 , and F_3 must be in static equilibrium; hence, the summing of forces in the x direction gives

$$F_3 = F_2 - F_1 \tag{b}$$

or

$$\tau b dx = \int \frac{(M + dM)y}{I} dA - \int \frac{My}{I} dA$$

from which

$$\tau = \frac{dM}{dx} \left(\frac{1}{Ib} \right) \int y dA$$

Substituting $V = dM/dx$ (see Eq. 4-3), we now obtain

$$\tau = \frac{V}{Ib} \int y dA \tag{5-20}$$

The integral in this equation represents the first moment of the shaded portion of the cross section (Fig. 5-24b) with respect to the neutral axis (the z axis); that is, the integral is the first moment of the cross-section area below the level y_1 at which the shear stress τ acts. When sectional area below the neutral axis, the integral is the first moment of the area above the level at which the shear stress is being calculated. Denoting the first moment by Q , we can write Eq. (5-20) in the form

$$\tau = \frac{VQ}{Ib} \tag{5-21}$$

This equation, known as the **shear formula**, can be used to determine the shear stress τ at any point in the cross section. To determine how the stress varies, we must examine how Q varies, because V , I , and b are constants for a given rectangular cross section.*

The first moment Q for the shaded area of Fig. 5-24b is obtained by multiplying the area by the distance from the centroid of the area to the neutral axis; thus,

$$Q = b \left(\frac{h}{2} - y_1 \right) \left(y_1 + \frac{h/2 - y_1}{2} \right) = \frac{b}{2} \left(\frac{h^2}{4} - y_1^2 \right) \tag{c}$$

Of course, the first moment can also be determined by integration:

$$Q = \int y dA = \int_{-h/2}^{h/2} \int_{y_1}^{h/2} y dy dz = \int_{y_1}^{h/2} y b dy = b \left[\frac{y^2}{2} \right]_{y_1}^{h/2} = \frac{b}{2} \left(\frac{h^2}{4} - y_1^2 \right)$$

as obtained before. Now substituting for Q (Eq. c) into the shear formula (Eq. 5-21), we get

$$\tau = \frac{V}{2I} \left(\frac{h^2}{4} - y_1^2 \right) \tag{5-22}$$

This equation shows that the shear stress in a rectangular beam varies quadratically with the distance y_1 from the neutral axis; thus, when plotted along the height of the beam, τ varies as shown in Fig. 5-24c. The stress is zero when $y_1 = \pm h/2$, and it has its maximum value at the neutral axis, where $y_1 = 0$; thus,

$$\tau_{\max} = \frac{Vh^2}{8I} = \frac{3V}{2A} \tag{5-23}$$

* In the derivation, Q is the first moment of the cross-sectional area shown shaded in Fig. 5-24b, and this area is usually used for calculating Q . However, we could also take the first moment of the remaining cross-sectional area, because it too is equal to Q (except for the value of Q for the area below the level y_1 is the negative of Q for the area above the level).

in which $A = bh$ is the cross-sectional area. Thus, the maximum shear stress is 50% larger than the average shear stress (which is equal to V/A). Note that the preceding equations for τ (Eqs. 5-20 through 5-23) can be used to calculate either vertical shear stresses acting on cross sections or horizontal shear stresses acting between horizontal layers of the beam. (The analysis presented in this section was developed by the Russian engineer D. J. Jourawski; Refs. 5-11 and 5-12.)

The preceding formulas for shear stresses were derived without regard to any particular sign conventions for V and τ . It is sufficient to observe that the shear force is the resultant of the shear stresses; hence, the stresses act in the same direction as the force. For most purposes, only absolute values are used in the shear formulas, and the directions of the stresses are determined by inspection, as in Fig. 5-22. If we use the sign convention for shear stresses described in Section 1.6 (see Fig. 1-23), then a positive shear force (Fig. 5-22a) produces a negative shear stress on the right-hand face of the element (Fig. 5-22c). Therefore, a minus sign is required in the shear formula in order to reconcile these sign conventions.

The formulas for shear stresses in rectangular beams are valid for beams of ordinary proportions and are subject to the same restrictions as the flexure formula from which they are derived; thus, the formulas are valid only for beams of linear elastic material with small deflections. The formulas may be considered to be exact for narrow beams (b much less than h), but they become less accurate as b increases relative to h . For instance, when $b = h$, the true maximum shear stress is about 13% larger than the value given by Eq. (5-23). For a discussion of the limitations of the shear formula, see Ref. 5-13.

Effect of shear strains. Because the shear stress τ varies parabolically from top to bottom of the beam, it follows that the shear strain $\gamma = \tau/G$ must vary in the same manner. Thus, cross sections of the beam that were originally plane surfaces become warped. This warping can be demonstrated by bending a beam on which vertical lines, such as lines mn and pq in Fig. 5-25, have been drawn. The lines will not remain straight, but will curve, with the maximum shear strain occurring at the neutral surface. At the points $m_1, p_1, n_1,$ and q_1 , the shear strain is zero and the curves m_1n_1 and p_1q_1 remain normal to the upper and lower surfaces of the bar after bending. At the neutral surface, the angles between the tangents to the curves m_1n_1 and p_1q_1 and the normal sections mn and pq are equal to the shear strain $\gamma = \tau_{\max}/G$. If the shear force V remains constant along the beam, the warping of all cross sections is the same, so that $m_1m = p_1p$ and $n_1n = q_1q$. Thus, the stretching or the shortening of the longitudinal fibers produced by the bending moment is unaffected by the shear strains, and the distribution of the normal stresses σ is the same as it is in pure bending.

A more elaborate investigation of this problem shows that the warping of cross sections due to shear strains does not substantially

affect the longitudinal strains even if a distributed load acts on the beam and the shear force varies continuously along the beam. For concentrated loads, the stress distribution near the loads is more complicated, but these irregularities are very localized and do not appreciably affect the overall stress distribution in the beam. Thus, it is quite justifiable to use the flexure formula derived for pure bending (Eq. 5-10) in the case of nonuniform bending.

Example 1

Calculate the normal and shear stresses acting at point C in the steel beam AB shown in Fig. 5-26. The beam is simply supported with a span length $L = 1$ m, and it has a $25 \text{ mm} \times 100 \text{ mm}$ rectangular cross section. The total uniform load on the beam (including its own weight) is $q = 28 \text{ kN/m}$. (The beam is adequately supported against sideways buckling.)

From static equilibrium, the bending moment M and shear force V at the cross section through point C are found to have the following values:

$$M = 2.24 \text{ kN}\cdot\text{m} \quad V = -8.4 \text{ kN}$$

The signs in these terms are based upon the sign conventions for M and V shown in Fig. 4-3. The moment of inertia of the cross-sectional area is

$$I = \frac{bh^3}{12} = \frac{1}{12} (25 \text{ mm})(100 \text{ mm})^3 = 2083 \times 10^3 \text{ mm}^4$$

Therefore, the bending stress at point C, which is located at $y = -25 \text{ mm}$, is

$$\sigma_x = \frac{My}{I} = \frac{(2.24 \times 10^6 \text{ N}\cdot\text{mm})(-25 \text{ mm})}{2083 \times 10^3 \text{ mm}^4} = -26.9 \text{ MPa}$$

The minus sign indicates a compressive stress.

To obtain the shear stress, we need to evaluate the first moment Q of the cross-sectional area between point C and the outer edge of the cross section; this area is shown shaded in Fig. 5-26b. The first moment of this area about the z axis is equal to the product of the area and its centroidal distance from the z axis; thus,

$$Q = (25 \text{ mm})(25 \text{ mm})(37.5 \text{ mm}) = 23,440 \text{ mm}^3$$

Now we can substitute into the shear formula and obtain the shear stress at C:

$$\tau = \frac{VQ}{Ib} = \frac{(8400 \text{ N})(23,440 \text{ mm}^3)}{(2083 \times 10^3 \text{ mm}^4)(25 \text{ mm})} = 3.8 \text{ MPa}$$

Because the shear force is negative, it acts upward on the left-hand part of the beam when the beam is cut by a section through C; therefore, the shear stress τ acts in this same direction. A convenient way to show the directions of the stresses is to draw a stress element at point C (see Fig. 5-26c).

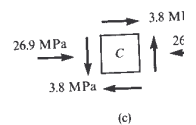
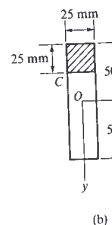
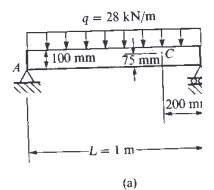
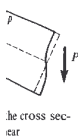
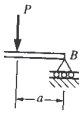


Fig. 5-26 Example 1



Example 2



A simple beam *AB* carrying two concentrated loads *P* (Fig. 5-27) has a rectangular cross section of width *b* = 100 mm and height *h* = 150 mm. The distance *a* from the end of the beam to one of the loads is 0.5 m. Determine the allowable value of *P* if the beam is constructed of wood having an allowable stress in bending $\sigma_{allow} = 11$ MPa and an allowable stress in horizontal shear $\tau_{allow} = 1.2$ MPa. Disregard the weight of the beam itself.

The maximum bending moment *M* and the maximum shear force *V* in the beam are

$$M = Pa \quad V = P$$

Also, the section modulus *S* and cross-sectional area *A* are

$$S = \frac{bh^2}{6} \quad A = bh$$

The maximum normal and shear stresses in the beam (from Eqs. 5-13 and 5-23) are

$$\sigma = \frac{M}{S} = \frac{6Pa}{bh^2} \quad \tau = \frac{3V}{2A} = \frac{3P}{2bh}$$

Therefore, the maximum permissible values of the load *P* are

$$P = \frac{\sigma_{allow}bh^2}{6a} \quad \text{and} \quad P = \frac{2\tau_{allow}bh}{3}$$

Substituting numerical values into these formulas, we get

$$P = 8.25 \text{ kN} \quad \text{and} \quad P = 12.0 \text{ kN}$$

Thus, the bending stress governs the design, and the allowable load is *P* = 8.25 kN.

5.6 SHEAR STRESSES IN THE WEBS OF BEAMS WITH FLANGES

When a beam of I-section (Fig. 5-28a) is subjected to a shear force *V*, shear stresses are developed throughout the cross section. Because of the shape, the distribution of these stresses is much more complicated than in the case of a rectangular beam. For instance, in the flanges of the beam, shear stresses act on the cross sections in both the horizontal and vertical directions. However, most of the vertical shear force *V* is carried by shear stresses in the web, and we can determine those stresses (which include the maximum shear stress) using the same techniques we used for rectangular beams.

Let us begin by considering the shear stresses at location *ef* in the web of the beam (Fig. 5-28a). We will make the same assumptions as in the case of a rectangular beam, that is, that the shear stresses are parallel to the *y* axis and are uniformly distributed across the thickness *t* of the web. Then the derivation made in the preceding section will still be valid, and the shear formula $\tau = VQ/Ib$ will still apply in general. However, the width *b* now becomes the thickness *t* of the web, and the area *A* used in calculating the first moment *Q* becomes the area between *ef* and the bottom edge of the cross section (that is, the shaded area of Fig. 5-28a). This area consists of two rectangles (disregarding the effects of the small fillets at the junction of the web and flange); the first rectangle is the flange, which has area

$$A_f = b \left(\frac{h}{2} - \frac{h_1}{2} \right)$$

The second rectangle is the part of the web between *ef* and the flange, and it has area

$$A_w = t \left(\frac{h_1}{2} - y_1 \right)$$

The first moments of these areas about the neutral axis are obtained by multiplying the areas by the distances from the *z* axis to the centroids of the areas; thus,

$$Q = b \left(\frac{h}{2} - \frac{h_1}{2} \right) \left(\frac{h_1}{2} + \frac{h/2 - h_1/2}{2} \right) + t \left(\frac{h_1}{2} - y_1 \right) \left(y_1 + \frac{h_1/2 - y_1}{2} \right)$$

or, upon simplifying,

$$Q = \frac{b}{8} (h^2 - h_1^2) + \frac{t}{8} (h_1^2 - 4y_1^2)$$

Therefore, the shear stress τ in the web of the beam is

$$\tau = \frac{VQ}{It} = \frac{V}{8It} [b(h^2 - h_1^2) + t(h_1^2 - 4y_1^2)] \quad (5-24)$$

When used for calculating shear stresses in the web. However, when considering the distribution of shear stresses in the flanges, the assumption of constant shear stress across the width *b* of the flanges cannot be made. For example, we see immediately that for $y_1 = h_1/2$ the shear stress over the free surfaces *ab* and *cd* (Fig. 5-28a) must be zero, whereas across the junction *bc* the stress is τ_{min} . This observation indicates that, at the junction of the web and flange, the distribution of shear stresses follows a more complicated law, one that cannot be investigated by an elementary analysis. The stresses would become very large at the corners if the internal corners were square; hence, fillets are used to reduce the stresses, as shown in the figure. Because of the localized nature of the stress distribution, the shear formula does not give accurate results for the vertical shear stresses in the flange. However, the formula can be used to calculate horizontal shear stresses in the flange, as discussed in Section 9.4.

Example

Determine the maximum shear stress in the web of a beam having the T-shaped cross section shown in Fig. 5-29 if *b* = 100 mm, *t* = 24 mm, *h* = 200 mm, *h*₁ = 176 mm, and *V* = 45 kN.

The distance *c* to the centroid of the cross section is determined as follows:

$$c = \frac{(76 \text{ mm})(24 \text{ mm})(12 \text{ mm}) + (200 \text{ mm})(24 \text{ mm})(100 \text{ mm})}{(76 \text{ mm})(24 \text{ mm}) + (200 \text{ mm})(24 \text{ mm})} = \frac{501,900 \text{ mm}^3}{6624 \text{ mm}^2} = 75.77 \text{ mm}$$

The moment of inertia *I* of the cross section about the neutral axis can be found by first obtaining the moment of inertia about axis *mn* and then using the parallel-axis theorem (see Appendix C). The calculations are as follows:

$$I = \frac{1}{3} (100 \text{ mm})(24 \text{ mm})^3 + \frac{1}{3} (24 \text{ mm})(176 \text{ mm})^3 - (6624 \text{ mm}^2)(75.77 \text{ mm})^2 = 26.3 \times 10^6 \text{ mm}^4$$

The maximum shear stress occurs at the neutral axis; the first moment *Q* of the area below the neutral axis is

$$Q = (24 \text{ mm})(124.2 \text{ mm})^2 \left(\frac{1}{2} \right) = 185 \times 10^3 \text{ mm}^3$$

Now, substituting into the shear formula, we get

$$\tau = \frac{VQ}{It} = \frac{(45,000 \text{ N})(185 \times 10^3 \text{ mm}^3)}{(26.3 \times 10^6 \text{ mm}^4)(24 \text{ mm})} = 13.2 \text{ MPa}$$

which is the maximum shear stress in the beam.

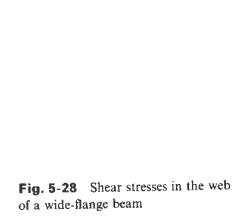


Fig. 5-28 Shear stresses in the web of a wide-flange beam

From this equation, we see that τ varies quadratically throughout the height of the web, as shown by the graph in Fig. 5-28b. Upon introducing the following expression for the moment of inertia *I*,

$$I = \frac{bh^3}{12} - \frac{(b-t)h_1^3}{12} = \frac{1}{12} (bh^3 - bh_1^3 + th_1^3) \quad (5-25)$$

we can rewrite Eq. (5-24) in the form

$$\tau = \frac{3V(bh^2 - bh_1^2 + th_1^2 - 4ty_1^2)}{2t(bh^3 - bh_1^3 + th_1^3)} \quad (5-26)$$

which expresses τ in terms of the dimensions of the cross section. The maximum shear stress occurs at the neutral axis ($y_1 = 0$), and the minimum shear stress in the web occurs at the junction with the flange ($y_1 = \pm h_1/2$). Thus, we find

$$\tau_{max} = \frac{V}{8It} (bh^2 - bh_1^2 + th_1^2) = \frac{3V(bh^2 - bh_1^2 + th_1^2)}{2t(bh^3 - bh_1^3 + th_1^3)} \quad (5-27)$$

and

$$\tau_{min} = \frac{Vb}{8It} (h^2 - h_1^2) = \frac{3Vb(h^2 - h_1^2)}{2t(bh^3 - bh_1^3 + th_1^3)} \quad (5-28)$$

Depending upon the beam dimensions, the maximum shear stress in the web typically is from 10% to 60% greater than the minimum stress.

The total shear force carried by the web may be determined by multiplying the area of the stress diagram (Fig. 5-28b) by the width *t* of the web itself. The area of the stress diagram consists of two parts, a rectangle of area $h_1\tau_{min}$ and a parabolic segment of area

$$\frac{2}{3} (h_1)(\tau_{max} - \tau_{min})$$

Thus, the shear force in the web is

$$V_{web} = h_1\tau_{min}t + \frac{2}{3} (h_1)(\tau_{max} - \tau_{min})t = \frac{th_1}{3} (2\tau_{max} + \tau_{min}) \quad (5-29)$$

For beams of typical proportions, the shear stresses in the web account for 90% to 98% of the total shear force; the remainder is carried by shear in the flanges.

In design work, it is common to calculate an approximation of the maximum shear stress by dividing the total shear force by the area of the web. This stress represents an average shear stress in the web:

$$\tau_{aver} = \frac{V}{th_1} \quad (5-30)$$

For typical I-section beams, the average shear stress is within 10% (plus or minus) of the actual maximum shear stress.

The elementary theory presented in this section is quite accurate

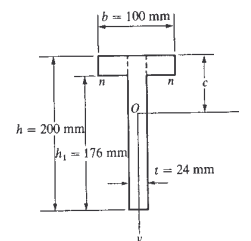
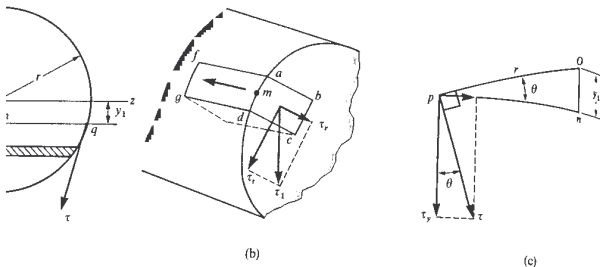


Fig. 5-29 Example

Stresses in Beams



Stresses in a beam of

5.7 SHEAR STRESSES IN CIRCULAR BEAMS

When a beam has a circular cross section (Fig. 5-30a), we can no longer assume that all of the shear stresses act parallel to the y axis. We can show that, at a point such as m on the boundary of the cross section, the shear stress must be tangent to the boundary. To demonstrate this fact, consider an infinitesimal element $abcd$ (Fig. 5-30b) in the form of a rectangular parallelepiped with the face $abcd$ on the surface of the beam and the face $abcd$ in the plane of the cross section. If the shear stress acting over the side $abcd$ of the element has a direction such as that shown by the stress τ_1 , it can always be resolved into two perpendicular components, a stress τ_r in the radial direction and a stress τ_t in the direction of the tangent to the boundary. We have already shown (by considering the equilibrium of an element) that, if a shear stress acts on one face of an element, a numerically equal shear stress will act on the perpendicular face. Applying this concept to the element shown in Fig. 5-30b, we conclude that, if a shear stress τ_r acts on the face $abcd$ in the radial direction, a numerically equal shear stress τ_t will act on the side $adgf$ of the element. But, since the outer surface of the beam is free of stresses, it follows that the radial component τ_r of the shear stress τ_1 must be equal to zero. Therefore, the stress τ_1 must act in the direction of the tangent to the boundary of the cross section of the beam.

Using this conclusion, let us now investigate the shear stresses acting along a chord pq at distance y_1 from the neutral axis (Fig. 5-30a). The shear stresses τ at the ends of the chord must be tangent to the boundary of the cross section, as shown in the figure. At the midpoint n of the chord, symmetry requires that the shear stress be parallel to the y axis. If follows that the lines of action of the shear stresses at points p and n will intersect at a point on the y axis. By assuming that the shear stress at any other point on line pq is also directed toward this same point, we will have defined the directions of the remaining shear stresses.

tion is required. Let us assume that the vertical components of the shear stresses are equal for all points along line pq . Because this assumption is the same as for a beam of rectangular cross section, we can use the shear formula (Eq. 5-21) for calculating the vertical components. In this case, the term b in the shear formula will denote the length of chord pq . Since the direction of the shear stress and its vertical component are now known, its magnitude may be calculated at any point of the cross section.

Let us now proceed to determine the shear stresses τ along line pq (Fig. 5-30a) in accord with the preceding assumptions. In order to use the shear formula for calculating the vertical component τ_y of the shear stresses, we must obtain the first moment Q of the area below line pq with respect to the z axis. The element of area at distance y from the z axis (shown shaded in the figure) has thickness dy and length $2\sqrt{r^2 - y^2}$ in which r is the radius of the cross section. The first moment of this element of area is found by multiplying the area by y . Thus, the first moment Q of the entire segment below line pq is

$$Q = \int_{y_1}^r 2y\sqrt{r^2 - y^2} dy = \frac{2}{3}(r^2 - y_1^2)^{3/2}$$

Also, the width b and moment of inertia I are

$$b = 2\sqrt{r^2 - y_1^2} \quad I = \frac{\pi r^4}{4}$$

Therefore, the vertical component of the shear stresses is

$$\tau_y = \frac{VQ}{Ib} = \frac{4V}{3\pi r^4}(r^2 - y_1^2) \tag{a}$$

At point p on the boundary of the cross section, the total shear stress τ is related to its vertical component τ_y (see Fig. 5-30c) by the equation

$$\tau = \frac{\tau_y}{\cos \theta} = \frac{r\tau_y}{\sqrt{r^2 - y_1^2}}$$

Substituting for τ_y from Eq. (a), we get

$$\tau = \frac{4V}{3\pi r^3} \sqrt{r^2 - y_1^2} \tag{5-31}$$

as the equation for the shear stress at any point p on the boundary at distance y_1 from the z axis. As we move along the line pn (Fig. 5-30a), the shear stress diminishes (because the vertical components are assumed to be constant) and reaches a minimum at point n , where $\tau = \tau_y$ (Eq. a).

The maximum shear stress occurs at the neutral axis; thus, substituting $y_1 = 0$ into Eq. (5-31), we get

$$\tau_{max} = \frac{4V}{3\pi r^2} = \frac{4V}{3A} \tag{5-32}$$

Stresses in Beams

in which A is the area of the cross section. This equation shows that the maximum shear stress in a circular beam is $4/3$ times the average shear stress V/A .

At the neutral axis, the shear stresses act parallel to the y axis and have constant magnitude (equal to τ_{max}) across the section. Inasmuch as these same assumptions are used in deriving the shear formula $\tau = VQ/Ib$, we may calculate the stresses at the neutral axis directly from that equation, as follows. For a circular cross section, we obtain $I = \pi r^4/4$, $b = 2r$, and

$$Q = \frac{\pi r^2}{2} \left(\frac{4r}{3\pi} \right) = \frac{2r^3}{3}$$

(see Case 11, Appendix D). By substituting these expressions for I , b , and Q into the shear formula, we again obtain the stresses at the neutral axis:

$$\tau = \frac{VQ}{Ib} = \frac{4V}{3\pi r^2} = \frac{4V}{3A}$$

which is the same as Eq. (5-32).

The approximate theory described in this section gives reasonably accurate results for the shear stresses in a solid circular beam. Exact results obtained by the theory of elasticity show that the stresses are not constant along the neutral axis (Refs. 5-13 and 5-14); however, the stresses found by the approximate solution are in error by only a few percent.

If a beam has a hollow circular cross section (Fig. 5-31), we may again assume with good accuracy that the shear stresses along the neutral axis are vertical and uniformly distributed. Therefore, we may obtain the maximum stress from the shear formula (Eq. 5-21). The properties of the cross section are

$$Q = \frac{2}{3}(r_2^3 - r_1^3) \quad I = \frac{\pi}{4}(r_2^4 - r_1^4) \quad b = 2(r_2 - r_1)$$

and the maximum stress is

$$\tau_{max} = \frac{VQ}{Ib} = \frac{4V}{3A} \frac{r_2^2 + r_2r_1 + r_1^2}{r_2^2 + r_1^2} \tag{5-33}$$

in which $A = \pi(r_2^2 - r_1^2)$ is the area of the hollow section.

5.8 BUILT-UP BEAMS

A built-up beam is fabricated of two or more pieces of material joined together to form a single, solid beam. Such beams can be constructed in a great variety of shapes to meet special needs or to provide larger cross sections than are ordinarily available. Figure 5-32 shows some typical cross sections of built-up beams. Part (a) of the figure

shows a wood box beam constructed of two planks, which serve as flanges, connected by plywood webs. The pieces are joined together with nails, screws, or glue; the design must ensure that the entire cross section acts as a single, solid unit. The second example is a glued laminated beam (called a glulam beam) made of boards glued together to form a much larger beam than could be cut from a tree as a single member. The last example is a welded steel plate girder, commonly used in bridge construction and fabricated from three steel plates by fillet weld-bridge construction and fabricated from three steel plates by fillet weld-bridge construction and fabricated from three steel plates by fillet weld-bridge construction and fabricated from three steel plates by fillet weld-

ing at the junctures. A built-up beam is usually designed with the assumption that the parts will be adequately connected so that the beam behaves as a single member. Then the design calculations involve two phases. First, the beam is proportioned as a solid beam, taking into account both bending and shear stresses, as explained in the preceding sections. In the second phase, the connecting elements (nails, welds, bolts, glue) are designed to ensure that the beam behaves as a solid beam. The loads transmitted between the parts of the beam.

A formula for the horizontal shear forces acting between the parts can be obtained by referring to the derivation of the shear formula (see Fig. 5-24, Section 5.5). In that derivation, we assumed that the shear stress τ acting on the top face of the element pp_1n_1n was uniformly distributed across the width b of the beam. However, in a more general case, this assumption may not be valid. Therefore, instead of calculating the shear stresses, we can calculate the total horizontal force F_3 acting on the top face of the element (see Eq. a of Section 5.5). This force may be expressed as $F_3 = f dx$, in which f is the shear force per unit distance along the axis of the beam. (When the shear stress is uniformly distributed across the width of the beam, as we assumed for a beam of rectangular cross section, then $f = \tau b$.) The quantity f , called the shear flow, has units of force per unit distance. To evaluate the shear flow, we proceed as in the derivation of the shear formula. Beginning with Eq. (b) of Section 5.5, we have

$$F_3 = f dx = F_2 - F_1$$

or, upon substituting for F_2 and F_1 and solving,

$$f = \frac{dM}{dx} \left(\frac{1}{I} \right) \int y dA$$

Again, replacing dM/dx with V and the integral with Q , we obtain

$$f = \frac{VQ}{I} \tag{5-34}$$

This equation gives the shear flow f acting between the shaded element shown in Fig. 5-24 and the remainder of the beam. In deriving Eq. (5-34),

5.8 Built-up Beams

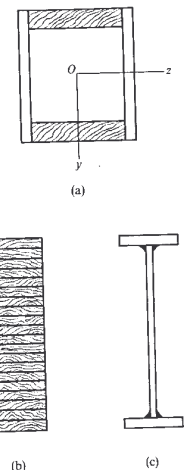


Fig. 5-32 Built-up beams: (a) wood box beam; (b) glulam beam; and (c) steel plate girder

we made no assumption about the distribution of shear stresses across the width of the section. Of course, if the stress distribution is uniform, then $\tau = fb$ and Eq. (5-34) is the same as the shear formula (Eq. 5-21).

The formula for shear flow f is not limited to beams of rectangular cross section; it is valid for any beam having a cross section that is symmetric about the y axis. In practice, the cross-sectional area of the shaded element of Fig. 5-24 may have a variety of shapes. In such cases, the shear flow f is the force per unit distance acting along the line in the cross section that divides the shaded area from the rest of the beam. To clarify this point, let us consider the cross sections shown in Fig. 5-33. In the case of a welded steel plate girder (Fig. 5-33a), the welds must transmit the horizontal shear force between the flanges and the web. This force (per unit distance) is the shear flow along the contact surface aa . It may be calculated from the shear-flow formula $f = VQ/I$ with Q as the first moment of the cross-sectional area above the contact surface aa . In other words, Q is the first moment of the flange area, shown shaded in the figure. Of course, the first moment is always calculated with respect to the z axis. Having calculated f in this manner, we then may select a weld size that is adequate to resist the force f per unit distance (acting longitudinally).

A second example is the beam of Fig. 5-33b, which consists of a wide-flange beam that is strengthened by riveting a channel section to each flange. The horizontal shear force acting between a channel and the main beam must be transmitted by the rivets. This force is calculated from the shear-flow formula using Q as the first moment of the entire channel (shown shaded in the figure). The resulting shear flow f is the longitudinal force per unit distance acting along the contact surface bb , and the rivets must be of adequate size and longitudinal spacing to resist this force. The last example (Fig. 5-33c) is similar, except that the shear flow is the force per unit distance along both contact surfaces cc and dd , and Q is calculated for the area shown shaded. In this case, the shear flow f is resisted by the combined action of the nails on both sides of the beam. These ideas will now be illustrated by an example.

Example

A wood box beam (Fig. 5-34a) is constructed of two boards (each 40 mm \times 180 mm in cross section) that serve as flanges and two webs of plywood, each 15 mm thick. The total height of the beam is 280 mm. The plywood is fastened to the flanges by screws having an allowable load in shear of $F = 1100$ N per screw. If the shear force V acting on the cross section is 10.5 kN, determine the maximum permissible longitudinal spacing s of the screws (Fig. 5-34b).

The horizontal shear force transmitted between one of the flanges and the two webs can be found from the shear-flow formula $f = VQ/I$. The quantity Q is the first moment of the cross-sectional area between the outer edge of the beam and the contact surfaces where the shear flow is being calculated. In this case, the section is cut along lines cc and dd of Fig. 5-33c; hence, the area is

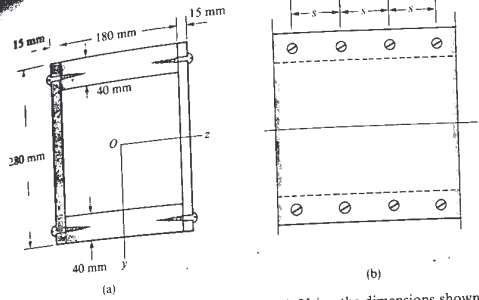


Fig. 5-34 Example

that of one flange (shown shaded in Fig. 5-33c). Using the dimensions shown in Fig. 5-34a, we calculate Q as follows:

$$Q = \bar{y}A = (120 \text{ mm})(180 \text{ mm})(40 \text{ mm}) = 864 \times 10^3 \text{ mm}^3$$

Also, the moment of inertia of the entire cross-sectional area about the neutral axis is

$$I = \frac{1}{12}(210 \text{ mm})(280 \text{ mm})^3 - \frac{1}{12}(180 \text{ mm})(200 \text{ mm})^3 = 264.2 \times 10^6 \text{ mm}^4$$

Now, substituting into the shear-flow formula, we obtain

$$f = \frac{VQ}{I} = \frac{(10,500 \text{ N})(864 \times 10^3 \text{ mm}^3)}{264.2 \times 10^6 \text{ mm}^4} = 34.3 \text{ N/mm}$$

which is the shear force per millimeter of length that must be carried by the screws.

The load capacity of the screws per unit length is $2F/s$, because there are two lines of screws (one on each side of the flange). Equating $2F/s$ to the shear flow, and solving for s , we obtain

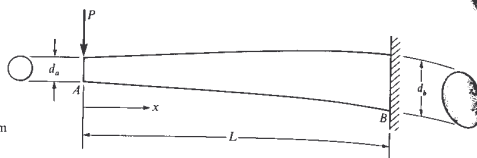
$$s = \frac{2F}{f} = \frac{2(1100 \text{ N})}{34.3 \text{ N/mm}} = 64.1 \text{ mm}$$

This value of s represents the maximum permissible spacing of the screws. For convenience in construction, a spacing such as $s = 60$ mm would be selected.

***5.9 STRESSES IN NONPRISMATIC BEAMS**

The beams analyses presented in the preceding sections of this chapter are restricted to prismatic beams (that is, beams with cross sections that remain the same throughout their lengths). In order to analyze

tapered cantilever beam section



such beams, we derived the flexure and shear formulas ($\sigma = My/I$, $\tau = VQ/Ib$, and $f = VQ/I$). A nonprismatic beam, such as the tapered cantilever beam of Fig. 5-35, will have stress distributions that differ from those given by these formulas. Hence, in this section, we discuss some approximate formulas for obtaining the stresses in nonprismatic beams, and we give some comparisons with exact results.

Normal stresses. If the cross-sectional dimensions change gradually as we move from one end of the beam to the other, we may calculate the normal stresses σ from the flexure formula $\sigma = My/I$ and obtain good accuracy. For instance, in Fig. 5-35, if the angle between the top edge of the beam and the horizontal is less than 20° , the error in calculating the normal stresses is less than 10% (see later discussion of exact results). Of course, for smaller angles, the error is less.

The maximum normal stresses in a prismatic beam always occur at a cross section of maximum bending moment, because σ varies along the axis of the beam in the same manner as M . However, this conclusion does not necessarily apply to nonprismatic beams, because for such beams σ varies along the axis not only in proportion to M but also in inverse proportion to the moment of inertia I . An illustration of this situation is a tapered cantilever beam of solid circular cross section subjected to a concentrated load, as shown in Fig. 5-35. In order to facilitate the analysis, let us assume that the fixed end B has a diameter twice that of the free end A :

$$\frac{d_b}{d_a} = 2$$

Then the diameter d of the bar at distance x from the left end is

$$d = d_a + (d_b - d_a)\frac{x}{L} = d_a\left(1 + \frac{x}{L}\right)$$

and the corresponding section modulus is

$$S = \frac{\pi d^3}{32} = \frac{\pi}{32} d_a^3 \left(1 + \frac{x}{L}\right)^3$$

Hence, the maximum normal stress σ at any cross section is

$$\sigma = \frac{M}{S} = \frac{Px}{S} = \frac{32Px}{\pi d_a^3 \left(1 + \frac{x}{L}\right)^3}$$

Taking the derivative $d\sigma/dx$ and equating it to zero, we can find the value of x for which σ is a maximum; the result is $x = L/2$. The corresponding maximum stress is

$$\sigma_{\max} = \frac{128PL}{27\pi d_a^3} = 4.741 \frac{PL}{\pi d_a^3}$$

At the section of maximum bending moment (support B), the largest stress is

$$\sigma_b = \frac{4PL}{\pi d_b^3}$$

Thus, in this particular example, the maximum stress occurs at the mid-section of the beam, and it is 19% greater than the stress at the built-in end where the bending moment reaches its maximum value. If the taper of the beam is reduced, the section of maximum normal stress will shift toward the fixed support. For very small tapers of the beam, the maximum stress occurs at end B just as it does in a prismatic cantilever.

Shear stresses. The shear stresses in a nonprismatic beam are quite different from those in a prismatic beam; therefore, the shear formula $\tau = VQ/Ib$ cannot be used. In its place, we must derive a new relationship that incorporates the effect of the changing height of the beam. For this purpose, let us consider an element of small length Δx cut out from a nonprismatic beam, as shown in Fig. 5-36. On the left-hand face m_1n_1 of this element, the bending moment is M_1 ; on the right-hand face m_2n_2 , it is M_2 . The corresponding heights of the beam are denoted by h_1 and h_2 , respectively, and y_1 is the distance from the neutral axis to the point where the shear stress τ acts (compare with Fig. 5-24a for a prismatic beam).

The shear flow f acting along the top face p_1p_2 of the shaded element $n_1p_1p_2n_2$ is obtained from an equation of static equilibrium for the element. The forces due to the normal bending stresses acting on the left-hand and right-hand faces of the element are M_1Q_1/I_1 and M_2Q_2/I_2 , respectively (see the equations for F_1 and F_2 in Section 5.5). In these expressions, I_1 and I_2 are the moments of inertia of the two cross sections, and Q_1 and Q_2 are the first moments about the neutral axis of the areas of the sides of the element labeled p_1n_1 and p_2n_2 , respectively. The total force on the top face p_1p_2 of the element is $f\Delta x$. Thus, the equation of static equilibrium becomes

$$f\Delta x = \frac{M_2Q_2}{I_2} - \frac{M_1Q_1}{I_1} \quad (5-35)$$

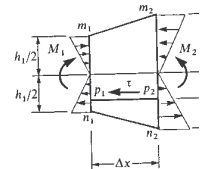


Fig. 5-36 Element of length Δx of a nonprismatic beam

If the shear stress τ is uniform across the width of the beam, then $f = \tau b$, where b is the width of the beam. For any particular beam, Eq. (5-35) can be used to find the average shear flow between the cross sections by substituting numerical values for M , Q , I , and Δx . The procedure is as follows. Select the cross section of the beam where the shear flow f is to be calculated. Then take an adjoining section a small distance Δx away; for instance, take $\Delta x = L/100$. At each of these sections determine the following: (1) bending moment M , (2) first moment Q of the part of the cross-sectional area located between the outer edge of the beam and the line in the cross section where f is to be determined, and (3) the moment of inertia I of the entire cross section. Then substitute these values into Eq. (5-35) and solve for f . The smaller the distance Δx , the more accurate the results will be (in theory). However, if Δx is too small, numerical accuracy may be inadequate because Eq. (5-35) requires taking the difference between two terms that are nearly equal. Equation (5-35) is quite general and is useful in many practical situations in order to obtain the shear flow for a beam of varying cross section when exact formulas are not available.

Shear stresses in rectangular beams. In the particular case of a beam of rectangular cross section with constant width b and varying height h , we can convert Eq. (5-35) to a more exact equation by letting Δx approach zero. Also, we note that, in a rectangular beam, it is reasonable to assume that the shear stresses τ are uniformly distributed across the width b of the beam, hence $f = \tau b$ in Eq. (5-35). To derive the desired formula, we begin by evaluating Q and I at cross sections 1 and 2, which are a distance Δx apart:

$$Q_1 = \frac{b}{2} \left(\frac{h_1^2}{4} - y_1^2 \right) \quad Q_2 = \frac{b}{2} \left(\frac{h_2^2}{4} - y_1^2 \right)$$

$$I_1 = \frac{bh_1^3}{12} \quad I_2 = \frac{bh_2^3}{12}$$

Now, letting $h_2 = h_1 + \Delta h$, where Δh is the increment in h as we go from section 1 to section 2, we obtain from the preceding equations

$$Q_2 = Q_1 + \frac{bh_1 \Delta h}{4} \quad I_2 = I_1 + \frac{bh_1^2 \Delta h}{4}$$

In deriving these equations, terms containing the square and cube of Δh have been dropped because they are small in comparison to the terms retained. Noting also that $M_2 = M_1 + \Delta M$, we now substitute the expressions for Q_2 , I_2 , and M_2 into Eq. (5-35):

$$\tau b \Delta x = \frac{(M_1 + \Delta M) \left(Q_1 + \frac{bh_1 \Delta h}{4} \right) - M_1 Q_1}{I_1 + \frac{bh_1^2 \Delta h}{4}}$$

In order to simplify this equation, we may multiply all terms by the de-

ominator of the second term and then expand the remaining products.

The result is

$$\tau b I_1 \Delta x + \frac{\tau b^2 h_1^2}{4} \Delta h \Delta x = \frac{M_1 b h_1}{4} \Delta h + Q_1 \Delta M + \frac{b h_1}{4} \Delta h \Delta M - \frac{M_1 Q_1}{4 I_1} b h_1^2 \Delta h$$

In this equation, terms containing the product of two small quantities may now be dropped, and then the equation may be divided by Δx . In the limit as Δx becomes smaller and smaller, the term $\Delta h/\Delta x$ becomes the limit dh/dx and the term $\Delta M/\Delta x$ becomes dM/dx , which is equal to the shear force V . Thus, the equation becomes

$$\tau b I_1 = \frac{M_1 b h_1}{4} \frac{dh}{dx} + Q_1 V - \frac{M_1 Q_1 b h_1^2}{4 I_1} \frac{dh}{dx}$$

As a final step, we divide all terms by $b I_1$, and then drop the numerical subscript, which is no longer needed. Thus, the final form of the expression for the shear stress τ in a nonprismatic beam of rectangular cross section is

$$\tau = \frac{VQ}{Ib} + \frac{Mh}{4I} \left(1 - \frac{Qh}{I} \right) \frac{dh}{dx} \quad (5-36)$$

This equation is valid for a beam of constant width b and varying height h . The height may vary in any manner, provided that the variation is gradual. We observe that the shear stress at any cross section is dependent not only upon the shear force V , but also upon the bending moment M and the rate of change of h with respect to x .

As a specific example, let us investigate the distribution of shear stresses in the cantilever beam of rectangular cross section shown in Fig. 5-37a. The beam has heights h_a and $h_b = 2h_a$ at its ends and a uniform taper. Therefore, the quantity dh/dx is constant and is equal to

$$\frac{dh}{dx} = \frac{h_b - h_a}{L} = \frac{h_a}{L}$$

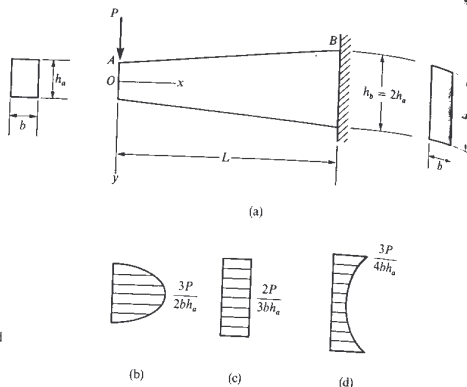
At the left end A , the bending moment is zero; hence, Eq. (5-36) gives the same parabolic distribution of shear stresses as in a prismatic beam. This distribution is plotted in Fig. 5-37b. The maximum shear stress occurs at the neutral axis, and it is equal to $1.5 P/bh_a$.

At the middle of the beam ($x = L/2$), the following values are obtained:

$$V = P \quad h = 1.5h_a \quad Q = \frac{b}{2} \left(\frac{h^2}{4} - y_1^2 \right) \quad M = \frac{PL}{2} \quad I = \frac{bh^3}{12}$$

Substituting into Eq. (5-36) yields

$$\tau = \frac{2P}{bh}$$



Shear stresses in a tapered beam of rectangular cross

section. The normal and shear stresses at any point p in cross section mn are given by the following formulas (Ref. 5-16):

$$\sigma = -\frac{Pxy \sin^4 \theta}{bx^2(\alpha - \sin \alpha \cos \alpha)} \quad \tau = \frac{Py^2 \sin^4 \theta}{bx^3(\alpha - \sin \alpha \cos \alpha)} \quad (a)$$

in which x and y are the coordinates of point p , θ is the angle between the line Op and the y axis, b is the thickness of the wedge (assumed constant), and α is the angle defining the taper of the wedge. These equations can be put in more convenient form by observing that the bending moment at section mn is $M = Px$, the height h of the wedge at the same moment at section mn is $h = 2x \tan \alpha$, and the moment of inertia at cross section mn is

$$I = \frac{bh^3}{12} = \frac{2bx^3 \tan^3 \alpha}{3}$$

Substituting the expressions for M , h , and I into Eqs. (a), we find

$$\sigma = -\frac{My}{I} \frac{2 \tan^3 \alpha \sin^4 \theta}{3(\alpha - \sin \alpha \cos \alpha)} \quad (5-37)$$

$$\tau = \frac{P}{bh} \frac{8y^2 \tan^3 \alpha \sin^4 \theta}{h^2(\alpha - \sin \alpha \cos \alpha)} \quad (5-38)$$

The normal stress σ given by Eq. (5-37) is equal to zero at the neutral axis ($\theta = \pi/2$, $y = 0$), and it reaches a maximum at the outer edge of the beam. At the top of the beam ($y = -h/2$, $\theta = \alpha + \pi/2$), the stress is

$$\sigma_{\max} = \frac{Mh}{2I} \frac{2 \sin^3 \alpha \cos \alpha}{3(\alpha - \sin \alpha \cos \alpha)} = \beta \frac{Mh}{2I} \quad (5-39)$$

For values of the angle α equal to 0° , 5° , 10° , 15° , and 20° , the factor β has the values 1, 0.994, 0.976, 0.946, and 0.906, respectively. Thus, we see that for small angles of taper there is little difference between the normal stresses calculated from the exact theory and those obtained from the flexure formula $\sigma = My/I$.

For the shear stresses, we see that Eq. (5-38) always gives $\tau = 0$ at the neutral axis ($y = 0$). The maximum stress is at the outer edges where

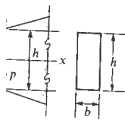
$$\tau_{\max} = \frac{P}{bh} \frac{2 \sin^3 \alpha \cos \alpha}{\alpha - \sin \alpha \cos \alpha} = \gamma \frac{P}{bh} \quad (5-40)$$

For values of α equal to 0° , 5° , 10° , 15° , and 20° , the factor γ is equal to 3, 2.98, 2.93, 2.84, and 2.72, respectively. Thus, the maximum shear stress is about three times the average shear stress P/bh , and it occurs at the outer edges.

If we apply the approximate theory for shear stresses in a tapered rectangular beam (see Eq. 5-36) to the wedge pictured in Fig. 5-38, we obtain for section mn :

$$V = P \quad Q = \frac{b}{2} \left(\frac{h^2}{4} - y_1^2 \right) \quad I = \frac{bh^3}{12} \quad M = Px \quad \frac{dh}{dx} = \frac{h}{x}$$

Exact results. The stresses in a cantilever wedge of rectangular cross section (Fig. 5-38) are found by the methods of the theory of elas-



wedge of rectangular cross section

Material 2 is in tension throughout. The maximum tensile stress σ_{t2} occurs at the bottom of the beam ($y = h_2 = 37.2$ mm); hence, from Eq. (5-46b) we get

$$\sigma_{t2} = 33.3 \text{ MPa}$$

The minimum tensile stress in material 2 is obtained at the junction of the two materials; this stress is 22.6 MPa.

Transformed-section method. The transformed-section method provides a convenient way to analyze a composite beam. The method is to transform the cross section, consisting of more than one material, into an equivalent cross section composed of only one material. Then the latter, called the **transformed section**, is analyzed in the usual manner for a beam of one material.

The transformed section must have the same location for the neutral axis and the same moment-resisting capacity as the original beam if it is to be equivalent. In order to see how this equivalence is accomplished, let us refer to the equation used for locating the neutral axis (Eq. 5-43). Introducing the notation

$$n = \frac{E_2}{E_1} \tag{5-47}$$

where n is the **modular ratio**, we can rewrite Eq. (5-43) in the form

$$\int_1 y dA + \int_2 yn dA = 0 \tag{5-48}$$

This equation shows that the neutral axis will be in the same position if each element of area dA in material 2 is multiplied by the factor n , provided that the distance y for each such element of area is unchanged. Therefore, we can consider the cross section as consisting of two parts: (1) area 1 with its dimensions unchanged and (2) area 2 with its width multiplied by n . Thus, we have a new cross section consisting of only one material, namely, material 1.

The transformed section for the composite beam of Fig. 5-41a is shown in Fig. 5-41d. As explained in the preceding paragraph, material 1 remains unchanged, but the width of material 2 is multiplied by n . (We assume in this illustration that $n > 1$, but this assumption is not necessary.) The transformed section consists entirely of material 1, and its neutral axis is in the same location as the neutral axis of the original beam (Fig. 5-41a).

Furthermore, the bending-moment capacity of the transformed section will be the same as for the original cross section. To establish this result, we note that the stresses in the transformed beam, which consists of only one material, are given by Eq. (5-5):

$$\sigma_x = -E_1 \kappa y$$

Therefore, the bending moment M can be obtained as follows (see Fig. 5-41d):

$$\begin{aligned} M &= \int \sigma_x y dA = \int_1 \sigma_x y dA + \int_2 \sigma_x y dA \\ &= -\kappa E_1 \int_1 y^2 dA - \kappa E_1 \int_2 y^2 dA \\ &= -\kappa(E_1 I_1 + E_1 n I_2) = -\kappa(E_1 I_1 + E_2 I_2) \end{aligned}$$

which is the same result as Eq. (5-44). Hence, we conclude that the bending moment is unchanged between the original beam and the transformed beam.

The stresses in the transformed beam can be found by the ordinary flexure formula for a beam of one material. Thus, the stresses in the beam transformed to material 1 are

$$\sigma_{x1} = \frac{My}{I_1} \tag{5-49}$$

where I_1 is the moment of inertia about the neutral axis of the transformed section; that is,

$$I_1 = I_1 + n I_2 = I_1 + \frac{E_2}{E_1} I_2 \tag{5-50}$$

Substituting the expression for I_1 from Eq. (5-50) into Eq. (5-49) gives

$$\sigma_{x1} = \frac{MyE_1}{E_1 I_1 + E_2 I_2} \tag{a}$$

which is the same as Eq. (5-46a). Hence, we observe that the stresses in material 1 in the original beam are the same as the stresses in the transformed beam. This conclusion results from the fact that we transformed the beam to material 1. However, the stresses in material 2 in the original beam are not the same as the stresses in the corresponding part of the transformed beam. Instead, the stresses in the transformed beam (Eq. a) must be multiplied by the modular ratio n to obtain the stresses in material 2 of the original beam (see Eq. 5-46b).

It is also possible to transform the original beam to a beam consisting entirely of material 2. In that case, the stresses in the original beam in material 2 are the same as the stresses in the corresponding parts of the transformed beam. However, the stresses in material 1 are obtained by multiplying the stresses in the transformed beam by n , which now is defined as

$$n = \frac{E_1}{E_2} \tag{5-51}$$

Example 3 illustrates these ideas.

The transformed-section method may be extended to composite beams of more than two materials. Also, it is possible to transform the

beam into a material having any arbitrary value of E , in which case all parts of the beam must be transformed to the fictitious material. Of course, it is simpler and more common to transform to one of the original materials, the choice among them being arbitrary.

Example 2

The composite beam described in Example 1 and pictured in Fig. 5-42 is to be analyzed by the transformed-section method. Let us transform the original beam into a beam of material 1 (Fig. 5-43a). Therefore, the upper part of the beam is not altered, but the lower part has its width multiplied by the modular ratio, which is

$$n = \frac{E_2}{E_1} = \frac{140 \text{ GPa}}{7 \text{ GPa}} = 20$$

Thus, the width of part 2 becomes 2 m in the transformed section.

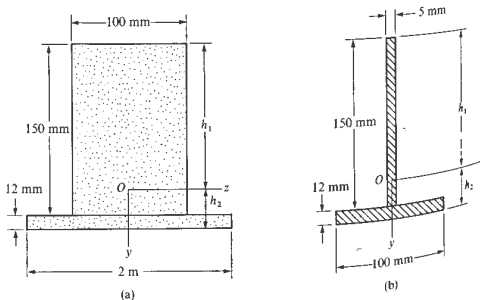
Because the transformed beam is of one material, the neutral axis must pass through the centroid of the cross-sectional area. Taking the top edge of the cross section as a reference line, we calculate the centroidal distance h_1 as follows:

$$\begin{aligned} h_1 &= \frac{\sum y_i A_i}{\sum A_i} = \frac{(75 \text{ mm})(100 \text{ mm})(150 \text{ mm}) + (156 \text{ mm})(2000 \text{ mm})(12 \text{ mm})}{(100 \text{ mm})(150 \text{ mm}) + (2000 \text{ mm})(12 \text{ mm})} \\ &= \frac{4869 \times 10^3 \text{ mm}^3}{39 \times 10^3 \text{ mm}^2} = 124.9 \text{ mm} \end{aligned}$$

Also, the distance h_2 is

$$h_2 = 162 \text{ mm} - h_1 = 37.2 \text{ mm}$$

Thus, the position of the neutral axis is determined.



Examples 2 and 3. Diagram (a) shows the original beam of material 1 and material 2. Diagram (b) shows the transformed section.

Utilizing the parallel-axis theorem, we calculate the moment of inertia I_1 of the entire cross-sectional area about the neutral axis as follows:

$$\begin{aligned} I_1 &= \frac{1}{12} (100 \text{ mm})(150 \text{ mm})^3 + (100 \text{ mm})(150 \text{ mm})(h_1 - 75 \text{ mm})^2 \\ &\quad + \frac{1}{12} (2000 \text{ mm})(12 \text{ mm})^3 + (2000 \text{ mm})(12 \text{ mm})(h_2 - 6 \text{ mm})^2 \\ &= 88.98 \times 10^6 \text{ mm}^4 \end{aligned}$$

The flexure formula is now used to calculate the stresses in the transformed beam at the top, at the junction of the two parts, and at the bottom, respectively:

$$\begin{aligned} \sigma &= \frac{My}{I_1} = \frac{(4 \times 10^6 \text{ N}\cdot\text{mm})(-124.9 \text{ mm})}{88.98 \times 10^6 \text{ mm}^4} = -5.61 \text{ MPa} \\ \sigma &= \frac{My}{I_1} = \frac{(4 \times 10^6 \text{ N}\cdot\text{mm})(25.15 \text{ mm})}{88.98 \times 10^6 \text{ mm}^4} = 1.13 \text{ MPa} \\ \sigma &= \frac{My}{I_1} = \frac{(4 \times 10^6 \text{ N}\cdot\text{mm})(37.15 \text{ mm})}{88.98 \times 10^6 \text{ mm}^4} = 1.67 \text{ MPa} \end{aligned}$$

The stresses in the original beam are the same as in the transformed beam for material 1; therefore, the maximum compressive stress in material 1 is

$$\sigma_{c1} = -5.61 \text{ MPa}$$

at the top of the beam. Also, the largest tensile stress in material 1 (at the junction) is

$$\sigma_{t1} = 1.13 \text{ MPa}$$

For material 2, we multiply the stresses in the transformed beam by n . The maximum tension occurs at the bottom of the beam:

$$\sigma_{t2} = n(1.67 \text{ MPa}) = 20(1.67 \text{ MPa}) = 33.4 \text{ MPa}$$

Also, the tension in material 2 at the junction is $20(1.13 \text{ MPa})$ or 22.6 MPa. All of these results agree with those found in Example 1.

Example 3

In order to illustrate more fully the transformed-section method, let us now analyze the composite beam of Fig. 5-42 by transforming the beam to material 2. The modular ratio for this analysis is

$$n = \frac{E_1}{E_2} = \frac{1}{20}$$

(see Eq. 5-51). The transformed section has the same dimensions as the original beam for material 2, but material 1 has its width multiplied by n ; thus, the width of the upper part of the beam is $\frac{1}{20}$ the original width (Fig. 5-43b).

We now follow the same steps as in the preceding example. The distance to the neutral axis are

$$h_1 = \frac{\sum y_i A_i}{\sum A_i} = \frac{(75 \text{ mm})(5 \text{ mm})(150 \text{ mm}) + (156 \text{ mm})(100 \text{ mm})(12 \text{ mm})}{(5 \text{ mm})(150 \text{ mm}) + (100 \text{ mm})(12 \text{ mm})}$$

$$= \frac{243,450 \text{ mm}^3}{1950 \text{ mm}^2} = 124.9 \text{ mm}$$

$$h_2 = 162 \text{ mm} - h_1 = 37.2 \text{ mm}$$

The moment of inertia is

$$I_x = \frac{1}{12} (5 \text{ mm})(150 \text{ mm})^3 + (5 \text{ mm})(150 \text{ mm})(h_1 - 75 \text{ mm})^2$$

$$+ \frac{1}{12} (100 \text{ mm})(12 \text{ mm})^3 + (100 \text{ mm})(12 \text{ mm})(h_2 - 6 \text{ mm})^2$$

$$= 4.449 \times 10^6 \text{ mm}^4$$

The stresses in the transformed section at the top, the junction, and the bottom are, respectively,

$$\sigma = \frac{My}{I_x} = \frac{(4 \times 10^6 \text{ N}\cdot\text{mm})(-124.9 \text{ mm})}{4.449 \times 10^6 \text{ mm}^4} = -112.3 \text{ MPa}$$

$$\sigma = \frac{My}{I_x} = \frac{4 \times 10^6 \text{ N}\cdot\text{mm}(25.2 \text{ mm})}{4.449 \times 10^6 \text{ mm}^4} = 22.6 \text{ MPa}$$

$$\sigma = \frac{My}{I_x} = \frac{4 \times 10^6 \text{ N}\cdot\text{mm}(37.2 \text{ mm})}{4.449 \times 10^6 \text{ mm}^4} = 33.4 \text{ MPa}$$

To obtain the stresses in the original beam, the stresses in material 1 are multiplied by n ; thus, at the top of the beam and at the junction, we obtain

$$\sigma_{t1} = n(-112.3 \text{ MPa}) = -5.61 \text{ MPa}$$

$$\sigma_{j1} = n(33.4 \text{ MPa}) = 1.13 \text{ MPa}$$

For material 2, the stresses in the original beam are the same as in the transformed beam (33.4 MPa and 22.6 MPa at the bottom and at the junction, respectively).

The calculations for Examples 2 and 3 are very similar; hence, it is apparent that no advantage is gained by transforming to one material rather than the other.

Sandwich beams. A sandwich beam consists of two thin layers of material, called the faces, on either side of a thick core (see Fig. 5-44). The core is usually of lightweight, low-strength material serving primarily as a filler or spacer, whereas the faces are of high-strength material. Sandwich construction is used where light weight combined with high strength and high stiffness are needed.

Sandwich beams can be analyzed for flexure in the manner just

described for beams of two materials. However, an approximate theory for bending of sandwich beams has been developed on the assumption that the faces carry all of the longitudinal bending stresses. This assumption is reasonable when the core has a low modulus of elasticity in the longitudinal direction relative to that of the faces. Thus, the normal stresses at the outermost edges of the beam (see Fig. 5-44) are

$$\sigma_x = \frac{Md}{2I_f} \quad (5-52)$$

where d is the depth of the beam and I_f is the moment of inertia of the faces about the z axis, as follows:

$$I_f = \frac{b}{12} (d^3 - h^3) \quad (5-53)$$

If the faces are thin, we can assume that the core carries all of the shear stresses. Therefore, the average shear stress and shear strain in the core are, respectively,

$$\tau = \frac{V}{bh} \quad \gamma = \frac{V}{bhG_c} \quad (5-54, b)$$

where h is the height of the core, V is the shear force, and G_c is the shear modulus of the core material.

More accurate theories of bending of sandwich beams also have been developed; for instance, bending of the faces as individual beams can be taken into account. For more detailed treatments of sandwich beams and other forms of composite construction, see Refs. 5-17 and 5-18.

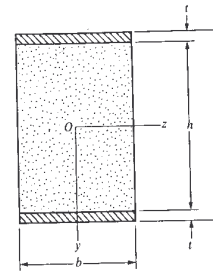


Fig. 5-44 Cross section of sandwich beam

5.11 BEAMS WITH AXIAL LOADS

Structural members may be subjected to the simultaneous action of bending loads and axial forces. An example is shown in Fig. 5-45a, which portrays a cantilever beam acted upon by an inclined force P acting through the centroid of the end cross section. The load P can be resolved into two components, a transverse load Q and an axial load S . These loads produce stress resultants in the form of bending moments M , shear forces V , and axial forces N . For a cross section at distance x from the support, these stress resultants are

$$M = Q(L - x) \quad V = -Q \quad N = S$$

The stresses due to each of these stress resultants can be determined at any point in the cross section by means of the appropriate formulas ($\sigma = My/I$, $\tau = VQ/Ib$, and $\sigma = N/A$). Then the final stress distribution can be obtained by combining the stresses associated with each stress resultant.

When determining the stresses in a bar due to the combined action of bending loads and axial forces, it is important to distinguish between

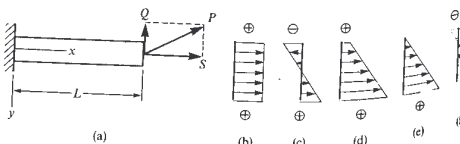
two possible situations, as follows: (1) The beam is relatively short and stiff, or stocky. Then the lateral deflections of the beam are very small compared to the length, and the presence of the deflections produces an insignificant change in the line of action of the axial load S . In such a case, the bending moment M does not depend upon the deflections (even though small in magnitude) may be large enough to affect the bending moments. The line of action of the axial force S is displaced every cross section equal to the product of the axial force and the deflection. In other words, there is an interaction, or coupling, between the axial effects and the bending effects. This type of beam behavior is discussed in Chapter 11. In this section, we will consider only beams that are relatively stiff and that meet the first set of conditions.

The distinction between a stocky beam and a slender beam is obviously not a precise one. In general, the only way to know whether interaction effects are important is to analyze the beam with and without the interaction effects and then notice whether the results differ significantly. However, this procedure may require considerable calculating effort. As a guideline for practical use, we may usually consider a beam with a length-to-depth ratio of 10 or less to be a stocky beam.

Let us now return to the investigation of the stresses in the cantilever beam of Fig. 5-45a. The resultant stresses acting at any cross section are obtained by superimposing the normal stresses due to the axial force N and those due to the bending moment M . The axial force N produces a uniform stress distribution $\sigma = N/A$, plotted in Fig. 5-45b, and the bending moment produces a linearly varying stress $\sigma = My/I$, plotted in Fig. 5-45c. The total stresses, shown in Fig. 5-45d, can be found from the following equation:

$$\sigma = \frac{N}{A} + \frac{My}{I} \quad (5-55)$$

Note that N is positive when it produces tension and that M is positive according to the bending-moment sign convention (positive M produces compression in the upper part of the beam; see Fig. 4-3). With these sign conventions, the sign of the normal stress σ in Eq. (5-55) is positive for tension and negative for compression, as expected. The final stress



beam subjected
ding load and

depends upon the relative algebraic values of the terms in the equation. The distribution may be such that the entire cross section is in tension, as shown in Fig. 5-45d. Other possibilities are that the stress distribution may be triangular (Fig. 5-45e), or the section may be partially in tension and partially in compression (Fig. 5-45f), or it may be entirely in compression if the axial force N is a compressive force instead of a tensile force.

When bending and axial loads are combined, the neutral axis (that is, the line in the cross section where the normal stress is zero) is not through the centroid of the cross section. As shown in Figs. 5-45d, e, and f, the neutral axis may be outside the cross section, at the edge of the cross section, or anywhere within the section.

Example

A simple beam AB having a rectangular cross section (width b and height h) and span length L is loaded by a force P acting at the end of an arm of length a (see Fig. 5-46a). Determine the maximum tensile and compressive stresses in the beam.

We begin by determining the reactions of the beam, which are shown in the force diagram of Fig. 5-46b. Next, we construct axial-force and bending-moment diagrams (Figs. 5-46c and d). The axial-force diagram shows that the axial force in the left-hand half of the beam is compressive and is equal to P . The bending-moment diagram shows that the maximum positive moment occurs just to the left of midspan and the maximum negative moment occurs just to the right of the midpoint. Thus, at a cross section located a small distance to the left of the midpoint of the beam, the axial force and the bending moment are, respectively,

$$N = -P \quad M = \frac{Pa}{2}$$

Therefore, we find from Eq. (5-55) that the stresses at the bottom and top edges of the beam ($y = h/2$, and $y = -h/2$, respectively) are as follows:

$$\sigma_b = \frac{P}{bh} + \frac{3Pa}{bh^2} \quad \sigma_t = -\frac{P}{bh} - \frac{3Pa}{bh^2}$$

Similarly, the stresses at a cross section just to the right of the center of the beam (where $M = -Pa/2$ and $N = 0$) are

$$\sigma_b = -\frac{3Pa}{bh^2} \quad \sigma_t = \frac{3Pa}{bh^2}$$

Upon comparing these stresses, we see that the maximum tensile stress in the beam occurs at the top to the right of the midpoint, and the maximum compressive stress occurs at the top to the left of the midpoint. These stresses are, respectively,

$$\sigma_{\text{tens}} = \frac{3Pa}{bh^2} \quad \sigma_{\text{comp}} = -\frac{P}{bh} - \frac{3Pa}{bh^2}$$

Thus, the compressive stress is numerically larger than the tensile stress.

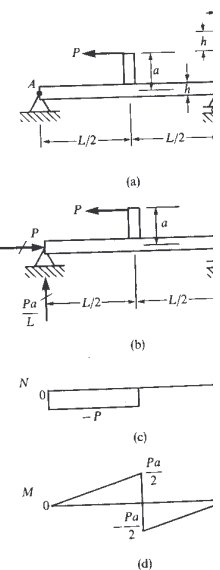
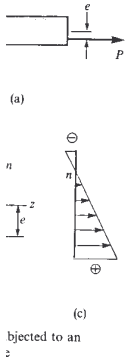


Fig. 5-46 Example



Eccentric axial load. An important case of practical interest is illustrated in Fig. 5-47. The tensile load P acts normal to the end cross section at a distance e from the z axis, which is a principal axis through the centroid C . (As in previous discussions, the y axis is an axis of symmetry.) The eccentric load P is statically equivalent to a force P applied at the centroid plus a couple Pe . Therefore, the normal stress at any point in the cross section (from Eq. 5-55) is

$$\sigma = \frac{P}{A} + \frac{Pe y}{I} \quad (5-56)$$

This stress distribution is shown in Fig. 5-47c. If the axial load is compression, the value of P in Eq. (5-56) is negative.

The equation of the neutral axis (line nn in Fig. 5-47b) can be obtained by setting the normal stress σ (Eq. 5-56) equal to zero, which gives

$$y = -\frac{l}{Ae} \quad (5-57)$$

This equation defines a straight line in the cross section parallel to the z axis. The minus sign shows that the neutral axis lies above the z axis when the axial load P acts below the z axis. (Note that e is positive when the load acts below the z axis.) If the eccentricity e is increased, the neutral axis will move closer to the centroid; if e is reduced, the neutral axis will move farther from the centroid. Of course, the neutral axis may be outside the cross section.

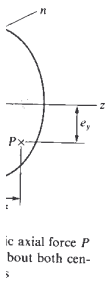
When the point of application of the eccentric force P is not on one of the principal axes of the cross section, there will be simultaneous bending about both centroidal principal axes. Denoting the coordinates of the point of application of P by e_y and e_z (see Fig. 5-48), we see that the bending moments about the y and z axes are numerically equal to Pe_z and Pe_y , respectively. The resultant normal stress σ at any point in the cross section (a point defined by coordinates y and z) then becomes

$$\sigma = \frac{P}{A} + \frac{Pe_z z}{I_y} + \frac{Pe_y y}{I_z} \quad (5-58)$$

where I_y and I_z are the moments of inertia about the y and z axes, respectively. In Eq. (5-58), the axial force P is positive if it is tension, and e_y and e_z are positive in the coordinate directions shown in Fig. 5-48. Equation (5-58) reduces to Eq. (5-56) when P lies on the y axis and e_z equals zero.

The equation of the neutral axis can be found by setting σ equal to zero, which gives

$$\frac{Ae_z}{I_z} y + \frac{Ae_y}{I_y} z + 1 = 0 \quad (5-59)$$



This equation is linear in y and z ; hence, the neutral axis is a straight line, such as line nn in Fig. 5-48. The neutral axis may or may not intersect the cross section, depending upon the shape of the cross section and the position of the point of application of the axial force P . The intercepts of line nn with the y and z axes can be found by setting z and y , respectively, equal to zero in Eq. (5-59) and solving for the intercepts. An interesting relationship exists between the point of application of the eccentric axial force P and the position of the neutral axis nn , as follows. If the force P moves along any straight line mm , the neutral axis follows. To demonstrate this fact, rotate about a fixed point R (see Fig. 5-49). To demonstrate this fact, observe first that the force P can be resolved into two parallel components, one acting at p_1 and the other at p_2 . The component at p_1 acts in a principal plane of bending; hence, the corresponding line of action is parallel to the z axis and is located at distance $s_1 = I_z/Ae_1$ from the z axis (see Fig. 5-49 and Eq. 5-57). Similarly, the component at p_2 produces bending about the y axis, and the line of zero stress is at distance $s_2 = I_y/Ae_2$ from the y axis. Point R , at the intersection of the two dashed lines in the figure, will always be on the neutral axis nn when both components of load act simultaneously. Thus, as the load P moves along line mm , point R remains fixed in position, and the neutral axis always passes through it.

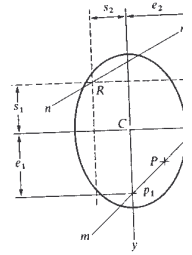


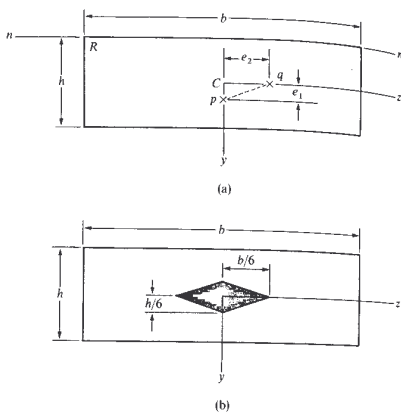
Fig. 5-49 Relationship between position of load P and neutral axis.

The core of a cross section. When the eccentricity e of the applied axial load P (Fig. 5-47) is small, the neutral axis will lie inside the cross section and the normal stresses will have the same sign throughout the cross section. A condition of this kind is important when a compressive load acts on a material that is very weak in tension, such as a ceramic material or concrete. For such materials, it may be necessary to ensure that the load produces no tension at any point of the cross section. This condition exists when the load remains within a certain small region surrounding the centroid. A compressive force acting within that region produces compression over the entire cross section, and a tensile force produces tension over the entire cross section. This region is called the **core** (or the **kern**) of the section.*

The core of a rectangular cross section (Fig. 5-50a) can be found in the following manner. If the load lies along the positive y axis, the neutral axis nn will coincide with the upper edge of the section when the load is at point p , a distance e_1 from the centroid. The distance e_1 can be found from Eq. (5-57) by substituting $y = -h/2$, $I = bh^3/12$, and $A = bh$; thus, $e_1 = h/6$. Similarly, the neutral axis coincides with the left-hand edge of the section when the load P acts on the positive z axis at point q , a distance $e_2 = b/6$ from the centroid. As the load moves along a straight line between points p and q , the neutral axis will rotate about point R at the corner of the rectangular cross section. Hence, line pq is

* The concept of the core of a cross section was introduced by the French engineer J. A. C. Bresse in 1854; see Ref. 5-19.

Stresses in Beams

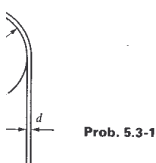


core of a rectangular

one of the sides of the core; the other three sides can be located by symmetry. We see that the core is a rhombus with diagonals of lengths $b/3$ and $h/3$ (Fig. 5-50b). If the point of application of a compressive load P is within this rhombus, the neutral axis will not intersect the cross section and the entire section will be in compression. The core of other cross-sectional shapes can be found by the same method as the one described for a rectangle.

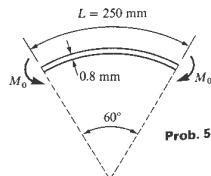
/ CHAPTER 5

e maximum stress σ_{max} produced in a wire of diameter $d = 0.8$ mm when the wire is bent into a circular arc subtending a central angle of 60° (see figure). What is the maximum stress σ_{max} in the wire?



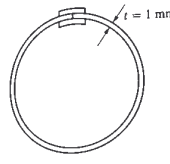
Prob. 5.3-1

5.3-2 A thin steel rule ($E = 200$ GPa) having thickness $t = 0.8$ mm and length $L = 250$ mm is bent by couples M_0 at the ends into a circular arc subtending a central angle of 60° (see figure). Determine the maximum bending stress σ_{max} in the rule.



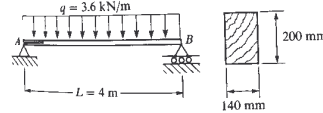
Prob. 5.3-2

5.3-3 A thin strip of copper ($E = 120$ GPa) having length $L = 1.5$ m and thickness $t = 1$ mm is bent into a circular arc with the ends just touching (see figure). Calculate the maximum bending stress σ_{max} in the strip.



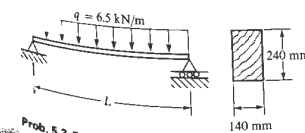
Prob. 5.3-3

5.3-4 A simple beam AB with span length $L = 4$ m carries a uniform load of intensity $q = 3.6$ kN/m (see figure). Calculate the maximum bending stress σ_{max} due to the load q if the beam is of rectangular cross section with width $b = 140$ mm and height $h = 200$ mm.



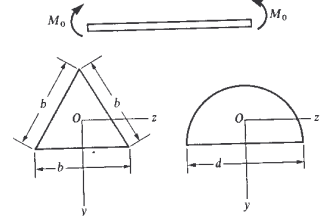
Prob. 5.3-4

5.3-5 Determine the maximum allowable span length L for a simple beam (see figure) of rectangular cross section (140 mm \times 240 mm) subjected to a uniformly distributed load $q = 6.5$ kN/m if the allowable bending stress is 8.2 MPa. (The weight of the beam is included in the load q .)



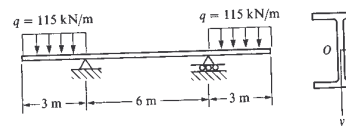
Prob. 5.3-5

5.3-6 The beam shown in the figure is subjected to bending by couples M_0 . Determine the ratio σ_t/σ_c of maximum tensile and compressive stresses if the cross section is (a) an equilateral triangle and (b) a semicircle.



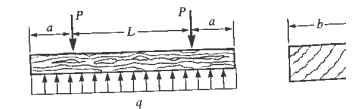
Prob. 5.3-6

5.3-7 A steel beam of wide-flange cross section is ported with overhanging ends, as shown in the figure. The beam carries a uniform load of intensity $q = 115$ kN/m on each overhang. Assuming that the section modulus of the cross-section is $S = 8.83 \times 10^6$ mm³, determine the maximum bending stress σ_{max} in the beam due to load q .



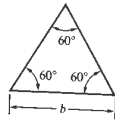
Prob. 5.3-7

5.3-8 A railroad tie (or sleeper) is subjected to two concentrated loads $P = 220$ kN, acting as shown in the figure. The reaction q of the ballast may be assumed uniformly distributed over the length of the tie, which has cross-sectional dimensions $b = 300$ mm and $h = 2$ m. Calculate the maximum bending stress σ_{max} in the tie assuming $L = 1.5$ m and $a = 0.5$ m.



Prob. 5.3-8

Determine the core of a cross section in the form of an equilateral triangle with sides of length b (see figure). Determine the core of a $203 \times 203 \times 60$ kg UC steel section (see Appendix E).



Prob. 5.11-17

Analysis of Stress and Strain

6.1 INTRODUCTION

Normal and shear stresses in beams, shafts, and bars can be obtained from the various formulas discussed in the preceding chapters. For instance, stresses in beams may be calculated from the flexure and shear formulas ($\sigma = My/I$ and $\tau = VQ/Ib$). The stresses given by these basic formulas act over cross sections of the members. In this chapter, we discuss methods for finding the normal and shear stresses acting on inclined sections through the members. For the special cases of uniaxial stress and pure shear, we derived expressions for the stresses on inclined planes in Sections 2.7 and 3.4, respectively. We found that the maximum shear stresses for an axially loaded bar occur on planes inclined at 45° , and the maximum tensile and compressive stresses for a bar in torsion also occur on 45° planes. In a similar manner, inclined sections cut through a beam may be subjected to both normal and shear stresses, and these stresses may be larger than the stresses acting on a cross section. To handle analyses of this type, we need a more general approach for determining the stresses on inclined planes.

Our approach uses **stress elements** to represent the state of stress at a point in a body. Stress elements were discussed previously in a specialized context (see Sections 2.7 and 3.4), but now we will use them in a more formalized manner. For instance, we will associate a set of coordinate axes with each position of a stress element. Our objective is to derive the transformation relationships that give the stress components for any orientation of these axes. In other words, we wish to determine the stresses acting on the sides of a stress element rotated to any desired position, assuming that the stresses are known for the reference position. This process is variously referred to as a **transformation of axes** or a **stress transformation**, although it must be emphasized that only one intrinsic state of stress exists at a point, regardless of the orientation of

the stress element being used to describe that state of stress. That is, when an element is rotated from one orientation to another, the stresses acting on the *faces* of the element are different but they still represent the same state of stress, namely, the stress at the point under consideration. The situation is analogous to the representation of a force vector by its components. The force is represented by different components when the coordinate axes are rotated to a new orientation, but the force itself is not changed. However, the state of stress at a point in a body is a more complex quantity than is a force, and the transformation relationships for stresses are more complicated than those for vectors. In mathematical terms, stress is known as a *tensor*; other tensor quantities in mechanics are strains and moments of inertia. The similarities between the transformation equations for stresses, strains, and moments of inertia are pointed out later in this chapter.

6.2 PLANE STRESS

The stress conditions encountered in axially loaded bars, shafts in torsion, and beams are examples of a state of stress called **plane stress**. To analyze plane stress, let us consider the infinitesimal element shown in Fig. 6-1a. This element is a rectangular parallelepiped with its edges parallel to the x , y , and z axes. The faces of the element are designated by the directions of their outward normals, as explained previously in Section 1.6. Thus, the right-hand face of the element in this figure is referred to as the positive x face, and the left-hand face (hidden from the viewer) is referred to as the negative x face. Similarly, the top face is the positive y face, and the front face is the positive z face.

In plane stress, only the x and y faces of the element are subjected to stresses, and all of the stresses act parallel to the x and y axes (Fig. 6-1a). The symbols for the stresses have the following meanings. A normal stress σ has a subscript that identifies the face on which the stress acts. Of course, equal normal stresses act on opposite faces of the element, and positive stress indicates tension. A shear stress τ has two sub-

scripts: the first denotes the face on which the stress acts, and the second gives the direction on that face. Thus, the stress τ_{xy} acts on the x face in the direction of the y axis, and the stress τ_{yx} acts on the y face in the direction of the x axis. A shear stress is positive when it acts on a positive face of the element in the positive direction of an axis, and it is negative when it acts on a positive face in the negative direction of an axis. Hence, the stresses τ_{xy} and τ_{yx} shown on the positive x and y faces (Fig. 6-1a) are positive shear stresses. Similarly, on a negative face of an element, the stresses τ_{xy} and τ_{yx} shown on the negative x and y faces of the element are also positive. This **sign convention** for shear stresses is easily remembered by the rule that, when the directions associated with the subscripts are plus-plus or minus-minus, the stress is positive; when the directions are plus-minus, the stress is negative.

The preceding sign convention for shear stresses is consistent with static equilibrium of the element, because we know that shear stresses on opposite faces of an element must be equal in magnitude and opposite in direction. Hence, according to our sign convention, a positive stress τ_{xy} acts upward on the positive face (Fig. 6-1a) and downward on the negative face. In a similar manner, the stresses τ_{yx} acting on the top and bottom faces of the element are positive and have opposite directions. Finally, we recall that shear stresses on perpendicular planes are equal in magnitude and have directions such that both stresses point toward, or away from, the line of intersection of the faces. Inasmuch as τ_{xy} and τ_{yx} are positive in the directions shown in the figure, they are consistent with this observation. Therefore, we note that

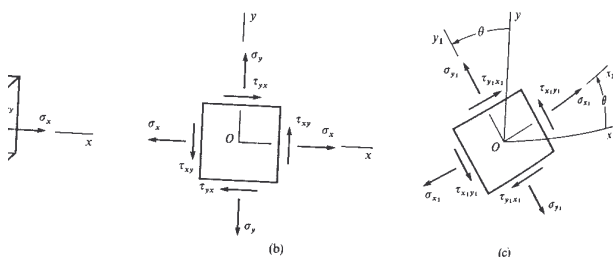
$$\tau_{xy} = \tau_{yx} \quad (6-1)$$

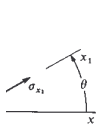
This relationship was derived previously from static equilibrium of the element (see Section 1.6).

For convenience in sketching plane stress elements, we usually draw only a two-dimensional view of the element, as shown in Fig. 6-1b. Although a figure of this kind shows clearly all of the stresses acting on a plane stress element, we must always keep in mind that the element is a solid body with a constant thickness perpendicular to the plane of the figure.

We are now ready to consider the stresses acting on **inclined sections**, our assumption being that the stresses σ_x , σ_y , and τ_{xy} are known (for example, from a bending or torsion analysis). To portray the stresses acting on an inclined section, we consider another stress element whose faces are parallel and perpendicular to the inclined section (Fig. 6-1c). Associated with this new element are axes x_1 , y_1 , and z_1 , such that the z_1 axis coincides with the z axis and the x_1 , y_1 axes are rotated counterclockwise through an angle θ with respect to the xy axes. The normal and shear stresses acting on this rotated element are denoted σ_{x_1} , σ_{y_1} ,

1 plane stress





$\tau_{x_1y_1}$, and $\tau_{y_1x_1}$, using the same subscript designations and sign conventions as for the stresses acting on the xy element. The previous conclusions regarding the shear stresses still apply, and we note that

$$\tau_{x_1y_1} = \tau_{y_1x_1} \quad (6-2)$$

An important observation is that the shear stresses acting on all four side faces of the element are known if we determine the shear stress acting on any one of the faces.

The stresses acting on the rotated x_1y_1 element can be expressed in terms of the stresses on the xy element by using equations of static equilibrium. For this purpose, we choose a wedge-shaped element whose inclined face is the x_1 face of the rotated element and whose other two side faces are parallel to the x and y axes (Fig. 6-2a). In order to write equations of equilibrium, we need to obtain the forces acting on these faces. Let us denote the area of the left-hand side face (that is, the negative x face) as A_0 . Then the normal and shear forces acting on this face are $\sigma_x A_0$ and $\tau_{xy} A_0$, as shown in the free-body diagram of Fig. 6-2b. The area of the bottom face (or negative y face) is $A_0 \tan \theta$, and the area of the inclined face (or positive x_1 face) is $A_0 \sec \theta$. Thus, the normal and shear forces acting on these faces have the magnitudes and directions shown. The four forces acting on the left-hand and bottom faces can now be resolved into orthogonal components acting in the x_1 and y_1 directions. Then we can sum forces in those directions and obtain two equations of equilibrium for the element. The first equation, obtained by summing forces in the x_1 direction, is

$$\begin{aligned} \sigma_{x_1} A_0 \sec \theta - \sigma_x A_0 \cos \theta - \tau_{xy} A_0 \sin \theta \\ - \sigma_y A_0 \tan \theta \sin \theta - \tau_{yx} A_0 \tan \theta \cos \theta = 0 \end{aligned}$$

In the same manner, summation of forces in the y_1 direction gives

$$\begin{aligned} \tau_{x_1y_1} A_0 \sec \theta + \sigma_x A_0 \sin \theta - \tau_{xy} A_0 \cos \theta \\ - \sigma_y A_0 \tan \theta \cos \theta + \tau_{yx} A_0 \tan \theta \sin \theta = 0 \end{aligned}$$

Using the relationship $\tau_{xy} = \tau_{yx}$, and also simplifying and rearranging, we obtain the following equations:

$$\begin{aligned} \sigma_{x_1} &= \sigma_x \cos^2 \theta + \sigma_y \sin^2 \theta + 2\tau_{xy} \sin \theta \cos \theta & (6-3a) \\ \tau_{x_1y_1} &= (\sigma_x - \sigma_y) \sin \theta \cos \theta + \tau_{xy} (\cos^2 \theta - \sin^2 \theta) & (6-3b) \end{aligned}$$

Equations (6-3) give the normal and shear stresses acting on the x_1 plane in terms of the angle of rotation θ and the stresses σ_x , σ_y , and τ_{xy} acting on the x and y planes.

For the special value $\theta = 0$, we note that Eqs. (6-3) give $\sigma_{x_1} = \sigma_x$ and $\tau_{x_1y_1} = \tau_{xy}$, as expected. Also, when $\theta = 90^\circ$, the equations give $\sigma_{x_1} = \sigma_y$ and $\tau_{x_1y_1} = -\tau_{xy}$. In the latter case, the x_1 axis is vertical; hence, the stress $\tau_{x_1y_1}$ is positive to the left, which is opposite to the positive direction of τ_{yx} .

Equations (6-3) can be expressed in a useful alternate form by introducing the following trigonometric identities:

$$\begin{aligned} \cos^2 \theta &= \frac{1}{2}(1 + \cos 2\theta) & \sin^2 \theta &= \frac{1}{2}(1 - \cos 2\theta) \\ \sin \theta \cos \theta &= \frac{1}{2} \sin 2\theta \end{aligned}$$

Then the equations become

$$\sigma_{x_1} = \frac{\sigma_x + \sigma_y}{2} + \frac{\sigma_x - \sigma_y}{2} \cos 2\theta + \tau_{xy} \sin 2\theta \quad (6-4a)$$

$$\tau_{x_1y_1} = -\frac{\sigma_x - \sigma_y}{2} \sin 2\theta + \tau_{xy} \cos 2\theta \quad (6-4b)$$

These equations will be used in the next section to construct Mohr's circle for plane stress.

The equations for σ_{x_1} and $\tau_{x_1y_1}$ are known as the **transformation equations for plane stress** because they transform the stress components from one set of axes to another. However, as explained previously, the intrinsic state of stress at the point under consideration is the same whether represented by the stresses on the xy element or by the rotated x_1y_1 element (Fig. 6-1). The transformation equations were derived solely from equilibrium considerations; hence, they are applicable to stresses in any kind of material.

An important observation concerning the normal stresses can be obtained from the transformation equations. As a preliminary matter, we note that the normal stress σ_{y_1} acting on the y_1 face of the rotated element (Fig. 6-1c) can be obtained from Eq. (6-4a) by substituting $\theta + 90^\circ$ for θ ; thus, we get the following equation for σ_{y_1} :

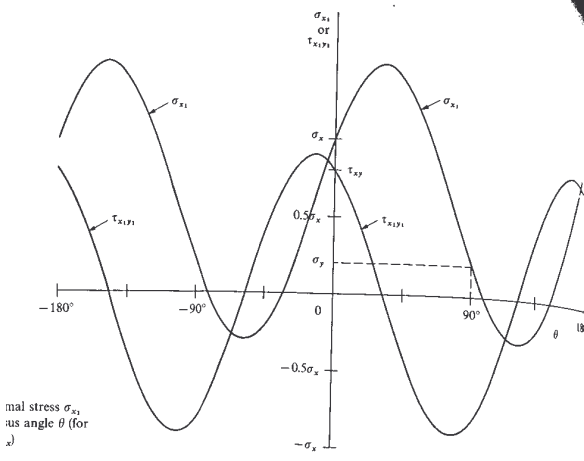
$$\sigma_{y_1} = \frac{\sigma_x + \sigma_y}{2} - \frac{\sigma_x - \sigma_y}{2} \cos 2\theta - \tau_{xy} \sin 2\theta \quad (6-5)$$

Summing Eqs. (6-4a) and (6-5) gives

$$\sigma_{x_1} + \sigma_{y_1} = \sigma_x + \sigma_y \quad (6-6)$$

This equation shows that the sum of the normal stresses acting on perpendicular faces of a plane stress element is constant and, hence, independent of the angle θ .

The general manner in which the normal and shear stresses vary is shown in Fig. 6-3, which is a graph of σ_{x_1} and $\tau_{x_1y_1}$ versus the angle of



Normal stress σ_{x_1} versus angle θ (for $\sigma_y = 0.2\sigma_x$ and $\tau_{xy} = 0.8\sigma_x$)

rotation θ (Eqs. 6-3). The graph is plotted for the particular case of $\sigma_y = 0.2\sigma_x$ and $\tau_{xy} = 0.8\sigma_x$. We see from the plot that the stresses vary continuously as the element is rotated. At certain angles of rotation, the normal stress reaches a maximum or minimum value; at other angles, it becomes zero. Similarly, the shear stress has maximum, minimum, and zero values at certain angles. A more detailed investigation of these special values of the stresses is made in the next section. Of course, the curves shown in Fig. 6-3 will be changed if the relative values of the stresses σ_x , σ_y , and τ_{xy} are changed.

The general case of plane stress reduces to simpler states of stress under special conditions. For instance, if all stresses acting on the xy element (Fig. 6-1b) are zero except for the normal stress σ_x , then the element is in **uniaxial stress** (Fig. 6-4). The corresponding transformation equations, obtained by setting σ_y and τ_{xy} equal to zero in Eqs. (6-3), are

$$\sigma_{x_1} = \sigma_x \cos^2 \theta \quad (6-7a)$$

$$\tau_{x_1y_1} = -\sigma_x \sin \theta \cos \theta \quad (6-7b)$$

These equations agree with the equations derived previously in Section 2.7 (see Eqs. 2-33), except that we are now using a more generalized notation for the stresses acting on a rotated element.

Another special case is **pure shear** (Fig. 6-5), for which the transfor-

Equation equations are obtained by substituting $\sigma_x = 0$ and $\sigma_y = 0$ into Eqs. (6-3):

$$\sigma_{x_1} = 2\tau_{xy} \sin \theta \cos \theta \quad (6-8a)$$

$$\tau_{x_1y_1} = \tau_{xy} (\cos^2 \theta - \sin^2 \theta) \quad (6-8b)$$

Again, the equations correspond to those derived earlier (see Eqs. 3-18 in Section 3.4).

The last special case is **biaxial stress**, a stress condition in which the element is subjected to normal stresses in both the x and y directions without shear stresses (Fig. 6-6). The equations for biaxial stress are obtained from Eqs. (6-3) or (6-4) by dropping the terms containing τ_{xy} . Biaxial stress, which occurs in thin-walled pressure vessels, is discussed in more detail in Section 6.6.

Example 1

An element in plane stress is subjected to stresses $\sigma_x = 110$ MPa, $\sigma_y = 40$ MPa and $\tau_{xy} = \tau_{yx} = 28$ MPa as shown in Fig. 6-7a. Determine the stresses acting on an element rotated through an angle $\theta = 45^\circ$.

Although the stresses acting on a rotated element can be obtained from either Eqs. (6-3) or (6-4), we usually find the latter more convenient for practical use. Using the given numerical values, we obtain

$$\frac{\sigma_x + \sigma_y}{2} = 75 \text{ MPa} \quad \frac{\sigma_x - \sigma_y}{2} = 35 \text{ MPa}$$

$$\sin 2\theta = \sin 90^\circ = 1 \quad \cos 2\theta = \cos 90^\circ = 0$$

Substituting these values and $\tau_{xy} = 28$ MPa into Eqs. (6-4), we get

$$\begin{aligned} \sigma_{x_1} &= \frac{\sigma_x + \sigma_y}{2} + \frac{\sigma_x - \sigma_y}{2} \cos 2\theta + \tau_{xy} \sin 2\theta \\ &= 75 \text{ MPa} + 35 \text{ MPa}(0) + 28 \text{ MPa}(1) = 103 \text{ MPa} \end{aligned}$$

$$\begin{aligned} \tau_{x_1y_1} &= -\frac{\sigma_x - \sigma_y}{2} \sin 2\theta + \tau_{xy} \cos 2\theta \\ &= -35 \text{ MPa}(1) + 28 \text{ MPa}(0) = -35 \text{ MPa} \end{aligned}$$

In addition, the stress σ_{y_1} may be obtained from Eq. (6-5):

$$\begin{aligned} \sigma_{y_1} &= \frac{\sigma_x + \sigma_y}{2} - \frac{\sigma_x - \sigma_y}{2} \cos 2\theta - \tau_{xy} \sin 2\theta \\ &= 75 \text{ MPa} - 35 \text{ MPa}(0) - 28 \text{ MPa}(1) = 47 \text{ MPa} \end{aligned}$$

From these results, we can obtain the stresses acting on the sides of an element at $\theta = 45^\circ$, as shown in Fig. 6-7b. The arrows show the true directions in which the stresses act. Note especially the directions of the shear stresses, all of which have the same magnitude. Also, observe that the sum of the normal stresses remains constant and equal to 150 MPa (Eq. 6-6). The stress components of Fig. 6-7b represent the same state of stress as that shown in Fig. 6-7a; the difference lies in the orientations of the planes on which the stress components act.

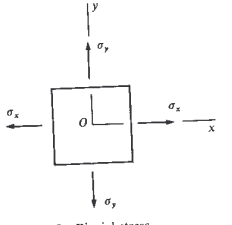


Fig. 6-6 Biaxial stress

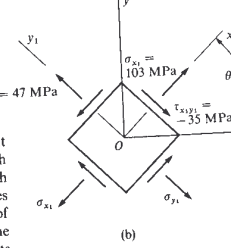
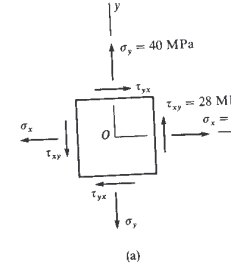


Fig. 6-7 Example 1

Example 2

A plane stress condition exists at a point in a loaded structure. The stresses have the magnitudes and directions shown on the stress element of Fig. 6-8a. Calculate the stresses acting on the planes obtained by rotating the element clockwise through an angle of 15°.

The stresses acting on the element shown in Fig. 6-8a have the following values:

$$\sigma_x = -46 \text{ MPa} \quad \sigma_y = 12 \text{ MPa} \quad \tau_{xy} = -19 \text{ MPa}$$

A clockwise rotation of the element through an angle of 15° puts the element in the position shown in Fig. 6-8b with the x_1 axis at an angle $\theta = -15^\circ$ to the x axis. (Alternatively, the x_1 axis could be placed at an angle $\theta = 75^\circ$.) Now we can readily calculate the stresses on the x_1 face of the rotated element by using Eqs. (6-4). The calculations proceed as follows:

$$\begin{aligned} \frac{\sigma_x + \sigma_y}{2} &= -17 \text{ MPa} & \frac{\sigma_x - \sigma_y}{2} &= -29 \text{ MPa} \\ \sin 2\theta &= \sin(-30^\circ) & \cos 2\theta &= \cos(-30^\circ) \\ \sigma_{x_1} &= \frac{\sigma_x + \sigma_y}{2} + \frac{\sigma_x - \sigma_y}{2} \cos 2\theta + \tau_{xy} \sin 2\theta \\ &= -17 \text{ MPa} - (29 \text{ MPa}) \cos(-30^\circ) - (19 \text{ MPa}) \sin(-30^\circ) \\ &= -32.6 \text{ MPa} \end{aligned}$$

$$\begin{aligned} \tau_{x_1 y_1} &= -\frac{\sigma_x - \sigma_y}{2} \sin 2\theta + \tau_{xy} \cos 2\theta \\ &= (29 \text{ MPa}) \sin(-30^\circ) - (19 \text{ MPa}) \cos(-30^\circ) \\ &= -31.0 \text{ MPa} \end{aligned}$$

Also, the normal stress acting on the y_1 face (Eq. 6-5) is

$$\begin{aligned} \sigma_{y_1} &= \frac{\sigma_x + \sigma_y}{2} - \frac{\sigma_x - \sigma_y}{2} \cos 2\theta - \tau_{xy} \sin 2\theta \\ &= -17 \text{ MPa} + (29 \text{ MPa}) \cos(-30^\circ) + (19 \text{ MPa}) \sin(-30^\circ) \\ &= -1.4 \text{ MPa} \end{aligned}$$

This stress can also be calculated by substituting $\theta = 75^\circ$ into Eq. (6-4a). Again we note that $\sigma_{x_1} + \sigma_{y_1} = \sigma_x + \sigma_y$. The stresses acting on the inclined planes are shown on the stress element of Fig. 6-8b, with the arrows indicating the true directions of the stresses.

selected combination of stresses. For design purposes, the largest positive and negative stresses are usually needed. To determine the maximum and minimum normal stresses, which are known as the principal stresses, we begin with the expression for σ_{x_1} (Eq. 6-4a):

$$\sigma_{x_1} = \frac{\sigma_x + \sigma_y}{2} + \frac{\sigma_x - \sigma_y}{2} \cos 2\theta + \tau_{xy} \sin 2\theta \quad (6-4a) \text{ repeated}$$

By taking the derivative of σ_{x_1} with respect to θ and setting it equal to zero, we obtain an equation that can be solved for the values of θ at which σ_{x_1} is a maximum or minimum. The equation is obtained as follows:

$$\frac{d\sigma_{x_1}}{d\theta} = -(\sigma_x - \sigma_y) \sin 2\theta + 2\tau_{xy} \cos 2\theta = 0 \quad (a)$$

from which we get

$$\tan 2\theta_p = \frac{2\tau_{xy}}{\sigma_x - \sigma_y} \quad (6-9)$$

The subscript p indicates that the angle θ_p defines the orientation of the principal planes, which are the planes on which the principal stresses act. Two values of $2\theta_p$ in the range from 0 to 360° can be obtained from Eq. (6-9). These values differ by 180°, with the lower value being between 0 and 180° and the higher between 180° and 360°. Therefore, the angle θ_p has two values that differ by 90°, one between 0 and 90° and the other between 90° and 180°. For one of these angles, the normal stress σ_{x_1} is a maximum principal stress; for the other, it is a minimum principal stress. Because the two values of θ_p differ by 90°, we conclude that the principal stresses occur on mutually perpendicular planes.

The values of the principal stresses can be readily calculated by substituting each of the two values of θ_p into the stress transformation equation (Eq. 6-4a) and solving for σ_{x_1} . By this procedure we also know which of the two principal stresses is associated with each of the two principal angles θ_p . However, it is also possible to obtain general formulas for the principal stresses. To do so, refer to Eq. (6-9) and Fig. 6-9 and note that

$$\cos 2\theta_p = \frac{\sigma_x - \sigma_y}{2R} \quad \sin 2\theta_p = \frac{\tau_{xy}}{R} \quad (6-10a,b)$$

$$R = \sqrt{\left(\frac{\sigma_x - \sigma_y}{2}\right)^2 + \tau_{xy}^2} \quad (6-11)$$

in which

When evaluating R , we always take the positive square root. Then we

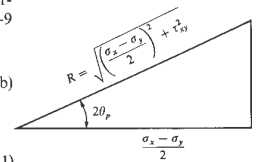


Fig. 6-9

6.3 PRINCIPAL STRESSES AND MAXIMUM SHEAR STRESSES

The transformation equations for plane stress show that the normal stress σ_{x_1} and shear stress $\tau_{x_1 y_1}$ vary continuously as the element is rotated through the angle θ . This variation is pictured in Fig. 6-3 for

6.3 Principal Stresses and Maximum Shear Stresses

substitute the expressions for $\cos 2\theta_p$ and $\sin 2\theta_p$ into Eq. (6-4a) and obtain the algebraically larger of the two principal stresses, denoted by σ_1 .

$$\sigma_1 = \frac{\sigma_x + \sigma_y}{2} + \sqrt{\left(\frac{\sigma_x - \sigma_y}{2}\right)^2 + \tau_{xy}^2}$$

The smaller of the principal stresses, denoted by σ_2 , may be found from the condition that

$$\sigma_1 + \sigma_2 = \sigma_x + \sigma_y \quad (6-12)$$

inasmuch as σ_1 and σ_2 act on perpendicular planes. Substituting the expression for σ_1 into Eq. (6-12) and solving for σ_2 , we get

$$\sigma_2 = \frac{\sigma_x + \sigma_y}{2} - \sqrt{\left(\frac{\sigma_x - \sigma_y}{2}\right)^2 + \tau_{xy}^2}$$

This expression has the same form as the expression for σ_1 but differs by the presence of the minus sign before the square root. Thus, the preceding formulas can be combined into a single formula for the principal stresses:

$$\sigma_{1,2} = \frac{\sigma_x + \sigma_y}{2} \pm \sqrt{\left(\frac{\sigma_x - \sigma_y}{2}\right)^2 + \tau_{xy}^2} \quad (6-13)$$

The plus sign gives the algebraically larger principal stress σ_1 and the minus sign gives the smaller principal stress σ_2 .

In summary, the two angles defining the principal planes are denoted θ_{p1} and θ_{p2} , corresponding to the principal stresses σ_1 and σ_2 , respectively. Both angles can be determined from the equation for $\tan 2\theta_p$ (Eq. 6-9), but we cannot tell from that equation which angle is θ_{p1} and which is θ_{p2} . A simple procedure for making this determination is to take one of the values and substitute it into the equation for σ_{x_1} (Eq. 6-4a). The resulting value of σ_{x_1} will be recognized as either σ_1 or σ_2 , thus correlating the principal angles with the principal stresses.

Another method for correlating the principal angles and stresses is to use Eqs. (6-10) for finding θ_p , since the only angle that satisfies both of those equations is θ_p . Thus, we can rewrite those equations as follows:

$$\cos 2\theta_p = \frac{\sigma_x - \sigma_y}{2R} \quad \sin 2\theta_p = \frac{\tau_{xy}}{R} \quad (6-14a,b)$$

Only one angle exists between 0 and 360° that satisfies both of these equations. Thus, the value of θ_{p1} , corresponding to the maximum principal stress σ_1 , can be determined uniquely from Eqs. (6-14). The angle θ_{p2} , corresponding to σ_2 , defines a plane that is perpendicular to the plane defined by θ_{p1} . Therefore, θ_{p2} can be taken as 90° larger or smaller than θ_{p1} .

An important characteristic concerning the principal planes can be

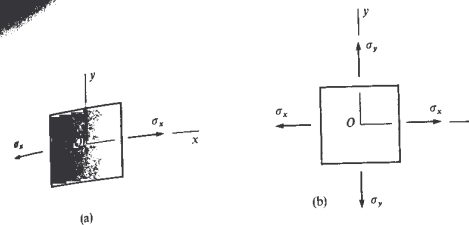


Fig. 6-10 Elements in uniaxial and biaxial stress

observed from the equation for the shear stresses (Eq. 6-4b), which is repeated here:

$$\tau_{x_1 y_1} = -\frac{\sigma_x - \sigma_y}{2} \sin 2\theta + \tau_{xy} \cos 2\theta \quad (6-4b) \text{ repeated}$$

If we set this stress equal to zero (compare with Eq. a) and solve for the angle 2θ , we obtain for $\tan 2\theta$ the same expression as before (see Eq. 6-9). Thus, we observe that the shear stresses are zero on the principal planes.

The principal planes for elements in uniaxial and biaxial stress are the x and y planes themselves (Fig. 6-10), because $\tan 2\theta_p = 0$ (see Eq. 6-9) and hence, the two values of θ_p are 0 and 90°.

For an element in pure shear (Fig. 6-11a), the principal planes are oriented at 45° to the x axis (Fig. 6-11b), because $\tan 2\theta_p$ is infinite and, hence, the two values of θ_p are 45° and 135°. If τ_{xy} is positive, the principal stresses are $\sigma_1 = \tau_{xy}$ and $\sigma_2 = -\tau_{xy}$ (see Section 3.4 for a discussion of pure shear).

The preceding discussion of principal stresses refers only to rotation of the stress element in the xy plane (that is, rotation about the z axis) (Fig. 6-12a). Therefore, the two principal stresses determined from Eq. (6-13) are sometimes called the in-plane principal stresses. We must not overlook the fact that the stress element is actually three-dimensional; hence, it has not two but three principal stresses acting on three mutually perpendicular planes. By making a more complete three-dimensional

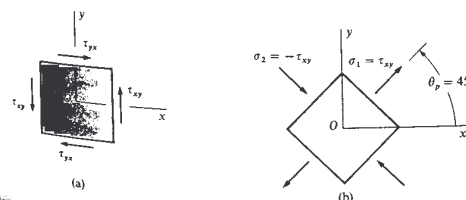
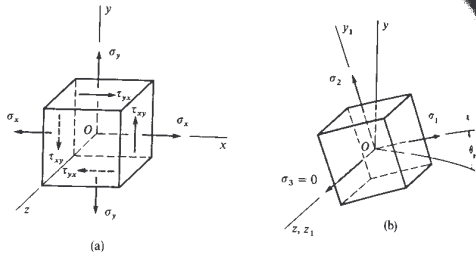


Fig. 6-11 Element in pure shear



anes for an

analysis, it can be shown that the three principal planes for a plane stress element are the two principal planes we have already described plus the z face of the element. These principal planes are shown in Fig. 6-12b, where the stress element of Fig. 6-12a has been rotated about the z axis through the principal angle θ_p , which is one of the two angles found from Eq. (6-9). The principal stresses are σ_1 , σ_2 , and σ_3 , where σ_1 and σ_2 are given by Eq. (6-13) and σ_3 equals zero. Of course, σ_1 is algebraically larger than σ_2 , but σ_3 may be algebraically larger or smaller than either or both of σ_1 and σ_2 . Note again that there are no shear stresses on the principal planes.*

Maximum shear stresses. Having found the maximum normal stresses acting on an element in plane stress, we now consider the determination of the maximum shear stresses and the planes on which they act. The shear stresses $\tau_{x_1y_1}$ acting on rotated elements are given by Eq. (6-4b). Taking the derivative of $\tau_{x_1y_1}$ with respect to θ and setting it equal to zero, we obtain

$$\frac{d\tau_{x_1y_1}}{d\theta} = -(\sigma_x - \sigma_y) \cos 2\theta - 2\tau_{xy} \sin 2\theta = 0 \quad (b)$$

from which

$$\tan 2\theta_s = -\frac{\sigma_x - \sigma_y}{2\tau_{xy}} \quad (6-15)$$

The subscript s indicates that the angle θ_s defines the orientation of the planes of maximum shear stresses. Equation (6-15) yields one value of θ_s between 0 and 90° and another between 90° and 180°; these two values

* The determination of principal stresses is an example of a type of mathematical analysis known as *eigenvalue analysis*, which is described in books on matrix algebra (such as Ref. 6-1). The stress transformation equations and the concept of principal stresses are due to the French mathematicians A. L. Cauchy (1789–1857) and Barré de Saint-Venant (1797–1886) and the Scottish scientist and engineer W. J. M. Rankine (1820–1872); see Refs. 6-2, 6-3, and 6-4, respectively.

... differ by 90°. Hence, the maximum and minimum values of $\tau_{x_1y_1}$ occur on perpendicular planes. Because shear stresses on perpendicular planes are equal in absolute value, the maximum and minimum shear stresses differ only in sign. Furthermore, comparing Eq. (6-15) with Eq. (6-9) shows that

$$\tan 2\theta_s = -\frac{1}{\tan 2\theta_p} = -\cot 2\theta_p \quad (6-16)$$

From trigonometry, we know that $\tan(\alpha \pm 90^\circ) = -\cot \alpha$

$$\text{Hence, we see that } 2\theta_s = 2\theta_p \pm 90^\circ, \text{ or } \theta_s = \theta_p \pm 45^\circ \quad (6-17)$$

Thus, we conclude that the planes of maximum shear stress occur at 45° to the principal planes.

The plane of the algebraically maximum shear stress τ_{max} is defined by the angle θ_{s1} , for which we can obtain the following equations:

$$\cos 2\theta_{s1} = \frac{\tau_{xy}}{R} \quad \sin 2\theta_{s1} = -\frac{\sigma_x - \sigma_y}{2R} \quad (6-18a,b)$$

in which R is given by Eq. (6-11). Also, the angle θ_{s1} is related to the angle θ_{p1} (see Eqs. 6-14) as follows:

$$\theta_{s1} = \theta_{p1} - 45^\circ \quad (6-19)$$

The corresponding maximum shear stress is obtained by substituting the expressions for $\cos 2\theta_{s1}$ and $\sin 2\theta_{s1}$ into Eq. (6-4b), yielding

$$\tau_{max} = \sqrt{\left(\frac{\sigma_x - \sigma_y}{2}\right)^2 + \tau_{xy}^2} \quad (6-20)$$

The algebraically minimum shear stress τ_{min} has the same magnitude but opposite sign.

A useful expression for the maximum shear stress can be obtained from the principal stresses σ_1 and σ_2 , which are given by Eq. (6-13). Subtracting the expression for σ_2 from that for σ_1 , and then comparing with Eq. (6-20), we see that

$$\tau_{max} = \frac{\sigma_1 - \sigma_2}{2} \quad (6-21)$$

Thus, the maximum shear stress is equal to one-half the difference of the principal stresses.

Normal stresses also act on the planes of maximum shear stresses. The normal stress on the plane of the maximum shear stress can be evaluated by substituting the expressions for the angle θ_{s1} (Eqs. 6-18)

Analysis of Stress and Strain

into the equation for σ_{x_1} (Eq. 6-4a). The resulting stress is equal to $(\sigma_x + \sigma_y)/2$, which is the average of the normal stresses on the x and y planes

$$\sigma_{aver} = \frac{\sigma_x + \sigma_y}{2} \quad (6-2)$$

The stress σ_{aver} acts on both the plane of maximum shear stress and the plane of minimum shear stress.

In the particular cases of uniaxial and biaxial stress (Fig. 6-10) the planes of maximum shear stress occur at 45° to the x and y axes. In the case of pure shear (Fig. 6-11), the maximum shear stresses occur on the x and y planes.

The preceding analysis of shear stresses has dealt only with in-plane stresses. If we make a three-dimensional analysis, we can establish that there are three possible positions of the element for maximum shear stress. With reference to the plane stress element of Fig. 6-12b, which is rotated to the principal directions, we can obtain the three positions by making 45° rotations (not shown in the figure) about the x_1 , y_1 , and z_1 axes. The corresponding maximum and minimum shear stresses (see Eq. 6-21) are

$$(\tau_{max})_{x_1} = \pm \frac{\sigma_2}{2} \quad (\tau_{max})_{y_1} = \pm \frac{\sigma_1}{2} \quad (\tau_{max})_{z_1} = \pm \frac{\sigma_1 - \sigma_2}{2} \quad (6-23a,b,c)$$

The algebraic values of σ_1 and σ_2 determine which of these expressions gives the numerically largest shear stress. If σ_1 and σ_2 are of the same sign, then one of the first two expressions is numerically largest; if they have opposite signs, then the last expression gives the largest value.

Example

An element in plane stress is subjected to stresses $\sigma_x = 84$ MPa, $\sigma_y = -30$ MPa and $\tau_{xy} = -32$ MPa, as shown in Fig. 6-13a. (a) Determine the principal stresses and show them on a sketch of a properly oriented element. (b) Determine the maximum shear stresses and show them on a sketch of a properly oriented element. (Consider only the in-plane stresses.)

(a) *Principal stresses.* The principal angles θ_p that locate the principal planes can be obtained by solving Eq. (6-9):

$$\tan 2\theta_p = \frac{2\tau_{xy}}{\sigma_x - \sigma_y} = \frac{2(-32 \text{ MPa})}{84 \text{ MPa} - (-30 \text{ MPa})} = -0.5614$$

from which

$$2\theta_p = 150.6^\circ \quad \text{and} \quad \theta_p = 75.3^\circ$$

or

$$2\theta_p = 330.6^\circ \quad \text{and} \quad \theta_p = 165.3^\circ$$

The principal stresses are obtained by substituting the two values of $2\theta_p$ into

6.3 Principal Stresses and Maximum Shear Stresses

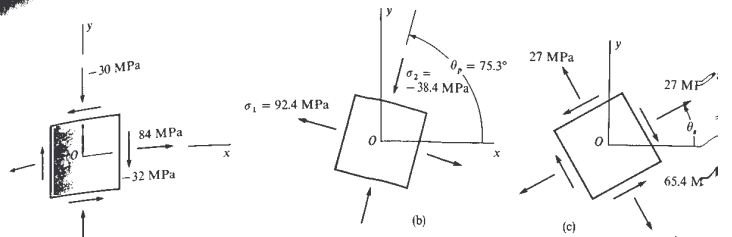


Fig. 6-13 Example. (a) Element in plane stress, (b) principal stresses, and (c) maximum shear stresses

the equation for σ_{x_1} (Eq. 6-4a). As a preliminary calculation, we determine the following quantities:

$$\frac{\sigma_x + \sigma_y}{2} = \frac{84 \text{ MPa} - 30 \text{ MPa}}{2} = 27 \text{ MPa}$$

$$\frac{\sigma_x - \sigma_y}{2} = \frac{84 \text{ MPa} + 30 \text{ MPa}}{2} = 57 \text{ MPa}$$

Now we substitute the first value of $2\theta_p$ into Eq. (6-4a):

$$\sigma_{x_1} = \frac{\sigma_x + \sigma_y}{2} + \frac{\sigma_x - \sigma_y}{2} \cos 2\theta + \tau_{xy} \sin 2\theta$$

$$= 27 \text{ MPa} + (57 \text{ MPa})(\cos 150.6^\circ) - (32 \text{ MPa})(\sin 150.6^\circ)$$

$$= -38.4 \text{ MPa}$$

In a similar manner, we substitute the second value of $2\theta_p$ and obtain $\sigma_{x_1} = 92.4$ MPa. Thus, the principal stresses and their corresponding principal angles are

$$\sigma_1 = 92.4 \text{ MPa} \quad \text{and} \quad \theta_{p1} = 165.3^\circ$$

$$\sigma_2 = -38.4 \text{ MPa} \quad \text{and} \quad \theta_{p2} = 75.3^\circ$$

Note that θ_{p1} and θ_{p2} differ by 90° and that $\sigma_1 + \sigma_2 = \sigma_x + \sigma_y$. The principal stresses are shown acting on a rotated stress element in Fig. 6-13b. Of course, no shear stresses act on the principal planes.

Alternate solution. The principal stresses may be calculated directly from Eq. (6-13):

$$\sigma_{1,2} = \frac{\sigma_x + \sigma_y}{2} \pm \sqrt{\left(\frac{\sigma_x - \sigma_y}{2}\right)^2 + \tau_{xy}^2}$$

$$= 27 \text{ MPa} \pm \sqrt{(57 \text{ MPa})^2 + (-32 \text{ MPa})^2}$$

$$= 27 \text{ MPa} \pm 65.4 \text{ MPa}$$

Therefore,

$$\sigma_1 = 92.4 \text{ MPa} \quad \sigma_2 = -38.4 \text{ MPa}$$

The angle θ_{p_1} to the plane on which σ_1 acts is obtained from Eqs. (6-14):

$$\cos 2\theta_{p_1} = \frac{\sigma_x - \sigma_y}{2R} = \frac{57 \text{ MPa}}{65.4 \text{ MPa}} = 0.8715$$

$$\sin 2\theta_{p_1} = \frac{\tau_{xy}}{R} = \frac{-32 \text{ MPa}}{65.4 \text{ MPa}} = -0.4893$$

in which we have noted that R is the square-root term in the preceding calculation for σ_1 and σ_2 . The only angle between 0 and 360° satisfying both of these conditions is $2\theta_{p_1} = 330.6^\circ$; hence, $\theta_{p_1} = 165.3^\circ$. This angle is associated with the algebraically larger principal stress $\sigma_1 = 92.4 \text{ MPa}$. The other angle is 90° larger or smaller than θ_{p_1} ; hence, $\theta_{p_2} = 75.3^\circ$, with $\sigma_2 = -38.4 \text{ MPa}$. These results agree with those found previously.

(b) *Maximum shear stresses.* The maximum shear stresses are given by Eq. (6-20):

$$\tau_{\max} = \sqrt{\left(\frac{\sigma_x - \sigma_y}{2}\right)^2 + \tau_{xy}^2} = 65.4 \text{ MPa}$$

which has already been calculated in part (a). The angle θ_{s_1} to the plane having the positive maximum shear stress is calculated from Eq. (6-19):

$$\theta_{s_1} = \theta_{p_1} - 45^\circ = 165.3^\circ - 45^\circ = 120.3^\circ$$

It follows that the negative shear stress acts on the plane for which $\theta_{s_2} = 120.3^\circ - 90^\circ = 30.3^\circ$. The normal stresses acting on the planes of maximum shear stresses are calculated from Eq. (6-22):

$$\sigma_{\text{aver}} = \frac{\sigma_x + \sigma_y}{2} = 27 \text{ MPa}$$

The rotated element subjected to the maximum shear stresses is shown in Fig. 6-13c.

As an alternative approach to finding the maximum shear stresses, we can use Eq. (6-15) to determine the angles θ_{s_1} and θ_{s_2} , and then we can use Eq. (6-4b) to obtain the corresponding shear stresses.

6.4 MOHR'S CIRCLE FOR PLANE STRESS

The transformation equations for plane stress (Eqs. 6-4) can be represented in a graphical form known as *Mohr's circle*. This representation is extremely useful in visualizing the relationships between normal and shear stresses acting on various inclined planes at a point in a stressed body. To establish Mohr's circle, we rearrange Eqs. (6-4) as follows:

$$\sigma_{x_1} - \frac{\sigma_x + \sigma_y}{2} = \frac{\sigma_x - \sigma_y}{2} \cos 2\theta + \tau_{xy} \sin 2\theta \quad (6-4a) \text{ repeated}$$

$$\tau_{x_1y_1} = -\frac{\sigma_x - \sigma_y}{2} \sin 2\theta + \tau_{xy} \cos 2\theta \quad (6-4b) \text{ repeated}$$

These equations are the equations of a circle in parametric form, with the angle 2θ as the parameter. Squaring both sides of each equation and then adding eliminates the parameter; the resulting equation is

$$\left(\sigma_{x_1} - \frac{\sigma_x + \sigma_y}{2}\right)^2 + \tau_{x_1y_1}^2 = \left(\frac{\sigma_x - \sigma_y}{2}\right)^2 + \tau_{xy}^2 \quad (a)$$

This equation can be written in simpler form by using the following notation from Section 6.3:

$$\sigma_{\text{aver}} = \frac{\sigma_x + \sigma_y}{2} \quad R = \sqrt{\left(\frac{\sigma_x - \sigma_y}{2}\right)^2 + \tau_{xy}^2} \quad (6-24a, b)$$

Equation (a) now becomes

$$(\sigma_{x_1} - \sigma_{\text{aver}})^2 + \tau_{x_1y_1}^2 = R^2 \quad (6-25)$$

which is the equation of a circle with σ_{x_1} and $\tau_{x_1y_1}$ as the coordinates. The circle has radius R , and its center has coordinates $\sigma_{x_1} = \sigma_{\text{aver}}$ and $\tau_{x_1y_1} = 0$.

Our next task is to construct Mohr's circle from Eqs. (6-4) and (6-25). To do so, we will take σ_{x_1} as the abscissa and $\tau_{x_1y_1}$ as the ordinate. However, there are two ways in which to draw the circle. In the first form of Mohr's circle, we plot σ_{x_1} positive to the right and $\tau_{x_1y_1}$ positive downward; then the angle 2θ is positive when counterclockwise (Fig. 6-14a). In the second form, $\tau_{x_1y_1}$ is positive upward and 2θ is positive clockwise (Fig. 6-14b). Both forms of the circle are mathematically correct and consistent with the equations; hence, the choice between them is a matter of personal preference. Because the angle θ for the stress element is positive when counterclockwise (see Fig. 6-1), we can avoid confusion by adopting the form of Mohr's circle in which the angle 2θ is positive when counterclockwise. Thus, we will opt for the first form of Mohr's circle (Fig. 6-14a).

Let us now proceed to construct Mohr's circle for an element in plane stress (Figs. 6-15a and b). The steps are as follows: (1) Locate the center C of the circle at the point having coordinates $\sigma_{x_1} = \sigma_{\text{aver}}$ and $\tau_{x_1y_1} = 0$ (Fig. 6-15c). (2) Locate point A , which is the point on the circle representing the stress conditions on the x face of the element ($\theta = 0$); for this point we have $\sigma_{x_1} = \sigma_x$ and $\tau_{x_1y_1} = \tau_{xy}$. (3) Locate point B , representing the stress conditions on the y face of the element ($\theta = 90^\circ$). The coordinates of this point are $\sigma_{x_1} = \sigma_y$ and $\tau_{x_1y_1} = -\tau_{xy}$, because, when the element is rotated through an angle $\theta = 90^\circ$, the normal stress σ_{x_1} becomes σ_y and the shear stress $\tau_{x_1y_1}$ becomes the negative of τ_{xy} . Note that a line from A to B passes through the center C . Hence, points A and B , representing the stresses on planes at 90° to each other, are

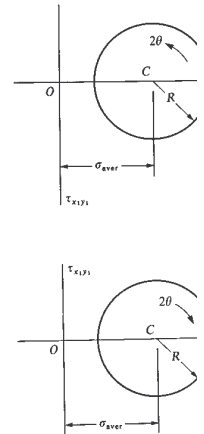
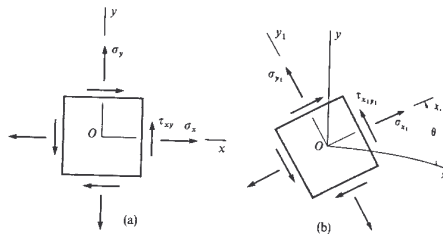


Fig. 6-14 Two forms of Mohr circle: (a) $\tau_{x_1y_1}$ is positive downward 2θ is positive counterclockwise (b) $\tau_{x_1y_1}$ is positive upward and positive clockwise. (Note: The first used in this book.)



A in the point for which $\theta = 0$. The angle 2θ locates point D on the circle; this point has coordinates σ_{x_1} and $\tau_{x_1y_1}$, representing the stresses on the x_1 face of the stress element. To show that the coordinates of point D are given by the stress transformation equations (Eqs. 6-4), we let β represent the angle between the radial line CD and the σ_{x_1} axis. Then, from the geometry of the figure, we obtain the following four relationships:

$$\begin{aligned} \sigma_{x_1} &= \frac{\sigma_x + \sigma_y}{2} + R \cos \beta & \tau_{x_1y_1} &= R \sin \beta \\ \cos(2\theta + \beta) &= \frac{\sigma_x - \sigma_y}{2R} & \sin(2\theta + \beta) &= \frac{\tau_{xy}}{R} \end{aligned} \quad (b)$$

Expanding the cosine and sine expressions gives

$$\begin{aligned} \cos 2\theta \cos \beta - \sin 2\theta \sin \beta &= \frac{\sigma_x - \sigma_y}{2R} \\ \sin 2\theta \cos \beta + \cos 2\theta \sin \beta &= \frac{\tau_{xy}}{R} \end{aligned}$$

Multiplying the first equation by $\cos 2\theta$ and the second by $\sin 2\theta$, and then adding the two equations, we obtain

$$\cos \beta = \frac{1}{R} \left(\frac{\sigma_x - \sigma_y}{2} \cos 2\theta + \tau_{xy} \sin 2\theta \right)$$

Also, multiplying the first equation by $\sin 2\theta$ and the second by $\cos 2\theta$ and then subtracting, we get

$$\sin \beta = \frac{1}{R} \left(-\frac{\sigma_x - \sigma_y}{2} \sin 2\theta + \tau_{xy} \cos 2\theta \right)$$

When these expressions for $\cos \beta$ and $\sin \beta$ are substituted into Eqs. (b), we obtain the stress transformation equations (Eqs. 6-4). Thus, we have shown that point D on Mohr's circle, defined by the angle 2θ , represents the stress conditions on the x_1 face of the stress element, defined by the angle θ .

Point D' , diametrically opposite point D , is located by an angle that is 180° greater than the angle 2θ to point D (see Fig. 6-15c). Therefore, point D' represents the stresses on a face of the stress element 90° from the face represented by point D ; hence, point D' gives the stresses on the y_1 face.

As we rotate the stress element counterclockwise through an angle θ (Fig. 6-15b), the point on Mohr's circle corresponding to the x_1 face element moves counterclockwise through an angle 2θ . Similarly, if we rotate the element clockwise, the point on the circle moves clockwise. At point P_1 on the circle, the normal stress reaches its algebraically largest value and the shear stress is zero. Hence, P_1 represents a principal plane. The other principal plane, associated with the algebraically smallest normal

Mohr's circle for plane

at opposite ends of a diameter (180° apart on the circle). (4) Draw the circle through points A and B with center at C .

Note that the radius R of the circle is the length of line CA . To calculate this length, we observe that the abscissas of points C and A are $(\sigma_x + \sigma_y)/2$ and σ_x , respectively. The difference in these abscissas is $(\sigma_x - \sigma_y)/2$, as shown in Fig. 6-15c. Also, the ordinate to point A is τ_{xy} . Therefore, line CA is the hypotenuse of a right triangle having one side of length $(\sigma_x - \sigma_y)/2$ and the other side of length τ_{xy} . Taking the square root of the sum of the squares of these two sides gives R (see Eq. 6-24b).

Let us now determine the stresses acting on an inclined face of the element oriented at an angle θ from the x axis (Fig. 6-15b). On Mohr's circle, we take an angle 2θ counterclockwise from the radius CA , because

stress, is represented by point P_2 . From the geometry of the circle, we see that the larger principal stress is

$$\sigma_1 = OC + CP_1 = \frac{\sigma_x + \sigma_y}{2} + R$$

which, upon substitution of the expression for R (Eq. 6-24b), agrees with Eq. (6-13). In a similar manner, we can verify the expression for σ_2 . The principal angle θ_{p_1} between the x axis and the plane of σ_2 , algebraically larger principal stress for the rotated stress element (Fig. 6-15b) is one-half the angle $2\theta_{p_1}$ between radii CA and CP_1 on Mohr's circle. The cosine and sine of the angle $2\theta_{p_1}$ can be obtained by inspection from the circle:

$$\cos 2\theta_{p_1} = \frac{\sigma_x - \sigma_y}{2R} \quad \sin 2\theta_{p_1} = \frac{\tau_{xy}}{R}$$

These expressions agree with Eqs. (6-14). The angle $2\theta_{p_2}$ to the other principal point is 180° larger than $2\theta_{p_1}$; hence, $\theta_{p_2} = \theta_{p_1} + 90^\circ$.

Points S and S' , representing the planes of maximum and minimum shear stresses, are located on the circle at 90° angles from points P_1 and P_2 . Therefore, the planes of maximum shear stress are at 45° to the principal planes, as discussed in Section 6.3. The maximum shear stress is numerically equal to the radius of the circle (compare Eq. 6-24b for R with Eq. 6-20 for τ_{max}). Also, the normal stresses on the planes of maximum shear stress are equal to the abscissa of point C , which is the average normal stress (see Eq. 6-22).

From the preceding discussions, it is apparent that we can find the stresses on any inclined planes, as well as the principal stresses and maximum shear stresses, from Mohr's circle. The diagram of Fig. 6-15 was drawn with both σ_x and σ_y as positive stresses, but the same procedures are followed if either or both stresses are negative. In such cases, part or all of Mohr's circle will be located to the left of the origin. We should also note that point A , representing the stresses on the plane $\theta = 0$, may be situated anywhere around the circle, depending upon the relative values of the stresses σ_x , σ_y , and τ_{xy} . However, the angle 2θ is always measured counterclockwise from the radius CA , regardless of where point A is located.

It is also possible to use Mohr's circle inversely. If we know the stresses σ_{x_1} , σ_{y_1} , and $\tau_{x_1y_1}$ acting on a rotated element, as well as the angle θ itself, then we can construct the circle and determine the stresses σ_x , σ_y , and τ_{xy} for $\theta = 0$. The procedure is to locate points D and D' from the known stresses and then draw the circle using line DD' as a diameter. By measuring the angle 2θ in a negative sense (that is, clockwise rather than counterclockwise) from radius CD , we can locate point A , corresponding to the x face of the element. Next, we locate point B by constructing a diameter from A . Finally, we use the coordinates of A and B to obtain the stresses acting on all faces of the element for which $\theta = 0$. It is quite possible to construct Mohr's circle to scale and measure values of stress from it; however, it is preferable to perform numerical

calculations for the stresses, using trigonometry and the geometry of the circle. Mohr's circle makes it possible to visualize the relationships between stresses acting on planes at various angles, and it also serves as a simple memory device for obtaining the stress transformation equations. Although most graphical techniques are no longer used in engineering work, Mohr's circle remains valuable because it provides a simple and clear picture of an otherwise complicated analysis. The circle is also applicable to transformations involving two-dimensional strains and moments of inertia of plane areas, because these quantities follow the same transformation laws as do stresses (see Section 6.11 and Appendix C, Section C.7).*

Example 1

An element in plane stress is subjected to stresses $\sigma_x = 100$ MPa, $\sigma_y = 34$ MPa, and $\tau_{xy} = 28$ MPa, as shown in Fig. 6-16a. Using Mohr's circle, determine (a) the stresses acting on an element rotated through an angle $\theta = 40^\circ$, (b) the principal stresses, and (c) the maximum shear stresses. Show all results on sketches of properly oriented elements.

The center C of the circle (Fig. 6-16b) is located on the σ_{x_1} axis at the point where σ_{x_1} equals σ_{aver} :

$$\sigma_{aver} = \frac{\sigma_x + \sigma_y}{2} = \frac{100 \text{ MPa} + 34 \text{ MPa}}{2} = 67 \text{ MPa}$$

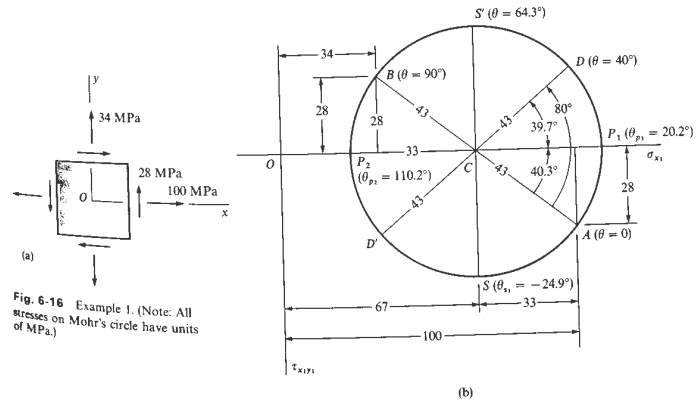


Fig. 6-16 Example 1. (Note: All stresses on Mohr's circle have units of MPa.)

* Mohr's circle is named after the famous German civil engineer Otto Christian Mohr (1835-1918), who developed the circle in 1882 (Ref. 6-5).

Point A , representing the stresses on the x face of the element, has coordinates

$$\sigma_{x_1} = 100 \text{ MPa} \quad \tau_{x_1y_1} = 28 \text{ MPa}$$

Similarly, the coordinates of point B , representing the stresses on the y face, are

$$\sigma_{y_1} = 34 \text{ MPa} \quad \tau_{x_1y_1} = -28 \text{ MPa}$$

The circle is now drawn through points A and B , with center at C and radius

$$R = \sqrt{(33 \text{ MPa})^2 + (28 \text{ MPa})^2} = 43 \text{ MPa}$$

The angle ACP_1 is the angle $2\theta_{p_1}$ from point A to point P_1 , representing the principal plane having the larger principal stress σ_1 ; this angle is obtained as follows:

$$\tan 2\theta_{p_1} = \frac{28 \text{ MPa}}{33 \text{ MPa}} = 0.848$$

from which

$$2\theta_{p_1} = 40.3^\circ \quad \theta_{p_1} = 20.2^\circ$$

Thus, we now have calculated the important angles and stresses that determine the geometry of Mohr's circle.

(a) The stresses acting on a plane at $\theta = 40^\circ$ are given by point D , which is at an angle $2\theta = 80^\circ$ from point A . Therefore, angle DCP_1 is

$$\text{Angle } DCP_1 = 80^\circ - 2\theta_{p_1} = 80^\circ - 40.3^\circ = 39.7^\circ$$

This angle is between line CD and the σ_{x_1} axis. Therefore, by inspection of the figure, we see that the coordinates of point D are

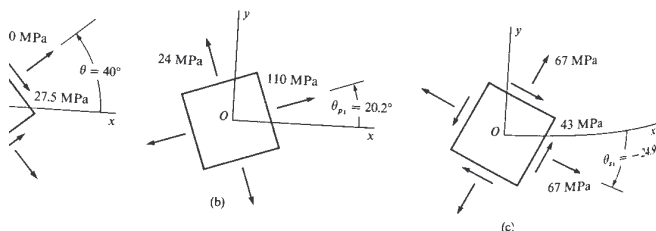
$$\begin{aligned} \sigma_{x_1} &= 67 \text{ MPa} + 43 \text{ MPa}(\cos 39.7^\circ) = 100 \text{ MPa} \\ \tau_{x_1y_1} &= -43 \text{ MPa}(\sin 39.7^\circ) = -27.5 \text{ MPa} \end{aligned}$$

In an analogous manner, we can find the stresses represented by point D' :

$$\begin{aligned} \sigma_{y_1} &= 67 \text{ MPa} - 43 \text{ MPa}(\cos 39.7^\circ) = 33.9 \text{ MPa} \\ \tau_{x_1y_1} &= 43 \text{ MPa}(\sin 39.7^\circ) = 27.5 \text{ MPa} \end{aligned}$$

These results are shown in Fig. 6-17a on a sketch of an element rotated through an angle $\theta = 40^\circ$.

Example 1 (continued). Element at $\theta = 40^\circ$, stresses, and shear stresses



(b) The principal stresses are represented by points P_1 and P_2 on Mohr's circle. The larger principal stress (point P_1) is

$$\sigma_1 = 67 \text{ MPa} + 43 \text{ MPa} = 110 \text{ MPa}$$

as seen by inspection of the circle. This stress acts on a plane defined by the angle $\theta_{p_1} = 20.2^\circ$. Similarly, the smaller principal stress is

$$\sigma_2 = 67 \text{ MPa} - 43 \text{ MPa} = 24 \text{ MPa}$$

The angle $2\theta_{p_2}$ is $40.3^\circ + 180^\circ = 220.3^\circ$; thus, the principal plane is defined by the angle $\theta_{p_2} = 110.2^\circ$. The principal stresses and principal planes are shown in Fig. 6-17b.

(c) The maximum and minimum shear stresses are represented by points S and S' ; therefore,

$$\tau_{max} = 43 \text{ MPa}$$

which is the radius of the circle. The angle ACS is $90^\circ - 40.3^\circ = 49.7^\circ$; hence, the angle $2\theta_{s_1}$ to point S on the circle is

$$2\theta_{s_1} = -49.7^\circ$$

because it is measured clockwise. The corresponding angle θ_{s_1} to the plane of the maximum shear stress is one-half that value, or $\theta_{s_1} = -24.9^\circ$. The maximum and minimum shear stresses are shown in Fig. 6-17c.

Example 2

An element in plane stress is subjected to stresses $\sigma_x = -50$ MPa, $\sigma_y = 10$ MPa, and $\tau_{xy} = -40$ MPa as shown in Fig. 6-18a. Using Mohr's circle, determine (a) the stresses acting on an element rotated through an angle $\theta = 45^\circ$, (b) the principal stresses, and (c) the maximum shear stresses. Show all results on sketches of properly oriented elements.

The center of the circle is on the σ_{x_1} axis at point C where σ_{x_1} equals σ_{aver} , which is

$$\sigma_{aver} = \frac{\sigma_x + \sigma_y}{2} = -20 \text{ MPa}$$

The stresses on the x face of the element determine the coordinates of point A :

$$\sigma_{x_1} = -50 \text{ MPa} \quad \tau_{x_1y_1} = -40 \text{ MPa}$$

The coordinates of point B represent the stresses on the y face of the element:

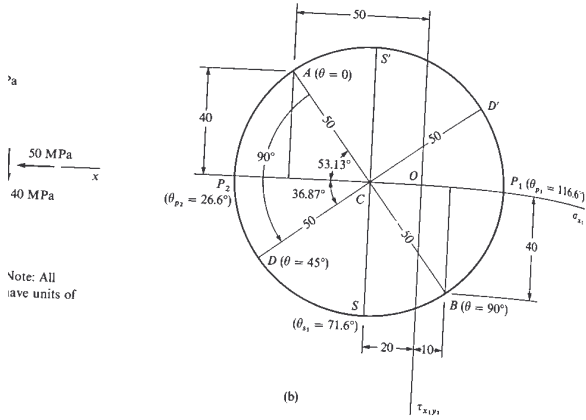
$$\sigma_{y_1} = 10 \text{ MPa} \quad \tau_{x_1y_1} = 40 \text{ MPa}$$

These points define the circle, which has radius

$$R = \sqrt{(30 \text{ MPa})^2 + (40 \text{ MPa})^2} = 50 \text{ MPa}$$

The angle ACP_2 is the angle $2\theta_{p_2}$ from point A to point P_2 , representing the principal plane having the algebraically smaller principal stress σ_2 . This angle is found by noting that

$$\tan 2\theta_{p_2} = \frac{40 \text{ MPa}}{30 \text{ MPa}} = \frac{4}{3}$$



Note: All have units of

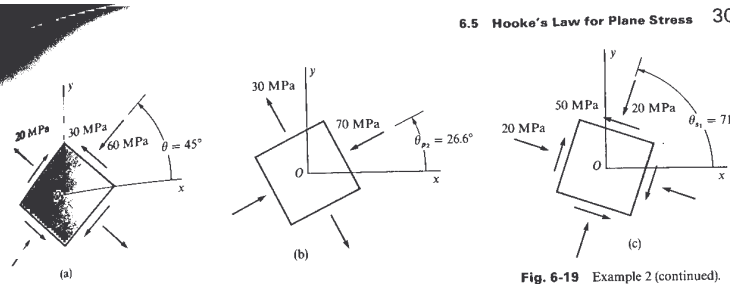


Fig. 6-19 Example 2 (continued). (a) Stresses on element at $\theta = 45^\circ$. (b) principal stresses, and (c) maximum shear stresses

The angle to point P_2 is $2\theta_{P_2} = 53.1^\circ$, or $\theta_{P_2} = 26.6^\circ$. The principal planes and principal stresses are shown in Fig. 6-19b.
 (c) The maximum and minimum shear stresses, represented by points S and S' , are $\tau_{max} = 50$ MPa and $\tau_{min} = -50$ MPa. The angle ACS (equal to $2\theta_{s_1}$) is $53.1^\circ + 90^\circ = 143.1^\circ$; hence, the angle $\theta_{s_1} = 71.6^\circ$. The maximum shear stresses are shown in Fig. 6-19c.

Hence,

$$2\theta_{P_2} = 53.13^\circ \quad \theta_{P_2} = 26.57^\circ$$

Thus, all of the required angles and stresses have been obtained, as shown on the circle.

(a) The stresses acting on a plane at $\theta = 45^\circ$ are represented by point D , which is at an angle $2\theta = 90^\circ$ from point A . The angle DCP_2 is

$$\text{Angle } DCP_2 = 90^\circ - 2\theta_{P_2} = 90^\circ - 53.13^\circ = 36.87^\circ$$

This angle is between line CD and the negative σ_{x_1} axis; therefore, by inspection we obtain the coordinates of point D :

$$\sigma_{x_1} = -20 \text{ MPa} - 50 \text{ MPa}(\cos 36.87^\circ) = -60 \text{ MPa}$$

$$\tau_{x_1y_1} = 50 \text{ MPa}(\sin 36.87^\circ) = 30 \text{ MPa}$$

Similarly, the coordinates of point D' are

$$\sigma_{x_1} = -20 \text{ MPa} + 50 \text{ MPa}(\cos 36.87^\circ) = 20 \text{ MPa}$$

$$\tau_{x_1y_1} = -50 \text{ MPa}(\sin 36.87^\circ) = -30 \text{ MPa}$$

These stresses, which act on an element at $\theta = 45^\circ$, are shown in Fig. 6-19a.
 (b) The principal stresses are represented by points P_1 and P_2 on the circle. Their values are

$$\sigma_1 = -20 \text{ MPa} + 50 \text{ MPa} = 30 \text{ MPa}$$

$$\sigma_2 = -20 \text{ MPa} - 50 \text{ MPa} = -70 \text{ MPa}$$

as obtained by inspection of the circle. The angle $2\theta_{P_1}$, on the circle (measured counterclockwise from A to P_1) is $53.1^\circ + 180^\circ = 233.1^\circ$; hence, $\theta_{P_1} = 116.6^\circ$

6.5 HOOKE'S LAW FOR PLANE STRESS

In the preceding sections, we analyzed the stresses acting on inclined planes for an element in plane stress (Fig. 6-20). In those discussions, we used statics only; hence, the properties of the material were not considered. Now let us assume that the material is homogeneous and isotropic; that is, the material is uniform throughout the body and has the same properties in all directions. Furthermore, we will assume that Hooke's law holds, which means that the material behaves in a linear elastic manner. Under these conditions, we can readily obtain the relationships between the stresses and the strains in the body.

Let us begin by considering the normal strains ϵ_x , ϵ_y , and ϵ_z , which are shown in Fig. 6-21 as the changes in dimensions of an infinitesimally small cube having edges of unit length. All three strains are shown positive in the figure. These strains can be expressed in terms of the stresses (Fig. 6-20) by superimposing the effects of the individual stresses. For instance, the stress σ_x produces a strain ϵ_x equal to σ_x/E , and the stress σ_y produces a strain ϵ_y equal to σ_y/E . Of course, the shear stress τ_{xy} produces no normal strain in the x direction. Thus, the resultant strain ϵ_x is

$$\epsilon_x = \frac{1}{E}(\sigma_x - \nu\sigma_y) \quad (6-26a)$$

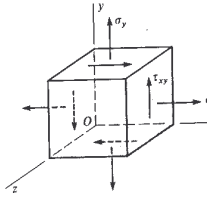
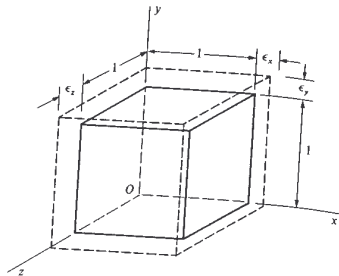


Fig. 6-20 Element in plane stress

6.5 HOOKE'S LAW FOR PLANE STRESS

6.5 HOOKE'S LAW FOR PLANE STRESS



Normal strains ϵ_x , ϵ_y , and ϵ_z .

In a similar way, we obtain the strains in the y and z directions:

$$\epsilon_y = \frac{1}{E}(\sigma_y - \nu\sigma_x) \quad (6-26b)$$

$$\epsilon_z = -\frac{\nu}{E}(\sigma_x + \sigma_y) \quad (6-26c)$$

These equations may be used to find the normal strains when the stresses are known.

The shear stress τ_{xy} causes a distortion of the element such that each z face becomes a rhombus (Fig. 6-22), and the shear strain γ_{xy} represents the decrease in angle between the positive (or negative) x and y faces of the element. Because no other shear stresses act on the sides of the plane stress element (Fig. 6-20), the x and y faces are not distorted and remain square. The shear strain is related to the shear stress by Hooke's law in shear, as follows:

$$\gamma_{xy} = \frac{\tau_{xy}}{G} \quad (6-27)$$

Of course, the normal stresses σ_x and σ_y have no effect on the shear strain γ_{xy} . Hence, Eqs. (6-26) and (6-27) give the strains due to all stresses (σ_x , σ_y , and τ_{xy}) acting simultaneously.

The first two equations for the normal strains (Eqs. 6-26a and b) can be solved simultaneously for the stresses in terms of the strains:

$$\sigma_x = \frac{E}{1-\nu^2}(\epsilon_x + \nu\epsilon_y) \quad (6-28a)$$

$$\sigma_y = \frac{E}{1-\nu^2}(\epsilon_y + \nu\epsilon_x) \quad (6-28b)$$

In addition, we have

$$\tau = G\gamma \quad (6-29)$$

These equations may be used to find the stresses when the strains are known.

The preceding equations (Eqs. 6-26 through 6-29) are known collectively as **Hooke's law for plane stress**. They contain three elastic constants (E , G , and ν), but only two are independent because of the relationship $G = E/2(1 + \nu)$.

Unit volume change. The unit volume change at a point in a body subjected to plane stress can be found by again considering the element of Fig. 6-21. The original volume of this element is $V_0 = (1)(1)(1) = 1$, and its final volume is

$$V_f = (1 + \epsilon_x)(1 + \epsilon_y)(1 + \epsilon_z)$$

or, disregarding products of small quantities,

$$V_f = 1 + \epsilon_x + \epsilon_y + \epsilon_z$$

Therefore, the change in volume is

$$\Delta V = V_f - V_0 = \epsilon_x + \epsilon_y + \epsilon_z$$

and the unit volume change (or dilatation) becomes

$$e = \frac{\Delta V}{V_0} = \epsilon_x + \epsilon_y + \epsilon_z \quad (6-30)$$

This equation is valid for any material. Note that shear strains produce no change in volume.

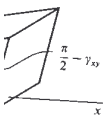
When the material follows Hooke's law, we can substitute Eqs. (6-26) into Eq. (6-30) and obtain the following expression for the unit volume change in plane stress:

$$e = \frac{\Delta V}{V_0} = \frac{1-2\nu}{E}(\sigma_x + \sigma_y) \quad (6-31)$$

If $\sigma_y = 0$, this equation reduces to Eq. (1-7) for the unit volume change in uniaxial stress. Knowing the value of e , we can find by integration the total volume change for any body subjected to plane stress.

Strain energy density. The strain energy density u is the strain energy stored in a unit volume of the material (see previous discussions in Sections 2.8 and 3.8). For an element in plane stress, we can use the element of unit volume shown in Figs. 6-21 and 6-22. Inasmuch as the normal and shear strains occur independently, we can add their strain energies to obtain the total energy.

Beginning with the normal strains (Fig. 6-21), we observe that the total force acting on the x face of the element is equal algebraically to σ_x , inasmuch as the area of the face is unity. This force moves through a distance equal to ϵ_x as the stresses are applied to the element. Assuming



this force is $\sigma_x \epsilon_x/2$. Similarly, the force σ_y on the y face does work equal to $\sigma_y \epsilon_y/2$. The sum of these work terms, which is the same as the strain energy density, is

$$\frac{1}{2}(\sigma_x \epsilon_x + \sigma_y \epsilon_y)$$

The strain energy density associated with the shear strains (Fig. 6-22) was evaluated in Section 3.8 (see Eq. 3-36) and equals $\tau_{xy} \gamma_{xy}/2$. By adding the strain energy densities for normal and shear strains, we obtain the following formula for plane stress:

$$u = \frac{1}{2}(\sigma_x \epsilon_x + \sigma_y \epsilon_y + \tau_{xy} \gamma_{xy}) \quad (6-32)$$

Substituting for the strains from Eqs. (6-26) and (6-27), we obtain the strain energy density in terms of stresses alone:

$$u = \frac{1}{2E}(\sigma_x^2 + \sigma_y^2 - 2\nu\sigma_x\sigma_y) + \frac{\tau_{xy}^2}{2G} \quad (6-33)$$

In the same manner, we can substitute for the stresses from Eqs. (6-28) and (6-29) to obtain the strain energy density in terms of strains:

$$u = \frac{E}{2(1-\nu^2)}(\epsilon_x^2 + \epsilon_y^2 + 2\nu\epsilon_x\epsilon_y) + \frac{G\gamma_{xy}^2}{2} \quad (6-34)$$

For the special case of uniaxial stress, we substitute the values

$$\sigma_y = 0 \quad \tau_{xy} = 0 \quad \epsilon_y = -\nu\epsilon_x \quad \gamma_{xy} = 0$$

into Eqs. (6-33) and (6-34) to obtain

$$u = \frac{\sigma_x^2}{2E} \quad \text{and} \quad u = \frac{E\epsilon_x^2}{2}$$

These equations agree with Eqs. (2-41) of Section 2.8.

6.6 SPHERICAL AND CYLINDRICAL PRESSURE VESSELS (BIAXIAL STRESS)

Pressure vessels are closed structures that contain liquids or gases under pressure. Familiar examples are spherical water-storage tanks, cylindrical tanks for compressed air, pressurized pipes, and inflated balloons. The curved walls of pressure vessels are often very thin in relation to the radius and the length, and in such cases they are in the general class of structural forms known as shells. Other examples of shell structures are thin curved roofs, domes, and fuselages.

In this section, we consider only thin-walled pressure vessels of spherical and circular cylindrical shape (Fig. 6-23). The term *thin-walled* is not precise, but a general rule is that the ratio of radius r to wall thickness t should be greater than 10 in order for us to determine the

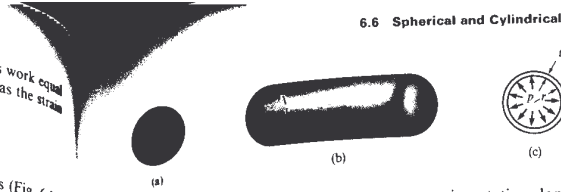


Fig. 6-23 Thin-walled pressure vessels: (a) spherical vessel, (b) cylindrical vessel, and (c) cross section showing internal pressure p

stresses in the walls with reasonable accuracy using statics alone. A second limitation is that the internal pressure must exceed the external pressure; otherwise, the shell may fail by collapsing due to buckling of the walls.

Spherical pressure vessels. A tank of spherical shape is the ideal container for resisting internal pressure. We need only contemplate the familiar soap bubble to recognize that a sphere is the "natural" shape for this purpose. To obtain the stresses in the wall, let us cut through the sphere on a vertical diametral plane and isolate half of the shell and its contents as a free body (Fig. 6-24a). Acting on this free body are the stresses σ in the wall and the internal pressure p . The weight of the tank and its contents is disregarded in this analysis. The pressure acts horizontally against the plane circular area formed by the cut, and the resultant force equals $p(\pi r^2)$, where r is the inside radius of the sphere. Note that the pressure p is the net internal pressure, or gage pressure (that is, the pressure above atmospheric, or external, pressure).

The tensile stress σ in the wall of the sphere is uniform around the circumference of the tank, because of the symmetry of the tank and its loading. Furthermore, because the wall is very thin, we can assume with good accuracy that the stress is uniform across the thickness t . The accuracy of this approximation increases as the shell becomes thinner and decreases as it becomes thicker. The resultant force obtained from the normal stress is $\sigma(2\pi r_m t)$, where t is the thickness and r_m is the mean radius of the shell ($r_m = r + t/2$). However, since our analysis is valid only for very thin shells, we can assume that $r_m \approx r$; then the resultant force becomes $\sigma(2\pi r t)$. Equilibrium of forces in the horizontal direction gives

$$\sigma(2\pi r t) - p(\pi r^2) = 0$$

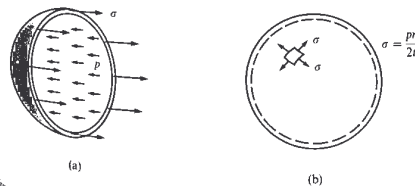


Fig. 6-24 Stresses in a spherical pressure vessel

from which we obtain

$$\sigma = \frac{pr}{2t} \quad (6-35)$$

As is evident from the symmetry of a spherical shell, this same equation for the stress σ will be obtained if we cut a plane through the center of the pressurized sphere in any direction whatsoever. Therefore, we conclude that a pressurized sphere is subjected to uniform tensile stresses σ in all directions. This stress condition is represented in Fig. 6-24b by the small stress element with stresses σ acting in mutually perpendicular directions. Stresses of this kind, which act tangential (rather than perpendicular) to the curved surface are known as **membrane stresses**. The name arises from the fact that stresses of this type exist in true membranes, such as soap films or thin sheets of rubber.

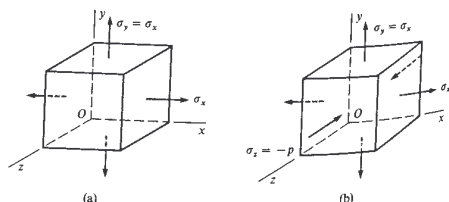
At the outer surface of a spherical pressure vessel, there are no stresses acting normal to the surface. Hence, the stress condition is a special case of biaxial stress in which σ_x and σ_y are the same (Fig. 6-25a). Because no shear stresses act on this element, we obtain exactly the same normal stresses when the element is rotated about the z axis through any angle. Thus, Mohr's circle for this stress condition reduces to a point, and every inclined plane is a principal plane. The principal stresses are

$$\sigma_1 = \sigma_2 = \frac{pr}{2t} \quad (6-36)$$

Also, the maximum in-plane shear stress is zero. However, as discussed in Section 6.3, we must not overlook the fact that the element is three-dimensional and that the third principal stress (in the z direction) is zero. Therefore, the absolute maximum shear stress, obtained by a 45° rotation of the element about either the x or y axis, is

$$\tau_{\max} = \frac{\sigma}{2} = \frac{pr}{4t} \quad (6-37)$$

as obtained from Eqs. (6-23).



in a spherical the outer surface face

At the inner surface of the wall of the spherical vessel, the stress element has the same membrane stresses (Eq. 6-35) but, in addition, a compressive stress equal to p acts in the z direction (Fig. 6-25b). These three normal stresses are the principal stresses:

$$\sigma_1 = \sigma_2 = \frac{pr}{2t} \quad \sigma_3 = -p \quad (6-38)$$

The maximum in-plane shear stress is zero, but the maximum out-of-plane shear stress (obtained by a 45° rotation about either the x or y axis) is

$$\tau_{\max} = \frac{\sigma + p}{2} = \frac{pr}{4t} + \frac{p}{2} \quad (6-39)$$

If the ratio r/t is sufficiently large, the last term in this equation can be disregarded. Then the equation becomes the same as Eq. (6-37), and we can assume that the maximum shear stress is constant across the thickness of the shell.

Every spherical tank used as a pressure vessel will have at least one opening in the wall as well as various attachments and supports. These features result in nonuniformities in the stress distribution that cannot be analyzed by elementary methods. High localized stresses are produced near the discontinuities in the shell, which must be reinforced in these regions. Therefore, the equations we have derived for the membrane stresses are valid everywhere in the wall of the vessel except close to the discontinuities. Other considerations entering into the design of tanks include effects of corrosion, accidental impacts, and temperature effects.

Cylindrical pressure vessels. Now let us consider a thin-walled circular cylindrical tank with closed ends and internal pressure p (Fig. 6-26a). A stress element with faces parallel and perpendicular to the axis of the tank is shown in the figure. The normal stresses σ_1 and σ_2 acting

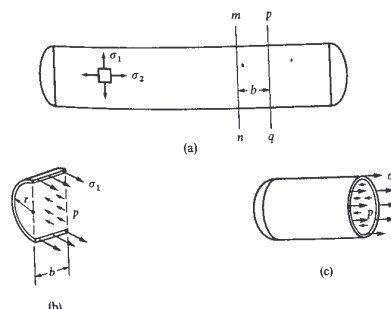


Fig. 6-26 Stresses in a circular cylindrical pressure vessel

on the side faces of this element represent the membrane stresses in the wall. No shear stresses act on the faces of this element because of the symmetry of the vessel. Therefore, the stresses σ_1 and σ_2 are principal stresses. Because of its direction, the stress σ_1 is called the circumferential stress or the hoop stress; similarly, the stress σ_2 is the longitudinal stress or the axial stress. Each of these stresses can be calculated from equilibrium by using appropriate free-body diagrams.

To calculate the circumferential stress σ_1 , we isolate a free body by making two cuts (mn and pq) a distance b apart and perpendicular to the longitudinal axis (Fig. 6-26a). Also, we make a third cut in a vertical plane through the axis itself; the resulting free-body is shown in Fig. 6-26b. Acting on the longitudinal vertical face of this free body are the stresses σ_1 in the wall and the internal pressure p . Stresses and pressures also act on the transverse faces of this free body, but they are not shown in the figure because they do not enter the equation of equilibrium that we will use. Also, we again disregard the weight of the vessel and its contents. The horizontal forces due to the stress σ_1 and the pressure p act in opposite directions; hence, we have the following equation of equilibrium:

$$\sigma_1(2bt) - p(2br) = 0$$

in which t is the thickness of the wall and r is the inside radius of the cylinder. From the preceding equation, we obtain

$$\sigma_1 = \frac{pr}{t} \quad (6-40)$$

as the formula for the circumferential stress. As discussed previously, this stress is uniformly distributed over the thickness of the wall provided the wall is very thin.

The longitudinal stress σ_2 is obtained from a free body of the part of the tank to the left of a section (such as mn) that is perpendicular to the longitudinal axis (Fig. 6-26c). In this case, the equation of equilibrium is

$$\sigma_2(2\pi rt) - p(\pi r^2) = 0$$

in which, as explained previously, we have used the inside radius of the shell in place of the mean radius when calculating the force due to the stress σ_2 . Solving the preceding equation for σ_2 , we obtain

$$\sigma_2 = \frac{pr}{2t} \quad (6-41)$$

which is the same as the membrane stress in a spherical shell. Comparing Eqs. (6-40) and (6-41), we see that

$$\sigma_2 = \frac{\sigma_1}{2} \quad (6-42)$$

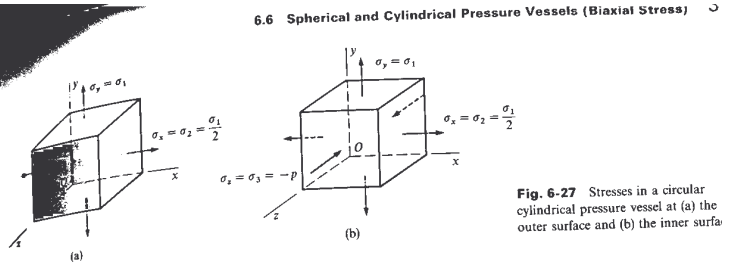


Fig. 6-27 Stresses in a circular cylindrical pressure vessel at (a) the outer surface and (b) the inner surface

Thus, the longitudinal stress in a cylindrical shell is one-half the circumferential stress.

The principal stresses σ_1 and σ_2 at the outer surface of the shell are shown acting on a stress element in Fig. 6-27a. The third principal stress, acting in the z direction, is zero. Thus, we again have biaxial stress. The in-plane maximum shear stresses occur when the element is rotated 45° about the z axis; this stress is

$$(\tau_{\max})_z = \frac{\sigma_1 - \sigma_2}{2} = \frac{\sigma_1}{4} = \frac{pr}{4t} \quad (6-43)$$

(see Eq. 6-21). The maximum shear stresses obtained by 45° rotations about the x and y axes are, respectively,

$$(\tau_{\max})_x = \frac{\sigma_1}{2} = \frac{pr}{2t} \quad (\tau_{\max})_y = \frac{\sigma_2}{2} = \frac{pr}{4t}$$

Thus, the absolute maximum shear stress is

$$\tau_{\max} = \frac{\sigma_1}{2} = \frac{pr}{2t} \quad (6-44)$$

and it occurs when the element is rotated 45° about the x axis.

The stress conditions at the inner surface of the shell are shown in Fig. 6-27b. The principal normal stresses are

$$\sigma_1 = \frac{pr}{t} \quad \sigma_2 = \frac{pr}{2t} \quad \sigma_3 = -p \quad (6-45)$$

The three maximum shear stresses, obtained by 45° rotations about the x , y , and z axes, are

$$(\tau_{\max})_z = \frac{\sigma_1 - p}{2} = \frac{pr}{2t} + \frac{p}{2} \quad (\tau_{\max})_y = \frac{\sigma_2 + p}{2} = \frac{pr}{4t} + \frac{p}{2} \quad (6-46)$$

$$(\tau_{\max})_x = \frac{\sigma_1 - \sigma_2}{2} = \frac{pr}{4t}$$

The first of these stresses is the largest. However, as explained in the discussion of shear stresses in a spherical shell, we often may disregard

the additional term $p/2$ in these expressions and assume that the maximum shear stress is constant across the thickness and is given by Eq. (6-44).

The preceding stress formulas are valid in parts of the cylinder away from any discontinuities. An obvious discontinuity exists at the end of the cylinder where the head is attached. Others occur at openings in the cylinder or where objects are attached to the cylinder.

Example 1

A spherical pressure vessel having 450 mm inside diameter and 6 mm wall thickness is to be constructed by welding two aluminium hemispheres (Fig. 6-28). From tests, it is found that the ultimate and yield stresses in tension at the weld are 165 MPa and 110 MPa, respectively. The tank must have a factor of safety of 2.1 with respect to the ultimate stress and 1.5 with respect to the yield stress. What is the maximum permissible pressure in the tank?

The allowable stress based upon the ultimate stress σ_u is

$$\sigma_{\text{allow}} = \frac{\sigma_u}{n} = \frac{165 \text{ MPa}}{2.1} = 78.6 \text{ MPa}$$

(see Eq. 1-12). Based upon the yield stress σ_y , the allowable stress (Eq. 1-12) is

$$\sigma_{\text{allow}} = \frac{\sigma_y}{n} = \frac{110 \text{ MPa}}{1.5} = 73.3 \text{ MPa}$$

The latter stress is lower, hence it governs the design.

The maximum tensile stress in the tank is given by the formula $\sigma = pr/2t$ (see Eq. 6-36). Solving this equation for the pressure, we get

$$p = \frac{2t\sigma_{\text{allow}}}{r} = \frac{2(6 \text{ mm})(73.3 \text{ MPa})}{225 \text{ mm}} = 3.91 \text{ MPa}$$

Thus, the maximum allowable pressure $p_{\text{max}} = 3.9 \text{ MPa}$. (Note that, in a calculation of this kind, we round downward, not upward.)

Example 2

A cylindrical pressure vessel is constructed with a helical weld that makes an angle of 55° with the longitudinal axis (Fig. 6-29a). The tank has inside radius $r = 1.8 \text{ m}$ and wall thickness $t = 8 \text{ mm}$. The maximum internal pressure is 600 kPa. Calculate the following quantities for the cylindrical part of the tank: (a) the circumferential and longitudinal stresses; (b) the maximum shear stress; and (c) the normal and shear stresses acting perpendicular and parallel to the weld, respectively.

(a) The circumferential and longitudinal stresses are obtained from Eqs. (6-40) and (6-42), respectively:

$$\sigma_1 = \frac{pr}{t} = \frac{(600 \text{ kPa})(1.8 \text{ m})}{8 \text{ mm}} = 135 \text{ MPa} \quad \sigma_2 = \frac{\sigma_1}{2} = 67.5 \text{ MPa}$$

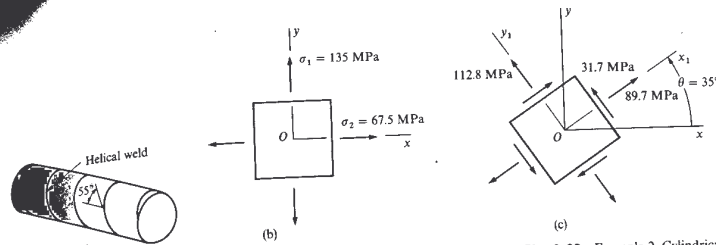


Fig. 6-29 Example 2. Cylindrical pressure vessel

These principal stresses are shown on the biaxial stress element of Fig. 6-29b. (b) The largest in-plane shear stress is obtained from Eq. (6-43):

$$\tau = \frac{\sigma_1 - \sigma_2}{2} = \frac{\sigma_1}{4} = 33.8 \text{ MPa}$$

However, the absolute maximum shear stress in the cylinder wall is

$$\tau_{\max} = \frac{\sigma_1}{2} = 67.5 \text{ MPa}$$

as obtained from Eq. (6-44).

(c) An element rotated through an angle $\theta = 35^\circ$ so that its sides are parallel and perpendicular to the weld is shown in Fig. 6-29c. Either the stress transformation equations (Eqs. 6-4) or Mohr's circle may be used to obtain the normal and shear stresses acting on the side faces of this element. The Mohr's-circle construction is shown in Fig. 6-30. Point A represents the stress σ_2 on the x face ($\theta = 0$), and point B represents the stress σ_1 on the y face ($\theta = 90^\circ$). A counterclockwise angle $2\theta = 70^\circ$ on the circle locates point D , which corresponds to the stresses on the x_1 face ($\theta = 35^\circ$). Since the radius of the circle is

$$R = \frac{135 \text{ MPa} - 67.5 \text{ MPa}}{2} = 33.75 \text{ MPa}$$

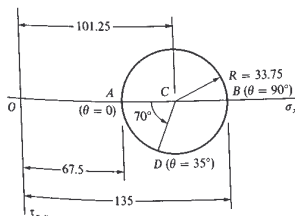


Fig. 6-30 Mohr's circle for the biaxial stress element of Fig. 6-29. (Note: All stresses have units of MPa)

we see that the coordinates of point *D* are

$$\sigma_{x_1} = 101.25 \text{ MPa} - (33.75 \text{ MPa}) \cos 70^\circ = 89.7 \text{ MPa}$$

$$\tau_{x_1 y_1} = (33.75 \text{ MPa}) \sin 70^\circ = 31.7 \text{ MPa}$$

These stresses act on the x_1 face of the element (Fig. 6-29c). The normal stress on the y_1 face is found from the equality of the sum of the normal stresses on perpendicular planes:

$$\sigma_1 + \sigma_2 = \sigma_{x_1} + \sigma_{y_1}$$

Hence,

$$\sigma_{y_1} = \sigma_1 + \sigma_2 - \sigma_{x_1} = 135 \text{ MPa} + 67.5 \text{ MPa} - 89.7 \text{ MPa} = 112.8 \text{ MPa}$$

Thus, the normal and shear stresses acting on planes parallel and perpendicular to the weld are as shown on the rotated stress element of Fig. 6-29c. We see that the tensile stress acting across the weld is 89.7 MPa and the shear stress acting along the weld is 31.7 MPa.

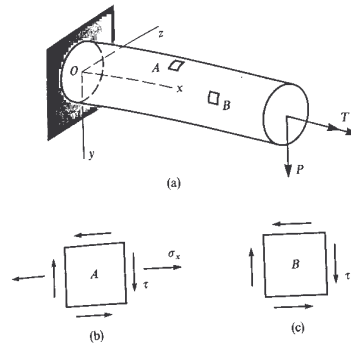


Fig. 6-31 Combined bending and torsion

6.7 COMBINED LOADINGS (PLANE STRESS)

Structural members often are required to resist more than one type of loading. For example, a shaft in torsion may also be subjected to bending, or a beam may be subjected to the simultaneous action of bending moments and axial forces. The stress analysis of a member subjected to such **combined loadings** can usually be performed by superimposing the stresses due to each load acting separately. Superposition is permissible if the stresses are linear functions of the loads and if there is no interaction effect between the various loads (that is, if the stresses due to one load are not affected by the presence of any other loads). The latter requirement is usually met if the deflections and rotations of the structure are small.

The analysis begins with the determination of the stresses due to the axial forces, torques, shear forces, and bending moments. Then these stresses are combined to obtain the resultant stresses, after which the stresses acting in inclined directions can be investigated by using either the stress transformation equations or Mohr's circle. In particular, the principal stresses and maximum shear stresses can be calculated. Any number of critical locations in the member can be analyzed in this manner, thereby either confirming the adequacy of the design or, if the stresses are too large or too small, showing that design changes are needed.

To illustrate the method, consider the solid circular cantilever bar shown in Fig. 6-31a. The bar is loaded at the free end by a twisting couple *T* and a lateral bending moment *P*. These loads produce at every cross section a bending moment *M*, a shear force *V*, and a twisting couple *T*, each of which produces stresses acting over the cross sections.

If we isolate a stress element *A* at the top of the bar, we see that it is subjected to bending stresses $\sigma_x = Mr/I$ and shear stresses $\tau = Tr/I_p$. In these expressions, *r* is the radius of the bar, *I* is the moment of inertia about the *z* axis (the neutral axis), and *I_p* is the polar moment of inertia. At the top of the bar, there are no shear stresses associated with the shear force *V*. Thus, the element at *A* is subjected to plane stress, as shown in Fig. 6-31b. Assuming that σ_x and τ have been calculated, we can proceed to determine the stresses on an element rotated through any desired angle. The maximum and minimum normal stresses at point *A* are the principal stresses, obtained from Eq. (6-13):

$$\sigma_{1,2} = \frac{\sigma_x}{2} \pm \sqrt{\left(\frac{\sigma_x}{2}\right)^2 + \tau^2}$$

Also, the maximum in-plane shear stress (from Eq. 6-20) is

$$\tau_{\max} = \sqrt{\left(\frac{\sigma_x}{2}\right)^2 + \tau^2}$$

which is larger than the out-of-plane shear stresses. These maximum stresses can be compared with the allowable normal and shear stresses when checking the adequacy of the bar. Of course, the stresses are largest when element *A* is located at the fixed end of the beam where the bending moment *M* has its maximum value. Hence, the top of the beam at the support is one of the critical points where the stresses must be investigated.

Another critical point is on the side of the bar at the neutral axis (point *B* in Fig. 6-31a). At this location, the bending stress σ_x is zero but the shear stress produced by the shear force *V* has its largest value. The

element at *B* is in a state of pure shear (Fig. 6-31c), with the shear stress τ consisting of two parts: first, the shear stress τ_1 due to the torque *T* and obtained from the formula $\tau_1 = Tr/I_p$; and, second, the shear stress τ_2 due to the shear force *V* (equal to the load *P*) and obtained from the formula $\tau_2 = 4V/3A$ for a solid circular bar (see Eq. 5-32). The total shear stress acting on the element is $\tau = \tau_1 + \tau_2$. The principal stresses occur on planes at 45° to the axis and have the same magnitude as the shear stress itself:

$$\sigma_{1,2} = \pm \tau$$

Of course, the maximum shear stress at *B* is the stress τ . These maximum normal and shear stresses should be compared with those obtained for elements at the top and bottom of the bar in order to ascertain the absolute maximum stresses for use in design.

The preceding discussion is intended to illustrate the general approach to problems that involve combined loadings. The variety of specific situations is seemingly endless, so it is not worthwhile to derive various critical points, and the results are compared. When selecting the points to be investigated, it is natural to choose those locations where either the normal or the shear stresses are a maximum. By using good judgment in the selection of the points, we can be reasonably certain of obtaining the absolute maximum stresses without analyzing a large number of stress elements.

6.8 PRINCIPAL STRESSES IN BEAMS

The normal and shear stresses acting at any point in the cross section of a beam can be obtained from the flexure and shear formulas ($\sigma = My/I$ and $\tau = VQ/Ib$). The normal stress is a maximum at the outer edges of the beam and equals zero at the neutral axis, whereas the shear stress is zero at the outer edges and usually is a maximum at the neutral axis. In most circumstances, only these stresses are needed in order to design the beam. However, a more detailed study requires that we calculate the principal stresses and maximum shear stresses at various locations.

To visualize how the principal stresses vary in a beam, let us examine the stresses in a beam of rectangular cross section (Fig. 6-32a). Five points, denoted in the figure by *A*, *B*, *C*, *D*, and *E*, are selected at the cross section. Points *A* and *E* are at the upper and lower surfaces, point *C* is at the midheight of the beam, and points *B* and *D* are in between. The cross-sectional stresses at each of these points can be readily calculated if the bending moment and shear force are known. These stresses can be pictured as acting on plane stress elements having horizontal and vertical faces (Fig. 6-32b). The stress condition of the beam is uniaxial at the top and bottom of the beam and pure shear at the neutral axis. At other locations, both normal and shear stresses act on the stress element. To find the principal stresses and maximum shear stresses at such locations, we may use either the equations of plane stress (Sec-

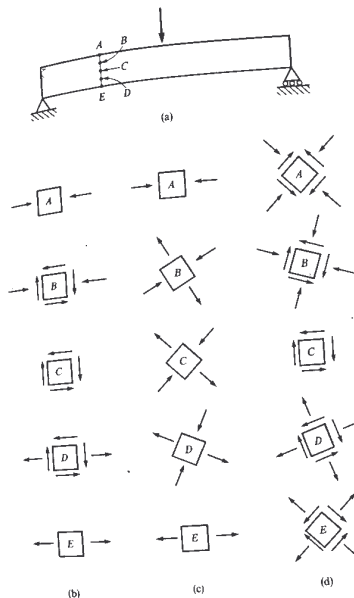
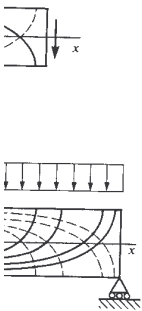


Fig. 6-32 Stresses in a beam of rectangular cross section: (a) points *A*, *B*, *C*, *D*, and *E* in the cross section, (b) normal and shear stresses acting on horizontal and vertical planes, (c) principal stresses, and (d) maximum shear stresses

tion 6.3) or Mohr's circle (Section 6.4). The directions of the principal stresses at each point are shown schematically in Fig. 6-32c, and the maximum shear stresses are shown in Fig. 6-32d.

From the sketches in Fig. 6-32c, we can observe how the principal stresses change. At the top of the beam, the compressive principal stress acts in the horizontal direction. As we move toward the neutral axis, this principal stress becomes inclined to the horizontal, and at the neutral axis (point *C*) it acts at 45°. As we approach the bottom of the beam, the direction of the compressive principal stress approaches the vertical direction. The magnitude of this stress varies continuously between the top of the beam and the bottom (where it becomes zero). The maximum numerical value of this stress (in a rectangular beam) usually occurs at point *A*, although it is theoretically possible (for deep beams with high shear) for the maximum value to occur at a point such as *B*. Analogous comments apply to the tensile principal stress, which also varies in both magnitude and direction as we move from *A* to *E*.



1 stress trajectories in a cantilever beam; (b) simple beam. (solid lines represent tensile principal stresses; dashed lines represent compressive principal stresses.)

Typical stress contours for a beam (principal stresses only) for a point load.

By investigating the stresses at many cross sections of the beam we can determine how the principal stresses vary throughout the beam. Then it is possible to construct two systems of orthogonal curves, called *stress trajectories*, that give the directions of the principal stresses. Two examples of stress trajectories for rectangular beams are shown in Fig. 6-33; part (a) shows a cantilever beam with a force acting at the free end and part (b) shows a simple beam with a uniform load. In the figure, solid lines are used for tensile principal stresses and dashed lines for compressive principal stresses. Only the stresses obtained from the flexure and shear formulas are considered in these figures; the direct compressive stresses caused by the uniform load bearing on the top of the beam are disregarded. The two sets of curves always intersect at right angles, and every trajectory crosses the neutral surface at 45°. At the top and bottom surfaces of the beam, where the shear stress is zero, the trajectories become either horizontal or vertical.*

Another type of curve that may be plotted from the principal stresses is a *stress contour*, which is a curve that connects points of equal principal stress. Stress contours for a cantilever beam of rectangular cross section are shown in Fig. 6-34 (for tensile principal stresses only).

Beams having other shapes of cross sections can be analyzed for the principal stresses in a manner similar to that described for rectangular beams. The maximum principal stress in a wide-flange or I-beam usually occurs at the top or bottom but may sometimes occur in the web at the junction with the flange. Similarly, the maximum shear stress usually occurs at the neutral axis, but under extraordinary loading conditions it may occur away from the neutral axis. (The location of maximum stresses in both rectangular and wide-flange beams is discussed in detail in Ref. 6-10.)



When analyzing a beam for the maximum stresses, remember that high stresses (or stress concentrations) exist near supports, points of load application, fillets, and holes. Such stresses are confined to the region very close to the discontinuity, and they cannot be calculated by the elementary beam formulas used in this chapter.

6.9 TRIAXIAL STRESS

An element of material subjected to normal stresses σ_x , σ_y , and σ_z acting in mutually perpendicular directions (Fig. 6-35a) is said to be in a state of *triaxial stress*.

* Stress trajectories were originated by the German engineer Karl Culmann (1821-1881); see Refs. 6-8 and 6-9.

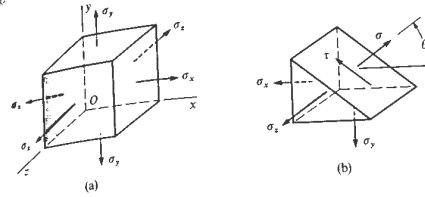


Fig. 6-35 Element in triaxial stress

a state of *triaxial stress*. Note that no shear stresses act on the x , y , and z faces of the element; hence, this stress condition is not the most general case of three-dimensional stress (which is discussed in the next section). The absence of shear stresses shows that the stresses σ_x , σ_y , and σ_z are the *principal stresses* for the element.

If an inclined plane parallel to the z axis is cut through the element (Fig. 6-35b), the only stresses on the inclined face are the normal stress σ and shear stress τ acting in the xy plane. Thus, these stresses are the same as the stresses σ_x and τ_{xy} encountered previously in our discussions of plane stress. Because these stresses are found from equations of force equilibrium in the xy plane, they are independent of the stress of force equilibrium in the xz plane, they are independent of the stress of plane stress, as well as Mohr's circle, when determining the stresses σ and τ . The same conclusion holds for the normal and shear stresses acting on inclined planes cut through the element parallel to the x and y axes.

From the previous discussions of plane stress, we know that the maximum shear stresses occur on planes oriented at 45° to the principal planes. To obtain these planes for an element in triaxial stress, we rotate the element through angles of 45° about the x , y , and z axes. For example, let us consider a 45° rotation about the z axis; then the maximum shear stresses acting on this element are

$$(\tau_{\max})_z = \pm \frac{\sigma_x - \sigma_y}{2} \quad (6-47a)$$

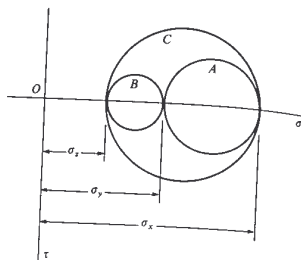
Similarly, if we rotate the element shown in Fig. 6-35a about the x axis through an angle of 45°, we obtain the following maximum shear stresses:

$$(\tau_{\max})_x = \pm \frac{\sigma_y - \sigma_z}{2} \quad (6-47b)$$

Finally, rotating the element about the y axis through a 45° angle gives the stresses

$$(\tau_{\max})_y = \pm \frac{\sigma_x - \sigma_z}{2} \quad (6-47c)$$

The **absolute maximum shear stress** is the algebraically largest of the stresses determined from Eqs. (6-47). It is equal to one-half the difference



36 Mohr's circles for an element in triaxial stress

between the algebraically largest and the algebraically smallest of the three principal stresses.

The stresses acting on elements rotated about the x , y , and z axes can be visualized with the aid of Mohr's circles. For elements obtained by rotation about the z axis, the corresponding circle is labeled *A* in Fig. 6-36; this circle is drawn for the case in which $\sigma_x > \sigma_y$ and both σ_x and σ_y are tension. In a similar manner, we can construct circles *B* and *C* for elements obtained by rotations about the x and y axes, respectively. The radii of the circles represent the maximum shear stresses given by Eqs. (6-47), and the absolute maximum shear stress is equal to the radius of the largest circle. The normal stresses acting on the planes of maximum shear stresses have magnitudes given by the abscissas of the centers of the circles.

In the preceding discussion, we considered only the stresses acting on planes obtained by rotating the element about the x , y , and z axes. Thus, every such plane is parallel to one of the axes. For instance, the inclined plane of Fig. 6-35b is parallel to the z axis, and its normal is parallel to the xy plane. Of course, we can also cut through the element in skew directions, so that the resulting inclined planes have normals that are skew to all three coordinate axes. The normal and shear stresses acting on such planes can be obtained by a more complicated three-dimensional analysis (see Section 6.10). However, those normal stresses are intermediate in value between the algebraically maximum and minimum principal stresses, and the shear stresses are less than the absolute maximum shear stress obtained from Eqs. (6-47).

Hooke's law for triaxial stress. The relationships between normal stresses and normal strains in the x , y , and z directions for triaxial stress can be obtained for a material that follows Hooke's law by using the same procedure as for plane stress (see Section 6.5). The strains produced by the stresses σ_x , σ_y , and σ_z acting independently are super-

imposed to obtain the resultant strains. Thus, we readily arrive at the following equations for the strains:

$$\epsilon_x = \frac{\sigma_x}{E} - \frac{\nu}{E}(\sigma_y + \sigma_z) \quad (6-48a)$$

$$\epsilon_y = \frac{\sigma_y}{E} - \frac{\nu}{E}(\sigma_x + \sigma_z) \quad (6-48b)$$

$$\epsilon_z = \frac{\sigma_z}{E} - \frac{\nu}{E}(\sigma_x + \sigma_y) \quad (6-48c)$$

In these equations, the standard sign conventions for σ and ϵ are used; that is, tensile stress σ and extensional strain ϵ are positive.

The preceding equations can be solved simultaneously for the stresses in terms of the strains:

$$\sigma_x = \frac{E}{(1 + \nu)(1 - 2\nu)} [(1 - \nu)\epsilon_x + \nu(\epsilon_y + \epsilon_z)] \quad (6-49a)$$

$$\sigma_y = \frac{E}{(1 + \nu)(1 - 2\nu)} [(1 - \nu)\epsilon_y + \nu(\epsilon_x + \epsilon_z)] \quad (6-49b)$$

$$\sigma_z = \frac{E}{(1 + \nu)(1 - 2\nu)} [(1 - \nu)\epsilon_z + \nu(\epsilon_x + \epsilon_y)] \quad (6-49c)$$

Equations (6-48) and (6-49) represent Hooke's law for triaxial stress.

Unit volume change. The unit volume change for an element in triaxial stress is obtained in the same manner as for plane stress (see Section 6.5). If we begin with a cube of unit dimensions (see Fig. 6-21), we see that its initial volume is $V_0 = 1$ and its final volume is

$$V_f = (1 + \epsilon_x)(1 + \epsilon_y)(1 + \epsilon_z) \quad (a)$$

The **unit volume change** is defined as

$$e = \frac{\Delta V}{V_0} = \frac{V_f - V_0}{V_0} = \frac{V_f}{V_0} - 1 \quad (6-50)$$

which, upon substitution from Eq. (a), becomes

$$e = (1 + \epsilon_x)(1 + \epsilon_y)(1 + \epsilon_z) - 1 = \epsilon_x + \epsilon_y + \epsilon_z + \epsilon_x\epsilon_y + \epsilon_x\epsilon_z + \epsilon_y\epsilon_z + \epsilon_x\epsilon_y\epsilon_z \quad (6-51)$$

When the strains are small quantities, we may disregard the terms containing their products and obtain the following simplified expression for the unit volume change:

$$e = \epsilon_x + \epsilon_y + \epsilon_z \quad (6-52)$$

Substituting for the strains from Eqs. (6-48), we get

$$e = \frac{1 - 2\nu}{E} (\sigma_x + \sigma_y + \sigma_z) \quad (6-53)$$

as the expression for the unit volume change in the general case of triaxial stress. (The quantity e is also called the dilatation or the volumetric strain.)

Strain energy density. Let us assume for convenience that the triaxial stress element of Fig. 6-35 has unit dimensions. Then the forces acting on its faces are equal algebraically to the respective stresses. Each force moves through a distance equal to the corresponding strain as the stresses are applied to the element. The work done by these forces is the same as the strain energy density u of the element, inasmuch as the element has unit volume. Therefore, assuming that Hooke's law holds for the material, we obtain the following expression for the strain energy density:

$$u = \frac{1}{2} (\sigma_x \epsilon_x + \sigma_y \epsilon_y + \sigma_z \epsilon_z) \quad (6-54)$$

Substituting for the strains from Eqs. (6-48), we obtain the strain energy density in terms of stresses only:

$$u = \frac{1}{2E} (\sigma_x^2 + \sigma_y^2 + \sigma_z^2) - \frac{\nu}{E} (\sigma_x \sigma_y + \sigma_x \sigma_z + \sigma_y \sigma_z) \quad (6-55a)$$

In a similar manner, we can express the strain energy density in terms of the strains:

$$u = \frac{E}{2(1+\nu)(1-2\nu)} [(1-\nu)(\epsilon_x^2 + \epsilon_y^2 + \epsilon_z^2) + 2\nu(\epsilon_x \epsilon_y + \epsilon_x \epsilon_z + \epsilon_y \epsilon_z)] \quad (6-55b)$$

When calculating from these expressions, we must substitute the stresses and strains with their proper algebraic signs.

Spherical stress. A special state of triaxial stress, called spherical stress, exists when all three normal stresses are equal (see Fig. 6-37):

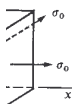
$$\sigma_x = \sigma_y = \sigma_z = \sigma_0 \quad (6-56)$$

Under these stress conditions, any plane cut through the element is subjected to the same normal stress σ_0 . Thus, we have equal normal stresses in every direction and no shear stresses. Every plane is a principal plane, and the three Mohr's circles shown in Fig. 6-36 reduce to a single point.

The normal strains ϵ_0 in spherical stress are also the same in all directions:

$$\epsilon_0 = \frac{\sigma_0}{E} (1-2\nu) \quad (6-57)$$

as obtained from Eqs. (6-48). Since there are no shear strains, a cube changes in size but remains a cube. In general, any body subjected to



stress

spherical stress will maintain its relative proportions but will either expand or contract in volume depending upon whether σ_0 is tension or compression.

The expression for the unit volume change can be obtained from Eq. (6-53) by substituting σ_0 for the stresses; the result is

$$e = \frac{\Delta V}{V_0} = \frac{3(1-2\nu)\sigma_0}{E} \quad (6-58a)$$

$$e = 3\epsilon_0 \quad (6-58b)$$

Equation (6-58a) is usually simplified by introducing a new quantity K called the volume modulus of elasticity or bulk modulus of elasticity:

$$K = \frac{E}{3(1-2\nu)} \quad (6-59)$$

With this notation, the expression for the volumetric strain becomes

$$e = \frac{\sigma_0}{K} \quad (6-60)$$

and, therefore,

$$K = \frac{\sigma_0}{e} \quad (6-61)$$

Thus, the volume modulus K can be defined as the ratio of the spherical stress to the volumetric strain, which is analogous to the definition of the modulus E . Note that the preceding formulas for e and K are based upon the assumption that the strains are small.

From Eq. (6-61) for K , we see that, if Poisson's ratio equals 1/3, the moduli K and E are equal. If $\nu = 0$, then K has the value $E/3$. When $\nu = 0.5$, K becomes infinite, which corresponds to a rigid material having no change in volume. Thus, the theoretical maximum value of Poisson's ratio is 0.5.

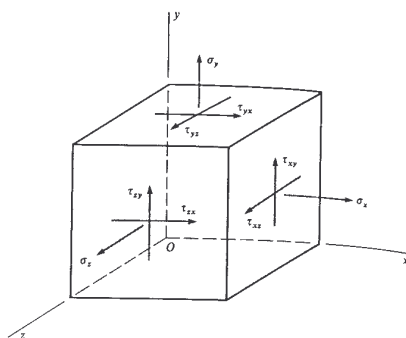
If the spherical stress σ_0 is a pressure p , as in the case of an object submerged in a fluid, or rock deep within the earth, the stress state is known as hydrostatic stress.

*6.10 THREE-DIMENSIONAL STRESS

In the most general case of three-dimensional stress, a stress element will be subjected to normal and shear stresses on all faces (see Fig. 6-38). As described in Section 6.2 for plane stress, the shear stresses have two subscripts, the first denoting the plane on which the stress acts and the second identifying the direction in that plane. All stresses are shown acting in their positive directions in Fig. 6-38.

From equilibrium of the element, it can be proven that shear stresses acting on perpendicular planes and directed perpendicular to the

is subjected to three-dimensional stress. (Only stresses acting on the faces are shown. All stresses act on the



three-dimensional stress element of Fig. 6-38 is as follows. After establishing the normal and shear stresses acting on the faces of the element, calculate the stress invariants A , B , and C . Then solve the cubic equation for its three roots; these roots are the principal stresses σ_1 , σ_2 , and σ_3 . The simplest procedure for solving the cubic equation is to use a computer program for obtaining roots of polynomials; another method is to use trial and error. Formal mathematical solutions, as given in mathematics handbooks, can also be used.

After finding the principal stresses, it is relatively easy to obtain the maximum shear stresses. Because no shear stresses act on the principal planes, it follows that an element rotated to the principal directions is in a state of triaxial stress. Therefore, the three maximum shear stresses (see Eqs. 6-47) are

$$\begin{aligned} (\tau_{\max})_3 &= \pm \frac{\sigma_1 - \sigma_2}{2} & (\tau_{\max})_2 &= \pm \frac{\sigma_1 - \sigma_3}{2} \\ (\tau_{\max})_1 &= \pm \frac{\sigma_2 - \sigma_3}{2} \end{aligned} \quad (6-64)$$

The absolute maximum shear stress is the numerically largest of the stresses determined from these three equations.

Hooke's law for three-dimensional stress consists of the triaxial equations relating normal stresses and strains (Eqs. 6-48 and 6-49) and the equations relating shear stresses and strains. The latter have the same form as Eqs. (6-27) and (6-29) for plane stress, but now there are three sets of shear equations instead of one. Thus, the equations for three-dimensional stress, giving the strains in terms of the stresses, are as follows:

$$\left. \begin{aligned} \epsilon_x &= \frac{\sigma_x}{E} - \frac{\nu}{E} (\sigma_y + \sigma_z) \\ \epsilon_y &= \frac{\sigma_y}{E} - \frac{\nu}{E} (\sigma_x + \sigma_z) \\ \epsilon_z &= \frac{\sigma_z}{E} - \frac{\nu}{E} (\sigma_x + \sigma_y) \\ \gamma_{xy} &= \frac{\tau_{xy}}{G} & \gamma_{xz} &= \frac{\tau_{xz}}{G} & \gamma_{yz} &= \frac{\tau_{yz}}{G} \end{aligned} \right\} \quad (6-65)$$

The inverse equations, giving the stresses in terms of the strains, are

$$\left. \begin{aligned} \sigma_x &= \frac{E}{(1+\nu)(1-2\nu)} [(1-\nu)\epsilon_x + \nu(\epsilon_y + \epsilon_z)] \\ \sigma_y &= \frac{E}{(1+\nu)(1-2\nu)} [(1-\nu)\epsilon_y + \nu(\epsilon_x + \epsilon_z)] \\ \sigma_z &= \frac{E}{(1+\nu)(1-2\nu)} [(1-\nu)\epsilon_z + \nu(\epsilon_x + \epsilon_y)] \\ \tau_{xy} &= G\gamma_{xy} & \tau_{xz} &= G\gamma_{xz} & \tau_{yz} &= G\gamma_{yz} \end{aligned} \right\} \quad (6-66)$$

line of intersection of the planes are equal in magnitude. Therefore, the following relationships hold:

$$\tau_{xy} = \tau_{yx} \quad \tau_{xz} = \tau_{zx} \quad \tau_{yz} = \tau_{zy} \quad (6-62)$$

This concept of equality of shear stresses has been discussed previously, and the first of Eqs. (6-62) was used in our discussion of plane stress (see Eq. 6-1).

Inclined planes cut through the element are subjected to normal and shear stresses, analogous to the stresses σ_{x_1} and $\tau_{x_1y_1}$ acting on inclined planes in plane stress (see Fig. 6-1). However, in the three-dimensional case, the normal to the inclined plane is not necessarily parallel to one of the coordinate planes; that is, it may be skew to all three axes. Nevertheless, the normal and shear stresses acting on any inclined plane can be determined by static equilibrium. The formulas for these stresses are rather long and complicated; hence, they are not given here. Instead, the reader is referred to textbooks on theory of elasticity (such as Ref. 2-1).

Of particular importance are the three principal stresses, which are obtained as the three real roots of the following cubic equation:

$$\sigma^3 - A\sigma^2 + B\sigma - C = 0 \quad (6-63)$$

in which

$$\begin{aligned} A &= \sigma_x + \sigma_y + \sigma_z \\ B &= \sigma_x \sigma_y + \sigma_x \sigma_z + \sigma_y \sigma_z - \tau_{xy}^2 - \tau_{xz}^2 - \tau_{yz}^2 \\ C &= \sigma_x \sigma_y \sigma_z + 2\tau_{xy} \tau_{xz} \tau_{yz} - \sigma_x \tau_{yz}^2 - \sigma_y \tau_{xz}^2 - \sigma_z \tau_{xy}^2 \end{aligned}$$

The quantities A , B , and C are known as stress invariants, because they do not change in value when the axes are rotated to new positions.

The procedure for evaluating the principal stresses for the three-

Equations (6-65) and (6-66) are often referred to as the **generalized Hooke's law**. Since the shear strains produce no change in volume, the expression for the unit volume change e is the same as for triaxial stress:

$$e = \frac{\Delta V}{V_0} = (1 + \epsilon_x)(1 + \epsilon_y)(1 + \epsilon_z) - 1 \quad (6-67a)$$

or, for small strains,

$$e = \epsilon_x + \epsilon_y + \epsilon_z \quad (6-67b)$$

Finally, the expression for strain energy density (see Eqs. 6-32 and 6-34) is

$$u = \frac{1}{2}(\sigma_x \epsilon_x + \sigma_y \epsilon_y + \sigma_z \epsilon_z + \tau_{xy} \gamma_{xy} + \tau_{xz} \gamma_{xz} + \tau_{yz} \gamma_{yz}) \quad (6-68)$$

By substituting from Hooke's law, we can express u in terms of stresses or strains only; thus, in terms of stresses,

$$u = \frac{1}{2E}(\sigma_x^2 + \sigma_y^2 + \sigma_z^2) - \frac{\nu}{E}(\sigma_x \sigma_y + \sigma_x \sigma_z + \sigma_y \sigma_z) + \frac{1}{2G}(\tau_{xy}^2 + \tau_{xz}^2 + \tau_{yz}^2) \quad (6-69a)$$

and, in terms of strains,

$$u = \frac{E}{2(1+\nu)(1-2\nu)} [(1-\nu)(\epsilon_x^2 + \epsilon_y^2 + \epsilon_z^2) + 2\nu(\epsilon_x \epsilon_y + \epsilon_x \epsilon_z + \epsilon_y \epsilon_z)] + \frac{G}{2}(\gamma_{xy}^2 + \gamma_{xz}^2 + \gamma_{yz}^2) \quad (6-69b)$$

The equations of three-dimensional stress are not usually needed in the study of mechanics of materials; nevertheless, we have given them in this section for reference.

6.11 PLANE STRAIN

The normal and shear strains at a point in a body vary with direction, in a manner analogous to that for stresses. In this section, we will derive the equations that give the strains in inclined directions in terms of the strains in the coordinate directions. These relationships are especially important in experimental investigations, where strains are measured with strain gages. The gages are oriented in specific directions and it is usually necessary to calculate the strains in other directions.

Recall that in the xy plane three strain components may exist, as shown in the three parts of Fig. 6-39. These strains are the normal strain ϵ_x in the x direction, the normal strain ϵ_y in the y direction, and the shear strain γ_{xy} . An element of material subjected only to these strains is said to be in a state of **plane strain**. It follows that an element in plane

strain has no normal strain ϵ_z and no shear strains γ_{xz} and γ_{yz} in the xz and yz planes, respectively. Thus, plane strain is defined by the following conditions:

$$\epsilon_z = 0 \quad \gamma_{xz} = 0 \quad \gamma_{yz} = 0 \quad (6-70)$$

The remaining strains (ϵ_x , ϵ_y , and γ_{xy}) may have nonzero values. The preceding definition of plane strain is analogous to that for plane stress. In plane stress, the following stresses must be zero:

$$\sigma_z = 0 \quad \tau_{xz} = 0 \quad \tau_{yz} = 0 \quad (6-71)$$

whereas the remaining stresses (σ_x , σ_y , and τ_{xy}) may have nonzero values.

A comparison of plane stress and plane strain is given in Fig. 6-40. It should not be inferred from the similarities in the definitions of plane stress and plane strain that both occur simultaneously. In general, plane stress and plane strain undergo a strain in the z direction (see Fig. 6-40); hence, it clearly is not in plane strain. Also, most elements subjected to plane strain will have stresses σ_z acting on them because of the requirement that $\epsilon_z = 0$; again, we see that plane strain and plane stress do not occur simultaneously. An exception is when an element in plane stress is subjected to equal and opposite normal stresses (that is, when $\sigma_x = -\sigma_y$). In this special case, there is no normal strain in the

	Plane stress	Plane strain
Stresses	$\sigma_z = 0$ $\tau_{xz} = 0$ $\tau_{yz} = 0$ $\sigma_x, \sigma_y,$ and τ_{xy} may have nonzero values	$\tau_{xz} = 0$ $\tau_{yz} = 0$ $\sigma_x, \sigma_y, \sigma_z,$ and τ_{xy} may have nonzero values
Strains	$\gamma_{xz} = 0$ $\gamma_{yz} = 0$ $\epsilon_x, \epsilon_y, \epsilon_z,$ and γ_{xy} may have nonzero values	$\epsilon_z = 0$ $\gamma_{xz} = 0$ $\gamma_{yz} = 0$ $\epsilon_x, \epsilon_y,$ and γ_{xy} may have nonzero values

Fig. 6-40 Comparison of plane stress and plane strain

z direction ($\epsilon_z = 0$; see Eq. 6-26c); hence, the element is in a state of plane strain as well as plane stress. Another special case, albeit a hypothetical one, is when a material has $\nu = 0$; then every plane stress element is also in plane strain because $\epsilon_z = 0$ (see Eq. 6-26c).

The stress transformation equations derived for plane stress in the xy plane (see Eqs. 6-4) may also be used if a normal stress σ_z is present. The reason is that the stress σ_z does not enter the equations of equilibrium used in determining the stresses σ_{x_1} and $\tau_{x_1 y_1}$, acting on inclined planes. An analogous situation exists for plane strain. We will derive the strain transformation equations for the case of plane strain, but the equations actually are valid even when a strain ϵ_z exists. Therefore, the transformation equations for plane stress can be used for the stresses in the xy plane that occur in the case of plane strain, and the transformation equations for plane strain can be used for the strains in the xy plane that occur in the case of plane stress.

In the derivation of the transformation equations for plane strain, we will use the coordinate axes shown in Fig. 6-41. We will assume that the normal strains ϵ_x and ϵ_y and the shear strain γ_{xy} associated with the xy axes are known (see Fig. 6-39). The objective of the analysis is to determine the normal strain ϵ_{x_1} and shear strain $\gamma_{x_1 y_1}$ associated with the $x_1 y_1$ axes, which are rotated counterclockwise through an angle θ from the xy axes. (We need not derive a separate equation for the normal strain ϵ_{y_1} , because it can be obtained from the equation for ϵ_{x_1} by substituting $\theta + 90^\circ$ for θ .)

The positive z face of a plane strain element having rectangular faces is shown in Fig. 6-42. The diagonal of the rectangle is in the direction of the x_1 axis, and the sides have lengths dx and dy . The strains ϵ_x , ϵ_y , and γ_{xy} in the xy plane produce an elongation of the element in the x direction equal to $\epsilon_x dx$ (Fig. 6-42a), an elongation in the y direction equal to $\epsilon_y dy$ (Fig. 6-42b), and a decrease in the angle between the x and y faces equal to γ_{xy} (Fig. 6-42c). These deformations cause the diagonal to increase in length by amounts equal to $\epsilon_x dx \cos \theta$, $\epsilon_y dy \sin \theta$, and $\gamma_{xy} dy \cos \theta$, respectively. The total increase Δd in the length of the diagonal is the sum of these three expressions:

$$\Delta d = \epsilon_x dx \cos \theta + \epsilon_y dy \sin \theta + \gamma_{xy} dy \cos \theta$$

The normal strain ϵ_{x_1} in the x_1 direction is equal to this increase in length divided by the initial length ds of the diagonal:

$$\epsilon_{x_1} = \frac{\Delta d}{ds} = \epsilon_x \frac{dx}{ds} \cos \theta + \epsilon_y \frac{dy}{ds} \sin \theta + \gamma_{xy} \frac{dy}{ds} \cos \theta$$

Observing that $dx/ds = \cos \theta$ and $dy/ds = \sin \theta$, we obtain the following equation for the normal strain:

$$\epsilon_{x_1} = \epsilon_x \cos^2 \theta + \epsilon_y \sin^2 \theta + \gamma_{xy} \sin \theta \cos \theta \quad (6-72a)$$

* In this discussion, we are not considering the effects of temperature changes and prestrains, both of which produce additional strains that would alter some of our comments.

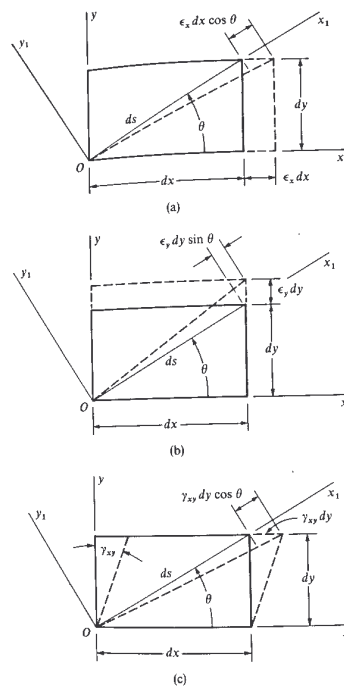


Fig. 6-42 Deformations of an element in plane strain due to: (a) normal strain ϵ_x , (b) normal strain ϵ_y , and (c) shear strain γ_{xy}

As mentioned previously, the normal strain ϵ_{y_1} in the y_1 direction is obtained from this equation by substituting $\theta + 90^\circ$ for θ .

Next, consider the shear strain $\gamma_{x_1 y_1}$ associated with the rotated axes. This strain is equal to the decrease in angle between lines in the material that were initially along the lines of the x_1 and y_1 axes. To clarify this idea, let line Oa in Fig. 6-43 represent a line in the material that initially was along the x_1 axis (that is, along the diagonal of the element). The deformations pictured in Fig. 6-42 cause this line to rotate

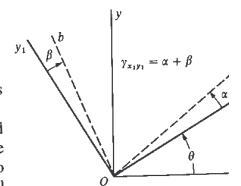


Fig. 6-43 Shear strain $\gamma_{x_1 y_1}$ associated with $x_1 y_1$ axes

through a counterclockwise angle α from the x_1 axis (Fig. 6-43). Similarly, line Ob was originally along the y_1 axis, but because of the deformation it rotates through a clockwise angle β . The shear strain $\gamma_{x_1y_1}$ is the total decrease in the angle between the two lines that originally were at right angles; thus,

$$\gamma_{x_1y_1} = \alpha + \beta$$

The angle α can be found from Fig. 6-42 as follows. The strain ϵ_x (Fig. 6-42a) produces a clockwise rotation of line Oa equal to the distance $\epsilon_x ds \sin \theta$ divided by ds . Therefore, the contribution of ϵ_x to the angle α is $-\epsilon_x ds \sin \theta$. Similarly, the strain ϵ_y produces a counterclockwise rotation of line Oa equal to $\epsilon_y ds \cos \theta$ divided by ds , and the strain γ_{xy} produces a clockwise rotation equal to $\gamma_{xy} dy \sin \theta$ divided by ds . Thus, the resultant counterclockwise rotation of line Oa is

$$\alpha = -\epsilon_x \frac{dx}{ds} \sin \theta + \epsilon_y \frac{dy}{ds} \cos \theta - \gamma_{xy} \frac{dy}{ds} \sin \theta$$

or

$$\alpha = -\epsilon_x \sin \theta \cos \theta + \epsilon_y \sin \theta \cos \theta - \gamma_{xy} \sin^2 \theta = -(\epsilon_x - \epsilon_y) \sin \theta \cos \theta - \gamma_{xy} \sin^2 \theta$$

The rotation of line Ob , which initially was at 90° to line Oa , can be found by substituting $\theta + 90^\circ$ for θ in the expression for α . The resulting expression is counterclockwise when positive, hence it is equal to the negative of the angle β , since β is a clockwise rotation. Thus, we get

$$\beta = (\epsilon_x - \epsilon_y) \sin(\theta + 90^\circ) \cos(\theta + 90^\circ) + \gamma_{xy} \sin^2(\theta + 90^\circ) = -(\epsilon_x - \epsilon_y) \sin \theta \cos \theta + \gamma_{xy} \cos^2 \theta$$

Adding α and β gives the shear strain $\gamma_{x_1y_1}$:

$$\gamma_{x_1y_1} = -2(\epsilon_x - \epsilon_y) \sin \theta \cos \theta + \gamma_{xy}(\cos^2 \theta - \sin^2 \theta)$$

To put the equation in a more useful form, we divide each term by 2 and write the equation as follows:

$$\frac{\gamma_{x_1y_1}}{2} = -(\epsilon_x - \epsilon_y) \sin \theta \cos \theta + \frac{\gamma_{xy}}{2}(\cos^2 \theta - \sin^2 \theta) \quad (6-72b)$$

Equations (6-72) give the normal and shear strains with respect to rotated axes in terms of the strains oriented to the x and y axes. These equations are similar in form to Eqs. (6-3) for plane stress, with ϵ_{x_1} corresponding to σ_{x_1} , $\gamma_{x_1y_1}/2$ corresponding to $\tau_{x_1y_1}$, ϵ_x corresponding to σ_x , ϵ_y corresponding to σ_y , and $\gamma_{xy}/2$ corresponding to τ_{xy} .

The equations for plane strain can be expressed in terms of the angle 2θ by substituting the following trigonometric identities:

$$\cos^2 \theta = \frac{1}{2}(1 + \cos 2\theta) \quad \sin^2 \theta = \frac{1}{2}(1 - \cos 2\theta)$$

$$\sin \theta \cos \theta = \frac{1}{2} \sin 2\theta$$

The transformation equations for plane strain now become

$$\epsilon_{x_1} = \frac{\epsilon_x + \epsilon_y}{2} + \frac{\epsilon_x - \epsilon_y}{2} \cos 2\theta + \frac{\gamma_{xy}}{2} \sin 2\theta \quad (6-73a)$$

$$\frac{\gamma_{x_1y_1}}{2} = -\frac{\epsilon_x - \epsilon_y}{2} \sin 2\theta + \frac{\gamma_{xy}}{2} \cos 2\theta \quad (6-73b)$$

These equations are the counterparts of Eqs. (6-4) for plane stress. The corresponding variables in the two sets of equations are listed in Table 6-1.

The analogy between the transformation equations for plane stress and plane strain shows that all of the observations made in Sections 6.2, 6.3, and 6.4 concerning plane stress have their counterparts in plane strain. For instance, the sum of the normal strains in perpendicular directions is a constant:

$$\epsilon_{x_1} + \epsilon_{y_1} = \epsilon_x + \epsilon_y \quad (6-74)$$

This equality can be verified easily by substituting the expressions for ϵ_{x_1} (Eq. 6-73a) and ϵ_{y_1} (obtained from Eq. 6-73a with θ replaced by $\theta + 90^\circ$) into Eq. (6-74).

Principal strains exist in perpendicular directions calculated from the following equation (compare with Eq. 6-9):

$$\tan 2\theta_p = \frac{\gamma_{xy}}{\epsilon_x - \epsilon_y} \quad (6-75)$$

The principal strains can be calculated from the equation

$$\epsilon_{1,2} = \frac{\epsilon_x + \epsilon_y}{2} \pm \sqrt{\left(\frac{\epsilon_x - \epsilon_y}{2}\right)^2 + \left(\frac{\gamma_{xy}}{2}\right)^2} \quad (6-76)$$

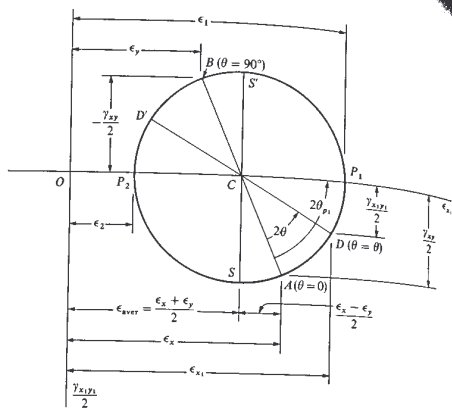
which corresponds to Eq. (6-13) for the principal stresses. In the directions of the principal strains, the shear strains are zero. The two principal strains can be correlated with the two principal directions by the techniques described in Section 6.3 for stresses. (Note that the third principal strain is $\epsilon_z = 0$.)

The maximum shear strains in the xy plane are associated with axes at 45° to the directions of the principal strains. The algebraically maximum shear strain (in the xy plane) is given by the following equation:

$$\frac{\gamma_{\max}}{2} = \sqrt{\left(\frac{\epsilon_x - \epsilon_y}{2}\right)^2 + \left(\frac{\gamma_{xy}}{2}\right)^2} \quad (6-77)$$

Stresses	Strains
σ_x	ϵ_x
σ_y	ϵ_y
τ_{xy}	$\gamma_{xy}/2$
σ_{x_1}	ϵ_{x_1}
$\tau_{x_1y_1}$	$\gamma_{x_1y_1}/2$

Table 6-1 Corresponding variables in the transformation equations for plane stress (Eqs. 6-3 and 6-4) and plane strain (Eqs. 6-72 and 6-73)



or plane

The minimum shear strain has the same magnitude but is negative. In the directions of maximum shear strain, the normal strains are equal to $(\epsilon_x + \epsilon_y)/2$.

An element in plane stress that is oriented to the principal directions (see Fig. 6-12b) has no shear stresses acting on its faces. Therefore, the shear strain $\gamma_{x_1y_1}$ for this element also is zero. It follows that the normal strains in this element are the principal strains. Thus, the principal planes are the same for both plane stress and plane strain.

Mohr's circle for plane strain is constructed in the same general manner as for plane stress, as illustrated in Fig. 6-44. Normal strains ϵ_{x_1} are plotted as the abscissas, and half the shear strains ($\gamma_{x_1y_1}/2$) are plotted downward as the ordinates. The center C of the circle has an abscissa equal to $(\epsilon_x + \epsilon_y)/2$. Point A , representing the strains associated with the x direction ($\theta = 0$), has coordinates ϵ_x and $\gamma_{xy}/2$. Point B , at the opposite end of a diameter from A , has coordinates ϵ_y and $-\gamma_{xy}/2$, representing the strains associated with a pair of axes rotated through an angle $\theta = 90^\circ$. The strains associated with axes at an angle θ are given by point D , which is located by measuring an angle 2θ from radius CA . The principal strains are represented by points P_1 and P_2 and the maximum shear strains by points S and S' . All of these strains can be determined directly from the circle or from the equations given previously.

An important use of the transformation equations for strain and Mohr's circle is the interpretation of strain-gage measurements, which are discussed further in Example 2. However, references on experimental stress analysis should be consulted for detailed information about experimental techniques (see, for example, Refs. 6-11 and 6-12).

Example 1

An element of material subjected to plane strain has strains as follows: $\epsilon_x = 340 \times 10^{-6}$, $\epsilon_y = 110 \times 10^{-6}$, and $\gamma_{xy} = 180 \times 10^{-6}$. These strains are shown highly exaggerated in Fig. 6-45a, which portrays an element of unit dimensions aligned with the x and y axes. Since the edges of the element have unit lengths, the changes in dimensions are equal to the normal strains. For convenience, the shear strain is shown as the change in angle at the corner of the element located at the origin.

Calculate the following quantities: (a) the strains for an element rotated through an angle $\theta = 30^\circ$, (b) the principal strains, and (c) the maximum shear strains. (Consider only the in-plane strains.)

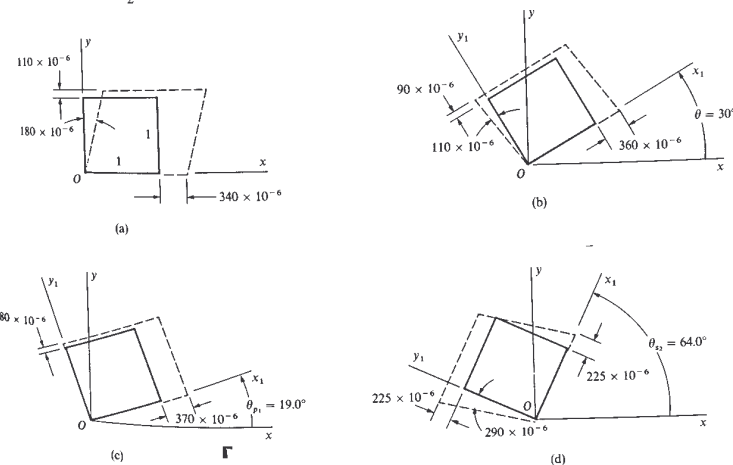
(a) The strains for an element rotated through an angle of 30° are found from the transformation equations (Eqs. 6-73). However, before substituting into those equations, we make the following preliminary calculations:

$$\frac{\epsilon_x + \epsilon_y}{2} = \frac{(340 + 110)10^{-6}}{2} = 225 \times 10^{-6}$$

$$\frac{\epsilon_x - \epsilon_y}{2} = \frac{(340 - 110)10^{-6}}{2} = 115 \times 10^{-6}$$

$$\frac{\gamma_{xy}}{2} = 90 \times 10^{-6}$$

Fig. 6-45 Example 1. (a) Element in plane strain, (b) element at $\theta = 30^\circ$, (c) principal strains, and (d) maximum shear strains. (Note: The edges of the elements have unit lengths.)



Now we substitute into Eqs. (6-73) and get

$$\begin{aligned} \epsilon_{x_1} &= \frac{\epsilon_x + \epsilon_y}{2} + \frac{\epsilon_x - \epsilon_y}{2} \cos 2\theta + \frac{\gamma_{xy}}{2} \sin 2\theta \\ &= (225 \times 10^{-6}) + (115 \times 10^{-6})(\cos 60^\circ) + (90 \times 10^{-6})(\sin 60^\circ) \\ &= 360 \times 10^{-6} \end{aligned}$$

$$\begin{aligned} \frac{\gamma_{x_1y_1}}{2} &= -\frac{\epsilon_x - \epsilon_y}{2} \sin 2\theta + \frac{\gamma_{xy}}{2} \cos 2\theta \\ &= -(115 \times 10^{-6})(\sin 60^\circ) + (90 \times 10^{-6})(\cos 60^\circ) \\ &= -55 \times 10^{-6} \end{aligned}$$

or

$$\gamma_{x_1y_1} = -110 \times 10^{-6}$$

The strain ϵ_{y_1} can be obtained from Eq. (6-74):

$$\epsilon_{x_1} + \epsilon_{y_1} = \epsilon_x + \epsilon_y$$

Thus,

$$\begin{aligned} \epsilon_{y_1} &= \epsilon_x + \epsilon_y - \epsilon_{x_1} \\ &= (340 + 110 - 360)10^{-6} = 90 \times 10^{-6} \end{aligned}$$

These strains are shown in Fig. 6-45b for an element at $\theta = 30^\circ$. Note that the angle at the corner of the element at the origin increases because $\gamma_{x_1y_1}$ is negative.

(b) The principal strains are calculated from Eq. (6-76), as follows:

$$\begin{aligned} \epsilon_{1,2} &= \frac{\epsilon_x + \epsilon_y}{2} \pm \sqrt{\left(\frac{\epsilon_x - \epsilon_y}{2}\right)^2 + \left(\frac{\gamma_{xy}}{2}\right)^2} \\ &= 225 \times 10^{-6} \pm \sqrt{(115 \times 10^{-6})^2 + (90 \times 10^{-6})^2} \\ &= 225 \times 10^{-6} \pm 146 \times 10^{-6} \end{aligned}$$

Therefore,

$$\epsilon_1 = 370 \times 10^{-6} \quad \epsilon_2 = 80 \times 10^{-6}$$

The angles to the principal directions can be obtained from Eq. (6-75):

$$\tan 2\theta_p = \frac{\gamma_{xy}}{\epsilon_x - \epsilon_y} = \frac{180}{340 - 110} = 0.783$$

Hence, the two values of $2\theta_p$ between 0 and 360° are 38.0° and 218° , and the angles to the principal directions are

$$\theta_p = 19.0^\circ \text{ and } 109.0^\circ$$

To determine which value of θ_p is associated with each principal strain, we substitute θ_p into Eq. (6-73a) and solve for the strain. Thus, using $\theta_p = 19.0^\circ$, we get

$$\begin{aligned} \epsilon_{x_1} &= \frac{\epsilon_x + \epsilon_y}{2} + \frac{\epsilon_x - \epsilon_y}{2} \cos 2\theta + \frac{\gamma_{xy}}{2} \sin 2\theta \\ &= (225 \times 10^{-6}) + (115 \times 10^{-6})(\cos 38.0^\circ) + (90 \times 10^{-6})(\sin 38.0^\circ) \\ &= 370 \times 10^{-6} \end{aligned}$$

This result shows that the larger principal strain ϵ_1 is at the angle $\theta_{p1} = 19.0^\circ$. Then the smaller strain ϵ_2 is 90° from that direction ($\theta_{p2} = 109.0^\circ$). The principal strains are portrayed in Fig. 6-45c.

(c) The maximum shear strain is calculated from Eq. (6-77):

$$\frac{\gamma_{\max}}{2} = \sqrt{\left(\frac{\epsilon_x - \epsilon_y}{2}\right)^2 + \left(\frac{\gamma_{xy}}{2}\right)^2} = 146 \times 10^{-6}$$

$$\gamma_{\max} = 290 \times 10^{-6}$$

to two significant digits. The orientation of the element for maximum shear strains is at 45° to the principal directions; therefore, $\theta_s = 19.0^\circ + 45^\circ = 64.0^\circ$ and $2\theta_s = 128.0^\circ$. By substituting into Eq. (6-73b) we can determine the sign of the shear strain associated with this direction. The calculations are as follows:

$$\begin{aligned} \frac{\gamma_{x_1y_1}}{2} &= -\frac{\epsilon_x - \epsilon_y}{2} \sin 2\theta + \frac{\gamma_{xy}}{2} \cos 2\theta \\ &= -(115 \times 10^{-6})(\sin 128.0^\circ) + (90 \times 10^{-6})(\cos 128.0^\circ) \\ &= -146 \times 10^{-6} \end{aligned}$$

This result shows that an element rotated through an angle $\theta_{s2} = 64.0^\circ$ has the maximum negative shear strain.

We can arrive at the same result by observing that the angle θ_{s1} to the direction of maximum positive shear strain is always 45° less than θ_{p1} . Hence,

$$\theta_{s1} = \theta_{p1} - 45^\circ = 19.0^\circ - 45^\circ = -26.0^\circ$$

and

$$\theta_{s2} = \theta_{s1} + 90^\circ = 64.0^\circ$$

The corresponding shear strains are $\gamma_{\max} = 290 \times 10^{-6}$ and $\gamma_{\min} = -290 \times 10^{-6}$, respectively.

The normal strains on an element having the maximum and minimum shear strains are

$$\epsilon_{\text{aver}} = \frac{\epsilon_x + \epsilon_y}{2} = 225 \times 10^{-6}$$

A sketch of this element is given in Fig. 6-45d. Note that $\gamma_{\max}/2$ is equal to one-half the difference of the principal strains.

In this example, we chose to solve for the strains by using the transformation equations. However, all of the results can be obtained just as easily from Mohr's circle.

Example 2

An electrical-resistance strain gage is a small device that is glued to the surface of an object. The gage contains wires that are stretched or shortened when the object is strained at that point. The electrical resistance of the wires is altered when the wires change in length. This change in resistance is measured and converted into a strain measurement. The gages are extremely sensitive and can

measure strains as small as 1×10^{-6} . Since each gage measures the normal strain in only one direction, it is often necessary to use three gages in combination with each gage measuring the strain in a different direction. From three such measurements, it is possible to calculate the strains in any direction on the surface. A group of three gages arranged in a particular pattern is called a strain rosette. Because the rosette is mounted on the surface of the body, where the strain material is in plane stress, we can use the transformation equations for plane strain to calculate the strains in various directions on the surface.

A 45° strain rosette consists of three electrical-resistance strain gages arranged as shown in Fig. 6-46. Gages A, B, and C measure the normal strains ϵ_a , ϵ_b , and ϵ_c in the directions of lines Oa , Ob , and Oc , respectively. Show how to obtain the strains ϵ_x , ϵ_y , and γ_{xy} associated with the xy axes.

Because gages A and C are aligned with the x and y axes, they give the strains ϵ_x and ϵ_y directly:

$$\epsilon_x = \epsilon_a \quad \epsilon_y = \epsilon_c$$

To obtain the shear strain γ_{xy} , we may use the transformation Eq. (6-73a) for the strain ϵ_{x_1} :

$$\epsilon_{x_1} = \frac{\epsilon_x + \epsilon_y}{2} + \frac{\epsilon_x - \epsilon_y}{2} \cos 2\theta + \frac{\gamma_{xy}}{2} \sin 2\theta$$

For the angle $\theta = 45^\circ$, we see that $\epsilon_{x_1} = \epsilon_b$; therefore, the preceding equation gives

$$\epsilon_b = \frac{\epsilon_a + \epsilon_c}{2} + \frac{\epsilon_a - \epsilon_c}{2} (\cos 90^\circ) + \frac{\gamma_{xy}}{2} (\sin 90^\circ)$$

Solving for γ_{xy} , we get

$$\gamma_{xy} = 2\epsilon_b - \epsilon_a - \epsilon_c$$

Thus, the strains ϵ_x , ϵ_y , and γ_{xy} are easily determined from the strain-gage readings. Knowing these strains, we can calculate the strains in any other directions by means of Mohr's circle or the transformation equations, as illustrated in the preceding example. Also, we can calculate the principal strains and maximum shear strains in the material.

Example 3

Derive the transformation equations for plane strain by using the transformation equations for plane stress and Hooke's law.

Let us begin with the plane stress element shown in Fig. 6-47a. Acting on this element are stresses σ_x , σ_y , and τ_{xy} . When the element is rotated through an angle θ , the stresses acting on the element become σ_{x_1} , σ_{y_1} , and $\tau_{x_1y_1}$ (Fig. 6-47b). The transformation equations for σ_{x_1} and $\tau_{x_1y_1}$ (see Eqs. 6-4) are as follows:

$$\sigma_{x_1} = \frac{\sigma_x + \sigma_y}{2} + \frac{\sigma_x - \sigma_y}{2} \cos 2\theta + \tau_{xy} \sin 2\theta$$

$$\tau_{x_1y_1} = -\frac{\sigma_x - \sigma_y}{2} \sin 2\theta + \tau_{xy} \cos 2\theta$$

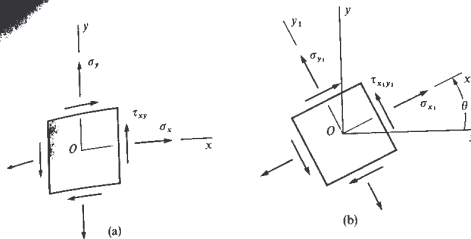


Fig. 6-47 Example 3

and the equation for σ_{y_1} (see Eq. 6-5) is

$$\sigma_{y_1} = \frac{\sigma_x + \sigma_y}{2} - \frac{\sigma_x - \sigma_y}{2} \cos 2\theta - \tau_{xy} \sin 2\theta$$

The strains ϵ_{x_1} and $\gamma_{x_1y_1}$ for the rotated element (Fig. 6-47b) can be expressed in terms of these stresses by using Hooke's law:

$$\epsilon_{x_1} = \frac{\sigma_{x_1}}{E} - \frac{\nu\sigma_{y_1}}{E} \quad \gamma_{x_1y_1} = \frac{\tau_{x_1y_1}}{G}$$

or, upon substituting for σ_{x_1} , σ_{y_1} , and $\tau_{x_1y_1}$:

$$\begin{aligned} \epsilon_{x_1} &= \frac{1}{E} \left(\frac{\sigma_x + \sigma_y}{2} + \frac{\sigma_x - \sigma_y}{2} \cos 2\theta + \tau_{xy} \sin 2\theta \right) \\ &\quad - \frac{\nu}{E} \left(\frac{\sigma_x + \sigma_y}{2} - \frac{\sigma_x - \sigma_y}{2} \cos 2\theta - \tau_{xy} \sin 2\theta \right) \\ \gamma_{x_1y_1} &= \frac{1}{G} \left(-\frac{\sigma_x - \sigma_y}{2} \sin 2\theta + \tau_{xy} \cos 2\theta \right) \end{aligned}$$

Finally, we again use Hooke's law (see Eqs. 6-28 and 6-29) and substitute into the last two equations the expressions for σ_x , σ_y , and τ_{xy} in terms of the strains ϵ_x , ϵ_y , and γ_{xy} . The results of this substitution are

$$\epsilon_{x_1} = \frac{\epsilon_x + \epsilon_y}{2} + \frac{\epsilon_x - \epsilon_y}{2} \cos 2\theta + \frac{\gamma_{xy}}{2} \sin 2\theta$$

$$\frac{\gamma_{x_1y_1}}{2} = -\frac{\epsilon_x - \epsilon_y}{2} \sin 2\theta + \frac{\gamma_{xy}}{2} \cos 2\theta$$

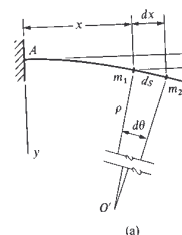
These equations are the transformation equations for plane strain (Eqs. 6-73).

This derivation shows that the strains for an element in plane stress transform in exactly the same manner as the stresses for an element in plane stress, provided that the strains are due to these same stresses (and not due to other causes, such as prestresses or temperature effects) and that Hooke's law holds.

Deflections of Beam

7.1 INTRODUCTION

When a beam is loaded, the initially straight longitudinal axis is deformed into a curve, called the **deflection curve** of the beam. In this chapter we describe methods for determining the equation of the deflection curve and for finding deflections at specific points along the axis of the beam. The calculation of deflections is essential to the analysis of statically indeterminate beams, as explained in the next chapter. In addition, deflections often must be calculated in order to verify that they do not exceed the maximum permissible values. This situation arises in building design, where there is usually an upper limit on deflections because large deflections are associated with poor appearance and with too much flexibility in the structure.



7.2 DIFFERENTIAL EQUATIONS OF THE DEFLECTION CURVE

To obtain the general equations for the deflection curve of a beam, let us consider the cantilever beam *AB* shown in Fig. 7-1a. We take the origin of coordinates at the fixed end, with the *x* axis directed to the right and the *y* axis directed downward. As in previous discussions, we assume that the *xy* plane is a plane of symmetry and that all loads act in this plane; thus, the *xy* plane is the plane of bending. The deflection *v* of the beam at any point *m*₁ at distance *x* from the origin (Fig. 7-1a) is the translation (or displacement) of that point in the *y* direction, measured from the *x* axis to the deflection curve. Thus, for the axes we have selected, a downward deflection is positive and an upward deflection is negative. When *v* is expressed as a function of *x*, we have the equation of the deflection curve.

The angle of rotation θ of the axis of the beam at any point *m*₁ is the angle between the *x* axis and the tangent to the deflection curve (Fig.

Fig. 7-1 Deflection curve.

7-1b). This angle is positive when clockwise, provided the *x* and *y* axes have the directions shown.

Now consider a second point *m*₂, located on the deflection curve at a small distance *ds* further along the curve and at distance *x + dx* (measured parallel to the *x* axis) from the origin. The deflection at this point is *v + dv*, where *dv* is the increment in deflection as we move from *m*₁ to *m*₂. Also, the angle of rotation at *m*₂ is $\theta + d\theta$, where *dθ* is the increment in angle of rotation. At points *m*₁ and *m*₂, we can construct lines normal to the tangents to the deflection curve. The intersection of these normals locates the **center of curvature** *O'*, and the distance from *O'* to the curve is the **radius of curvature** ρ . From the figure, we see that $\rho d\theta = ds$ hence, the **curvature** κ (equal to the reciprocal of the radius of curvature) is given by the following equation:

$$\kappa = \frac{1}{\rho} = \frac{d\theta}{ds} \quad (7-1)$$

The **sign convention** for curvature is pictured in Fig. 5-3. Note that positive curvature corresponds to a positive value of $d\theta/ds$, which means that the angle θ increases as we move along the beam in the positive *x* direction.

The **slope** of the deflection curve is the first derivative dv/dx , as we know from calculus. From Fig. 7-1b, we see that the slope is equal to the tangent of the angle of rotation θ , because *dx* is infinitesimally small; thus,

$$\frac{dv}{dx} = \tan \theta \quad \text{or} \quad \theta = \arctan \frac{dv}{dx}$$

Equations (7-1) and (7-2) are based upon geometric considerations; thus they apply to a beam of any material. Furthermore, there is no restriction on the magnitudes of the slopes and deflections.

Most beams undergo only very small rotations when they are loaded; hence, their deflection curves are very flat with extremely small curvatures. Under these conditions, the angle θ is a very small quantity; hence, we can make some approximations that simplify our work. From Fig. 7-1b we see that

$$ds = \frac{dx}{\cos \theta} \quad (a)$$

Since $\cos \theta \approx 1$ when θ is small, we obtain

$$ds \approx dx$$

Therefore, Eq. (7-1) becomes

$$\kappa = \frac{1}{\rho} = \frac{d\theta}{dx} \quad (7-3)$$

Also, since $\tan \theta \approx \theta$ when θ is a small quantity, we can approximate Eq. (7-2a) as follows:

$$\theta \approx \tan \theta = \frac{dv}{dx} \quad (b)$$

Thus, for small rotations of a beam, the angle of rotation and the slope are equal. (Note that the angle of rotation is measured in radians.) Taking the derivative of θ with respect to *x*, we get

$$\frac{d\theta}{dx} = \frac{d^2v}{dx^2} \quad (c)$$

Now combining this equation with Eq. (7-3), we obtain

$$\kappa = \frac{1}{\rho} = \frac{d\theta}{dx} = \frac{d^2v}{dx^2} \quad (7-4)$$

This equation relates the curvature to the deflection *v* of the beam. It is valid for a beam of any material, provided the rotations are small.

If the material of the beam is linearly elastic and if it follows Hooke's law, the curvature (see Eq. 5-9) is:

$$\kappa = \frac{1}{\rho} = -\frac{M}{EI} \quad (7-5)$$

in which *M* is the bending moment and *EI* is the flexural rigidity of the beam. Note that Eq. (7-5) is valid for large rotations as well as small rotations. The relationships between the signs for bending moments and for curvatures are portrayed in Fig. 5-11. Combining Eq. (7-4), which is limited to small rotations, with Eq. (7-5) yields

$$\frac{d\theta}{dx} = \frac{d^2v}{dx^2} = -\frac{M}{EI} \quad (7-6)$$

which is the basic **differential equation of the deflection curve** of a beam. This equation can be integrated in each particular case to find the angle of rotation θ or the deflection *v*, provided the bending moment *M* is known.

In summary, the **sign conventions** to be used with Eq. (7-6) are as follows: (1) the *x* and *y* axes are positive to the right and downward, respectively; (2) the angle of rotation θ is positive when clockwise from the *x* axis; (3) the deflection *v* is positive downward; (4) the bending

moment M is positive when it produces compression in the upper part of the beam; and (5) the curvature is positive when the beam is bent concave downward. If the sign convention for M is reversed, or if the axis (and hence v) is taken positive upward, then the minus sign in Eq. (7-6) should be changed to a plus sign. If both M and y are reversed in sign, the equation is unchanged.

By differentiating Eq. (7-6) with respect to x and then substituting the equations $q = -dV/dx$ and $V = dM/dx$ (see Eqs. 4-1 and 4-3), we obtain:

$$\frac{d^3v}{dx^3} = -\frac{V}{EI} \tag{7-7}$$

$$\frac{d^4v}{dx^4} = \frac{q}{EI} \tag{7-8}$$

where V is the shear force and q is the intensity of distributed load. The deflection v can be found by solving any one of Eqs. (7-6) through (7-8), depending on mathematical convenience and personal preference. The sign conventions for M , V , and q are repeated in Fig. 7-2.

For simplicity in succeeding discussions, we often will use primes to denote differentiation; thus,

$$v' \equiv \frac{dv}{dx} \quad v'' \equiv \frac{d^2v}{dx^2} \quad v''' \equiv \frac{d^3v}{dx^3} \quad v'''' \equiv \frac{d^4v}{dx^4} \tag{7-9}$$

Using this notation, we can express the differential equations given above in the following form:

$$EIv' = -M \qquad EIv'' = -V \qquad EIv'''' = q \tag{7-10a,b,c}$$

In the next two sections, we will use these equations to find deflections of beams. The procedure consists of successive integrations of the equations, with the resulting constants of integration being evaluated from the boundary conditions of the beam.

From the derivation of Eqs. (7-10), we see that they are valid only when Hooke's law applies for the material and when the slopes of the deflection curve are very small. Also, it should be realized that the equations were derived by considering the deformations due to pure bending and disregarding the shear deformations. These limitations are satisfactory for most practical purposes, although on rare occasions it may be necessary to consider the additional deflections due to shear effects (see Section 7.12).

Exact expression for curvature. If the deflection curve of a beam has large slopes, we cannot use the approximations given by Eqs.

Eq. (7-1) and angle of rotation (Eq. 7-2b). Combining those expressions, we get

$$\kappa = \frac{1}{\rho} = \frac{d\theta}{ds} = \frac{d(\arctan v')}{dx} \frac{dx}{ds}$$

Noting from Fig. 7-1b that $ds^2 = dx^2 + dv^2$, we obtain

$$\frac{ds}{dx} = \left[1 + \left(\frac{dv}{dx} \right)^2 \right]^{1/2} = [1 + (v')^2]^{1/2}$$

Also, by differentiation, we get

$$\frac{d}{dx}(\arctan v') = \frac{v''}{1 + (v')^2}$$

Substitution of these expressions into the equation for curvature yields

$$\kappa = \frac{1}{\rho} = \frac{v''}{[1 + (v')^2]^{3/2}} \tag{7-11}$$

Comparing this equation with Eq. (7-4), we see that the assumption of small slopes is equivalent to disregarding $(v')^2$ in comparison to unity, thus making the denominator in Eq. (7-11) equal to one. Equation (7-11) must be used for the curvature when solving problems that involve large deflections of beams (see Section 7.13).*

7.3 DEFLECTIONS BY INTEGRATION OF THE BENDING-MOMENT EQUATION

The equation of the deflection curve in terms of the bending moment (Eq. 7-10a) may be integrated to obtain the deflection v as a function of x . Since the differential equation is of second order, two integrations are required. The first step in the solution is to write the equations for the bending moment, using free-body diagrams and static equilibrium to obtain the equations.** If the loading on the beam changes abruptly as we move along the axis of the beam, there will be separate moment expressions for each region of the beam between the points at which such changes occur. For each of these regions, we substitute the expression for M into the differential equation. Then the equation can be integrated to obtain the slope v' , and a constant of integration is introduced by this process. A second integration gives the

* The basic relationship stating that the curvature of a beam is proportional to the bending moment (see Eq. 7-5) was first obtained by Jacob Bernoulli, although he obtained an incorrect value for the constant of proportionality. The relationship was used later by Euler, who solved the differential equation of the deflection curve both for large deflections (using Eq. 7-11 for the curvature) and for small deflections (using Eq. 7-6). For the history of elastic curves, see Ref. 7-1.

** Only statically determinate beams are considered in this chapter. The analysis of statically indeterminate beams is described in Chapter 8.



Fig. 7-2. Sign conventions for bending moment M , shear force V , and intensity of distributed load q .

deflection v , and another constant of integration is introduced. Thus, there are two constants of integration for each region of the beam. These constants can be evaluated from boundary conditions of the beam. These conditions are v and v' at the supports of the beam and from continuity conditions on v and v' at the points where the regions of integration meet. Each such condition gives an equation containing one or more of the constants of integration. Since the number of conditions always matches the number of constants, we can solve these equations for the constants. Then the evaluated constants can be substituted back into the expressions for v and v' , thus yielding the final equations of the deflection curve. This method for finding deflections is sometimes called the **method of successive integrations**. The following examples illustrate the procedure for both simple and cantilever beams.

Example 1

Determine the equation of the deflection curve for a simple beam AB supporting a uniform load of intensity q (Fig. 7-3). Also, determine the maximum deflection δ at the middle of the beam and the angles of rotation θ_a and θ_b at the supports.

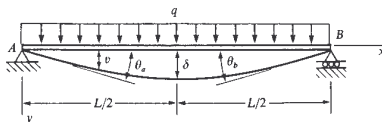


Fig. 7-3. Deflections of a simple beam AB supporting a uniform load.

With the origin of coordinates taken at the left-hand support, the equation for the bending moment is

$$M = \frac{qLx}{2} - \frac{qx^2}{2}$$

Hence, the second-order differential equation (Eq. 7-10a) becomes

$$EIv'' = -\frac{qLx}{2} + \frac{qx^2}{2}$$

Multiplying both sides of this equation by dx and integrating, we obtain

$$EIv' = -\frac{qLx^2}{4} + \frac{qx^3}{6} + C_1 \tag{a}$$

where C_1 is a constant of integration. To evaluate this constant, we observe from symmetry that the slope v' of the deflection curve at midspan is zero. Thus, we have the condition

$$v' = 0 \quad \text{when } x = \frac{L}{2}$$

which may be expressed more succinctly as

$$v' \left(\frac{L}{2} \right) = 0$$

Applying this condition to Eq. (a) gives

$$C_1 = \frac{qL^3}{24}$$

and Eq. (a) then becomes

$$EIv' = -\frac{qLx^2}{4} + \frac{qx^3}{6} + \frac{qL^3}{24} \tag{7-12}$$

Again multiplying both sides of the equation by dx and integrating, we get

$$EIv = -\frac{qLx^3}{12} + \frac{qx^4}{24} + \frac{qL^3x}{24} + C_2 \tag{b}$$

The constant of integration C_2 may be evaluated from the condition that $v = 0$ when $x = 0$, or

$$v(0) = 0$$

Applying this condition to Eq. (b) yields $C_2 = 0$; hence, the equation for the deflection curve is

$$v = \frac{qx}{24EI} (L^3 - 2Lx^2 + x^3) \tag{7-13}$$

This equation gives the deflection at any point along the beam.

The maximum deflection δ occurs at the middle of the span and is obtained by setting x equal to $L/2$ in Eq. (7-13). The result is

$$\delta = v_{\max} = \frac{5qL^4}{384EI} \tag{7-14}$$

The maximum angles of rotation occur at the supports of the beam. At the left-hand end, the angle θ_a is equal to the slope v' ; thus, by substituting $x = 0$ into Eq. (7-12), we obtain

$$\theta_a = v'(0) = \frac{qL^3}{24EI} \tag{7-15}$$

In a similar manner, we obtain the angle θ_b at the other end:

$$\theta_b = -v'(L) = \frac{qL^3}{24EI} \tag{7-16}$$

Since the beam and loading are symmetric about the midpoint, the angles of rotation at the ends are equal. Note that the angles of rotation are assumed to be positive when the ends of the beam rotate as shown in Fig. 7-3. Of course, the positive sense of the slope v' is determined by the directions of the coordinate axes. For the beam in this example, v' is positive at support A , negative at B , and zero at the midpoint.

Example 2

Determine the equation of the deflection curve for a cantilever beam AB subjected to a uniform load of intensity q (Fig. 7-4). Also, determine the deflection δ_b and angle of rotation θ_b at the free end.

We again take the origin of coordinates at the left-hand support. Then the expression for the bending moment is

$$M = -\frac{q(L-x)^2}{2}$$

and the differential equation (Eq. 7-10a) becomes

$$EIv'' = \frac{q(L-x)^2}{2}$$

The first integration of this equation gives

$$EIv' = -\frac{q(L-x)^3}{6} + C_1$$

The constant of integration C_1 can be found from the condition that the slope of the beam is zero at the support; thus, we have $v'(0) = 0$, which gives $C_1 = qL^3/6$. Therefore,

$$v' = \frac{qx}{6EI}(3L^2 - 3Lx + x^2) \quad (7-17)$$

Integration of this equation yields

$$v = \frac{qx^2}{24EI}(6L^2 - 4Lx + x^2) + C_2$$

The boundary condition on the deflection at the support is $v(0) = 0$, which shows that $C_2 = 0$. Thus, the equation of the deflection curve is

$$v = \frac{qx^2}{24EI}(6L^2 - 4Lx + x^2) \quad (7-18)$$

The angle of rotation θ_b and the deflection δ_b at the free end of the beam (Fig. 7-4) are readily found by substituting $x = L$ into Eqs. (7-17) and (7-18), as follows:

$$\theta_b = v'(L) = \frac{qL^3}{6EI} \quad \delta_b = v(L) = \frac{qL^4}{8EI} \quad (7-19a,b)$$

These quantities are the maximum angle of rotation and maximum deflection, respectively.

Example 3

Determine the equations of the deflection curve for a simple beam AB supporting a concentrated load P (Fig. 7-5). Also, determine the angles of rotation θ_a and θ_b at the supports, the maximum deflection v_{max} , and the deflection δ_c at the center C of the beam. (Note that the position of the load P is defined by the distances a and b from the supports A and B , respectively.)

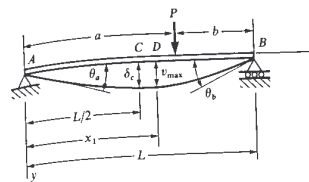


Fig. 7-5 Example 3. Deflections of a simple beam with a concentrated load

To obtain the deflections, we first must determine the expression for the bending moment in each part of the beam. Then we must write Eq. (7-10a) twice, once for each part of the beam, as follows:

$$EIv'' = -\frac{Pbx}{L} \quad (0 \leq x \leq a)$$

$$EIv'' = -\frac{Pbx}{L} + P(x-a) \quad (a \leq x \leq L)$$

Integration of these equations gives

$$EIv' = -\frac{Pbx^2}{2L} + C_1 \quad (0 \leq x \leq a) \quad (c)$$

$$EIv' = -\frac{Pbx^2}{2L} + \frac{P(x-a)^2}{2} + C_2 \quad (a \leq x \leq L) \quad (d)$$

Performing a second integration, we obtain

$$EIv = -\frac{Pbx^3}{6L} + C_1x + C_3 \quad (0 \leq x \leq a) \quad (e)$$

$$EIv = -\frac{Pbx^3}{6L} + \frac{P(x-a)^3}{6} + C_2x + C_4 \quad (a \leq x \leq L) \quad (f)$$

The four constants of integration appearing in the preceding equations can be found from the following conditions: (1) at $x = a$, the slopes v' for the two parts of the beam must be equal; (2) at $x = a$, the deflections v for the two parts of the beam must be equal; (3) at $x = 0$, the deflection is zero; and (4) at $x = L$, the deflection is zero. From the first condition we see that the slopes determined from Eqs. (c) and (d) must be equal when $x = a$; thus,

$$-\frac{Pba^2}{2L} + C_1 = -\frac{Pba^2}{2L} + C_2$$

from which $C_1 = C_2$. The second condition means that the deflections found from Eqs. (e) and (f) must be equal when $x = a$:

$$-\frac{Pba^3}{6L} + C_1a + C_3 = -\frac{Pba^3}{6L} + C_2a + C_4$$

which gives $C_3 = C_4$. Finally, when conditions (3) and (4) are applied to Eqs. (e) and (f), respectively, we obtain

$$C_3 = 0 \quad \text{and} \quad -\frac{PbL^2}{6} + \frac{Pb^3}{6} + C_2L = 0$$

From the preceding results, we see that

$$C_1 = C_2 = \frac{Pb(L^2 - b^2)}{6L} \quad C_3 = C_4 = 0$$

Substitution of these values into Eqs. (e) and (f) gives the equations for the deflection curve:

$$EIv = \frac{Pbx}{6L}(L^2 - b^2 - x^2) \quad (0 \leq x \leq a) \quad (7-20a)$$

$$EIv = \frac{Pbx}{6L}(L^2 - b^2 - x^2) + \frac{P(x-a)^3}{6} \quad (a \leq x \leq L) \quad (7-20b)$$

The first of these equations gives the deflection curve for the part of the beam to the left of the load P , and the second gives the deflection to the right of the load.

The slopes for the two parts of the beam are found by substituting the values of C_1 and C_2 into Eqs. (c) and (d), which gives

$$EIv' = \frac{Pb}{6L}(L^2 - b^2 - 3x^2) \quad (0 \leq x \leq a) \quad (7-21a)$$

$$EIv' = \frac{Pb}{6L}(L^2 - b^2 - 3x^2) + \frac{P(x-a)^2}{2} \quad (a \leq x \leq L) \quad (7-21b)$$

From these equations the slope at any point of the deflection curve can be calculated.

To obtain the angles of rotation θ_a and θ_b at the ends of the beam, we substitute $x = 0$ into Eq. (7-21a) and $x = L$ into Eq. (7-21b), as follows:

$$\theta_a = v'(0) = \frac{Pb(L^2 - b^2)}{6LEI} = \frac{Pab(L+b)}{6LEI} \quad (7-22a)$$

$$\theta_b = -v'(L) = \frac{Pab(L+a)}{6LEI} \quad (7-22b)$$

The angle θ_a has its maximum value when $b = L/\sqrt{3}$.

The maximum deflection of the beam occurs at point D (Fig. 7-5) where the deflection curve has a horizontal tangent. If $a > b$, this point is in the part of the beam to the left of the load. We can locate this point by equating the slope v' from Eq. (7-21a) to zero. Denoting the distance from end A of the beam to the point of maximum deflection by x_1 , we find from Eq. (7-21a) the following formula for x_1 :

$$x_1 = \sqrt{\frac{L^2 - b^2}{3}} \quad (a \geq b) \quad (7-23)$$

From this equation we see that, as the load P moves from the middle of the beam ($b = L/2$) to the right-hand end (b approaches 0), the distance x_1 varies

7.4 Deflections by Integration of the Shear-Force and Load Equations

from $L/2$ to $L/\sqrt{3} = 0.577L$. Thus, the maximum deflection occurs at a point very close to the center of the beam and always between the center of the beam and the load. The maximum deflection is found by substituting x_1 from Eq. 7-23 into Eq. (7-20a), yielding

$$v_{max} = \frac{Pb(L^2 - b^2)^{3/2}}{9\sqrt{3}LEI} \quad (a \geq b) \quad (7-24)$$

The deflection at the middle of the beam is obtained by substituting $x = L/2$ into Eq. (7-20a):

$$\delta_c = v\left(\frac{L}{2}\right) = \frac{Pb(3L^2 - 4b^2)}{48EI} \quad (a \geq b) \quad (7-25)$$

Because the maximum deflection always occurs near the midpoint of the beam, Eq. (7-25) gives a good approximation of the maximum deflection. In the most unfavorable case (when b approaches zero), the difference between the maximum deflection and the deflection at the midpoint is less than 3% of the maximum deflection.

An important special case occurs when the load P acts at the midpoint of the beam. Then $a = b = L/2$, and the preceding results simplify to the following:

$$v' = \frac{P}{16EI}(L^2 - 4x^2) \quad \left(0 \leq x \leq \frac{L}{2}\right) \quad (7-26)$$

$$v = \frac{Px}{48EI}(3L^2 - 4x^2) \quad \left(0 \leq x \leq \frac{L}{2}\right) \quad (7-27)$$

$$\theta_a = \theta_b = \frac{PL^2}{16EI} \quad (7-28)$$

$$\delta_c = v_{max} = \frac{PL^3}{48EI} \quad (7-29)$$

In this case the deflection curve is symmetric about the midpoint of the beam; however, the preceding equations for v' and v are valid only for the left-hand half of the beam.

7.4 DEFLECTIONS BY INTEGRATION OF THE SHEAR-FORCE AND LOAD EQUATIONS

The equations of the deflection curve in terms of the shear force V and the load q (Eqs. 7-10b and c, respectively) may be used to obtain beam deflections. The procedure is similar to that for the bending-moment equation, except that more integrations are required. For instance, if we begin with the load equation, which is of fourth order, four integrations are needed in order to arrive at the deflection equation. These additional steps introduce additional constants of integration, but these constants can be obtained from boundary and continuity conditions. The conditions now include conditions on the shear forces and bending moments, as well as on the slopes and deflections.

The choice among the three differential equations depends upon mathematical convenience and personal preference. For instance, if the expression for the load q is easy to write but the expression for the bending moment M is not easily obtained by static equilibrium for the free-body diagrams, then the load equation should be used. The following examples illustrate the techniques for making the analyses.

Example 1

Determine the equation of the deflection curve for a cantilever beam AB supporting a triangularly distributed load of maximum intensity q_0 (Fig. 7-6). Also determine the deflection δ_b and angle of rotation θ_b at the free end.

The intensity of the distributed load is given by the following equation

$$q = \frac{q_0(L-x)}{L}$$

Hence, the fourth-order differential equation (Eq. 7-10c) becomes

$$EIv'''' = \frac{q_0(L-x)}{L}$$

The first integration gives

$$EIv''' = \frac{q_0x}{2L}(2L-x) + C_1 \tag{a}$$

The right-hand side of this equation represents the negative of the shear force V (see Eq. 7-10b). Because the shear force is zero at $x = L$, we obtain the following boundary condition:

$$v'''(L) = 0$$

Using this condition with Eq. (a), we get $C_1 = -q_0L/2$. When this expression for C_1 is substituted into Eq. (a), it becomes

$$EIv'' = -\frac{q_0}{2L}(L^2 - 2Lx + x^2) = -\frac{q_0}{2L}(L-x)^2$$

Integrating a second time, we obtain

$$EIv' = \frac{q_0}{6L}(L-x)^3 + C_2 \tag{b}$$

which is the bending-moment equation (Eq. 7-10a). A second boundary condition is obtained at the free end of the beam, where the bending moment is zero

$$v''(L) = 0$$

Applying this condition to Eq. (b), we obtain $C_2 = 0$; therefore,

$$EIv' = \frac{q_0}{6L}(L-x)^3$$

Integrating and fourth integrations yield

$$EIv = -\frac{q_0}{24L}(L-x)^4 + C_3 \tag{c}$$

$$EIv = \frac{q_0}{120L}(L-x)^5 + C_3x + C_4 \tag{d}$$

From the boundary conditions at the fixed support, which are

$$v'(0) = 0 \quad v(0) = 0$$

we obtain

$$C_3 = \frac{q_0L^3}{24} \quad C_4 = -\frac{q_0L^4}{120}$$

Substituting these expressions for the constants into Eqs. (c) and (d), we obtain the following equations for the slope and deflection of the beam:

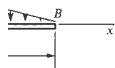
$$v' = \frac{q_0x}{24LEI}(4L^3 - 6L^2x + 4Lx^2 - x^3) \tag{7-30}$$

$$v = \frac{q_0x^2}{120LEI}(10L^3 - 10L^2x + 5Lx^2 - x^3) \tag{7-31}$$

The angle of rotation θ_b and deflection δ_b at the free end ($x = L$) are now easily obtained from Eqs. (7-30) and (7-31); the results are

$$\theta_b = \frac{q_0L^3}{24EI} \quad \delta_b = \frac{q_0L^4}{30EI} \tag{7-32a, b}$$

Thus, we have determined the required deflections and slopes of the beam by solving the fourth-order differential equation of the deflection curve.



Deflections of a cantilever beam with a triangular load

Example 2

Determine the equations of the deflection curve for a simple beam with an overhang subjected to a concentrated load P (Fig. 7-7). The main span has length L and the overhang has length $L/2$.

Because reactive forces act at supports A and B , we must write separate differential equations for parts AB and BC of the beam. The shear forces in those parts are as follows:

$$V = -\frac{P}{2} \quad (0 < x < L)$$

$$V = P \quad (L < x < \frac{3L}{2})$$

found from equilibrium. Thus, the third-order differential equations (see Eq. 7-10b) are

$$EIv''' = \frac{P}{2} \quad (0 < x < L)$$

$$EIv''' = -P \quad (L < x < \frac{3L}{2})$$

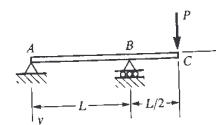


Fig. 7-7 Example 2. Deflections of beam with an overhang

Integration of these equations yields the following bending-moment equations

$$EIv'' = \frac{Px}{2} + C_1 \quad (0 \leq x \leq L)$$

$$EIv'' = -Px + C_2 \quad (L \leq x \leq \frac{3L}{2})$$

The bending moments at points A and C are zero; hence, we have the following boundary conditions:

$$v''(0) = 0 \quad v''(\frac{3L}{2}) = 0$$

Using these conditions with Eqs. (e) and (f), we get

$$C_1 = 0 \quad C_2 = \frac{3PL}{2}$$

from which

$$EIv' = \frac{Px^2}{2} \quad (0 \leq x \leq L)$$

$$EIv' = \frac{P(3L-2x)}{2} \quad (L \leq x \leq \frac{3L}{2})$$

From the next integration, we get

$$EIv = \frac{Px^3}{4} + C_3 \quad (0 \leq x \leq L)$$

$$EIv = \frac{Px(3L-x)}{2} + C_4 \quad (L \leq x \leq \frac{3L}{2})$$

The only condition on the slope is the continuity condition at support B :

$$v'(L) \text{ for } AB = v'(L) \text{ for } BC$$

or

$$\frac{PL^2}{4} + C_3 = PL^2 + C_4$$

This equation eliminates one constant of integration because we can express C_4 in terms of C_3 :

$$C_4 = C_3 - \frac{3PL^2}{4} \tag{g}$$

The third and last integration gives

$$EIv = \frac{Px^3}{12} + C_3x + C_5 \quad (0 \leq x \leq L)$$

$$EIv = \frac{Px^2(9L-2x)}{12} + C_4x + C_6 \quad (L \leq x \leq \frac{3L}{2})$$

Since the deflections at points A and B are zero, we obtain three more boundary conditions:

$$v(0) = 0 \quad v(L) \text{ for } AB = 0 \quad v(L) \text{ for } BC = 0$$

Integrating equations for the constants are

$$C_5 = 0 \quad C_3 = -\frac{PL^2}{12}$$

$$C_4L + C_6 = -\frac{7PL^3}{12}$$

Combining these equations with Eq. (g), we get

$$C_4 = -\frac{5PL^2}{6} \quad C_6 = \frac{PL^3}{4}$$

Thus, the deflection equations for the beam are

$$v = -\frac{Px}{12EI}(L^2 - x^2) \quad (0 \leq x \leq L) \tag{7-33a}$$

$$v = \frac{P}{12EI}(3L^3 - 10L^2x + 9Lx^2 - 2x^3) \tag{7-33b}$$

$$= \frac{P}{12EI}(3L-x)(L-x)(L-2x) \quad (L \leq x \leq \frac{3L}{2})$$

From Eq. (7-33b) we find the deflection at the end of the overhang ($x = 3L/2$):

$$\delta_c = \frac{PL^3}{8EI} \tag{7-34}$$

Note that the deflection of the beam is downward between B and C and upward between A and B .

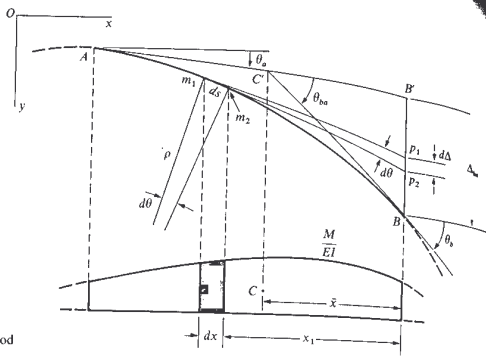
7.5 MOMENT-AREA METHOD

In this section we consider another method for finding deflections of beams. Known as the **moment-area method**, it utilizes properties of the area of the bending-moment diagram. The method is especially suitable when the deflection or angle of rotation at only one point of the beam is desired, because it is possible to find those quantities without first finding the complete equation of the deflection curve.

To explain the method, let us consider a segment AB of the deflection curve of a beam in a region where the curvature is positive (Fig. 7-8, page 366). At point A the tangent AB' to the deflection curve has a positive angle of rotation θ_a from the x axis, and at point B the tangent CB is at an angle θ_b . The angle between the tangents, denoted θ_{ba} , is equal to the difference between θ_b and θ_a :

$$\theta_{ba} = \theta_b - \theta_a \tag{7-35}$$

Thus, θ_{ba} represents the relative angle of rotation of the tangent at B with respect to the tangent at A . The relative angle θ_{ba} is positive when θ_b is larger than θ_a , as shown in the figure.



8 Moment-area method

Next, consider two points m_1 and m_2 on the axis of the beam, a distance ds apart. The tangents to the deflection curve at these points are shown in the figure as lines m_1p_1 and m_2p_2 . The normals to these tangents intersect at the center of curvature at an angle $d\theta$, which is equal to ds/ρ , where ρ is the radius of curvature. It follows that the angle between the two tangents is also equal to $d\theta$. The angle $d\theta$ can be obtained from Eq. (7-6):

$$d\theta = -\frac{M dx}{EI} \quad (a)$$

in which M is the bending moment in the beam and EI is the flexural rigidity.

The quantity $M dx/EI$ has a simple geometric interpretation. Directly below the beam in Fig. 7-8, we draw the M/EI diagram (that is, a diagram in which the ordinate at any point is equal to the bending moment M at that point divided by the flexural rigidity EI at that point). Thus, the M/EI diagram has the same shape as the bending-moment diagram only when EI is constant. The term $M dx/EI$ is the area of the shaded strip (Fig. 7-8) within the M/EI diagram.

Let us now integrate Eq. (a) between points A and B :

$$\int_A^B d\theta = -\int_A^B \frac{M dx}{EI} \quad (b)$$

The integral on the left is equal to $\theta_b - \theta_a$, which is the relative angle θ_{ba} between the tangents at B and A . The integral on the right is equal to the area of the M/EI diagram between points A and B . Note that the area of the M/EI diagram is an algebraic quantity and that it may

be positive or negative, depending upon whether the bending moment is positive or negative. Now we can write Eq. (b) as follows:

$$\theta_{ba} = -\int_A^B \frac{M dx}{EI} = -[\text{area of } M/EI \text{ diagram between } A \text{ and } B] \quad (7-36)$$

This equation may be stated as a theorem:

First moment-area theorem: The angle θ_{ba} between the tangents to the deflection curve at two points A and B is equal to the negative of the area of the M/EI diagram between those points.

The sign conventions used with this theorem are summarized as follows: (1) The relative angle θ_{ba} between the tangents is positive when the angle θ_b is algebraically larger than the angle θ_a , as illustrated in Fig. 7-8. Note that point B must be to the right of point A ; that is, it must be further along the axis of the beam as we move in the x direction. (2) The bending moment M is positive according to our usual sign convention; that is, M is positive when it produces compression in the upper part of the beam. (3) The area of the M/EI diagram is given a positive or negative sign according to whether the bending moment is positive or negative. If part of the bending-moment diagram is positive and part is negative, then the corresponding parts of the M/EI diagram are given those same signs. Thus, the areas of the M/EI diagram are treated as algebraic quantities.

The first moment-area theorem is used in deflection calculations to relate the angles of rotation between selected points along the axis of the beam, as illustrated later.

As the next step in the analysis, let us consider the vertical offset Δ_{ba} between point B on the deflection curve and point B' on the tangent at A (Fig. 7-8). Recalling that the angles of rotation θ_a and θ_b are very small quantities (and, hence, the tangents at A and B are nearly horizontal lines), we observe from the figure that the vertical distance $d\Delta$ (equal to p_1p_2) is $x_1 d\theta$, where x_1 is the horizontal distance from the element m_1m_2 to point B . Since $d\theta = -M dx/EI$, we can write

$$d\Delta = x_1 d\theta = -x_1 \frac{M dx}{EI} \quad (c)$$

The distance $d\Delta$ represents the contribution made by the bending of element m_1m_2 to the total offset Δ_{ba} . The expression $x_1 M dx/EI$ may be interpreted geometrically as the first moment of the shaded element of area ($M dx/EI$) of the M/EI diagram taken about a vertical line through B . Integrating Eq. (c) between points A and B , we get

$$\int_A^B d\Delta = -\int_A^B x_1 \frac{M dx}{EI} \quad (d)$$

The integral on the left is equal to Δ_{ba} , which is the vertical offset of point B from the tangent at A . The integral on the right represents the first moment with respect to point B of the area of the M/EI diagram between A and B . Hence, we can write Eq. (d) as follows:

$$\Delta_{ba} = -\int_A^B x_1 \frac{M dx}{EI} = -[\text{first moment of the area of the } M/EI \text{ diagram between } A \text{ and } B, \text{ taken with respect to } B] \quad (7-37)$$

This equation represents the second theorem:

Second moment-area theorem: The offset Δ_{ba} of point B from the tangent at A is equal to the negative of the first moment of the area of the M/EI diagram between A and B , taken with respect to B .

Note that the offset Δ_{ba} is positive in the y direction. If, as we move from A to B in the x direction, the area of the M/EI diagram is negative, then the first moment is also negative and the offset is positive, which means that point B is below the tangent at A . This situation is illustrated in Fig. 7-8. If the area is positive, then the first moment is positive, the offset is negative, and point B is above the tangent at A . When calculating the first moment, the distance x_1 is positive from B toward A , as shown in Fig. 7-8.

The first moment of the area of the M/EI diagram can be obtained by taking the product of the area of the diagram and the distance \bar{x} from point B to the centroid C of the area (Fig. 7-8). This procedure is usually more convenient than integrating, because the diagram usually consists of familiar geometric figures such as rectangles, triangles, and parabolic segments. The areas and centroidal distances of such figures are tabulated in Appendix D.

The second moment-area theorem is useful for finding deflections because it relates the position of a point on the beam to the tangent at some other point. The techniques to be used are illustrated in the examples that follow.

In many beams, it is obvious whether the beam deflects upward or downward and whether the angle of rotation is clockwise or counterclockwise. In such cases, it is not necessary to follow the sign conventions that have been described for the moment-area method, which may seem complicated at first. Instead, we can calculate with absolute values and determine the directions by inspection.

The moment-area theorems apply only to linear elastic beams, because they are based upon Eq. (7-6). Later, in Chapter 10, we will use more general curvature-area theorems that apply to inelastic beams.*

* The moment-area method was introduced by Saint-Venant (Refs. 7-6 and 7-7). The method was developed more fully by Mohr (Refs. 7-8 and 7-9) and by Greene (Ref. 7-10).

Example 1

Determine the angle of rotation θ_b and deflection δ_b at the free end B of a cantilever beam AB supporting a concentrated load P (Fig. 7-9).

The bending-moment diagram for this beam is triangular in shape, as shown in the lower part of the figure. Since the flexural rigidity EI is constant, the M/EI diagram has the same shape as the bending-moment diagram. From the first moment-area theorem, we know that the relative angle of rotation θ_{ba} between the tangents at B and A is equal to the negative of the area of the M/EI diagram. The area of the diagram is

$$A_1 = \frac{1}{2}(L)(-PL)\left(\frac{1}{EI}\right) = -\frac{PL^2}{2EI}$$

and, therefore,

$$\theta_{ba} = \theta_b - \theta_a = -A_1 = \frac{PL^2}{2EI}$$

The tangent to the deflection curve at A is horizontal ($\theta_a = 0$); hence,

$$\theta_b = \frac{PL^2}{2EI} \quad (7-38)$$

The end of the beam rotates clockwise, as shown in the figure.

The deflection δ_b at the free end can be obtained from the second theorem. The offset Δ_{ba} of point B from the tangent at A is the same as the deflection δ_b in this case. The first moment of the area of the M/EI diagram, taken with respect to point B , is

$$Q_1 = A_1 \left(\frac{2L}{3}\right) = -\frac{PL^2}{2EI} \left(\frac{2L}{3}\right) = -\frac{PL^3}{3EI}$$

From the second moment-area theorem, we obtain $\delta_b = -Q_1$, or

$$\delta_b = \frac{PL^3}{3EI} \quad (7-39)$$

A positive value means that both the offset and the deflection are downward.

Example 2

Find the angle of rotation θ_b and deflection δ_b at the free end B of a cantilever beam AB with a uniform load of intensity q acting over part of the length (Fig. 7-10).

The bending-moment diagram consists of a parabolic spandrel of second degree (see Case 19, Appendix D, for properties of this area). The M/EI diagram has the same shape, inasmuch as EI is constant. Note that the deflected axis of the beam is curved in the region under the uniform load and is straight in the unloaded part.

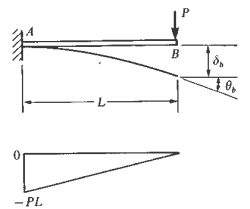


Fig. 7-9 Example 1. Cantilever beam with a concentrated load



The angle of rotation θ_A is equal to the relative angle $\theta_{B/A}$, inasmuch as the tangent at A is horizontal. The area of the M/EI diagram is

$$A_1 = \frac{1}{3} \left(a \right) \left(-\frac{qa^2}{2} \right) \left(\frac{1}{EI} \right) = -\frac{qa^3}{6EI}$$

Hence, from the first moment-area theorem, we obtain $\theta_A = -A_1$, or

$$\theta_A = \frac{qa^3}{6EI} \quad (7-40)$$



This angle is equal to the slope of the beam throughout the unloaded region. The deflection δ_B is equal to the offset $\Delta_{B/A}$ in this case. Hence, δ_B equals the negative of the first moment of the area of the M/EI diagram, taken with respect to B. The centroid C of the diagram is at distance $3a/4$ from the edge of the load, or distance $b + 3a/4$ from B. Thus, the first moment is

$$Q_1 = A_1 \left(b + \frac{3a}{4} \right) = \left(-\frac{qa^3}{6EI} \right) \left(b + \frac{3a}{4} \right) = -\frac{qa^3}{24EI} (4L - a)$$

since $b = L - a$. The deflection at the end is $\delta_B = -Q_1$, or

$$\delta_B = \frac{qa^3}{24EI} (4L - a) \quad (7-41)$$

If $a = L$, this equation becomes $\delta_B = qL^4/8EI$, which is the deflection of a fully loaded cantilever beam (Eq. 7-19b).

antilever over part

Example 3

Find the angle of rotation θ_B and deflection δ_B at the free end B of a cantilever beam AB with a uniform load of intensity q acting over the right-hand half of the length (Fig. 7-11).



The bending-moment diagram consists of a parabolic curve from B to C and a straight line from C to A. The M/EI diagram has the same shape, since EI is constant. For the purpose of evaluating the area and first moment of the M/EI diagram, it is convenient to divide this diagram into three parts having areas A_1 , A_2 , and A_3 . These parts are a parabolic spandrel, a rectangle, and a triangle, respectively, with areas as follows:

$$A_1 = \frac{1}{3} \left(\frac{L}{2} \right) \left(-\frac{qL^2}{8EI} \right) = -\frac{qL^3}{48EI}$$

$$A_2 = \frac{L}{2} \left(-\frac{qL^2}{8EI} \right) = -\frac{qL^3}{16EI}$$

$$A_3 = \frac{1}{2} \left(\frac{L}{2} \right) \left(-\frac{qL^2}{4EI} \right) = -\frac{qL^3}{16EI}$$

The angle of rotation θ_B is equal to the negative of the area of the M/EI diagram

$$\theta_B = -(A_1 + A_2 + A_3) = \frac{7qL^3}{48EI} \quad (7-42)$$

antilever over one-

The deflection δ_B is equal to the negative of the first moment of the M/EI diagram, taken about B:

$$\delta_B = -(A_1 \bar{x}_1 + A_2 \bar{x}_2 + A_3 \bar{x}_3)$$

in which \bar{x}_1 , \bar{x}_2 , \bar{x}_3 are the distances from B to the centroids of the respective areas. Thus,

$$\delta_B = \frac{qL^3}{48EI} \left(\frac{3L}{8} \right) + \frac{qL^3}{16EI} \left(\frac{3L}{4} \right) + \frac{qL^3}{16EI} \left(\frac{5L}{6} \right) = \frac{41qL^4}{384EI} \quad (7-43)$$

This example illustrates how the area and first moment of a complicated M/EI diagram can be determined easily by dividing the diagram into parts having known properties.

Example 4

A simple beam AB supports a concentrated load P as shown in Fig. 7-12. Determine the angle of rotation θ_A at support A, the deflection δ under the load P , and the maximum deflection δ_{max} .

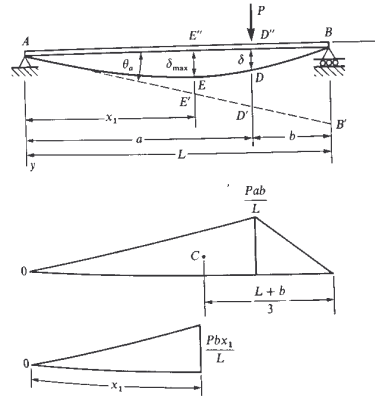


Fig. 7-12 Example 4. Simple beam with a concentrated load

We begin by constructing the tangent AB' at support A. Then we note that the distance BB' is the offset $\Delta_{B/A}$ of point B from the tangent. Hence, we can calculate the distance BB' by evaluating the first moment of the M/EI diagram with respect to B and using the second moment-area theorem. The bending-moment diagram is triangular, with maximum ordinate Pab/L , as shown in the

figure, and the M/EI diagram has the same shape, since EI is constant. Thus the area of the M/EI diagram is

$$A_1 = \frac{1}{2} (L) \left(\frac{Pab}{L} \right) \left(\frac{1}{EI} \right) = \frac{Pab}{2EI}$$

The centroid C of this area is at distance $(L + b)/3$ from B (see Case 3, Appendix D). Therefore, the offset $\Delta_{B/A}$ is

$$\Delta_{B/A} = -A_1 \left(\frac{L + b}{3} \right) = -\frac{Pab}{6EI} (L + b)$$

The minus sign shows that the offset is in the negative y direction, or upward; that is, point B is above the tangent. The distance BB' is numerically equal to $\Delta_{B/A}$, as follows:

$$BB' = \frac{Pab}{6EI} (L + b)$$

Also, we see from the figure that the angle θ_A is equal to the distance BB' divided by the length of the beam:

$$\theta_A = \frac{BB'}{L} = \frac{Pab}{6LEI} (L + b) \quad (7-44)$$

Thus, the angle of rotation at support A has been found.

As can be seen from Fig. 7-12, the deflection δ under the load P is equal to the distance $D'D''$ minus the distance $D'D$. The distance $D'D''$ is equal to $a\theta_A$, and the distance $D'D$ can be found from the second moment-area theorem. This latter distance is numerically equal to the offset of point D from the tangent at A. Hence, we take the first moment of the area of the M/EI diagram between A and D with respect to D. The area of the diagram is the area of the left-hand triangle divided by 2:

$$A_2 = \frac{1}{2} (a) \left(\frac{Pab}{L} \right) \left(\frac{1}{EI} \right) = \frac{Pa^2b}{2LEI}$$

Its first moment about D is

$$Q_1 = A_2 \left(\frac{a}{3} \right) = \frac{Pa^3b}{6LEI}$$

The offset $\Delta_{D/A}$ is the negative of this expression; however, we need the actual distance $D'D$, which is equal to Q_1 itself.

$$D'D = \frac{Pa^3b}{6LEI}$$

Thus, for the deflection δ at point D, we obtain

$$\delta = D'D'' - D'D = a\theta_A - \frac{Pa^3b}{6LEI} = \frac{Pa^2b^2}{3LEI} \quad (7-45)$$

The preceding formulas for θ_A and δ are valid for any position of the load P . To determine the maximum deflection, let us assume that $a \geq b$, so that the maximum deflection occurs to the left of the load (or under the load in the special case when $a = b$). The maximum deflection occurs at point E (distance x_1 from

A), where the deflection curve has a horizontal tangent. The relative angle $\theta_{E/A}$ between the tangents at E and A is equal to the negative of the area of the M/EI diagram between A and E, according to the first moment-area theorem. The portion of the bending-moment diagram between A and E is shown in the lowest part of Fig. 7-12. The area of the corresponding M/EI diagram is

$$A_3 = \frac{1}{2} (x_1) \left(\frac{Pbx_1}{L} \right) \left(\frac{1}{EI} \right) = \frac{Pbx_1^2}{2LEI}$$

From the first theorem, we now obtain

$$\theta_{E/A} = \theta_E - \theta_A = -A_3 = -\frac{Pbx_1^2}{2LEI}$$

The angle θ_E is zero, and the angle θ_A is given by Eq. (7-44); substituting these values, we get an equation that can be solved for the distance x_1 :

$$-\frac{Pab}{6LEI} (L + b) = -\frac{Pbx_1^2}{2LEI}$$

from which

$$x_1 = \sqrt{\frac{a(2L - a)}{3}} = \sqrt{\frac{L^2 - b^2}{3}} \quad (7-46)$$

Thus, the distance to point E is determined.

The maximum deflection δ_{max} is equal to $E'E''$ minus $E'E$; the former is equal to $x_1\theta_E$, and the latter can be obtained from the second moment-area theorem in the same way that we found the distance $D'D$. The resulting calculation is as follows:

$$\delta_{max} = x_1\theta_E - A_3 \left(\frac{x_1}{3} \right) = \frac{Pb}{9\sqrt{3}LEI} (L^2 - b^2)^{3/2} \quad (7-47)$$

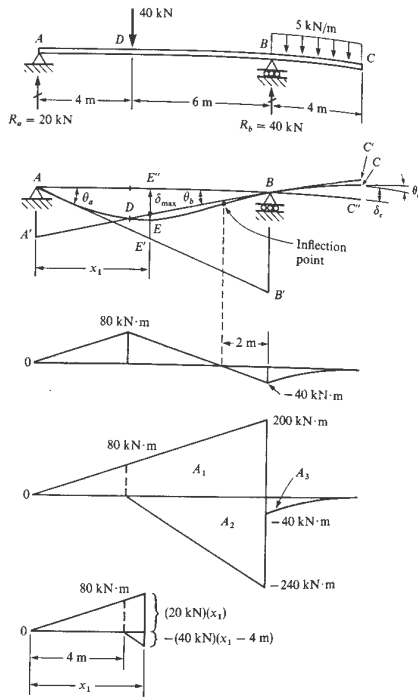
An alternate and slightly simpler scheme for finding δ_{max} is to note that δ_{max} is numerically equal to the offset of point A from the tangent at E. Hence, we can find δ_{max} by determining the first moment of the area of the M/EI diagram between A and E with respect to A:

$$\delta_{max} = A_3 \left(\frac{2x_1}{3} \right) = \frac{Pbx_1^2}{3LEI} \quad (7-48)$$

Substituting for x_1 from Eq. (7-46), we get the same expression as before (Eq. 7-47). Equations (7-46) through (7-48) are valid when $a \geq b$.

Example 5

A beam ABC is simply supported at A and B, and it overhangs from B to C (Fig. 7-13). The span from A to B has a length of 10 m, and the overhang has a length of 4 m. A concentrated load of 40 kN acts at point D, which is 4 m from the support at A, and a uniform load of 5 kN/m acts on the overhang. The beam is a standard wide-flange section with $E = 200$ GPa and $I = 1.28 \times 10^9$ mm⁴. (a) Calculate the angles of rotation θ_A , θ_B , and θ_C at A, B, and C, respectively, assuming



Example 5. Beam with an

that the angles are positive as shown in the figure. (b) Calculate the deflection δ_c at the free end C. (c) Calculate the maximum deflection δ_{max} in span AB. δ_c at the free end C. (c) Calculate the maximum deflection δ_{max} in span AB. (a) To find the various angles of rotation and deflections, we need the bending-moment diagram. From static equilibrium, we construct the diagram shown below the sketch of the deflection curve. The bending moment under the concentrated load is $80 \text{ kN}\cdot\text{m}$ and at support B is $-40 \text{ kN}\cdot\text{m}$. Between these points, the bending moment varies linearly and becomes zero at a point located 2 m from B. At the point of zero moment, the bending moment changes sign; hence, the curvature also changes sign. Consequently, there is a point of zero curvature, called an inflection point, or point of contraflexure, in the deflection curve of the beam. To the left of the inflection point, the beam bends concave upward; to the right, it bends concave downward.

For convenience in calculating areas and first moments of the M/EI diagram, we shall redraw the bending-moment diagram as shown in the fourth sketch in the figure. This moment diagram is equivalent to the one just above it, as can easily be verified by calculating the bending moment at a few selected points. The upper triangle in this sketch represents the moment from A to B of the reaction at A, and the lower triangle represents the moment of the concentrated load from D to B. A bending-moment diagram constructed in this form is referred to as a moment diagram drawn by "parts," for the obvious reason that, instead of giving the total bending moment at any cross section, the diagram gives the moment in parts. We can use either form of the bending-moment diagram when making calculations by the moment-area theorems, but in this example it is easier to use the diagram drawn by parts. Of course, the total bending moment is needed when designing the beam. As a preliminary matter, let us calculate the areas A_1 , A_2 , and A_3 of the three parts of the bending-moment diagram:

$$A_1 = \frac{1}{2} (10 \text{ m})(200 \text{ kN}\cdot\text{m}) = 1000 \text{ kN}\cdot\text{m}^2$$

$$A_2 = \frac{1}{2} (6 \text{ m})(-240 \text{ kN}\cdot\text{m}) = -720 \text{ kN}\cdot\text{m}^2$$

$$A_3 = \frac{1}{3} (4 \text{ m})(-40 \text{ kN}\cdot\text{m}) = -53.33 \text{ kN}\cdot\text{m}^2$$

The corresponding areas of the M/EI diagram are obtained by dividing these areas by EI .

Now we are ready to calculate the angle of rotation θ_a (Fig. 7-13). This angle equals the distance BB' divided by the span length of 10 m. The distance BB' equals the first moment of the area of the M/EI diagram between A and B, taken about B. Therefore, the quantity EI times the distance BB' is calculated as follows:

$$EI(BB') = A_1 \left(\frac{10 \text{ m}}{3} \right) + A_2 \left(\frac{6 \text{ m}}{3} \right)$$

$$= (1000 \text{ kN}\cdot\text{m}^2) \left(\frac{10 \text{ m}}{3} \right) - (720 \text{ kN}\cdot\text{m}^2) \left(\frac{6 \text{ m}}{3} \right)$$

$$= 1893 \text{ kN}\cdot\text{m}^3$$

The quantity $EI\theta_a$ can now be calculated:

$$EI\theta_a = \frac{EI(BB')}{10 \text{ m}} = 189.3 \text{ kN}\cdot\text{m}^2$$

Note that, for convenience in the calculations, we keep EI as a common factor. Later, we will substitute numerical values for E and I and determine the value of θ_a in radians.

The angle of rotation θ_b is determined in a similar manner. We first find the distance AA' from the second moment-area theorem:

$$EI(AA') = A_1 \left(\frac{2}{3} \right) (10 \text{ m}) + A_2 \left[4 \text{ m} + \frac{2}{3} (6 \text{ m}) \right]$$

$$= (1000 \text{ kN}\cdot\text{m}^2) \left(\frac{20 \text{ m}}{3} \right) - (720 \text{ kN}\cdot\text{m}^2)(8 \text{ m})$$

$$= 906.7 \text{ kN}\cdot\text{m}^3$$

Hence, the angle θ_b (times EI) is

$$EI\theta_b = \frac{EI(AA')}{10 \text{ m}} = 90.67 \text{ kN}\cdot\text{m}^2$$

The angle of rotation θ_c is equal to the angle θ_b at support B plus the area of the M/EI diagram between B and C, in accord with the first moment-area theorem. Hence,

$$EI\theta_c = EI\theta_b + A_3$$

$$= 90.67 \text{ kN}\cdot\text{m}^2 - 53.33 \text{ kN}\cdot\text{m}^2 = 37.33 \text{ kN}\cdot\text{m}^2$$

Now we can determine the actual angles of rotation by substituting $E = 200 \text{ GPa}$ and $I = 1.28 \times 10^9 \text{ mm}^4$ into the preceding equations. The product EI equals $256.0 \text{ MN}\cdot\text{m}^2$; therefore,

$$\theta_a = \frac{189.3 \text{ kN}\cdot\text{m}^2}{256.0 \text{ MN}\cdot\text{m}^2} = 739 \times 10^{-6} \text{ rad}$$

$$\theta_b = \frac{90.67 \text{ kN}\cdot\text{m}^2}{256.0 \text{ MN}\cdot\text{m}^2} = 354 \times 10^{-6} \text{ rad}$$

$$\theta_c = \frac{37.33 \text{ kN}\cdot\text{m}^2}{256.0 \text{ MN}\cdot\text{m}^2} = 146 \times 10^{-6} \text{ rad}$$

Thus, the required angles of rotation have been calculated.

(b) From Fig. 7-13, we see that the deflection δ_c equals the distance CC' minus the distance $C'C$. The first of these distances is obtained by multiplying θ_b by the distance from B to C:

$$EI(C'C) = EI\theta_b(4 \text{ m}) = (90.67 \text{ kN}\cdot\text{m}^2)(4 \text{ m})$$

$$= 362.7 \text{ kN}\cdot\text{m}^3$$

The distance CC' is the offset of point C from the tangent at B, which is equal to the negative of the first moment of the area of the M/EI diagram between B and C, with respect to C:

$$EI(C'C) = -A_3 \left(\frac{3}{4} \right) (4 \text{ m}) = (53.33 \text{ kN}\cdot\text{m}^2)(3 \text{ m})$$

$$= 160.0 \text{ kN}\cdot\text{m}^3$$

Therefore, the deflection (times EI) is

$$EI\delta_c = EI(C'C) - EI(C'C)$$

$$= 362.7 \text{ kN}\cdot\text{m}^3 - 160.0 \text{ kN}\cdot\text{m}^3 = 202.7 \text{ kN}\cdot\text{m}^3$$

Substituting the value of EI , we get

$$\delta_c = \frac{202.7 \text{ kN}\cdot\text{m}^3}{256.0 \text{ MN}\cdot\text{m}^2} = 0.792 \text{ mm}$$

This deflection is upward, as shown in the figure.

(c) The maximum downward deflection δ_{max} occurs in span AB at a point E to be located. Let us assume that this point is between D and B. (If it is not, the calculations will so indicate, and then we can begin again by assuming that E is between A and D.) At point E, the deflection curve has a horizontal tangent.

Therefore, the area of the M/EI diagram between A and E must equal the angle of rotation θ_a . Denoting the distance from A to E by x_1 , we can write the following equation (see the last part of Fig. 7-13):

$$EI\theta_a = \frac{1}{2} (x_1)(20 \text{ kN})(x_1) - \frac{1}{2} (x_1 - 4 \text{ m})(40 \text{ kN})(x_1 - 4 \text{ m})$$

$$= x_1^2(-10 \text{ kN}) + x_1(160 \text{ kN}\cdot\text{m}) - 320 \text{ kN}\cdot\text{m}^2$$

in which x_1 has units of meters. Substituting $EI\theta_a = 189.3 \text{ kN}\cdot\text{m}^2$ into this equation, we get the following quadratic equation for x_1 :

$$x_1^2 - 16x_1 + 50.93 = 0$$

Solving by the quadratic formula, we get $x_1 = 4.385 \text{ m}$ (the other root has no physical meaning in this problem). The position of point E between D and B is now determined.

The maximum deflection δ_{max} is numerically equal to the offset of point A from the horizontal tangent at E. Therefore, we can calculate δ_{max} by taking the first moment of the area between A and E with respect to A (see the last part of Fig. 7-13):

$$EI\delta_{max} = \frac{1}{2} (x_1)(20 \text{ kN})(x_1) \left(\frac{2x_1}{3} \right)$$

$$- \frac{1}{2} (x_1 - 4 \text{ m})(40 \text{ kN})(x_1 - 4 \text{ m}) \left[4 \text{ m} + \frac{2}{3} (x_1 - 4 \text{ m}) \right]$$

Substituting $x_1 = 4.385 \text{ m}$ into the above expressions, we get

$$EI\delta_{max} = 562.2 \text{ kN}\cdot\text{m}^3 - 12.63 \text{ kN}\cdot\text{m}^3 = 549.6 \text{ kN}\cdot\text{m}^3$$

Finally, we calculate δ_{max} in numerical terms:

$$\delta_{max} = \frac{549.6 \text{ kN}\cdot\text{m}^3}{256.0 \text{ MN}\cdot\text{m}^2} = 2.15 \text{ mm}$$

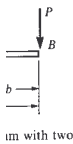
Thus, the maximum downward deflection of the beam has been determined.

In this example, we relied on the geometry of the deflection curve to obtain the desired relationships between angles of rotation and deflections. Such a common-sense procedure often is more efficient than using the proper sign conventions associated with the moment-area theorems.

7.6 METHOD OF SUPERPOSITION

The differential equations of the deflection curve of a beam (Eqs. 7-10) are linear differential equations; that is, all terms containing the deflection v and its derivatives are raised to the first power only. Therefore, solutions of the equations for various loading conditions may be superimposed. Thus, the deflection of the beam caused by several different loads acting simultaneously can be found by superimposing the deflections caused by the loads acting separately. For instance, if v_1 , v_2 ,

flections of Beams



resents the deflection due to a load q_1 and if v_2 represents the deflection due to a load q_2 , the total deflection produced by q_1 and q_2 acting simultaneously is $v_1 + v_2$.

To illustrate this idea, consider the cantilever beam shown in Fig. 7-14. This beam supports a uniform load of intensity q over part of the span and a concentrated load P acting at the end. Assume that we want to find the deflection δ_b at the free end. When the load P acts alone, the deflection at B is $PL^3/3EI$, as shown in Example 1 of the preceding section (Eq. 7-39). Also, due to the uniform load acting alone, the deflection is $qa^3(4L - a)/24EI$, as obtained in Example 2 of the preceding section (Eq. 7-41). Hence, the deflection δ_b due to the combined loading is

$$\delta_b = \frac{PL^3}{3EI} + \frac{qa^3(4L - a)}{24EI} \quad (7-49)$$

The deflection and angle of rotation at any point of the beam can be found by this procedure.

The method of superposition is most useful when the loading system on the beam can be subdivided into loading conditions that produce deflections that are already known, as illustrated in the example just given. For convenient use in cases of this kind, tables of beam deflections are given in Appendix G. Using these tables and the method of superposition, we can find deflections and angles of rotation for many different loading conditions for beams. Some additional examples of this type are given at the end of this section.

Superposition may also be used for distributed loadings by considering an element of the distributed load as if it were a concentrated load and then integrating throughout the region of the load. This procedure can be easily understood from the example shown in Fig. 7-15. The load on the simple beam AB is triangularly distributed over the left-hand half of the beam, and we will assume that the deflection δ at the midpoint is to be found. An element $q dx$ of the distributed load can be visualized as a concentrated load. The deflection at the midpoint produced by a concentrated load P acting at distance x from the left end is

$$\frac{Px}{48EI} (3L^2 - 4x^2)$$

which is obtained from Case 5 of Table G-2 in Appendix G. Substituting $q dx$ for P in this expression, and noting that $q = 2q_0x/L$, we obtain for the deflection

$$\delta = \int_0^{L/2} \frac{q_0 x dx}{48EI} (3L^2 - 4x^2) = \frac{q_0}{24LEI} \int_0^{L/2} (3L^2 - 4x^2)x^2 dx = \frac{q_0 L^4}{240EI} \quad (7-50)$$

By this same procedure of superimposing elements of the distributed load, we can calculate the angle of rotation θ_a at the left end of the beam. The expression for this angle due to a concentrated load P (see Case 5 of Table G-2) is

$$\frac{Pab(L + b)}{6LEI}$$

In this expression, we must replace P with $2q_0x dx/L$, a with x , and b with $L - x$; thus:

$$\theta_a = \int_0^{L/2} \frac{2q_0x dx}{3L^2EI} (x)(L - x)(2L - x) = \frac{41q_0L^3}{2880EI} \quad (7-51)$$

Another illustration of this technique is given in Example 2.

In each of the preceding illustrations, we have used the principle of superposition to obtain deflections of beams. This concept is widely used in mechanics and is valid whenever the quantity to be determined is a linear function of the applied loads. Under such conditions, the desired quantity may be found due to each load acting separately, and then the results may be superimposed to obtain the total value due to all loads acting simultaneously. In the case of deflections of beams, the principle of superposition is valid if Hooke's law holds for the material and if the deflections and rotations of the beam are small. The requirement of small deflections ensures that the differential equation of the deflection curve is linear, and the requirement of small deflections ensures that the lines of action of the loads and reactions are not changed significantly from their original positions.

The following examples further illustrate the use of the principle of superposition for calculating deflections of beams.

Example 1

A simple beam AB is acted upon by couples M_0 and $2M_0$ at the ends (see Fig. 7-16). Obtain expressions for the angles of rotation θ_a and θ_b at the ends of the beam and the deflection δ at the middle.

Using Case 7 of Table G-2, we obtain by superposition

$$\theta_a = \frac{M_0L}{3EI} + \frac{(2M_0)L}{6EI} = \frac{2M_0L}{3EI}$$

$$\theta_b = \frac{M_0L}{6EI} + \frac{(2M_0)L}{3EI} = \frac{5M_0L}{6EI}$$

$$\delta = \frac{M_0L^2}{16EI} + \frac{(2M_0)L^2}{16EI} = \frac{3M_0L^2}{16EI}$$

Thus, the required quantities have been found.

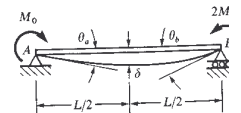
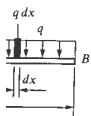


Fig. 7-16 Example 1. Simple beam with couples acting at the ends

7.7 Deflections of Beams



Example 2. Cantilever beam with uniform load over one-half of its length

Example 2

A cantilever beam AB carries a uniform load of intensity q over the right-hand half of its length, as shown in Fig. 7-17. Find the deflection δ_b and the angle of rotation θ_a at the free end.

We begin by considering an element $q dx$ of the load located at distance x from the support. This element of load produces a deflection $d\delta$ and an angle $d\theta$ at the free end equal to

$$d\delta = \frac{(q dx)(x^2)(3L - x)}{6EI} \quad d\theta = \frac{(q dx)(x^2)}{2EI}$$

as found from Case 5 of Table G-1. Hence, by integrating, we get

$$\delta_b = \frac{q}{6EI} \int_{L/2}^L x^2(3L - x) dx = \frac{41qL^4}{384EI} \quad (7-52)$$

$$\theta_a = \frac{q}{2EI} \int_{L/2}^L x^2 dx = \frac{7qL^3}{48EI} \quad (7-53)$$

These same results can be obtained more simply by using the formulas in Case 3 of Table G-1 and substituting $a = b = L/2$.

Example 3

A simple beam with an overhang is loaded as shown in Fig. 7-18a. Find the deflection δ_c at the end of the overhang.

The deflection of point C is made up of two parts: (1) a deflection δ_1 caused by the rotation of the beam axis at support B and (2) a deflection δ_2 caused by the bending of part BC acting as a cantilever beam. To obtain the first part of the deflection, we observe that portion AB of the beam is in the same condition as a simple beam carrying a uniform load and subjected to a couple M_b (equal to $qa^2/2$) and a vertical load (equal to qa) acting at the right-hand end, as shown in Fig. 7-18b. The angle θ_b at end B (see Cases 1 and 7 of Table G-2) is:

$$\theta_b = \frac{qL^3}{24EI} + \frac{M_bL}{3EI} = \frac{qL(4a^2 - L^2)}{24EI}$$

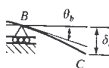
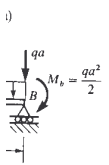
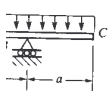
in which clockwise rotation is positive. The deflection δ_1 of point C , due to the rotation at B , is equal to $a\theta_b$, or

$$\delta_1 = \frac{qaL(4a^2 - L^2)}{24EI}$$

This deflection is positive when downward.

The bending of the overhang itself produces a downward deflection δ_2 at C . This deflection is equal to the deflection of a cantilever beam of length a (see Case 1 of Table G-1):

$$\delta_2 = \frac{qa^4}{8EI}$$



3. Simple beam

total deflection of point C , assumed to be positive when downward, is

$$\delta_c = \delta_1 + \delta_2 = \frac{qa}{24EI} (3a^3 + 4a^2L - L^3) \quad (7-54)$$

From this result, we can show that, when a is less than $L(\sqrt{13} - 1)/6$, or $0.434L$, the deflection δ_c is negative and point C deflects upward.

The shape of the deflection curve for the beam in this example is shown in Fig. 7-18c for the case where a is large enough ($a > 0.434L$) to produce a downward deflection at C and small enough ($a < L$) to ensure that the reaction at A is upward. Under these conditions the beam has a positive bending moment from A to a point such as D ; hence, the deflection curve is convex downward in this part of the beam. From D to C , the bending moment is negative, and the deflection curve is convex upward. Point D , at which the curvature of the axis of the beam is zero (because the bending moment is zero), is a point of inflection. The curvature of the deflection curve changes sign at this point.

Example 4

Determine the deflection δ_b at the hinge B for the compound beam shown in Fig. 7-19. Note that the beam is composed of two parts: (1) a beam AB , simply supported at A , and (2) a cantilever beam BC , fixed at C . The two beams are linked together by a pin connection at B .

Considering beam AB as a free body, we see that it has vertical reactions $P/3$ and $2P/3$ at ends A and B , respectively. Therefore, beam BC is in the condition of a cantilever beam subjected to a uniform load of intensity q and a concentrated load at the end equal to $2P/3$. The deflection of the end of this cantilever, which is the same as the deflection of the hinge, is

$$\delta_b = \frac{qb^4}{8EI} + \frac{2Pb^3}{9EI}$$

as found from Cases 1 and 4 of Table G-1.

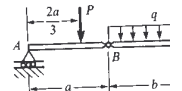
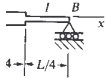


Fig. 7-19 Example 4. Compound beam with a hinge

7.7 NONPRISMATIC BEAMS

The methods presented in the preceding sections for calculating deflections of prismatic beams (that is, beams with constant cross sections throughout their lengths) can also be used to find deflections of nonprismatic beams. Such beams include those with different cross-sectional areas in various parts of the beam (see Fig. 7-20 for an example) and tapered beams (see Fig. 7-21). When a beam has abrupt changes in cross-sectional dimensions, there are local stress concentrations at the points where changes occur; however, these local stresses have no noticeable effect on the calculation of deflections. For a tapered beam, the bending theory derived previously for a prismatic beam gives satisfactory results provided that the angle of taper is small.



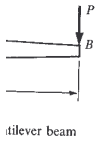
The first method for finding deflections is integration of the differential equation of the deflection curve. To illustrate this method, consider the example pictured in Fig. 7-20a. This beam is assumed to be reinforced along its central region so that the moment of inertia in that part of the beam is twice the moment of inertia in the end regions. The differential equation of the deflection curve in terms of bending moment (Eq. 7-5) for the left-hand half of the beam may be written in two parts, as follows:

$$EIv'' = -\frac{Px}{2} \quad \left(0 \leq x \leq \frac{L}{4}\right) \quad (a)$$

$$E(2I)v'' = -\frac{Px}{2} \quad \left(\frac{L}{4} \leq x \leq \frac{L}{2}\right) \quad (b)$$



beam with two different moments of inertia



cantilever beam

Each of these equations can be integrated twice to obtain expressions for the slopes and the deflections. The four constants of integration can be found from the following conditions: (1) at $x = 0$, $v = 0$; (2) at $x = L/2$, $v' = 0$; (3) at $x = L/4$, the slope of the beam obtained from Eq. (a) is equal to the slope obtained from Eq. (b); and (4) at $x = L/4$, the deflection obtained from Eq. (a) is equal to the deflection obtained from Eq. (b). Having found the constants of integration from these conditions, we then will know the deflection curve of the beam for each of the two regions under consideration.

The use of the differential equation for finding deflections is practical only if the number of equations to be solved is limited to one or two and only if the integrations are easily performed, as in the preceding illustration. In the case of a tapered beam (Fig. 7-21), it may be difficult (or even impossible) to solve the differential equation mathematically. The reason is that the expression for the moment of inertia I as a function of x is often complicated and produces a differential equation with a variable coefficient instead of constant coefficients.

The method of integration for nonprismatic beams should be performed in most cases with the moment equation (Eq. 7-10a) rather than with the shear and load equations (Eqs. 7-10b and c). The reason is that the moment equation can be written in the following simple form:

$$v'' = -\frac{M}{EI_x} \quad (7-5)$$

in which I_x is the moment of inertia of the cross section at distance x from the origin of coordinates. If the right-hand side of Eq. (7-5) can be integrated, then the method of integration is feasible. However, the shear and load equations are obtained by differentiating Eq. (7-5), which leads to much more complicated differential equations when I_x is also a variable and must be differentiated.

The second method for finding deflections is the moment-area method. The use of this method is illustrated in Fig. 7-20 for the beam discussed previously. The bending-moment diagram for the beam is given in Fig. 7-20b and the M/EI diagram in Fig. 7-20c. The areas and

moments of the various parts of the M/EI diagram are used to find the angles of rotation and the deflections. For example, let us find the angle of rotation at the left-hand support and the deflection at the middle of the beam. From the symmetry of the beam, we know that the tangent to the deflection curve at the center C is horizontal. It follows from the first moment-area theorem that the angle of rotation θ_a at the left support is equal to the area of the M/EI diagram between points A and C . Therefore, this angle is obtained as follows:

$$\theta_a = (\text{area of triangle}) + (\text{area of trapezoid})$$

$$= \frac{1}{2} \left(\frac{L}{4}\right) \left(\frac{PL}{8EI}\right) + \frac{1}{2} \left(\frac{PL}{16EI} + \frac{PL}{8EI}\right) \left(\frac{L}{4}\right) = \frac{5PL^2}{128EI} \quad (c)$$

The offset of point A from a tangent to the deflection curve at point C , which is equal to the deflection δ_c at the middle of the beam, is obtained by taking the first moment of the area of the M/EI diagram between A and C about point A , in accordance with the second moment-area theorem. Thus,

$$\delta_c = (\text{first moment of triangle}) + (\text{first moment of trapezoid})$$

$$= \left(\frac{2}{3}\right) \left(\frac{L}{4}\right) \left(\frac{PL^2}{64EI}\right) + \left(\frac{L}{4} + \frac{5L}{36}\right) \left(\frac{3PL^2}{128EI}\right) = \frac{3PL^3}{256EI} \quad (d)$$

This example shows that the use of the moment-area theorem for nonprismatic beams is similar to that for prismatic beams.

Another method for finding deflections is the method of superposition. To illustrate this method for a nonprismatic beam, consider the cantilever beam of Fig. 7-22 and assume that we wish to calculate the deflection δ_a at the free end. This deflection can be obtained in two steps. First, we imagine that the beam is held rigidly at point C , so that it neither deflects nor rotates at that point. Then we can calculate the deflection of A due to bending of AC as a cantilever beam. Since this beam has length $L/2$ and moment of inertia I , its deflection δ_1 is

$$\delta_1 = \frac{P(L/2)^3}{3EI} = \frac{PL^3}{24EI}$$

In addition, part CB of the beam also behaves like a cantilever (Fig. 7-22b) and contributes to the deflection of point A . The deflection δ_c and angle of rotation θ_c of the free end of this cantilever are

$$\delta_c = \frac{P(L/2)^3}{3(2EI)} + \frac{(PL/2)(L/2)^2}{2(2EI)} = \frac{5PL^3}{96EI}$$

$$\theta_c = \frac{P(L/2)^2}{2(2EI)} + \frac{(PL/2)(L/2)}{2EI} = \frac{3PL^2}{16EI}$$

The deflection δ_c and angle of rotation θ_c make an additional contribution δ_2 to the deflection under the load P , as follows:

$$\delta_2 = \delta_c + \theta_c \left(\frac{L}{2}\right) = \frac{7PL^3}{48EI}$$

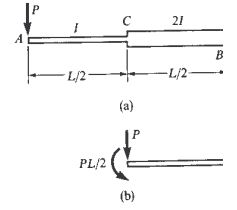


Fig. 7-22 Cantilever beam with two different moments of inertia

Therefore, the total deflection of the free end A is

$$\delta_a = \delta_1 + \delta_2 = \frac{3PL^3}{16EI}$$

Thus, the techniques of the method of superposition may be readily adapted to certain kinds of nonprismatic beams, as this example shows. The choice of method to be used for finding deflections of nonprismatic beams and the details of the procedure depend upon the problem to be solved and the preferences of the analyst.

7.8 STRAIN ENERGY OF BENDING

The concept of strain energy was explained previously in our discussions of axially loaded members and bars in torsion (see Sections 2.8 and 3.8, respectively). Now we will apply those concepts to bending of beams. Only beams that behave in a linear elastic manner are considered; hence, the material must follow Hooke's law and the deflections and rotations must be small.

Let us begin with a beam in pure bending subjected to couples M (Fig. 7-23a). The deflection curve is a circular arc of constant curvature $\kappa = -M/EI$ (see Eq. 7-5). The angle θ subtended by this arc equals L/ρ , where L is the length of the beam and ρ is the radius of curvature; thus, considering only absolute values, we obtain

$$\theta = \frac{ML}{EI} \quad (7-56)$$

This linear relationship between the couples M and the angle θ is shown graphically in Fig. 7-23b by line OA on the moment-rotation diagram. As the bending couples are gradually increased in magnitude from zero to their maximum values M , they perform work W represented by the area below line OA (the shaded area in Fig. 7-23b). This work, which is equal to the strain energy U stored in the beam, is

$$U = W = \frac{M\theta}{2} \quad (7-57)$$

This equation is analogous to Eqs. (2-38) and (3-39) for the strain energies in axial load and torsion, respectively.

By combining Eqs. (7-56) and (7-57), we can express the strain energy stored in a beam in pure bending in either of the following forms:

$$U = \frac{M^2 L}{2EI} \quad U = \frac{EI\theta^2}{2L} \quad (7-58a, b)$$

Each of these equations expresses the strain energy in terms of the bending moment M and the second expresses it in terms of the angle θ . The equations are similar in form to those for strain energy in axial load and torsion (see Eqs. 2-39 and 3-38, respectively).

If the bending moment M varies along the length of the beam (nonuniform bending), then we may obtain the strain energy by applying Eq. (7-58) to an element of length dx subjected to a moment M (Fig. 7-24). Considering an element of length dx subjected to a moment M (Fig. 7-24), we note that the angle $d\theta$ between the sides of the element (see Eq. 7-6) is

$$d\theta = \frac{d^2v}{dx^2} dx = \frac{M dx}{EI}$$

in which only absolute values are considered. Thus, the strain energy dU stored in the element (from Eqs. 7-58) is

$$dU = \frac{M^2 dx}{2EI} \quad \text{or} \quad dU = \frac{EI}{2} \left(\frac{d^2v}{dx^2}\right)^2 dx$$

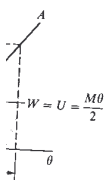
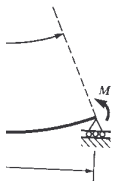
By integrating the preceding equations, we can express the total strain energy stored in the beam in either of the following forms:

$$U = \int \frac{M^2 dx}{2EI} \quad U = \int \frac{EI}{2} \left(\frac{d^2v}{dx^2}\right)^2 dx \quad (7-59a, b)$$

in which the integrations are carried out over the length of the beam. The first equation is used when the bending moment is known, and the second is used when the equation of the deflection curve is known.

Equations (7-59) give the strain energy in a beam when only the effects of bending moments are taken into account. In addition to the strain energy of bending, strain energy of shear will be stored in the elements of the beam; this strain energy is discussed in Section 7.12. However, for beams of usual proportions in which the lengths are much greater than the depths (say, $L/d > 6$), the strain energy of shear is relatively small in comparison with the strain energy of bending and may be disregarded.

Principles of mechanics based upon strain energy have an important role in structural analysis and in the design of structures to resist dynamic loads. Some of these principles are discussed in Chapter 12. In this section, however, we are concerned primarily with evaluating strain energy in beams and then using the strain energy to solve simple deflection and impact problems. For instance, if a beam is subjected to only one concentrated load P or one couple M_0 , we can find the deflection δ or the angle of rotation θ at the point where the load acts, in the direction of the load, by equating the work done by the load ($P\delta/2$ or $M_0\theta/2$) to the strain energy of the beam. This same technique was dis-



pure bending by a moment showing the strain energy of bending and rotation θ

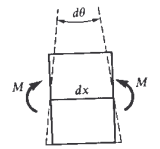


Fig. 7-24 Element of a beam

discussed in Section 2.8. However, the method is limited in its usefulness because there can be only one load on the structure, and the only deflection that can be found is the one corresponding to that load.

Example 1

Determine the strain energy U stored in a cantilever beam of length L carrying a concentrated load P at the free end (Fig. 7-25a). Also, find the vertical deflection δ_b at the free end.

The bending moment at a cross section located at distance x from the free end is $M = -Px$. Substituting this expression for M into Eq. (7-59a) gives

$$U = \int_0^L \frac{M^2 dx}{2EI} = \int_0^L \frac{(-Px)^2 dx}{2EI} = \frac{P^2 L^3}{6EI} \quad (a)$$

as the strain energy of the beam. Note that the strain energy is always a positive quantity and that the load appears to the second power.

To obtain the deflection under the load P , we equate the work done by the load with the strain energy:

$$\frac{P\delta_b}{2} = \frac{P^2 L^3}{6EI}$$

from which

$$\delta_b = \frac{PL^3}{3EI} \quad (b)$$

This expression agrees with the result obtained in Example 1, Section 7.5 (see Eq. 7-39). Again, it is important to observe that the only deflection we can find in this example is the deflection corresponding to P (that is, the downward deflection at the free end).

Example 2

The cantilever beam shown in Fig. 7-25b is subjected to a couple M_0 acting at the free end. Determine the strain energy U of the beam and the angle of rotation θ_b at the free end.

In this case the bending moment is constant and is equal to $-M_0$; hence, from Eq. (7-59a) we obtain

$$U = \int_0^L \frac{M^2 dx}{2EI} = \int_0^L \frac{(-M_0)^2 dx}{2EI} = \frac{M_0^2 L}{2EI} \quad (c)$$

The work done by the couple M_0 during loading of the beam is $M_0\theta_b/2$; hence,

$$\frac{M_0\theta_b}{2} = \frac{M_0^2 L}{2EI}$$

and

$$\theta_b = \frac{M_0 L}{EI} \quad (d)$$

The angle of rotation has the same sense as the moment, which is clockwise for this beam.

Example 3

In this example the cantilever beam is subjected simultaneously to both a concentrated load P and a couple M_0 (Fig. 7-25c). Determine the strain energy U of the beam.

The bending moment in the beam is given by the expression

$$M = -Px - M_0$$

where x is measured from the free end. Therefore, the strain energy is

$$U = \int_0^L \frac{M^2 dx}{2EI} = \frac{1}{2EI} \int_0^L (-Px - M_0)^2 dx$$

$$= \frac{P^2 L^3}{6EI} + \frac{PM_0 L^2}{2EI} + \frac{M_0^2 L}{2EI} \quad (e)$$

The first term in the last expression gives the strain energy due to P acting alone ($M_0 = 0$) and the last term gives the strain energy due to M_0 alone ($P = 0$). However, when both loads act simultaneously, the term in the middle also appears in the expression for strain energy. This result shows that the strain energy in a structure due to two or more loads cannot be obtained by adding the strain energies due to the loads acting separately. The explanation is that strain energy is a quadratic function of the loads, not a linear function; hence, the principle of superposition does not apply.

We also observe that we cannot calculate a deflection for the beam of Fig. 7-25c by equating work and strain energy because there are too many unknowns in the expression for work:

$$W = \frac{P\delta_b}{2} + \frac{M_0\theta_b}{2}$$

When this expression is equated with U , we have one equation with two unknowns. Hence, although the equation is quite correct, we cannot obtain any useful information from it.

Example 4

The equation of the deflection curve for a simple beam with a uniform load of intensity q (Fig. 7-26) is

$$v = \frac{qx}{24EI} (L^3 - 2Lx^2 + x^3)$$

as given in Case 1 of Table G-2. Using this expression, determine the strain energy U stored in the beam.

To obtain the strain energy, we will use Eq. (7-59b), which contains d^2v/dx^2 . Taking derivatives of the expression for v , we get

$$\frac{dv}{dx} = \frac{q}{24EI} (L^3 - 6Lx^2 + 4x^3)$$

$$\frac{d^2v}{dx^2} = -\frac{qx}{2EI} (L - x)$$

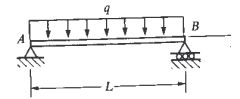


Fig. 7-26 Example 4. Strain energy of a beam

Deflections of Beams

Now substituting into Eq. (7-59b) and integrating, we obtain

$$U = \int_0^L \frac{EI}{2} \left(\frac{d^2v}{dx^2} \right)^2 dx = \frac{EI}{2} \int_0^L \left[-\frac{qx}{2EI} (L - x) \right]^2 dx = \frac{q^2 L^3}{240EI}$$

as the amount of strain energy stored in the beam. Note again that the load appears to the second power.

Deflection produced by impact.

The dynamic deflection of a beam subjected to an impact load may be determined under certain simplified conditions by equating the work done by the load with the strain energy stored in the beam. This approach was described in Section 2.9 for impact loads on an axially loaded bar. The assumptions described in that discussion apply also to beams; namely, the falling weight sticks to the beam and moves with it, no energy losses occur, the beam is linearly elastic, the deflected shape of the beam is the same under a dynamic load as under a static load, and the potential energy of the beam due to its change in position is disregarded. In general, these assumptions are reasonable if the mass of the falling object is very large compared to the mass of the beam. Otherwise, this approximate analysis is not valid and a more advanced analysis is required (Refs. 2-12 and 2-13).

As an illustration of this approach, consider a simple beam AB that is struck at the middle by a falling body of weight W (Fig. 7-27). In accord with the preceding idealizations, we may assume that all of the work done by the body during its fall is transformed into elastic strain energy of the beam. Since the distance through which it falls is $h + \delta$, where h is the initial height of the weight above the beam and δ is the maximum dynamic deflection of the beam, the work done is

$$W(h + \delta) \quad (e)$$

If we let P denote the force exerted on the beam when its deflection is a maximum, then the relationship between P and δ is

$$\delta = \frac{PL^3}{48EI} \quad \text{or} \quad P = \frac{48EI\delta}{L^3}$$

because we have assumed that the deflection shape under a dynamic load is the same as under a static load. Therefore, the strain energy of the beam, equal to the work of the force P , is

$$U = \frac{P\delta}{2} = \frac{24EI\delta^2}{L^3}$$

Equating the work done by the falling mass (Eq. g) with the strain energy gives

$$W(h + \delta) = \frac{24EI\delta^2}{L^3}$$

This equation is quadratic in δ and can be solved for its positive root:

$$\delta = \frac{WL^3}{48EI} + \left[\left(\frac{WL^3}{48EI} \right)^2 + 2h \left(\frac{WL^3}{48EI} \right) \right]^{1/2} \quad (7-60)$$

Let us denote the static deflection of the beam due to the weight W as δ_{st} :

$$\delta_{st} = \frac{WL^3}{48EI} \quad (7-61)$$

Then Eq. (7-60) for the maximum dynamic deflection can be written in simpler form as follows:

$$\delta = \delta_{st} + (\delta_{st}^2 + 2h\delta_{st})^{1/2} \quad (7-62)$$

From this equation we observe that the dynamic deflection is always larger than the static deflection. If the height $h = 0$, which means that the load is applied suddenly but without any free fall, the dynamic deflection is twice the static deflection. If h is very large compared to the deflection, then the term containing h in Eq. (7-62) predominates, and the equation can be simplified to

$$\delta = \sqrt{2h\delta_{st}} \quad (7-63)$$

These and other observations are analogous to those encountered previously for impact on a bar in tension (Section 2.9).

The deflection δ calculated from Eq. (7-62) generally represents an upper limit, because we assumed there were no losses of energy during impact. Local deformation of the contact surfaces, the tendency of the falling mass to bounce upward, and the mass of the beam itself tend to reduce the deflection.

***7.9 DISCONTINUITY FUNCTIONS**

Discontinuity functions are utilized in a variety of engineering applications, including beam analysis, electrical circuits, and heat transfer. These functions probably are the easiest to use and understand when applied to beams; hence, the study of mechanics of materials offers an excellent opportunity to become familiar with them. The mathematics of the functions are described in this section, and we also will see how the functions are used to represent loads on beams. Then, in the next section, we will use them for finding slopes and deflections of beams.



and 3. Strain



a beam

The unique feature of discontinuity functions is that they permit the writing of a discontinuous function by a single expression, whereas the more conventional approach requires that a discontinuous function be described by a series of expressions, one for each region in which the function is distinct. For instance, if the loading on a beam consists of a mixture of concentrated and distributed loads, we can write with a single continuity function a single equation that applies throughout the entire length, whereas ordinarily we must write separate equations for each segment of the beam between changes in loading. In a similar manner we can express shear forces, bending moments, slopes, and deflections of a beam by one equation each, even though there may be several changes in loads along the axis of the beam.

These results are achievable because the functions themselves are discontinuous; that is, they have different values in different regions of the independent variable. In effect, these functions can pass through discontinuities in a manner that is not possible with ordinary continuous functions. However, because they differ significantly from the functions we are accustomed to, discontinuity functions must be used with care and caution.

Two kinds of functions, called **Macaulay functions** and **singularity functions**, will be discussed in this section. Although these functions have different definitions and properties, together they form a family of **discontinuity functions**.*

Macaulay functions. Macaulay functions are used to represent quantities that "begin" at some particular point on the x axis (such as at the point $x = a$) and that have the value zero to the left of that point. For instance, one of the Macaulay functions, denoted F_1 , is defined as follows:

$$F_1(x) = \langle x - a \rangle^1 = \begin{cases} 0 & \text{when } x \leq a \\ x - a & \text{when } x \geq a \end{cases} \quad (7-64)$$

In this equation, x is the independent variable and a is the value of x at which the function "begins." The *pointed brackets* (or *angle brackets*) are the mathematical symbol for a discontinuity function. In the case of the function F_1 , the pointed brackets tell us that the function has the value zero when x is less than or equal to a (that is, when the expression within the brackets is negative or zero), and a value equal to $x - a$ when x is greater than or equal to a . A graph of this function, called the **unit ramp function**, is given in Fig. 7-28.

In general terms, the Macaulay functions are defined by the following expressions:

$$F_n(x) = \langle x - a \rangle^n = \begin{cases} 0 & \text{when } x \leq a \\ (x - a)^n & \text{when } x \geq a \end{cases} \quad (7-65)$$

$n = 0, 1, 2, 3, \dots$

* Sometimes both kinds of discontinuity functions are called *singularity functions*, but this usage obscures the distinctions between the two functions, which obey different mathematical laws. Furthermore, Macaulay functions do not have singularities.

From this definition that the Macaulay functions have the value zero to the left of the point $x = a$ and the value $(x - a)^n$ to the right of that point. Except for the case $n = 0$, which is discussed later, the function equals zero at $x = a$. Another way to express this definition is as follows: If the quantity $x - a$ within the pointed brackets is negative or zero, the Macaulay function has the value zero; if the function $x - a$ is positive or zero, the Macaulay function has the value obtained by replacing the pointed brackets with parentheses.

The preceding definition of the Macaulay functions holds for values of n equal to positive integers and zero. When $n = 0$, note that the function takes on the following special values:

$$F_0(x) = \langle x - a \rangle^0 = \begin{cases} 0 & \text{when } x \leq a \\ 1 & \text{when } x \geq a \end{cases} \quad (7-66)$$

This function has a vertical "step" at the point of discontinuity $x = a$; thus, at $x = a$ it has two values, zero and one. The function F_0 , called the **unit step function**, is pictured in Table 7-1 along with other Macaulay functions.*

The Macaulay functions of higher degree can be expressed in terms of the unit step function, as follows:

$$F_n(x) = \langle x - a \rangle^n = (x - a)^n \langle x - a \rangle^0 \quad (7-67)$$

This equation is easily confirmed by comparing Eqs. (7-65) and (7-66).

Some of the basic algebraic operations, such as addition, subtraction, and multiplication by a constant, can be performed on the Macaulay functions. Illustrations of these elementary operations are given in Fig. 7-29. The important thing to note from these examples is that a function y having different algebraic expressions for different regions along the x axis can be written as a single equation through the use of Macaulay functions. The reader should verify each of the graphs in Fig. 7-29 in order to become familiar with the functions.

The Macaulay functions can be integrated and differentiated according to the formulas given in the last column of Table 7-1. These formulas can be verified by ordinary differentiation and integration of the functions in the two regions $x \leq a$ and $x \geq a$.

The units of the Macaulay functions are the same as the units of x^n ; that is, F_0 is dimensionless, F_1 has units of x , F_2 has units of x^2 , and so forth.

The use of special brackets for discontinuity functions was introduced by the English mathematician W. H. Macaulay in 1919 (Ref. 7-11); hence, the brackets are often called *Macaulay's brackets*. However, Macaulay used braces $\{ \}$ to identify the functions; the pointed brackets $\langle \rangle$ in common use today were introduced at a later time. The general concept of combining two or more expressions into a single function by using a special symbol predates Macaulay's work (see Refs. 7-12 through 7-15).

* The unit step function is also known as the *Heaviside step function*, denoted by $u(x - a)$, after Oliver Heaviside (1850-1925), an English physicist and electrical engineer.

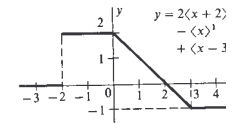
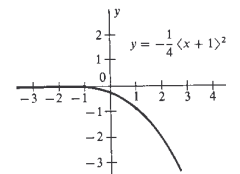
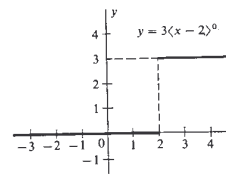
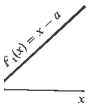


Fig. 7-29 Graphs of expressions involving Macaulay functions



Macaulay function

Singularity functions. The second kind of discontinuity functions are the singularity functions, defined by the following expressions:

$$F_n(x) = \langle x - a \rangle^n = \begin{cases} 0 & \text{when } x \neq a \\ \pm \infty & \text{when } x = a \end{cases} \quad (7-68)$$

$n = -1, -2, -3, \dots$

Note that singularity functions are defined for negative integer values of n , whereas Macaulay functions are defined for positive integers and for zero. The pointed brackets identify both kinds of functions, but the brackets have different meanings in the two cases (compare Eqs. 7-65 and 7-68).

The singularity functions have the value zero everywhere except at the singular point $x = a$. The singularities arise because, when n is a negative integer, the function $(x - a)^n$ can be written as a fraction with the expression $x - a$ in the denominator; thus, when $x = a$ the function becomes infinite.

The nature of the singularities depends upon the value of n , and the two most important cases are pictured in Table 7-1. The **unit doublet function** ($n = -2$) has a singularity that can be pictured by two arrows of infinite extent, one directed upward and the other downward, with the arrows being infinitesimally close to each other. For convenience, these arrows can be visualized as forces, and then the doublet can be represented by a curved arrow that is the moment of the two forces. This moment is equal to the product of an infinite force and a vanishingly small distance; the moment turns out to be finite and equal to unity. For this reason, the doublet is also known as the **unit moment**. (A third name in common usage is **dipole**.)

The **unit impulse function** ($n = -1$) is also infinite at $x = a$, but in a different way. It can be pictured by a single arrow, as shown in Table 7-1. If the arrow is visualized as a force, then the force has infinite intensity and acts over an infinitesimally small distance along the x axis. The force is equal to the intensity times the distance over which it acts; this product also turns out to be finite and equal to unity. Thus, the name **unit force** is sometimes used for this function.*

Singularity functions are sometimes referred to as *pathological functions* or *improper functions*, because they are neither continuous nor differentiable at $x = a$. However, singularity functions can be integrated through the singularities; the integration formula is as follows:

$$\int_{-\infty}^x F_n dx = \int_{-\infty}^x \langle x - a \rangle^n dx = \langle x - a \rangle^{n+1} = F_{n+1} \quad (7-69)$$

$n = -1, -2, -3, \dots$

* The terminology *unit impulse function* comes from the use of this function in dynamics, in which the x axis is the time axis. In physics and mathematics, this function is denoted by $\delta(x - a)$ and is called the *Dirac delta function*, named for the English theoretical physicist Paul A. M. Dirac (born in 1902) who developed it.

Table 7-1 Discontinuity functions

Name	Definition	Graph	Derivative and integral
Singularity functions	Unit doublet function $F_{-2} = \langle x - a \rangle^{-2} = \begin{cases} 0 & x \neq a \\ \pm \infty & x = a \end{cases}$		$\int_{-\infty}^x F_{-2} dx = F_{-1}$
	Unit impulse function $F_{-1} = \langle x - a \rangle^{-1} = \begin{cases} 0 & x \neq a \\ +\infty & x = a \end{cases}$		$\int_{-\infty}^x F_{-1} dx = F_0$
Macaulay functions	Unit step function $F_0 = \langle x - a \rangle^0 = \begin{cases} 0 & x \leq a \\ 1 & x \geq a \end{cases}$		$\int_{-\infty}^x F_0 dx = F_1$
	Unit ramp function $F_1 = \langle x - a \rangle^1 = \begin{cases} 0 & x \leq a \\ x - a & x \geq a \end{cases}$		$\frac{d}{dx} F_1 = F_0$ $\int_{-\infty}^x F_1 dx = \frac{F_2}{2}$
	Unit second-degree function $F_2 = \langle x - a \rangle^2 = \begin{cases} 0 & x \leq a \\ (x - a)^2 & x \geq a \end{cases}$		$\frac{d}{dx} F_2 = 2F_1$ $\int_{-\infty}^x F_2 dx = \frac{F_3}{3}$
	General Macaulay function $F_n = \langle x - a \rangle^n = \begin{cases} 0 & x \leq a \\ (x - a)^n & x \geq a \end{cases}$ $n = 0, 1, 2, 3, \dots$		$\frac{d}{dx} F_n = nF_{n-1}$ $n = 1, 2, 3, \dots$ $\int_{-\infty}^x F_n dx = \frac{F_{n+1}}{n+1}$ $n = 0, 1, 2, 3, \dots$

Note that this formula is not the same as the integration formula for the Macaulay functions, which is given in the last line of Table 7-1. Equation (7-69) shows that the integral of the unit impulse function is the unit step function, and the integral of the unit doublet function is the unit step function (see last column of Table 7-1).

The units of the singularity functions, like those of the Macaulay functions, are the same as the units of x^n . Thus, the doublet function has units of $1/x^2$ and the impulse function has units of $1/x$.

Representation of loads on beams by discontinuity functions. The discontinuity functions listed in Table 7-1 are ideally suited for representing loads on beams, such as couples, forces, uniform loads, and varying loads. The shapes of the various loading diagrams exactly match the shapes of the corresponding functions F_{-2}, F_{-1}, F_0, F_1 , and so on. It is necessary only to multiply the functions given in the table (which are the unit functions) by the appropriate loads intensities in order to obtain mathematical representations of the loads. Several standard load cases, explained in detail in the following paragraphs, are listed in Table 7-2 for ready reference. More complicated cases of loading can be handled by superposition of these elementary ones.

To explain how the expressions in Table 7-2 are obtained, let us consider first the uniform load of Case 3. This load can be expressed in terms of the unit step function F_0 (see Table 7-1), which is given by the formula

$$F_0(x) = \langle x - a \rangle^0$$

This function has the value 0 for $x \leq a$ and the value +1 for $x \geq a$. If the function is multiplied by the constant q_0 , representing intensity of uniform load, it becomes an expression for the uniformly distributed load on a beam:

$$q(x) = q_0 \langle x - a \rangle^0 \quad (a)$$

The load $q(x)$ defined by this expression has the value 0 for $x \leq a$ and the value q_0 for $x \geq a$. Thus, at $x = a$, the function equals zero if we approach from the left and equals q_0 if we approach from the right. Equation (a) is listed for Case 3 in the last column of Table 7-2. The direction of the load that is represented by Eq. (a) can be either upward or downward, depending upon the sign convention that we adopt for distributed loads. Since we assumed previously that downward uniform load is positive, the expression for $q(x)$ represents the load pictured in the middle column of the table. With our sign convention, the quantity q_0 is positive for downward load and negative for upward load.* Note that the uniform load q_0 continues indefinitely to the right along the x axis.

Cases 4 and 5 in Table 7-2 can be explained in a manner similar

* If we had assumed positive load to be upward, the equation for $q(x)$ would still be the same, but q_0 would be positive for upward load and negative for downward load because $\langle x - a \rangle^0$ equals 1 for $x \geq a$.

Table 7-2 Load intensities represented by discontinuity functions

Case	Load on beam (shown positive)	Intensity $q(x)$ of equivalent distributed load (positive downward)
1		$q(x) = P \langle x - a \rangle^{-1}$
2		$q(x) = M_0 \langle x - a \rangle^{-2}$
3		$q(x) = q_0 \langle x - a \rangle^0$
4		$q(x) = \frac{q_0}{b} \langle x - a \rangle^1$
5		$q(x) = \frac{q_0}{b^2} \langle x - a \rangle^2$
6		$q(x) = q_0 \langle x - a_1 \rangle^0 - q_0 \langle x - a_2 \rangle^0$
7		$q(x) = \frac{q_0}{b} \langle x - a_1 \rangle^1 - \frac{q_0}{b} \langle x - a_2 \rangle^1 - q_0 \langle x - a_2 \rangle^0$
8		$q(x) = q_0 \langle x - a_1 \rangle^2 - \frac{q_0}{b} \langle x - a_1 \rangle^1 + \frac{q_0}{b} \langle x - a_2 \rangle^1$

to that for Case 3, using the ramp and second-degree functions. Both loading functions continue indefinitely to the right. To define the function to do so is to give the ordinate q_0 at some arbitrarily selected point located at distance b from the point $x = a$, as shown in the table.

The loading in Case 6 is a segment of uniform load that begins at $x = a_1$ and ends at $x = a_2$. This loading can be expressed as the superposition of two loads. The first load is a uniform load of intensity q_0 that begins at $x = a_1$ and continues indefinitely to the right (see Case 3); the second load has intensity $-q_0$, begins at $x = a_2$, and also continues indefinitely to the right. Thus, the second load cancels the first load in the region to the right of the point $x = a_2$.

The loads in Cases 7 and 8 also consist of segments of distributed loads and are obtained by combining more elementary load patterns. The reader can easily verify the expressions given in the last column of the table for these two cases. More complicated loading patterns that involve distributed loads are obtained by similar techniques of superposition using the Macaulay functions.

Loads in the form of couples or forces (Cases 1 and 2) are handled by the singularity functions, with the unit doublet function representing a unit couple and the unit impulse function representing a unit force. When the unit doublet function is multiplied by M_0 , it represents a couple as an equivalent distributed load of intensity $q(x)$. The units of M_0 are force times length, and the units of the unit doublet function are length to the power -2 . Thus, their product has units of force divided by length, which are the correct units for intensity $q(x)$ of distributed load. The situation is similar for a concentrated load; the product of force P and the unit impulse function has units of load intensity. The equations for $q(x)$ given in Cases 1 and 2 are mathematical expressions that define the equivalent load intensities for a moment and a force. Their signs have physical meaning only when we adopt sign conventions for the loads themselves. We will assume that loads in the form of couples and forces are positive as shown in the table (that is, positive when counterclockwise and downward, respectively). As before, the equivalent loads $q(x)$ are positive when downward.

Example 1

The simple beam AB shown in Fig. 7-30a supports a concentrated load P and a couple M_0 . (a) Write the expression for the intensity $q(x)$ of the equivalent distributed loads acting on the beam in the region between the supports ($0 < x < L$). (b) Write the expression for the intensity $q(x)$ including the reactions ($0 \leq x \leq L$).

(a) The loads on the beam between the supports are the concentrated load P and the couple M_0 . Their equivalent distributed loads are obtained from

Cases 2 and 1, respectively, of Table 7-2. Thus, with the origin of coordinates at support A , we can write by inspection the following expression:

$$q(x) = P \langle x - \frac{L}{3} \rangle^{-1} + M_0 \langle x - \frac{2L}{3} \rangle^{-2} \quad (b)$$

This single equation gives the equivalent distributed load at any point along the axis of the beam (except at the supports). Note that each term on the right-hand side is zero everywhere except at the point where the load acts.

(b) It is sometimes desirable to include the reactions in the expression for the load $q(x)$; this expression then is valid at all points along the axis of the beam, including the end points. To obtain the expression for $q(x)$, we begin by determining the reactions from static equilibrium and showing them on a free-body diagram of the beam (Fig. 7-30b). Then we can write the expression for $q(x)$ by inspection, using Table 7-2:

$$q(x) = -\left(\frac{2P}{3} + \frac{M_0}{L}\right) \langle x \rangle^{-1} + P \langle x - \frac{L}{3} \rangle^{-1} + M_0 \langle x - \frac{2L}{3} \rangle^{-2} - \left(\frac{P}{3} - \frac{M_0}{L}\right) \langle x - L \rangle^{-1} \quad (c)$$

The last term in this equation, containing $\langle x - L \rangle^{-1}$, is zero at every point along the beam except at the right support. Hence, it has no role in calculation of the deflections and may be omitted.

In the next section, we will integrate equations for the load $q(x)$, such as Eqs. (b) and (c), to obtain successively the shear forces, bending moments, slopes, and deflections of beams in terms of discontinuity functions.

Example 2

A cantilever beam AB supports a distributed load of varying intensity as shown in Fig. 7-31a. (a) Write the expression for the intensity $q(x)$ of the distributed load acting on the beam to the right of the support. (b) Write the expression for the intensity $q(x)$ including the reactions.

(a) The loads on the beam can be divided into two parts, a uniform load acting from $x = L/3$ to $x = L$ and a triangular load acting from $x = 2L/3$ to $x = L$. Thus, using Cases 6 and 7 of Table 7-2, we get

$$q(x) = q_1 \langle x - \frac{L}{3} \rangle^0 - q_1 \langle x - L \rangle^0 + \frac{3(q_2 - q_1)}{L} \langle x - \frac{2L}{3} \rangle^1 - \frac{3(q_2 - q_1)}{L} \langle x - L \rangle^1 - (q_2 - q_1) \langle x - L \rangle^0$$

The three terms containing $\langle x - L \rangle$ are zero at every point along the axis of the beam; hence, they have no physical meaning and will not affect the calculation of the deflections. Thus, those terms may be omitted, and the expression for $q(x)$ becomes

$$q(x) = q_1 \langle x - \frac{L}{3} \rangle^0 + \frac{3(q_2 - q_1)}{L} \langle x - \frac{2L}{3} \rangle^1$$

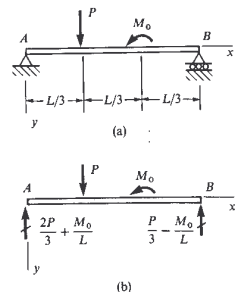


Fig. 7-30 Example 1. Representation of loads by discontinuity functions

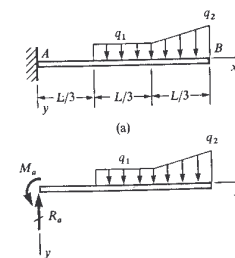


Fig. 7-31 Example 2. Representation of loads by discontinuity functions

As a check on this expression, we can substitute specific values of x and determine the load. For instance, if $x = L/6$, we get $q(x) = 0$; if $x = L/2$, we get $q(x) = q_1$; if $x = L$, we get $q(x) = q_1 + (3/L)(q_2 - q_1)(L - 2L/3) = q_2$; and so on.

(b) To obtain an expression for $q(x)$ that includes the reactions, we draw the free-body diagram of Fig. 7-31b. The vertical reaction R_a and the moment reaction M_a at support A are

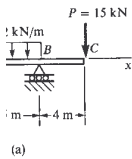
$$R_a = \frac{(3q_1 + q_2)L}{6} \quad M_a = \frac{4(2q_1 + q_2)L^2}{27} \quad (d)$$

Using Table 7-2, we obtain the following expression for $q(x)$:

$$q(x) = -R_a \langle x \rangle^{-1} + M_a \langle x \rangle^{-2} + q_1 \left\langle x - \frac{L}{3} \right\rangle^0 + \frac{3(q_2 - q_1)}{L} \left\langle x - \frac{2L}{3} \right\rangle^1$$

To put this equation in final form, we merely substitute the expressions for R_a and M_a from Eqs. (d).

Example 3



A beam ABC with simple supports at A and B and an overhang from B to C (Fig. 7-32a) supports a uniform load $q = 12 \text{ kN/m}$ over part of the span and a concentrated load $P = 15 \text{ kN}$ at the free end. Write the expression for the intensity $q(x)$ of the equivalent distributed loads acting on the beam.

We begin by calculating the reactions of the beam, which are shown on the free-body diagram of Fig. 7-32b. Also, we take the origin of coordinates at support A . Then we can write the expression for $q(x)$ with the aid of Table 7-2, as follows:

$$q(x) = -(9 \text{ kN}) \langle x \rangle^{-1} + (12 \text{ kN/m}) \langle x - 5 \text{ m} \rangle^0 - \langle x - 10 \text{ m} \rangle^0 - (66 \text{ kN}) \langle x - 10 \text{ m} \rangle^{-1} + (15 \text{ kN}) \langle x - 14 \text{ m} \rangle^{-1}$$

in which x has units of meters. The last term equals zero at all points along the beam except at the right end; hence, it may be omitted. Also, it is cumbersome to write the units with every term. Hence, in practical calculations we would write $q(x)$ as

$$q(x) = -9 \langle x \rangle^{-1} + 12 \langle x - 5 \rangle^0 - 12 \langle x - 10 \rangle^0 - 66 \langle x - 10 \rangle^{-1}$$

and we would accompany this equation with the following note:

x has units of meters
 $q(x)$ has units of kN/m

Without this note, the equation could easily be misinterpreted and erroneous results could be obtained.

Example 3. Representation of discontinuity functions

10 USE OF DISCONTINUITY FUNCTIONS TO OBTAIN BEAM DEFLECTIONS

In the conventional integration method for finding beam deflections (see Eqs. 7-10 and Sections 7.3 and 7.4), we write an expression for the load q , shear force V , or bending moment M for each segment of the beam between points where the load changes. These expressions are then integrated separately for each segment of the beam. Both boundary and continuity conditions are needed in order to evaluate the resulting constants of integration. Thus, this method of integration is quite satisfactory for very simple loadings but is likely to become unwieldy if the number of segments exceeds two. The use of discontinuity functions makes it possible to write one expression that is valid throughout the entire length of the beam. When this expression is integrated, only one constant of integration appears. Thus, in certain types of problems, the use of discontinuity functions can be very helpful.

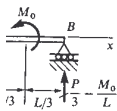
The procedure for the use of discontinuity functions is quite straightforward. First, we write the expression for the equivalent distributed load $q(x)$, using the techniques described in the preceding section. This expression is then substituted into the differential equation of the deflection curve (Eq. 7-10c). Next, the differential equation is integrated successively to obtain the shear force V , the bending moment M , the slope v' , and the deflection v . Each integration produces one constant of integration, which can be evaluated from known boundary conditions. Thus, we ultimately arrive at a single expression that gives the deflection v at every point of the beam. We need not integrate a separate differential equation for each segment of the beam, because the use of discontinuity functions makes it possible to integrate across discontinuities and singularities without introducing conditions of continuity of slope and deflection. Continuity of slopes and deflections is ensured automatically by the integration process.

The discontinuity method for obtaining beam deflections is also called **Clebsch's method**, after the German engineer who developed it in 1883 (Refs. 7-12 through 7-15). There are many variations in the details of the procedure, depending upon the particular beam being analyzed as well as the personal preferences of the analyst. Some of these variations are brought out in the examples that follow; others will be encountered in the problems. The analysis may begin with the load, shear-force, or bending-moment equation (Eqs. 7-10a, b, or c); however, in our examples we will start with the load equation because the solution then automatically includes the other two equations.

Example 1

Obtain the equation of the deflection curve for a simple beam AB supporting a concentrated load P and a couple M_0 (Fig. 7-33).

Deflections of Beams



Example 1. Discontinuity

We will begin by setting up the differential equation of the deflection curve in terms of the distributed load q (Eq. 7-10c). With the origin of coordinates at end A , the loads P and M_0 can be expressed in terms of an equivalent distributed load $q(x)$ as follows:

$$q(x) = P \left\langle x - \frac{L}{3} \right\rangle^{-1} + M_0 \left\langle x - \frac{2L}{3} \right\rangle^{-2}$$

(see Eq. b of Example 1, Section 7.9). Therefore, the differential equation becomes

$$EIv'''' = q = P \left\langle x - \frac{L}{3} \right\rangle^{-1} + M_0 \left\langle x - \frac{2L}{3} \right\rangle^{-2} \quad (b)$$

Integration of this equation yields

$$EIv''' = -V = P \left\langle x - \frac{L}{3} \right\rangle^0 + M_0 \left\langle x - \frac{2L}{3} \right\rangle^{-1} + C_1 \quad (c)$$

The constant of integration is evaluated from a condition on the shear force. Let us use the shear condition at the left end of the beam, namely, when $x = 0$ (or, more precisely, when x is slightly greater than zero), the shear force equals the reaction R_a ; thus,

$$V(0) = R_a = \frac{2P}{3} + \frac{M_0}{L}$$

Applying this condition to Eq. (c), we obtain

$$C_1 = -R_a = -\left(\frac{2P}{3} + \frac{M_0}{L}\right)$$

Hence, we get

$$EIv''' = -V = -\left(\frac{2P}{3} + \frac{M_0}{L}\right) + P \left\langle x - \frac{L}{3} \right\rangle^0 + M_0 \left\langle x - \frac{2L}{3} \right\rangle^{-1} \quad (d)$$

as the differential equation in terms of the shear force.

Instead of beginning with Eq. (a), which represents only the applied loads between the supports, we could have started the analysis with an expression for $q(x)$ that contains the reactions in addition to the loads. For the beam of Fig. 7-33, this expression was obtained in the preceding section (see Eq. c in Example 1, Section 7.9). Using that expression for $q(x)$, we get the following differential equation:

$$EIv'''' = q = -\left(\frac{2P}{3} + \frac{M_0}{L}\right) \langle x \rangle^{-1} + P \left\langle x - \frac{L}{3} \right\rangle^{-1} + M_0 \left\langle x - \frac{2L}{3} \right\rangle^{-2} - \left(\frac{P}{3} - \frac{M_0}{L}\right) \langle x - L \rangle^{-1} \quad (e)$$

The last term in this equation, representing the reaction at support B , is zero at every point along the axis of the beam up to the support. Because this term will have no effect on the calculation of shear forces, bending moments, slopes, and

... of the beam, it can be omitted. Then we proceed to integrate Eq. (e) to obtain the equation for the shear force:

$$EIv''' = -V = -\left(\frac{2P}{3} + \frac{M_0}{L}\right) \langle x \rangle^0 + P \left\langle x - \frac{L}{3} \right\rangle^0 + M_0 \left\langle x - \frac{2L}{3} \right\rangle^{-1} + C_1 \quad (f)$$

The constant of integration can be evaluated from the known shear force at any point along the beam; for variety, let us evaluate it at a point just to the left of support B :

$$V(L) = R_a - P = \frac{2P}{3} + \frac{M_0}{L} - P$$

Then from Eq. (f) we find

$$-\left(\frac{2P}{3} + \frac{M_0}{L} - P\right) = -\left(\frac{2P}{3} + \frac{M_0}{L}\right) + P(1) + M_0(0) + C_1$$

from which $C_1 = 0$. We could have anticipated this result, because, when the expression for $q(x)$ includes all forces (both loads and reactions), no constant of integration is required. Also, we note that the term $\langle x \rangle^0$ in Eq. (f) is equal to unity at every point along the axis of the beam. Therefore, substituting 1 for $\langle x \rangle^0$ and 0 for C_1 into Eq. (f), we get

$$EIv''' = -V = -\left(\frac{2P}{3} + \frac{M_0}{L}\right) + P \left\langle x - \frac{L}{3} \right\rangle^0 + M_0 \left\langle x - \frac{2L}{3} \right\rangle^{-1} \quad (g)$$

which is identical to Eq. (d).

Thus, the two preceding methods lead to the same equation for the shear force. One method begins with an equation for the loads only, after which the shear force is evaluated from a boundary condition; the other method begins with an equation that includes the reactions but requires no boundary condition. The two methods differ only in the details, and the choice between them is a matter of individual preference.

Now let us examine Eq. (g) for the shear force. The first term on the right-hand side is the shear force due to the reaction R_a , and the second term is the shear force due to the load P . In an ordinary analysis using free-body diagrams, these two terms would be the only ones to appear in an expression for V . The third term, involving the couple M_0 , represents a singularity in the shear-force diagram. This term is present because the action of the couple M_0 , applied at a point, must produce concentrations of shear force. However, this term has no effect on the construction of the shear-force diagram; for all practical purposes, it can be disregarded when considering the shear force. Nevertheless, the term must be retained in the equation, because it affects the next integration, which gives the bending moment.

A second integration of the differential equation produces the equation for the bending moment M :

$$EIv'' = -M = -\left(\frac{2P}{3} + \frac{M_0}{L}\right)x + P \left\langle x - \frac{L}{3} \right\rangle^1 + M_0 \left\langle x - \frac{2L}{3} \right\rangle^0 + C_2 \quad (h)$$

We can evaluate the constant C_2 from the known bending moment at the end of the beam. At the left end we have $M(0) = 0$, from which we get $C_2 = 0$. Again we could have anticipated this result, because, when we get $C_2 = 0$, the shear force includes the effects of all loads and reactions (both forces and couples), no constant of integration is required.

Note that we could have obtained Eq. (h) for the bending moment directly from free-body diagrams and static equilibrium; then we could have started the deflection analysis with the second-order differential equation (Eq. 7-10a).

The slopes and deflections of the beam are obtained by two more integrations, each of which requires the introduction of a constant of integration:

$$EIv' = -\left(\frac{2P}{3} + \frac{M_0}{L}\right)\frac{x^2}{2} + \frac{P}{2}\left\langle x - \frac{L}{3} \right\rangle^2 + M_0\left\langle x - \frac{2L}{3} \right\rangle + C_3$$

$$EIv = -\left(\frac{2P}{3} + \frac{M_0}{L}\right)\frac{x^3}{6} + \frac{P}{6}\left\langle x - \frac{L}{3} \right\rangle^3 + \frac{M_0}{2}\left\langle x - \frac{2L}{3} \right\rangle^2 + C_3x + C_4$$

The two additional boundary conditions are $v(0) = 0$ and $v(L) = 0$

from which we find

$$C_4 = 0 \quad C_3 = \frac{5PL^2}{81} + \frac{M_0L}{9}$$

Hence, the final equations for the slope and deflection are

$$EIv' = -\left(\frac{2P}{3} + \frac{M_0}{L}\right)\frac{x^2}{2} + \frac{P}{2}\left\langle x - \frac{L}{3} \right\rangle^2 + M_0\left\langle x - \frac{2L}{3} \right\rangle + \frac{5PL^2}{81} + \frac{M_0L}{9}$$

$$EIv = -\left(\frac{2P}{3} + \frac{M_0}{L}\right)\frac{x^3}{6} + \frac{P}{6}\left\langle x - \frac{L}{3} \right\rangle^3 + \frac{M_0}{2}\left\langle x - \frac{2L}{3} \right\rangle^2 + \left(\frac{5PL^2}{81} + \frac{M_0L}{9}\right)x$$

From these equations we can find the slope and deflection at any point of the beam. For instance, at the left-hand support ($x = 0$), Eq. (k) yields

$$\theta_a = v'(0) = \frac{5PL^2}{81EI} + \frac{M_0L}{9EI}$$

At the center of the beam ($x = L/2$), the angle of rotation and deflection are, respectively,

$$\theta_c = v'\left(\frac{L}{2}\right) = \frac{5PL^2}{648EI} - \frac{M_0L}{72EI}$$

$$\delta_c = v\left(\frac{L}{2}\right) = \frac{23PL^3}{1296EI} + \frac{5M_0L^2}{144EI}$$

In a similar manner, we can find any other desired deflections and angles of rotation. Thus, the analysis of the beam by the use of discontinuity functions is complete.

Example 2

Obtain the equation of the deflection curve for the cantilever beam AB shown in Fig. 7-34. Let us begin by determining the reactions at the fixed support:

$$R_a = qa \quad M_a = \frac{qa^2}{2}$$

Then we can express the intensity $q(x)$ of the equivalent distributed load as follows:

$$q(x) = -R_a\langle x \rangle^{-1} + M_a\langle x \rangle^{-2} + q\langle x \rangle^0 - q\langle x - a \rangle^0$$

Substituting from Eqs. (p) into Eq. (q), and then using the differential equation in terms of the load (Eq. 7-10c), we obtain

$$EIv''' = q = -qa\langle x \rangle^{-1} + \frac{qa^2}{2}\langle x \rangle^{-2} + q\langle x \rangle^0 - q\langle x - a \rangle^0$$

Replacing $\langle x \rangle^0$ with unity and then integrating, we get

$$EIv'' = -V = -qa\langle x \rangle^0 + \frac{qa^2}{2}\langle x \rangle^{-1} + qx - q\langle x - a \rangle^1$$

Because we began with the complete expression for q , including the reactions, no constant of integration is required. Also, note that the second term on the right comes from the moment reaction; it has no effect on the shear-force diagram, but it must be retained because it affects the next step of integration. Also, a disadvantage of using discontinuity functions is evident from Eq. (s): for the right-hand part of the beam (where $a < x < L$), the shear force V equals zero, but this fact may not be recognized from the equation.

The next step is to integrate Eq. (s) to obtain the bending moment. Again we replace $\langle x \rangle^0$ with unity before integrating:

$$EIv' = -M = -qax + \frac{qa^2}{2}\langle x \rangle^0 + \frac{qx^2}{2} - \frac{q}{2}\langle x - a \rangle^2$$

Since we retained all terms in the equation for V , including the term based upon the couple M_a , no constant of integration is needed in the preceding equation. Now we can replace $\langle x \rangle^0$ with unity and perform two more integrations:

$$EIv = \frac{q}{6}(x^3 - 3ax^2 + 3a^2x) - \frac{q}{6}\langle x - a \rangle^3 + C_1$$

$$EIv = \frac{q}{24}(x^4 - 4ax^3 + 6a^2x^2) - \frac{q}{24}\langle x - a \rangle^4 + C_1x + C_2$$

The constants C_1 and C_2 are evaluated from the conditions at the fixed support:

$$v'(0) = 0 \quad v(0) = 0$$

These conditions give $C_1 = 0$ and $C_2 = 0$; hence, the final equations for v' and v are

$$EIv' = \frac{qx}{6}(3a^2 - 3ax + x^2) - \frac{q}{6}\langle x - a \rangle^3$$

$$EIv = \frac{qx^2}{24}(6a^2 - 4ax + x^2) - \frac{q}{24}\langle x - a \rangle^4$$

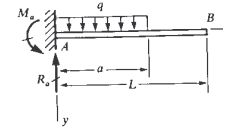


Fig. 7-34 Example 2. Discontinuity functions

Deflections of Beams

Thus, we have obtained the equation of the entire deflection curve in terms of discontinuity functions.

The slope and deflection at any specific point may be obtained by substituting the appropriate value of x into Eqs. (w) and (x). For example, at the point $x = a$ we get

$$v'(a) = \frac{qa^3}{6EI} \quad v(a) = \frac{qa^4}{8EI}$$

and at $x = L$ we get

$$\theta_b = v'(L) = \frac{qa^3}{6EI} \quad \delta_b = v(L) = \frac{qa^3}{24EI}(4L - a)$$

Note that the deflection curve is actually a straight line in the unloaded part of the beam.

which we get $C_1 = \frac{475}{4} \quad C_2 = 0$

Thus, the final expressions for v' and v are

$$EIv' = -\frac{9x^2}{2} + \frac{475}{4} + 2\langle x - 5 \rangle^3 - 2\langle x - 10 \rangle^3 - 33\langle x - 10 \rangle^2$$

$$EIv = -\frac{3x^3}{2} + \frac{475x}{4} + \frac{1}{2}\langle x - 5 \rangle^4 - \frac{1}{2}\langle x - 10 \rangle^4 - 11\langle x - 10 \rangle^3$$

in which the variables have the following units:

- x has units of meters (m)
- v has units of meters (m)
- E has units of kilonewtons per square meter (kPa)
- I has units of meters to fourth power (m^4)

The deflection δ_d at point D is found by substituting the following numerical values into the preceding equation:

$$x = 5 \text{ m} \quad E = 200 \text{ GPa} = 200 \times 10^6 \text{ kPa}$$

$$I = 118 \times 10^6 \text{ mm}^4 = 118 \times 10^{-6} \text{ m}^4$$

The calculations proceed as follows:

$$EI\delta_d = EIv(5) = -\frac{3}{2}(5)^3 + \frac{475(5)}{4} = 406.25 \text{ kN}\cdot\text{m}^3$$

$$\delta_d = \frac{406.25 \text{ kN}\cdot\text{m}^3}{(200 \times 10^6 \text{ kPa})(118 \times 10^{-6} \text{ m}^4)} = 0.0172 \text{ m} = 17.2 \text{ mm}$$

In a similar manner, we calculate the deflection δ_e at the end of the overhang:

$$x = 14 \text{ m} \quad E = 200 \times 10^6 \text{ kPa} \quad I = 118 \times 10^{-6} \text{ m}^4$$

$$EI\delta_e = EIv(14) = -\frac{3}{2}(14)^3 + \frac{475(14)}{4} + \frac{1}{2}(14 - 5)^4$$

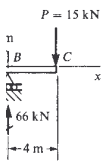
$$= -\frac{1}{2}(14 - 10)^4 - 11(14 - 10)^3$$

$$= -5.00 \text{ kN}\cdot\text{m}^3$$

$$\delta_e = \frac{-5.00 \text{ kN}\cdot\text{m}^3}{(200 \times 10^6 \text{ kPa})(118 \times 10^{-6} \text{ m}^4)} = -0.00021 \text{ m} = -0.21 \text{ mm}$$

The minus sign means that the deflection is upward.

Example 3



The beam ABC shown in Fig. 7-35 consists of a simple span AB with an overhang BC . Determine the vertical deflections δ_c and δ_d at points C and D , respectively. The beam has modulus of elasticity $E = 200 \text{ GPa}$ and moment of inertia $I = 118 \times 10^6 \text{ mm}^4$.

The loads and reactions of this beam were expressed in terms of discontinuity functions in Example 3 of the preceding section. Therefore, we can take the expression for $q(x)$ from that example:

$$q(x) = -9\langle x \rangle^{-1} + 12\langle x - 5 \rangle^0 - 12\langle x - 10 \rangle^0 - 66\langle x - 10 \rangle^{-1}$$

in which x has units of meters (m) and $q(x)$ has units of kilonewtons per meter (kN/m). Substituting into Eq. (7-10c), we get the differential equation of the deflection curve:

$$EIv''' = q = -9\langle x \rangle^{-1} + 12\langle x - 5 \rangle^0 - 12\langle x - 10 \rangle^0 - 66\langle x - 10 \rangle^{-1}$$

In this equation, v has units of meters (m), E has units of kilonewtons per square meter (kPa), and I has units of meters to the fourth power (m^4). (Note that v' has units of m^{-3} .)

The first and second integrations give the equations for the shear force and bending moment:

$$EIv'' = -V = -9\langle x \rangle^0 + 12\langle x - 5 \rangle^1 - 12\langle x - 10 \rangle^1 - 66\langle x - 10 \rangle^0$$

$$EIv' = -M = -9x + 6\langle x - 5 \rangle^2 - 6\langle x - 10 \rangle^2 - 66\langle x - 10 \rangle^1$$

As explained previously, no integration constants for V and M are required when we use the complete expression for $q(x)$, that is, the expression that includes the reactions and the loads.

The next two integrations give the slope and deflection:

$$EIv' = -\frac{9x^2}{2} + 2\langle x - 5 \rangle^3 - 2\langle x - 10 \rangle^3 - 33\langle x - 10 \rangle^2 + C_1$$

$$EIv = -\frac{3x^3}{2} + \frac{1}{2}\langle x - 5 \rangle^4 - \frac{1}{2}\langle x - 10 \rangle^4 - 11\langle x - 10 \rangle^3 + C_1x + C_2$$

The boundary conditions on the deflection are

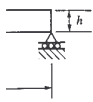
$$v(0) = 0 \quad v(10) = 0$$

***7.11 TEMPERATURE EFFECTS**

A uniform temperature increase causes an unconstrained bar or beam to have its length increased by the amount

$$\delta_t = \alpha(\Delta T)L \quad (7-70)$$

Deflections of Beams



in which α is the coefficient of thermal expansion,* ΔT is the increase in temperature, and L is the length of the bar (see Fig. 7-20 and Eq. 7-20). If a beam is supported in such a manner that longitudinal expansion is free to occur, as is the case for all beams considered in this chapter, then a uniform temperature change will not produce any stresses in the beam. Neither will there be any lateral deflections of such a beam because there is no tendency for the beam to bend.

The behavior of a beam is quite different if the temperature is not constant across its height. For example, assume that a simple beam, initially straight and at a uniform temperature T_0 , has its temperature changed to T_1 on its upper surface and T_2 on its lower surface, as pictured in Fig. 7-36a. If we assume that the variation in temperature is linear between the top and bottom of the beam, then the average temperature of the beam is $T_{aver} = (T_1 + T_2)/2$ and it occurs at the midheight. Any difference between this average temperature and the initial temperature T_0 results in a change in the length of the beam, as described in the preceding paragraph. The temperature differential $T_2 - T_1$ between the bottom and top of the beam results in a curvature of the axis of the beam, which means that lateral deflections are produced.

To investigate the deflections, we consider the deformation of an element having length dx (Fig. 7-36b). The changes in length of the element at the lower and upper surfaces are $\alpha(T_2 - T_0)dx$ and $\alpha(T_1 - T_0)dx$, respectively. If T_1 is greater than T_2 , the sides of the element will rotate with respect to each other through an angle $d\theta$, as shown in Fig. 7-36b. The angle $d\theta$ is related to the changes in dimension by the following equation, obtained from the geometry of the figure:

$$h d\theta = \alpha(T_1 - T_0)dx - \alpha(T_2 - T_0)dx$$

or

$$\frac{d\theta}{dx} = \frac{\alpha(T_2 - T_1)}{h} \tag{7-71}$$

in which h is the height of the beam. We have already seen that the quantity $d\theta/dx$ represents the curvature of the deflection curve of the beam (see Eq. 7-4); therefore, we are led to the following differential equation of the deflection curve:

$$\frac{d^2v}{dx^2} = -\frac{\alpha(T_2 - T_1)}{h} \tag{7-72}$$

Note that, when T_2 is greater than T_1 , the curvature is negative and the beam is bent concave upward. The quantity $\alpha(T_2 - T_1)/h$ is the counterpart of the quantity M/EI , which appears in the differential equation for the deflection curve that we used previously (Eq. 7-6). Now that we have established Eq. (7-72) as the basic differential

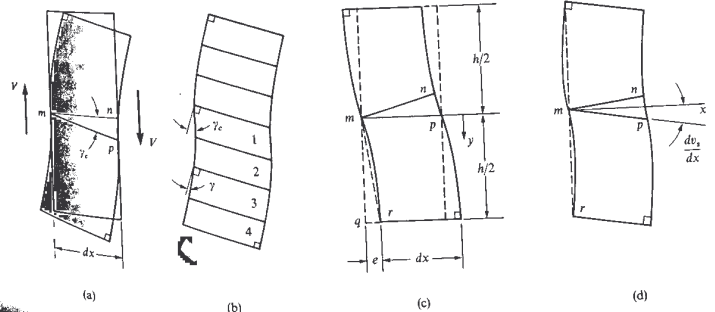
*Values of the thermal coefficient α are given in Appendix H, Table H-4.

...for a beam subjected to a temperature change between top and bottom of the beam, we can proceed to solve this equation using the same techniques as already described for the effects of bending moments. That is, we can integrate the equation successively to obtain dv/dx and v , and then we can use boundary conditions to evaluate the constants of integration. Alternatively, theorems of the moment-area method may be used; all that is required is to replace M/EI by $\alpha(T_2 - T_1)/h$ in those theorems.

7.12 EFFECTS OF SHEAR DEFORMATIONS

In the preceding sections of this chapter, only the effects of bending deformations were considered in finding deflections. An additional deflection is produced by the shear deformations which, for a beam of rectangular cross section, cause an element of the beam of length dx to be deformed as shown in Fig. 7-37a. Because the shear stresses vary over the depth of the beam, the cross sections become curved surfaces. The depth of the beam, the cross sections become curved surfaces. The figure shows the deformations due to shear only; hence, the bending deformations and the bending moment acting on the element are omitted from the sketch. Line mn represents the original axis of the beam, assumed to be horizontal, and line mp shows the original axis of the beam after the shear deformations have occurred. If the sides of the element at points m and n are assumed to remain vertical, then the top and bottom edges of the beam will be parallel to line mp , which makes an angle γ_c with the horizontal (γ_c is the shear strain at the neutral axis). The deformation of the element can be visualized easily if it is divided into thin layers, each of which is assumed to be in pure shear (Fig. 7-37b). The shear strain in layer 1 is γ_1 , whereas in layers 2 and 3 the shear strain γ will be less than γ_c . At the outermost layer 4, the shear strain must be zero; hence, the sides of this layer are at right angles.

Fig. 7-37 Shear deformations in a beam



Deflections of Beams

The slope of the deflection curve of the beam due to shear alone is approximately equal to the shear strain at the neutral axis (see Fig. 7-37a). Thus, denoting by v_s the deflections due to shear alone, we obtain the following expression for the slope:

$$\frac{dv_s}{dx} = \gamma_c = \frac{\alpha_s V}{GA} \tag{7-73}$$

in which V/A is the average shear stress obtained by dividing the shear force by the cross-sectional area of the beam, α_s is a numerical factor (or shear coefficient) by which the average shear stress must be multiplied to obtain the shear stress at the centroid of the cross section, and G is the modulus of elasticity in shear. For a rectangular cross section $\alpha_s = \frac{3}{2}$ (see Eq. 5-23), for a circular cross section $\alpha_s = \frac{8}{5}$ (see Eq. 5-32), and for an I-beam, α_s is approximately equal to A_w/A_w , where A_w is the area of the web of the beam. The quantity GA/α_s is known as the shearing rigidity of the beam.*

When there is a continuously distributed load q acting on the beam, the shear force V is a continuous function that may be differentiated with respect to x . Then the curvature caused by the shear alone is

$$\frac{d^2v_s}{dx^2} = \frac{\alpha_s}{GA} \frac{dV}{dx} = -\frac{\alpha_s q}{GA} \tag{a}$$

The total deflection v of the beam is the sum of the bending deflection v_b , found as explained in the preceding sections of this chapter, and the shear deflection v_s ; thus, $v = v_b + v_s$. The total curvature, therefore, is

$$\frac{d^2v}{dx^2} = \frac{d^2v_b}{dx^2} + \frac{d^2v_s}{dx^2} = -\frac{M}{EI} - \frac{\alpha_s q}{GA} \tag{7-74}$$

This equation can be solved by successive integrations to determine deflections of beams in those instances where the effect of shear must be considered.

The boundary conditions for the beam are used in evaluating the constants of integration that arise in the solution of Eq. (7-74). For instance, at a simple support the deflection is zero ($v = v_b = v_s = 0$). At a fixed support the deflection is also zero, but the condition on the slope depends upon how the end of the beam is held. If the sides of the element at the neutral axis remain vertical (as in Fig. 7-37a), then the conditions for the slope are

$$\frac{dv_b}{dx} = 0 \quad \frac{dv_s}{dx} = \gamma_c \tag{b}$$

because, in this situation, the axis of the beam at the support will have zero slope due to bending deformations and a slope γ_c due to shear de-

*The shearing rigidity of a beam as determined by the method of virtual work is GA/f_s , where f_s (called the form factor for shear) may be different from the shear coefficient α_s ; see Section 12.9.

formations. If the beam is constrained in such a manner that the total deflection curve has zero slope at the end, then the conditions are

$$\frac{dv_b}{dx} = 0 \quad \frac{dv_s}{dx} = 0 \tag{c}$$

and the end of the beam is oriented as shown in Fig. 7-37c with line mp being horizontal.

Another possibility is that the top and bottom of the beam are held in a vertical line (Fig. 7-37d). In this case, neither line mn nor line mp remains horizontal. Instead, the slope dv_s/dx can be found by rotating the element in Fig. 7-37c until line mr is vertical. The angle clockwise the element in Fig. 7-37c until line mr is vertical. The distance e is seen to be

$$e = \int_0^{h/2} \gamma dy \tag{d}$$

where γ is the shear strain (Fig. 7-37b) at distance y (Fig. 7-37c) from the neutral axis. The boundary conditions for this case are as follows:

$$\frac{dv_b}{dx} = 0 \quad \frac{dv_s}{dx} = \frac{2e}{h} \tag{e}$$

The quantity e , given by Eq. (d), can be evaluated for any particular shape of cross section. For a beam of rectangular cross section with width b , we have

$$e = \int_0^{h/2} \gamma dy = \frac{1}{G} \int_0^{h/2} \tau dy = \frac{1}{bG} \int_0^{h/2} tb dy = \frac{V}{2bG} \tag{f}$$

and Eqs. (e) become

$$\frac{dv_b}{dx} = 0 \quad \frac{dv_s}{dx} = \frac{V}{GA} \tag{g}$$

where $A = bh$ is the cross-sectional area. For an I-beam the web carries almost all of the shear force, and the shear stress is approximately uniform throughout the height of the web; then we have

$$e = \int_0^{h/2} \gamma dy = \frac{1}{G} \int_0^{h/2} \tau dy = \frac{1}{t_w G} \int_0^{h/2} t_w dy \approx \frac{V}{2t_w G} \tag{h}$$

and the boundary conditions become

$$\frac{dv_b}{dx} = 0 \quad \frac{dv_s}{dx} = \frac{V}{GA_w} \tag{i}$$

where $A_w \approx ht_w$ is the area of the web of the beam.

To illustrate the calculation of shear deflections, let us take as a first example a simple beam with a uniform load q (see Fig. 7-3). The equation for the curvature of this beam (see Eq. 7-74) becomes:

$$\frac{d^2v}{dx^2} = -\frac{q}{2EI} (xL - x^2) - \frac{\alpha_s q}{GA}$$

which, after two successive integrations, gives the deflection v .

$$v = \frac{q}{24EI} (x^4 - 2x^3L) - \frac{\alpha_s q}{2GA} x^2 + C_1 x + C_2$$

At the ends of the beam ($x = 0$ and $x = L$), the deflection v is zero, which gives for C_1 and C_2 the following values:

$$C_1 = \frac{qL^3}{24EI} + \frac{\alpha_s qL}{2GA} \quad C_2 = 0$$

Therefore, the deflection curve of the beam is

$$v = \frac{qL^4}{24EI} \left(\frac{x}{L} \right) \left(\frac{x^3}{L^3} - 2 \frac{x^2}{L^2} + 1 \right) + \frac{\alpha_s qL^2}{2GA} \left(\frac{x}{L} \right) \left(1 - \frac{x}{L} \right) \quad (7-75)$$

This equation has two terms on the right-hand side; the first is the deflection due to bending (compare with Eq. 7-13), and the second gives the additional deflection due to shear deformations.

At the center of the beam ($x = L/2$), the deflection is

$$v_c = \frac{5qL^4}{384EI} + \frac{\alpha_s qL^2}{8GA} = \frac{5qL^4}{384EI} \left(1 + \frac{48\alpha_s EI}{5GA L^2} \right) \quad (7-76)$$

The relative importance of the shear effects can be judged by examining the last term in this equation. If shear deformations are disregarded, the effect is the same as if we assume that the beam is infinitely rigid in shear ($GA/\alpha_s = \infty$); then the last term in the preceding equation becomes zero and only the bending deflection remains. When the shear effect is included, the deflection is increased. The last term has a value that is small in comparison to unity for solid beams, such as beams of rectangular cross section; but in other beams, such as sandwich beams, it may be quite large.

In order to obtain some numerical results, consider a beam of rectangular cross section with height h (thus, $\alpha_s = 1.5$ and $I/A = h^2/12$) and with $E/G = 2.5$. The central deflection for this case is

$$v_c = \frac{5qL^4}{384EI} \left(1 + 3 \frac{h^2}{L^2} \right) \quad (7-77)$$

If $L/h = 10$ the effect of shear deformations is to increase the deflection by 3%. For smaller ratios of L/h (that is, for short, deep beams), the effect of shear increases. For I-beams the effects are similar to those for rectangular beams, except that the relative magnitude of the shear deflection is usually two or three times greater. For beams of sandwich construction, the increase in deflection due to shear may be as high as 50%.

The differential equation used in solving for the shear deflection was derived on the assumption that each cross section of the beam can warp freely, as pictured in Fig. 7-37a. The uniformly loaded simple beam is a case in which this assumption is nearly satisfied. At the middle of

the beam, there can be no warping of the cross section (by symmetry). However, since $V = 0$ at the middle, there is no tendency to warp at this section. Warping increases gradually from the middle toward the end of the beam, as does the shear force itself. Thus, the additional restraint against deflection that is provided by the warping has only a minor effect. In general, the effect of restrained warping is to reduce the deflections calculated above.

By the methods of theory of elasticity, the deflection curve for a simple beam of rectangular cross section carrying a uniform load has been determined (Ref. 7-18). For the case when Poisson's ratio $\nu = 0.25$, the deflection at the middle is

$$v_c = \frac{5qL^4}{384EI} \left(1 + 2.2 \frac{h^2}{L^2} \right) \quad (7-78)$$

which gives a smaller deflection than does Eq. (7-77). The second term in Eq. (7-78) takes into account not only the effects of shear, but also the effects of stresses σ_y in the vertical direction (due to the uniform load q acting on the top of the beam).

The second example we will consider is a simple beam with a concentrated load P at the center. In the left-hand half of the beam, the expressions for the bending moment, shear force, and intensity of load are, respectively, $M = Px/2$, $V = P/2$, and $q = 0$. Hence, the equations for the curvatures due to bending and shear become

$$\frac{d^2 v_b}{dx^2} = -\frac{Px}{2EI} \quad \frac{d^2 v_s}{dx^2} = 0 \quad \left(0 \leq x \leq \frac{L}{2} \right)$$

These two equations must be integrated separately, rather than in combined form as was done for the first example, because the boundary conditions for the slopes associated with the bending and shear deflections are different at the middle of the beam. Two successive integrations of the differential equation for v_b , using as boundary conditions the fact that $dv_b/dx = 0$ at $x = L/2$ and $v_b = 0$ at $x = 0$, give the bending deflection:

$$v_b = \frac{PL^3}{48EI} \left(\frac{x}{L} \right) \left(3 - 4 \frac{x^2}{L^2} \right) \quad \left(0 \leq x \leq \frac{L}{2} \right)$$

Integration of the differential equation for v_s gives

$$\frac{dv_s}{dx} = C_1$$

which shows that the slope due to shear is constant throughout the left-hand half of the beam. This slope is equal to $\alpha_s V/GA$, as given by Eq. (7-73). A second integration, combined with the condition that $v_s = 0$ when $x = 0$, yields the deflection equation due to shear alone:

$$v_s = \frac{\alpha_s Px}{2GA} \quad \left(0 \leq x \leq \frac{L}{2} \right)$$

The total deflection (for $0 \leq x \leq L/2$) is

$$v = v_b + v_s = \frac{PL^3}{48EI} \left(\frac{x}{L} \right) \left(3 - 4 \frac{x^2}{L^2} \right) + \frac{\alpha_s Px}{2GA} \quad (7-79)$$

The deflection at the center of the beam is

$$v_c = \frac{PL^3}{48EI} \left(1 + \frac{12\alpha_s EI}{GA L^2} \right) \quad (7-80)$$

Again, the relative importance of the shear deformations can be determined in each particular instance by evaluating numerically the last term in the parentheses.

The preceding solution (Eq. 7-79) gives deflections that are too large because the effects of warping are ignored, as previously pointed out. From symmetry we know that the middle cross section of the beam must remain plane, and no warping can occur there. However, adjacent sections to the left and right of the middle carry shear forces $P/2$ and $-P/2$, respectively, and warping of these sections should occur. Since they tend to warp in opposite directions, but are restrained from doing so, additional stresses develop. The additional warping restraint tends to resist deflection of the beam; hence, the actual shear deflections will be less than those determined above.

For a beam of rectangular cross section with $E/G = 2.5$, the central deflection given by Eq. (7-80) is

$$v_c = \frac{PL^3}{48EI} \left(1 + 3.75 \frac{h^2}{L^2} \right) \quad (7-81)$$

which can be compared with the following, more exact result obtained by the theory of elasticity for the case when $\nu = 0.25$ and $E/G = 2.5$ (Ref. 7-19):

$$v_c = \frac{PL^3}{48EI} \left(1 + 2.78 \frac{h^2}{L^2} - 0.84 \frac{h^3}{L^3} \right) \quad (7-82)$$

This last equation gives a smaller deflection than does Eq. (7-81) because it takes into account the localized stresses near the middle of the beam where the load is applied.

The third example to be considered is a cantilever beam, fixed at the left-hand end and carrying a concentrated load P at the free end (see Appendix G, Table G-1, Case 4). The bending deflection v_b is given in Appendix G, and only the shear deflection v_s will be discussed here. Because the shear force is constant, the slope dv_s/dx of the beam due to shear is also constant. The magnitude of this slope depends on how the beam is supported at the left-hand end. If the sides of the element at the neutral axis remain vertical and the end of the beam is free to warp (see Fig. 7-37a), the slope is

$$\frac{dv_s}{dx} = \frac{\alpha_s P}{GA}$$

Since, the shear deflection is
$$v_s = \frac{\alpha_s P}{GA} x \quad (j)$$

If the deflection distorts as shown in Fig. 7-37c, then $dv_s/dx = 0$, and there is no shear deflection v_s . Finally, if the top and bottom edges of the beam remain vertically above each other at the support and the beam warps as shown in Fig. 7-37d, then the slope due to shear is

$$\frac{dv_s}{dx} = \frac{2e}{h}$$

and the deflection curve due to shear alone is

$$v_s = \frac{2e}{h} x \quad (k)$$

The total deflection at the free end of the cantilever is found by substituting $x = L$ into the preceding equations for v_b and adding the result to $PL^3/3EI$, which is the deflection at the free end due to bending alone.

The deflection at the end of a cantilever beam as found by the methods of theory of elasticity can be obtained from the formula given above for a simply supported beam with a concentrated load at the middle (see Eq. 7-82) by replacing P with $2P$ and L with $2L$. The resulting deflection is valid for a cantilever beam with the fixed end prevented from warping (that is, with the end cross section assumed to remain plane).*

In the preceding derivations we made use of the shear coefficient α_s , defined as the ratio of the shear stress (or strain) at the neutral axis to the average shear stress (or strain) on the cross section. The value of α_s determined in this manner was used in calculating the shearing rigidity GA/α_s . However, more accurate determinations of the shearing rigidity have been made by using elasticity theory. The following formulas for α_s are taken from Ref. 7-21, which also contains a bibliography on the subject of the shear coefficient. For solid rectangular and circular cross sections, respectively, the coefficients are:

$$\alpha_s = \frac{12 + 11\nu}{10(1 + \nu)} \quad \alpha_s = \frac{7 + 6\nu}{6(1 + \nu)} \quad (7-83a,b)$$

For the case of $\nu = 0.3$, we obtain from these equations $\alpha_s = 1.18$ and $\alpha_s = 1.13$ for a rectangle and a circle, respectively. Using these new values (instead of the values $\frac{3}{2}$ and $\frac{4}{3}$) in the previously derived equations for shear deflections, we obtain smaller values for those deflections. Of course, it must always be kept in mind that, for static deflection problems, great accuracy in calculating the shear deflection is not warranted because it represents only a few percent of the total deflection.

* The shear effect in deflection formulas for beams was introduced by Poncelet and Rankine (Ref. 7-20).

Another method for determining shear deflections of beams is the unit-load method (see Section 12.9), which is based upon the principle of virtual work. This method generally gives results for the shear deflections of a rectangular beam that are slightly less than those obtained from the solutions of the differential equation using a shear coefficient of $\frac{3}{2}$ but that are very close to the results obtained using a shear coefficient of $\frac{3}{2}$.

In obtaining deflections for a sandwich beam (see Section 5.10), it is usually necessary to take into account the effects of shear deformations and, hence, the shear rigidity is small. The methods already described in this section can be used to calculate the deflections of such beams. The flexural rigidity EI of the beam is replaced by the quantity $E_f I_f$, where E_f is the modulus of elasticity of the faces and I_f is their moment of inertia (see Eq. 5-53). The shear rigidity GA/α_s becomes $G_c A_c$, because we may assume that the shear stress is uniformly distributed over the core area A_c ; hence, the shear coefficient α_s becomes equal to one. In practical applications, because of the variety of materials used in sandwich beams, it often happens that the flexural and shearing rigidities cannot be obtained by calculation because of a lack of accurate data. In such instances, the rigidities must be determined experimentally for the particular materials and types of construction being used.

Strain energy of shear. An expression for the strain energy stored in a beam due to the effect of the shear force V can be obtained readily. From Fig. 7-37a we see that the work done by the shear force, equal to the strain energy dU_s stored in the element, is

$$dU_s = \frac{V\gamma_c dx}{2}$$

Using Eq. (7-73), we can rewrite this expression as

$$dU_s = \frac{\alpha_s V^2 dx}{2GA}$$

Thus, the strain energy stored in a beam due to the effect of shear alone is

$$U_s = \int \frac{\alpha_s V^2 dx}{2GA} \quad (7-84)$$

The strain energy of shear can be added to the strain energy of bending (Eqs. 7-59) to obtain the total strain energy. Of course, in most instances the shear strain energy is negligible compared to the bending strain energy.*

* 7.13 LARGE DEFLECTIONS OF BEAMS

The beam deflections discussed previously in this chapter were obtained by solving the differential equations for a beam with small angles of rotation (Eqs. 7-10). When the slopes and deflections become large,

* The method of virtual work leads to an expression for the strain energy of shear in a beam that is similar to Eq. (7-84) except that the shear coefficient α_s is replaced by the form factor f_s ; see Section 12.9.

The exact differential equation of the deflection curve must be used. This equation, which is also based upon the assumption that the material of the beam remains linearly elastic, is:

$$\kappa = \frac{d\theta}{ds} = -\frac{M}{EI} \quad (7-85)$$

(see Eqs. 7-1 and 7-5). The quantity $d\theta/ds$, which is the curvature of the beam, is the rate of change of θ (the angle of rotation of the deflection curve) with respect to s (the distance measured along the curve itself). When the rotations are very small, the distance s becomes the same as the distance x , and the angle of rotation θ becomes the same as the slope dv/dx ; hence, $d\theta/ds$ is approximated by d^2v/dx^2 . However, for large deflections these simplifications are not valid, and Eq. (7-85) must be solved using the exact expression for curvature (Eq. 7-11). Thus, the differential equation of the deflection curve becomes

$$\frac{d^2v}{dx^2} \left[1 + \left(\frac{dv}{dx} \right)^2 \right]^{3/2} = -\frac{M}{EI} \quad (7-86)$$

The exact shape of the elastic deflection curve, as found from this equation, is called the *elastica*.

The mathematical solution of the problem of the elastica has been obtained for many different types of beams and loading conditions. Because the solutions are lengthy, they will not be worked out here. Instead, we will give the final results for one beam of practical interest* together with references showing where other solutions can be found.

Let us consider the cantilever beam AB shown in Fig. 7-38. The load P is assumed to produce large deflections of the beam, resulting in the end of the beam moving from point B to B' . The angle of rotation of the end of the beam is denoted θ_b , and the horizontal and vertical displacements are δ_h and δ_v , respectively. The length AB' of the deflection curve is equal to the initial length L because axial changes in length due to direct tension are disregarded. Because the beam is statically determinate, the expression for the bending moment M can be obtained easily and substituted into the differential equation (Eq. 7-86). Then, after considerable manipulation of the equation, including a change of the dependent variable, and also after applying the appropriate boundary conditions, the solution of the equation can be obtained in terms of

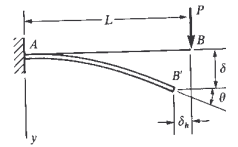


Fig. 7-38 Large deflections of a cantilever beam

* The problem of the elastica was first investigated by Jacob Bernoulli, Euler, Lagrange, and Plana (Refs. 7-22 through 7-27). Solutions to the problem of the elastica can be found in Refs. 7-28 through 7-31. A complete reference on large deflections of beams is given in the book by R. Frisch-Fay (Ref. 7-31), which contains many references. Another bibliography can be found in Ref. 7-32.

elliptic functions.* From this solution, expressions for θ_b , δ_h , and δ_v can be obtained in terms of elliptic integrals. For instance, the equation for finding the angle θ_b is as follows:

$$F(k) - F(k, \phi) = \sqrt{\frac{PL^2}{EI}} \quad (7-87)$$

The terms in this equation have the following definitions:

$$k = \sqrt{\frac{1 + \sin \theta_b}{2}} \quad (a)$$

$$\phi = \arcsin \frac{1}{k\sqrt{2}} \quad (b)$$

$$F(k) = \text{complete elliptic integral of the first kind} = \int_0^{\pi/2} \frac{dt}{\sqrt{1 - k^2 \sin^2 t}} \quad (c)$$

$$F(k, \phi) = \text{incomplete elliptic integral of the first kind} = \int_0^{\phi} \frac{dt}{\sqrt{1 - k^2 \sin^2 t}} \quad (d)$$

Elliptic integrals can be evaluated by numerical integration using a programmable calculator. Also, mathematical handbooks contain tables that give numerical values of the elliptic integrals for various values of the modulus k and the amplitude ϕ (for example, see Ref. 7-33). Note that the difference of the two elliptic integrals in Eq. (7-87) can be expressed as a single integral with limits from ϕ to $\pi/2$.

Because of the transcendental nature of Eq. (7-87), it must be solved by trial and error to obtain θ_b . The procedure is as follows: (1) Assume a value of θ_b between 0 and 90°; (2) calculate k from Eq. (a); (3) obtain the corresponding value of $F(k)$ from Eq. (c); (4) calculate ϕ from Eq. (b); (5) knowing k and ϕ , obtain the value of $F(k, \phi)$ from Eq. (d); and (6) calculate the load P from Eq. (7-87). This process gives the load P that corresponds to the particular assumed value of θ_b . By repeating the calculations for other values of θ_b , we can determine as many corresponding values of P and θ_b as we desire. A listing of values determined in this manner is presented in Table 7-3, which is adapted from Ref. 7-34.

The equation for the vertical deflection at the end of the cantilever beam is

$$\frac{\delta_v}{L} = 1 - \sqrt{\frac{4EI}{PL^2}} [E(k) - E(k, \phi)] \quad (7-88)$$

in which

$$E(k) = \text{complete elliptic integral of the second kind} = \int_0^{\pi/2} \sqrt{1 - k^2 \sin^2 t} dt \quad (e)$$

* Elliptic functions are discussed in textbooks and handbooks of advanced mathematics.

Table 7-3 Angle of rotation and deflections of a cantilever beam with a concentrated load at the free end (see Fig. 7-38)

$\frac{PL^2}{EI}$	$\frac{\theta_b}{\pi/2}$	$\frac{\delta_v}{L}$	$\frac{\delta_h}{L}$
0	0	0	0
0.2	0.063	0.066	0.003
0.4	0.126	0.131	0.010
0.6	0.185	0.192	0.022
0.8	0.241	0.249	0.038
1.0	0.294	0.302	0.056
1.5	0.407	0.411	0.108
2	0.498	0.493	0.161
3	0.574	0.603	0.254
4	0.628	0.670	0.329
5	0.714	0.714	0.388
6	0.774	0.745	0.435
7	0.817	0.767	0.473
8	0.850	0.785	0.505
9	0.875	0.799	0.532
10	0.895	0.811	0.555
15	0.911	0.811	0.555
∞	0.956	0.848	0.635
∞	1	1	1

$E(k, \phi) = \text{incomplete elliptic integral of the second kind}$

$$= \int_0^{\phi} \sqrt{1 - k^2 \sin^2 t} dt \quad (f)$$

Equation (7-88) can be solved by using the values of θ_b , k , ϕ , and PL^2/EI that were obtained in the solution of Eq. (7-87). The only additional step is to determine the values of $E(k)$ and $E(k, \phi)$ and substitute them into Eq. (7-88). Again we note that for purposes of calculation the difference between the elliptic integrals in Eq. (7-88) is equal to the value of a single integral having limits from 0 to $\pi/2$. Some numerical results are given in Table 7-3.

Finally, we can obtain the horizontal deflection from the equation

$$\frac{\delta_h}{L} = 1 - \sqrt{\frac{2EI \sin \theta_b}{PL^2}} \quad (7-89)$$

The results for this case are shown in the last column of Table 7-3. The angle of rotation θ_b and the deflections δ_h and δ_v are also shown graphically in Figs. 7-39a, b, and c, respectively. In each instance, the large deflection results merge with those obtained by small-deflection theory as the load approaches zero.

The complete solution for a cantilever beam with a vertical load at the end (Fig. 7-38) is given in Refs. 7-31, 7-35, and 7-36, and the deflec-

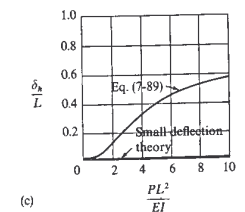
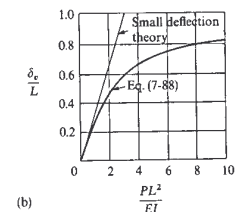
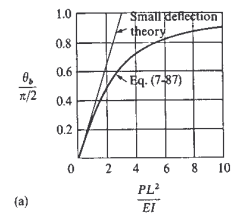
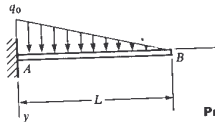


Fig. 7-39 Large deflections of a cantilever beam with a concentrated load P at the free end (Fig. 7-38): (a) angle of rotation θ_b , (b) vertical deflection δ_v , and (c) horizontal deflection δ_h

tion of a cantilever beam with a uniform load is given in Ref. 7-37. The solutions for cantilever beams can be adapted to symmetrically loaded, simply supported beams by considering one-half of the simple beam to be the same as a cantilever beam. Many other cases of large deflections are described in Ref. 7-31.

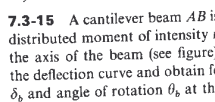
In the general three-dimensional case of a beam bent by couples and forces at the ends, the differential equations of the elastica have the same form as those for the motion of a heavy body moving about a fixed point. This analogy was observed by Kirchhoff in 1859 and is known as Kirchhoff's dynamical analogy (Ref. 7-38). In the special case of only axial forces at the ends of the bar, the differential equation for the elastica is the same as for an ordinary pendulum having large angles of rotation. Reference 7-39 should be consulted for information about the Kirchhoff analogy between elastic and dynamic systems.

7.3-9 Calculate the maximum deflection δ of a uniformly loaded simple beam (see Fig. 7-3 and Example 1) if the span length $L = 2$ m, $q = 2.5$ kN/m, and the maximum bending stress $\sigma = 60$ MPa. The beam has a square cross section and is made of aluminum having modulus of elasticity $E = 70$ GPa.



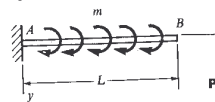
Prob. 7.3-14

7.3-10 A simple beam AB supports a concentrated load P as shown in Fig. 7-5 and discussed in Example 3. Plot a graph showing how the ratio θ_a/θ_b of the angles of rotation at the supports varies with the ratio a/L that defines the position of the load P ($0 < a/L < 1$).



Prob. 7.3-15

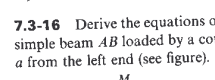
7.3-11 Obtain a formula for the ratio δ_c/δ_{max} of the deflection at the midpoint to the maximum deflection for a simple beam supporting a concentrated load P (see Fig. 7-5 and Example 3). From the formula, plot a graph of δ_c/δ_{max} versus the ratio a/L that defines the position of the load ($0.5 < a/L < 1$).



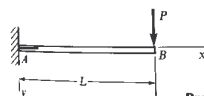
Prob. 7.3-16

Problems 7.3-12 through 7.3-19 are to be solved by integrating the second-order differential equation of the deflection curve (the bending-moment equation).

7.3-12 Determine the equation of the deflection curve for a cantilever beam AB supporting a load P at the free end (see figure). Also, determine the deflection δ_b and angle of rotation θ_b at the free end.

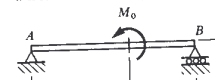


Prob. 7.3-17



Prob. 7.3-12

7.3-13 Determine the equation of the deflection curve for a simple beam AB loaded by a couple M_0 at the end (see figure). Also, determine the maximum deflection v_{max} .

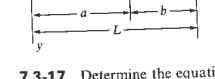


Prob. 7.3-18

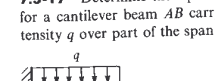


Prob. 7.3-13

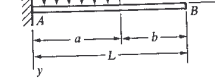
7.3-14 A cantilever beam AB supporting a triangularly distributed load of maximum intensity q_0 is shown in the figure. Obtain formulas for the deflection δ_b and angle of rotation θ_b at the free end.



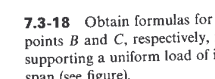
Prob. 7.3-19



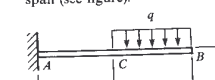
Prob. 7.3-17



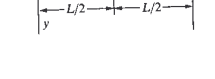
Prob. 7.3-18



Prob. 7.3-19



Prob. 7.3-18



Prob. 7.3-19

CHAPTER 7

rentiations of the equation of the ple beam with a uniform load 1), obtain expressions for the rear force V in the beam. Verify equilibrium.

ie deflection curve for a simple

$$\delta = 10L^2x^2 + 3x^4$$

am?



Probs. 7.3-2 and 7.3-3

deflection curve for a simple

$$\frac{L^4}{EI} \sin \frac{\pi x}{L}$$

im?

g Universal Beam supporting -3 and Example 1) has a span be maximum deflection δ and supports if $q = 26$ kN·m and

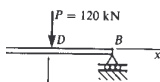
7.3-5 A simple beam of rectangular cross section supports a uniform load that deflects the beam 12 mm at the midpoint (see Fig. 7-3 and Example 1). The beam is to be replaced by a new beam of the same material and also of rectangular cross section. However, the width of the new beam is only one-half the width of the original beam. What must be the height h_2 of the new beam compared to the height h_1 of the original beam if the new beam is to deflect only 3 mm under the same load?

7.3-6 A cantilever beam with a uniform load (see Fig. 7-4 and Example 2) has a height h equal to one-tenth the length L . The beam is a steel I-section with $E = 200$ GPa and an allowable stress of 140 MPa in both tension and compression. Calculate the ratio δ/L of the deflection at the free end to the length, assuming that the beam carries the maximum allowable load.

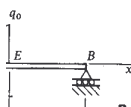
7.3-7 What is the span length L for a uniformly loaded simple beam (see Fig. 7-3 and Example 1) of wide-flange cross section if the maximum bending stress is 72 MPa, the maximum deflection is 3.0 mm, the height of the beam is 400 mm, and the modulus of elasticity is 200 GPa?

7.3-8 A uniformly loaded I-beam of steel with simple supports (see Fig. 7-3 and Example 1) has a deflection of 8 mm at the midpoint and a slope of 0.01 radians at the ends. Calculate the height h of the beam if the maximum bending stress σ is 124 MPa and E equals 200 GPa.

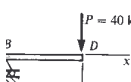
lections of Beams



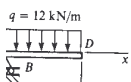
Probs. 7.9-9 and 7.10-9



Probs. 7.9-10 and 7.10-10



Probs. 7.9-11 and 7.10-11



Probs. 7.9-12 and 7.10-12

7.10 are to be solved by using

3 Determine the equation of cantilever beam AB shown in angle of rotation θ_b and deflection δ_b at point B. (For Problem 7.10-3, $E = 200 \times 10^6$ mm².)

and 7.10-7 Determine the curve for the simple beam AB obtain the angle of rotation θ_a , deflection δ_a at point D. (For 7-7, assume $E = 210$ GPa and

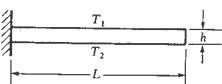
10 Obtain the equation of simple beam AB (see figure). i rotation θ_b at the right sup-clockwise) and the deflection δ_b at point B. (For Problem 7.10-9, assume $E = 200 \times 10^6$ mm².)

7.10-11 A simple beam AB with an overhang BD is shown in the figure. Obtain the equation of the deflection curve for the beam. Also, determine the deflections δ_c and δ_d at points C and D, respectively. (Assume $E = 200$ GPa and $I = 100 \times 10^6$ mm⁴.)

7.10-12 The overhanging beam shown in the figure is supported at A and B. Obtain the equation of the deflection curve and the deflections δ_c and δ_d at points C and D, respectively. (Assume $E = 200$ GPa and $I = 12 \times 10^6$ mm⁴.)

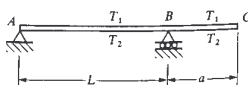
7.11-1 A simple beam of length L and height h undergoes a temperature change such that the bottom of the beam is at temperature T_2 and the top of the beam is at temperature T_1 (see Fig. 7-36a). Determine the equation of the deflection curve of the beam, the angle of rotation θ at the supports, and the deflection δ at the middle.

7.11-2 A cantilever beam of length L and height h is subjected to a temperature change such that the temperature on the upper surface is T_1 and on the lower surface is T_2 . Obtain expressions for the angle of rotation θ (assumed positive when clockwise) and the deflection δ (assumed positive when downward) at the free end.



Prob. 7.11-2

7.11-3 An overhanging beam ABC of height h is heated to a temperature T_1 on the top and T_2 on the bottom (see figure). Determine the deflection δ_c (assumed positive when downward) at the end of the overhang.



Prob. 7.11-3

7.11-4 A simple beam of length L and height h (see Fig. 7-36a) is heated nonuniformly so that the temperature difference $T_2 - T_1$ between the bottom and top of the beam varies linearly along the length of the beam; that is, $T_2 - T_1 = T_0x$, where T_0 is a constant. Determine the maximum deflection δ_{max} of the beam.

CHAPTER 8

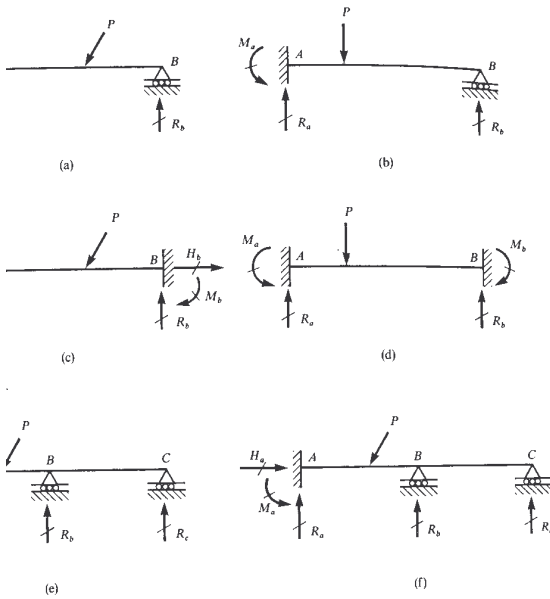
Statically Indeterminate Beams

8.1 STATICALLY INDETERMINATE BEAMS

In this chapter we will consider the analysis of beams that have a larger number of reactions than can be found from equations of static equilibrium. Such beams are said to be statically indeterminate, and their analysis requires that deflections be calculated. Only statically determinate beams were considered in the previous chapters, and in each instance we could immediately obtain the reactions of the beam by solving equations of static equilibrium. Knowing the reactions, we then could obtain the bending moments and shear forces, which in turn made it possible to find the stresses and deflections. However, when the beam is statically indeterminate, we cannot solve for the forces on the basis of equilibrium alone. Instead, we must take into account the deflections of the beam and obtain equations of compatibility to supplement the equations of equilibrium. This same procedure was discussed in Chapter 2 for statically indeterminate structures involving members in tension and compression.

Several types of statically indeterminate beams are illustrated in Fig. 8-1. The beam in part (a) of the figure is fixed (or clamped) at support A and is simply supported at B; such a beam is called either a propped cantilever beam or a fixed-simple beam. The reactions of the beam consist of horizontal and vertical forces at A, a couple at A, and a vertical force at B. Because there are only three independent equations of static equilibrium for the beam, it is not possible to calculate all four of these reactions by statics. The number of reactions in excess of the number of equilibrium equations is called the degree of statical indeterminacy. Thus, the beam pictured in Fig. 8-1a is said to be statically indeterminate to the first degree. Any reactions in excess of the number needed to support the structure in a statically determinate manner are called statical redundants, and the number of such redundants necessarily is the same

Statically Indeterminate Beams



indeterminate

as the degree of statical indeterminacy. For example, the reaction R_b shown in Fig. 8-1a may be considered as a redundant reaction. Note that the structure becomes a cantilever beam when the support at B is removed. The statically determinate structure that remains when the redundant is released is called the **released structure** or the **primary structure**.

Another approach to the beam in Fig. 8-1a is to consider the reactive moment M_a as the redundant; if the moment restraint is removed, the released structure is a simple beam with a pin support at A and a roller support at B.

A special case arises if all loads on the beam are vertical (Fig. 8-1e) because then the horizontal reaction vanishes. However, the beam is still statically indeterminate to the first degree inasmuch as there are now two independent equations of static equilibrium and three reactions.

A **fixed-end beam**, sometimes called a **fixed-fixed beam** or a **clamped beam**, is shown in Fig. 8-1c. At each support there are three reactive

quantities; hence, the beam has a total of six unknown reactions. Because there are three equations of equilibrium, the beam is statically indeterminate to the third degree. If we take the reactions at one end as the three redundants, and if we remove them from the structure, a cantilever beam will remain as the released structure. If we remove the two fixed-end moments and one horizontal reaction, the released structure is a simple beam.

Again considering the special case of vertical loads only (Fig. 8-1d), we find that there are only four reactions to be determined. The number of static equilibrium equations is two; therefore, the beam is statically indeterminate to the second degree.

The remaining two beams shown in Fig. 8-1 are examples of continuous beams, so called because they have more than one span and are continuous over a support. The beam shown in Fig. 8-1e is statically indeterminate to the first degree because there are four reactive forces and only three equations of static equilibrium. If R_b is selected as the redundant, and if we remove support B from the beam, there will remain a statically determinate simple beam AC. If R_c is selected as the redundant, the released structure will be a simple beam AB with an overhang BC.

The last beam shown in Fig. 8-1 is statically indeterminate to the second degree. If we select R_b and R_c as the redundant reactions, the released structure is a cantilever beam.

In the following sections, we will discuss various methods for analyzing statically indeterminate beams. The objective in each case is to determine the redundant reactions because, after they are known, the remaining force quantities always can be found from equilibrium. With the forces known, we then can determine the stresses and deflections at any point using the methods of beam analysis described in preceding chapters.

8.2 ANALYSIS BY THE DIFFERENTIAL EQUATIONS OF THE DEFLECTION CURVE

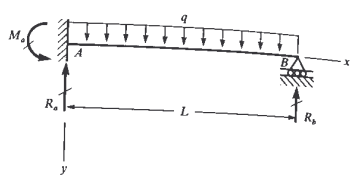
Statically indeterminate beams may be analyzed by solving one of the differential equations of the deflection curve. The procedure is essentially the same as that for a determinate beam (see Sections 7.2, 7.3, and 7.4) and consists of writing the differential equation, integrating to obtain its general solution, and then applying boundary conditions to evaluate the constants of integration. There will always be enough boundary conditions only to ascertain the constants of integration but also to find the redundant reactions that appear in the solution. Either the second-order equation in terms of the bending moment (Eq. 7-10a), the third-order equation in terms of the shear force (Eq. 7-10b), or the fourth-order equation in terms of the intensity of distributed load (Eq. 7-10c) may be used.

8.2 Analysis by the Differential Equations of the Deflection Curve 41

Because of the computational difficulties that arise when a large number of constants is to be evaluated, the method is practical only for relatively simple cases of loading and for beams of only one span. The following examples illustrate the procedure.*

Example 1

A propped cantilever beam AB with a uniform load of intensity q is shown in Fig. 8-2. Determine the reactions R_a , R_b , and M_a for this beam.



Example 1. Propped beam

Let us begin with the second-order differential equation of the deflection curve. Then it is necessary to obtain an expression for the bending moment M at any cross section of the beam. This expression will be in terms of not only the load but also the redundant reaction. Therefore, we need to select a redundant reaction and express the other reactions in terms of it. Let us choose the reaction R_b as the redundant; then, from equations of static equilibrium, we obtain the reactions at A in terms of R_b as follows:

$$R_a = qL - R_b \quad M_a = \frac{qL^2}{2} - R_b L \quad (a)$$

Now we can obtain a general expression for the bending moment in terms of R_b

$$M = R_a x - M_a - \frac{qx^2}{2} = qLx - R_b x - \frac{qL^2}{2} + R_b L - \frac{qx^2}{2}$$

The second-order differential equation of the deflection curve is

$$EIv'' = -M = -qLx + R_b x + \frac{qL^2}{2} - R_b L + \frac{qx^2}{2}$$

and two successive integrations give

$$EIv' = -\frac{qLx^2}{2} + \frac{R_b x^2}{2} + \frac{qL^2 x}{2} - R_b Lx + \frac{qx^3}{6} + C_1$$

$$EIv = -\frac{qLx^3}{6} + \frac{R_b x^3}{6} + \frac{qL^2 x^2}{4} - \frac{R_b Lx^2}{2} + \frac{qx^4}{24} + C_1 x + C_2$$

* The earliest use of the differential equation for analyzing statically indeterminate beams appears in Navier's book on strength of materials (Ref. 8-1).

There are three unknown quantities in these equations (C_1 , C_2 , and R_b) and three boundary conditions:

$$v(0) = 0 \quad v'(0) = 0 \quad v(L) = 0$$

Application of these conditions to the preceding equations gives $C_1 = 0$, $C_2 = 0$, and

$$R_b = \frac{3qL}{8} \quad (8-1)$$

With the value of the redundant R_b now established, we can easily find the remaining reactions from Eqs. (a):

$$R_a = \frac{5qL}{8} \quad M_a = \frac{qL^2}{8} \quad (8-2a, b)$$

Also, we can now substitute these quantities into the equations for the deflection v , the slope v' , and the bending moment M and thus obtain a complete analysis of the beam.

An alternate way to analyze this beam is to take the reactive moment M_a as the redundant. Then we express the bending moment M in terms of M_a , substitute the resulting expression into the second-order differential equation, and solve as before. Still another approach is to begin with the fourth-order equation, as illustrated in the next example. Also, the differential equations can be solved with the aid of discontinuity functions if desired.

Example 2

Analyze the fixed-end beam shown in Fig. 8-3 by solving the fourth-order differential equation of the deflection curve.

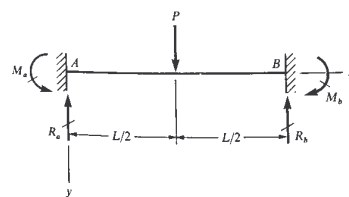


Fig. 8-3 Example 2. Fixed-end beam

The concentrated load P acts at the midpoint of the beam; hence, we conclude from symmetry that $M_b = M_a$ and $R_b = R_a = P/2$. Thus, only one redundant quantity (M_a) remains to be determined. No load acts on the beam in the region between $x = 0$ and $x = L/2$, so the differential equation becomes

$$EIv'''' = 0$$

Integration yields

$$\begin{aligned}
 Elv''' &= C_1 & (b) \\
 Elv'' &= C_1x + C_2 & (c) \\
 Elv' &= \frac{C_1x^2}{2} + C_2x + C_3 & (d) \\
 Elv &= \frac{C_1x^3}{6} + \frac{C_2x^2}{2} + C_3x + C_4
 \end{aligned}$$

The boundary conditions applicable to the left-hand half of the beam are as follows: First, the shear force throughout this part of the beam is equal to R_a , hence, from Eq. (b) we get $C_1 = -P/2$. Next, we observe that the bending moment at $x = 0$ is equal to $-M_a$; therefore, from Eq. (c) we get $C_2 = M_a$. The two conditions on the slope, namely, that $v' = 0$ when $x = 0$ and when $x = L/2$, yield $C_3 = 0$ and

$$M_a = \frac{PL}{8} \quad (8-3)$$

Thus, the redundant moment M_a has been found. Finally, we have the condition that $v = 0$ when $x = 0$, which gives $C_4 = 0$. Combining these results enables us to write the equation of the deflection curve:

$$v = \frac{Px^2}{48EI}(3L - 4x) \quad \left(0 \leq x \leq \frac{L}{2}\right) \quad (8-4)$$

From this equation we may find by differentiation the equations for the slope, the bending moment, and the shear force.

As we observed in this example, a sufficient number of boundary conditions always exists to evaluate not only the constants of integration but also the redundant reactions. Sometimes it is necessary to set up the differential equations for more than one region of the beam and then make use of conditions of continuity between regions, as was done previously for statically determinate beams. However, such analyses are very long and tedious.

released structure. Next we place the loads on the released structure and draw the corresponding diagram of bending moment divided by flexural rigidity (that is, the M/EI diagram). In a similar manner, the redundants are applied as loads acting on the released structure, and again the M/EI diagram is drawn. Finally, we invoke the moment-area theorems to provide the necessary equations for calculating the redundant reactions. These equations pertain to the areas and first moments of the M/EI diagrams; the particular relations to be used depend upon the type of beam and the choice of redundants. The following examples illustrate the techniques to be used.

Example 1

Using the moment-area method, determine the reactions for the propped cantilever beam AB shown in Fig. 8-4a.

This beam is statically indeterminate to the first degree, hence we select one reaction as the redundant. If R_b is selected as the redundant and removed, the released structure is a cantilever beam supported at A (Fig. 8-4b). On this beam we place P and R_b as loads, thus producing the bending-moment diagram shown in Fig. 8-4c. Since the beam has constant flexural rigidity EI , the M/EI diagram has the same shape as the moment diagram.

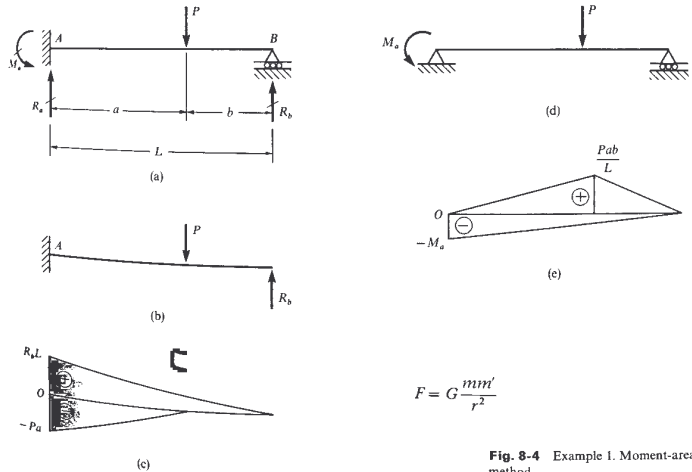
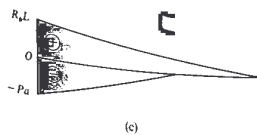


Fig. 8-4 Example 1. Moment-area method

8.3 MOMENT-AREA METHOD

Another method for analyzing a statically indeterminate beam is the moment-area method, described in Section 7.5 for finding beam deflections. In the case of an indeterminate beam, the procedure consists of using the two moment-area theorems to obtain the additional equations that are needed to calculate the redundant reactions. These additional equations represent conditions on the slopes and deflections of the beam, and the number of such conditions will always equal the number of redundants.

The analysis of a statically indeterminate beam by the moment-area method begins with the selection of the redundant reactions. Then these reactions are removed from the beam, leaving a statically determinate



8.3 Moment-Area Method

Statically Indeterminate Beams

Now we are ready to use the moment-area theorems. Because the slope of the deflection curve at support A is zero (Fig. 8-4a), we note that the tangent to the curve at point A passes through point B . In other words, the offset Δ_{AB} of area theorem that the first moment of the area of the M/EI diagram between A and B , taken with respect to point B , must equal zero. This relation gives the equation

$$\frac{L}{2} \left(\frac{R_b L}{EI} \right) \left(\frac{2L}{3} \right) - \frac{a}{2} \left(\frac{Pa}{EI} \right) \left(L - \frac{a}{3} \right) = 0$$

from which

$$R_b = \frac{Pa^2}{2L^3}(3L - a) \quad (8-5)$$

Knowing this redundant reaction, we can find from static equilibrium the other two reactions; the results are

$$R_a = \frac{Pb}{2L^3}(3L^2 - b^2) \quad M_a = \frac{Pab}{2L^2}(L + b) \quad (8-6a, b)$$

With all reactions known, we can proceed to calculate stresses and deflections as needed.

As an alternative solution, we can solve this same problem by considering the reactive moment M_a as the redundant. In that event, the released structure is a simple beam (Fig. 8-4d), and the corresponding bending-moment diagram due to P and M_a is shown in Fig. 8-4e. Again using the second moment-area theorem and taking the first moment of the area of the M/EI diagram about point B , we get

$$\frac{L}{2} \left(\frac{Pab}{LEI} \right) \left(\frac{L + b}{3} \right) - \frac{L}{2} \left(\frac{M_a}{EI} \right) \left(\frac{2L}{3} \right) = 0$$

Solving this equation, we obtain the same result for M_a as before (see Eq. 8-6b).

From the preceding results, we obtain the reactions for a beam with a concentrated load at the middle by substituting $a = b = L/2$; thus,

$$R_a = \frac{11P}{16} \quad R_b = \frac{5P}{16} \quad M_a = \frac{3PL}{16} \quad (8-7a, b, c)$$

Note that the vertical reaction at the fixed support is over twice as large as the reaction at the simple support, although the load is at the middle.

Example 2

Determine the reactions for a fixed-end beam loaded by a couple M_0 (Fig. 8-5a). Also, find the deflection of the beam at point C where the couple acts.

This beam is statically indeterminate to the second degree, hence two redundants must be selected. The three useful possibilities are as follows: R_a and M_a , which gives a released structure in the form of a cantilever beam fixed at B ; R_b and M_b , which gives a cantilever beam fixed at A ; and M_a and M_b , which gives a simple beam. Let us select the first alternative, taking R_a and M_a as

the redundants. Then the released structure is the cantilever beam of Fig. 8-5b. We can easily draw the shear-force and bending-moment diagrams (Fig. 8-5c) for this beam, which is subjected to R_a , M_a , and M_0 as loads. Again, the M/EI diagram has the same shape, because EI is assumed to be constant.

Two conditions concerning the deflections of the beam are required for finding the two redundants. As a first condition, we note that both ends of the beam have zero slopes; hence, the change in slope between A and B is zero. It follows from the first moment-area theorem that the area of the M/EI diagram between A and B must be zero; thus,

$$\frac{L}{2} \left(\frac{R_a L}{EI} \right) - \frac{M_a}{EI}(L) - \frac{M_0}{EI}(b) = 0$$

$$R_a L^2 - 2M_a L = 2M_0 b \quad (a)$$

or

The second condition is obtained from the fact that the tangent to the deflection curve at A passes through point B , which means that the first moment of the area of the M/EI diagram between A and B , taken about B , is zero. The resulting equation is

$$\frac{L}{2} \left(\frac{R_a L}{EI} \right) \left(\frac{L}{3} \right) - L \left(\frac{M_a}{EI} \right) \left(\frac{L}{2} \right) - b \left(\frac{M_0}{EI} \right) \left(\frac{b}{2} \right) = 0$$

$$R_a L^3 - 3M_a L^2 = 3M_0 b^2 \quad (b)$$

Now we can solve simultaneously Eqs. (a) and (b) and obtain the redundants:

$$R_a = \frac{6M_0 ab}{L^3} \quad M_a = \frac{M_0 b}{L^2}(2a - b) \quad (8-8a, b)$$

The other two reactions are

$$R_b = -R_a \quad M_b = \frac{M_0 a}{L^2}(a - 2b) \quad (8-9a, b)$$

found from static equilibrium equations.

The deflection δ_c at the point where the load is applied can be found from the second moment-area theorem. We observe that δ_c is equal to the offset of point C from the tangent at A, because the tangent at A is horizontal. Therefore, δ_c is equal to the first moment of the area of the M/EI diagram between A and C, taken about point C. Referring to Fig. 8-5c, we see that this deflection is calculated as follows:

$$\delta_c = \frac{a}{2} \left(\frac{a}{L} \right) \left(\frac{R_a L}{EI} \right) \left(\frac{a}{3} \right) - a \left(\frac{M_a}{EI} \right) \left(\frac{a}{2} \right) = \frac{R_a a^3}{6EI} - \frac{M_a a^2}{2EI}$$

Substituting the expressions for R_a and M_a (see Eqs. 8-8), we get

$$\delta_c = \frac{M_0 a^2 b^2 (b-a)}{2L^3 EI} \tag{8-10}$$

for the deflection under the load.

If the couple M_0 acts at the midpoint of the span ($a = b = L/2$), the reactions are

$$M_a = -M_b = \frac{M_0}{4} \quad R_a = -R_b = \frac{3M_0}{2L} \tag{8-11a, b}$$

and the deflection at the middle is zero.

The area of the M/EI diagram between A and B equals zero (from the first moment-area theorem):

$$L \left(\frac{M_b}{EI} \right) - \frac{L}{2} \left(\frac{R_b L}{EI} \right) = 0$$

$$2M_b = R_b L \tag{c}$$

The second condition relates to the offset of point B from the tangent at A. Since this offset is Δ , it follows from the second moment-area theorem that Δ is equal to the negative of the first moment of the area of the M/EI diagram between A and B, taken with respect to B:

$$\Delta = -L \left(\frac{M_b}{EI} \right) \left(\frac{L}{2} \right) + \frac{L}{2} \left(\frac{R_b L}{EI} \right) \left(\frac{2L}{3} \right)$$

$$2R_b L - 3M_b = \frac{6EI\Delta}{L^2} \tag{d}$$

Solving Eqs. (c) and (d), we get

$$R_b = \frac{12EI\Delta}{L^3} \quad M_b = \frac{6EI\Delta}{L^2} \tag{8-12a, b}$$

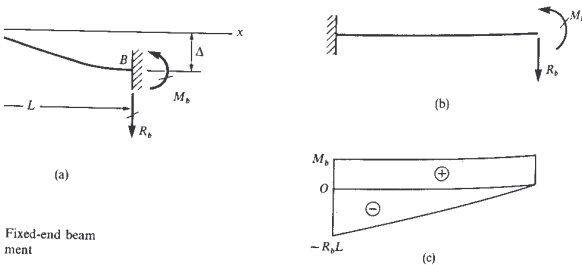
From the symmetry of the beam, we note that $R_a = R_b$ and $M_a = M_b$.

Example 3

A fixed-end beam AB has its right-hand support lowered vertically without rotation by an amount Δ (Fig. 8-6a). Determine the reactions for this beam.

Let us select the reactions R_b and M_b at support B as the redundants. The corresponding released structure, subjected to loads R_b and M_b , is shown in Fig. 8-6b. The bending-moment diagram is shown in the last part of the figure.

Two equations are required to solve for both R_b and M_b . The first equation expresses the condition that the slope of the beam is zero at each support. Hence,



Fixed-end beam ment

8.4 METHOD OF SUPERPOSITION (FLEXIBILITY METHOD)

The method of superposition is of great importance in the analysis of statically indeterminate structures. It is applicable to many different types of structures, such as trusses and frames, in addition to beams, which are our primary concern in this chapter. We have previously used the method in analyzing statically indeterminate systems composed of members in tension and compression (see Section 2.4).

The essence of the superposition method can be described in simple terms. We begin by identifying the statical redundants, as explained in the preceding sections. Then the redundants are removed from the indeterminate beam, leaving a statically determinate released structure. The displacements of the released structure can be found by the techniques described in Chapter 7. In particular, the displacements (either translations or rotations) corresponding to the redundants and caused by the loads can be ascertained. Next, the redundants themselves are visualized as loads acting on the released structure, and the corresponding displacements are calculated. From the principle of superposition, we know that the final displacements due to both the actual loads and the redundants must be equal to the sum of those displacements as

calculated separately. In the case of redundant constraints, the corresponding displacements either are zero or have known magnitudes; hence, we can write equations of superposition expressing these relationships. Finally, these equations can be solved for the values of the redundant reactions, after which all other reactions can be determined from equations of static equilibrium.

The steps described in the preceding paragraph can be made clearer through an illustration. Let us again analyze a propped cantilever beam supporting a uniform load (see Fig. 8-7a). If the reaction R_b is selected as the statical redundant and the corresponding constraint is removed, we obtain a cantilever beam for the released structure (Fig. 8-7b). The deflection of this beam at end B due to the uniform load is denoted δ_b' , and the deflection caused by the redundant is δ_b'' (see Fig. 8-7c). The total deflection δ_b in the original structure, obtained by superimposing the deflections δ_b' and δ_b'' , must be zero. This conclusion leads to the following equation:

$$\delta_b = \delta_b' - \delta_b'' = 0 \tag{a}$$

The minus sign appears in this equation because δ_b' is downward whereas δ_b'' is upward. The deflections δ_b' and δ_b'' due to the uniform load q and the redundant R_b are easily found with the aid of Table G-1 in Appendix G (see Cases 1 and 4). Using the formulas given there, we get from Eq. (a):

$$\delta_b = \frac{qL^4}{8EI} - \frac{R_b L^3}{3EI} = 0$$

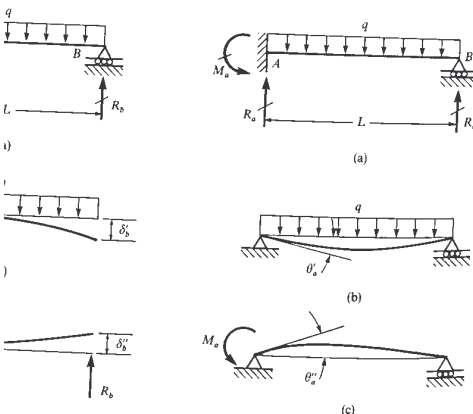


Fig. 8-8 Method of superposition

$$R_b = \frac{3qL}{8} \tag{8-13}$$

The reaction R_a and the moment M_a can now be found from the equilibrium of the beam; the results are

$$R_a = \frac{5qL}{8} \quad M_a = \frac{qL^2}{8} \tag{8-14a, b}$$

This same beam (Fig. 8-8a) could have been analyzed in a different way by taking the moment M_a as the redundant; then the released structure is a simple beam (Figs. 8-8b and c). The angle of rotation produced by the uniform load acting on the released structure (Table G-2, Case 1) is

$$\theta_a = \frac{qL^3}{24EI}$$

and the corresponding angle caused by the redundant M_a (Table G-2, Case 7) is

$$\theta_a' = \frac{M_a L}{3EI}$$

The equation of superposition, stating that the angle of rotation at support A of the original beam is zero, becomes

$$\theta_a = \theta_a' - \theta_a'' = \frac{qL^3}{24EI} - \frac{M_a L}{3EI} = 0 \tag{b}$$

Solving this equation, we get $M_a = qL^2/8$, which agrees with the previous result.

After finding the reactions of a statically indeterminate beam, the calculation of all stress resultants (axial forces, shear forces, and bending moments) presents no further difficulty because equations of static equilibrium are sufficient for this purpose. Furthermore, deflections and slopes can also be obtained at any point, either by using the differential equation of the deflection curve or by using the principle of superposition in conjunction with the deflection formulas listed in Appendix G. In the illustrative examples that follow, and also in the problems, attention will be directed primarily to finding the reactions, which is the key step in the solution.

The method of analysis described in this section is called the flexibility method or the force method of analysis. The latter name arises from the use of force quantities (forces and couples) as the redundants; the former name is used because the coefficients of the unknowns (terms such as $L/3EI$ in Eq. (b)) are flexibilities (that is, deflections produced by a unit load). The equations of superposition that express conditions imposed on the deflections (see Eqs. (a) and (b)) are usually called equations of compatibility. The method of superposition, like the moment-area method and the differential equation of the deflection curve, applies only to linear elastic structures.

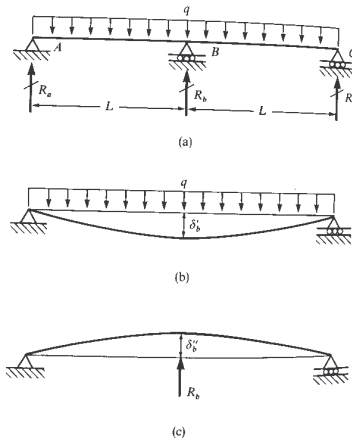
Example 1

The reactions for the two-span continuous beam *ABC* shown in Fig. 8-9a are to be determined by the method of superposition. Note that the beam supports a uniform load of intensity *q*.

Selecting the middle reaction *R_b* as the redundant, the released structure is a simple beam (Fig. 8-9b). Under the action of the uniform load, the deflection at point *B* in the released structure (see Table G-2, Case 1) is

$$\delta_b = \frac{5q(2L)^4}{384EI} = \frac{5qL^4}{24EI}$$

where *L* is the length of each span. The deflection in the upward direction produced by the redundant (see Fig. 8-9c) is



8-9 Example 1. Two-span continuous beam

$$\delta_b'' = \frac{R_b(2L)^3}{48EI} = \frac{R_b L^3}{6EI}$$

as obtained from Table G-2, Case 4. The equation of compatibility pertaining to the vertical deflection at point *B* is

$$\delta_b = \delta_b' - \delta_b'' = \frac{5qL^4}{24EI} - \frac{R_b L^3}{6EI} = 0$$

from which

$$R_b = \frac{5qL}{4}$$

Since the reactions have the values *R_a* = *R_c* = 3*qL*/8, as found from static equilibrium. With all the reactions known, we will have no difficulty in proceeding to find the stresses and deflections.

Example 2

A beam with fixed ends is loaded by a force *P* acting at the position shown in Fig. 8-10a. Find the reactive forces and moments at the ends of the beam. Let us select the reactive moments *M_a* and *M_b* for the redundants, thereby giving a released structure in the form of a simple beam (Fig. 8-10b). The angles at the ends produced by the load *P* are obtained from Case 5 of Table G-2:

$$\theta_a' = \frac{Pab(L+b)}{6LEI} \quad \theta_b' = \frac{Pab(L+a)}{6LEI}$$

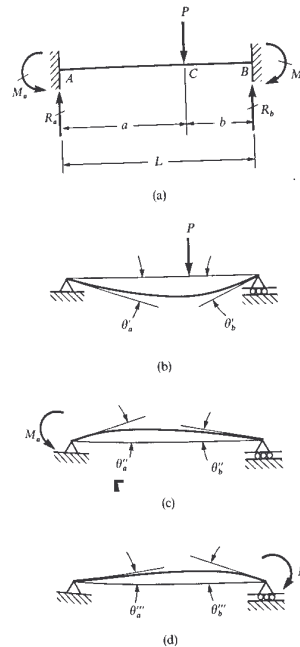


Fig. 8-10 Example 2. Fixed-end beam with a concentrated load

Now we apply the redundant moments *M_a* and *M_b* as if they were loads on the released structure (Figs. 8-10c and d). The angles at the ends due to *M_a* are

$$\theta_a'' = \frac{M_a L}{3EI} \quad \theta_b'' = \frac{M_b L}{6EI}$$

and due to *M_b* are

$$\theta_a''' = \frac{M_b L}{6EI} \quad \theta_b''' = \frac{M_b L}{3EI}$$

Because the angles of rotation at both ends in the original beam are zero, we have two equations of compatibility:

$$\theta_a = \theta_a' - \theta_a'' - \theta_a''' = 0$$

$$\theta_b = \theta_b' - \theta_b'' - \theta_b''' = 0$$

When the various expressions for the angles are substituted into these equations, we arrive at two simultaneous equations containing *M_a* and *M_b* as unknowns

$$\frac{M_a L}{3EI} + \frac{M_b L}{6EI} = \frac{Pab(L+b)}{6LEI}$$

$$\frac{M_a L}{6EI} + \frac{M_b L}{3EI} = \frac{Pab(L+a)}{6LEI}$$

The solutions are

$$M_a = \frac{Pab^2}{L^2} \quad M_b = \frac{Pa^2b}{L^2} \quad (8-16a, b)$$

Using these results and also equations of equilibrium, we obtain the following formulas for the vertical reactions:

$$R_a = \frac{Pb^2}{L^2}(L+2a) \quad R_b = \frac{Pa^2}{L^2}(L+2b) \quad (8-17a, b)$$

To illustrate how the principle of superposition may be used to obtain deflections, let us now calculate the deflection of the fixed-end beam at point *C* where the load is applied (Fig. 8-10a). The deflection at this point in the released structure under the action of the load *P* (Fig. 8-10b) is

$$\delta_c' = \frac{Pa^2b^2}{3LEI}$$

from Case 5, Table G-2. The upward deflections at this same point of the released structure due to the couples *M_a* and *M_b* (see Figs. 8-10c and d) are

$$\delta_c'' = \frac{M_a ab}{6LEI} \quad \delta_c''' = \frac{M_b ab}{6LEI}(L+a)$$

as found from Case 7, Table G-2. Substituting the values of *M_a* and *M_b* from Eqs. (8-16), we get

$$\delta_c'' = \frac{Pa^2b^3}{6L^3EI}(L+b) \quad \delta_c''' = \frac{Pa^3b^2}{6L^3EI}(L+a)$$

Therefore, the total deflection at point *C* is

$$\delta_c = \delta_c' - \delta_c'' - \delta_c''' = \frac{Pa^2b^3}{3L^3EI} \quad (8-18)$$

In the special case when the load *P* is at the middle of the beam, the deflection at the center is

$$\delta_c = \frac{PL^3}{192EI} \quad (8-19)$$

and the reactions are

$$M_a = M_b = \frac{PL}{8} \quad R_a = R_b = \frac{P}{2} \quad (8-20a, b)$$

Example 3

Find the reactions for a fixed-end beam with a uniform load over part of the span (Fig. 8-11).

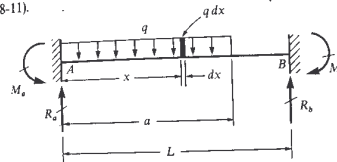


Fig. 8-11 Example 3. Fixed-end beam with a uniform load over part of the span

Let us isolate an element *q dx* of the load at distance *x* from the left-hand end of the beam. By treating this element as a concentrated load, we can utilize the formulas derived in the preceding example. Beginning with the formulas for the moments *M_a* and *M_b* (see Eqs. 8-16), we can replace *P* with *q dx*, *a* with *x*, and *b* with *L - x*; hence, the fixed-end moments due to the element of load are

$$dM_a = \frac{qx(L-x)^2 dx}{L^2} \quad dM_b = \frac{qx^2(L-x) dx}{L^2}$$

Integration over the loaded part of the beam yields

$$M_a = \int dM_a = \frac{q}{L^2} \int_0^a x(L-x)^2 dx = \frac{qa^2}{12L^2}(6L^2 - 8aL + 3a^2) \quad (8-21)$$

$$M_b = \int dM_b = \frac{q}{L^2} \int_0^a x^2(L-x) dx = \frac{qa^3}{12L^2}(4L - 3a) \quad (8-22)$$

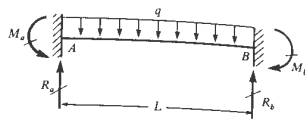
Similarly, the vertical reactions at the ends can be found with the aid of Eqs. (8-17):

$$R_a = \frac{q}{L^3} \int_0^a (L-x)^2(L+2x) dx = \frac{qa}{2L^3}(2L^3 - 2a^2L + a^3) \quad (8-23)$$

$$R_b = \frac{q}{L^3} \int_0^a x^2(3L-2x) dx = \frac{qa^3}{2L^3}(2L-a) \quad (8-24)$$

Thus, the desired results have been found.

Example 3. Fixed-end beam with a uniform load



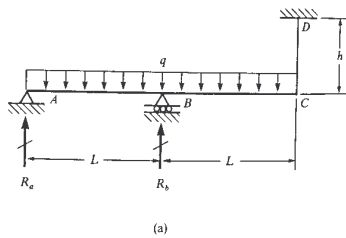
If a fixed-end beam has a uniform load over the entire span (Fig. 8-12), we can obtain the reactions by substituting $a = L$ into the preceding equations yielding

$$M_a = M_b = \frac{qL^2}{12} \quad R_a = R_b = \frac{qL}{2} \quad (8-25a, b)$$

The reactions at the supports of a beam with fixed ends are called **fixed-end moments** and **fixed-end forces**. They have an important role in several methods of structural analysis.

Example 4

A beam ABC (Fig. 8-13a) is simply supported at A and B and is hung from a cable CD at point C. Prior to the application of the uniform load q , there is no force in the cable nor is there any slack in the cable. When the load q is applied,



Example 4. Beam supported

the beam deflects downward at C and a tensile force T develops in the cable. Find the magnitude of this force.

It is convenient in this analysis to select the unknown force T in the cable as the redundant and to cut the structure into two parts (Fig. 8-13b). The released structure then consists of the beam ABC and the cable CD as independent structures, with the force T acting upward on the beam and downward on the cable. The deflection at point C on the beam will consist of two parts, a downward deflection δ_c' due to the uniform load and an upward deflection δ_c'' due to the force T . At the same time, the end of the cable (point C) will deflect downward by an amount δ_c''' , equal to the elongation of the cable. Therefore, the equation of compatibility, expressing the fact that the downward displacement of the end of the beam is equal to the elongation of the cable, is

$$\delta_c' - \delta_c'' = \delta_c'''$$

Having formulated this equation, we now turn to the task of evaluating the three deflection terms.

The deflection at the end of the overhang produced by the uniform load can be found from the results given in Example 3 of Section 7.6. Using Eq. (7-54) of that example, and substituting $a = L$, we get

$$\delta_c' = \frac{qL^3}{4EI}$$

where EI is the flexural rigidity of the beam. The deflection of the beam at C due to the force T can be taken from the answer to Problem 7.5-14 by again substituting $a = L$; hence,

$$\delta_c'' = \frac{2TL^3}{3EI}$$

Finally, the stretch of the cable is

$$\delta_c''' = \frac{Th}{EA}$$

where h is the length of the cable and EA is its axial rigidity.

By substituting the preceding deflection formulas into the equation of compatibility and solving for the force T , we get

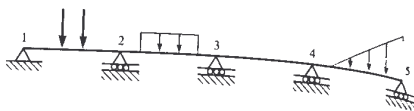
$$T = \frac{3qAL^4}{8AL^3 + 12th} \quad (8-26)$$

Note that in this example the redundant was selected as an internal force quantity instead of an external reaction.

8.5 CONTINUOUS BEAMS

Beams that are continuous over many supports (see Fig. 8-14) are known as **continuous beams** and are commonly encountered in buildings, pipelines, bridges, and various kinds of specialized structures. If the loads on a continuous beam are vertical and if there are no axial deformations,

Fig. 8-14 Continuous beam



then all reactions will be vertical. To represent this behavior schematically, we can consider one of the supports to be a pin support and all the others to be roller supports, as shown in the figure. Then the total number of reactions will be the same as the number of supports, and the degree of statical indeterminacy will be two less than this number. Thus, for the beam shown in Fig. 8-14, there are five vertical reactions, of which three are redundants.

Although we may analyze a continuous beam by any of the methods described in the preceding sections, only the method of superposition is practical. When using this method, one possibility is to select the reactions at the intermediate supports as the redundants, which means that the released structure is a simple beam. This technique was used in Example 1 of Section 8.4 (see Fig. 8-9) and is satisfactory for beams of only two or three spans. When there are more than two redundants, it is advantageous to select the bending moments in the beam at the intermediate supports as the redundants. This choice greatly simplifies the calculations because it leads to a set of simultaneous equations in which no more than three unknowns appear in each equation regardless of the number of redundants.

Let us now develop in more detail this procedure for analyzing continuous beams. When the bending moments at the supports are released from the structure, the continuity of the beam at the supports is broken; hence, the released structure consists of a series of simple beams. Each such beam is subjected to the external loads that normally act on it, together with the two redundant moments at its ends. Under the action of these loads, we can determine the angles of rotation at the ends of each simple beam. The equations of compatibility, which express the fact that at each support the adjacent beams must have the same angle of rotation, provide the necessary equations to solve for the unknown bending moments.

Consider, for example, the portion of a continuous beam shown in Fig. 8-15a. The three consecutive supports are identified as A, B, and C, and the lengths and moments of inertia of the two adjacent spans are denoted by L_a, I_a and L_b, I_b , respectively. Let M_a, M_b , and M_c denote the bending moments at the three supports. The true directions of these moments will depend upon the loads on the beam, but for purposes of this derivation we will assume they are positive (that is, causing compression on the top of the beam). The released structure, consisting of two simple beams, is shown in Fig. 8-15b for the two adjacent spans. Each span is loaded by the applied external loads plus the redundant bending moments. These loads produce deflections and rotations of the two sim-

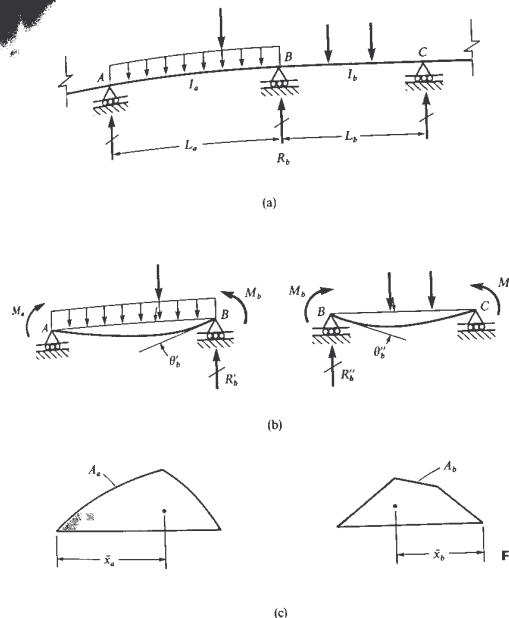


Fig. 8-15 Three-moment equation

ple beams. The angle of rotation of the left-hand beam at support B is indicated in the figure as θ_b' , and the rotation of the right-hand beam at this same support is θ_b'' . These angles are taken to be positive as shown in the figure (that is, in the same directions as the positive bending moments M_b). Because the axis of the beam is actually continuous across support B, the equation of compatibility is

$$\theta_b' = -\theta_b'' \quad (8-27)$$

which expresses the fact that the slopes of the two simple beams must match each other at B. The next step is to develop appropriate expressions for the angles θ_b' and θ_b'' and substitute into Eq. (8-27).

The bending-moment diagrams associated with the external loads acting on the released structure are shown in Fig. 8-15c. The particular shapes of these diagrams will depend upon the nature of the loads. How-

ever, in all instances, we can characterize the bending-moment diagrams by their areas and centroidal distances. Let us denote the areas of the two diagrams as A_a and A_b , respectively. Also, the distance from the centroid of A_a to the centroid of A_b is denoted by \bar{x}_a , and the distance from point c to the centroid of A_b is denoted by \bar{x}_b . We can use these properties of the bending-moment diagrams to evaluate the angles θ'_b and θ''_b . We note from the second moment-area theorem that the contribution to the angle θ'_b from the external loads on beam AB is

$$\frac{A_a \bar{x}_a}{EI_a L_a}$$

In addition, the moments M_a and M_b contribute to θ'_b in the following amounts:

$$\frac{M_a L_a}{6EI_a} \quad \text{and} \quad \frac{M_b L_a}{3EI_a}$$

Thus, the angle θ'_b is

$$\theta'_b = \frac{M_a L_a}{6EI_a} + \frac{M_b L_a}{3EI_a} + \frac{A_a \bar{x}_a}{EI_a L_a} \quad (a)$$

Considering the right-hand span BC , we obtain in an analogous manner the following equation for θ''_b :

$$\theta''_b = \frac{M_b L_b}{3EI_b} + \frac{M_c L_b}{6EI_b} + \frac{A_b \bar{x}_b}{EI_b L_b} \quad (b)$$

Thus, the angles of rotation at support B are expressed in terms of the bending moments at the supports and the properties of the M/EI diagrams for the two adjacent spans.

Next, we substitute the expressions for θ'_b and θ''_b (Eqs. a and b) into the equation of compatibility (Eq. 8-27) and rearrange the terms; in this manner, we obtain the following equation:

$$M_a \left(\frac{L_a}{I_a} \right) + 2M_b \left(\frac{L_a}{I_a} + \frac{L_b}{I_b} \right) + M_c \left(\frac{L_b}{I_b} \right) = - \frac{6A_a \bar{x}_a}{I_a L_a} - \frac{6A_b \bar{x}_b}{I_b L_b} \quad (8-28)$$

This equation is called the **three-moment equation** because it relates three consecutive bending moments in the beam. If all spans have the same moment of inertia I , the three-moment equation simplifies to the following:

$$M_a L_a + 2M_b(L_a + L_b) + M_c L_b = - \frac{6A_a \bar{x}_a}{L_a} - \frac{6A_b \bar{x}_b}{L_b} \quad (8-29)$$

If all spans have the same length L , the equation becomes even simpler:

$$M_a + 4M_b + M_c = - \frac{6}{L^2} (A_a \bar{x}_a + A_b \bar{x}_b) \quad (8-30)$$

The procedure when using the three-moment equation is to write the equation once for each intermediate support of the continuous beam, thus providing as many equations as there are redundant bending moments. Then these equations can be solved simultaneously for the moments.

The terms on the right-hand sides of the three-moment equations can be evaluated from the loads on the beam. For instance, if a uniform load of intensity q acts on span AB , we have

$$A_a = \frac{2}{3} \left(\frac{qL_a^2}{8} \right) (L_a) = \frac{qL_a^3}{12} \quad \bar{x}_a = \frac{L_a}{2}$$

and, hence,

$$A_a \bar{x}_a = \frac{qL_a^4}{24} \quad (8-31)$$

For a concentrated load P at the center of the span, the terms are

$$A_a = \frac{1}{2} \left(\frac{PL_a}{4} \right) (L_a) = \frac{PL_a^2}{8} \quad \bar{x}_a = \frac{L_a}{2}$$

and

$$A_a \bar{x}_a = \frac{PL_a^3}{16} \quad (8-32)$$

These two examples are sufficient to show that there is no major difficulty in evaluating the terms involving the bending-moment diagrams. Once this step is accomplished, the equations can be formulated by merely writing them down, after which they can be solved for the unknown bending moments.*

Throughout the foregoing discussion, it has been assumed that the two extreme ends of the continuous beam were simply supported. If either or both of these ends should be a **fixed support**, the number of redundant moments will be increased (see Fig. 8-16a). An easy way to handle this situation is to replace the fixed support by an additional span having an infinite moment of inertia (Fig. 8-16b). The effect of this extra span having infinitely large stiffness is to prevent rotation at support 1, which is the same condition imposed by the fixed support. The bending moments found at points 1, 2, and 3 in the continuous beam shown in Fig. 8-16b will be identical to those in the original beam. The

* The three-moment equation was developed by the French engineers B.P.E. Clapeyron and H. Bertot in the middle of the 19th century (see Ref. 8-3).

Statically Indeterminate Beams

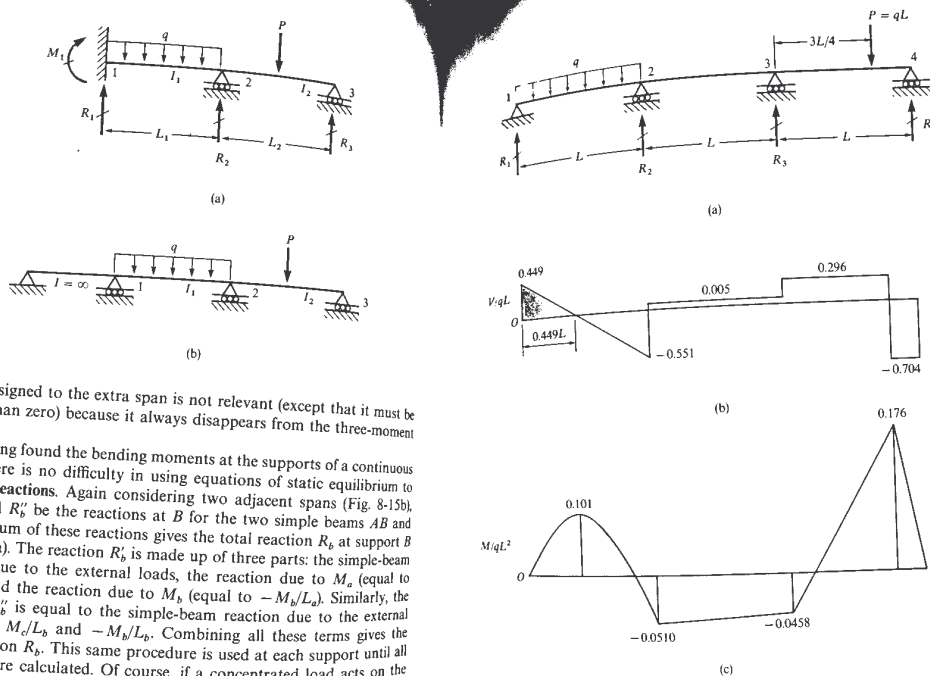


Fig. 8-17 Example 1. Three-moment equation

length assigned to the extra span is not relevant (except that it must be greater than zero) because it always disappears from the three-moment equation.

Having found the bending moments at the supports of a continuous beam, there is no difficulty in using equations of static equilibrium to find the reactions. Again considering two adjacent spans (Fig. 8-15b), let R'_b and R''_b be the reactions at B for the two simple beams AB and BC . The sum of these reactions gives the total reaction R_b at support B (Fig. 8-15a). The reaction R'_b is made up of three parts: the simple-beam reaction due to the external loads, the reaction due to M_a (equal to M_a/L_a), and the reaction due to M_b (equal to $-M_b/L_a$). Similarly, the reaction R''_b is equal to the simple-beam reaction due to the external loads plus M_c/L_b and $-M_b/L_b$. Combining all these terms gives the total reaction R_b . This same procedure is used at each support until all reactions are calculated. Of course, if a concentrated load acts on the beam over a support, it will be transmitted directly into the reaction.

Example 1

As an illustration of the use of the three-moment equation, we will analyze the continuous beam shown in Fig. 8-17. The beam has three spans of equal length and constant moment of inertia, and it is loaded in the first and third spans. The concentrated load P is assumed to be equal to qL .

Equation (8-30) can be used in this example because the moments of inertia and the lengths are the same for all spans. As a preliminary matter, we will determine the terms of the form $A\bar{x}$ that appear on the right-hand side of the equation, for each of the three spans. For span 1-2 this term is $qL^4/24$, as given

by Eq. (8-31). For span 2-3 this term becomes zero because there is no load. Finally, for span 3-4 we observe that the bending-moment diagram is a triangle with maximum ordinate equal to $3PL/16$. The area of the triangle is $3PL^2/32$, and its centroidal distance from point 4 is $5L/12$ (see Appendix D, Case 3). Therefore, the term $A\bar{x}$ has the value $5qL^4/128$, which becomes $5qL^4/128$ because we assumed that P equals qL .

Now we are ready to write the three-moment equations for the interior supports. Considering support 2, we recognize that M_a in the general equation (Eq. 8-30) becomes M_1 (which is zero), M_b becomes M_2 , and M_c becomes M_3 ; thus

$$4M_2 + M_3 = - \frac{qL^2}{4} \quad (c)$$

which converges provided that t is numerically less than one. If t is very small compared to unity, we can disregard the terms involving $t^2, t^3,$ and so on, in comparison with the first two terms, and obtain

$$(1+t)^{1/2} \approx 1 + \frac{t}{2} \tag{8-37}$$

The term $(dv/dx)^2$ in Eq. (a) is very small in ordinary beams; hence, using Eq. (8-37), we can rewrite Eq. (a) as

$$ds - dx = dx \left[1 + \frac{1}{2} \left(\frac{dv}{dx} \right)^2 \right] - dx = \frac{1}{2} \left(\frac{dv}{dx} \right)^2 dx$$

If this expression is integrated over the length of the beam, we obtain the difference λ between the total length of the beam and the chord AB :

$$\lambda = \frac{1}{2} \int_0^L \left(\frac{dv}{dx} \right)^2 dx \tag{8-38}$$

Thus, whenever the equation of the deflection curve of the beam is known, we can use Eq. (8-38) to obtain the horizontal displacement λ .

If the ends of the beam are prevented from translating horizontally, as shown in Fig. 8-20b, then a horizontal reaction H will develop at each end. This force will cause the axis of the beam to elongate as bending occurs. In addition, the force H itself will have an effect upon the bending moments in the beam and hence also upon the deflection curve of the beam. Rather than attempt an exact analysis of this complicated problem, let us instead obtain an approximate expression for the force H in order to ascertain its importance. A reasonable approximation to the shape of the deflection curve of the beam is a parabola having the equation

$$v = \frac{4\delta x(L-x)}{L^2} \tag{b}$$

where δ is the deflection at the middle. The distance λ corresponding to this assumed deflected shape can be found by substituting Eq. (b) into Eq. (8-38), which gives

$$\lambda = \frac{8\delta^2}{3L}$$

The force H required to elongate the beam by this amount is

$$H = \frac{EA\lambda}{L} = \frac{8EA\delta^2}{3L^2}$$

and the corresponding axial tensile stress is

$$\sigma = \frac{H}{A} = \frac{8E\delta^2}{3L^2} \tag{c}$$

The deflection δ at the middle of a beam is ordinarily very small compared to the length; for example, the ratio δ/L might be $1/500$. Using this number, and also assuming that the material is steel with $E = 30 \times 10^6$ psi, we see from Eq. (c) that the stress σ is only 320 psi. Thus, the axial stress due to H is very small compared to the allowable bending stress in the beam. Furthermore, in practice, the ends of the beam cannot be held rigidly, and some small horizontal movement always will occur, thereby reducing the axial force calculated above. Thus, we conclude that the customary practice of disregarding the effects of any horizontal restraint, and assuming that one end of the beam is on a roller, is justified. (For a more exact analysis of beams with immovable supports, see Ref. 8-6.)

PROBLEMS/CHAPTER 8

The problems for Section 8.2 are to be solved by integrating the differential equation of the deflection curve.

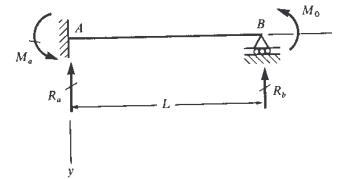
8.2-1 Determine the reactions for the propped cantilever beam AB shown in Fig. 8-2 (Example 1) by taking the reactive moment M_0 as the redundant and using the second-order differential equation. Then obtain the equation of the deflection curve and the location and magnitude of the maximum deflection δ_{max} .

8.2-2 Beginning with the fourth-order differential equation in terms of the intensity of the distributed load, obtain the reactions for the propped cantilever beam AB of Fig. 8-2 (Example 1). Then draw the shear-force and bending-moment diagrams for the beam, labeling all critical ordinates including maximum and minimum values.

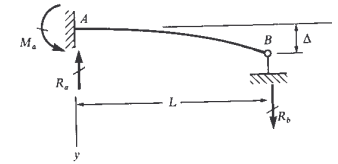
8.2-3 Determine the reactions for the fixed-end beam with a concentrated load P shown in Fig. 8-3 (Example 2) by starting with the second-order differential equation in terms of the bending moment. Also, determine the maximum deflection δ_{max} of the beam and draw the shear-force and bending-moment diagrams, labeling all critical ordinates including maximum and minimum values.

8.2-4 A propped cantilever beam AB is subjected to a couple M_0 acting at support B (see figure). Derive the equation of the deflection curve and determine the reactions at the supports. Also, construct the shear-force and bending-moment diagrams, labeling all critical ordinates.

8.2-5 A cantilever beam AB has a fixed support at A (see figure). At end B , the beam is pulled downward by a wire. Determine the equation of the deflection in terms of the deflection Δ at end B . Also, determine reactions R_A , R_B , and M_A in terms of Δ .



Prob. 8.2-4



Prob. 8.2-5

CHAPTER

Unsymmetric Bending

9.1 INTRODUCTION

The theories for bending of beams that we developed in preceding chapters are restricted to beams having a plane of symmetry through the longitudinal axis. A beam of this kind is shown in Fig. 9-1a, where the xy plane is an axial plane of symmetry for the cantilever beam. We also assume that the lateral loads act in the plane of symmetry, from which it follows that the beam deflects only in the y direction. The xy plane is known as the **plane of bending**. Because the y axis is an axis of symmetry, it is a principal axis of the cross section (Fig. 9-1b). Furthermore, the neutral axis (the z axis), which is perpendicular to the y axis, is also a principal axis. If the material of the beam is linearly elastic, then the neutral axis passes through the centroid C . Thus, the y and z axes are centroidal principal axes of the cross section (Fig. 9-1b). Under these conditions, the normal bending stresses acting on the cross sections vary linearly with the distance from the neutral axis and are calculated from the flexure formula $\sigma_x = My/I$ (Eq. 5-10).

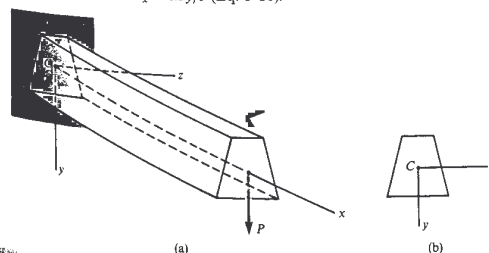


Fig. 9-1 Beam with an axial plane of symmetry (the xy plane)

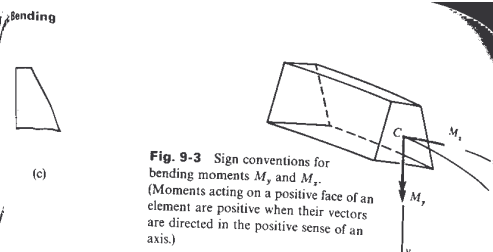


Fig. 9-3 Sign conventions for bending moments M_y and M_z . (Moments acting on a positive face of an element are positive when their vectors are directed in the positive sense of an axis.)

In this chapter we consider **unsymmetric bending** of beams, which occurs when the cross sections are not symmetric or when the loads do not act in a plane of symmetry. We will describe the cross section of a beam as doubly symmetric, singly symmetric, or unsymmetric according to whether it has two, one, or no axes of symmetry (Fig. 9-2).

Beams in unsymmetric bending generally are subjected to bending moments acting about both principal axes of the cross section; hence, we need to establish a consistent sign convention for such moments. Because of the generalized nature of the analyses, we will adopt a more formalized **sign convention** than before. A segment of a beam subjected to bending moments M_y and M_z acting at an arbitrarily selected cross section is shown in Fig. 9-3. These moments are represented vectorially by double-headed arrows and are taken as positive in the positive directions of the y and z axes, as shown in the figure. When using this vectorial representation, the right-hand rule gives the sense of the moment (that is, the direction of rotation of the moment). Note that the bending moments act on the positive x face of the segment of the beam. (Recall that a positive face has its outward normal in the positive direction of an axis.) If it is necessary to show the bending moments M_y and M_z acting on a negative x face, we must keep in mind that they then act in opposite directions to the moments on the positive face. In other words, bending moments M_y and M_z acting on the negative x face are positive when their vectors are in the negative directions of the y and z axes, respectively.

9.2 DOUBLY SYMMETRIC BEAMS WITH SKEW LOADS

The simplest case of unsymmetric bending arises when a doubly symmetric beam is subjected to loads acting in directions that are skew to the axes of symmetry, as illustrated in Fig. 9-4a by a cantilever beam subjected to a load P acting at the free end. This load may be resolved into two components, one in each plane of symmetry, and a bending analysis can be performed for each component acting separately. The final

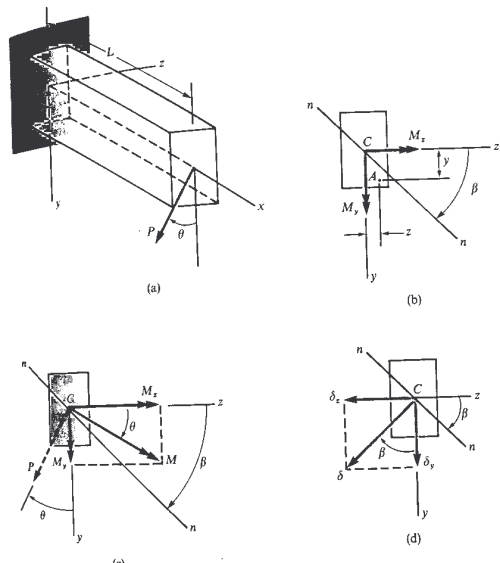


Fig. 9-4 Doubly symmetric beam with a skew load

stresses and deflections of the beam are obtained by superimposing the results. Of course, the load must act through the centroid of the cross section if there is to be no twisting about the longitudinal axis.

To illustrate this method of analysis, let us investigate in detail the beam of Fig. 9-4a. The load components are $P \cos \theta$ in the positive y direction and $P \sin \theta$ in the negative z direction. Therefore, the bending moments acting on a cross section (Fig. 9-4b) at distance x from the fixed support are

$$M_y = (P \cos \theta)(L - x) \quad M_z = (P \sin \theta)(L - x) \quad (a)$$

where L is the length of the beam.

Inasmuch as the bending moments M_y and M_z act in the planes of symmetry of the beam, the corresponding bending stresses can be obtained from the flexure formula. Let us consider a point A having co-

ordinates y and z in the cross section (Fig. 9-4b). The normal stress at this point is

$$\sigma_x = \frac{M_y z}{I_y} - \frac{M_z y}{I_z} \quad (9.1)$$

in which I_y and I_z are the moments of inertia of the cross-sectional area with respect to the y and z axes, respectively.

The equation of the neutral axis of the cross section can be determined by equating the stress σ_x (see Eq. 9-1) to zero:

$$\frac{M_y}{I_y} z - \frac{M_z}{I_z} y = 0 \quad (9.2)$$

Thus, the neutral axis mn (Fig. 9-4b) is an inclined line through the centroid. The angle β between this line and the z axis is defined as follows:

$$\tan \beta = \frac{y}{z} = \frac{M_y I_z}{M_z I_y} \quad (9.3)$$

Depending upon the magnitudes and directions of the bending moments, β may vary from -90° to $+90^\circ$. The maximum normal stresses occur at points located farthest from the neutral axis.

For the cantilever beam of Fig. 9-4a, the bending moments are given by Eqs. (a) and are in the ratio

$$\frac{M_y}{M_z} = \tan \theta \quad (9.4)$$

Hence, the resultant moment vector M is at the angle θ with the z axis (Fig. 9-4c). This vector is perpendicular to the longitudinal plane containing the force P , which is shown by a dashed arrow. In this case, the neutral axis is located as follows:

$$\tan \beta = \frac{M_y I_z}{M_z I_y} = \frac{I_z}{I_y} \tan \theta \quad (9.5)$$

From this equation we see that the angle β is generally not equal to θ , which means that the neutral axis is not perpendicular to the plane of the load. Exceptions occur in three special cases: (1) if $\theta = 0$, the load lies in the xy plane, and the z axis ($\beta = 0$) is the neutral axis. (2) If $\theta = 90^\circ$, the load lies in the xz plane, and the y axis ($\beta = 90^\circ$) is the neutral axis. (3) If $I_z = I_y$, the principal moments of inertia are equal; hence, all axes through the centroid are principal axes with the same moment of inertia. Thus, the plane of loading, no matter what its direction, is always a principal plane, and the neutral axis is always perpendicular to it ($\beta = \theta$).

The deflections of a doubly symmetric beam with skew loads can be determined for each component of the load acting independently, and

then the deflections can be superimposed. For instance, in the case of the cantilever beam of Fig. 9-4a, the deflections at the free end in the positive y direction and negative z direction are

$$\delta_y = \frac{(P \cos \theta)L^3}{3EI_z} \quad \delta_z = \frac{(P \sin \theta)L^3}{3EI_y}$$

as shown in Fig. 9-4d. The resultant deflection δ is

$$\delta = \sqrt{\delta_y^2 + \delta_z^2} \quad (9.6)$$

The angle β between the resultant deflection and the y axis is given by the following equation:

$$\tan \beta = \frac{\delta_z}{\delta_y} = \frac{I_z}{I_y} \tan \theta$$

which is the same as Eq. (9-5). Thus, the resultant deflection lies in a plane that is perpendicular to the neutral plane, a result that we could have anticipated.

Example

If a beam has a cross section for which the moment of inertia I_z is much larger than the moment of inertia I_y , it will be very sensitive to the direction of application of the loads. To illustrate this point, let us analyze a cantilever beam made of an I-section that is very narrow compared to its height. The beam selected is 610 x 305 x 149 kg UB (see Appendix E), with a length $L = 4$ m (Fig. 9-5a). A load $P = 45$ kN acts in the vertical direction at the free end of the beam.

If the beam is constructed in perfect alignment, the load P will act in the direction of the y axis and the z axis will be the neutral axis. Then the maximum stress in the beam (at the fixed end) is obtained from the flexure formula:

$$\sigma_{\max} = \frac{Mc}{I_z} = \frac{PLc}{I_z} = \frac{(45 \text{ kN})(4 \text{ m})(305 \text{ mm})}{124,341 \times 10^6 \text{ mm}^4} = 44.2 \text{ MPa}$$

This stress occurs in tension at the top of the beam and in compression at the bottom of the beam.

Now let us suppose that the beam is constructed with a very slight inclination (Fig. 9-5b), so that the angle between the load P and the y axis is $\theta = 1^\circ$. This inclination may be caused by defects in manufacture and construction or by a small movement of the supporting structure. The angle β giving the orientation of the neutral axis mn is obtained from Eq. (9-5):

$$\tan \beta = \frac{I_z}{I_y} \tan \theta = \frac{124,341 \text{ cm}^4}{8471 \text{ cm}^4} \tan(1^\circ) = 0.2562$$

and $\beta = 14.4^\circ$. This calculation shows that, even though the plane of the load is inclined by only 1° , the neutral axis is inclined 14.4° from the z axis. The great sensitivity of the position of the neutral axis to the angle of the load is a consequence of the large I_z/I_y ratio.

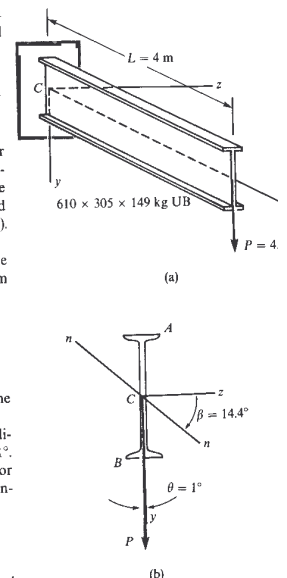


Fig. 9-5 Example. Cantilever beam with moment of inertia I_z much larger than I_y

The maximum stresses in the beam occur at the support at points A and B (Fig. 9-5b), which are located at the farthest distances from the neutral axis. At the support, the bending moments (see Eqs. a) are

$$M_z = (P \cos \theta)L = (45 \text{ kN})(\cos 1^\circ)(4 \text{ m}) = 180 \text{ kN}\cdot\text{m}$$

$$M_y = (P \sin \theta)L = (45 \text{ kN})(\sin 1^\circ)(4 \text{ m}) = 3.14 \text{ kN}\cdot\text{m}$$

The coordinates of point A are

$$z = 152 \text{ mm} \quad y = -305 \text{ mm}$$

Hence, the tensile stress at A (see Eq. 9-1) is

$$\sigma_A = \frac{M_y z}{I_y} - \frac{M_z y}{I_z}$$

$$= \frac{(3.14 \times 10^6 \text{ N}\cdot\text{mm})(152 \text{ mm})}{8471 \times 10^6 \text{ mm}^4} - \frac{(180 \times 10^6 \text{ N}\cdot\text{mm})(-305 \text{ mm})}{124,341 \times 10^6 \text{ mm}^4}$$

$$= 5.6 \text{ MPa} + 44.2 \text{ MPa} = 49.8 \text{ MPa}$$

The stress at B has the same magnitude but is a compressive stress:

$$\sigma_B = -49.8 \text{ MPa}$$

These stresses are 13% larger than the maximum stress $\sigma_{\max} = 44.2 \text{ MPa}$ obtained for the ideal beam with $\theta = 0$. In addition, the beam undergoes a lateral deflection in the z direction, whereas the ideal beam does not.

This example shows that beams with I_z much larger than I_y may develop large stresses if the beam or its loads deviate even a small amount from their planned alignment. Therefore, such beams should be used with caution, because they are highly susceptible to lateral or sideways buckling. The remedy is to provide adequate lateral support for the beam, thereby preventing lateral bending.

9.3 PURE BENDING OF UNSYMMETRIC BEAMS

If the cross section of a beam is unsymmetric, the analysis for bending becomes more complicated. Let us begin with a discussion of pure bending for such beams, and then in later sections we will consider the effects of transverse loads. Assume that a beam having the cross section shown in Fig. 9-6 is subjected to a bending moment M . Then we consider two perpendicular axes y and z in the plane of the cross section, and our task is to determine what conditions must be met in order for these axes to be the neutral axes for bending under the action of the moment M .

We begin by assuming that the beam is bent in such a manner that the z axis is the neutral axis. Then the xy plane is the plane of bending, and the beam deflects in that plane. The curvature κ_y of the bent beam in the xy plane is positive or negative according to the mathematical sign convention shown in Fig. 9-7a. The normal stress acting on an

element of area dA at distance y from the neutral axis (see Fig. 9-6 and Eq. 5-5) is

$$\sigma_x = -\kappa_y E y \tag{9-7}$$

The minus sign is needed because positive curvature means that the part of the beam below the neutral axis is in compression. The force on the element of area is $\sigma_x dA$, and the resultant force is the integral of this elemental force taken over the entire cross-sectional area. Since we are considering pure bending, the resultant force must be zero; hence,

$$\int \sigma_x dA = -\kappa_y E \int y dA = 0$$

or

$$\int y dA = 0 \tag{a}$$

This equation shows that the neutral axis (the z axis) must pass through the centroid C of the cross section.

As an alternative, we could have assumed that the y axis was the neutral axis, in which case the xz plane is the plane of bending. The sign convention for the curvature κ_z in the xz plane is shown in Fig. 9-7b. The corresponding normal stress acting on the element of area dA (Fig. 9-6) is

$$\sigma_x = -\kappa_z E z \tag{9-8}$$

where again the minus sign is needed because positive curvature produces compression on the element dA . The resultant force for this case is

$$\int \sigma_x dA = -\kappa_z E \int z dA = 0$$

or

$$\int z dA = 0 \tag{b}$$

and we again see that the neutral axis passes through the centroid. Thus, the origin of the y and z axes is located at the centroid C .

Now let us consider the moment resultant of the stresses σ_x . We assume first that bending takes place about the z axis as the neutral axis,

in which case the stresses σ_x are obtained from Eq. (9-7). The corresponding bending moments about the y and z axes are

$$M_z = -\int \sigma_x y dA = \kappa_y E \int y^2 dA = \kappa_y E I_{zz} \tag{9-9a}$$

$$M_y = \int \sigma_x z dA = -\kappa_y E \int y z dA = -\kappa_y E I_{yz} \tag{9-9b}$$

in which I_{yz} is the product of inertia of the cross-sectional area with respect to the y and z axes. The positive directions of the moments M_y and M_z are shown in Fig. 9-8. From Eqs. (9-9) we can draw certain conclusions. If the z axis is selected in an arbitrary direction through the centroid, it will be the neutral axis only if there are moments M_y and M_z acting about both the y and z axes and only if these moments are in the ratio established by Eqs. (9-9). However, if the z axis is a principal axis, then $I_{yz} = 0$ and the only moment acting is M_z . In that event, we have bending in the xy plane with the moment M_z acting in that same plane. In other words, bending takes place in the same manner as for a symmetric beam.

We arrive at similar conclusions if we assume that the y axis is the neutral axis. In that case, the stresses σ_x are given by Eq. (9-8), and the bending moments are

$$M_y = \int \sigma_x z dA = -\kappa_z E \int z^2 dA = -\kappa_z E I_{yy} \tag{9-10a}$$

$$M_z = -\int \sigma_x y dA = \kappa_z E \int y z dA = \kappa_z E I_{yz} \tag{9-10b}$$

Again we observe that, if the neutral axis (the y axis) is oriented arbitrarily, moments M_y and M_z must exist. However, if the y axis is a principal axis, the only moment is M_y , and we have ordinary bending in the xz plane.

Thus, we have arrived at the following important conclusion. *When an unsymmetric beam is in pure bending, the plane of the bending moment is perpendicular to the neutral surface only if the y and z axes are principal centroidal axes of the cross section.* Then, if a bending moment acts in one of the principal planes, this plane will be the plane of bending (perpendicular to the neutral axis), and the usual bending theory is valid.

The preceding conclusion suggests a direct method for analyzing an unsymmetric beam subjected to any bending moment M (Fig. 9-9).

We begin by locating the principal centroidal axes y and z , using the techniques described in Appendix C. Then the applied couple M is resolved into components M_y and M_z , assumed to be positive in the directions shown in the figure. These components are

$$M_y = M \sin \theta \quad M_z = M \cos \theta \tag{9-11}$$

where θ is the angle between the vector M and the z axis. Each of these components acts in a principal plane and produces pure bending in that same plane. Thus, the usual stress and deflection formulas for pure bending apply. The stresses and deflections obtained from M_y and M_z acting separately may be superimposed to obtain the corresponding quantities due to the original bending moment M . For instance, the resultant bending stress at any point A in the cross section is

$$\sigma_x = \frac{M_y z}{I_y} - \frac{M_z y}{I_z} \tag{9-12a}$$

or

$$\sigma_x = \frac{(M \sin \theta) z}{I_y} - \frac{(M \cos \theta) y}{I_z} \tag{9-12b}$$

in which y and z are the coordinates of point A .

The equation of the neutral axis nn (Fig. 9-9) is obtained by setting σ_x equal to zero:

$$\frac{\sin \theta}{I_y} z - \frac{\cos \theta}{I_z} y = 0 \tag{9-13}$$

The angle β between this line and the z axis is obtained as follows:

$$\tan \beta = \frac{y}{z} = \frac{I_z}{I_y} \tan \theta \tag{9-14}$$

This equation shows that in general the angles β and θ are not equal, hence the neutral axis is not perpendicular to the plane in which the applied couple M acts. The only exceptions are the three special cases ($\theta = 0$, $\theta = 90^\circ$, and $I_z = I_y$) described in the preceding section.

The deflections produced by the bending couples M_y and M_z can be obtained from the usual deflection formulas. These deflections take place in the principal planes and can be superimposed to obtain the resultant deflections, which lie in a plane that is normal to the neutral axis nn .

Throughout the preceding discussion, we directed our attention to unsymmetric beams (Fig. 9-9). Of course, symmetric beams can be viewed as special cases of unsymmetric beams. If a beam is singly symmetric, one of the centroidal principal axes of the cross section is the axis of symmetry; the other principal axis is perpendicular to the axis of symmetry at the centroid. If a beam is doubly symmetric, the centroidal principal axes are the axes of symmetry.

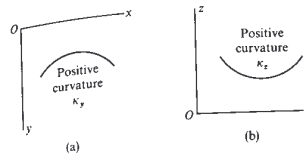
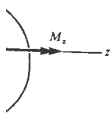
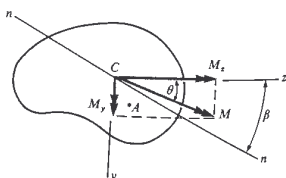


Fig. 9-7 Sign conventions for curvatures κ_y and κ_z in the xy and xz planes, respectively



moments M_y and M_z , respectively

cross section of the beam with the bending moment M resolved into components M_y and M_z acting in the principal planes



In this section we have discussed only pure bending, which means that no lateral loads act on the beam. When bending is produced by the lateral loads, the possibility arises of twisting of the beam about the longitudinal axis. Twisting is avoided when the loads act through the shear centre (see Section 9.5).

Another method for determining the stresses in an unsymmetric beam is described in the next section. This method has the advantage of not requiring that the principal axes be located; however, it is not a convenient method to use if deflections must be determined.

Example 1

A 254 × 76 × 28.3 kg channel section is subjected to a bending couple $M = 1.7 \text{ kN}\cdot\text{m}$ having its vector at an angle $\theta = 10^\circ$ to the z axis (Fig. 9-10). Calculate the stresses σ_a and σ_b at points A and B , respectively.

The centroid C is located on the axis of symmetry (the z axis) at a distance $c = 18.6 \text{ mm}$ from the back of the angle (see Table E-4, Appendix E). Then the y and z axes are principal centroidal axes with moments of inertia

$$I_y = 163 \text{ cm}^4 \quad I_z = 3367 \text{ cm}^4$$

The coordinates of points A and B are as follows:

$$y_a = -127 \text{ mm} \quad z_a = 76.2 - 18.6 = 57.6 \text{ mm}$$

$$y_b = 127 \text{ mm} \quad z_b = -18.6 \text{ mm}$$

Also, the moments about the y and z axes are

$$M_y = M \sin \theta = (1.7 \text{ kN}\cdot\text{m})(\sin 10^\circ) = 0.295 \text{ kN}\cdot\text{m}$$

$$M_z = M \cos \theta = (1.7 \text{ kN}\cdot\text{m})(\cos 10^\circ) = 1.674 \text{ kN}\cdot\text{m}$$

We can now calculate the stress at point A from Eq. (9-12a):

$$\sigma_a = \frac{M_y z_a}{I_y} - \frac{M_z y_a}{I_z}$$

$$= \frac{(0.295 \times 10^6 \text{ N}\cdot\text{m})(57.6 \text{ mm})}{163 \times 10^4 \text{ mm}^4} - \frac{(1.674 \times 10^6 \text{ N}\cdot\text{m})(-127 \text{ mm})}{3367 \times 10^4 \text{ mm}^4}$$

$$= 10.4 \text{ MPa} + 6.3 \text{ MPa} = 16.7 \text{ MPa}$$

By a similar calculation we obtain the stress at B :

$$\sigma_b = -9.7 \text{ MPa}$$

These stresses are the maximum tensile and compressive stresses in the cross section, because they are located at the farthest distances from the neutral axis mn (see Fig. 9-10).

The angle β that locates the neutral axis (see Eq. 9-14) is

$$\beta = \arctan\left(\frac{I_z}{I_y} \tan \theta\right) = \arctan\left(\frac{3367}{163} \tan 10^\circ\right) = 74.6^\circ$$

This angle is much larger than θ because the ratio I_z/I_y is large. As discussed in the example of Section 9.2, beams with large I_z/I_y ratios are very sensitive to the direction of loading. In this example, the angle β to the neutral axis goes from 0 to 74.6° as the angle θ to the moment vector goes only from 0 to 10° . Thus, beams of this kind should be provided with lateral support to prevent excessive lateral deflections.

Example 2

An angle section with unequal legs ($150 \times 90 \times 15$) is shown in Fig. 9-11. The section is subjected to a bending moment $M = 1 \text{ kN}\cdot\text{m}$ having its vector along axis 1-1, which is parallel to the short leg of the angle section. Determine the maximum tensile and compressive stresses in the beam.

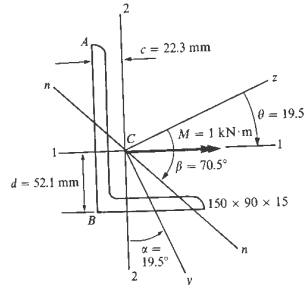


Fig. 9-11 Example 2. Angle section with unequal legs

The properties of the angle section are listed in Table E-6, Appendix E. The centroid is located at distance $c = 22.3 \text{ mm}$ from the back of the long leg and distance $d = 52.1 \text{ mm}$ from the back of the short leg. The principal centroidal axes are shown as axes 3-3 and 4-4 in Table E-6; however, we will label them as the y and z axes to be consistent with our earlier discussions. From Table E-6 we find that the angle α between axis 2-2 and principal axis 3-3 is

$$\alpha = \arctan 0.354 = 19.5^\circ$$

This angle is the same as the angle between the z axis and the axis 1-1 (Fig. 9-11). Since in our particular problem the vector M is directed along the 1-1 axis, it follows that the angle θ between the z axis and the vector M is equal to α :

$$\theta = \alpha = 19.5^\circ$$

The principal moments of inertia I_y and I_z can be found from Table E-6. The table gives the radius of gyration about the 3-3 (or y) axis; therefore,

$$I_y = Ar_{\min}^2 = (33.9 \text{ cm}^2)(1.93 \text{ cm})^2 = 126.3 \text{ cm}^4$$

The other principal moment of inertia is obtained from the fact that the sum of the moments of inertia for perpendicular axes is a constant:

$$I_y + I_z = I_{11} + I_{22}$$

or

$$I_z = I_{11} + I_{22} - I_y = 761 + 205 - 126 = 840 \text{ cm}^4$$

If a table of properties were not available, it would be necessary to calculate the orientation of the principal axes and the principal moments of inertia using the transformation equations given in Appendix C.

The neutral axis mn is oriented at an angle β from the z axis; this angle is determined as follows (see Eq. 9-14):

$$\beta = \arctan\left(\frac{I_z}{I_y} \tan \theta\right) = \arctan\left(\frac{840}{126} \tan 19.5^\circ\right) = 67.0^\circ$$

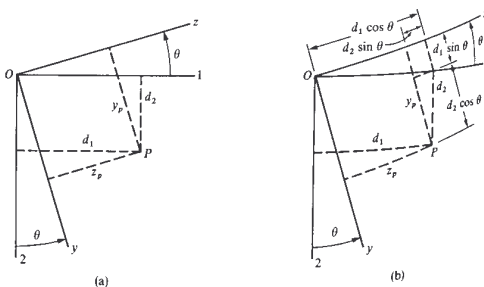
By inspection of the figure, we see that points A and B are located farthest from the neutral axis; therefore, the maximum compressive stress occurs at B and the maximum tensile stress occurs at A . (Actually, the maximum tensile stress occurs at a point located on the curved surface near A . However, it is not worth the effort to locate this point precisely, so we will consider the stress at A to be the maximum stress for practical purposes.)

The coordinates of points A and B are needed when determining the stresses. Unfortunately, the coordinates with respect to the y and z axes are not easy to calculate. To make the task easier, we will derive a general formula that can be used. In Fig. 9-12a are shown two sets of axes (axes 1-2 and axes yz) with an angle θ between them. Point P has coordinates d_1 and d_2 with respect to the 1-2 axes, and we wish to determine the coordinates y_p and z_p with respect to the yz axes. From the geometry of the figure (see Fig. 9-12b), we obtain the following expressions for these coordinates:

$$y_p = d_1 \sin \theta + d_2 \cos \theta \tag{9-15a}$$

$$z_p = d_1 \cos \theta - d_2 \sin \theta \tag{9-15b}$$

Thus, knowing the coordinates of a point with respect to the 1-2 axes, we can use the preceding equations to obtain the coordinates for the yz axes.



Coordinates of point P axes yz and axes 1-2

Returning now to the angle section of Fig. 9-11, we obtain the coordinates of point A with respect to the 1-2 axes by using the dimensions given in Table E-6:

$$d_1 = -22.3 \text{ mm} \quad d_2 = -(150 \text{ mm} - 52.1) = -97.9 \text{ mm}$$

Then the y and z coordinates of A are obtained from Eqs. (9-15):

$$y_a = (-22.3 \text{ mm})(\sin 19.5^\circ) + (-97.9 \text{ mm})(\cos 19.5^\circ)$$

$$= -99.7 \text{ mm}$$

$$z_a = (-22.3 \text{ mm})(\cos 19.5^\circ) - (-97.9 \text{ mm})(\sin 19.5^\circ)$$

$$= 11.7 \text{ mm}$$

In a similar manner, we find for point B the following coordinates:

$$d_1 = -22.3 \text{ mm} \quad d_2 = 52.1 \text{ mm}$$

$$y_b = 41.7 \text{ mm} \quad z_b = -38.4 \text{ mm}$$

An alternate method for finding these coordinates is to draw the cross section of the angle to scale and then measure the distances.

The components of the moment M about the y and z axes are

$$M_y = M \sin \theta = (1 \text{ kN}\cdot\text{m})(\sin 19.5^\circ) = 334 \text{ N}\cdot\text{m}$$

$$M_z = M \cos \theta = (1 \text{ kN}\cdot\text{m})(\cos 19.5^\circ) = 943 \text{ N}\cdot\text{m}$$

The stress at point A (from Eq. 9-12a) is

$$\sigma_a = \frac{M_y z_a}{I_y} - \frac{M_z y_a}{I_z}$$

Substituting numerical values, we get

$$\sigma_a = 14.3 \text{ MPa}$$

By a similar calculation, we get the stress σ_b :

$$\sigma_b = \frac{M_y z_b}{I_y} - \frac{M_z y_b}{I_z}$$

$$= -14.8 \text{ MPa}$$

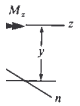
Thus, we have calculated the maximum tensile and compressive stresses produced by the bending couple M . In the next section, we will analyze this same beam by a different method.

9.4 GENERALIZED THEORY OF PURE BENDING

In the preceding sections, we analyzed unsymmetric beams by locating the principal centroidal axes of the cross section and then resolving the bending moment into components in those directions. The advantage of this method is that we can use all of the standard formulas for stresses and deflections because bending takes place in a principal plane. However, the method is inconvenient when the orientation of the prin-



Z-section 1 axes



cross section axes

principal axes cannot be obtained by inspection (as when an axis of symmetry exists) or from tables (as in the case of standard angle sections). If it is necessary to calculate the orientation of the principal axes and the magnitudes of the principal moments of inertia, it may be easier to work with axes in the cross section that are not principal axes. An example of this kind is a Z-section (Fig. 9-13), for which the principal axes must be located by calculation. The y and z axes shown in the figure are nonprincipal centroidal axes, but they are convenient axes to use in calculations because they are parallel to the sides of the cross section.

To derive the equations of a **generalized bending theory** (that is, a theory related to nonprincipal axes rather than restricted to principal axes), let us consider the unsymmetric cross section of Fig. 9-14. The y and z axes have their origin at the centroid but they are not principal axes. In the most general situation, bending moments M_y and M_z act on the cross section and bending of the beam occurs in both the xy and xz planes. (Since the xy and xz planes are not principal planes, each moment produces bending in both planes. If they were principal planes, only M_z would produce bending in the xy plane, and only M_y would produce bending in the xz plane.) Let us again denote the curvatures in the xy and xz planes by κ_y and κ_z , respectively, with sign conventions as portrayed in Fig. 9-7. Then the normal stress σ_x at point A, which has coordinates y and z (see Fig. 9-14), is

$$\sigma_x = -\kappa_y E y - \kappa_z E z \quad (9-16)$$

as given by Eqs. (9-7) and (9-8) or as obtained by inspection from Fig. 9-14.

The resultant force acting on the cross section in the x direction (that is, the axial force) can now be evaluated and equated to zero:

$$\int \sigma_x dA = 0 \quad \text{or} \quad \kappa_y E \int y dA + \kappa_z E \int z dA = 0$$

We see that this equation is satisfied automatically because the origin of the axes is at the centroid of the cross-sectional area.

The moment M_y is the moment stress resultant about the y axis:

$$M_y = \int \sigma_x z dA = -\kappa_y E \int y z dA - \kappa_z E \int z^2 dA$$

or

$$M_y = -\kappa_y E I_{yz} - \kappa_z E I_y \quad (9-17a)$$

in which I_{yz} is the product of inertia of the cross-sectional area with respect to the y and z axes. In a similar way, we get for the moment about the z axis

$$M_z = - \int \sigma_x y dA = \kappa_y E \int y^2 dA + \kappa_z E \int y z dA$$

or

$$M_z = \kappa_y E I_z + \kappa_z E I_{yz} \quad (9-17b)$$

Solving simultaneously Eqs. (9-17), we obtain the following expressions for the curvatures in terms of the bending moments:

$$\kappa_y = \frac{M_z I_z + M_y I_{yz}}{E(I_y I_z - I_{yz}^2)} \quad \kappa_z = -\frac{M_y I_z + M_z I_{yz}}{E(I_y I_z - I_{yz}^2)} \quad (9-18a, b)$$

Now substituting these expressions for the curvatures into Eq. (9-16), we obtain the **normal stress** σ_x :

$$\sigma_x = \frac{(M_y I_z + M_z I_{yz})z - (M_z I_y + M_y I_{yz})y}{I_y I_z - I_{yz}^2} \quad (9-19)$$

This equation is a **generalized flexure formula** that can be used to calculate the bending stress at any point in an unsymmetric beam when the moments M_y and M_z are known. These moments act about the y and z axes, which are perpendicular centroidal axes but not necessarily principal axes.

The orientation of the **neutral axis** nm (Fig. 9-14) is obtained by equating σ_x to zero:

$$(M_y I_z + M_z I_{yz})z - (M_z I_y + M_y I_{yz})y = 0$$

From this equation we find

$$\tan \phi = \frac{y}{z} = \frac{M_y I_z + M_z I_{yz}}{M_z I_y + M_y I_{yz}} \quad (9-20)$$

in which ϕ is the angle between the z axis and the neutral axis. Knowing the position of the neutral axis is helpful in identifying the points of maximum stress. Also, the orientation of the neutral axis determines the direction in which the deflections occur, because the plane of bending is perpendicular to the neutral axis.

If either bending moment is zero, the preceding formulas can be simplified. For instance, if $M_y = 0$ we obtain

$$\sigma_x = \frac{M_z (I_{yz} z - I_y y)}{I_y I_z - I_{yz}^2} \quad (9-21a)$$

$$\tan \phi = \frac{I_{yz}}{I_y} \quad (9-21b)$$

If $M_z = 0$, we get

$$\sigma_x = \frac{M_y (I_z z - I_{yz} y)}{I_y I_z - I_{yz}^2} \quad (9-22a)$$

$$\tan \phi = \frac{I_z}{I_{yz}} \quad (9-22b)$$

These formulas are applicable in many cases of practical interest because the y and z axes often are aligned with the loads.

As a special case, let us assume that the y and z axes are principal axes. Then $I_{yz} = 0$ and Eqs. (9-19) and (9-20) reduce to

$$\sigma_x = \frac{M_y z}{I_y} - \frac{M_z y}{I_z}$$

$$\tan \phi = \frac{y}{z} = \frac{M_y I_z}{M_z I_y}$$

The first of these equations is the same as Eq. (9-12a), and the second agrees with Eq. (9-14) if we note that $\tan \theta = M_y/M_z$.

Example

An angle section with unequal legs (150 × 90 × 15) is subjected to a bending moment $M_z = 1 \text{ kN}\cdot\text{m}$ acting in the xy plane (Fig. 9-15). Determine the maximum tensile and compressive stresses in the beam using the generalized flexure formula.

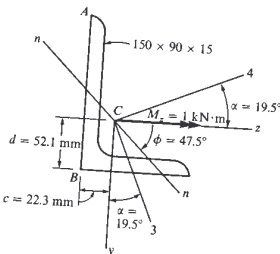


Fig. 9-15. Angle section

The properties of the angle section are given in Appendix E, Table E-6. The centroidal axes y and z are located at distance $c = 22.3 \text{ mm}$ from the back of the long leg and distance $d = 52.1 \text{ mm}$ from the back of the short leg. The corresponding moments of inertia are

$$I_y = 205 \text{ cm}^4 \quad I_z = 761 \text{ cm}^4$$

as obtained from the table.

In order to use the generalized flexure formula, we also need the product of inertia I_{yz} . Because it is not a tabulated quantity, we must calculate I_{yz} from the other properties. One method is to use the formula for rotation of axes for products of inertia (Eq. C-15b, Appendix C). We must apply this formula to a rotation from the principal axes to the yz axes, and then, because the product of inertia is zero for the principal axes, we can solve for I_{yz} . The orientation of the principal axes 3-4 is given in Table E-6 by the angle α . For the angle section in this problem, we obtain

$$\alpha = \arctan 0.354 = 19.5^\circ$$

Also, the principal moments of inertia are obtained from the tabulated data, as follows:

$$I_3 = A r^2 = (33.9 \text{ cm}^2)(1.93 \text{ cm})^2 = 126.3 \text{ cm}^4$$

$$I_4 = I_y + I_z - I_3 = 761 + 205 - 126 = 840 \text{ cm}^4$$

Rotation from the principal axes 3-4 to the yz axes is clockwise in Fig. 9-15 instead of counterclockwise as in Fig. C-16 of Appendix C because the y axis is downward in Fig. 9-15. Thus, substituting into Eq. (C-15b) of Appendix C, and converting to the notation of Fig. 9-15, we get

$$I_{yz} = \frac{I_4 - I_3}{2} \sin 2\alpha \quad (9-23)$$

This equation gives I_{yz} in terms of the moments of inertia with respect to the principal axes 3-4 and the angle α to the principal axes.

For the angle section being analyzed, we calculate I_{yz} as follows:

$$I_{yz} = \frac{840 \text{ cm}^4 - 126 \text{ cm}^4}{2} \sin 2(19.5^\circ) = 224 \text{ cm}^4$$

Now that I_{yz} is known, we can proceed to locate the neutral axis and calculate the stresses.

From Eq. (9-21b) we obtain the angle ϕ that locates the neutral axis nm:

$$\phi = \arctan \frac{I_{yz}}{I_y} = \arctan \frac{224}{205} = 47.5^\circ$$

The neutral axis nm is shown in Fig. 9-15. We see that the maximum tensile stress occurs at point A (or at least very close to point A) and that the maximum compressive stress occurs at point B. The coordinates of point A are

$$y_A = -(150 \text{ mm} - 52.1 \text{ mm}) = -97.9 \text{ mm} \quad z_A = -22.3 \text{ mm}$$

Then the flexure formula (Eq. 9-21a) with $M_z = 1 \text{ kN}\cdot\text{m}$ yields

$$\begin{aligned} \sigma_A &= \frac{M_z (I_{yz} z_A - I_y y_A)}{I_y I_z - I_{yz}^2} \\ &= \frac{(1 \text{ kN}\cdot\text{m})[(224 \text{ cm}^4)(-22.3 \text{ mm}) - (205 \text{ cm}^4)(-97.9 \text{ mm})]}{(205 \text{ cm}^4)(761 \text{ cm}^4) - (224 \text{ cm}^4)^2} \\ &= 14.3 \text{ MPa} \end{aligned}$$

By a similar calculation we get the stress at B:

$$y_B = 52.1 \text{ mm} \quad z_B = -22.3 \text{ mm}$$

$$\begin{aligned} \sigma_B &= \frac{M_z (I_{yz} z_B - I_y y_B)}{I_y I_z - I_{yz}^2} \\ &= \frac{(1 \text{ kN}\cdot\text{m})[(224 \text{ cm}^4)(-22.3 \text{ mm}) - (205 \text{ cm}^4)(52.1 \text{ mm})]}{(205 \text{ cm}^4)(761 \text{ cm}^4) - (224 \text{ cm}^4)^2} \\ &= -14.8 \text{ MPa} \end{aligned}$$

These stresses are the maximum tensile and compressive stresses in the beam. Within the limits of accuracy of the calculations, they agree with the results obtained in Example 2 of the preceding section, where we analyzed the same angle by considering bending about the principal axes.

9.5 BENDING OF BEAMS BY LATERAL LOADS; SHEAR CENTER

In the preceding sections we considered pure bending of unsymmetric beams, hence we dealt only with bending couples acting on the cross sections. Now we will consider the effects of lateral loads that produce shear forces in addition to bending moments. To show the effects of lateral loads, let us consider a cantilever beam of singly symmetric cross section supporting a load P at the free end (Fig. 9-16a). The force P acts perpendicular to the z axis, which is an axis of symmetry of the cross section (Fig. 9-16b). The origin of coordinates is taken at the centroid C of the cross section, hence the y and z axes are principal centroidal axes.

Let us make the assumption that, under the action of the load P , the beam bends with the z axis as the neutral axis. Then, on any cross section of the beam, two stress resultants exist; these resultants are the bending moment M_z about the z axis and the shear force V_y (equal to P) acting in the y direction (Fig. 9-16b). The moment M_z is the resultant of the normal stresses acting on the cross section, and the force P is the resultant of the shear stresses. If the material follows Hooke's law, the normal stresses will vary linearly with the distance from the neutral axis. Since we obtain the shear stresses from the normal stresses by means of static equilibrium, the distribution of normal stresses also determines the distribution of the shear stresses. Thus, the shear stresses have a specific resultant force P that has its line of action through a point S lying on the z axis (Fig. 9-16b). This point is known as the **shear center** (or the **center of flexure**) of the cross section. It does not coincide with the centroid C except in special cases that are mentioned later.

From this discussion, we see that the load P must act through the shear center S if the only resultant of the shear stresses is to be the force P itself. Under these conditions, bending occurs about the z axis as the neutral axis with the beam deflecting in the xy plane as the plane of bending. If P does not act through S , it can be replaced by a force P

through S plus a twisting couple (that is, a couple having its vector in the x direction). The effect of the force is to produce bending about the z axis as just described, and the effect of the couple is to produce torsion of the beam. Thus, we observe that a lateral load acting on a beam will produce bending without twisting only if it acts through the shear center. As a consequence, locating the shear center S is important in beam design.

The shear center of the singly symmetric I-beam shown in Fig. 9-16b can be determined as follows. We consider the cross section to consist of three rectangular parts: the two flanges and the web (Fig. 9-17). All three parts are subject to the same curvature when bending takes place, because they are parts of the same cross section. Therefore, the bending moment carried by each part is in proportion to its moment of inertia about the z axis:

$$\kappa = \frac{M_1}{EI_1} = \frac{M_2}{EI_2} = \frac{M_3}{EI_3} \quad (a)$$

in which M_1 , M_2 , and M_3 are the moments resisted by parts 1, 2, and 3, respectively, and I_1 , I_2 , and I_3 are their respective moments of inertia about the z axis. If the web is thin, its moment of inertia I_3 will be very small compared to I_1 and I_2 . Then we may disregard the effect of the web and assume that all of the moment is resisted by the flanges:

$$M_z = M_1 + M_2$$

Also, from Eq. (a) we get

$$\frac{M_1}{I_1} = \frac{M_2}{I_2}$$

Combining the preceding two equations, we obtain

$$M_1 = \frac{M_z I_1}{I_1 + I_2} \quad M_2 = \frac{M_z I_2}{I_1 + I_2} \quad (b)$$

The shear forces V_1 and V_2 in the flanges are in the same proportions as the bending moments (because $V = dM/dx$); hence,

$$\frac{V_1}{V_2} = \frac{M_1}{M_2}$$

Also, the total shear force V_y (equal to P) is

$$V_y = V_1 + V_2$$

By comparing this equation with Eqs. (b), we see that the shear forces are

$$V_1 = \frac{V_y I_1}{I_1 + I_2} \quad V_2 = \frac{V_y I_2}{I_1 + I_2} \quad (c)$$

The line of action of the resultant of these two shear forces determines the location of the shear center S .

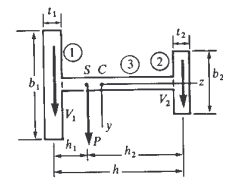
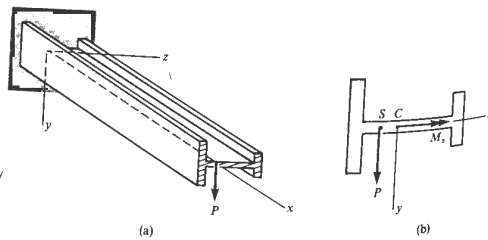


Fig. 9-17 Cross section of singly symmetric I-beam showing location of shear center S



with singly symmetric beam with shear center S

Unsymmetric Bending

To locate S in terms of the dimensions of the cross section, let us denote the distance between the centerlines of the flanges by h , the widths of the flanges by b_1 and b_2 , and their thicknesses by t_1 and t_2 (Fig. 9-17). We wish to determine the distances h_1 and h_2 from the center of the flanges to the shear center S . Inasmuch as P is the resultant about point S ; therefore,

$$V_1 h_1 = V_2 h_2$$

or, using Eqs. (c),

$$\frac{h_1}{h_2} = \frac{I_2}{I_1} \quad (d)$$

The moments of inertia I_1 and I_2 are

$$I_1 = \frac{t_1 b_1^3}{12} \quad I_2 = \frac{t_2 b_2^3}{12}$$

Substituting these expressions into Eq. (d), and also noting that $h = h_1 + h_2$, we find

$$h_1 = \frac{t_2 b_2^3 h}{t_1 b_1^3 + t_2 b_2^3} \quad h_2 = \frac{t_1 b_1^3 h}{t_1 b_1^3 + t_2 b_2^3} \quad (9-24a, b)$$

These expressions can be used to locate the shear center S of a singly symmetric I-beam. Note particularly that h , h_1 , and h_2 are measured to the centerlines of the flanges. If $b_1 > b_2$ and $t_1 \geq t_2$, or if $t_1 > t_2$ and $b_1 \geq b_2$, the shear center is located to the left of the centroid C in Fig. 9-17; that is, it is located between C and the larger flange.

A special case occurs when the beam has only one flange and is a T-beam (Fig. 9-18). For a beam of this shape, we substitute $b_2 = t_2 = 0$ into Eqs. (9-24) and obtain

$$h_1 = 0 \quad h_2 = h$$

This result shows that the shear center is located at the intersection of the centerlines of the flange and web. We could have anticipated this result because in the derivation we assumed that the web was very thin so that the shear force was carried entirely by the flanges.

If the beam has two identical flanges, we have a doubly symmetric I-beam for which the y and z axes are axes of symmetry. Then we have $t_1 = t_2$ and $b_1 = b_2$, and Eqs. (9-24) yield

$$h_1 = h_2 = \frac{h}{2}$$

This result shows that the shear center coincides with the centroid. In general, the shear center (like the centroid) lies on any axes of symmetry; hence, the two points always coincide for doubly symmetric cross sections. Thus, any transverse load that acts through the centroid of a doubly symmetric cross section will produce bending without torsion. The method of finding stresses and deflections for such beams was discussed in Section 9.2.

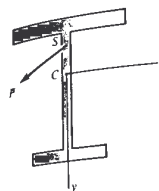


Fig. 9-19 Singly symmetric beam with transverse load P acting through the shear center S

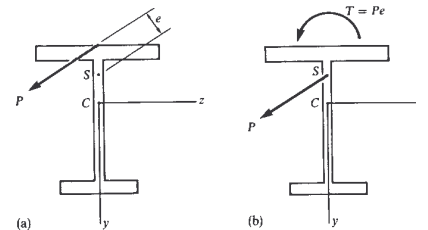


Fig. 9-20 Singly symmetric beam with transverse load P that does not act through the shear center S

If a beam is singly symmetric, both the centroid and the shear center lie on the axis of symmetry, as already mentioned. Then, if a transverse load acts through the shear center in any direction (Fig. 9-19), it can be resolved into two components, one in the direction of the y axis and the other parallel to the z axis. The first component will produce bending in the xy plane with the z axis as the neutral axis. The second component will produce bending (without torsion) in the xz plane with the y axis as the neutral axis. The stresses and deflections produced by these loads acting separately can be superimposed to obtain the stresses and deflections caused by the original inclined load P , as described in Section 9.3.

If the transverse load P does not act through the shear center (Fig. 9-20a), it can be replaced by a statically equivalent system consisting of a parallel force P acting through the shear center and a twisting couple T (Fig. 9-20b). The couple T has a magnitude equal to the product of the force P and the distance e between its old and new lines of action. The effects of the load P acting through the shear center can be determined as described in the preceding paragraph, and the effects of the twisting couple can be handled by a torsion analysis. Of course, in this discussion we are assuming that the beam is free to deflect sideways and to rotate. If it is laterally supported, sideways bending and rotation will be prevented and additional stresses will be introduced by the action of the supports.

Locating the shear center for singly symmetric or unsymmetric cross sections is not always an easy task. For solid sections and closed hollow sections, it is usually located near the centroid. Such sections have high torsional rigidities; hence, we usually can ignore the effects of twisting if the load is applied at or near the centroid. Beams with thin-walled open cross sections (such as channels, angles, T-beams, and Z-sections) are torsionally very weak; therefore, it is important to locate the shear centers and to take into account the effects of twisting. Cross sections of this type are considered in the following sections.

9.6 SHEAR STRESSES IN BEAMS OF THIN-WALLED OPEN CROSS SECTIONS

We have already described the distribution of shear stresses in rectangular beams and in the webs of beams with flanges (see Sections 9.5 and 5.6). In beams of those shapes, the shear stresses are given by the shear formula

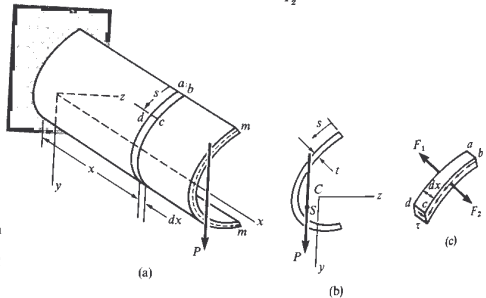
$$\tau = \frac{VQ}{Ib} \tag{9-25}$$

provided that the shear stresses are distributed uniformly across the width b of the beam. This requirement is met with good accuracy for beams of thin rectangular cross section, for the webs of wide-flange beams, and for a few other shapes.

We will now consider a special class of beams, known as beams of **thin-walled open cross section**, for which we can determine the shear stresses by the same method that we used when deriving the shear formula. Beams of this kind are distinguished by two features: (1) the cross section has a wall thickness that is small compared to its overall height or width and (2) the cross section is open, as in the case of an I-beam or channel beam, rather than closed, as in the case of a hollow box beam. Beams of thin-walled open sections are widely used in engineering work and are also called **structural sections** or **profile sections**.

We shall begin our study of shear stresses in structural sections by examining a beam having its cross-sectional centerline mm of arbitrary shape (Fig. 9-21a). The y and z axes are principal centroidal axes of the cross section, and the load P acts parallel to the y axis (Fig. 9-21b). If the load P acts through the shear center S , there will be no twisting of the beam; bending will occur in the xy plane and the z axis will be the neutral axis. The normal stresses at any point in the beam are given by

$$\sigma_x = -\frac{M_x y}{I_z} \tag{9-26}$$



Stresses in a beam cross section. y and z axes are principal

where M_x is the bending moment about the z axis and y is the ordinate to the point under consideration.

Now consider an element $abcd$ cut out between two cross sections, a distance dx apart, and having length s measured along the centerline of the cross section (Fig. 9-21a). The resultant of the normal stresses acting on the face ad is denoted F_1 (Fig. 9-21c) and the resultant on the face bc is denoted F_2 . Since the bending moment at face ad is larger than at bc , the force F_1 will be larger than F_2 ; hence, shear stresses τ must act along the face cd in order to have static equilibrium of the element. These shear stresses must be parallel to the top and bottom surfaces of the element, which are free of stress, and must be accompanied by complementary shear stresses acting on the cross sections ad and bc . Summing forces in the x direction for the element $abcd$ (Fig. 9-21c), we get

$$\tau t dx = F_1 - F_2 \tag{a)}$$

where t is the thickness of the cross section at cd ; that is, t is the thickness at distance s from the free edge of the cross section (Fig. 9-21b). Using Eq. (9-26), we conclude that

$$F_1 = \int_0^s \sigma_x dA = -\frac{M_{z1}}{I_z} \int_0^s y dA$$

where dA is an element of area on the side ad of the element, y is the coordinate of the element dA , and M_{z1} is the bending moment at this cross section. An analogous expression is obtained for the force F_2 :

$$F_2 = \int_0^s \sigma_x dA = -\frac{M_{z2}}{I_z} \int_0^s y dA$$

Substituting the expressions for F_1 and F_2 into Eq. (a), we get

$$\tau = \frac{M_{z2} - M_{z1}}{dx} \frac{1}{I_z t} \int_0^s y dA$$

The quantity $(M_{z2} - M_{z1})/dx$ is the rate of change of the bending moment and is equal to $-V_y$, where V_y is the shear force in the y direction (equal to P in Fig. 9-21). Therefore, the equation for the shear stresses is

$$\tau = -\frac{V_y}{I_z t} \int_0^s y dA$$

This equation gives the shear stresses at any point in the cross section at distance s from the free edge. The integral on the right-hand side represents the first moment with respect to the neutral axis (the z axis) of the area of the cross section from $s = 0$ to $s = s$. Denoting this first moment by Q_z , and using only the absolute value of the shear stress because its direction can be determined by inspection, we can write the

equation for the shear stresses τ in the simpler form

$$\tau = \frac{V_y Q_z}{I_z t} \tag{9-27}$$

which is analogous to Eq. (9-25). The shear stresses τ are directed along the median line of the cross section, parallel to the edges of the section, and are assumed to be of constant intensity across the thickness t of the wall. The thickness itself need not be a constant, but may vary as a function of s .

The **shear flow** at any point in the cross section, equal to the product of the shear stresses and the thickness at that point, is

$$f = \tau t = \frac{V_y Q_z}{I_z} \tag{9-28}$$

Because V_y and I_z are constants, we see that the shear flow is directly proportional to Q_z . At the top and bottom edges of the cross section, Q_z is zero and hence the shear flow is zero. The shear flow varies continuously between these end points and reaches its maximum value when Q_z is a maximum, which occurs at the neutral axis.

If the beam shown in Fig. 9-21 is bent by loads acting through the shear center and parallel to the z axis, then the y axis will be the neutral axis for bending. In such a case, we can repeat the same type of analysis and arrive at the following equations in place of Eqs. (9-27) and (9-28):

$$\tau = \frac{V_z Q_y}{I_y t} \quad f = \tau t = \frac{V_z Q_y}{I_y} \tag{9-29a, b}$$

In these equations, V_z is the shear force parallel to the z axis and Q_y is the first moment with respect to the y axis.

In summary, we have derived equations for the shear stresses in beams of thin-walled open cross sections provided that the shear force acts through the shear center S and is parallel to one of the principal centroidal axes. If the shear force is inclined to the y and z axes (but still acts through the shear center), it can be resolved into components parallel to the principal axes. Then two separate analyses can be made, and the results may be superimposed.

Example

Investigate the shear stresses in a wide-flange beam loaded by a force P acting in the vertical direction in the plane of the web (Fig. 9-22a).

Let us begin by taking an intermediate cross section of the beam (Fig.

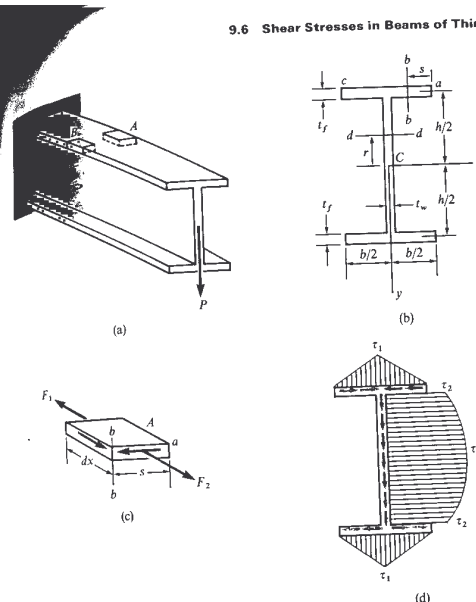


Fig. 9-22 Example. Shear stresses in a wide-flange beam

9-22b) and considering the stresses in the right-hand part of the top flange. The distance s for this part of the beam will be measured from point a , where the shear stress is zero, leftward to section bb . The cross-sectional area between point a and section bb is st_f , where t_f is the thickness of the flange. The distance from the centroid of this area to the neutral axis is $h/2$ (note that h is the height of the beam between the centerlines of the flanges). Thus, for section bb we have $Q_z = st_f h/2$; therefore, the shear stress at bb is

$$\tau = \frac{shP}{2I_z} \tag{9-30}$$

as obtained from Eq. (9-27). The direction of this stress can be found by considering the forces acting on an element cut out of the flange between point a and section bb (see element A in Fig. 9-22a). This element is drawn to a larger scale in Fig. 9-22c, in order to show clearly the forces acting on it. We see immediately that the tensile force F_1 is larger than the force F_2 , because the bending moment is larger on the rear face of the element than it is on the front face. Hence, it follows that, for equilibrium, the shear stress τ on the left face of element A must act toward the reader. This conclusion then dictates the direction

of the shear stresses on the cross section; namely, they must act toward the web. Returning now to Fig. 9-22b, we see that we have completely determined the magnitude and direction of the shear stress at section bb . This section may be taken anywhere between point a and the juncture of the flange and web, because throughout this region the shear stress is horizontal and to the left, and its magnitude is given by Eq. (9-30). We see also from Eq. (9-30) that the stress increases linearly with the distance s , as shown graphically in Fig. 9-22d. The maximum value τ_1 is reached when $s = b/2$, where b is the flange width; thus

$$\tau_1 = \frac{bhP}{4I_z} \quad (9-31)$$

and the corresponding shear flow is

$$f_1 = \tau_1 t_f = \frac{bht_f P}{4I_z} \quad (9-32)$$

Note that we have calculated the shear stress at the centerline juncture of the flange and web, without taking into account the thickness of the cross section. This approximate procedure is satisfactory for thin-walled sections.

By beginning at point c on the left part of the top flange (Fig. 9-22b) and measuring s toward the right, we can repeat the same kind of analysis. We will find that the magnitude of the shear stresses is again given by Eqs. (9-30) and (9-31). However, by cutting out an element B (Fig. 9-22a) and considering its equilibrium, we will find that the shear stresses on the cross section now act toward the right, as shown in Fig. 9-22d.

The next step is to determine the shear stresses in the web. Considering a horizontal cut at the top of the web, just below the flange, we find the first moment to be

$$Q_2 = \frac{bt_f h}{2}$$

and the corresponding shear stress is

$$\tau_2 = \frac{bht_f P}{2I_z t_w} \quad (9-33)$$

where t_w is the thickness of the web. The associated shear flow is

$$f_2 = \tau_2 t_w = \frac{bht_f P}{2I_z} \quad (9-34)$$

which is equal to twice the shear flow f_1 , as expected. The shear stresses in the web act vertically downward and increase in magnitude until the neutral axis is reached. At section dd , located at distance r from the neutral axis, the shear stress is calculated as follows:

$$Q_2 = \frac{bt_f h}{2} + \left(\frac{h}{2} - r\right)(t_w) \left(\frac{h/2 + r}{2}\right) = \frac{bt_f h}{2} + \frac{t_w}{2} \left(\frac{h^2}{4} - r^2\right)$$

and

$$\tau = \left(\frac{bt_f h}{t_w} + \frac{h^2}{4} - r^2\right) \frac{P}{2I_z} \quad (9-35)$$

When $r = h/2$, this equation reduces to Eq. (9-33); and, when $r = 0$, it gives the maximum shear stress:

$$\tau_{\max} = \left(\frac{bt_f}{t_w} + \frac{h}{4}\right) \frac{Ph}{2I_z} \quad (9-36)$$

Again it should be pointed out that we have made all calculations on the basis of the centerline dimensions of the cross section, which gives reasonably accurate results for thin sections. For this reason, however, the shear stresses calculated for the web of a wide-flange beam by using Eq. (9-35) may be slightly different from those obtained in our previous analysis (see Eq. 5-24).

The shear stresses in the web vary parabolically, as shown in Fig. 9-22d, although the variation is not great. This fact can be seen from the ratio of τ_{\max} to τ_2 , which is

$$\frac{\tau_{\max}}{\tau_2} = 1 + \frac{ht_w}{4bt_f} \quad (9-37)$$

The second term is usually small; for example, if we take typical values such as $h = 2b$ and $t_f = 2t_w$, the ratio is $\tau_{\max}/\tau_2 = 1.25$.

Finally, we may investigate the shear stresses in the lower flange by the same methods used for the top flange. We will find that the magnitudes of the stresses are the same as in the top flange, but they have the directions shown in Fig. 9-22d.

From Fig. 9-22d, we see that the shear stresses on the cross section "flow" inward from the outermost edges of the top flange, then down through the web, and finally outward to the edges of the bottom flange. This flow is always continuous in any structural section; therefore, it serves as a convenient way to determine the directions of the stresses. Because the shear force acts downward on the beam, we know that the shear flow in the web must be downward. Then, knowing the direction of the shear flow in the web, we immediately know the directions in the flanges also, because of the required continuity in the shear flow. Using this simple technique to get the directions of the stresses is easier than visualizing elements such as A (Fig. 9-22c) cut out from the beam.

The resultant of all shear stresses on the cross section is clearly a vertical force, because the horizontal stresses in the flanges produce no resultant. The shear stresses in the web have a resultant R , which can be found by integrating the shear stresses over the height of the web, as follows:

$$R = \int \tau dA = 2 \int_0^{h/2} \tau t_w dr$$

Now substituting from Eq. (9-35), we get

$$R = 2t_w \int_0^{h/2} \left(\frac{bt_f h}{t_w} + \frac{h^2}{4} - r^2\right) \left(\frac{P}{2I_z}\right) dr = \left(\frac{bt_f}{t_w} + \frac{h}{6}\right) \frac{h^2 t_w P}{2I_z} \quad (b)$$

The term I_z can be calculated as follows:

$$I_z = \frac{t_w h^3}{12} + \frac{bt_f h^2}{2} \quad (9-38)$$

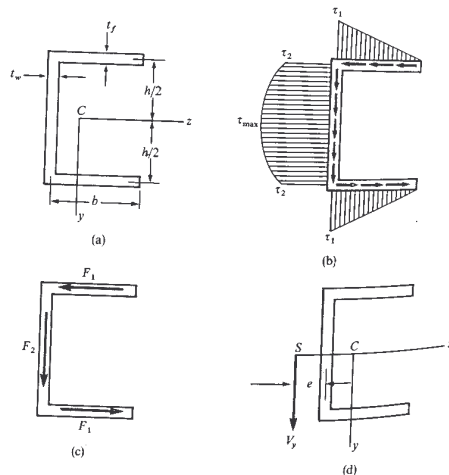
where the first term is the moment of inertia of the web and the second term is the moment of inertia of the flanges, again calculated by using centerline dimensions. When this expression for I_z is substituted into Eq. (b), we get $R = P$, which establishes the fact that the resultant of the shear stresses acting on the cross section is equal to the vertical force P . The resultant passes through the centroid C , which is also the shear center for a doubly symmetric beam.

9.7 SHEAR CENTERS OF THIN-WALLED OPEN SECTIONS

In the preceding section we developed techniques for determining the shear stresses in beams of thin-walled open cross sections. Now we will use those techniques to locate the shear centers. Inasmuch as the shear center is the point through which the resultant shear force acts and not only evaluating the shear stresses but also locating the line of action of the resultant of those stresses. To illustrate the method, as well as to obtain some useful results, we will derive formulas for locating the shear centers of several common sections.

The first beam we consider is a channel section (Fig. 9-23a) bent about the z axis and subjected to a vertical shear force V_y acting parallel to the y axis. The distribution of shear stresses for the channel is shown in Fig. 9-23b. To find the maximum stress τ_1 in the flange, we use Eq. (9-27) with Q_2 equal to the first moment of the flange area about the z axis:

$$Q_2 = \frac{bt_f h}{2}$$



the stress τ_1 in the flange is

$$\tau_1 = \frac{bhV_y}{2I_z} \quad (9-39)$$

In the same manner, we find that the stress τ_2 at the top of the web is

$$\tau_2 = \frac{bt_f h V_y}{2I_z t_w} \quad (9-40)$$

Also, at the neutral axis the stress is

$$\tau_{\max} = \left(\frac{bt_f}{t_w} + \frac{h}{4}\right) \frac{h V_y}{2I_z} \quad (9-41)$$

These stresses are shown in Fig. 9-23b.

The total shear force F_1 in either flange (Fig. 9-23c) can be found from the triangular diagrams of shear stress. Each force is equal to the area of the stress triangle multiplied by the thickness of the flange over which the stress acts:

$$F_1 = \left(\frac{\tau_1 b}{2}\right)(t_f) = \frac{hb^2 t_f V_y}{4I_z} \quad (a)$$

The vertical force F_2 in the web must be equal to the shear force V_y , since the forces in the flanges are horizontal and have no vertical components. We can easily verify that $F_2 = V_y$ by considering the parabolic stress diagram of Fig. 9-23b. We note that the diagram is made up of two parts: a rectangle of dimensions τ_2 and h , and a parabolic area equal to

$$\frac{2}{3}(\tau_{\max} - \tau_2)h$$

Thus, the total shear force, equal to the area of the stress diagram times the web thickness, is

$$F_2 = \tau_2 h t_w + \frac{2}{3}(\tau_{\max} - \tau_2) h t_w$$

Substituting the expressions for τ_2 and τ_{\max} , we obtain

$$F_2 = \left(\frac{t_w h^3}{12} + \frac{bh^2 t_f}{2}\right) \frac{V_y}{I_z}$$

Finally, we note that the expression for the moment of inertia is

$$I_z = \frac{t_w h^3}{12} + \frac{bt_f h^2}{2} \quad (9-42)$$

in which we again base the calculations upon centerline dimensions only. Substituting this expression for I_z into the equation for F_2 , we get

$$F_2 = V_y \quad (b)$$

as expected.

The three forces acting on the cross section (see Fig. 9-23c) must be statically equivalent to the resultant force V_y acting through the shear center S (see Fig. 9-23d). Hence, the moment of the force V_y about any point in the cross section is equal to the moment about that same point of the three forces. This moment relationship provides an equation from which the distance e to the shear center may be found. It is usually convenient to select the center of moments at the shear center S . Then, for the channel being analyzed, the equation of moments is

$$\int (F_1 \frac{h}{2}) - F_2 e = V_y(0) = 0$$

Substituting the expressions for F_1 and F_2 (Eqs. a and b) and solving for e , we find

$$e = \frac{b^2 h^2 t_f}{4I_z} \tag{9.43}$$

When the expression for I_z (Eq. 9.42) is substituted, Eq. (9.43) becomes

$$e = \frac{3b^2 t_f}{ht_w + 6bt_f} \tag{9.44}$$

Note that e is the distance from the centerline of the web to the shear center.

Instead of taking moments about the shear center, we can use a point on the centerline of the web as the center of moments. Then the moment equation for the channel beam is

$$F_1 h = V_y e$$

from which

$$e = \frac{b^2 h^2 t_f}{4I_z}$$

as before. This alternate choice of the center of moments is sometimes convenient, although it offers no significant reduction in calculating effort.

As explained in Section 9.5, a channel beam will undergo simple bending whenever it is loaded by forces acting through the shear center S . If the loads act parallel to the y axis but through some point other than the shear center (for example, the loads might act in the plane of the web), then they can be replaced by a statically equivalent force system consisting of loads through the shear center and twisting couples. We then have a combination of bending and torsion of the beam. If the loads act in the direction of the z axis, through points S and C , we will have simple bending about the y axis. If the loads act in skew directions, they can be replaced by statically equivalent loads parallel to the y and z axes.

The next shape to be considered is an equal-leg angle section (Fig. 9-24a), which we assume is subjected to a shear force V_y . Each leg of the

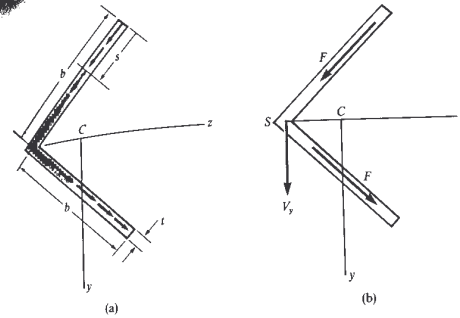


Fig. 9-24 Shear center of an equal-leg angle section

angle has length b and thickness t . At distance s from one end, the shear stress is

$$\tau = \frac{V_y Q_z}{I_z t} = \frac{3sV_y}{\sqrt{2} b^2 t} \left(b - \frac{s}{2} \right) \tag{c}$$

in which we have used the relations

$$Q_z = \frac{st}{\sqrt{2}} \left(b - \frac{s}{2} \right)$$

and

$$I_z = \frac{b^3 t}{3} \tag{9.45}$$

Equation (c) shows that τ varies quadratically with s ; it reaches its maximum value when $s = b$:

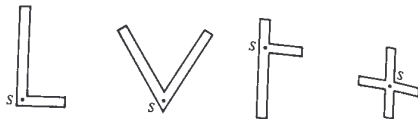
$$\tau_{\max} = \frac{3V_y}{2\sqrt{2}bt} \tag{d}$$

The total shear force F in each leg (see Fig. 9-24b) is

$$F = \int_0^b \tau t ds = \frac{3V_y}{\sqrt{2} b^3} \int_0^b \left(bs - \frac{s^2}{2} \right) ds = \frac{V_y}{\sqrt{2}} \tag{e}$$

Taking the vertical components of the forces F , we see that the resultant of these forces is a vertical force equal to V_y , as expected. Furthermore, we see that this resultant force must pass through the point where the lines of action of the two forces F intersect. Hence, the shear center S of the angle section is at the junction of the two legs.

Shear centers S of sections intersecting narrow



For all cross sections consisting of two narrow intersecting rectangles, as in the examples of Fig. 9-25, the shear stresses have resultant forces that intersect at the junction of the rectangles. Therefore, the shear center S is located at the junction, as shown in the figure. The locations of the shear centers for most structural shapes are given in this section, either in the preceding discussions or in the examples and problems that follow.*

Example 1

Locate the shear center S of the thin-walled semicircular cross section shown in Fig. 9-26.

Let us consider a section bb defined by the distance s measured along the median line of the cross section. The central angle subtended between point a , which is at the edge of the section, and section bb is denoted by θ . Therefore, we have $s = r\theta$, where r is the radius of the median line. The first moment of the area between a and section bb is

$$Q_z = \int y dA = \int_0^\theta (r \cos \phi)(rt) d\phi = r^2 t \sin \theta$$

where t is the thickness of the section. Thus, the shear stress τ at section bb is

$$\tau = \frac{V_y Q_z}{I_z t} = \frac{V_y r^2 \sin \theta}{I_z}$$

Substituting $I_z = \pi r^3 t/2$, we get

$$\tau = \frac{2V_y \sin \theta}{\pi r t} \tag{9.46}$$

When $\theta = 0$ or π , this expression gives $\tau = 0$; and, when $\theta = \pi/2$, it gives the maximum shear stress.

The moment about the center O due to the shear stresses τ is

$$T = \int \tau r dA = \int_0^\pi \frac{2V_y r \sin \theta}{\pi} \sin \theta d\theta = \frac{4rV_y}{\pi}$$

which must be the same as the moment due to the force V_y acting at the shear center; hence,

$$T = V_y e = \frac{4rV_y}{\pi}$$

* The first determination of a shear center was made by Timoshenko in 1913 (Ref. 9-1). For additional information and for the historical development of the shear-center concept, see Refs. 9-1 through 9-20.

Thus, the distance e from point O to the shear center is

$$e = \frac{4r}{\pi} \approx 1.27r \tag{9.47}$$

The shear center of a more general thin-walled circular section is given in Problem 9.7-10.

Example 2

Locate the shear center of the Z-section shown in Fig. 9-27a. (The y and z axes shown in the figure are principal axes through the centroid C .)

Let us assume that a shear force V_y acts parallel to the y axis. Then the shear stresses in the flanges and web will be directed as shown in Fig. 9-27b. From symmetry considerations, we see that the forces F_1 in the two flanges must be equal to each other (Fig. 9-27b). The resultant of all three forces acting on the cross section (F_1 in the flanges and F_2 in the web) must be equal to the shear force V_y . The forces F_1 have a resultant $2F_1$ acting through the centroid shear force V_y . The forces F_2 have a resultant F_2 acting through the centroid, and parallel to the flanges. This force intersects the force F_2 at the centroid; hence, this point must be the shear center. The composition of the forces $2F_1$ and F_2 into the resultant shear force V_y is shown in Fig. 9-27b.

If the beam is subjected to a shear force V_y parallel to the z axis, we arrive at a similar conclusion, namely, that the shear center coincides with the centroid.

The calculation of the shear stresses in a Z-section becomes complicated if principal axes are used, for the obvious reason that the flanges and web are skew to the axes. In the next section we will show how to calculate the shear stresses in a Z-section by using nonprincipal axes that are parallel to the web and flanges.

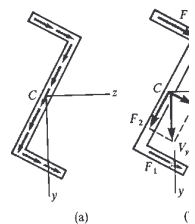


Fig. 9-27 Example 2. Shear in a Z-section

***9.8 GENERAL THEORY FOR SHEAR STRESSES**

In our previous derivations of formulas for the shear stresses in beams of thin-walled open cross sections, we arrived at Eqs. (9-27) through (9-29) for the case in which the y and z axes are principal axes. Now we will derive more general equations related to nonprincipal centroidal axes y and z (Fig. 9-28).

Let us assume that the loads on the beam are parallel to the y axis and that they produce a bending moment M_z and a shear force V_y . Let us also assume that the forces act through the shear center S . The bending moment M_z will produce bending about both the y and z axes; the corresponding stresses are given by Eq. (9-21a):

$$\sigma_x = \frac{M_z(I_{yz}z - I_y y)}{I_y I_z - I_{yz}^2}$$

where y and z are the coordinates of a point in the cross section. We now proceed to cut out an element from the beam in the manner illustrated in Fig. 9-21. The forces F_1 and F_2 acting on the element (Fig.

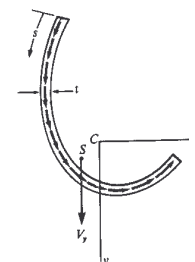


Fig. 9-28 Shear stresses in thin-walled open cross section. The y and z axes are nonprincipal centroidal axes.

9-21c) are found by the same procedure as before, except that the preceding equation must be used for the normal stresses; thus,

$$F_1 = \int_0^s \sigma_x dA = \frac{M_{z1}}{I_y I_z - I_{yz}^2} \int_0^s (I_{yz} z - I_{yz} y) dA$$

$$F_2 = \int_0^s \sigma_x dA = \frac{M_{z2}}{I_y I_z - I_{yz}^2} \int_0^s (I_{yz} z - I_{yz} y) dA$$

and

$$\tau = \frac{M_{z1} - M_{z2}}{dx} \frac{1}{(I_y I_z - I_{yz}^2)} \int_0^s (I_{yz} z - I_{yz} y) dA$$

Again we note that the quantity $(M_{z2} - M_{z1})/dx$ is equal to $-V_y$; hence,

$$\tau = \frac{V_y}{(I_y I_z - I_{yz}^2)} \left[I_{yz} \int_0^s z dA - I_{yz} \int_0^s y dA \right] \quad (9-48)$$

This equation is a **generalized shear formula** that gives the shear stress τ in a beam when the shear force V_y acts parallel to a nonprincipal axis.

By proceeding in the same manner as above, we can derive a formula for the shear stresses caused by a shear force V_z acting through the shear center and parallel to the z axis; the result is

$$\tau = \frac{V_z}{(I_y I_z - I_{yz}^2)} \left[I_{yz} \int_0^s y dA - I_z \int_0^s z dA \right] \quad (9-49)$$

Note that, when the y and z axes are principal axes ($I_{yz} = 0$), Eqs. (9-48) and (9-49) reduce (except for sign) to Eqs. (9-27) and (9-29a). In our previous work, we always took Q_y and Q_z as positive and obtained the directions of the shear stresses from physical considerations. However, in Eqs. (9-48) and (9-49), it is necessary to follow a sign convention for the first moments because they may be either positive or negative. This refinement is readily accomplished by treating y and z as algebraic quantities.

Having derived the generalized shear formulas (Eqs. 9-48 and 9-49), we may now proceed to find the distribution of shear stresses in any particular beam. Also, the shear center of the section can be located by finding the lines of action of the shear forces V_y and V_z and noting their point of intersection. These procedures are illustrated in the following examples.

Example 1

Determine the shear stresses in a Z-section (Fig. 9-29a) due to shear forces V_y and V_z (Figs. 9-29c and e).

We begin by calculating the properties of the section on the basis of centerline dimensions, as follows:

$$I_x = \frac{h^3 t_w}{12} + \frac{b h^2 t_f}{2} \quad I_y = \frac{2b^3 t_f}{3} \quad I_{yz} = \frac{b^2 h t_f}{2} \quad (a)$$

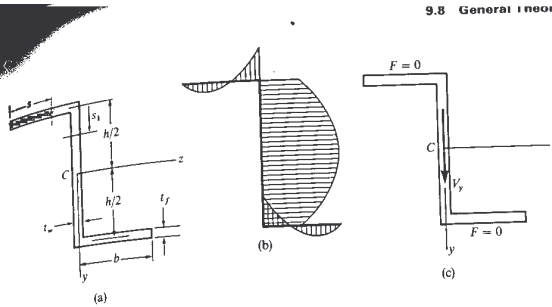


Fig. 9-29 Example 1. Shear stresses in a Z-section

in which the dimensions h, b, t_w , and t_f are defined as shown in the figure. Due to the shear force V_y , the shear stresses in the upper flange (from Eq. 9-48) are

$$\tau = \frac{V_y}{t_f(I_y I_z - I_{yz}^2)} \left[I_{yz} \int_0^s (s-b)t_f ds + I_y \int_0^s \frac{h}{2} t_f ds \right]$$

where s is measured from left to right along the flange. Carrying out the integrations, we find that the term in brackets in the preceding equation is equal to

$$\frac{b^2 h t_f^2}{12} (3s^2 - 2bs)$$

Substituting this expression, along with the expressions for I_y, I_z , and I_{yz} into the equation for τ , we get the following formula for the stresses in the flange:

$$\tau = \frac{3V_y(3s^2 - 2bs)}{bh(2ht_w + 3bt_f)} \quad (0 \leq s \leq b) \quad (b)$$

These shear stresses in the upper flange act toward the left when s is less than

$2b/3$; then they reverse in direction and act toward the right when s is between $2b/3$ and b . The resultant shear force in the flange is

$$F = \int_0^b \tau t_f ds = 0$$

An analogous condition exists in the lower flange.

The shear stresses in the web can also be found from Eq. (9-48), and it can be shown that the resultant force in the web is equal to V_y . At the neutral axis, the stress is

$$\tau_{\max} = \frac{3V_y(ht_w + bt_f)}{ht_w(2ht_w + 3bt_f)} \quad (c)$$

The distribution of the shear stresses due to V_y is shown in Fig. 9-29b, and the resultant forces in the flanges and web are shown in Fig. 9-29c.

Now let us consider a horizontal shear force V_z acting on the cross section. For the upper flange, we make use of Eq. (9-49), which becomes

$$\tau = \frac{V_z}{t_f(I_y I_z - I_{yz}^2)} \left[-I_{yz} \int_0^s t_f ds + I_z \int_0^s (b-s)t_f ds \right]$$

Evaluating the term in brackets, we get

$$\frac{h^2 t_f}{24} [bs(2ht_w + 6bt_f) - s^2(ht_w + 6bt_f)]$$

Hence, the final expression for τ becomes

$$\tau = \frac{3V_z}{2b^3 t_f(2ht_w + 3bt_f)} [bs(2ht_w + 6bt_f) - s^2(ht_w + 6bt_f)] \quad (d)$$

These stresses act toward the right in the upper flange and have the distribution shown in Fig. 9-29d. The resultant force F in the flange is

$$F = \int_0^b \tau t_f ds = \frac{V_z}{2}$$

as shown in Fig. 9-29e.

The shear stresses in the web due to V_z , found from Eq. (9-49), are

$$\tau = \frac{3V_z(h^2 + 6s_1^2 - 6hs_1)}{2bh(2ht_w + 3bt_f)} \quad (e)$$

where s_1 is measured from the juncture of the flange and web (Fig. 9-29a). This shear stress reverses its direction in the middle region of the web (see Fig. 9-29d), and the resultant shear force in the web is zero.

Example 2

Locate the shear center S of the unsymmetric channel section shown in Fig. 9-30a.

We begin by noting that the flange widths are b_1 and b_2 for the upper and lower flanges, respectively, and that the height of the section is h . The thickness is constant and is equal to t . The y and z axes are through the centroid C par-

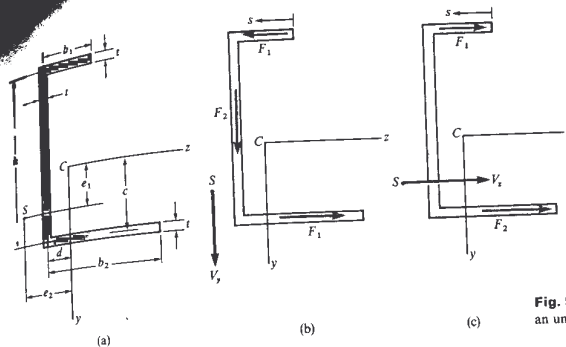


Fig. 9-30 Example 2. Shear stresses in an unsymmetric channel section

allel to the web and flanges, hence they are nonprincipal axes. The centroid is located by the dimensions c and d , which are

$$c = \frac{h^2 + 2b_1 h}{2(h + b_1 + b_2)} \quad d = \frac{b_1^2 + b_2^2}{2(h + b_1 + b_2)} \quad (f)$$

The shear center S is located by the distances e_1 and e_2 from the centroidal axes, and these distances must be determined next.

Let us assume that a shear force V_y acts through the shear center (Fig. 9-30b). The shear stresses in the top flange, found from Eq. (9-48), are

$$\tau = \frac{V_y}{t(I_y I_z - I_{yz}^2)} \left[I_{yz} \int_0^s (b_1 - d - s)t ds + I_y \int_0^s (h - c)t ds \right]$$

$$= \frac{V_y}{I_y I_z - I_{yz}^2} \left[I_{yz}(b_1 - d)s + I_y(h - c)s - \frac{I_{yz}s^2}{2} \right] \quad (g)$$

where s is measured as shown in the figure. The total force F_1 in the flange is

$$F_1 = \int_0^{b_1} \tau t ds = \frac{b_1^2 t V_y}{6(I_y I_z - I_{yz}^2)} [I_{yz}(2b_1 - 3d) + 3I_y(h - c)] \quad (h)$$

Because no external horizontal force acts on the beam, the shear force in the lower flange must also equal F_1 and the force F_2 in the web must equal V_y . Because the moment about C of the force V_y acting through the shear center must equal the moment about C of the three forces in the flanges and web, we get

$$V_y e_2 = F_2 d + F_1 h$$

or

$$e_2 = d + \frac{F_1 h}{V_y}$$

Substituting for F_1 from Eq. (h), we obtain the following equation, for e_1 :

$$e_2 = d + \frac{b^2 h t}{6(I_y I_z - I_{yz}^2)} [I_{yz}(2b_1 - 3d) + 3I_y(h - c)] \quad (9-50)$$

In the special case when the flanges are equal, the y and z axes become principal axes, and we have $I_{yz} = 0$, $c = h/2$, and $b_1 = b_2 = b$; then, from Eq. (9-50), we obtain

$$e_2 = d + \frac{b^2 h^2 t}{4I_z}$$

which is in agreement with our previous result (Eq. 9-43).

Now let us assume that a shear force V_z acts on the beam (Fig. 9-30c). In this case we can use Eq. (9-49) to calculate the shear stresses in the top flange:

$$\tau = \frac{V_z}{t(I_y I_z - I_{yz}^2)} \left[I_{yz} \int_0^s (c-h)t ds - I_z \int_0^s (b_1 - d - s)t ds \right] \\ = \frac{V_z}{I_y I_z - I_{yz}^2} \left[I_{yz}(c-h)s + I_z(d-b_1)s + \frac{I_z s^2}{2} \right] \quad (i)$$

The total force F_1 in the flange is

$$F_1 = - \int_0^{b_1} \tau t ds = \frac{b_1^2 t V_z}{6(I_y I_z - I_{yz}^2)} [3I_{yz}(h-c) + I_z(2b_1 - 3d)] \quad (j)$$

where we have introduced the minus sign in front of the equation because τ is positive to the left in Eq. (i) and we prefer to take F_1 positive to the right, as shown in Fig. 9-30c. The resultant force in the web must equal zero because there is no external force in the y direction. The force in the lower flange is denoted by F_2 , as shown in the figure. Taking moments about the lower flange gives the equation

$$V_z(c - e_1) = F_1 h$$

from which

$$e_1 = c - \frac{F_1 h}{V_z}$$

Substituting for F_1 from Eq. (j), we get the following equation for e_1 :

$$e_1 = c - \frac{b_1^2 h t}{6(I_y I_z - I_{yz}^2)} [3I_{yz}(h-c) + I_z(2b_1 - 3d)] \quad (9-51)$$

Again considering the special case of equal flanges, we have $I_{yz} = 0$, $c = h/2$, $b_1 = b_2 = b$, and $d = b^2/(h + 2b)$; therefore,

$$e_1 = \frac{h}{2} - \frac{b^3 h t (b + 2h)}{6I_y (h + 2b)}$$

Now substituting

$$I_y = \frac{b^3 t (b + 2h)}{3(h + 2b)}$$

which is the moment of inertia for a symmetric channel, we get $e_1 = 0$, as anticipated.

Thus, in any particular case of an unsymmetric channel, we can substitute the dimensions and properties of the cross section into Eqs. (9-50) and (9-51) and obtain the location of the shear centre. As a specific example, let us take the following dimensions:

$$b_1 = b \quad b_2 = 2b \quad h = 3b$$

Then we find

$$c = \frac{5b}{4} \quad d = \frac{5b}{12}$$

$$I_y = \frac{47}{24} b^3 t \quad I_z = \frac{69}{8} b^3 t \quad I_{yz} = \frac{13}{8} b^3 t$$

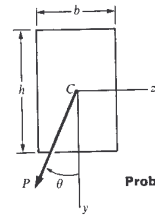
Substituting into Eqs. (9-50) and (9-51), we obtain

$$e_1 = \frac{55b}{76} \quad e_2 = \frac{187b}{228}$$

as the distances from the centroidal axes to the shear centre.

PROBLEMS/CHAPTER 9

9.2-1 A cantilever beam of rectangular cross section (see figure) supports an inclined load P at its free end. Demonstrate that, if the load P has its line of action along a diagonal of the cross section, then the neutral axis will lie along the other diagonal.



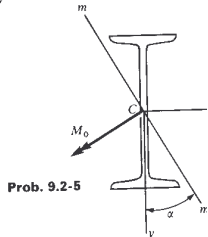
Probs. 9.2-1, 9.2-2, 9.2-3.

9.2-2 A wood cantilever beam of rectangular cross section (see figure) supports an inclined load P at its free end. Calculate the maximum tensile stress σ_{max} and the maximum deflection δ of the beam due to the load P . Data for the beam are as follows: $b = 75$ mm, $h = 150$ mm, $L = 1.5$ m, $P = 800$ N, $\theta = 29.52^\circ$, and $E = 12$ GPa.

9.2-3 Solve the preceding problem for a cantilever beam with data as follows: $b = 100$ mm, $h = 175$ mm, $L = 2$ m, $P = 2$ kN, $\theta = 45^\circ$, and $E = 12$ GPa.

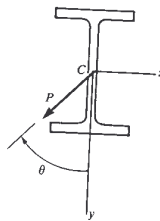
9.2-4 A cantilever beam of rectangular cross section (see figure) carries an inclined load P at its free end. What curve will be described by the end of the beam as the angle θ varies from 0 to 360° ?

9.2-5 A steel beam of I-section (see figure) is simply supported at the ends. Two equal and oppositely directed bending couples M_0 act at the ends of the beam; thus, the beam is in pure bending. The couples act in plane mn , which is oriented at an angle α to the xy plane. Determine the maximum tensile stress σ_{max} and the maximum deflection δ of the beam due to the couples M_0 . Data for the beam are as follows: $254 \times 102 \times 28$ kg UB, $L = 4$ m, $M_0 = 6$ kN·m, $\alpha = 30^\circ$, and $E = 200$ GPa.



Prob. 9.2-5

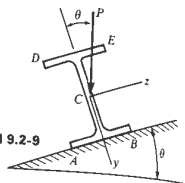
9.2-6 A cantilever beam of wide-flange cross section supports an inclined load P at its free end. Calculate the maximum tensile stress σ_{max} and the maximum deflection δ of the beam due to the load P . Data for the beam are as follows: $356 \times 171 \times 67$ kg UB, $L = 2$ m, $P = 10$ kN, $\theta = 45^\circ$, and $E = 200$ GPa.



Probs. 9.2-6 and 9.2-7

9.2-7 Solve the preceding problem using the following data: 54 kg UB, $L = 2$ m, $P = 10$ kN, $\theta = 45^\circ$, and $E = 200$ GPa.

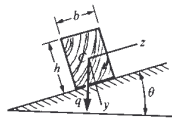
9.2-8 A cantilever beam of wide-flange cross section is supported at the free end by a vertical concentrated load P acting at the midpoint C of the span. The beam is inclined at an angle θ to the horizontal. Calculate the maximum deflection δ of the beam. Data for the beam are as follows: 171×67 kg UB, $L = 2.5$ m, $P = 25$ kN, and $E = 200$ GPa.



Probs. 9.2-8 and 9.2-9

9.2-9 Solve the preceding problem using the following data: 54 kg UB, $L = 2.4$ m, $P = 20$ kN and $E = 200$ GPa.

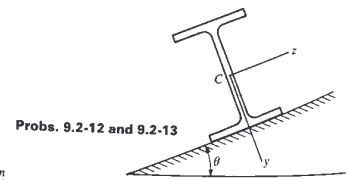
9.2-10 A beam of rectangular cross section is supported at the ends. The longitudinal axis is horizontal, but the cross section is inclined at an angle θ to the horizontal. The load on the beam is a uniform load of intensity q that is applied perpendicular to the cross section. Calculate the maximum deflection δ of the beam. Data for the beam are as follows: $h = 200$ mm, $L = 3$ m, $\tan \theta = 3/4$, and $E = 10$ GPa.



Probs. 9.2-10 and 9.2-11

9.2-11 Solve the preceding problem using the following data: $h = 75$ mm, $L = 3$ m, $\theta = 30^\circ$, $q = 11$ kPa, and $E = 10$ GPa.

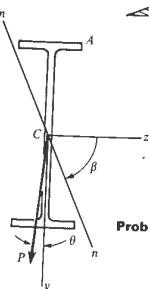
9.2-12 A beam of rectangular cross section is supported at the ends. The beam is inclined at an angle θ to the horizontal. Calculate the maximum deflection δ of the beam. Data for the beam are as follows: $h = 100$ mm, $L = 3$ m, $\theta = 30^\circ$, and $E = 10$ GPa.



Probs. 9.2-12 and 9.2-13

9.2-13 Solve the preceding problem using the following data: $h = 100$ mm, $L = 3$ m, $\theta = 30^\circ$, and $E = 10$ GPa.

9.2-14 A beam of rectangular cross section is supported at the ends. The beam is inclined at an angle θ to the horizontal. Calculate the maximum deflection δ of the beam. Data for the beam are as follows: $h = 100$ mm, $L = 3$ m, $\theta = 30^\circ$, and $E = 10$ GPa.



Prob. 9.2-14

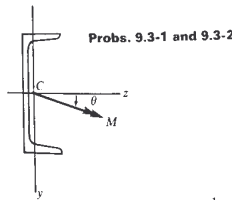
9.3-1 A channel section is subjected to a bending couple M having its vector at an angle θ to the z axis (see figure). Calculate the maximum tensile stress σ_t and maximum compressive stress σ_c in the beam. Use the following data: 203×76 section, $M = 4$ kN·m, $\tan \theta = 3/4$.

9.3-2 Solve the preceding problem for a 152×76 channel section.

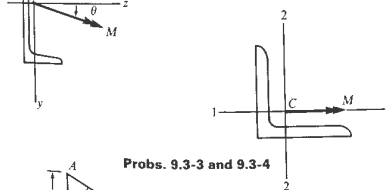
9.3-3 An angle section with equal legs is subjected to a bending moment M having its vector along the 1-1 axis, as shown in the figure. Calculate the maximum tensile stress σ_t and maximum compressive stress σ_c if the angle is an $L 150 \times 150 \times 18$ section and $M = 2$ kN·m.

9.3-4 Solve the preceding problem for an $L 100 \times 100 \times 15$ angle section with $M = 1$ kN·m.

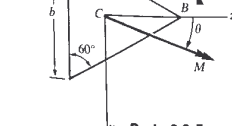
9.3-5 The cross section of a beam is in the form of an equilateral triangle with sides of length b (see figure). The beam is subjected to a bending couple M having its vector at an angle θ to the z axis. (a) Derive formulas for the stresses σ_x and σ_y at points A and B , respectively, in terms of M , b , and θ . (b) Plot a graph of the maximum tensile stress σ_{max} as a function of the angle θ for θ varying from 0 to 90° . Let the ordinate of the graph be the nondimensional quantity $\sigma_{max} b^3 / 32M$.



Probs. 9.3-1 and 9.3-2



Probs. 9.3-3 and 9.3-4



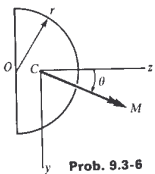
Prob. 9.3-5

9.3-6 A beam of semicircular cross section is subjected to a bending couple M having its vector along the z axis (see figure). Determine the maximum tensile stress σ_{max} in the beam for $\theta = 45^\circ$.

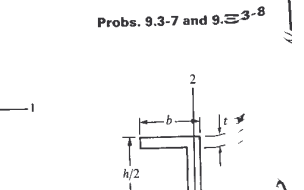
9.3-7 An angle section with unequal legs is subjected to a bending moment M having its vector along the 1-1 axis, as shown in the figure. Calculate the maximum tensile stress σ_t and the maximum compressive stress σ_c if the angle is an $L 200 \times 150 \times 18$ section and $M = 2$ kN·m.

9.3-8 Solve the preceding problem for an $L 100 \times 100 \times 15$ angle section with $M = 2$ kN·m.

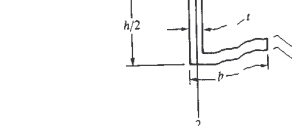
9.3-9 A beam of Z-section is subjected to a bending moment M acting in the 2-2 plane, as shown in the figure. Calculate the maximum tensile stress σ_t and maximum compressive stress σ_c if the moment M has dimensions are $b = 90$ mm, $h = 180$ mm, and $E = 200$ GPa.



Prob. 9.3-6

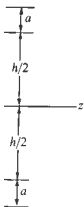


Probs. 9.3-7 and 9.3-8



Prob. 9.3-9

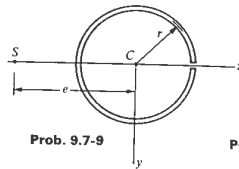
Unsymmetric Bending



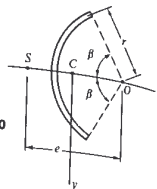
Prob. 9.7-8



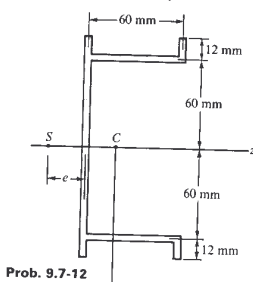
Prob. 9.7-11



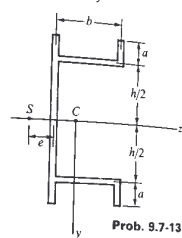
Prob. 9.7-9



Prob. 9.7-10



Prob. 9.7-12



Prob. 9.7-13

Derive the following formula for the distance e from the wall to the shear center S for a constant thickness t shown in the figure:

$$\frac{h^2(b+2a) - 8ba^3}{4b+6a + 4a^2(2a+3h)}$$

for the special case in which $a = 0$

Derive the following formula for the distance e from the center of the circle to the shear center S :

$$e = 2r$$

Derive the following formula for the distance e from the center of the circle to the shear center S :

$$\frac{(\sin \beta - \beta \cos \beta)}{2 - \sin \beta \cos \beta}$$

Derive the following formula for the distance e from the center of the circle to the shear center S :

9.7-11 A U-shaped cross section of constant thickness t is shown in the figure. Derive the following formula for the distance e from the center of the semicircle to the shear center S :

$$e = \frac{2(2r^2 + b^2 + \pi br)}{4b + \pi r}$$

Also, plot a graph showing how the distance e (expressed as the nondimensional ratio e/r) varies as a function of the ratio b/r .

9.7-12 Calculate the distance e from the centerline of the wall to the shear center S for the singly symmetric cross section of constant thickness shown in the figure. (Procedure: Determine the shear stresses acting on the cross section and find the line of action of their resultant. Use the formula of Problem 9.7-13 only as a check.)

9.7-13 Derive the following formula for the distance e from the centerline of the web to the shear center S for the singly symmetric cross section of constant thickness shown in the figure:

$$e = \frac{3bh^2(b+2a) - 8ba^3}{h^2(h+6b) + 4a(3h^2 + 4a^2 + 6bh)}$$

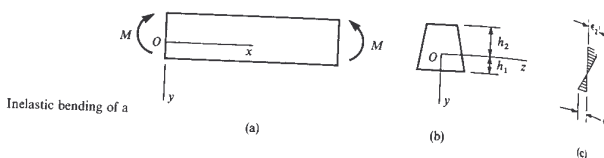
Also, check the formula for the special case in which $a = 0$ (channel section).

10.1 INTRODUCTION

Inelastic bending refers to the bending of beams when the material does not follow Hooke's law. Thus, it occurs whenever the beam is loaded in such a manner that the stresses in the beam exceed the proportional limit of the material. Naturally, the behavior of a beam in inelastic bending depends upon the shape of the stress-strain diagram. The material may be aluminum, which has a stress-strain diagram that is curved beyond the proportional limit, as shown in Fig. 10-1, or the material may be steel, which exhibits pronounced yielding and has the idealized stress-strain diagram shown in Fig. 10-2. In either case, if the stress-strain diagram is known, it is always possible to determine the stresses, strains, and deflections of the beam, as will be shown in this chapter.

The analysis of an inelastic beam is based on the fact that plane cross sections of a beam remain plane under pure bending, a condition that is valid for both nonlinear inelastic materials and linear elastic materials (see Section 5.2). Therefore, the strains in an inelastic beam vary linearly over the height of the beam. Then, with the aid of the stress-strain diagram and equations of statics, we can determine the magnitudes of the stresses. We can also calculate the curvature of the beam and the deflections.

By making an inelastic analysis of a beam, we can determine the ultimate load-carrying capacity, which is usually much greater than the load at the proportional limit (that is, the greatest load the beam can carry without exceeding the proportional limit at any point). For design purposes, we often need the ultimate load in order to ascertain the factor of safety against failure. Of course, this factor is much larger than the factor of safety with respect to the proportional limit. The concepts of ultimate-load design (see Section 1.7) are often used in the design of steel and concrete structures.



Inelastic bending of a

10.2 EQUATIONS OF INELASTIC BENDING

To obtain the basic equations for inelastic bending, let us consider a beam in pure bending subjected to a positive bending moment M (see Fig. 10-1a). The bending couples act in the xy plane, which is assumed to be a plane of symmetry of the cross section (Fig. 10-1b). Thus, the beam will deflect in this same plane, which is the plane of bending. We may consider the z axis as the neutral axis of the cross section, but its location remains to be determined.

From considerations of symmetry we know that the strains in the beam have a linear distribution irrespective of the nature of the material, as discussed in Section 5.2. Therefore, the strains vary from top to bottom of the beam in the manner pictured in Fig. 10-1c, with the strains at the lower and upper surfaces being denoted by ϵ_1 and ϵ_2 , respectively. Denoting by ρ the radius of curvature of the deflection curve, we see that the strain at distance y from the neutral surface (see Eq. 5-2) is

$$\epsilon = -\frac{y}{\rho} = -\kappa y \quad (10-1)$$

in which $\kappa = 1/\rho$ is the curvature. The strains at the outermost surfaces are

$$\epsilon_1 = -\kappa h_1 \quad \epsilon_2 = \kappa h_2 \quad (10-2a,b)$$

where h_1 and h_2 are the distances from the neutral axis to the lower and upper surfaces of the beam, respectively. From these equations we see that the strains can be readily determined provided that we know the curvature and the position of the neutral axis.

The location of the neutral axis can be found by making use of the stress-strain diagram for the material and an equation of statics expressing the fact that the resultant horizontal force due to the normal stresses σ acting on any cross section of the beam vanishes; thus,

$$\int \sigma dA = 0 \quad (10-3)$$

in which dA is an element of area in the cross section and the integration is performed over the entire cross section.

The curvature can be obtained by making use of a second equation

of statics, namely, an equation stating that the resultant of the stresses acting on the cross section is equal to the bending moment M :

$$\int \sigma y dA = M \quad (10-4)$$

Of course, Eqs. (10-3) and (10-4) are the same equations used previously in analyzing beams of linear elastic material (see Section 5.3). In this chapter we will use these equations to solve problems of inelastic bending.

After the curvature of the beam has been calculated, we can find the deflections of the beam by equating the curvature to d^2v/dx^2 (see Eq. 7-4) and then solving for the deflection v . Some of the same techniques developed earlier for finding deflections of elastic beams can be applied for inelastic bending; however, it is necessary to use more complicated expressions for curvature in place of the quantity M/EI , as described in Section 10.6.

10.3 PLASTIC BENDING

The simplest case of inelastic bending is plastic bending, which occurs when the material of the beam is elastic-plastic. Such a material follows Hooke's law up to the yield stress and then yields plastically under constant stress. The stress-strain diagram for an elastic-plastic material having the same yield stress σ_y and the same modulus of elasticity E in both tension and compression is shown in Fig. 10-2. We see that an elastic-plastic material has a region of linear elasticity between regions of perfect plasticity. For this reason, the term perfectly plastic material is often applied to an elastic-plastic material.

Structural steels may be idealized as elastic-plastic materials because they have sharply defined yield points and undergo large strains during yielding. The assumption of perfect plasticity after the yield stress is reached means that the effects of strain hardening are disregarded, but, since strain hardening provides an increase in the strength of the steel, it is generally safe to disregard it.

Now let us consider a beam of elastic-plastic material subjected to pure bending (Fig. 10-1). When the applied bending couples M are small, the maximum stress in the beam is less than the yield stress σ_y , and the beam is in the condition of ordinary elastic bending with a linear stress distribution, as shown in Fig. 10-3a. Under these conditions we learn from Eqs. (10-1) through (10-4) that the neutral axis passes through the centroid of the cross section, that the normal stress is $\sigma = My/I$, and that the curvature is $-M/EI$. These results are valid until the stress in the beam at the point farthest from the neutral axis reaches the yield stress (Fig. 10-3b). The corresponding moment acting on the beam is called the yield moment M_y :

$$M_y = \frac{\sigma_y I}{c} = \sigma_y S \quad (10-5)$$

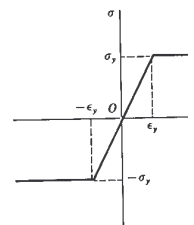
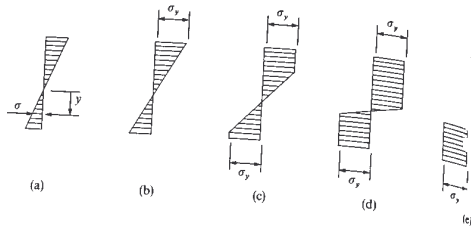


Fig. 10-2 Stress-strain diagram for an elastic-plastic material

distributions in a
tic material



in which S is the smaller of the two section moduli of the cross section. As an example, the yield moment for a beam of rectangular cross section is

$$M_y = \frac{\sigma_y b h^2}{6} \quad (10-6)$$

in which b is the width and h is the height of the cross section.

If we now increase the bending moment above the yield moment M_y , the strains at the extreme points of the cross section will continue to increase and the maximum strain will exceed the yield strain ϵ_y . However, because of perfectly plastic yielding, the maximum stresses will remain constant and equal to σ_y . Thus, the stress condition will be as pictured in Fig. 10-3c. The outer regions of the beam will have become plastic while a central core remains elastic. Also, the position of the neutral axis changes, unless the cross section is doubly symmetric. However, this shift in the neutral axis is too small to be shown in Fig. 10-3.

As the bending moment increases, the plastic region extends farther inward toward the neutral axis until the condition shown in Fig. 10-3d is reached. At this stage the strains in the extreme fibers are perhaps 10 or 15 times the yield strain ϵ_y , and the elastic core has almost disappeared. Thus, for all practical purposes the beam has reached its ultimate moment-resisting capacity, and we can idealize the ultimate stress distribution as consisting of two rectangular parts (Fig. 10-3e). The bending moment corresponding to this idealized stress distribution is called the **plastic moment** M_p , and it represents the maximum moment that can be sustained by a beam of elastic-plastic material.

The determination of the plastic moment is obviously of great importance because it is the limiting or maximum moment for the beam. In order to find M_p , we begin by locating the neutral axis of the cross section (Fig. 10-4a). Above the neutral axis, every element in the cross section has a compressive stress equal to σ_y (Fig. 10-4b); below the neutral axis, the stress is tension and also is equal to σ_y . The total tensile force T is equal to $\sigma_y A_1$, where A_1 is the area of the cross section below the neutral axis. Similarly, the compressive force C is $\sigma_y A_2$, where A_2

is the cross-sectional area above the neutral axis. As shown by Eq. (10-3), the resultant force on the cross section must be zero, so that

$$T - C = 0 \quad \text{or} \quad A_1 = A_2 \quad (a)$$

Since the total area of the cross section is $A = A_1 + A_2$, it is apparent from the preceding equation that

$$A_1 = A_2 = \frac{A}{2} \quad (10-7)$$

and we conclude that the neutral axis divides the cross section into two equal areas. Thus, in general, the neutral axis for the plastic moment M_p is in a different location from that for linear elastic bending. For instance, for a trapezoidal cross section that is narrower at the top than at the bottom, as shown in Fig. 10-4a, the neutral axis is slightly lower for the plastic than for the elastic case. Of course, if the cross section is doubly symmetric, as for a rectangular beam or a wide-flange beam, the neutral axis will have the same position for both plastic and elastic bending.

The plastic moment M_p can now be found from Eq. (10-4) by integrating or by the equivalent procedure of simply taking the moments about the neutral axis of the forces T and C shown in Fig. 10-4b; thus, we obtain

$$M_p = T y_1 + C y_2$$

where y_1 and y_2 are the distances from the neutral axis to the centroids c_1 and c_2 of the areas A_1 and A_2 , respectively. Replacing T and C by $\sigma_y A/2$, we get

$$M_p = \frac{\sigma_y A (y_1 + y_2)}{2} \quad (10-8)$$

The procedure for each particular beam is to divide the cross section into two equal areas, locate the centroid of each half, and then use Eq. (10-8) to calculate M_p .

The expression for the plastic moment can be written in a form analogous to that for the yield moment (see Eq. 10-5), as follows:

$$M_p = \sigma_y Z \quad (10-9)$$

in which

$$Z = \frac{A(y_1 + y_2)}{2} \quad (10-10)$$

is the **plastic modulus** for the cross section. The plastic modulus may be interpreted geometrically as the first moment (taken about the neutral axis) of the area of the cross section above the neutral axis plus the first moment of the area below the neutral axis.

The ratio of the plastic moment for a beam to its yield moment is solely a function of the shape of the cross section and is called the **shape factor** f :

$$f = \frac{M_p}{M_y} = \frac{Z}{S} \quad (10-11)$$

If we take a beam of rectangular cross section ($b =$ width, $h =$ height), the plastic modulus (see Eq. 10-10) becomes

$$Z = \frac{bh}{2} \left(\frac{h}{4} + \frac{h}{4} \right) = \frac{bh^2}{4} \quad (10-12)$$

Recalling that the section modulus is $S = bh^2/6$, we see that the shape factor for a rectangular beam is

$$f = \frac{3}{2} \quad (10-13)$$

Thus, the plastic moment for a rectangular beam is 50% greater than the yield moment.

For an I-section beam (see Fig. 10-5), the plastic modulus is easily calculated by taking the first moment of one flange and the part of the web above the neutral axis and then multiplying by 2; thus,

$$Z = bt_f(h - t_f) + t_w \left(\frac{h}{2} - t_f \right)^2 \quad (10-14)$$

in which the first term on the right-hand side represents the contribution of the flanges and the second term is from the web. For standard shapes of wide-flange beams, values of Z are tabulated in the BCSA/Constrado Handbook (Ref. 5-5). The shape factor f for wide-flange beams is typically in the range of 1.1 to 1.2, depending upon the proportions of the cross section.

Moment-curvature relation. It has already been observed that, for values of bending moment less than the yield moment M_y , the curvature κ is $-M/EI$. If we denote by κ_y the yield curvature (that is, the curvature when M equals M_y), we have

$$\kappa_y = -\frac{M_y}{EI} \quad (10-15)$$

Hence, the moment-curvature relation for a beam in the linear elastic range can be expressed in a nondimensional form as follows:

$$\frac{M}{M_y} = \frac{\kappa}{\kappa_y} \quad (0 \leq M \leq M_y) \quad (10-16)$$

This equation is represented by the straight-line portion of the moment-curvature diagram shown in Fig. 10-6.

When the moment becomes greater than M_y , part of the beam will

become fully plastic as discussed earlier in connection with Fig. 10-3c. The moment-curvature relationship then becomes nonlinear, as shown in Fig. 10-6. As the plastic zone penetrates farther toward the neutral axis of the beam, the curve in Fig. 10-6 becomes flatter and approaches a horizontal line as an asymptote. This asymptote represents the plastic moment M_p ; hence, the ordinate to the asymptote is the shape factor f . The equation of the curved line naturally will depend upon the shape of the cross section.

Let us take again the case of a beam of rectangular cross section (Fig. 10-7a), and let e represent the distance from the neutral axis to the edge of the elastic core. The fully plastic zone is shown dark in part (a) of the figure and the stress distribution in the beam is shown in part (b). The bending moment represented by this stress distribution is

$$M = \sigma_y b \left(\frac{h}{2} - e \right) \left(\frac{h}{2} + e \right) + \sigma_y b \left(\frac{2e^2}{3} \right) \quad (b)$$

in which the first term on the right-hand side is the moment due to the stresses in the fully plastic zone and the second term is due to the stresses in the elastic core. Simplifying Eq. (b), we get

$$M = \frac{\sigma_y b h^2}{6} \left(\frac{3}{2} - \frac{2e^2}{h^2} \right) = M_y \left(\frac{3}{2} - \frac{2e^2}{h^2} \right) \quad (c)$$

Note that, when $e = h/2$, we get $M = M_y$ from Eq. (c); and, when $e = 0$, we get $M = 3M_y/2$, which is equal to the plastic moment M_p for a rectangular cross section.

The curvature of the rectangular beam shown in Fig. 10-7 can easily be found by applying the equation $\kappa = -\epsilon/y$ (see Eq. 10-1) to a point in the beam at the outer edge of the elastic core. At such a point we have $\epsilon = \sigma_y/E$ and $y = e$, so that

$$\kappa = -\frac{\sigma_y}{Ee} \quad (d)$$

This equation can be expressed in nondimensional form by introducing the following expression for the yield curvature κ_y for a rectangular beam:

$$\kappa_y = -\frac{M_y}{EI} = -\frac{2\sigma_y}{Eh} \quad (e)$$

Combining Eqs. (d) and (e), we get

$$\frac{\kappa}{\kappa_y} = \frac{h^2}{2e^2} \quad (f)$$

We can now eliminate e/h between Eqs. (c) and (f) and obtain the moment-curvature equation in the following nondimensional form:

$$\frac{M}{M_y} = \frac{3}{2} - \frac{\kappa^2}{2\kappa_y^2} \quad (M_y \leq M \leq M_p) \quad (10-17)$$

10.3 Plastic Bending

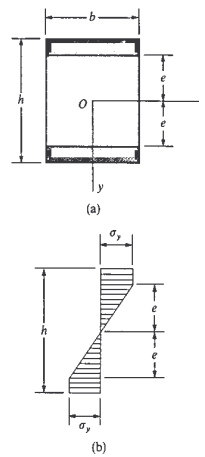
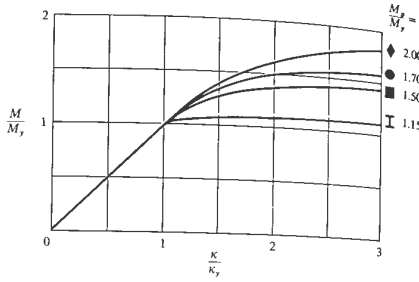


Fig. 10-7 Stress distribution in beam of rectangular cross section



moment-curvature diagrams of elastic-plastic

Solving Eq. (10-17) for the curvature in terms of the moment, we get

$$\frac{\kappa}{\kappa_y} = \frac{1}{\sqrt{3 - 2M/M_y}} \quad (M_y \leq M \leq M_p) \quad (10-18)$$

A graph of the moment-curvature relationship for a rectangular beam from either Eq. 10-17 or Eq. 10-18 is given in Fig. 10-8.

For other cross sections, a similar procedure can be followed to obtain moment-curvature equations. Graphs of these equations for a rhombus, a circle, and a typical wide-flange beam are also plotted in Fig. 10-8. In each instance the diagram consists of a straight line representing the linear elastic region followed by a curved line representing the region where the beam is partially plastic and partially elastic. In the latter region of the diagram, additional yielding may occur in the plastic zone of the beam without an increase in stress; whereas, in the central elastic zone of the beam, additional deformation occurs simultaneously with an increase in stress. Thus, the deformation of the beam is controlled by the elastic zone; this type of behavior is sometimes called *contained plastic flow*. When the curvature becomes very large, each curve in Fig. 10-8 approaches a horizontal asymptote. At this stage the beam can continue to deform without any increase in the applied bending moment. Thus we have the condition of *unrestricted plastic flow*, and the corresponding bending moment is the plastic moment M_p . The presence of unrestricted plastic flow leads to the concept of a plastic hinge, as described in the following section.

10.4 PLASTIC HINGES

To illustrate the concept of a plastic hinge, let us consider the behavior of a simple beam of elastic-plastic material subjected to a con-

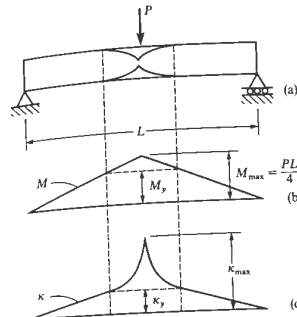


Fig. 10-9 Partially plastic beam: (a) plastic zone, (b) bending-moment diagram, and (c) curvature diagram

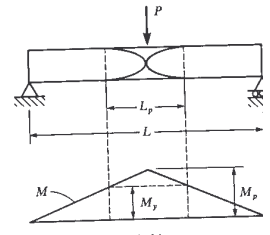


Fig. 10-10 Plastic hinge

centrated load P at the midpoint (Fig. 10-9a). The bending-moment diagram is triangular in shape with the maximum moment M_{max} equal to $PL/4$ (Fig. 10-9b). If the maximum moment is larger than M_y but less than M_p , a region of contained plastic flow will exist in the central part of the beam. The regions where the beam has become fully plastic are shown shaded in Fig. 10-9a. The height of the elastic zone at any cross section can be calculated from the bending moment, using the theory for pure bending described in the preceding section. This theory disregards the effects of the shear forces, but these effects are usually very small. Also, in this example we are disregarding the weight of the beam and considering only the bending moments produced by the applied load. Within these limitations, we can calculate the dimensions of the plastic zone for any specific beam and loading.

The curvature of the beam varies as shown in Fig. 10-9c. The curvature increases linearly from the ends of the beam toward the middle until we reach the edges of the plastic region where the curvature is equal to its yield value κ_y . Then the curvature increases at a faster rate and reaches a maximum value, κ_{max} at the midpoint of the beam. The maximum curvature remains finite as long as an elastic core continues to exist at the middle of the beam.

As the load is increased and the maximum bending moment approaches the plastic moment M_p , the regions of plasticity extend farther inward toward the neutral axis of the beam. Finally, when M_{max} becomes equal to M_p , the cross section at the center of the beam is completely plastic (Fig. 10-10). The curvature at the center of the beam

then becomes extremely large, and unrestrained plastic flow may take place. No further increase in the maximum moment can occur, and the load on the beam is at its maximum value. The beam fails by excessive rotations that occur at the middle cross section, while the two halves of the beam remain comparatively rigid. Thus, the beam behaves like two rigid bars linked by a plastic hinge that permits the two bars to rotate relative to each other under the action of a constant moment M_p .

The length L_p of the plastic zone surrounding the plastic hinge (Fig. 10-10) can easily be calculated from the fact that the bending moment at the edge of the zone is equal to M_y . Therefore, we have

$$M_y = \frac{P}{2} \left(\frac{L - L_p}{2} \right) \quad (a)$$

In addition, we know that the maximum moment $PL/4$ is equal to M_p , so that the load on the beam is

$$P = \frac{4M_p}{L} \quad (b)$$

Substituting Eq. (b) into Eq. (a) and solving for L_p , we get

$$L_p = L \left(1 - \frac{M_y}{M_p} \right) = L \left(1 - \frac{1}{f} \right) \quad (10-19)$$

for a simple beam with a concentrated load at the middle. For a rectangular beam ($f = 1.5$) we obtain $L_p = L/3$, and for a wide-flange beam ($f = 1.1$ to 1.2) we get $L_p = 0.09L$ to $0.17L$. Thus, the plastic zone is much smaller in a wide-flange beam than in a rectangular beam.

Even though the plastic zone extends over an appreciable length of the beam, the curvature tends to be concentrated at the hinge cross section (see Fig. 10-9c). Therefore, for most purposes we may consider a plastic hinge as having no dimensions; that is, we may consider the hinge as being located at a single cross section of the beam. The presence of the plastic hinge means that the beam will rotate at the hinge cross section while the bending moment remains constant and equal to M_p . Of course, plastic hinges always form at sections where the bending moment reaches a maximum value.

10.5 PLASTIC ANALYSIS OF BEAMS

The concept of plastic hinges provides a useful method for determining the maximum load that an elastic-plastic beam can support. We have already observed in connection with the illustration in the preceding section that the presence of a plastic hinge permits unlimited rotation to occur. Therefore, if the beam is statically determinate, the formation of a single hinge is sufficient to produce failure. The magnitude of the load required to develop the hinge (that is, the *ultimate load*) can

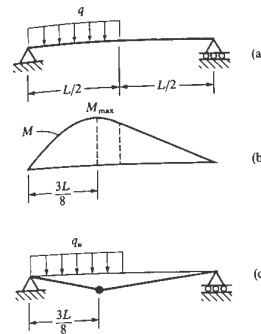


Fig. 10-11 Plastic analysis of a statically determinate beam

be calculated from static equilibrium. For instance, the ultimate load P_u for the beam pictured in Fig. 10-10a is

$$P_u = \frac{4M_p}{L}$$

as found from Eq. (b) of the preceding section. The task of calculating the ultimate loads and locating the plastic hinges for elastic-plastic beams is referred to as *plastic analysis*.

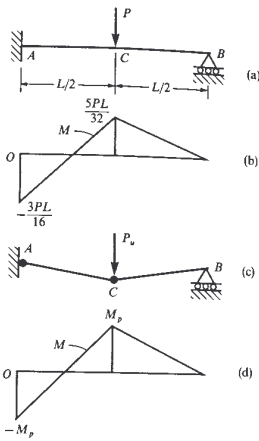
Now consider another example of a statically determinate beam. The beam shown in Fig. 10-11a has a uniform load of intensity q acting over the left-hand half. The bending-moment diagram is shown in part (b) of the figure, and we find that the maximum moment is $M_{max} = 9qL^2/128$. Note that the bending-moment diagram for a statically determinate beam is found from static equilibrium and is independent of whether the material of the beam is elastic or inelastic.

As the load q is gradually increased, we encounter initial yielding when the maximum moment becomes equal to the yield moment M_y for the beam; the corresponding load is called the *yield load*. Thus, the yield load for this beam is

$$q_y = \frac{128M_y}{9L^2}$$

With further increase in the load, a plastic hinge eventually will form at the section of maximum bending moment, shown by the heavy dot in Fig. 10-11c. The corresponding ultimate load is

$$q_u = \frac{128M_p}{9L^2}$$



Plastic analysis of a propped cantilever beam

where M_p is the plastic moment for the beam. After the hinge forms, the beam may be visualized as consisting of two bars linked together by the hinge. A beam in this condition forms a **mechanism** that may continue to deflect under the ultimate load. The terms *collapse mechanism* and *failure mechanism* are used to describe this condition.

The ratio of the ultimate load to the yield load for a statically determinate beam is M_p/M_y , which is equal to the shape factor f for the cross section. However, for statically indeterminate beams this ratio varies with the type of beam and its loading.

To demonstrate the behavior of **statically indeterminate beams**, we will take as an illustration a propped cantilever beam carrying a concentrated load P at the center (Fig. 10-12a). For any value of the load less than the yield load P_y , the bending-moment diagram has the shape shown in Fig. 10-12b. The maximum bending moment occurs at the fixed end A and is equal numerically to $3PL/16$; hence, the yield load is

$$P_y = \frac{16M_y}{3L} \quad (a)$$

If P is increased beyond the value P_y , additional yielding takes place at section A . Then, at a load larger than P_y , yielding also begins at section C where there is a peak in the bending-moment diagram. If we continue to increase the load, a plastic hinge will form at end A of the

beam. However, this single hinge will not cause complete failure of the beam. Instead, the beam will behave as a statically determinate simple beam acted upon by the load P at section C and by a moment M_p at end A . Thus, the structure will withstand further increase in the load until finally the bending moment at C also reaches the plastic moment M_p . At this stage plastic hinges will have formed at both A and C , hence the structure has formed a failure mechanism (Fig. 10-12c). Unrestricted deflection can now occur, and no further increase in the load is possible; thus, we have reached the ultimate load, we need not investigate in detail the behavior of the beam from initial loading up to collapse as was described in the preceding paragraph. Instead, we can go directly to the failure condition shown in Fig. 10-12c and calculate P_u from static equilibrium. Because the bending moments at the plastic hinges are equal to M_p , the complete bending-moment diagram for the failure condition is known immediately (see Fig. 10-12d). Hence, the load P_u can be found from equilibrium considerations. For instance, we can find the reaction R_b at support B from a free-body diagram of the entire beam. Taking moments about A (Fig. 10-12c), we obtain

$$M_p - \frac{P_u L}{2} + R_b L = 0 \quad \text{or} \quad R_b = \frac{P_u}{2} - \frac{M_p}{L}$$

Next, using a free-body diagram of part CB of the beam and taking moments about C , we get

$$-M_p + \frac{R_b L}{2} = 0$$

Combining this equation with the preceding one, we obtain

$$P_u = \frac{6M_p}{L} \quad (b)$$

as the ultimate load for the beam.

From Eqs. (a) and (b) we now obtain the ratio of the ultimate load to the yield load:

$$\frac{P_u}{P_y} = \frac{9M_p}{8M_y}$$

which is larger than the ratio M_p/M_y for statically determinate beams. The reason for this increase can readily be seen. Although the shape of the bending-moment diagram always remains the same for determinate beams, a *redistribution of moments* occurs with indeterminate beams. In the example of the beam shown in Fig. 10-12, the initial moment diagram has a maximum value at section A (Fig. 10-12b). After a hinge forms at that cross section, the bending moment there remains constant, although the moments will continue to increase elsewhere until the condition shown in Fig. 10-12d is reached. This redistribution of moments

increases the ultimate strength of a statically indeterminate structure as compared to a determinate structure, because as soon as one section fails other parts of the structure begin to support additional load.

One of the convenient features of plastic analysis is the ease with which the ultimate load can be calculated from equilibrium. A purely static analysis is naturally much simpler than the statically indeterminate analysis required for the linear elastic range. Furthermore, the results obtained by plastic analysis are insensitive to imperfections in the boundary conditions. A small rotation of a fixed support or a slight lowering of a simple support has no effect on the ultimate load, whereas the same kind of imperfections will have an appreciable effect on the elastic behavior of the structure.

When calculating the ultimate load by statics, we may use the principle of **virtual displacements**. This principle states that if a system of rigid bodies is in equilibrium under the action of a set of forces, then the work done by those forces during a small virtual displacement of the system must be zero. Let us apply this principle to the beam shown in Fig. 10-12. We consider the failure mechanism to consist of two bars AC and CB with plastic hinges at A and C , as shown in Fig. 10-13. We can introduce a virtual displacement by rotating bar AC through a small angle θ . During this displacement, bar CB will rotate through the same angle θ , and point C will move downward by the distance $\theta L/2$. The work done by the force P_u is positive and equal to P_u times $\theta L/2$. The work done by the plastic moments M_p is negative because they oppose the rotation of the bars; at section A the work is $-M_p\theta$, and at section C the work is $-M_p(2\theta)$. Therefore, the equation of virtual work for the beam is

$$\frac{P_u \theta L}{2} - M_p \theta - 2M_p \theta = 0$$

Note that the angle θ cancels out of the equation. Solving for the ultimate load, we get

$$P_u = \frac{6M_p}{L}$$

as before. The advantage of using the principle of virtual displacements lies in its simplicity; we merely introduce the virtual displacement and then write one equation of virtual work. By contrast, the more conventional approach of statics requires that we make use of free-body diagrams, not only for the structure as a whole but also for its parts.

In the preceding example there was only one possible way of positioning the plastic hinges; hence, only one failure mechanism had to be considered. However, often there will be several different possible mechanisms, and it may not be obvious which is the correct one. In that event we must consider in turn each mechanism and calculate the value of the corresponding load (or loads); naturally, the correct failure mechanism is the one that occurs at the smallest value of the load. This load is the true ultimate load for the structure.

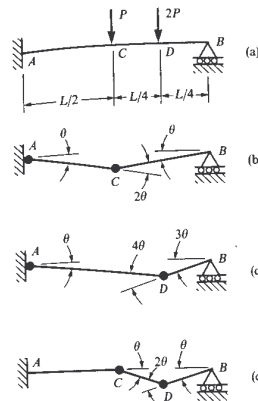


Fig. 10-14 Example illustrating possible failure mechanisms

To illustrate the proper selection of the failure mechanism, let us take the beam AB shown in Fig. 10-14a as an example. This beam supports two concentrated loads acting at sections C and D . The peak values of the bending moment in such a beam will occur at the cross sections where loads or reactions are acting (that is, at A , C , or D). A failure mechanism will be formed if plastic hinges exist at two of these three cross sections, and the three possibilities are shown in Fig. 10-14b, c, and d. The magnitude of the load P for each assumed mechanism can readily be calculated from the principle of virtual displacements. Thus, for the mechanism shown in Fig. 10-14b, we obtain

$$P \left(\frac{\theta L}{2} \right) + 2P \left(\frac{\theta L}{4} \right) - M_p \theta - M_p (2\theta) = 0$$

or $P = 3M_p/L$. Similarly, the load P corresponding to the mechanism shown in Fig. 10-14c is found to be $5M_p/2L$ and corresponding to Fig. 10-14d is $6M_p/L$. Comparing these three results, we conclude that the ultimate load for the beam shown in Fig. 10-14a is

$$P_u = \frac{5M_p}{2L}$$

and the collapse mechanism has plastic hinges at sections A and D . As yet another example of plastic analysis, let us examine a propped cantilever beam with a uniform load (Fig. 10-15a). The maximum nega-

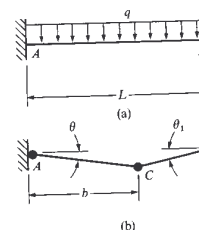


Fig. 10-15 Plastic analysis of beam with a uniform load

tive bending moment in the beam occurs at the fixed support *A*, and the maximum positive moment occurs somewhere near the middle of the beam. Thus, the collapse mechanism will have plastic hinges at *A* and *C*, as pictured in Fig. 10-15b. If we introduce a virtual displacement of the vertical displacement of the hinge at *C* will be θb , where b is the distance to the hinge. Also, the angle of rotation of part *CB* becomes $\theta_1 = \theta b / (L - b)$. Thus, the virtual work done by the plastic moments M_p at the hinges is

$$-M_p\theta - M_p(\theta + \theta_1) \tag{c}$$

The work done by the applied load q can be found by taking an element $q dx$ of the load, multiplying by the virtual displacement through which it moves, and then integrating along the length of the beam. Because q is constant, the result is equal to the product of q and the area of the displacement diagram shown in Fig. 10-15b. Thus, the virtual work of the load q is

$$q\left(\frac{L}{2}\right)(\theta b) \tag{d}$$

The equation of virtual work is obtained by adding expressions (c) and (d) and equating the sum to zero; solving the resulting equation, we get

$$q_u = \frac{2M_p}{bL} \left(\frac{2L - b}{L - b} \right) \tag{e}$$

This equation gives the ultimate load in terms of the distance b , which is an unknown quantity. However, we have already observed that, when considering various possible failure mechanisms, the correct mechanism is the one that gives the lowest value for the ultimate load. Applying this concept to the present problem, we conclude that the distance b must be such as to make q_u a minimum. Therefore, we can take the derivative of q_u with respect to b , set this derivative equal to zero, and solve for b . The result is

$$b = L(2 - \sqrt{2}) \tag{f}$$

An alternative procedure is to set up an expression for the bending moment in the beam with hinges and then find the location of the maximum moment; this point will be the location of the plastic hinge. Of course, calculations of the type just described (either minimizing q_u or locating the point of maximum moment) are possible only in the simplest problems where the mathematical steps are easy to handle. In more complicated situations it is easier to obtain a numerical solution by assuming several positions of the plastic hinge and then calculating the corresponding load q for each case by using the principle of virtual displacements. From such calculations both the smallest load q_u and the hinge location can be found with good accuracy.

Returning now to the problem at hand, we take the distance b from Eq. (f) and substitute it into the expression for q_u (see Eq. e), obtaining

$$q_u = \frac{2M_p}{L^2} (3 + 2\sqrt{2}) \approx \frac{11.66M_p}{L^2} \tag{g}$$

as the expression for the ultimate load on the beam. The ratio of the ultimate load q_u to the yield load $q_y = 8M_y/L^2$ can be readily calculated for this beam; the ratio is $1.46M_p/M_y$, which is 46% larger than for a statically determinate beam.

The plastic analysis of fixed-end beams and continuous beams can be performed in a manner analogous to that described in the preceding examples. A fixed-end beam will become a mechanism when three plastic hinges form; usually, there will be a hinge at each support plus one at some intermediate location. Continuous beams collapse when a mechanism forms in one span. For an interior span, three hinges are required: one at each end of the span and one at an intermediate location. For an end span having simple supports, two hinges, one at the first interior support and one within the span itself, are needed to form a mechanism.

The most important applications of plastic analysis are in the design of plane frames. Such frames form mechanisms when the ultimate load is reached, but their analysis is much more complicated than for beams. The interested reader may study some of the general references (see Refs. 10-1 through 10-8) for further information on methods of plastic analysis.

When analyzing a beam or other structure in the inelastic range, we must keep in mind that the principle of superposition does not hold and that the behavior of the structure depends not only upon the final values of the loads but also upon the order in which they are applied. To illustrate this point, consider the beam *AB* with two loads P acting as shown in Fig. 10-16a. If both loads are applied simultaneously, the bending-moment diagram has the shape shown in part (b) of the figure and the yield load is $P_y = 9M_y/L$. Now suppose that the load acting at

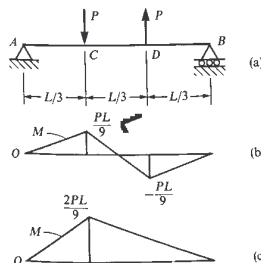


Fig. 10-16 Beam with two loads

point *C* is applied first, and then the load at *D* is applied. When only the load at *C* is acting, the bending-moment diagram has the shape shown in Fig. 10-16c. The maximum moment is twice its value for the preceding case; hence, the load P acting alone at *C* may produce plastic behavior even though it is less than the value P_y calculated above. This point *D*; hence, it is obvious that the final condition of the beam differs from the case in which the loads are applied simultaneously.

For this reason we will always assume in our studies that the forces are applied simultaneously to the structure and that the ratios of the loads remain constant during the loading process.

Plastic design. The design of steel structures on the basis of their ultimate-load capacity is referred to as **plastic design, ultimate-load design, or limit design**. In plastic design we first establish the service loads for the structure and then multiply those loads by a **load factor**, such as 1.7, to obtain the ultimate loads. The structure is designed for ultimate-load conditions, using the concepts of plastic analysis. This approach contrasts with the more familiar **elastic design, or allowable-stress design**, in which a safety factor is applied to the yield stress to give an allowable stress, after which the structure is designed (using the concepts of elastic analysis) so that the allowable stress is not exceeded.

The essential difference in the two methods of design is that plastic design produces a structure having a more or less uniform factor of safety against failure of all its parts, whereas an elastically designed structure has a uniform factor of safety against yielding. From the earlier discussion of how the bending moments in a structure redistribute during inelastic action, we can readily understand that structures designed by these two methods will have different relative proportions of their parts.

*10.6 DEFLECTIONS

The deflections of inelastic beams may be determined by methods that are similar to those used for elastic beams. However, the calculations are usually much more complicated because of the nonlinear relationships between bending moments and curvatures. We begin with the basic relationship between curvature and deflection (see Eq. 7-4):

$$\kappa = \frac{d^2v}{dx^2} \tag{10-20}$$

Because this equation was derived solely from geometric considerations, it is valid for a beam of any material. The principal limitations of the equation are that it is valid only for small deflections and that the effects of shear are disregarded. However, the equation is sufficiently accurate for ordinary purposes.

To use Eq. (10-20) for finding deflections, we must know the curvature κ , which is equal to $-M/EI$ for a beam of linear elastic material.

In the case of an inelastic beam, the appropriate expression for curvature (such as Eq. 10-18) must be used instead of $-M/EI$. Once the curvature is known, we may solve Eq. (10-20) for the deflections using some of the same methods that were described in Chapter 7 for elastic beams. For instance, we may use the successive-integration method and integrate Eq. (10-20) twice; however, there are practical difficulties in performing the integrations in all but the most elementary beam problems.

Another method is a generalized version of the moment-area method (Section 7.5), which we shall call the **curvature-area method**. This method is based upon the properties of the curvature diagram instead of the M/EI diagram, and hence it uses the following **curvature-area theorems**:

1. The angle θ_{AB} between the tangents to the deflection curve at two points *A* and *B* is equal to the negative of the area of the curvature diagram between those points.
2. The offset Δ_{AB} of point *B* from the tangent at *A* is equal to the negative of the first moment of the area of the curvature diagram between *A* and *B*, taken with respect to *B*.

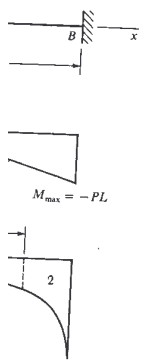
These theorems can be used to find slopes and deflections for inelastic beams in the same manner that the moment-area theorems were used for elastic beams.

Because the curvature diagram usually cannot be expressed in terms of simple functions, numerical techniques are generally needed for finding the deflections. For instance, the curvature can be calculated at a set of discrete points along the axis of the beam, and ordinates of the curvature diagram can be plotted at each of these points. These ordinates can be connected by straight lines to give an approximation of the exact diagram. Then the areas and first moments of the approximate diagram can be found numerically, after which the deflections and slopes can be determined from the curvature-area theorems. Only very simple problems can be handled by these methods, which in a strict sense are valid only for beams with doubly-symmetric cross sections and for materials having the same stress-strain diagrams in both tension and compression. The references should be consulted for further information on finding deflections.

When calculating deflections, we must keep in mind that the principle of superposition does not apply to any beam for which the proportional limit has been exceeded. Therefore, we cannot use the method of superposition when determining deflections of inelastic beams.

Example

A cantilever beam *AB* supporting a concentrated load P at the free end (see Fig. 10-17a) is constructed of an elastic-plastic material. Determine the angle of rotation θ and the deflection δ at the free end of the beam from the onset of loading up to failure, assuming that the beam is of rectangular cross section.



Let us begin by sketching the bending-moment diagram for the beam (Fig. 10-17b). We see that the maximum moment is equal to PL , and, as long as its value is less than the yield moment M_y , the beam is fully elastic. For the elastic range we have

$$\theta = \frac{PL^2}{2EI} \quad \delta = \frac{PL^3}{3EI}$$

The yield load P_y that first produces yielding of the beam is given by the equation

$$P_y = \frac{M_y}{L} \tag{a}$$

The angle θ_y and the deflection δ_y caused by this load are

$$\theta_y = \frac{P_y L^2}{2EI} \quad \delta_y = \frac{P_y L^3}{3EI} \tag{b}$$

In nondimensional form we can express the angle of rotation and the deflection for the entire elastic range by the following equations:

$$\frac{\theta}{\theta_y} = \frac{P}{P_y} \quad \frac{\delta}{\delta_y} = \frac{P}{P_y} \quad \left(0 \leq \frac{P}{P_y} \leq 1 \right) \tag{c}$$

When the maximum moment in the beam exceeds M_y , the beam will have two regions: (1) a region of fully elastic behavior and (2) a region of elastic-plastic behavior, as shown in the curvature diagram of Fig. 10-17c. In region 1 the curvature is

$$\kappa = \frac{Px}{EI} \tag{d}$$

and in region 2 (see Eq. 10-18) it is

$$\kappa = \frac{\kappa_y}{\sqrt{3 - 2Px/M_y}} \tag{e}$$

where $\kappa_y = M_y/EI$. The length x_1 of the elastic region is found from the equation $Px_1 = M_y$, so that

$$x_1 = \frac{M_y}{P} \tag{f}$$

The angle at the end of the beam, from the first curvature-area theorem, is equal to the total area of the curvature diagram:

$$\begin{aligned} \theta &= \int_0^{x_1} \frac{Px \, dx}{EI} + \int_{x_1}^L \frac{\kappa_y \, dx}{\sqrt{3 - 2Px/M_y}} \\ &= \frac{Px_1^2}{2EI} + \frac{\kappa_y M_y}{P} \left[\sqrt{3 - 2Px_1/M_y} - \sqrt{3 - 2PL/M_y} \right] \end{aligned}$$

If we substitute M_y/EI for κ_y , M_y/P for x_1 , and $P_y L$ for M_y , the preceding equation becomes

$$\frac{\theta}{\theta_y} = \frac{P}{P_y} \left[3 - 2\sqrt{3 - 2P/P_y} \right] \quad \left(1 \leq \frac{P}{P_y} \leq \frac{3}{2} \right) \tag{g}$$

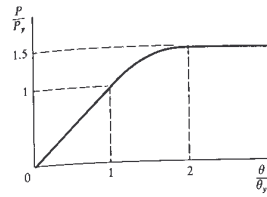


Fig. 10-18 Load versus angle of rotation for cantilever beam shown in Fig. 10-17

in which θ_y is given by Eq. (b). This equation is valid until the maximum moment in the beam becomes equal to the plastic moment M_p , which corresponds to $P/P_y = 3/2$. At the instant when P/P_y reaches this value, the angle of rotation $P/P_y = 3/2$. Subsequently, this angle increases indefinitely. A graph of load P/P_y versus angle of rotation θ/θ_y is shown in Fig. 10-18.

The deflection at the end of the beam is calculated from the second curvature-area theorem as follows:

$$\delta = \int_0^{x_1} \frac{Px^2 \, dx}{EI} + \int_{x_1}^L \frac{\kappa_y x \, dx}{\sqrt{3 - 2Px/M_y}}$$

By evaluating these integrals and making the same substitutions as for Eq. (g), we get

$$\frac{\delta}{\delta_y} = \left(\frac{P_y}{P} \right)^2 \left[5 - \left(3 + \frac{P}{P_y} \right) \sqrt{3 - \frac{2P}{P_y}} \right] \quad \left(1 \leq \frac{P}{P_y} \leq \frac{3}{2} \right) \tag{h}$$

in which δ_y is given by Eq. (b). When P/P_y equals $3/2$, the deflection is $\delta/\delta_y = 20/9$. The load-deflection diagram is plotted in Fig. 10-19.

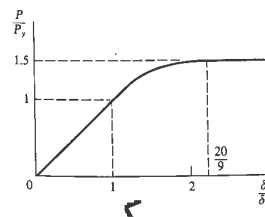
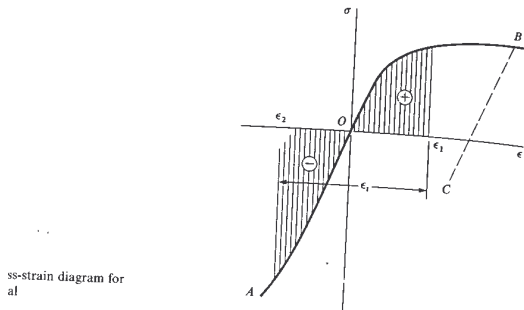


Fig. 10-19 Load versus deflection for cantilever beam shown in Fig. 10-17

*10.7 INELASTIC BENDING

In the preceding four sections we dealt in detail with the special case of an elastic-plastic material. Because this idealized material represents very accurately the behavior of structural steel, it is especially



Stress-strain diagram for beam

important in engineering work. We shall now consider the more general case of inelastic bending in which the material has a stress-strain diagram of any shape, typified by curve AOB in Fig. 10-20. Let us also consider a beam of rectangular cross section (Fig. 10-21), and let us denote by h_1 and h_2 the distances from the neutral axis to the lower and upper surfaces of the beam, respectively. These distances are equal only if the stress-strain diagram has the same shape in both tension and compression.

In order to locate the neutral axis of the rectangular beam, we use Eqs. (10-1) and (10-3). From Eq. (10-1) we get

$$y = -\rho\epsilon \quad dy = -\rho d\epsilon \tag{a}$$

Substituting into Eq. (10-3), we obtain

$$\int \sigma \, dA = \int_{-h_2}^{h_1} \sigma b \, dy = -\rho b \int_{\epsilon_2}^{\epsilon_1} \sigma \, d\epsilon = 0$$

in which ϵ_1 and ϵ_2 are the strains at the bottom and top of the beam, respectively (see Fig. 10-1). Note that these strains are also indicated on the stress-strain curve of Fig. 10-20, assuming that the curvature is negative and that the bottom of the beam is in tension. The preceding equation shows that the position of the neutral axis is such that

$$\int_{\epsilon_2}^{\epsilon_1} \sigma \, d\epsilon = 0 \tag{10-21}$$

Let us now denote by ϵ_n the sum of the absolute values of the maximum positive and negative strains in the beam:

$$\epsilon_n = \epsilon_1 - \epsilon_2 = -\kappa h_1 - \kappa h_2 = -\kappa h \tag{10-22}$$

To satisfy Eq. (10-21) and thereby locate the neutral axis, we begin by assuming a value of ϵ_n . Then we mark the length ϵ_n on the horizontal axis in Fig. 10-20 in such a way as to make the tension area of the dia-

gram equal to the compression area. In this manner we obtain the strains ϵ_1 and ϵ_2 in the extreme fibers; these strains correspond to the assumed value of the total strain ϵ_n . The corresponding position of the neutral axis is then obtained from Eq. (10-2), as follows:

$$\frac{h_1}{h_2} = \frac{\epsilon_1}{-\epsilon_2} = \left| \frac{\epsilon_1}{\epsilon_2} \right| \tag{10-23}$$

Because the strains ϵ are linear with distance from the neutral axis (see Fig. 10-1c), we conclude that the stress-strain diagram AOB in Fig. 10-20 represents the distribution of bending stresses over the height of the beam if the distance h is substituted for ϵ_n . Thus, for an assumed value of ϵ_n , we now know the position of the neutral axis and the stresses and strains over the height of the beam. From Eq. (10-22) we also know the curvature of the beam.

The next step is to find the bending moment M (through the use of Eq. (10-4)). Substituting from Eqs. (a), we can put Eq. (10-4) into the form

$$\int \sigma y \, dA = \int_{-h_2}^{h_1} \sigma y b \, dy = \rho^2 b \int_{\epsilon_2}^{\epsilon_1} \sigma \epsilon \, d\epsilon = M \tag{b}$$

By observing from Eq. (10-22) that $\rho = 1/\kappa = -h/\epsilon_n$, we can write Eq. (b) in the form

$$M = \frac{bh^2}{\epsilon_n^2} \int_{\epsilon_2}^{\epsilon_1} \sigma \epsilon \, d\epsilon \tag{10-24}$$

The integral in this expression represents the first moment with respect to the vertical axis of the area under the stress-strain curve (the shaded area) in Fig. 10-20. Note that the first moments of both areas are positive, because both σ and ϵ are positive to the right of the vertical axis and negative to the left. By evaluating these first moments and adding them, we obtain the value of the integral in Eq. (10-24). Then we can easily calculate the bending moment M , thereby completing the analysis of the beam in pure bending for the assumed value of ϵ_n .

The entire process can be repeated for other values of ϵ_n , each such calculation giving a value of curvature and a corresponding bending moment. From these data the moment-curvature diagram can be plotted (Fig. 10-22). Such a diagram is for a particular stress-strain curve and for a particular beam of rectangular cross section.

The calculations are simplified if the tension and compression parts of the stress-strain diagram are the same, because then we know immediately that the neutral axis passes through the centroid of the rectangular cross section. The following equations apply to this case:

$$h_1 = h_2 = \frac{h}{2} \tag{10-25}$$

$$\epsilon_1 = -\epsilon_2 = \frac{\epsilon_n}{2} \tag{10-26}$$

$$M = \frac{2bh^2}{\epsilon_n^2} \int_{-\epsilon_n/2}^{\epsilon_n/2} \sigma \epsilon \, d\epsilon \tag{10-27}$$

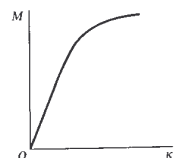


Fig. 10-22 Moment-curvature diagram for inelastic bending

From the last of these equations, we can calculate M for any assumed value of ϵ_1 , and the corresponding curvature can be found from Eq. (10-22).
 In the special case of a rectangular beam of linear elastic material, we have $\sigma = E\epsilon$, and Eq. (10-27) gives

$$M = \frac{2bh^2}{\epsilon_1^2} \int_0^{\epsilon_1} E\epsilon^2 d\epsilon = \frac{2bh^2 E \epsilon_1^3}{3\epsilon_1^2} \quad (c)$$

Now substituting $\epsilon_1 = 2\epsilon_1$ and $\sigma_{max} = E\epsilon_1$ into Eq. (c), we get

$$M = \frac{\sigma_{max} bh^2}{6} = \sigma_{max} S \quad (d)$$

where σ_{max} is the stress at the bottom of the beam. Also, if we substitute $\epsilon_1 = 2\epsilon_1$ and $\epsilon_1 = -\kappa h/2$ into Eq. (c), we get

$$\kappa = -\frac{M}{Ebh^3/12} = -\frac{M}{EI} \quad (e)$$

Equations (d) and (e) are the familiar equations of linear elastic bending. If instead of a rectangle we have some other shape of cross section for which the width b is variable (see Fig. 10-1b, for instance), then instead of Eqs. (10-21) and (10-24) we get

$$\int_{\epsilon_2}^{\epsilon_1} \sigma b d\epsilon = 0 \quad (10-28)$$

$$M = \frac{h^2}{\epsilon_1^2} \int_{\epsilon_2}^{\epsilon_1} \sigma b \epsilon d\epsilon \quad (10-29)$$

Note that the width b has been retained under the integral sign. As a specific example, let us consider a T-section (Fig. 10-23). Denoting by ϵ_3 the strain at the junction of the web and the flange, we can write the preceding equations in the following form:

$$\int_{\epsilon_3}^{\epsilon_1} \sigma d\epsilon + \int_{\epsilon_3}^{\epsilon_1} \sigma \frac{b_1}{b_2} d\epsilon = 0 \quad (f)$$

$$M = \frac{b_2 h^2}{\epsilon_1^2} \left[\int_{\epsilon_2}^{\epsilon_3} \sigma \epsilon d\epsilon + \int_{\epsilon_3}^{\epsilon_1} \sigma \frac{b_1}{b_2} \epsilon d\epsilon \right] \quad (g)$$

We see from these equations that the ordinates of the stress-strain diagram in the region corresponding to the flange of the cross section must be magnified in the ratio b_1/b_2 (see Fig. 10-24). In determining the position of the neutral axis, we proceed as in the earlier case and mark off the horizontal axis of Fig. 10-24 the position of the assumed distance ϵ_1 such that the two shaded areas become numerically equal. The position must be found, of course, by trial and error. For each trial position, the strain ϵ_3 at the junction of web and flange is obtained from the equation

$$\frac{\epsilon_1 - \epsilon_3}{\epsilon_1} = \frac{c}{h} \quad (h)$$

By proceeding in this manner, we can obtain the strains ϵ_1 and ϵ_2 in the extreme fibers.

Having located the neutral axis from Eq. (f), we can now find the bending moment from Eq. (g). We note that the two integrals within the brackets represent the first moments of the shaded areas in Fig. 10-24 with respect to the vertical axis through the origin O . By calculating this first moment, and then substituting into Eq. (g), we get the bending moment M corresponding to the assumed value of ϵ_1 . We can also find the corresponding curvature κ from Eq. (10-22), and then we can construct the moment-curvature diagram for the beam of T-section. An analogous process can be used for a wide-flange beam.

The preceding description of the analysis of a beam in inelastic bending is quite general and can be used for any stress-strain curve and any shape of cross section. However, the stress-strain curve sometimes may be approximated by an analytical expression; in that event it may be possible to determine the stresses, strains, and curvature by direct calculation. This procedure is feasible only in relatively simple cases, as illustrated in the following example for a beam of rectangular cross section.

Example

A beam of rectangular cross section (see Fig. 10-21) is constructed of material having a stress-strain diagram consisting of two straight lines, as shown in Fig. 10-25. The modulus of elasticity in tension is E_1 and in compression is E_2 , so that

$$\sigma = E_1 \epsilon \quad (\epsilon \geq 0) \quad (i)$$

$$\sigma = E_2 \epsilon \quad (\epsilon \leq 0) \quad (j)$$

The beam is assumed to be subjected to a positive bending moment M . The objectives of the analysis are to locate the neutral axis, obtain the moment-curvature expression, and find the maximum stresses and strains in the beam.

Let us denote the strains at the bottom and top of the beam as ϵ_1 and ϵ_2 , respectively. The corresponding maximum stresses are σ_1 and σ_2 . These stresses and strains are indicated in Fig. 10-25. To locate the neutral axis, we observe that the two shaded areas under the stress-strain curve must be equal, so that

$$\frac{\sigma_1 \epsilon_1}{2} = \frac{\sigma_2 \epsilon_2}{2} \quad (k)$$

From Eqs. (i) and (j) we know that

$$\sigma_1 = E_1 \epsilon_1 \quad \sigma_2 = E_2 \epsilon_2 \quad (l)$$

Also, we have the relations

$$\epsilon_1 = -\kappa h_1 \quad \epsilon_2 = \kappa h_2 \quad (m)$$

Substituting from Eqs. (l) and (m) into Eq. (k), we get

$$E_1 h_1^2 = E_2 h_2^2 \quad (n)$$

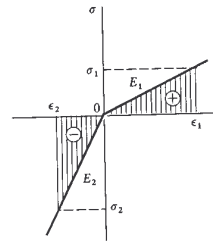


Fig. 10-25 Example. Stress-strain diagram consisting of two straight lines

10 Inelastic Bending

as the first equation relating h_1 and h_2 . In addition, we have the equation

$$h = h_1 + h_2$$

The distances h_1 and h_2 can now be found by simultaneous solution of Eqs. (n) and (o), yielding

$$h_1 = \frac{h\sqrt{E_2}}{\sqrt{E_1} + \sqrt{E_2}} \quad h_2 = \frac{h\sqrt{E_1}}{\sqrt{E_1} + \sqrt{E_2}} \quad (10-30a,b)$$

Thus, the position of the neutral axis is determined.

Next we calculate the bending moment by substituting from Eqs. (i) and (j) into Eq. (10-24); thus,

$$M = \frac{bh^2}{\epsilon_1^2} \left[\int_{\epsilon_2}^0 E_2 \epsilon^2 d\epsilon + \int_0^{\epsilon_1} E_1 \epsilon^2 d\epsilon \right]$$

which becomes

$$M = \frac{bh^2}{3\epsilon_1^2} [-E_2 \epsilon_2^3 + E_1 \epsilon_1^3] \quad (p)$$

The strains ϵ_1 and ϵ_2 are related to the curvature by Eqs. (m). Substituting for h_1 and h_2 (Eqs. 10-30), we get

$$\epsilon_1 = -\kappa h \frac{\sqrt{E_2}}{\sqrt{E_1} + \sqrt{E_2}} \quad \epsilon_2 = \kappa h \frac{\sqrt{E_1}}{\sqrt{E_1} + \sqrt{E_2}}$$

Also, the strain ϵ_1 is equal to $-\kappa h$ (see Eq. 10-22). We can now substitute these expressions for ϵ_1 , ϵ_2 , and ϵ_1 into Eq. (p), obtaining

$$M = -\frac{4E_1 E_2 I \kappa}{(\sqrt{E_1} + \sqrt{E_2})^2} \quad (q)$$

in which $I = bh^3/12$. Finally, let us introduce the notation

$$E_r = \frac{4E_1 E_2}{(\sqrt{E_1} + \sqrt{E_2})^2} \quad (10-31)$$

so that Eq. (q) becomes $M = -E_r I \kappa$ and, hence, the curvature becomes

$$\kappa = -\frac{M}{E_r I} \quad (10-32)$$

The quantity E_r is called the *reduced modulus of elasticity* and has a value between E_1 and E_2 . In the special case when both moduli are equal to E , the reduced modulus E_r also equals E .

The stresses and strains at the extreme fibers of the beam are now readily found in terms of the bending moment. We take Eqs. (m) for ϵ_1 and ϵ_2 and substitute Eq. (10-32) for the curvature, obtaining

$$\epsilon_1 = \frac{M h_1}{E_r I} \quad \epsilon_2 = -\frac{M h_2}{E_r I} \quad (10-33a,b)$$

Next, the stress-strain equations (Eqs. l) yield

$$\sigma_1 = \frac{M h_1 E_1}{I E_r} \quad \sigma_2 = -\frac{M h_2 E_2}{I E_r} \quad (10-34a,b)$$

and the analysis of the beam is completed.

Deflections. The deflections of a statically determinate inelastic beam can be found if we know the moment-curvature diagram. The techniques for making the calculations were discussed in Section 10.6. However, in the case of a statically indeterminate beam, the analysis is much more complicated because we cannot use the principle of superposition to find redundant reactions. Let us consider a simple example to show the method of analysis.

Suppose we have an inelastic beam that is fixed at one end and simply supported at the other. The reactive moment at the fixed support can be obtained by trial and error in the following manner. A trial value of this moment is assumed, and then the corresponding bending-moment diagram is constructed. Next, the curvature diagram for the beam is drawn by making use of the moment-curvature relationship. From the curvature diagram, we can calculate the angle of rotation at the fixed support. If the trial value of the redundant moment were correctly chosen, this angle would be zero. By making repeated trials, we can eventually arrive at the true value of the redundant moment. Similar techniques can be used to analyze any indeterminate beam.

***10.8 RESIDUAL STRESSES**

When a beam is bent inelastically and then the load is removed, some permanent set of the beam is produced, and the beam does not return to its original configuration. Those fibers of the beam that are stressed beyond the elastic limit will have a permanent set and will prevent the elastically stressed fibers from recovering their initial lengths after unloading. Hence, some residual stresses will exist in the beam.

The pattern of residual stresses in a beam is not difficult to determine if the stresses due to the initial inelastic bending are known. Suppose that the stress distribution in a beam due to a positive bending moment M is given by the diagram shown in Fig. 10-26a. For simplicity, we have assumed that the cross section of the beam has two axes of symmetry and that the material has the same properties in both tension and compression; it follows that the neutral axis is at the midheight of the beam and that the maximum tensile and compressive stresses (equal to σ_1) are numerically equal. Unloading of this beam is equivalent to bending of the beam by a negative bending moment equal to M . During unloading, the material of the beam is assumed to behave elastically and to follow Hooke's law, as shown by the line BC on the stress-strain diagram of Fig. 10-20. Therefore, the stress distribution that is superimposed during unloading is linear (Fig. 10-26b); hence, these stresses are obtained from the formula $\sigma = My/I$. The maximum unloading stress is $\sigma_2 = M/S$.

The superposition of the initial inelastic bending stresses and the linear unloading stresses will give the stresses remaining in the beam after the load is removed. These residual stresses are pictured in Fig. 10-26c and can easily be calculated as the algebraic sum of the stresses pictured in Figs. 10-26a and b. For instance, at the lower edge of the

10.8 Residual Stress

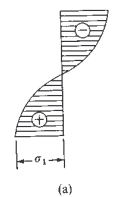


Fig. 10-26 Residual inelastic bending

beam, the residual stress is $\sigma_r = \sigma_1 + \sigma_2$. For the case pictured, σ_2 is negative and is numerically larger than σ_1 ; hence, σ_r also will be negative. Now suppose that the original positive bending moment M is re-applied to the beam having the residual stresses shown in Fig. 10-26c. Each fiber of the beam will remain elastic and follow Hooke's law until its stress reaches the original value before unloading took place. Therefore, the moment M now being applied will produce stresses having a linear relationship, and the beam will behave in a linear elastic manner as long as the applied moment does not exceed M . The stresses due to M will be the same as shown in Fig. 10-26b, except reversed in direction, and the final stresses will be as shown in Fig. 10-26a. Hence, the effect of the initial inelastic bending, with its attendant residual stresses due to unloading, is to produce a beam that will behave in a linear elastic manner, provided that the direction of bending is unchanged and that the moment does not exceed the initial moment.

As implied in this discussion, residual stresses are stresses that remain after the structure is loaded and unloaded. Another kind of residual stress exists in rolled structural shapes due to the manufacturing process. The rolling operation and the uneven heating and cooling of the section causes stresses to exist in a structural beam as received from the producer. Such stresses, often called residual stresses or *initial stresses*, may be as large as 70 or 100 MPa. For information on residual stresses in structural beams, see Refs. 10-8 through 10-10.

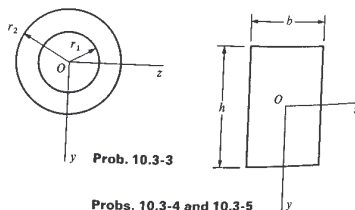
/ CHAPTER 10

on 10.3 are to be solved using the material is elastic-plastic.

ic shape factor f for a solid circular (ure).

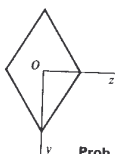
ic shape factor f for a cross section us (see figure).

: the shape factor f for a hollow ce figure). (b) In the special case of at is the shape factor f ?



Prob. 10.3-3

Probs. 10.3-4 and 10.3-5



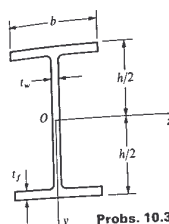
Prob. 10.3-2

10.3-4 A beam of rectangular cross section (see figure) with height $h = 100$ mm and width $b = 50$ mm is constructed of steel with yield stress $\sigma_y = 230$ MPa and $E = 200$ GPa. Calculate the yield moment M_y , the plastic moment M_p , and the plastic modulus Z for this beam. Also, plot to scale the moment-curvature diagram.

10.3-5 Solve the preceding problem for a rectangular beam with $h = 100$ mm, $b = 40$ mm, $\sigma_y = 250$ MPa, and $E = 210$ GPa.

10.3-6 Calculate the plastic moment M_p , the plastic modulus Z , and the shape factor f for the wide-flange beam shown in the figure. Assume $h = 400$ mm, $b = 150$ mm, $t_f = 12$ mm, $t_w = 8$ mm, and $\sigma_y = 290$ MPa.

10.3-7 Solve the preceding problem for a wide-flange beam with $h = 320$ mm, $b = 160$ mm, $t_f = 15$ mm, $t_w = 8$ mm, and $\sigma_y = 250$ MPa.



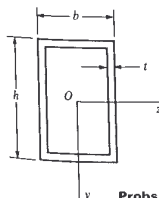
Probs. 10.3-6 and 10.3-7

10.3-8 Determine the plastic modulus Z and the shape factor f for a 305 x 165 x 40 kg UB section (see Appendix E). (Note: Obtain these properties by calculation using the dimensions of the cross section.)

10.3-9 Solve the preceding problem for a 254 x 102 x 28 kg UB section.

10.3-10 A doubly-symmetric hollow box section with height $h = 400$ mm, width $b = 250$ mm, and constant wall thickness $t = 20$ mm is shown in the figure. The beam is constructed of steel with yield stress $\sigma_y = 250$ MPa. Calculate the plastic moment M_p , the plastic modulus Z , and the shape factor f .

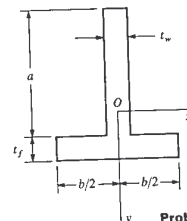
10.3-11 Solve the preceding problem for a box beam with dimensions $h = 0.5$ m, $b = 0.3$ m and $t = 25$ mm. (Assume $\sigma_y = 230$ MPa.)



Probs. 10.3-10 and 10.3-11

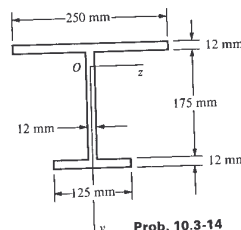
10.3-12 A singly-symmetric beam of T-section (figure) has dimensions $b = 150$ mm, $a = 200$ mm, 50 mm, and $t_f = 50$ mm. Calculate the plastic moment and the shape factor f .

10.3-13 Solve the preceding problem for a T-beam dimensions $b = 120$ mm, $a = 200$ mm, $t_w = 20$ mm, and $t_f = 25$ mm.



Probs. 10.3-12 and 10.3-13

10.3-14 A singly-symmetric I-section beam ($\sigma_y = 250$ MPa) has the cross section shown in Determine the plastic moment M_p .



Prob. 10.3-14

10.3-15 A 356 x 127 x 39 kg Universal Be appendix E) is subjected to a bending mom produces plastic yielding throughout the flat web remains elastic. Calculate the moment corresponding curvature κ , assuming $\sigma_y = 2$, $E = 200$ GPa.

10.3-16 Solve the preceding problem for a 40 kg UB section.

CHAPTER
Colum

11.1 BUCKLING AND STABILITY

Structures and machines may fail in a variety of ways, depending upon the materials, kinds of loads, and conditions of support. For instance, ductile members may stretch or bend excessively if overloaded, allowing the structure to come apart or collapse. Fractures can occur from repeated cycles of loading (fatigue failures) or from the overstressing of brittle members. Most of these types of failures are avoided by designing the members so that their maximum stresses and maximum deflections remain within tolerable limits. Thus, the **strength** and **stiffness** of a member are the important criteria in design. These subjects were considered in preceding chapters.

Another type of failure is **buckling**, which is the subject matter of this chapter. We will consider specifically the buckling of **columns** (that is, long, slender structural members loaded axially in compression) (Fig. 11-1a). If such a member is slender, then, instead of failing by direct compression, it may bend and deflect laterally (Fig. 11-1b), and we say that the column has buckled. Under an increasing axial load, the lateral deflections increase too, and eventually the column will collapse completely. Of course, buckling can occur in many different kinds of structures and can take a variety of forms. When you step on an empty aluminum can, the thin cylindrical walls buckle under your weight; and, when a large bridge collapsed a few years ago, it was due to buckling of a flat steel plate that wrinkled under compressive stresses.

To illustrate the phenomenon of buckling in an elementary manner, we will consider the **idealized structure** shown in Fig. 11-2a. Member AB is a rigid bar that is pinned at the base and supported by an elastic spring of stiffness β at the top. (The stiffness β is also known as the *spring constant*.) The bar supports a centrally applied load P that is perfectly aligned with the axis of the bar, hence the spring has no initial force in

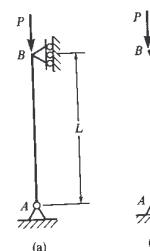
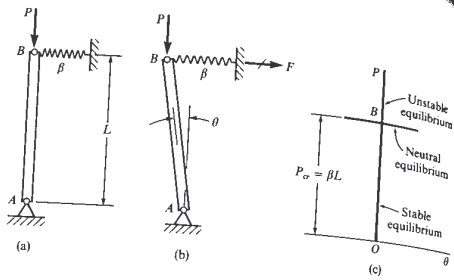


Fig. 11-1 Buckling of to an axial compressive

3 of a rigid bar
g



it. Now suppose that the bar is disturbed by some external force so that it rotates slightly through a small angle θ about support A (Fig. 11-2b). If the force P is small, the bar-spring system is **stable** and will return to its initial position when the disturbing force is removed. But if the force P is very large, the bar will continue to rotate and the system will collapse; thus, for a large force, the system is **unstable** and buckles by undergoing large rotations of the bar.

We can analyze the bar-spring system in more detail by considering its static equilibrium. When the bar is rotated slightly (Fig. 11-2b), the spring is elongated by an amount equal to θL , where L is the length of the bar. The corresponding force F in the spring is

$$F = \beta \theta L$$

This force creates a clockwise moment about point A equal to FL , or $\beta \theta L^2$. The tendency of this moment is to return the bar to its original position, hence we shall refer to $\beta \theta L^2$ as the **restoring moment**. The force P creates a counterclockwise moment about A that tends to overturn the bar; thus, the **overturning moment** is $P\theta L$. If the restoring moment exceeds the overturning moment, the system is stable and the bar returns to the initial vertical position; if the overturning moment exceeds the restoring moment, the system is unstable and the bar collapses by rotating through large angles. Therefore, we have the following conditions:

- If $P\theta L < \beta \theta L^2$, or $P < \beta L$, the system is stable.
- If $P\theta L > \beta \theta L^2$, or $P > \beta L$, the system is unstable.

The transition from a stable to an unstable system occurs when $P\theta L = \beta \theta L^2$, or $P = \beta L$; this value of the load is called the **critical load**:

$$P_{cr} = \beta L \tag{11-1}$$

We see that the system is stable when $P < P_{cr}$ and unstable when $P > P_{cr}$.

As long as P remains less than P_{cr} , the system returns to its initial position and $\theta = 0$. In other words, the bar is in equilibrium only when $\theta = 0$. When P is greater than P_{cr} , the bar is still in equilibrium when $\theta = 0$ (because the bar is in direct compression and there is no force in the spring), but the equilibrium is unstable and cannot be maintained. The slightest disturbance will cause the bar to collapse. At the critical load, the restoring and overturning moments are equal for any small value of θ (note that θ cancels out of the equilibrium equation). Thus, the bar is in equilibrium for any small angle θ ; this condition is referred to as **neutral equilibrium**.

These equilibrium relationships are shown in the graph of P versus θ (Fig. 11-2c), in which the two heavy lines represent the equilibrium conditions. Point B , where the equilibrium diagram branches, is called a **bifurcation point**. The horizontal line for neutral equilibrium extends to the left and right of the vertical axis because the angle θ may be clockwise or counterclockwise. The line extends only a short distance, however, because our analysis is based upon the assumption that θ is a small angle. Of course, this assumption is quite valid, because θ is indeed small when buckling begins and the bar first departs from the vertical position. (If θ becomes large, the equilibrium line curves away from the horizontal.)



Fig. 11-3 Ball in stable, unstable, and neutral equilibrium

The equilibrium of the bar described in Fig. 11-2 is analogous to that of a ball placed upon a surface (Fig. 11-3). If the surface is concave upward, like the inside of a dish, the equilibrium is stable and the ball always returns to the low point; if it is convex upward, like a dome, then the ball theoretically can be in equilibrium on top of the surface, but the equilibrium is unstable and in reality the ball rolls away. When placed on a flat surface, the ball is in neutral equilibrium and remains wherever it is placed.

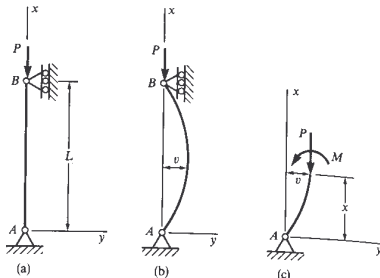
As we will see in the next section, the behavior of an ideal elastic column is analogous to that of the bar-spring system shown in Fig. 11-2. Furthermore, many kinds of buckling and stability problems in both structural and mechanical systems fit this model.

11.2 COLUMNS WITH PINNED ENDS

To investigate the stability behavior of columns, we will begin by considering a slender column with pinned ends (Fig. 11-4a). The column is loaded by a vertical force P that is applied through the centroid of the cross section and aligned with the longitudinal axis of the column. The column itself is perfectly straight and is made of a linear elastic material

Columns

in with pinned ends:
) buckled shape, and
m of part of column



that follows Hooke's law. Thus, we are going to analyze the behavior of an **ideal column**. The xy plane is a plane of symmetry, and we assume that any bending of the column takes place in that plane (Fig. 11-4b).

When the axial load P has a small value, the column remains straight and undergoes only axial compression. The uniform compressive stresses are obtained from the equation $\sigma = P/A$. This straight form of equilibrium is **stable**, which means that the column returns to the straight position if it is disturbed. For instance, if we apply a small lateral load and cause the column to bend, the deflection will disappear and the column will return to its original position when the lateral load is removed. As the axial load P is gradually increased, we reach a condition of **neutral equilibrium** in which the column may have a bent shape. The corresponding value of the load is the **critical load** P_{cr} . At this load the ideal column may undergo small lateral deflections with no change in the axial force, and a small lateral load will produce a bent shape that does not disappear when the lateral load is removed. Thus, the critical load can maintain the column in static equilibrium either in the straight position or in a slightly bent position. At higher values of the load, the column is **unstable** and will collapse by bending. For the ideal case that we are discussing, the column is in equilibrium in the straight position even when P is greater than P_{cr} . However, the equilibrium is unstable, and the smallest imaginable disturbance will cause the column to deflect sideways; the deflections will increase immediately and the column will collapse. The situation is analogous to balancing a pencil on its point. In theory, the pencil is in equilibrium when so balanced, but the position cannot be maintained.

The behavior of an ideal column compressed by an axial load P (Fig. 11-4) may be summarized as follows:

If $P < P_{cr}$, the column is in stable equilibrium in the straight position.

If $P = P_{cr}$, the column is in neutral equilibrium in either the straight or a slightly bent position.
If $P > P_{cr}$, the column is in unstable equilibrium in the straight position, and hence it buckles.

Of course, actual columns do not behave in this idealized manner because imperfections always exist. Nevertheless, we begin by studying ideal columns because they provide insight into the behavior of real columns.

To determine the critical load and the deflected shape of the buckled column (Fig. 11-4b), we use one of the differential equations of the deflection curve of a beam (see Eqs. 7-10). These equations are applicable to a column because, when buckling occurs, bending moments are developed in the column, which bends as though it were a beam. Although the fourth-order differential equation in terms of load intensity q and the fourth-order equation in terms of shear force V are suitable for the third-order equation in terms of bending moment M because its general solution is the simplest. This equation (Eq. 7-10a) is

$$EIv'' = -M \tag{11-2}$$

in which v is the lateral deflection in the y direction. For a column, we orient the x and y axes as shown in Fig. 11-4b, which corresponds to a beam AB that has been rotated 90° from the horizontal. The bending moment M at distance x from end A of the buckled column can be obtained from the free-body diagram shown in Fig. 11-4c. We cut the column at distance x from support A and observe from static equilibrium that a vertical force P and a bending moment M (equal to Pv) must act on the cut cross section. Therefore, the differential equation becomes

$$EIv'' = -M = -Pv$$

or

$$EIv'' + Pv = 0 \tag{11-3}$$

The quantity EI is the flexural rigidity for bending in the xy plane, which we have assumed to be the plane of buckling.

The solution of Eq. (11-3), which is a homogeneous linear differential equation of second order with constant coefficients, gives the deflection v as a function of x . For convenience in writing the general solution of the equation, we introduce the notation

$$k^2 = \frac{P}{EI} \tag{11-4}$$

Then we can rewrite Eq. (11-3) in the form

$$v'' + k^2v = 0 \tag{11-5}$$

The general solution of this equation is

$$v = C_1 \sin kx + C_2 \cos kx \tag{11-6}$$

where C_1 and C_2 are constants to be evaluated from the boundary conditions (or end conditions) of the column. Note that the number of arbitrary constants (two in this case) must agree with the order of the differential equation. Also, the fact that Eq. (11-6) represents the general solution of Eq. (11-5) may be verified easily by substituting the expression for v into the differential equation and observing that the equation is satisfied.

To evaluate the constants of integration, we use the boundary conditions at the ends:

$$v(0) = 0 \quad \text{and} \quad v(L) = 0$$

The first condition gives $C_2 = 0$, and the second gives

$$C_1 \sin kL = 0 \tag{a}$$

From this equation we conclude that either $C_1 = 0$ or $\sin kL = 0$. If $C_1 = 0$, the deflection v is zero and the column remains straight. In that case, Eq. (a) is satisfied for any value of the quantity kL . Therefore, the axial load P also may have any value (see Eq. 11-4). This solution of the differential equation (often called the *trivial solution*) is represented by the vertical axis of the load-deflection diagram shown in Fig. 11-5. This solution corresponds to an ideal column that is in equilibrium (either stable or unstable) under the action of the compressive load P .

The other possibility for satisfying Eq. (a) is to meet the following condition:

$$\sin kL = 0 \tag{b}$$

This equation is satisfied when $kL = 0, \pi, 2\pi, \dots$. Since $kL = 0$ means that $P = 0$, this solution is not of interest. Therefore, the solutions we will consider are

$$kL = n\pi \quad n = 1, 2, 3, \dots \tag{c}$$

or

$$P = \frac{n^2\pi^2 EI}{L^2} \quad n = 1, 2, 3, \dots \tag{d}$$

(see Eq. 11-4). This equation gives the values of P that satisfy Eq. (a) and hence provide solutions (other than the trivial solution) to the differential equation. Thus, the equation of the deflection curve is

$$v = C_1 \sin kx = C_1 \sin \frac{n\pi x}{L} \quad n = 1, 2, 3, \dots \tag{e}$$

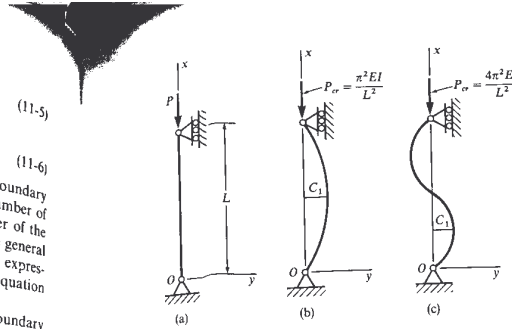


Fig. 11-6 Buckled shapes for an ideal column with pinned ends: (a) initial straight column, (b) buckled shape for $n = 1$, and (c) buckled shape for $n = 2$

Only when P has one of the values given by Eq. (d) is it theoretically possible for the column to have a bent shape; for all other values of P , the column is in equilibrium only if it remains straight. Therefore, the values of P given by Eq. (d) are the **critical loads** for the column.

The smallest critical load for the column is obtained when $n = 1$:

$$P_{cr} = \frac{\pi^2 EI}{L^2} \tag{11-7}$$

The corresponding buckled shape (sometimes called a *mode shape*) is

$$v = C_1 \sin \frac{\pi x}{L} \tag{11-8}$$

as shown in Fig. 11-6b. The constant C_1 represents the deflection at the midpoint of the column and may be positive or negative. Therefore, the part of the load-deflection diagram corresponding to P_{cr} is a horizontal straight line (Fig. 11-5). The deflection at this load is undefined, although it must remain small because we used the differential equation for small deflections. The bifurcation point B is at the critical load; above point B the equilibrium is unstable, and below it is stable. Buckling of a pinned-end column in the first mode ($n = 1$) is called the **fundamental case** of column buckling.

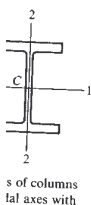
The critical load for an ideal elastic column is also known as the **Euler load**. The famous mathematician Leonhard Euler (1707–1783), whom many consider to be the greatest mathematician of all time, was the first person to investigate the bending of a slender column and determine its critical load (in 1744); see Refs. 1-1 through 1-3 and 11-1 through 11-7. For brief information about Euler's life and works, see the note to Ref. 11-3.

table
librium
—
utrial
uilibrium
de
librium
—
v
on diagram
1

By taking higher values of the index n in Eqs. (d) and (e), we obtain an infinite number of critical loads and corresponding mode shapes. The mode shape for $n = 2$ is pictured in Fig. 11-6c; the corresponding critical load is four times larger than that for the fundamental case. We see that the magnitudes of the critical loads are proportional to the square of n , and the number of half-waves in the buckled shape is equal to n . Such buckled shapes are usually of no practical interest because the column will always buckle when the axial load P reaches its lowest critical value (Eq. 11-7). The only way to obtain higher modes of buckling is to provide lateral support of the column at the inflection points (or nodal points).

The critical load of a column is proportional to the flexural rigidity EI and inversely proportional to the square of the length. However, the strength of the material itself (for instance, the proportional limit) does not appear in the equation for the critical load. Thus, the critical load is not increased by using a stronger material. However, the load can be increased by using a stiffer material (that is, a material with larger modulus of elasticity E). Also, the load can be increased by distributing the material in such a way as to increase the moment of inertia I of the cross section, just as a beam can be made stiffer by increasing the value of I . The moment of inertia is increased by distributing the material away from the centroid of the cross section. Hence, hollow tubular members are more economical for columns than are solid members having the same cross-sectional areas. Reducing the wall thickness of a tubular member and increasing its lateral dimensions, while keeping the cross-sectional area constant, increases the critical load because I is increased. This process has a practical limit, however, because eventually the wall itself becomes unstable. Then localized buckling occurs in the form of small corrugations or wrinkles. Thus, we must distinguish between overall buckling of a column, as shown in Fig. 11-6, and local buckling of its parts. The latter requires more detailed investigations, such as those found in books on buckling and stability (Refs. 11-1, 11-2, 11-8, 11-9, and 11-10). In this chapter we consider only overall buckling of columns.

In the preceding analysis we assumed that the xy plane was a plane of symmetry of the column and that buckling took place in that plane (Fig. 11-6). The latter assumption is met if the column has lateral supports perpendicular to the plane of the figure, so that the column is constrained to buckle in the xy plane. If the column is supported only at its ends, so that it is free to buckle in any direction, then bending will occur about the principal centroidal axis having the smaller moment of inertia. For instance, consider the rectangular and wide-flange cross sections shown in Fig. 11-7. In each case, the moment of inertia I_1 is greater than I_2 ; hence, the column will buckle in the 1-1 plane, and the smaller moment of inertia I_2 should be used in the formula for the critical load. If the cross section is square or circular, all centroidal axes have the same moment of inertia and buckling may occur in any longitudinal plane.



Effects of large deflections, imperfections, and inelastic behavior.

The equation for the critical load was derived for an ideal column in which the deflections are small, the construction is perfect, and the material follows Hooke's law. As a consequence, we found that the magnitudes of the deflections at buckling were undefined.* Thus, the column may have any small deflection, a condition at $P = P_{cr}$, the column may have any small deflection, a condition represented by the horizontal line A in the load-deflection diagram of Fig. 11-8. (In this figure, we show only the right-hand half of the diagram, but the two halves are symmetric about the vertical axis.) The theory is limited to small deflections because we used v'' for the curvature. A more exact analysis based upon the exact expression for curvature (see Eq. 7-11) shows that there is no indefiniteness in the magnitudes of the load-deflections at buckling. Instead, for an ideal elastic column, the load-deflection diagram goes upward in accord with curve B of Fig. 11-8. Thus, after an elastic column begins to buckle, a larger and larger load is required to cause an increase in the deflections.

Now suppose that the column is not constructed perfectly; for instance, it could have an imperfection in the form of a small initial curvature, so that the unloaded column is not perfectly straight. Such imperfections produce deflections from the onset of loading, as shown by curve C in Fig. 11-8. For small deflections, curve C approaches line A ; as the deflections become large, it approaches curve B . The larger the imperfections, the further curve C moves to the right. If the column is constructed with great accuracy, curve C approaches more closely to the straight line A (one vertical and one horizontal). From lines A , B , and C , we see that the critical load represents the maximum load-carrying capacity of an elastic column for practical purposes, because large deflections usually are not acceptable.

Finally, we consider what happens when the stresses exceed the proportional limit and the column material no longer follows Hooke's law. Of course, the load-deflection diagram is unchanged up to the level of load at which the proportional limit is reached. Then the curve for inelastic behavior (curve D) departs from the elastic curve, continues upward, reaches a maximum, and turns downward. Naturally, the detailed shapes of these curves depend upon the material properties and column dimensions, but the general nature of the behavior is typified by the curves shown.

Only extremely slender columns remain elastic up to the critical load P_{cr} . Stockier columns behave inelastically and follow a curve such as D . It is important to recognize that the maximum load P that can be supported by an inelastic column may be considerably less than the critical load P_{cr} . Furthermore, the descending part of curve D represents catastrophic collapse, because it takes smaller and smaller loads to maintain larger and larger deflections. By contrast, the curves for elastic

* Using mathematical terminology, we solved a *linear eigenvalue problem*. The critical load is an *eigenvalue* and the corresponding buckled mode shape is an *eigenfunction*.

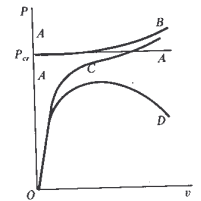
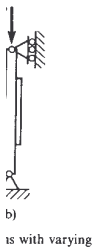


Fig. 11-8 Load-deflection diagram for columns: Lines A , ideal elastic with small deflections; Curve B , elastic column with large deflection; Curve C , elastic column with imperfections; Curve D , inelastic column with imperfections



columns are quite stable, because they continue upward as the deflections increase; that is, it takes larger and larger loads to cause an increase in deflection.

Optimum columns. Most columns are prismatic members; that is, they have the same cross sections throughout their lengths. Only such columns are analyzed in this chapter. However, the critical load of a column consisting of a given amount of material may be increased by tapering the column so that it has larger cross sections in regions where the bending moments are larger. Consider, for instance, a column of solid circular cross section with pinned ends. A "submarine-shaped" column with appropriately varying cross section (Fig. 11-9a) will have a larger critical load than if the same volume of material is made into a prismatic column. Of course, it is not practical to construct such a column, but prismatic columns sometimes are reinforced over part of their lengths (Fig. 11-9b) in order to approximate the optimum conditions.

Now consider a prismatic column with pinned ends that is free to buckle in any direction (Fig. 11-10a). Also, consider only solid convex cross sections, such as a circle, square, triangle, rectangle, or hexagon (Fig. 11-10b). For a given cross-sectional area, which of these shapes makes the most efficient column? Or, in more precise terms, we wish to know which cross section gives the largest critical load, considering that the critical load is calculated from the formula $P_{cr} = \pi^2 EI/L^2$ using the smallest moment of inertia for the cross section. For most people, intuition suggests that the circular shape is best. However, you can easily prove that a cross section in the shape of an equilateral triangle gives a 21% higher critical load than does a circular cross section of the same area (see Problem 11.2-10). The equilateral triangle also gives higher loads than any of the other shapes, hence it is the optimum cross section. (For a mathematical analysis of optimum column shapes, see Ref. 11-11.)

In practice, columns often are constrained to buckle in only one plane, hence a shape should be chosen that gives a large moment of inertia for bending in that plane. In steel construction, wide-flange sections are commonly used for columns; in both reinforced concrete and wood construction, rectangular and circular sections are used. The shapes used in aircraft and space structures, as well as in machine design, are quite varied, depending upon the particular application. In general, hollow sections are more efficient than solid sections because they provide a larger moment of inertia for the same cross-sectional area.

11.3 COLUMNS WITH OTHER SUPPORT CONDITIONS

Buckling of a column with pinned ends is often called the fundamental case of buckling. However, many other conditions, such as fixed ends, elastic supports, and free ends, are encountered in practice. The

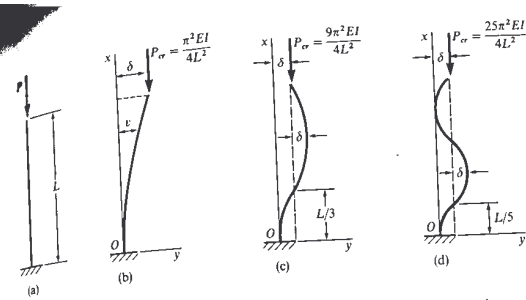


Fig. 11-11 Ideal column shapes and buckled shapes for $n = 1, 3, 5$.

critical loads for columns with various kinds of supports can be determined from the differential equation of the deflection curve, in a manner similar to that for a pinned-end column. We begin by drawing free-body diagrams of the column in order to obtain expressions for the bending moment M . Then we solve the differential equation in terms of the deflection v and slope v' . Boundary conditions on the deflection v and slope v' are used to evaluate the arbitrary constants and any other unknowns that appear in the solution. The final solution consists of the critical load P_{cr} and the deflected shape of the buckled column.

To illustrate this procedure, let us analyze an ideal elastic column that is fixed at the base, free at the top, and subjected to a vertical axial load P (Fig. 11-11a). This particular column is of historical interest because it is the one first analyzed by Euler in 1744. The deflected column is shown in Fig. 11-11b, and from this figure we can see that the bending moment at distance x from the base is

$$M = -P(\delta - v)$$

where δ is the deflection at the free end. The differential equation of the deflection curve (Eq. 11-2) then becomes

$$EIv'' = -M = P(\delta - v) \quad (a)$$

in which I is the moment of inertia for buckling in the xy plane.

Using the notation $k^2 = P/EI$ (see Eq. 11-4), we can write Eq. (a) in the form

$$v'' + k^2v = k^2\delta \quad (b)$$

This equation is another linear differential equation of second order with constant coefficients. However, it is more complicated than the equation for a column with pinned ends (see Eq. 11-5) because it has a nonzero term on the right-hand side. Its general solution consists of two parts: (1) the homogeneous solution, which is the solution of the corresponding homogeneous equation obtained by replacing the right-hand side with zero, and (2) the particular solution, which is a solution of the equation that produces the actual right-hand side. The homo-

geneous solution v_H (also called the complementary solution) is the same as the solution of Eq. (11-5); hence,

$$v_H = C_1 \sin kx + C_2 \cos kx \quad (c)$$

where C_1 and C_2 are arbitrary constants. When v_H is substituted into the left-hand side of the differential equation (Eq. b), it produces zero. The particular solution is

$$v_p = \delta \quad (d)$$

When v_p is substituted into the left-hand side of the differential equation, it produces the right-hand side. Therefore, the general solution of the equation is the sum of v_H and v_p :

$$v = C_1 \sin kx + C_2 \cos kx + \delta \quad (e)$$

This equation contains three unknowns, C_1 , C_2 , and δ ; hence, three boundary conditions are needed to obtain the solution.

At the fixed base of the column, we have two conditions:

$$v(0) = 0 \quad v'(0) = 0$$

The first condition gives

$$C_2 = -\delta \quad (f)$$

To use the second condition, we first differentiate Eq. (e) to obtain the slope:

$$v' = C_1 k \cos kx - C_2 k \sin kx$$

Then the second condition yields $C_1 = 0$. Substituting the values of C_1 and C_2 into the general solution, we get the equation of the deflection curve:

$$v = \delta(1 - \cos kx) \quad (g)$$

This equation gives the shape of the deflection curve, but the amplitude of the deflection is undefined.

The third boundary condition is at the upper end of the column where the deflection v is equal to δ :

$$v(L) = \delta$$

Using this condition with Eq. (g), we get

$$\delta \cos kL = 0 \quad (h)$$

from which we conclude that either $\delta = 0$ or $\cos kL = 0$. If $\delta = 0$, there is no deflection of the bar, and hence buckling does not occur (Fig. 11-11a). In that case, Eq. (h) will be satisfied for any value of the quantity kL . Therefore, the load P can have any value also. This result is represented by the vertical axis of the load-deflection diagram shown in Fig. 11-5.

The other possibility is that $\cos kL = 0$. In this case, Eq. (h) is

satisfied regardless of the value of the deflection δ ; thus, δ is undefined and may have any (small) value. The condition $\cos kL = 0$ requires that

$$kL = \frac{n\pi}{2} \quad n = 1, 3, 5, \dots \quad (i)$$

The corresponding formula for the critical loads is

$$P_{cr} = \frac{n^2 \pi^2 EI}{4L^2} \quad n = 1, 3, 5, \dots \quad (11-9)$$

Also, the buckled mode shapes (see Eq. g) are given by the following equation:

$$v = \delta \left(1 - \cos \frac{n\pi x}{2L} \right) \quad n = 1, 3, 5, \dots \quad (11-10)$$

The smallest critical load ($n = 1$) is the only load of practical interest:

$$P_{cr} = \frac{\pi^2 EI}{4L^2} \quad (11-11)$$

The corresponding buckled shape is

$$v = \delta \left(1 - \cos \frac{\pi x}{2L} \right) \quad (11-12)$$

which is shown in Fig. 11-11b. As previously mentioned, the deflection δ is undefined; hence, we obtain a horizontal line on the load-deflection diagram (Fig. 11-5).

By taking higher values of the index n , we obtain an infinite number of critical loads from Eq. (11-9). The corresponding buckled mode shapes have more and more waves in them. When $n = 3$, P_{cr} is nine times larger than for $n = 1$, and the buckled shape is shown in Fig. 11-11c. Similarly, the shape for $n = 5$ is pictured in part (d) of the figure.

Effective lengths of columns. The critical loads for columns with various support conditions can be related to the critical load of a pinned-end column through the concept of an effective length. To explain the idea, let us observe the deflected shape of a column fixed at the base and free at the top (Fig. 11-12a). This column buckles in a curve that is one-fourth of a full sine wave. If we extend the deflection curve (Fig. 11-12b), we see that it becomes the deflection curve for a pinned-end column, or one-half of a sine wave. The effective length L_e is the length of the equivalent pinned-end column, or the distance between points of inflection in the deflection curve. Thus, for the fixed-free column, the effective length is

$$L_e = 2L \quad (j)$$

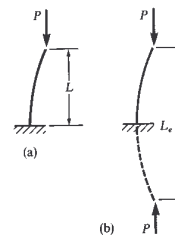


Fig. 11-12 Effective length of a column fixed at the base and free at the top.

Since the effective length is the length of an equivalent pinned-end column, we can write a general formula for the critical load as follows:

$$P_{cr} = \frac{\pi^2 EI}{L_e^2} \quad (11-13)$$

Substituting $L_e = 2L$, we get the critical load for a fixed-free column (Eq. 11-11).

The effective length is often expressed in terms of an effective length factor K :

$$L_e = KL \quad (11-14)$$

Hence, the critical load is

$$P_{cr} = \frac{\pi^2 EI}{(KL)^2} \quad (11-15)$$

The factor K equals 2 for a column fixed at the base and free at the top and equals 1 for a pinned-end column.

Column with fixed ends. Now consider a column with both ends fixed against rotation (Fig. 11-13a). We assume that the ends of the column are free to move toward each other. Then, when the axial load P is applied at the top, an equal reactive force develops at the base. When buckling occurs, reactive moments M_0 also develop at the supports (Fig. 11-13b). The deflection curve for the first mode of buckling is a trigonometric curve having inflection points at distance $L/4$ from the ends. Thus, the effective length, equal to the distance between inflection points, is

$$L_e = \frac{L}{2} \quad (k)$$

Substituting into Eq. (11-13) gives the critical load:

$$P_{cr} = \frac{4\pi^2 EI}{L^2} \quad (11-16)$$

We see that the critical load for a column with fixed ends is four times that for a column with pinned ends. This result can also be obtained by solving the differential equation of the deflection curve (Problem 11.3-6).

Column fixed at the base and pinned at the top. The critical load and buckled mode shape for a column that is fixed at the base and pinned at the top (Fig. 11-14a) cannot be determined by

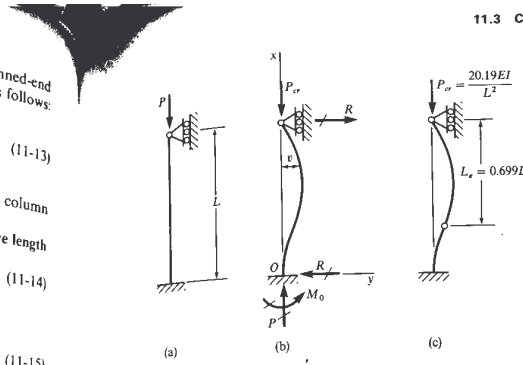


Fig. 11-14 Column fixed at the base and pinned at the top

inspection of the buckled mode shape (Fig. 11-14b) because the location of the point of inflection is not apparent. Hence, we must solve the differential equation in order to find P_{cr} .

When the column buckles, horizontal reactive forces R develop at the supports and a reactive couple M_0 develops at the base (Fig. 11-14b). From static equilibrium we know that the horizontal forces are equal in magnitude and opposite in direction and that

$$M_0 = RL$$

The bending moment in the buckled column, at distance x from the base, is

$$M = Pv - R(L - x)$$

By proceeding as in previous analyses, we arrive at the following differential equation:

$$v'' + k^2 v = \frac{R}{EI} (L - x) \quad (l)$$

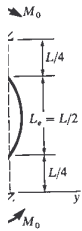
in which $k^2 = P/EI$.

The general solution of the differential equation is

$$v = C_1 \sin kx + C_2 \cos kx + \frac{R}{P} (L - x) \quad (m)$$

which has three unknown constants (C_1 , C_2 , and R). The three boundary conditions required are

$$v(0) = 0 \quad v'(0) = 0 \quad v(L) = 0$$



Length for a fixed against

11.4 Columns with Eccentric Axial Loads

11.4 COLUMNS WITH ECCENTRIC AXIAL LOADS

In the preceding sections we analyzed ideal columns for which the axial load P acted at the centroid of the cross section. In such cases the column remains straight until the critical load is reached. Now we will assume that the load is applied with a small eccentricity e from the axis of the column (Fig. 11-15a). As a consequence of the eccentricity, the load P produces bending of the column even when the load is small. Therefore, the column deflects from the onset of loading, and the deflection becomes steadily larger as P increases. In this situation, the allowable load for the column may be determined by the magnitude of the deflection or the bending stress, rather than by the critical load.

To analyze the column, we represent it by the idealized pinned-end column shown in Fig. 11-15b; that is, we assume that the xy plane is a plane of symmetry, the column is initially straight, and the material is linearly elastic. The bending moment in the column at distance x from the lower end is

$$M = P(e + v)$$

where v is the deflection measured from the axis of the column. The differential equation of the deflection curve is

$$EIv'' = -M = -P(e + v)$$

$$v'' + k^2 v = -k^2 e \quad (a)$$

in which $k^2 = P/EI$, as before. The general solution of this equation is the sum of the homogeneous solution and the particular solution, as follows:

$$v = C_1 \sin kx + C_2 \cos kx - e \quad (b)$$

in which C_1 and C_2 are constants in the homogeneous solution and $-e$ is the particular solution.

The boundary conditions from which we obtain C_1 and C_2 are obtained from the deflection v at the ends of the column:

$$v(0) = 0 \quad v(L) = 0$$

These conditions yield

$$C_2 = e \quad C_1 = \frac{e(1 - \cos kL)}{\sin kL} = e \tan \frac{kL}{2}$$

Therefore, the equation of the deflection curve is

$$v = e \left(\tan \frac{kL}{2} \sin kx + \cos kx - 1 \right) \quad (11-19)$$

For a column with a known load P and known eccentricity e , we can use this equation to calculate the deflection at any point. Thus, the

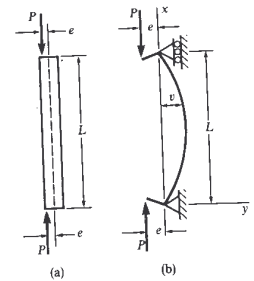


Fig. 11-15 Column with eccentric axial loads

Applying these conditions to Eq. (m) yields

$$C_2 + \frac{RL}{P} = 0 \quad C_1 k - \frac{R}{P} = 0 \quad C_1 \tan kL + C_2 = 0 \quad (n)$$

All three equations are satisfied if $C_1 = C_2 = R = 0$, in which case we have the trivial solution and the deflection is zero. To obtain the solution for buckling, we must solve the equations in a more general manner. One method of solution is to eliminate R from the first two equations, which yields

$$C_1 kL + C_2 = 0$$

or $C_2 = -C_1 kL$. Now we substitute this expression for C_2 into the third of Eqs. (n) and obtain the buckling equation:

$$kL = \tan kL \quad (o)$$

The solution of the buckling equation gives the critical load.

Since the buckling equation is a transcendental equation,* it cannot be solved explicitly. However, the value of kL can be determined by trial and error or by using a calculator that has a program for finding roots of equations. The smallest nonzero value of kL that satisfies Eq. (o) is

$$kL = 4.4934 \quad (p)$$

The corresponding critical load is

$$P_{cr} = \frac{20.19EI}{L^2} = \frac{2.046\pi^2 EI}{L^2} \quad (11-17)$$

which is between the values of the critical loads for columns with pinned ends and fixed ends (see Eqs. 11-7 and 11-16). The effective length for the column is obtained by comparing Eqs. (11-17) and (11-13); thus, we find

$$L_e = 0.699L \approx 0.7L \quad (q)$$

This length represents the distance from the pinned end of the column to the point of inflection in the buckled shape (Fig. 11-14c).

The equation of the buckled mode shape is obtained by substituting $C_2 = -C_1 kL$ and $R/P = kC_1$ into the general solution (Eq. m):

$$v = C_1 [\sin kx - kL \cos kx + k(L - x)] \quad (11-18)$$

in which $k = 4.4934/L$. The term in brackets gives the mode shape for the deflection of the buckled column, but the amplitude of the deflection is undefined because C_1 may have any value (with the limitation that v must remain small).

* A transcendental function cannot be expressed by a finite number of algebraic operations; hence, trigonometric, logarithmic, exponential, and other such functions are transcendental.

condition of the column is quite different from what we encountered when discussing critical loads; in those cases, the magnitude of the deflection either is zero or is undefined, because at the critical load the column is in neutral equilibrium. Now, however, each value of the load P produces a definite value of the deflection. Of course, our results are still limited to small deflections.

The maximum deflection δ occurs at the midpoint of the column and is obtained by setting x equal to $L/2$ in Eq. (11-19);

$$\delta = v_{\max} = v\left(\frac{L}{2}\right) = e\left(\sec \frac{kL}{2} - 1\right) \quad (11-20)$$

As special cases, note that we get $\delta = 0$ if $e = 0$ or if $P = 0$.

A load-deflection diagram for the column can be plotted from Eq. (11-20). We select a particular value e_1 of the eccentricity and then calculate corresponding values of P and δ . The resulting diagram is shown in Fig. 11-16 by the curve labeled $e = e_1$. We note immediately that the deflection δ increases as P increases, but the relationship is nonlinear. Hence, we cannot use the principle of superposition for calculating deflections due to more than one load. However, the deflection δ is linear with e , so the curve for $e = e_2$ has the same shape as the curve for e_1 but the abscissas are increased in the ratio e_2/e_1 .

ram
rads

As the load P approaches the critical load ($P_{cr} = \pi^2 EI/L^2$), the value of kL approaches π and the secant term in Eq. (11-20) approaches infinity. Therefore, the deflection δ increases without limit as the load approaches P_{cr} . Hence, the horizontal line corresponding to $P = P_{cr}$ in Fig. 11-16 is an asymptote for the curves. In the limit, as e becomes smaller and approaches zero, the curve on the diagram approaches two straight lines, one vertical and one horizontal. Thus, an ideal column with a centrally applied load is the limiting case of a column with an eccentric load. The curves plotted in Fig. 11-16 are mathematically correct, but again we must recall that the differential equation is valid only for small deflections. Hence, for large values of δ , the curves must be modified to take into account either the presence of large deflections or inelastic bending effects (see Fig. 11-8).

The reason for the nonlinear relationship between load and deflection, even when the deflections are small and Hooke's law holds, can be understood if we observe that the axial loads P (Fig. 11-15b) are equivalent to centrally applied loads P plus couples Pe acting at the ends. The couples Pe , if acting alone, would produce bending deflections of the column in the same manner as for a beam. In a beam, the presence of the deflections does not change the action of the loads, and the bending moments are the same whether the deflections exist or not. However, when an axial load acts on the member, the presence of the deflections increases the bending moments produced by the axial forces (because of the additional moments Pe). When the moments are increased, the deflections are further increased, hence the moments increase even more, and so on. Thus, the bending moments depend upon the deflections,

columns

of two kinds: first, the uniformly distributed normal stresses produced by the axial load, and second, the normal stresses produced by the bending moment. Because the material of the column is assumed to follow Hooke's law, the stresses due to the bending moment vary linearly across the section and can be obtained from the flexure formula. Thus, the maximum compressive stress in the column (on the concave side) is

$$\sigma_{\max} = \frac{P}{A} + \frac{M_{\max}}{S} \quad (a)$$

where A is the cross-sectional area and S is the section modulus. Note that for a column we assume compressive stresses to be positive. Substitution of the expression for M_{\max} (see Eq. 11-21) yields

$$\sigma_{\max} = \frac{P}{A} + \frac{Pe}{S} \sec \frac{kL}{2} \quad (b)$$

We can put this equation in a more useful form by making three substitutions. First, the section modulus S is replaced by I/c , where c is the distance from the centroidal axis to the extreme fiber on the concave side of the column. Second, we introduce the notation

$$r = \sqrt{\frac{I}{A}} \quad (11-22)$$

for the **radius of gyration** of the cross section in the plane of bending. Third, we replace k by $\sqrt{P/EI}$. With these substitutions, Eq. (b) becomes

$$\sigma_{\max} = \frac{P}{A} \left[1 + \frac{ec}{r^2} \sec \left(\frac{L}{2r} \sqrt{\frac{P}{EA}} \right) \right] \quad (11-23)$$

This equation is known as the **secant formula** for an eccentrically loaded column. It gives the maximum compressive stress in the column as a function of the average compressive stress P/A and two nondimensional ratios, called the **eccentricity ratio** and the **slenderness ratio**:

$$\text{Eccentricity ratio} = \frac{ec}{r^2} \quad (11-24)$$

$$\text{Slenderness ratio} = \frac{L}{r} \quad (11-25)$$

The first of these ratios is a measure of the eccentricity of the load as compared to properties of the cross section, and the second represents the extent to which the column is long and slender. A slenderness ratio of 200 is extremely large for a column.

exists in a nonlinear relationship between the axial loads and the deflections.

When the axial load P is very small compared to the critical load, the load-deflection relationship can be approximated by a straight line near the origin (Fig. 11-16). The curves have a steep slope near the origin, but the slope is finite. To determine the equation of the initial part of the curves, we use the series expansion for the secant function:

$$\sec t = 1 + \frac{t^2}{2!} + \frac{5t^4}{4!} + \dots$$

In the present case, the quantity $kL/2$ corresponds to t (see Eq. 11-20). When the axial load is very small compared to the critical load (and hence kL is very small), we can disregard the higher-power terms in the series and use only the first two terms:

$$\sec \frac{kL}{2} = 1 + \frac{k^2 L^2}{8}$$

Substitution of this expression into Eq. (11-20) yields

$$\delta = \frac{k^2 L^2 e}{8} = \frac{PeL^2}{8EI} \quad (c)$$

This equation gives the deflection at the middle of a simple beam loaded by couples Pe at the ends (see Case 10, Table G-2, Appendix G). It also gives the slope of the load-deflection curves at the origin:

$$\text{Slope at origin} = \frac{P}{\delta} = \frac{8EI}{eL^2} \quad (d)$$

If $e = 0$, the slope becomes infinite, as expected.

The maximum bending moment in the eccentrically loaded column (Fig. 11-15b) occurs at the midpoint where the deflection is a maximum; it is given by the equation

$$M_{\max} = P(e + \delta) = Pe \sec \frac{kL}{2} \quad (11-21)$$

The manner in which M_{\max} varies as a function of the axial load P is shown in Fig. 11-17. When P is small, the maximum moment is equal to Pe , which means that the effect of the deflections is negligible. As P increases, the bending moment grows nonlinearly and theoretically becomes very large as P approaches the critical load. However, as explained before, our equations are not valid when the deflections become large and other effects become important.

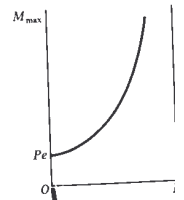


Fig. 11-17 Graph of maximum bending moment for a column subjected to eccentric axial loads (Fig. 11-15).

11.5 SECANT FORMULA

In the preceding section we analyzed a column subjected to eccentric axial loads P (Fig. 11-15), and we determined the maximum bending moment in the column as a function of the axial load P .

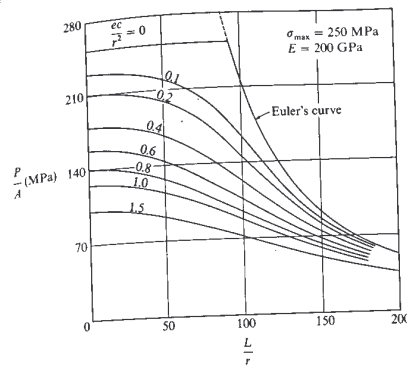


Fig. 11-18 Graph of the secant formula (Eq. 11-23) for $\sigma_{\max} = 250$ MPa and $E = 200$ GPa.

The secant formula relates the maximum stress in the column to the average stress P/A . If we set a limit on the maximum stress (for example, we might set σ_{\max} equal to the yield stress σ_y), then we can calculate the corresponding value of P from the secant formula. Because the equation is transcendental, we must solve it by trial and error. To assist in using the formula, we can plot graphs such as the one shown in Fig. 11-18. This graph is plotted for a maximum stress $\sigma_{\max} = 250$ MPa and for steel with modulus of elasticity $E = 200$ GPa. The abscissa is the slenderness ratio L/r , and the ordinate is the average compressive stress P/A . Curves are plotted for several values of the eccentricity ratio ec/r^2 . Of course, the secant formula is valid only when the maximum stress is less than (or, at most, equal to) the proportional limit of the material, because the formula was derived using Hooke's law.

When the eccentricity e is zero, the secant formula no longer applies. Instead, we have an ideal column with a centrally applied load; hence, the maximum load is the critical load ($P_{cr} = \pi^2 EI/L^2$), and the corresponding critical stress is

$$\sigma_{cr} = \frac{P_{cr}}{A} = \frac{\pi^2 EI}{AL^2} = \frac{\pi^2 E}{(L/r)^2} \quad (11-26)$$

This equation shows that the critical stress is inversely proportional to the square of the slenderness ratio. Equation (11-26) is valid as long as σ_{cr} does not exceed the proportional limit of the material.

Since Eq. (11-26) relates the average stress P/A to the slenderness ratio L/r , we can also plot it on the graph shown in Fig. 11-18. The corresponding curve is labeled **Euler's curve** to distinguish it from the plots

of the secant formula.* However, the curves from the secant formula approach Euler's curve as e approaches zero. As already mentioned Euler's curve is valid only if the stress P/A is less than the proportional limit. In the present case, we are assuming that the maximum stress is 250 MPa and that this value does not exceed the proportional limit. Thus we construct a horizontal line on the graph at this value of stress; the horizontal line and Euler's curve represent the limits of the secant formula curves as the eccentricity e approaches zero.

Both the secant formula (Eq. 11-23) and the equation for the critical stress (Eq. 11-26) may be used with columns having other end conditions by replacing the length L by the effective length L_e (described in Section 11.3).

We see from Fig. 11-18 that the load-carrying capacity of a column decreases significantly as the slenderness ratio L/r increases, especially in the middle region of L/r values. Thus, long, slender columns are much less stable than short, stocky columns. The graph also shows that the load-carrying capacity decreases with increasing eccentricity, and this effect is relatively greater for short columns than for long ones.

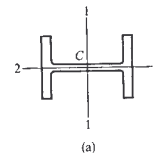
The load P in the secant formula is the load that produces the maximum stress σ_{max} under ideal, linearly elastic conditions. In design, we usually assign to σ_{max} a limiting stress value, such as the yield stress σ_y . Then the corresponding value of P is the axial load that will produce that maximum stress. The allowable load P_{allow} is obtained by dividing P by a factor of safety n . Although the secant formula gives an excellent theoretical description of column behaviour, difficulties arise when using it in practical design because the eccentricity e of the load may not be known accurately.

Now let us consider an actual column, which inevitably differs from an ideal column because of imperfections such as initial curvature of the axis, imperfect support conditions, and nonhomogeneity of the material. Furthermore, even when the load is supposed to be a centrally applied load, unavoidable eccentricities in its point of application and direction will exist. The extent of these imperfections and eccentricities varies from one column to another and produces scatter in the results of column tests. Of course, all of these imperfections have the effect of subjecting the column to bending in addition to direct compression. Hence, actual columns with centrally applied loads depart from the idealized behaviour described in Sections 11.2 and 11.3. It is reasonable to assume that the behaviour of an imperfect, centrally loaded column is similar to that of an ideal, eccentrically loaded column. Hence, it is reasonable to use the secant formula for the design of supposedly straight, centrally loaded columns by choosing an appropriate value of the eccentricity ratio ec/r^2 to account for the effects of all imperfections. However, the value of

* Euler's curve is not a common geometric shape. It is sometimes mistakenly called a hyperbola, but hyperbolas are plots of polynomial equations of the second degree in two variables whereas Euler's curve is a plot of an equation of the third degree in two variables.

ec/r^2 must be based upon test results because there is no theoretical way to know what the imperfections are. For instance, a commonly used value of the eccentricity ratio for pinned-end columns in structural-steel design is $ec/r^2 = 0.25$. The use of the secant formula in this manner for columns with centrally applied loads provides a rational means of accounting for the effects of imperfections, rather than allowing for them simply by increasing the factor of safety.

The method for analyzing a column with a centrally applied load by means of the secant formula can be summarized as follows. Assume a value of the eccentricity ratio ec/r^2 based upon test results and other experience. Substitute this value into the secant formula, along with the values of L/r , A , and E . Assign a value to σ_{max} representing the yield stress of the material (or use the proportional limit). Then solve the secant formula for the load P_y that produces the stress σ_y in the column. This load is always less than the critical load P_{cr} for the column. The allowable load on the column equals the load P_y divided by a factor of safety n . A reasonable value for n is 2.



Example

A steel wide-flange column of 254 × 254 × 167 kg UC section (Fig. 11-19) with pinned ends is 8 m long. It supports a centrally applied load $P_1 = 1400$ kN and an eccentrically applied load $P_2 = 180$ kN; the eccentric load acts on axis 2-2 at a distance of 340 mm from the centroid (Fig. 11-19b). Buckling occurs in plane 2-2. (a) Using the secant formula, calculate the maximum compressive stress in the column. (b) If the yield stress for the steel is $\sigma_y = 290$ MPa, what is the factor of safety with respect to initial yielding of the steel?

(a) The two loads P_1 and P_2 acting as shown in Fig. 11-19b are statically equivalent to a single load $P = 1580$ kN acting with an eccentricity $e = 38.7$ mm (Fig. 11-19c). Using the properties of the UC section from Appendix E, we find

$$\frac{P}{A} = \frac{1580 \text{ kN}}{212.4 \text{ cm}^2} = 74.4 \text{ MPa} \quad \frac{L}{r} = \frac{8 \text{ m}}{11.9 \text{ cm}} = 67.2$$

$$\frac{ec}{r^2} = \frac{eA}{S} = \frac{(38.7 \text{ mm})(212.4 \text{ cm}^2)}{2070 \text{ cm}^3} = 0.3971$$

Substituting these values into the secant formula, and also using $E = 200$ GPa, we get

$$\sigma_{max} = \frac{P}{A} \left[1 + \frac{ec}{r^2} \sec \left(\frac{L}{2r} \sqrt{\frac{P}{EA}} \right) \right] = 111.5 \text{ MPa}$$

Thus, this stress is the largest compressive stress in the column.

(b) We now wish to determine the load P that will bring the maximum stress up to yield stress $\sigma_y = 290$ MPa. Since this value of the load is just sufficient to produce initial yielding of the material, we will denote it as P_y . Note that we cannot determine P_y by multiplying P by the ratio σ_y/σ_{max} ; the reason, of course, is that we are dealing with a nonlinear relationship between load and

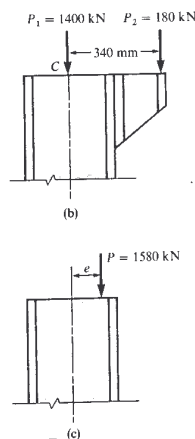


Fig. 11-19 Example. Use of the secant formula for a column with eccentric axial loads

stress. Instead, we substitute $\sigma_{max} = \sigma_y = 290$ MPa into the secant formula and then solve by trial and error for the corresponding load P_y . Thus, we have to find the value of P_y that satisfies the following equation:

$$290 \text{ MPa} = \frac{P_y}{212.4 \text{ cm}^2} \left[1 + 0.3971 \sec \left(33.6 \sqrt{\frac{P_y}{(200 \text{ GPa})(212.4 \text{ cm}^2)}} \right) \right]$$

or

$$6.16 \times 10^6 = P_y [1 + 0.3971 \sec(0.000516 \sqrt{P_y})]$$

in which P_y has units of Newtons. The result is

$$P_y = 3600 \text{ kN}$$

Since the actual load P is 360 k, we obtain

$$n = \frac{P_y}{P} = \frac{3600 \text{ kN}}{1580 \text{ kN}} = 2.28$$

as the factor of safety with respect to yielding of the column.

***11.6 IMPERFECTIONS IN COLUMNS**

In the discussion at the end of the preceding section, we described how to account for the effects of imperfections in the construction of the column and eccentricities in the line of application of the load by using the secant formula with an assumed value of the eccentricity ratio. Another approach to the problem is to assume that the inaccuracies are equivalent to an initial deflection, or crookedness, of the column. For a column with pinned ends, we may assume that the initial deflection v_0 of the column is a half-wave of a sine curve with maximum deflection equal to a (Fig. 11-20a):

$$v_0 = a \sin \frac{\pi x}{L} \tag{a}$$

This equation gives an initial shape that is a good approximation of any actual shape that a bent member may have. The bending moment in the column when the axial load P is applied centrally (Fig. 11-20b) then becomes

$$M = P(v_0 + v)$$

where v is the additional deflection of the column due to bending. This expression for M can be substituted into the differential equation of the deflection curve, which then can be solved in the manner described previously. The resulting expression for the deflection at the middle of the column is

$$\delta_{max} = a + v_{max} = \frac{a}{1 - \alpha} \tag{11-27}$$

where α is the ratio of the axial load P to the critical load for the column:

$$\alpha = \frac{P}{P_{cr}} = \frac{PL^2}{\pi^2 EI} \tag{11-28}$$

Equation (11-27) shows that the axial load causes the initial deflection of the column to increase by the factor $1/(1 - \alpha)$. Because $\alpha < 1$, this factor is always greater than unity. Note that when $\alpha = 0$ the maximum deflection is a , and when $\alpha = 1$ the maximum deflection becomes infinitely large, as expected.

The maximum bending moment in the column is

$$M_{max} = P\delta_{max} = \frac{Pa}{1 - \alpha} \tag{b}$$

and the maximum compressive stress is

$$\sigma_{max} = \frac{P}{A} + \frac{M_{max}c}{I} = \frac{P}{A} \left[1 + \frac{ac}{r^2(1 - \alpha)} \right]$$

in which $r^2 = I/A$. Substituting for α from Eq. (11-28), we get

$$\sigma_{max} = \frac{P}{A} \left[1 + \frac{ac}{r^2} \frac{1}{1 - \frac{PL^2}{\pi^2 EI} \left(\frac{L}{r} \right)^2} \right] \tag{11-29}$$

in which ac/r^2 is the **imperfection ratio**. If we now proceed as with the secant formula (Section 11.5) and set a limit on the maximum stress σ_{max} , we can calculate from Eq. (11-29) the corresponding value of P/A for any given ratio ac/r^2 .

Equation (11-29) can be represented graphically in a manner similar to that for the secant formula. The graph of Eq. (11-29) is almost identical to that for the secant formula (Fig. 11-18) except that the term ac/r^2 replaces the eccentricity ratio ec/r^2 . When $L/r = 0$, both formulas give the same value of P/A . When $L/r > 0$, the curves obtained from Eq. (11-29) are always slightly above those for the secant formula. In addition, they are always below Euler's curve (except in the limiting case when $a = 0$).

For purposes of calculation, Eq. (11-29) can be rewritten as a quadratic equation with P/A as the unknown:

$$b_1 \left(\frac{P}{A} \right)^2 - b_2 \left(\frac{P}{A} \right) + \sigma_{max} = 0 \tag{11-30}$$

in which

$$b_1 = \frac{1}{\pi^2 E} \left(\frac{L}{r} \right)^2 \quad b_2 = 1 + \frac{ac}{r^2} + \frac{\sigma_{max}}{\pi^2 E} \left(\frac{L}{r} \right)^2$$

Thus, if σ_{max} is given, we can solve Eq. (11-30) for P/A . (Use the smaller of the two values obtained from the quadratic formula.) If P/A is given,

we can solve Eq. (11-29) for σ_{max} . Of course, P must be less than the critical load P_{cr} . Also, Eqs. (11-29) and (11-30) are valid only for linear elastic behaviour of the material.

The initial deflection a for columns is usually in the range $L/1000$ to $L/400$. If a can be estimated, then ac/r^2 can be calculated and we can use Eq. (11-29) to obtain the maximum stress σ_{max} for any given load P . Conversely, if the maximum stress is given, we can solve by trial and error for the corresponding load P . (For further discussions of the effects of imperfections, see Refs. 11-1, 11-2, 11-8, and 11-12.)

11.7 ELASTIC AND INELASTIC COLUMN BEHAVIOUR

In the preceding sections we discussed the behaviour of columns when the material follows Hooke's law. We began by considering an ideal column subjected to a centrally applied load, and we arrived at the concept of a critical load P_{cr} . The behaviour of an ideal column is represented by Euler's curve on a diagram of average compressive stress P/A versus slenderness ratio L/r (Fig. 11-21). This curve is valid only in the region CD below the proportional limit σ_{pl} of the material. The value of slenderness ratio above which the Euler curve applies is obtained by setting σ_{cr} equal to σ_{pl} in Eq. (11-26) and solving for L/r ; thus, letting $(L/r)_c$ represent the critical value of slenderness ratio, we get

$$\left(\frac{L}{r}\right)_c = \sqrt{\frac{\pi^2 E}{\sigma_{pl}}} \tag{11-31}$$

As an example, consider steel with $\sigma_{pl} = 250$ MPa and $E = 200$ GPa; then $(L/r)_c = 88.9$.

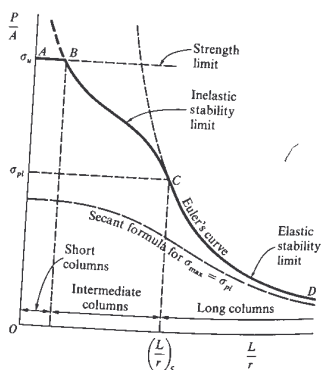


Diagram of average compressive stress P/A versus slenderness ratio L/r .

If we take into account the effects of eccentricities in loading or imperfections in the column, and still assume that the material follows Hooke's law, then we obtain a curve such as the one labeled **secant formula** in Fig. 11-21. This curve is plotted for a maximum stress equal to the proportional limit σ_{pl} . Thus, when comparing the curve for the secant formula with Euler's curve, we must keep in mind the distinctions between them. In the case of Euler's curve, the stress P/A not only is proportional to the applied load P but also is the maximum stress in the column when buckling occurs. Hence, as we move from C to D , both the load P and the maximum stress are decreasing in the same proportions. However, for the secant formula, the load P decreases as we move from left to right along the curve, but the maximum stress does not change.

From Euler's curve, we see that columns with large slenderness ratios buckle at low values of the average compressive stress P/A . This condition cannot be improved by using a higher-strength material, because collapse is by instability of the column as a whole and not by failure of the material itself. The critical stress can be raised by reducing L/r or by using a material with higher modulus of elasticity E .

When a compression member is very short, it fails by yielding or crushing of the material; hence, there are no buckling or stability considerations. In such a case, we can define a maximum compressive stress σ_s as the failure stress for the material. This stress establishes a **strength limit** for the column, represented by the horizontal line AB in the figure. This stress is much higher than the proportional limit, since it represents the ultimate stress in compression.

Between the regions of short and long columns, there is a range of intermediate slenderness ratios too small for elastic stability to govern and too large for strength considerations alone to govern. Such an intermediate-length column fails by **inelastic buckling**. Instability of the column occurs, but the maximum stresses exceed the proportional limit. The slope of the stress-strain curve diminishes after the proportional limit is passed; hence, the critical load for inelastic buckling is less than the Euler load, as explained in the next section. The dividing lines between short, intermediate, and long columns are not precise; nevertheless, it is useful to distinguish between these three types of column behavior. The curve $ABCD$ in Fig. 11-21 represents the maximum load-carrying capacity of a typical column. The diagram applies to columns with any end conditions if the length L is replaced by the effective length L_e .

Tests of columns show reasonably good agreement with curve $ABCD$. When the test results are plotted on the diagram, they generally form a band that lies just below curve $ABCD$. Considerable scatter of test results is to be expected with columns, because they are sensitive to the accuracy of the construction, alignment of loads, and support conditions. To account for this variability, we obtain the allowable stress for a column by dividing the maximum stress (curve $ABCD$) by a suitable **factor of safety**, often having a value of about 2. Because imperfections are apt to increase as a column becomes longer, a variable factor of safety

(increasing as L/r increases) is sometimes used. In Section 11.9 we will give some typical formulas for allowable stresses.

*11.8 INELASTIC BUCKLING

The critical load (or Euler load) for elastic buckling is valid only for long columns, as discussed in the preceding section. For ideal columns of intermediate lengths, the stress in the column exceeds the proportional limit before buckling begins (Fig. 11-21). Hence, we need a theory of **inelastic buckling** for calculating critical loads in this range of slenderness ratios.

Let us again consider an ideal pinned-end column subjected to an axial force P (Fig. 11-22a). The column has a slenderness ratio L/r that is less than $(L/r)_c$, hence the axial stress P/A reaches the proportional limit before the elastic critical load is reached (see Fig. 11-21). The compression stress-strain diagram for the material of the column is shown in Fig. 11-23. Let us assume that the stress σ_0 in the column is above the proportional limit, so that we are at a point such as A on the stress-strain diagram. Then, if a small increase in stress is produced, the relationship between the increment of stress and the corresponding increment of strain is given by the slope of the tangent line at A . This slope, equal to the slope of the tangent line at A , is called the **tangent modulus** and is denoted by E_t ; thus,

$$E_t = \frac{d\sigma}{d\epsilon} \tag{11-32}$$

The tangent modulus is a variable property of the material that decreases as the stress increases beyond the proportional limit. When the stress is below the proportional limit, E_t is the same as the elastic modulus E .

According to the **tangent-modulus theory** of inelastic buckling, the column shown in Fig. 11-22a remains straight until the critical load is reached. At that value of load, the column may undergo a small lateral deflection (Fig. 11-22b). The resulting bending stresses are superimposed upon the axial compressive stresses σ_0 . Since the column starts bending from the straight position, the bending stresses initially represent only a small increment of stress. Therefore, the relationship between the bending stresses and strains is given by the tangent modulus E_t . Since the strains vary linearly across the section, the initial bending stresses also vary linearly and the expressions for curvature are the same as for elastic bending except that E_t replaces E :

$$\kappa = \frac{1}{\rho} = \frac{d^2v}{dx^2} = -\frac{M}{E_t I} \tag{11-33}$$

Because the bending moment $M = Pv$, the differential equation of the deflection curve is

$$E_t I v'' + Pv = 0 \tag{11-34}$$

This equation has the same form as the equation for elastic buckling (see Eq. 11-3) except that E_t appears in place of E . Therefore, we can solve the equation in the same manner as before and obtain the following equation for the **tangent-modulus load**:

$$P_t = \frac{\pi^2 E_t I}{L^2} \tag{11-35}$$

This load represents the critical load for the column according to the tangent-modulus theory. The corresponding critical stress is

$$\sigma_t = \frac{\pi^2 E_t}{(L/r)^2} \tag{11-36}$$

which is similar in form to Eq. (11-26).

Inasmuch as the tangent modulus E_t varies with the compressive stress $\sigma = P/A$ (Fig. 11-23), we usually must find P_t by an iterative procedure. We begin by estimating the value of P_t ; this trial value P_1 should be slightly larger than $\sigma_{pl} A$, which is the load when the stress reaches the proportional limit. Knowing P_1 , we can calculate the corresponding proportional limit. Knowing P_1 , we can calculate the corresponding axial stress $\sigma_1 = P_1/A$ and determine the tangent modulus E_t from the stress-strain diagram. Next, we use Eq. (11-35) to obtain a second estimate of P_t . Let us call this value P_2 . If P_2 is close enough to P_1 , then we may take the load P_2 as the tangent-modulus load P_t . However, it is more likely that additional cycles of iteration will be required until we reach a calculated load that is in close agreement with the trial load. In this manner, we arrive at a value for the tangent-modulus load.

A diagram showing how the critical stress σ_t , calculated from the tangent-modulus load, varies with the slenderness ratio is given in Fig. 11-24 for a typical metal column. The tangent-modulus formulas may be used for columns with other support conditions by using the effective length L_e for L .

The tangent-modulus theory is distinguished by its simplicity and ease of use. However, it is conceptually deficient in that it does not

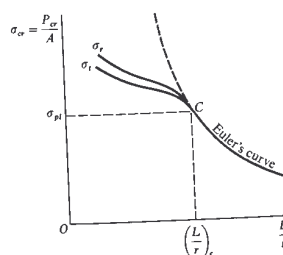
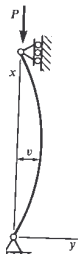


Fig. 11-24 Diagram of critical stress versus slenderness ratio



(b) In that



E

epsilon diagram

account for the complete behavior of the column, as follows. When the column shown in Fig. 11-22 first departs from the straight position, the fibers on the concave side are subjected to compressive bending stresses, and the fibers on the convex side are subjected to tensile bending stresses. These stresses are superimposed on the pre-existing large compressive stresses $\sigma_a = P/A$ at point A on the stress-strain diagram (Fig. 11-23). Hence, the fibers on the concave side have their compressive stresses increased, and the fibers on the convex side have their compressive stresses decreased. When the stress at point A is increased, the stress-strain relation is given by the tangent modulus E_t . However, when the stress is decreased, the material follows the unloading line AB on the stress-strain diagram. This line is parallel to the initial linear part of the diagram, and its slope is equal to the elastic modulus E . Thus, during the initial bending, the column behaves as if it were made of two different materials, a material of modulus E_t on the concave side and a material of modulus E on the convex side. A bending analysis of such a column can be made using the theory for a beam of two materials (see Section 5.10). The results of such analyses show that the column bends as though it had a modulus of elasticity intermediate between the values of E and E_t . This effective modulus is known as the **reduced modulus E_r** , and its value depends not only upon the magnitude of the stress (because E_t depends upon the magnitude of the stress) but also upon the shape of the column cross section. Thus, E_r is more difficult to determine than E_t . Hence, we shall not derive formulas for E_r here but, instead, will give one result as an example. If a column has a **rectangular cross section**, the equation for the reduced modulus is

$$E_r = \frac{4EE_t}{(\sqrt{E} + \sqrt{E_t})^2} \quad (11-37)$$

Further discussion of the reduced modulus, which is also known as the *double modulus*, is given in Refs. 11-1, 11-2, and 11-10.

Since the reduced modulus represents an effective modulus that governs the bending of the column when it first departs from the straight position, we can formulate a **reduced-modulus theory** of inelastic buckling. Proceeding in the same manner as for the tangent-modulus theory, we can write an equation for the curvature and then we can write the differential equation of the deflection curve. These equations are the same as Eqs. (11-33) and (11-34) except that E_t appears instead of E_r . Thus, we arrive at the following equation for the reduced-modulus load:

$$P_r = \frac{\pi^2 E_r I}{L^2} \quad (11-38)$$

The corresponding equation for the critical stress is

$$\sigma_r = \frac{\pi^2 E_r}{(L/r)^2} \quad (11-39)$$

the load increases but doesn't reach the reduced-modulus load until the deflection becomes infinite. However, other effects become important as the deflection increases, and in reality the curve eventually goes downward as shown by the dashed line.

The Shanley concept of inelastic buckling has been verified by numerous investigators and by many tests. However, the maximum load attained in real columns (see the dashed curve in Fig. 11-25) is only slightly above the tangent-modulus load P_t . Fortunately, the tangent-modulus load is very simple to calculate, and for all practical purposes it is reasonable to adopt the tangent-modulus load as the critical load for inelastic buckling of a column.

The preceding discussions of elastic and inelastic buckling are based upon idealized conditions. The theoretical concepts are important in understanding column behavior, but the design of actual columns must take into account additional factors not considered in the theory. For instance, steel columns always contain residual stresses from the rolling process. Because of these stresses, which vary greatly in different parts of the cross section, the stress level required to produce yielding also varies over the cross section. For such reasons a variety of empirical design formulas are used for designing columns. Some of the most commonly used formulas are given in the next section.

Historical note. The critical-load formulas for elastic buckling originated with Euler in 1744, as explained in the note to Ref. 11-3. Very little additional progress was made for a hundred years. Then, in 1845, A. H. E. Lamarle pointed out that Euler's formula should be used only for slenderness ratios beyond a certain limit and that experimental data should be relied upon for smaller ratios (Ref. 11-13). In 1889, the French engineer A. Considère performed a series of 32 tests on columns (Ref. 11-14). He observed that the stresses on the concave side of the column increased with E_t and the stresses on the convex side decreased with E . Thus, he showed why the Euler formula was not applicable to inelastic buckling, and he stated that the effective modulus was between E and E_t . Although he made no attempt to evaluate the effective modulus, he is responsible for beginning the reduced-modulus theory. In the same year, and quite independently, the German engineer F. Engesser suggested the tangent-modulus theory (Ref. 11-15). He denoted the tangent modulus by the symbol T (equal to $d\sigma/de$) and proposed that T be substituted for E in Euler's formula for the critical load. Later, in March 1895, Engesser again presented the tangent-modulus theory (Ref. 11-16). Obviously without knowledge of Considère's work. Three months later, Polish-born F. Jasinsky, then a professor in St. Petersburg, pointed out that Engesser's tangent-modulus theory was incorrect, called attention to Considère's work, and presented the reduced-modulus theory (Ref. 11-17). He also stated that the reduced modulus could not be calculated theoretically. In response, and only one month later, Engesser acknowledged the error in the tangent-modulus approach and showed how to

find the reduced-modulus load P_r , we must use a trial-and-error procedure, because E_r depends upon E_t . The critical stress according to the reduced-modulus theory is also shown in Fig. 11-24. Note that the curve for σ_r is above that for σ_t , because E_r is always greater than E_t .

The reduced-modulus theory is difficult to use in practice because E_r depends upon the shape of the cross section as well as the stress-strain curve and must be evaluated for each particular column. (The only exception is a rectangular cross section, for which Eq. 11-37 is available.) Moreover, this theory also has a conceptual defect. In order for the reduced modulus E_r to apply, the fibers on the convex side of the column must be undergoing a reduction in stress. But such a reduction in stress cannot occur until bending takes place. Therefore, the load P_r , applied to an ideal straight column, can never reach the reduced-modulus load P_r to reach that load would require that bending already exists, which is a contradiction.

Thus, neither the tangent-modulus theory nor the reduced-modulus theory is adequate by itself to explain the phenomenon of inelastic buckling, although an understanding of both theories is necessary in order to develop a more complete and logically consistent theory. Such a theory was developed by F. R. Shanley (see the historical note that follows), and it is called the **Shanley theory of inelastic buckling**. This theory overcomes the difficulties with both the tangent-modulus and reduced-modulus theories by recognizing that it is not possible to have buckling of the Euler type when the column becomes inelastic. In Euler buckling, a critical load is reached at which the column is in neutral equilibrium, represented by a horizontal line on the load-deflection diagram (Fig. 11-25). As already explained, neither the tangent-modulus load P_t nor the reduced-modulus load P_r can represent this type of behavior; in both cases, we are led to contradictions if we try to associate these loads with a condition of neutral equilibrium. Instead, we must think of a column that has an ever-increasing axial load. When the load reaches P_t , bending can begin *provided the load continues to increase*. Under these conditions, bending occurs simultaneously with an increase in load, resulting in a decrease in strain on the convex side of the column. Thus, the effective modulus of the material throughout the cross section becomes greater than E_t , and therefore an increase in load is possible. However, the effective modulus is not as great as E_r , because E_r is based upon full strain reversal on the convex side of the column. In other words, E_r is based upon the amount of strain reversal that exists if the column bends without a change in the axial force, whereas the presence of an increasing axial force means that the reduction in strain is not as great. Thus, instead of neutral equilibrium, where the relationship between load and deflection is undefined, we now have a definite relationship between each value of the load and the corresponding deflection. This behavior is shown by the curve labeled *Shanley theory* in Fig. 11-25. Note that buckling begins at the tangent-modulus load; then

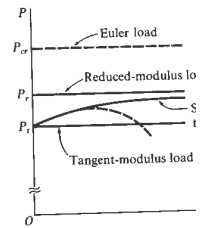


Fig. 11-25 Load-deflection d for elastic and inelastic buckling

obtain the reduced modulus for any cross section (Ref. 11-18). Thus, the tangent-modulus theory is sometimes called the *Engesser theory*, and the reduced-modulus theory is called the *Considère-Engesser theory*.

The reduced-modulus theory was also presented by the famous scientist Theodore von Kármán in 1908 and 1910 (Refs. 11-19 and 11-20), apparently independently of the earlier investigations. In the latter paper, he derived formulas for E_r for rectangular and idealized wide-flange sections (that is, sections without a web). He extended the theory to include the effects of eccentricities on the buckling load, and he showed that the maximum load decreases rapidly as the eccentricity increases. The English elastician R. V. Southwell also presented the reduced-modulus theory. In a paper in 1912 (Ref. 11-22), he derived the theory but used a modified length for the column instead of a reduced modulus for the material. His work appears to be independent of the others, although the basic concepts are the same. The reduced-modulus theory was the accepted theory of inelastic buckling until 1946, when the American aeronautical-engineering professor F. R. Shanley pointed out the logical paradoxes in both theories. In a remarkable one-page paper (Ref. 11-23), Shanley not only explained what was wrong with the generally accepted theories but also proposed his own theory that resolved the paradoxes. In a second paper, five months later, he gave further analyses to support his earlier theory and gave results from tests on columns (Ref. 11-24). Other investigators have confirmed and expanded Shanley's concept (Refs. 11-25 through 11-31). The background of the inelastic-buckling theories is described in Refs. 11-1, 11-2, and 11-8. For excellent discussions of the column-buckling problem, see the comprehensive papers by Hoff (Refs. 11-6 and 11-32); and for a historical account, see the paper by Johnston (Ref. 11-7).

11.9 COLUMN DESIGN FORMULAS

In the preceding sections we discussed the load-carrying capacity of columns based only upon theoretical considerations. The next step is to determine allowable loads on columns considering not only the theoretical results but also the behavior of real columns as observed in laboratory tests. A common procedure is to employ empirical design formulas that fit the test data in the inelastic range of column behavior (low values of slenderness ratio) and to use the Euler formula for the critical load in the elastic range (high values of slenderness ratio). A factor of safety must be applied to obtain allowable loads from the maximum loads (or allowable stresses from the maximum stresses). The use of empirical design formulas is quite satisfactory within the limits for which they were established, provided there is adequate experimental data. Thus, the following restrictions should be noted when using a column design formula: (1) The formula is valid only for a particular material. (2) The formula is valid only for a specified range of slenderness

ratios. (3) The formula may specify the allowable stress or it may specify the maximum stress; if the latter, a factor of safety must be applied to obtain the allowable stress.

The following examples of column design formulas are applicable to centrally loaded columns. However, many factors besides those discussed here enter into the design of columns, so other references should be consulted before designing a column for a specific application.

Column design using these formulas requires trial-and-error calculations. Knowing the axial compressive load, we begin by estimating the allowable stress σ_{allow} and calculating approximately the required cross-sectional area. Then a section is selected from tables of available sizes. This section is checked with the aid of the appropriate design formulas to see if it is adequate to support the load. If it is not, then a heavier section is selected and the process repeated; if it appears to be oversized, a lighter section is selected and checked.

Structural steel. For the design of centrally loaded, structural-steel columns, the Structural Stability Research Council (SSRC) proposed design formulas that are in common use in the United States.* The SSRC formulas give the maximum stress or critical stress in the column (that is, the stress obtained by dividing the assumed maximum load that the column can carry by the cross-sectional area).

When the slenderness ratio L/r is large, the maximum stress is based upon the Euler load:

$$\sigma_{max} = \frac{\pi^2 E}{(KL/r)^2} \quad (a)$$

where the effective length KL (see Eqs. 11-14 and 11-15) is used so that the formula may be applied to a variety of support conditions. Equation (a) is valid only when the stresses in the column do not exceed the proportional limit σ_{pl} , as discussed previously (see Fig. 11-21). For structural steel, we normally assume that the proportional limit is equal to the yield stress σ_y . However, rolled sections (such as wide-flange sections) have large residual stresses in them; the compressive residual stresses may be as large as one-half the yield stress. Hence, for such a column, the proportional limit is

$$\sigma_{pl} = \sigma_y - \sigma_{rc} = 0.5\sigma_y \quad (b)$$

where σ_{rc} represents the compressive residual stress in the column and is assumed to be equal to $0.5\sigma_y$.

To determine the smallest slenderness ratio for which Eq. (a) is applicable, we set σ_{max} equal to σ_{pl} (Eq. b) and solve for the corresponding

* The Structural Stability Research Council was founded in 1944 as the Column Research Council (CRC). It publishes the *Guide to Stability Design Criteria for Metal Structures* (Ref. 11-8).

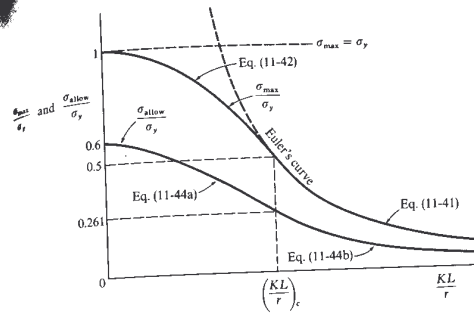


Fig. 11-26 Design formulas for structural-steel columns

value of KL/r , denoted by $(KL/r)_c$:

$$\left(\frac{KL}{r}\right)_c = \sqrt{\frac{2\pi^2 E}{\sigma_y}} \quad (11-40)$$

If the effective slenderness ratio is equal to or larger than $(KL/r)_c$, the Euler formula for the critical stress (Eq. a) may be used. This equation may be expressed in a convenient nondimensional form by dividing by the yield stress σ_y and also substituting from Eq. (11-40):

$$\frac{\sigma_{max}}{\sigma_y} = \frac{\pi^2 E}{\sigma_y \left(\frac{KL}{r}\right)^2} = \frac{\left(\frac{KL}{r}\right)_c^2}{2 \left(\frac{KL}{r}\right)^2} \quad \frac{KL}{r} \geq \left(\frac{KL}{r}\right)_c \quad (11-41)$$

This equation is plotted in Fig. 11-26 and labeled *Euler's curve*.

For the region of inelastic buckling, that is, the region where $KL/r \leq (KL/r)_c$, the maximum stress is given by a parabolic curve:

$$\frac{\sigma_{max}}{\sigma_y} = 1 - \frac{\left(\frac{KL}{r}\right)^2}{2 \left(\frac{KL}{r}\right)_c^2} \quad \frac{KL}{r} \leq \left(\frac{KL}{r}\right)_c \quad (11-42)$$

This empirical formula is also plotted in Fig. 11-26. The curve has a horizontal tangent at $KL/r = 0$, where the maximum stress is equal to σ_y . At $KL/r = (KL/r)_c$, the curve merges smoothly with Euler's curve (both curves have the same slope at the point where they meet).

The American Institute of Steel Construction (AISC), an organization that prepares specifications for structural steel design, has adopted the formulas for σ_{max} proposed by the SSRC. To obtain allowable

stresses, the AISC specifies that the maximum stresses be divided by the following factors of safety:

$$n_1 = \frac{5}{3} + \frac{3 \left(\frac{KL}{r}\right) - \left(\frac{KL}{r}\right)^3}{8 \left(\frac{KL}{r}\right)_c} \quad \frac{KL}{r} \leq \left(\frac{KL}{r}\right)_c \quad (11-43a)$$

$$n_2 = \frac{23}{12} \approx 1.92 \quad \frac{KL}{r} \geq \left(\frac{KL}{r}\right)_c \quad (11-43b)$$

Thus, the factor of safety is $5/3$ when $KL/r = 0$ and gradually increases to $23/12$ when $KL/r = (KL/r)_c$. For higher slenderness ratios, the factor of safety remains constant at that value. The AISC formulas for the allowable stresses are obtained by dividing the maximum stresses σ_{max} by the appropriate factors of safety; thus,

$$\frac{\sigma_{allow}}{\sigma_y} = \frac{1}{n_1} \left[1 - \frac{\left(\frac{KL}{r}\right)^2}{2 \left(\frac{KL}{r}\right)_c^2} \right] \quad \frac{KL}{r} \leq \left(\frac{KL}{r}\right)_c \quad (11-44a)$$

$$\frac{\sigma_{allow}}{\sigma_y} = \frac{\left(\frac{KL}{r}\right)_c^2}{2n_2 \left(\frac{KL}{r}\right)^2} \quad \frac{KL}{r} \geq \left(\frac{KL}{r}\right)_c \quad (11-44b)$$

These equations for the allowable stresses are also plotted in Fig. 11-26. They may be used with either USCS or SI units. The maximum value of KL/r permitted by the AISC specifications is 200; also, the modulus of elasticity E is specified as 200 GPa. Finally, we note that the AISC uses the symbols C_c for $(KL/r)_c$, F_a for σ_{allow} , and F_y for σ_y .

Aluminium. The design of aluminium columns is in accord with the specifications of the Aluminium Association (Ref. 5-6) and follows a pattern similar to that for structural steel columns. Euler's curve is used for large values of slenderness ratio. For smaller slenderness ratios, two straight lines, one horizontal and one inclined, are used (Fig. 11-27). The slenderness ratios that separate short, intermediate, and long columns are denoted by S_1 and S_2 . The formulas for the allowable stresses are as follows:

$$\sigma_{allow} = \frac{\sigma_y}{k_c n_y} \quad 0 \leq \frac{L}{r} \leq S_1 \quad (11-45a)$$

$$\sigma_{allow} = \frac{1}{n_u} (B_c - D_c \frac{L}{r}) \quad S_1 \leq \frac{L}{r} \leq S_2 \quad (11-45b)$$

$$\sigma_{allow} = \frac{\pi^2 E}{n_u \left(\frac{L}{r}\right)^2} \quad S_2 \leq \frac{L}{r} \quad (11-45c)$$

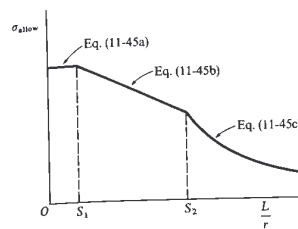


Fig. 11-27 Design formulas for aluminium columns

In these equations, the length L is defined as the distance between points of lateral support, or twice the length of a cantilever column. Thus, L may be interpreted as the effective length. The stress σ_y is the compressive yield stress (0.2% offset), k_c is a constant, n_y is the factor of safety with respect to the yield stress, n_u is the factor of safety with respect to the ultimate stress, and B_c , D_c , S_1 , and S_2 are constants. The values of these quantities vary according to the alloy, temper, and usage. Numerous aluminium alloys and tempers are available, so the Aluminium Association specifications give tables of the various constants according to the material. As examples, the following are some typical formulas for alloys used in buildings and similar structures.

1. Alloy 2014-T6

$$\sigma_{allow} = 193 \text{ MPa} \quad 0 \leq \frac{L}{r} \leq 12 \quad (11-46a)$$

$$\sigma_{allow} = 212 - 1.58 \left(\frac{L}{r}\right) \text{ MPa} \quad 12 \leq \frac{L}{r} \leq 55 \quad (11-46b)$$

$$\sigma_{allow} = \frac{372 \text{ GPa}}{\left(\frac{L}{r}\right)^2} \quad 55 \leq \frac{L}{r} \quad (11-46c)$$

2. Alloy 6061-T6

$$\sigma_{allow} = 131 \text{ MPa} \quad 0 \leq \frac{L}{r} \leq 9.5 \quad (11-47a)$$

$$\sigma_{allow} = 139 - 0.868 \left(\frac{L}{r}\right) \text{ MPa} \quad 9.5 \leq \frac{L}{r} \leq 66 \quad (11-47b)$$

$$\sigma_{allow} = \frac{350 \text{ GPa}}{\left(\frac{L}{r}\right)^2} \quad 66 \leq \frac{L}{r} \quad (11-47c)$$

These formulas give the allowable stresses, hence they incorporate the safety factors, which vary from 1.65 to 2.20.

Wood. The design of wood structural members is governed by the National Design Specification for Wood Construction, published by the National Forest Products Association (Ref. 5-8). The formulas for allowable stresses in rectangular wood columns for short, intermediate, and long columns are as follows:

$$\sigma_{\text{allow}} = F_c \quad 0 \leq \frac{L}{d} \leq 11 \quad (11-48a)$$

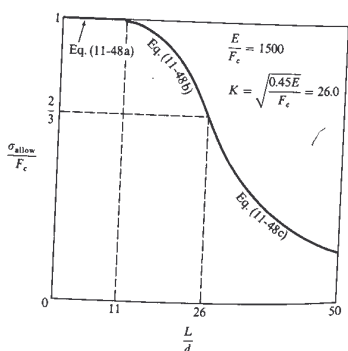
$$\sigma_{\text{allow}} = F_c \left[1 - \frac{1}{3} \left(\frac{L/d}{K} \right)^4 \right] \quad 11 < \frac{L}{d} \leq K \quad (11-48b)$$

$$\sigma_{\text{allow}} = \frac{0.3E}{(L/d)^2} = \frac{2F_c}{3} \left(\frac{K}{L/d} \right)^2 \quad K \leq \frac{L}{d} \leq 50 \quad (11-48c)$$

The stress F_c is the design value in compression parallel to the grain as modified for duration of loading and other service conditions; typical values of F_c for structural timber are in the range of 5 to 12.5 MPa. The slenderness ratio L/d is the effective length L of the column for buckling in a principal plane divided by the cross-sectional dimension d in that same plane. The factor K is the slenderness ratio that separates intermediate from long columns:

$$K = \sqrt{\frac{0.45E}{F_c}} \quad (11-49)$$

Values of K are usually in the range from 18 to 30. The modulus of elasticity E , like the compressive stress F_c , varies with species and grade, but typical values are in the range of 7 to 12.5 GPa. A graph of Eqs. (11-48a, b, and c) is shown in Fig. 11-28 for $E/F_c = 1500$. Equations (11-48) may be used with either SI or USCS units.



formulas for
unns with

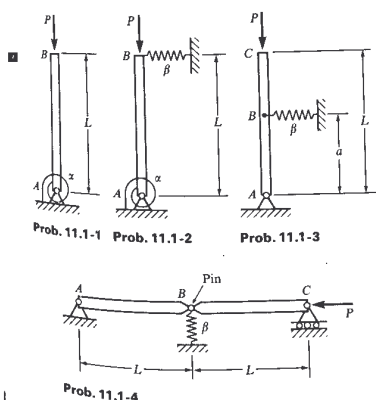
The column formulas for steel, aluminium, and wood given in this section are for use in solving problems, but they should not be used by inexperienced persons for the design of actual columns, because they represent only a small part of the complete design process for columns. All design formulas taken from specifications and building codes require informed judgment in their use. There are many cases of structures that "met the building code" but nevertheless collapsed or failed to perform adequately. In addition, codes specify many additional limitations that are not described here.

PROBLEMS/CHAPTER 11

The problems for Section 11.1 are to be solved using the assumptions that the bars are rigid, the springs are elastic, and the deflections and angles of rotation are small.

11.1-1 Determine the critical load P_{cr} for the bar-spring system shown in the figure. The bar is free at B and supported at A by a rotational spring of stiffness α ; that is, $M = \alpha\theta$ where M is the moment acting on the spring and θ is the angle of rotation.

11.1-2, 11.1-3, 11.1-4, and 11.1-5 Determine the critical load P_{cr} for the bar-spring system shown in the figure.



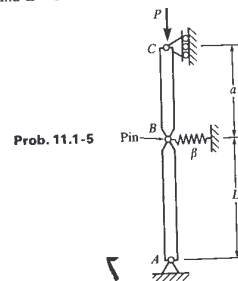
The problems for Section 11.2 are to be solved using the assumptions of ideal, slender, prismatic, elastic columns. Buckling occurs in the plane of the figure unless otherwise stated.

11.2-1 Calculate the critical load for a 254 x 254 107 kg UC steel column having length $L = 4$ m. $E = 200$ GPa. Assume that the column has pinned ends and may buckle in any direction.

11.2-2 Solve the preceding problem for a 305 x 305 158 kg UC steel column having length $L = 7$ m.

11.2-3 A pinned-end column must support an axial load $P = 1$ MN with a factor of safety $n = 2.5$ with respect to buckling. The column has length $L = 4$ m and n buckle in any direction. Select from Table E-2 in Appendix E the lightest steel UC section ($E = 200$ GPa) that support the load.

11.2-4 Solve the preceding problem for a column $P = 1.25$ MN and $L = 5$ m.



Columns

Problems 11.9 are to be solved assuming centrally applied axial loads at the ends of columns supported only at the ends in the direction.

11.9-1 Determine the allowable axial load P for a 203 x 203 mm UC steel column with pinned ends for each of the following lengths: 3 m, 6 m, 9 m, and 12 m. (Assume $E = 200$ GPa and $F_c = 250$ MPa.)

11.9-2 Determine the allowable axial load P for a 254 x 254 mm UC steel column with pinned ends for each of the following lengths: 3 m, 6 m, 9 m, and 12 m. (Assume $E = 200$ GPa and $F_c = 250$ MPa.)

11.9-3 Determine the allowable axial load P for a 203 x 203 mm UC steel column with pinned ends for each of the following lengths: 1 m, 2 m, 3 m, and 5 m. (Assume $E = 200$ GPa and $F_c = 250$ MPa.)

11.9-4 Determine the allowable axial load P for a 305 x 305 mm UC steel column with pinned ends for each of the following lengths: 3 m, 6 m, 9 m, and 12 m. (Assume $E = 200$ GPa and $F_c = 250$ MPa.)

11.9-5 Determine the allowable axial load P for a steel column with pinned ends having outside diameter 100 mm and inside diameter 75 mm for each of the following lengths: 10 m, and 12 m. (Assume $E = 200$ GPa and $F_c = 250$ MPa.)

11.9-6 Determine the allowable axial load P for a steel column with pinned ends having outside diameter 100 mm and inside diameter 75 mm for each of the following lengths: 8 m and 10 m. (Assume $E = 200$ GPa and $F_c = 250$ MPa.)

11.9-7 Determine the allowable axial load P for a steel column with pinned ends having outside diameter 100 mm and inside diameter 75 mm for each of the following lengths: 7 m for each of the following lengths: 10 m, and 12 m. (Assume $E = 200$ GPa and $F_c = 250$ MPa.)

11.9-8 Determine the allowable axial load P for a steel column with pinned ends having outside diameter 100 mm and inside diameter 75 mm for each of the following lengths: 5 m, 7.5 m, and 10 m. (Assume $E = 200$ GPa and $F_c = 250$ MPa.)

11.9-9 A column with pinned ends supports an axial load P . The pipe has outside and inside diameters of 70 mm, respectively. What is the longest permissible length L of the column if $E = 200$ GPa and $F_c = 250$ MPa?

11.9-10 A 43 kg UB column with pinned ends supports an axial load P . What is the longest permissible length L of the column if $E = 200$ GPa and $F_c = 250$ MPa?

What is the longest permissible length L of the column if $P = 225$ kN and if $P = 450$ kN? (Assume $E = 200$ GPa and $F_c = 250$ MPa.)

11.9-11 A 203 x 203 x 60 kg UC steel column with pinned ends carries an axial load P . What is the longest permissible length L of the column if $P = 330$ kN and if $P = 670$ kN? (Assume $E = 200$ GPa and $F_c = 250$ MPa.)

11.9-12 What is the minimum permissible diameter d of a solid steel column of circular cross section with pinned ends and length 2 m if it must support an axial load $P = 800$ kN? (Assume $E = 200$ GPa and $F_c = 250$ MPa.)

11.9-13 What is the minimum permissible width b of a solid steel column of square cross section with pinned ends and length $L = 1.5$ m if it must support an axial load $P = 250$ kN? (Assume $E = 200$ GPa and $F_c = 250$ MPa.)

11.9-14 Determine the allowable axial load P for an aluminium pipe column (alloy 2014-T6) with pinned ends for each of the following lengths: $L = 1$ m, 2 m, 3 m, and 5 m. The column has outside diameter 140 mm and inside diameter 120 mm.

11.9-15 Solve the preceding problem for an aluminium pipe with outside diameter 170 mm and inside diameter 150 mm.

11.9-16 A square aluminium bar of width 50 mm is loaded in compression by a force P . The bar has pinned ends and is constructed of alloy 2014-T6. What is the longest permissible length L of the bar if $P = 400$ kN and if $P = 130$ kN.

11.9-17 What is the minimum permissible diameter d of a solid aluminium column of circular cross section with pinned ends and length 0.6 m if it must support an axial load $P = 50$ kN? (Assume the alloy is 2014-T6.)

11.9-18 Determine the allowable axial load P for a 150 mm x 150 mm wood column (actual dimensions 140 mm x 140 mm) with pinned ends for each of the following lengths: $L = 1.5$ m, 3 m, 4.5 m and 6 m. (Assume $E = 12$ GPa and $F_c = 8$ MPa.)

11.9-19 Determine the allowable axial load P for a 100 mm x 200 mm wood column (actual dimensions 90 mm x 185 mm) with pinned ends for each of the following lengths: $L = 1$ m, 2 m, 3 m, and 4 m. (Assume $E = 11$ GPa and $F_c = 7$ MPa.)

11.9-20 A square wood column of width 120 mm (actual dimensions) is supported with pinned ends. Determine the longest permissible length L of the column for each of the following axial loads: $P = 90$ kN, 60 kN, and 30 kN. (Assume $E = 12$ GPa and $F_c = 8$ MPa.)

11.9-21 What is the minimum permissible width b of a square wood column with pinned ends and length 3 m if it must support an axial load $P = 150$ kN? (Assume $E = 12$ GPa and $F_c = 9$ MPa.)

CHAPTER 11

Energy Method

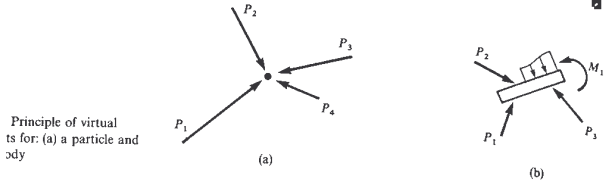
12.1 INTRODUCTION

The concepts of work and strain energy were introduced in earlier chapters, and expressions for the strain energy stored in linear elastic structures subjected to axial loads, torsion, and bending were derived. Now we will consider some additional concepts, including virtual work and complementary energy. The principle of virtual work leads to the unit-load method, which is a powerful method for finding displacements (or deflections) of structures of all kinds.* Strain energy and complementary energy provide methods for analyzing both linear and nonlinear structures, whether statically determinate or indeterminate. We will consider only simple trusses, beams, and frames in this chapter, but the concepts are applicable to more complex structures. Thus, this chapter provides an introduction to principles of applied mechanics that are fundamental to advanced structural analysis.

12.2 PRINCIPLE OF VIRTUAL WORK

The principle of virtual displacements and the principle of virtual work are usually introduced in the study of statics, in which they are used to solve problems of static equilibrium. The word *virtual* means that the quantities are hypothetical and do not exist in a real or physical sense. Thus, a *virtual displacement* is an imaginary displacement that is arbitrarily imposed upon a structural or mechanical system; it is not an actual displacement, such as the deflection caused by a load acting on a structure. The work done by the real forces during a virtual displacement is called *virtual work*.

* A deflection is the translation of a point in a deformable structure. However, a displacement is a more general quantity that includes not only translations but also rotations.

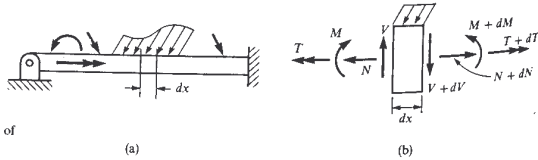


Principle of virtual work for: (a) a particle and (b) a beam element

When a single particle is acted upon by a set of forces in static equilibrium (see Fig. 12-1a), we may impart to the particle a virtual displacement consisting of a translation of the particle in any direction. During this virtual displacement the virtual work done by the forces must be zero because the forces are in equilibrium. This seemingly simple statement is the **principle of virtual displacements**. As shown in the study of statics, this principle may be used instead of the more familiar equations of equilibrium for the purpose of solving statics problems.

The principle of virtual displacements is also applicable to a rigid body that is held in equilibrium by the action of a set of loads that may include forces, couples, and distributed loads (Fig. 12-1b). The rigid body may be given a virtual displacement consisting of a translation in any direction, a rotation about any axis, or a combination of translation and rotation. In all instances the virtual work done by the forces will be zero if the body is in equilibrium. Usually we must restrict the virtual displacement to a very small displacement in order that the lines of action of the forces will not be altered during the virtual displacement.*

For use in finding displacements of deformable structures, we must extend the principle of virtual displacements to take into account not only the virtual work of the external forces, or loads, but also the virtual work associated with the internal forces, or stress resultants. To show how this is accomplished, let us consider the beam shown in Fig. 12-2a, although any other structure could be used. This structure is assumed to be loaded in a completely general fashion by forces, bending couples, torques, and distributed loads. The structure is at rest and in equilibrium under the action of these loads. At any cross section of the structure,



Principle of virtual work

* The principle of virtual displacements was first formulated by John Bernoulli, 1667-1748 (see Ref. 7-1).

stress resultants may exist in the form of an axial force N , bending moment M , shear force V , and twisting couple T , as shown on the left-hand face of an element of length dx cut out from the member (Fig. 12-2b). On the opposite face of the element, the stress resultants may have changed by small amounts; hence, they are shown as $N + dN$, $M + dM$, $V + dV$, and $T + dT$.

Assume now that the beam (Fig. 12-2a) is given a virtual deformation consisting of a small change in its deflected shape. This virtual deformation is imposed upon the beam in some unspecified manner, and deformation is independent of the fact that the structure has already been subjected to real deflections caused by the loads acting on it. Such real deflections have definite magnitudes dictated by the nature of both the loads and the structure. The virtual deformation, however, represents an additional deformation that is imparted arbitrarily to the structure. The only restriction on the virtual deformation is that it must represent a deformed shape that could actually occur physically; that is, the virtual change in shape must be compatible with the conditions of support for the structure and must maintain continuity between elements of the structure. As a consequence of the virtual deformation of the beam, points on the axis of the beam will undergo virtual displacements, such as deflections in the vertical direction.

During the virtual deformation each element of the beam will be displaced to a new location and also will be deformed in shape. Therefore, the forces acting on an element (both stress resultants and external loads, as shown in Fig. 12-2b) will perform virtual work. Let us denote the total amount of this virtual work by dW_e . This work may be considered to be composed of two parts: (1) the work dW_r due to the displacement (both translation and rotation) of the element as a rigid body and (2) the work dW_d associated with the deformation of the element. Thus,

$$dW_e = dW_r + dW_d$$

Because the element is in equilibrium, the virtual work dW_e done by the forces (both external and internal) during the displacement of the element as a rigid body must be zero; hence, the preceding equation reduces to

$$dW_r = dW_d \quad (a)$$

This equation states that the total virtual work done by all forces acting on the element during its virtual displacement is equal to the virtual work done by those same forces during only the virtual deformation of the element. Summing up the virtual-work terms in Eq. (a) for all elements of the structure, we get

$$\int dW_e = \int dW_d \quad (b)$$

in which it is understood that the integrations are performed over the entire structure.

The integrals in Eq. (b) can be simply interpreted. The integral on the left-hand side of the equation is the total virtual work done during the virtual deformation of the structure by all the forces, both loads and stress resultants, acting on all faces of all elements, of which the element shown in Fig. 12-2b is typical. We note, however, that the sides of each element are in direct contact with the sides of adjacent elements. Therefore, the virtual work of the stress resultants acting on one element exactly cancels the virtual work of the equal and opposite stress resultants acting on adjacent elements. The only remaining virtual work is the work of the external forces acting on the external boundaries of the elements (such as the top and bottom of the element in Fig. 12-2b). Thus, we conclude that the integral on the left-hand side of Eq. (b) is equal to the virtual work of the external forces acting on the structure. We will refer to this quantity as the **external virtual work** and will designate it by W_{ext} .

The term on the right-hand side of Eq. (b) was obtained by integrating the virtual work associated with the deformation of an element. This work includes the effects of all forces acting on the element, both stress resultants and external forces. However, when an element deforms (for example, when it elongates) only the stress resultants perform work. Thus, the second term in Eq. (b) actually represents the virtual work of the stress resultants alone. This virtual work is equal to the work done by the stress resultants when the elements on which they act are deformed virtually. The total amount of this virtual work, obtained by summing over all elements, is called the **internal virtual work** and is denoted by W_{int} . Thus, Eq. (b) becomes

$$W_{ext} = W_{int} \quad (12-1)$$

This equation represents the **principle of virtual work**, and it may be stated as follows:

If a deformable structure in equilibrium under the action of a system of loads is given a small virtual deformation, then the virtual work done by the external forces (or loads) is equal to the virtual work done by the internal forces (or stress resultants).

The principle of virtual work is extremely general and has many applications in structural analysis and applied mechanics. We will use it in the next section to derive the unit-load method for finding deflections. However, before proceeding to use the principle, it is important to emphasize some of its features. First, the virtual deformation or virtual displacement must be compatible with the supports of the structure and must maintain the continuity of the structure. Second, the deformations and displacements must be sufficiently small so that the geometry of the structure is not altered, allowing all calculations to be based upon the initial configuration of the structure. Except for these restrictions, the virtual change in shape may be arbitrarily imposed on the structure. However, the virtual deformations should not be confused with the de-

formed shape of the structure caused by the real loads. Finally, a review of the development of the principle will show that the properties of the material of the structure never entered the derivation. Therefore, the principle of virtual work applies to all structures irrespective of whether the material behaves linearly or nonlinearly, elastically or inelastically.

Now let us consider the evaluation of the terms for external and internal virtual work appearing in Eq. (12-1). The external work W_{ext} is the work performed by the loads acting on the structure during the virtual displacement. Since these loads are acting at their full values when the virtual displacement is imposed, the virtual work they perform is simply the product of load and displacement. Specifically, the virtual work of a concentrated load is the product of the force and the virtual displacement of its point of application. In such a case the positive direction of the displacement must be taken in the same direction as the positive direction of the force. If the load is a couple, then the virtual work is the product of the moment and the virtual angle through which it rotates.

The evaluation of the internal work W_{int} of the stress resultants is more involved. The virtual work done by the stress resultants acting on an element (Fig. 12-2b) depends upon the deformation of the element during the virtual displacement. The various kinds of small virtual deformations are shown in Fig. 12-3. Part (a) of the figure shows a virtual deformation consisting of a uniform axial strain in the element; thus, the length of the element has increased by an amount denoted by $d\delta$. This virtual deformation results in virtual work $(N + dN)d\delta$ being done by the axial force (Fig. 12-2b), but no virtual work is done by the bending moment, shear force, or twisting couple. Again we should note that nothing is said at this time about the cause of the virtual deformation $d\delta$; it is clearly not caused by the axial force N itself.

The next type of virtual displacement is a flexural deformation consisting of a relative rotation $d\theta$ between two sides of the element (Fig. 12-3b). During such a virtual deformation, the only stress resultant that does work is the bending moment, and its virtual work is $(M + dM)d\theta$. A shearing virtual deformation and a torsional virtual deformation are shown in Figs. 12-3c and d, respectively. The former

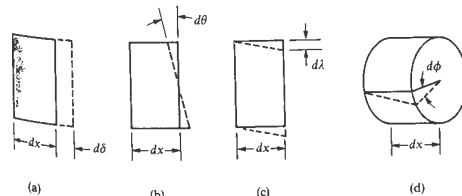


Fig. 12-3 Virtual deformation of an element of a structure: (a) axial, (b) flexural, (c) shearing, and (d) torsional

consists of a lateral translation $d\lambda$ of one side of the element with respect to the other, and the latter consists of a relative rotation $d\phi$ about the longitudinal axis. The virtual-work terms associated with these virtual deformations are $(V + dV)d\lambda$ and $(T + dT)d\phi$.

Each of the four preceding expressions for internal virtual work can be simplified by disregarding the product of two differentials (such as $dN d\delta$) in comparison with the product of the finite term and the differential (such as $N d\delta$). Thus, the expression for the internal virtual work done by the stress resultants acting on one element of the structure becomes

$$N d\delta + M d\theta + V d\lambda + T d\phi$$

Integrating over all elements of the structure gives the complete expression for the internal virtual work:

$$W_{int} = \int N d\delta + \int M d\theta + \int V d\lambda + \int T d\phi \quad (12-2)$$

In this expression the stress resultants N , M , V , and T are the actual stress resultants in the structure due to the real loads, whereas the deformations $d\delta$, $d\theta$, $d\lambda$, and $d\phi$ are the fictitious deformations associated with the virtual displacement of the structure. In the next section we will develop a method for finding displacements of structures based upon Eqs. (12-1) and (12-2).

12.3 UNIT-LOAD METHOD FOR CALCULATING DISPLACEMENTS

The determination of displacements in structures is an essential part of structural analysis and design. We discussed methods for finding deflections of simple trusses and beams in Section 2.3 and Chapter 7, respectively. However, those methods are limited to structures containing relatively few members. In this section, we will use the principle of virtual work to derive the **unit-load method**, which is widely used for finding displacements of structures. This method can be used not only for beams and trusses but also for very complicated structures having many members. Furthermore, the unit-load method is suitable for finding all types of displacements, including the deflection of a point in the structure, the rotation of the axis of a member, and the relative displacement between two points. Theoretically it may be used for either statically determinate or indeterminate structures, although for practical purposes the method is limited to determinate structures because its use requires that the stress resultants be known throughout the structure.

Because the basic equation of the unit-load method may be derived from the principle of virtual work, the method itself is sometimes called the **method of virtual work**. It is also known as the **dummy-load method** and the **Maxwell-Mohr method**. The former name arose because the method requires the use of a fictitious, or dummy, load (that is, the unit load), and the latter name is used because J. C. Maxwell in 1864

and O. Mohr in 1874 independently developed the method (Refs. 12-1 and 12-4).

Two loading systems must be considered when using the unit-load method to find the displacements of a structure. The first system consists of the structure subjected to the actual loads, temperature changes, or other causes that are responsible for producing the displacement to be calculated. The second system consists of a unit load acting alone on the structure. The unit load is a fictitious, or dummy, load that is introduced solely for the purpose of calculating a displacement Δ of the structure due to the actual loads. The unit load must correspond to the desired displacement Δ . A load that corresponds to a displacement is a load that acts on the structure at the point where the displacement is to be determined and has its positive direction in the same direction as a positive displacement. As previously mentioned, the term *displacement* is used in a generalized sense; thus, the displacement Δ may be a translation, a rotation, a relative displacement, or a relative rotation. If the displacement to be calculated is a translation, then the corresponding unit load is a force acting at the point where the translation occurs and having its positive direction in the positive direction of the translation. If the displacement to be calculated is a rotation, then the unit load is a couple acting at the point on the structure where the rotation occurs; the positive sense of the unit couple must be the same as the positive sense of the rotation. If the displacement is the relative translation of two points along the line joining them, the unit load will consist of two collinear and oppositely directed forces acting at the two points. Each of these possibilities will be illustrated by examples.

The unit load acting on the structure produces reactions at the supports and stress resultants within the members. Let us designate these stress resultants by the symbols N_U , M_U , V_U , and T_U . These quantities, in combination with the unit load and the reactions, constitute a force system that is in equilibrium. According to the principle of virtual work, if the structure is given a small virtual deformation (or change in shape), then the virtual work of the external forces is equal to the virtual work of the internal forces (see Eq. 12-1). Now we come to the key step in the development of the unit-load method; namely, we must make the proper choice of the virtual deformation. Let us take the actual deformations of the structure caused by the first system of loading as the virtual deformations to be imposed upon the second system (the structure with the unit load). During this virtual deformation the only external virtual work is the work performed by the unit load itself, because it is the only external load on the structure. This virtual work is the product of the unit load and the displacement Δ through which it moves; thus,

$$W_{ext} = 1 \cdot \Delta \quad (a)$$

where Δ represents the displacement of the structure due to the actual loads (recall that the unit load was intentionally selected to correspond to Δ).

The internal virtual work is the work performed by the stress resultants (N_U , M_U , V_U , and T_U) when the elements of the structure are deformed virtually. However, the virtual deformations are chosen to be the same as the actual deformations that occur in the structure supporting the real loads. Denoting those deformations by $d\delta$, $d\theta$, $d\lambda$, and $d\phi$, as shown in Fig. 12-3, we get for the internal work (see Eq. 12-2)

$$W_{int} = \int N_U d\delta + \int M_U d\theta + \int V_U d\lambda + \int T_U d\phi \quad (b)$$

Finally, by equating external and internal work (see Eqs. a and b), we obtain the **equation of the unit-load method**:

$$\Delta = \int N_U d\delta + \int M_U d\theta + \int V_U d\lambda + \int T_U d\phi \quad (12-3)$$

In this equation, Δ represents the displacement to be calculated, which may be a translation, a rotation, or a relative displacement; the stress resultants N_U , M_U , V_U , and T_U represent the axial force, bending moment, shear force, and twisting couple caused by the unit load corresponding to Δ ; and $d\delta$, $d\theta$, $d\lambda$, and $d\phi$ represent deformations caused by the actual loads. Because the unit load has been divided from the left-hand side of Eq. (12-3), leaving only the term Δ , it is necessary to consider the quantities N_U , M_U , V_U , and T_U as having the dimensions of force or moment per unit of the applied unit load.

The equation of the unit-load method (Eq. 12-3) is quite general and is not subject to any restrictions concerning linear behavior of the material or the structure. In other words, the principle of superposition need not be valid in order to use Eq. (12-3). However, the deformations $d\delta$, $d\theta$, $d\lambda$, and so on, must be small in order not to change the geometry of the structure, as explained in the preceding section.

The most common situation occurs when the material of the structure follows Hooke's law and the structure behaves linearly. In this case we can readily obtain expressions for the deformations $d\delta$, $d\theta$, $d\lambda$, and $d\phi$ caused by the real loads acting on the structure. If we denote the stress resultants in the structure due to the real loads as N_L , M_L , V_L , and T_L , then the deformations of an element are

$$d\delta = \frac{N_L dx}{EA} \quad d\theta = \frac{M_L dx}{EI} \quad d\lambda = \frac{\alpha V_L dx}{GA} \quad d\phi = \frac{T_L dx}{GI_p} \quad (c)$$

The first of these equations gives the elongation of an element (Fig. 12-3a) due to the axial force N_L . Similarly, the remaining three terms give the deformations associated with flexure, shear, and torsion (Figs. 12-3b, c, and d). These expressions are based upon equations derived in earlier chapters (see Eqs. 2-1, 7-6, 7-73, and 3-8). Substituting these four expressions into Eq. (12-3) gives the equation of the unit-load method for **linear elastic structures** in the following form:

$$\Delta = \int \frac{N_U N_L dx}{EA} + \int \frac{M_U M_L dx}{EI} + \int \frac{\alpha V_U V_L dx}{GA} + \int \frac{T_U T_L dx}{GI_p} \quad (12-4)$$

This equation can be used to find the displacement Δ at any point of a structure when the material is linearly elastic and the principle of superposition is valid. Each integral in the equation represents the contribution of one type of deformation to the total displacement. Thus, the first integral gives the contribution to the displacement Δ from the effects of axial deformations, the second term gives the contribution from flexural deformations, and so forth, for the remaining terms.

The **sign conventions** used for the stress resultants appearing in Eq. (12-4) must be consistent; thus, the axial forces N_U and N_L must be obtained according to the same sign convention, as must M_U and M_L , V_U and V_L , and T_U and T_L . Only under these conditions will the displacement Δ have the same positive sense as the unit load.

The procedure for calculating a displacement by means of the unit-load method using Eq. (12-4) may be summarized as follows: (1) determine the stress resultants N_L , M_L , V_L , and T_L in the structure due to the actual loads; (2) place a unit load on the structure corresponding to the displacement Δ that is to be found; (3) determine the stress resultants N_U , M_U , V_U , and T_U due to the unit load; (4) form the terms shown in Eq. (12-4) and integrate each term for the entire structure; and (5) sum the results to obtain the displacement Δ . These steps are illustrated in the examples given later.

Depending upon the type of structure, we can anticipate that some of the terms in Eq. (12-4) will not be needed. For example, if a truss with pinned joints has loads acting only at the joints, then there will be no flexural, shearing, or torsional deformations in the members and only the first term in Eq. (12-4) is required. Furthermore, the axial forces in the members will be constant throughout the lengths of the members; hence, if the members are prismatic, the integration for one member yields $N_U N_L L / EA$, where L is the length of the member. Then a summation for all members yields the following equation for a **truss**:

$$\Delta = \sum \frac{N_U N_L L}{EA} \quad (12-5)$$

This equation shows that the deflection Δ at any joint of the truss can be found by the following procedure: (1) determine the axial forces N_U and N_L in all members due to the unit load and the actual loads, respectively; (2) form the expression $N_U N_L L / EA$ for each member; and (3) add these expressions for all members to obtain the deflection.

Only flexural deformations are apt to be important in a beam or plane frame. Therefore, the unit-load equation for a **beam** is

$$\Delta = \int \frac{M_U M_L dx}{EI} \quad (12-6)$$

This expression can be integrated for each member of the structure, and then the resulting terms can be summed for all members of the structure. In general, it is possible to calculate displacements of structures by using any appropriate combination of terms from Eq. (12-4), depending upon the type of structure and loading.

Temperature effects. If the displacements are caused by effects other than loads, such as temperature changes, then we must use the appropriate expressions for $d\delta$, $d\theta$, $d\lambda$, and $d\phi$ in place of the expressions given in Eqs. (c), which are for the effects of loads only. For instance, a temperature increase produces an increase in length (see Fig. 12-3a) given by the equation

$$d\delta = \alpha(\Delta T) dx$$

in which α is the coefficient of thermal expansion and ΔT is the increase in temperature (see Eq. 2-22). Then the unit-load equation (Eq. 12-3) takes the form

$$\Delta = \int N_U \alpha(\Delta T) dx \quad (12-7)$$

This equation may be used even when the temperature change ΔT varies along the axes of the members; it is necessary only to express ΔT as a function of x and then integrate. However, for the common case in which the temperature change is constant along the length of each member, we can replace the expression in Eq. (12-7) by a summation that includes all members:

$$\Delta = \sum N_U \alpha L(\Delta T) \quad (12-8)$$

where L is the length of a member. Thus, the term $N_U \alpha L(\Delta T)$ must be evaluated for each member of the structure, and then these terms must be summed to obtain the displacement.

When the temperature varies linearly from top to bottom of the member but is constant along the length, the deformation is of the type pictured in Fig. 12-3b in which the deformation $d\theta$ is

$$d\theta = \frac{\alpha(T_2 - T_1) dx}{h}$$

as given by Eq. (7-71) with h being the height of the beam. T_2 is the temperature on the lower surface, and T_1 is the temperature on the upper surface. Thus, under these conditions we get

$$\Delta = \int \frac{M_U \alpha(T_2 - T_1) dx}{h} \quad (12-9)$$

In this equation $d\theta$ is assumed to be positive when the top fibers of the beam shorten and the lower fibers lengthen, as pictured in Fig. 12-3b. Therefore, the bending moment M_U must be taken as positive for the same conditions; this means that M_U is positive when it produces compression on the top of the beam.

Evaluation of product integrals. When evaluating the integrals in Eq. (12-4), we are usually dealing with members for which the material properties and cross-sectional dimensions are constant from one end of the member to the other. Therefore, the rigidities EA , EI , GJ/x , and GI_p may be placed outside the integral signs. The remaining integrals are in the form of a product, such as

$$\int M_U M_L dx \quad (12-10)$$

These product integrals must be evaluated over the length of each member and then added for all members. For any particular member, each quantity (such as M_U or M_L) is a function of the distance x measured along the axis of the member; specifically, the quantity may be constant along the length, may vary linearly along the length, or may be a function of higher order, such as quadratic or cubic. To save time when performing calculations, these product integrals can be evaluated in advance and the results tabulated for ready use. A compilation of product integrals, covering the most commonly encountered functions, is given in Table 12-1. The table is presented in terms of the functions M_U and M_L , but it is apparent that these functions can be replaced by others, such as V_U and V_L or T_U and T_L . Illustrations of the use of the table are given in some of the examples.

Example 1

The truss pictured in Fig. 12-4a is subjected to loads P and $2P$ at joint A . All members of the truss are assumed to be prismatic and to have the same axial rigidity EA . Calculate the horizontal and vertical deflections of joint B of the truss using the unit-load method.

Because the loads act only at the joints, the axial force in each member is constant throughout the length of the member. Therefore, we can use Eq. (12-5) to determine the desired deflections. It is helpful to record the calculations in a systematic manner, as shown in Table 12-2. The first two columns in the table identify the members of the truss and their lengths. The axial forces N_L , obtained by static-equilibrium analysis of the truss shown in Fig. 12-4a, are listed in column 3 of the table (tensile forces are positive).

In order to find the horizontal deflection δ_h of joint B , we introduce a horizontal unit load on the structure at B (see Fig. 12-4b). The axial forces N_U produced by this unit load are given in column 4 of the table; again, tensile forces are positive. Next, the products $N_U N_L L$ are calculated for each member and summed (column 5). Dividing this result by EA gives the desired displacement (see Eq. 12-5):

$$\delta_h = -3.828 \frac{PL}{EA}$$

The negative sign in this expression means that the deflection is in the direction opposite to the direction of the unit load; that is, the deflection is toward the left. The same general procedure is used to find the vertical deflection δ_v of joint

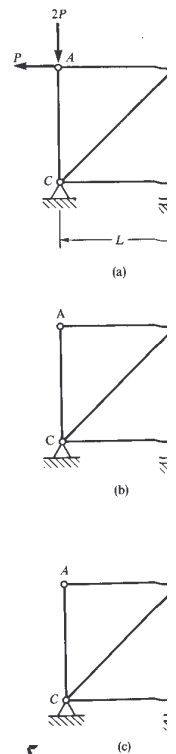


Fig. 12-4 Example 1. I of a truss by the unit-load

of product integrals $\int_0^L M_U M_L dx$

$\frac{L}{2} M_1 M_3$	$\frac{L}{2} (M_1 + M_2) M_3$	$\frac{L}{2} M_1 M_3$	$\frac{2L}{3} M_1 M_3$
$\frac{L}{3} M_1 M_3$	$\frac{L}{6} (M_1 + 2M_2) M_3$	$\frac{L}{6} \left(1 + \frac{a}{L}\right) M_1 M_3$	$\frac{L}{3} M_1 M_3$
$\frac{L}{6} M_1 M_3$	$\frac{L}{6} (2M_1 + M_2) M_3$	$\frac{L}{6} \left(1 + \frac{b}{L}\right) M_1 M_3$	$\frac{L}{3} M_1 M_3$
$\frac{L}{6} M_1 (M_3 + 2M_4)$	$\frac{L}{6} M_1 (2M_3 + M_4) + \frac{L}{6} M_2 (M_3 + 2M_4)$	$\frac{L}{6} \left(1 + \frac{b}{L}\right) M_1 M_3 + \frac{L}{6} \left(1 + \frac{a}{L}\right) M_1 M_4$	$\frac{L}{3} M_1 (M_3 + M_4)$
$\frac{L}{6} \left(1 + \frac{c}{L}\right) M_1 M_3$	$\frac{L}{6} \left(1 + \frac{d}{L}\right) M_1 M_3 + \frac{L}{6} \left(1 + \frac{c}{L}\right) M_2 M_3$	For $c \leq a$: $\frac{L}{3} M_1 M_3 - \frac{L(a-c)^2}{6ad} M_1 M_3$	$\frac{L}{3} \left(1 + \frac{cd}{L^2}\right) M_1 M_3$
$\frac{L}{3} M_1 M_3$	$\frac{L}{3} (M_1 + M_2) M_3$	$\frac{L}{3} \left(1 + \frac{ab}{L^2}\right) M_1 M_3$	$\frac{8L}{15} M_1 M_3$
$\frac{L}{4} M_1 M_3$	$\frac{L}{12} (M_1 + 3M_2) M_3$	$\frac{L}{12} \left(1 + \frac{a}{L} + \frac{a^2}{L^2}\right) M_1 M_3$	$\frac{L}{5} M_1 M_3$

1-degree parabolas with vertices shown by heavy dots.

Table 12-2 Calculations for Example 1

(1) Member	(2) Length	(3) N_L	(4) N_U	(5) $N_U N_L L$	(6) N_U	(7) $N_U N_L L$
AB	L	P	0	0	0	0
AC	L	-2P	0	0	0	0
BC	L	P	-1	-PL	1	PL
BD	L	0	0	0	0	0
CD	L	$-\sqrt{2}P$	$\sqrt{2}$	$-2.828PL$	0	0
CB	$\sqrt{2}L$	$-\sqrt{2}P$	$\sqrt{2}$	$-2.828PL$		PL

B . The corresponding unit load (taken as positive when upward) is portrayed in Fig. 12-4c, and the axial forces N_U for this loading condition are listed in column 4 of the table. In the last column, the products $N_U N_L L$ are calculated and summed. Finally, dividing the sum by EA yields

$$\delta_v = \frac{PL}{EA}$$

Because this result is positive, we know that the vertical deflection of joint B produced by the loads P and $2P$ is upward.

In this example we assumed for simplicity that all bars had the same cross-sectional area. If such were not the case, it would be necessary to insert an additional column in Table 12-2 in order to list the areas. Then, instead of calculating $N_U N_L L$ in columns 5 and 7, we would calculate $N_U N_L L/A$. The possibility of different moduli of elasticity for the members can be accommodated with equal ease.

Example 2

In this example we again consider the truss shown in Fig. 12-4a. However, rather than find the deflection of a joint, let us determine the angle of rotation of member AB and the change in distance between joints A and D .

The unit load corresponding to a rotation is a unit couple. In this example we create a unit couple consisting of equal and opposite forces acting at the ends of member AB (see Fig. 12-5a). Each force has a magnitude equal to the unit couple divided by the length of bar AB . We can easily show that the displacement corresponding to this couple is the counterclockwise rotation of bar AB ; we merely need to note that the external work done by these two forces during the virtual deformation of the truss is

$$W_{ext} = \frac{1}{L} (\delta_a) + \frac{1}{L} (\delta_b) = \frac{1}{L} (\delta_a + \delta_b) \quad (d)$$

where δ_a is the downward deflection of joint A and δ_b is the upward deflection of joint B . The units of the terms appearing in Eq. (d) are consistent because each "1" represents the unit couple and has units of length times force. The sum

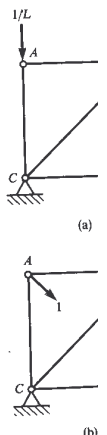


Fig. 12-5 E

Table 12-3 Calculations for Example 2

(1) Member	(2) Length	(3) N_L	(4) N_U	(5) $N_U N_L L$	(6) N_U	(7) $N_U N_L L$
AB	L	P	0	0	$-1/\sqrt{2}$	$-0.707PL$
AC	L	$-2P$	$-1/L$	$2P$	$-1/\sqrt{2}$	$1.414PL$
BD	L	P	$1/L$	P	$-1/\sqrt{2}$	$-0.707PL$
CD	L	0	0	0	$-1/\sqrt{2}$	0
CB	$\sqrt{2}L$	$-\sqrt{2}P$	0	0	1	$-2PL$
				3P		$-2PL$

of the two deflections δ_a and δ_b , when divided by the length L of the member, is the angle of rotation of member AB:

$$\theta_{ab} = \frac{\delta_a + \delta_b}{L} \quad (e)$$

From Eqs. (d) and (e) we get

$$W_{ext} = 1 \cdot \theta_{ab} \quad (f)$$

as expected. Thus, the application of a unit couple in the form of the two forces shown in Fig. 12-5a will enable us to find the angle of rotation θ_{ab} .

The calculations for this example are given in Table 12-3; the first three columns are the same as in Table 12-2, but the last four columns differ because we are calculating different deflections. Column 4 contains the axial forces N_U for the loads shown in Fig. 12-5a, and column 5 gives the products $N_U N_L L$. From the sum of those terms we get

$$\theta_{ab} = \frac{3P}{EA}$$

in which a positive result means that the bar rotates counterclockwise. Thus, the desired angle of rotation produced by the loads P and 2P has been found. A similar procedure can be followed to determine the angle of rotation for any other member.

Next, let us consider the change in distance between points A and D of the truss shown in Fig. 12-4a. In other words, we wish to determine the relative translation δ_{ad} of joints A and D along the line that joins them. The corresponding unit load consists of two equal and opposite unit forces acting along the line from A to D (see Fig. 12-5b). The resulting axial forces N_U in the truss are listed in column 6 of Table 12-3, and the products $N_U N_L L$ are listed in column 7. Thus, the relative translation of joints A and D is

$$\delta_{ad} = -\frac{2PL}{EA}$$

in which the minus sign indicates that the distance between points A and D has increased (that is, the relative translation is opposite to the sense of the unit loads).

Example 3

Let us consider the effects of a uniform temperature change in one of the bars of the truss shown in Fig. 12-4a. Assume that member BD has its temperature increased uniformly by an amount ΔT , so that the length of the member is increased by $\alpha(\Delta T)L$. We wish to calculate the horizontal deflection of joint B of the truss.

To obtain the deflection of a joint, we use Eq. (12-8). However, because only one bar of the truss has a change in length due to a temperature change, there is only one term in the summation. When finding the horizontal deflection of joint B due to the temperature change, we use the unit load shown in Fig. 12-4b, and therefore we take N_U from column 4 of Table 12-2. Thus, the force in bar BD is $N_U = -1$, and the horizontal deflection (from Eq. 12-8) is

$$\delta_h = -\alpha L(\Delta T)$$

in which the minus sign means that the deflection is toward the left (that is, opposite to the direction of the unit load). By a similar procedure we can easily calculate any other joint displacements caused by the temperature change.

Example 4

A prismatic cantilever beam AB supporting a uniform load of intensity q acting over part of the span is shown in Fig. 12-6a. We want to determine the deflection δ and angle of rotation θ at the free end B.

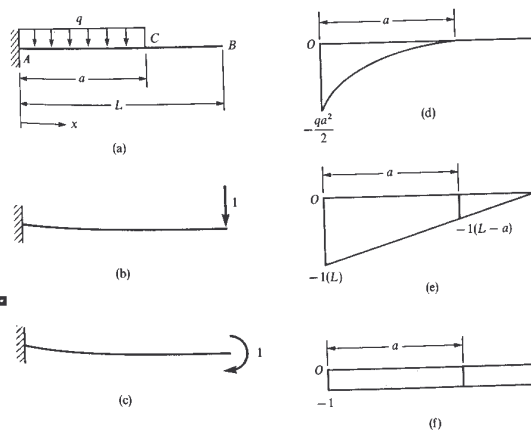


Fig. 12-6 Example 4. Displacement of a beam by the unit-load method

When finding beam deflections, we use the form of the unit-load equation that considers only the effects of flexural deformations (Eq. 12-6). If we take the origin of coordinates at the left end A and measure x to the right (Fig. 12-6a), then the equations for the bending moment M_L due to the load are

$$M_L = -\frac{q}{2}(a-x)^2 \quad (0 \leq x \leq a)$$

$$M_L = 0 \quad (a \leq x \leq L)$$

in which a positive bending moment causes compression on the top of the beam. The unit load corresponding to a downward deflection δ is shown in Fig. 12-6b; this load produces a bending moment as follows:

$$M_U = -1(L-x) \quad (0 \leq x \leq L)$$

Substituting M_U and M_L into Eq. (12-6) and integrating, we obtain the deflection of point B:

$$\delta = \frac{1}{EI} \int_0^a (-1)(L-x) \left(-\frac{q}{2} \right) (a-x)^2 dx = \frac{qa^3}{24EI} (4L-a)$$

This result is positive, hence the deflection is downward.

The procedure for finding the angle of rotation θ is similar except that the unit load is a unit couple, as shown in Fig. 12-6c. The bending moment due to this load is

$$M_U = -1 \quad (0 \leq x \leq L)$$

and the unit-load equation becomes

$$\theta = \frac{1}{EI} \int_0^a (-1) \left(-\frac{q}{2} \right) (a-x)^2 dx = \frac{qa^3}{6EI}$$

This result is positive, which indicates that the angle θ has the same sense (clockwise) as the unit couple.

An alternative procedure for finding the displacements is to use Table 12-1 for the product integrals. The bending-moment diagram for the load q is a parabola over part AC of the beam, as shown in Fig. 12-6d. The moment diagrams in this region of the beam for the unit loads are a trapezoid and a rectangle, respectively (see Figs. 12-6e and f). Taking the case of a parabola and a trapezoid from Table 12-1, we get for the value of the product integral

$$\frac{a}{12} [-1(L-a) - 3(L)] \left(-\frac{qa^2}{2} \right) = \frac{qa^3}{24} (4L-a)$$

Now dividing by EI, we obtain the same expression for the deflection δ as before. Also, the case of a parabola and a rectangle* yields

$$\frac{a}{12} (-4) \left(-\frac{qa^2}{2} \right) = \frac{qa^3}{6}$$

which leads to the previous result for the angle of rotation θ . The use of the table of product integrals in conjunction with bending-moment diagrams is often faster than writing the equations for the bending moments and then integrating.

* Note that the formulas for a rectangle can be obtained from Table 12-1 by taking a trapezoid with $M_1 = M_2$.

Example 5

A beam ABC with a span of length L and an overhang of length b (Fig. 12-7a) undergoes a change in temperature such that the top surface of the beam is at temperature T_1 while the lower surface is at temperature T_2 . Calculate the vertical deflection δ_c of the end of the overhanging portion of the beam.

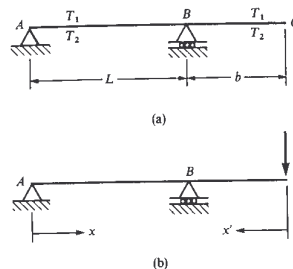


Fig. 12-7 Example 5. Beam temperature differential

The unit load corresponding to δ_c is pictured in Fig. 12-7b. The bending moment caused by this unit load, for region AB, is

$$M_U = -1 \left(\frac{b}{L} \right) x \quad (0 \leq x \leq L)$$

where x is the distance measured from A toward the right. Also, the bending moment in region BC is

$$M_U = -1(x') \quad (0 \leq x' \leq b)$$

where x' is measured from C toward the left. In both parts of the beam, the bending moment M_U is negative because it causes tension on the top of the beam.

Knowing the bending moments, we can now substitute directly into Eq. (12-9) and obtain the deflection:

$$\delta_c = \int_0^L -1 \left(\frac{b}{L} \right) (x) \frac{\alpha(T_2 - T_1)}{h} dx + \int_0^b -1(x') \frac{\alpha(T_2 - T_1)}{h} dx'$$

from which

$$\delta_c = \frac{\alpha b(T_1 - T_2)(L+b)}{2h} \quad (g)$$

where h is the height of the beam and α is the coefficient of thermal expansion. If the calculated value of δ_c is negative, then the deflection is upward; this condition exists whenever T_2 is greater than T_1 .

Example 6

The plane frame *ABC* shown in Fig. 12-8a has a fixed support at point *A* and carries a vertical load *P* at the free end *C*. The members *AB* and *BC* are joined rigidly at *B*, and both members of the frame have constant flexural rigidity *EI*. Determine the horizontal deflection δ_h , the vertical deflection δ_v , and the angle of rotation θ at point *C*.

The bending moments M_L caused by the load *P* are portrayed in Fig. 12-8b, in which the bending-moment diagrams are plotted on the sides of the members that are in tension. The unit loads corresponding to the horizontal deflection, vertical deflection, and angle of rotation at point *C* are shown in the last three parts of the figure. In each case the complete bending-moment diagram for M_U is also shown, again plotted on the tension sides of the members.

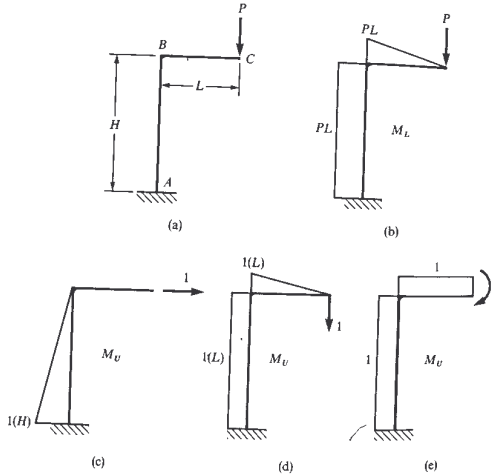


Fig. 12-8 Examples 6 and 7. a plane frame

Knowing the bending moments, we can now obtain the deflections either by integrating (see Eq. 12-6) or by using the formulas for the product integrals listed in Table 12-1. The latter approach seems simpler in this example. For instance, to find δ_h , we take M_U from Fig. 12-8c and M_L from Fig. 12-8b. Then using Table 12-1 we get

$$\frac{H}{2} (1)(H)(PL)$$

Dividing this expression by *EI*, we get

$$\delta_h = \frac{PLH^2}{2EI} \tag{h}$$

for the horizontal deflection of point *C*.

The vertical deflection is calculated in a similar manner from the diagrams of Figs. 12-8b and d. For member *BC* we have the case of two triangles, and for member *AB* the case of two rectangles; thus, from Table 12-1 we find

$$\frac{L}{3} (1)(L)(PL) + \frac{H}{2} (2L)(PL) = \frac{PL^3}{3} + PL^2H$$

and the vertical deflection is

$$\delta_v = \frac{PL^2(L + 3H)}{3EI} \tag{i}$$

Finally, using Figs. 12-8b and e and Table 12-1, we obtain

$$\frac{L}{2} (PL)(1) + \frac{H}{2} (2)(PL) = \frac{PL^2}{2} + PLH$$

from which

$$\theta = \frac{PL(L + 2H)}{2EI} \tag{j}$$

Thus, the desired displacements of the frame have been determined.

Example 7

Referring to the plane frame described in Example 6, let us determine the additional contributions to the displacements δ_h , δ_v , and θ caused by axial deformations in the members. Assume that both members have constant axial rigidity *EA*.

The additional displacements will be found with the aid of Eq. (12-5). The axial forces N_L in that equation are the axial forces caused by the load *P* shown in Fig. 12-8a; the only such force is $N_L = -P$ in member *AB*. To find the horizontal deflection δ_h , we take the axial forces N_U from Fig. 12-8c. The only such force is $N_U = 1$ in member *BC*; therefore, we conclude that the horizontal deflection δ_h is not affected by the presence of axial deformations.

To obtain the vertical deflection δ_v , we observe from Fig. 12-8d that the only axial force caused by the unit load is $N_U = -1$ for member *AB*. Hence, the vertical deflection due to axial deformations (from Eq. 12-5) is

$$\sum \frac{N_U N_L L}{EA} = \frac{(-1)(-P)(H)}{EA} = \frac{PH}{EA}$$

This quantity can be added to the earlier result obtained in Example 6 to give the total vertical deflection of joint *C*:

$$\delta_v = \frac{PL^2(L + 3H)}{3EI} + \frac{PH}{EA} \tag{k}$$

Energy Methods

When numerical values are substituted into this expression, it is found that the last term, representing the effects of axial deformations, is extremely small compared to the first term. For this reason it is common practice to consider only the effects of flexural deformations when analyzing plane frames and to disregard completely the contribution of the axial deformations.

To complete this example, we consider the angle of rotation θ and observe that the corresponding unit load (Fig. 12-8e) produces no axial forces in the members. Hence, θ is unaffected by the presence of axial deformations.

Example 8

A curved bar *AB* has a centerline in the form of a quarter circle of radius *R*, as shown in Fig. 12-9a. The bar has a fixed support at *A* and carries a vertical load *P* at the free end *B*. Obtain an expression for the horizontal deflection δ_h of point *B*.

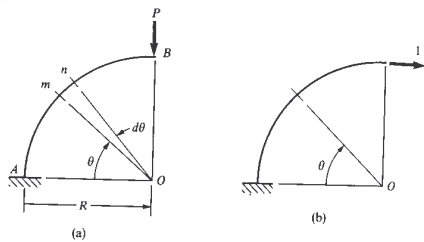


Fig. 12-9 Deflection of a

The unit-load equation for finding displacements of the curved bar can be expressed in the general form

$$\Delta = \int \frac{M_U M_L ds}{EI} \tag{12-11}$$

where *ds*, equal to *R dθ*, is the length of an element *mn* of the bar. It is assumed that the bar is thin compared to the radius *R* so that the above formula, originally derived for the bending of a straight bar, can be used. Also, only the effects of flexural deformations are considered in Eq. (12-11).

The bending moment M_L caused by the load *P* is $M_L = -PR \cos \theta$, where a positive moment is assumed to cause compression on the outside of the curved bar. Also, the bending moment M_U due to a horizontal unit load (Fig. 12-9b) is $M_U = -R(1 - \sin \theta)$. Substituting for M_U and M_L in Eq. (12-11) and integrating, we obtain

$$\delta_h = \frac{1}{EI} \int_0^{\pi/2} (-R)(1 - \sin \theta)(-PR \cos \theta)R d\theta = \frac{PR^3}{2EI}$$

Thus, the horizontal deflection of point *B* has been found by the unit-load method.

12.4 RECIPROCAL THEOREMS

The reciprocal theorems are important concepts in applied mechanics and structural analysis. They apply only to linear elastic structures (that is, structures for which the principle of superposition is valid). Thus, two basic conditions must be satisfied: (1) the material must follow Hooke's law and (2) the displacements must be small enough that all calculations can be based upon the undeformed geometry of the structure. We will use the concepts of work and strain energy to derive the theorems.

Reciprocal-displacement theorem. To illustrate the reciprocal-displacement theorem, let us take as an example a cantilever beam *AB* subjected to a concentrated load *P* at the free end (Fig. 12-10a). We can obtain the deflection at the midpoint *C* of this beam from the formulas in Appendix G; thus,

$$\delta_{cb} = \frac{5PL^3}{48EI}$$

The subscript notation used with the symbol δ is based upon the following scheme: the first subscript denotes the point at which the deflection occurs, and the second subscript denotes the point at which the load is applied. Thus, the symbol δ_{cb} identifies the deflection at point *C* caused by a load acting at point *B*.

Now let us consider the same cantilever beam subjected to a load *P* acting at the midpoint *C* (Fig. 12-10b). In this case we wish to find the deflection at the free end *B*, denoted by the symbol δ_{bc} . Again referring to the formulas in Appendix G, we find

$$\delta_{bc} = \frac{5PL^3}{48EI}$$

Thus, we observe that the deflection at *C* due to the load acting at *B* is equal to the deflection at *B* due to the load acting at *C*. This statement is an example of the **reciprocal-displacement theorem**.

To prove the theorem in more general terms, let us consider a structure of any type (that is, a truss, beam, three-dimensional body of arbitrary shape, and so on). For convenience a simple beam will be discussed (see Fig. 12-11), but any other structure would be satisfactory. Also, let us consider two states of loading acting on the structure. In the first state of loading, a force *P* acts at any point *A* (Fig. 12-11a); in the second state, the same load *P* acts at any other point *B* (Fig. 12-11b). The deflections at points *A* and *B* for the first state of loading are denoted by δ_{aa} and δ_{ba} , respectively, in accordance with the subscript notation already described. In an analogous manner, the deflections for the second state of loading are identified as δ_{ab} and δ_{bb} .

The deflections of the beam may be described by using the notion of correspondence between loads and displacements (see Section 12.3).

12.4 Reciprocal Theorems

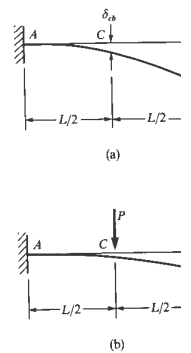


Fig. 12-10 Reciprocal-displacement theorem

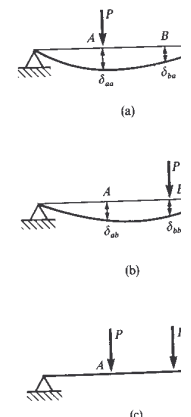


Fig. 12-11 Reciprocal-displacement theorem

For instance, the deflections δ_{aa} and δ_{ab} both correspond to the load P acting at A (Fig. 12-11a). To clarify this idea, recall that the displacement force acts; this deflection is measured along the line of action of the force and is positive in the direction of the force. However, the deflection need not be caused by the force to which it corresponds. The deflection δ_{aa} is caused by the force P from the first state of loading and the deflection δ_{ab} is caused by the force P from the second state of loading. Nevertheless, both deflections correspond to the load P of Fig. 12-11a. Similarly, the deflections δ_{ba} and δ_{bb} both correspond to the load P from the second state of loading, although δ_{ba} is caused by the first load and δ_{bb} is caused by the second load. This concept of correspondence as a means of identifying a displacement will be very useful in subsequent discussions.

Now returning to the derivation of the reciprocal-displacement theorem, let us suppose that both forces P act simultaneously on the beam (Fig. 12-11c). If the material of the beam is linearly elastic and if the deflections are small, we can use the principle of superposition to obtain the deflections for this beam. The deflection corresponding to the load P acting at A is $\delta_{aa} + \delta_{ab}$, and the deflection corresponding to the load P acting at B is $\delta_{ba} + \delta_{bb}$. Knowing these deflections, we can easily calculate the work done by the two loads P as they are slowly and simultaneously applied to the beam. This work, equal to the total strain energy U of the beam, is

$$U = \frac{1}{2} P(\delta_{aa} + \delta_{ab}) + \frac{1}{2} P(\delta_{ba} + \delta_{bb}) \quad (a)$$

as obtained from Clapeyron's theorem (Eq. 2-38).

The total strain energy of the beam subjected to two loads (Fig. 12-11c) does not depend upon the order in which the two loads are applied. Because the beam behaves linearly, the strain energy must be the same when the two loads are applied simultaneously and when one load is applied before the other load. The final state of the beam is the same in both cases. Let us assume that the load at A is applied first, followed by the load at B . Then the strain energy of the beam during the application of the first load is

$$\frac{1}{2} P\delta_{aa} \quad (b)$$

because this load causes the deflection δ_{aa} , shown in Fig. 12-11a. When the second load is applied, an additional deflection results at B equal to δ_{bb} ; hence, the second load does work equal to

$$\frac{1}{2} P\delta_{bb} \quad (c)$$

and an equal amount of strain energy is developed in the beam. However, we must not overlook the fact that, while the load at B is being

applied, the load P acting at A undergoes an additional deflection δ_{ab} . The corresponding amount of work done by that load is

$$P\delta_{ab} \quad (d)$$

Thus, this additional strain energy is produced. Equation (d) does not contain the factor $1/2$ because the force P remains constant during the time that the additional deflection δ_{ab} occurs. Summing Eqs. (b), (c), and (d), we get the total strain energy for the case when one load is applied before the other:

$$U = \frac{1}{2} P\delta_{aa} + \frac{1}{2} P\delta_{bb} + P\delta_{ab} \quad (e)$$

This amount of strain energy must be equal to the strain energy produced when the two loads are applied simultaneously (Eq. a). Equating the two expressions for strain energy leads to the following result:

$$\delta_{ab} = \delta_{ba} \quad (12-12)$$

This equation represents the **reciprocal-displacement theorem**, which may be stated as follows:

The deflection at A due to a load acting at B is equal to the deflection at B due to the same load acting at A .

The positive directions of the deflections are understood to be the same as the positive directions of the corresponding loads.

The reciprocal-displacement theorem is also applicable if one load is a force and the other is a couple, or if both loads are couples. To illustrate the former possibility, consider again a simple beam subjected to two states of loading (Fig. 12-12). The first loading consists of a couple

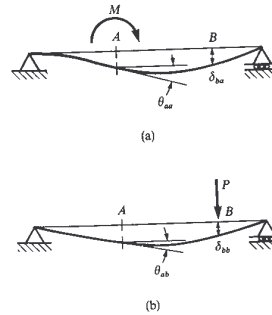


Fig. 12-12 Reciprocal-displacement theorem

M acting at point A (Fig. 12-12a). The displacement corresponding to M in the first beam is the angle of rotation θ_{aa} , and in the second beam it is the angle θ_{ab} . The second loading is the force P acting at B . Repeating the same steps as in the preceding derivation, we get the following expression for the strain energy of the beam when the two loads M and P are applied simultaneously:

$$U = \frac{1}{2} M(\theta_{aa} + \theta_{ab}) + \frac{1}{2} P(\delta_{ba} + \delta_{bb})$$

When the couple M is applied first, followed by the force P , the strain energy is

$$U = \frac{1}{2} M\theta_{aa} + \frac{1}{2} P\delta_{bb} + M\theta_{ab}$$

Equating these two expressions for strain energy yields

$$M\theta_{ab} = P\delta_{ba} \quad (12-13)$$

If the loads M and P are numerically equal, then θ_{ab} and δ_{ba} also will be numerically equal. Therefore, for this case we may state the reciprocal-displacement theorem as follows:

The angle of rotation at A due to a force acting at B is equal numerically to the deflection at B due to a couple acting at A if the force and couple are numerically equal.

Of course, consistent units must be used for all quantities.

If both loads acting on the structure consist of couples M (Fig. 12-13), then we find

$$\theta_{ab} = \theta_{ba} \quad (12-14)$$

In this situation the theorem is as follows:

The angle of rotation at A due to a couple acting at B is equal to the angle of rotation at B due to the same couple acting at A .

The positive senses of the angles are understood to be the same as the positive senses of the corresponding couples.

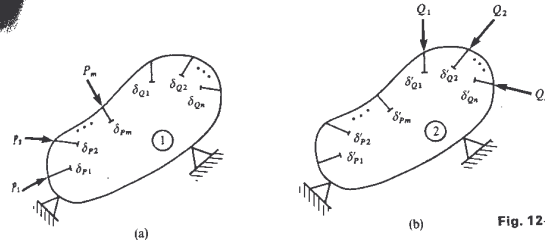
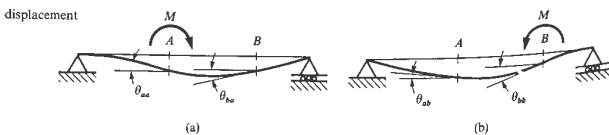


Fig. 12-14 Reciprocal-work theorem

The preceding derivations of the reciprocal-displacement theorem used a simple beam for illustrative purposes. Any other type of structure, such as a truss, frame, or massive body, could have been used, because the derivation was based only on strain-energy considerations and the principle of superposition. Thus, the theorem is quite general and applies to structures having axial, flexural, shearing, or torsional deformations. The only restriction on the use of the theorem is that the principle of superposition must be valid, which requires that the structure be linearly elastic. The theorem was first derived by J. C. Maxwell and published in 1864 (see Ref. 12-1); it is often called **Maxwell's reciprocal theorem**.

Reciprocal-work theorem. The reciprocal-work theorem is much more general than the reciprocal-displacement theorem and contains the latter as a special case. To derive the theorem, let us consider any linear elastic body for which the principle of superposition holds (Fig. 12-14). This body could represent a beam, truss, frame, or other kind of structure. Two states of loading on the structure must be considered. In the first state (Fig. 12-14a) there are m loads P_1, P_2, \dots, P_m ; in the second state (Fig. 12-14b) there are n loads Q_1, Q_2, \dots, Q_n . The deflections in the first state are designated by the symbol δ , with the subscript identifying the particular load to which each deflection corresponds. For instance, δ_{Q_2} represents the deflection corresponding to the force Q_2 . It follows that this deflection must be measured in the direction of the force Q_2 , although there is no implication that the point where Q_2 is applied moves only in the direction of Q_2 . This point may also have a component of displacement normal to the direction of δ_{Q_2} , but this component does not enter into our discussion because it does not correspond to Q_2 .

In the second state of loading (Fig. 12-14b), the situation is similar; the loads Q cause displacements, some of which correspond to the forces P and some of which correspond to the forces Q . These displacements



are denoted by the symbol δ_i , and again the subscripts denote the forces to which the deflections correspond.

To derive the reciprocal-work theorem, we use the same ideas about strain energy that we used in deriving the reciprocal-displacement theorem. If both load systems P and Q are applied simultaneously to the body, the strain energy (equal to the work done by the forces) is

$$U = \frac{1}{2} P_1(\delta_{P1} + \delta_{Q1}) + \frac{1}{2} P_2(\delta_{P2} + \delta_{Q2}) + \dots + \frac{1}{2} P_m(\delta_{Pm} + \delta_{Qm}) + \frac{1}{2} Q_1(\delta_{Q1} + \delta_{P1}) + \frac{1}{2} Q_2(\delta_{Q2} + \delta_{P2}) + \dots + \frac{1}{2} Q_n(\delta_{Qn} + \delta_{Pn}) \quad (f)$$

This strain energy must be the same as the strain energy obtained when we apply first the entire P -load system and then the entire Q -load system. When the loads P are applied alone, the strain energy is

$$\frac{1}{2} P_1 \delta_{P1} + \frac{1}{2} P_2 \delta_{P2} + \dots + \frac{1}{2} P_m \delta_{Pm} \quad (g)$$

When the second set of loads is applied, we get the following amount of strain energy due to the work done by the loads Q :

$$\frac{1}{2} Q_1 \delta_{Q1} + \frac{1}{2} Q_2 \delta_{Q2} + \dots + \frac{1}{2} Q_n \delta_{Qn} \quad (h)$$

At the same time, we get the following additional amount of strain energy due to the work done by the loads P :

$$P_1 \delta_{P1} + P_2 \delta_{P2} + \dots + P_m \delta_{Pm} \quad (i)$$

Therefore, the total strain energy (for the case when the loads P are applied first, followed by the loads Q) is the sum of expressions (g), (h), and (i). Equating this sum with the strain energy associated with simultaneous application of the loads (see Eq. f) gives

$$P_1 \delta_{P1} + P_2 \delta_{P2} + \dots + P_m \delta_{Pm} = Q_1 \delta_{Q1} + Q_2 \delta_{Q2} + \dots + Q_n \delta_{Qn}$$

or

$$\sum_{i=1}^m P_i \delta_{Pi} = \sum_{j=1}^n Q_j \delta_{Qj} \quad (12-15)$$

The expression on the left-hand side of this equation is the sum of the products of the P forces and their corresponding displacements caused by the Q forces. On the right-hand side appears the sum of the products of the Q forces and their corresponding displacements caused by the P forces. This equation represents the **reciprocal-work theorem**, and it may be stated as follows:

The work done by the forces in the first state of loading when they move through their corresponding displacements in the second state of loading is equal to the work done by the forces in the second state of loading when they move through their corresponding displacements in the first state of loading.

The reciprocal-work theorem applies to both forces and couples. For instance, P_i may represent either a force or a couple, and then the corresponding displacement δ_{Pi} is either a deflection or an angle of rotation, respectively.

Although in the derivation of the reciprocal-work theorem we portrayed the two sets of forces as acting at different points of the structure (see Fig. 12-14), it is not necessary that they do so. The force structure (see Fig. 12-14), it is not necessary that they do so. The force structure, for example, could act at the same point on the body as one of the Q_i , for example, could even act in the same direction and have the same P forces; it could even act in the same direction and have the same P magnitude. In other words, no restriction is imposed on either the P forces or the Q forces as to the number of forces, the locations of their points of application, or their directions. This generality makes the reciprocal-work theorem a very useful principle in structural mechanics. As in the case of the reciprocal-displacement theorem, the reciprocal-work theorem is valid only for structures for which the principle of superposition may be used. The theorem was derived by E. Betti (Ref. 12-5) and Lord Rayleigh (Refs. 12-6 through 12-8); hence, it is often called the **Betti-Rayleigh reciprocal theorem**.

It is evident that the reciprocal-displacement theorem is a special case of the reciprocal-work theorem. For instance, we can apply the reciprocal-work theorem to the two cases of loading shown in Figs. 12-11a and b; then we obtain $P\delta_{ab} = P\delta_{ba}$, which immediately gives Eq. (12-12) for the reciprocal-displacement theorem. Similarly, application of the theorem to the two loading conditions pictured in Fig. 12-12 gives $M\theta_{ab} = P\delta_{ba}$, which is the same as Eq. (12-13). Finally, we can get Eq. (12-14) by applying the reciprocal-work theorem to the two states of loading shown in Fig. 12-13.

12.5 STRAIN ENERGY AND COMPLEMENTARY ENERGY

The dual concepts of strain energy and complementary energy provide the bases for some extremely powerful methods of analysis. In their most general form, these methods are applicable to both linear and nonlinear structures. Our approach will be to describe the concepts for nonlinear structures and then to consider linear structures as a special case. We used this procedure when discussing the unit-load method in Section 12.3, where we first derived Eq. (12-3) for nonlinear structures and then specialized to Eq. (12-4) for linear structures.

Nonlinearities in the behavior of a structure have two primary causes. The most obvious cause is a material having a nonlinear stress-strain curve; in this case we refer to the structure as having **material**

nonlinearities. The second cause of nonlinearities is a change in the geometry of the structure. This situation occurs whenever the displacements of the structure alter the action of the applied loads or the reactions. An example is a column with an eccentric axial load (Section 11.4), for which we observe that lateral deflections of the column have a significant effect upon the deflections and bending moments in the column. Another example is a beam with large deflections, as described in Section 7.13. In both of these examples, the material of the beam was assumed to follow Hooke's law, but, because of the changing geometry of the deformed structure, we found that the deflections and stress resultants were related nonlinearly to the applied loads. These examples are illustrations of **geometric nonlinearities**. When analyzing a nonlinear structure, it is important to remember that the principle of superposition is not applicable except in very special cases.

Independently of whether material or geometric nonlinearities are present, we assume that the material of the structure is **elastic**. This requirement is necessary in order that the various energy principles, including conservation of energy, will be valid.

To illustrate the energy concepts, let us consider a prismatic bar subjected to an axial force P that produces a uniformly distributed stress $\sigma = P/A$ (Fig. 12-15a). The strain in the bar is $\epsilon = \delta/L$, where δ is the elongation of the bar and L is the length. The material of the bar is assumed to have the nonlinear stress-strain curve shown in Fig. 12-15b.

The load-deflection diagram (Fig. 12-15c) has the same shape as the stress-strain curve.

The work done by the load P during loading of the bar is

$$W = \int_0^\delta P_1 d\delta_1$$

In this equation, P_1 represents any value of the axial load between zero and the maximum value P ; δ_1 is the corresponding elongation; and δ is the maximum elongation. Because the bar behaves elastically and because we are disregarding any losses of energy during loading and unloading (in other words, because we are dealing with a conservative system), all of the work done by the load will be stored in the bar in the form of elastic strain energy that can be recovered during unloading. Therefore, the **strain energy** is equal to the work W , as follows:

$$U = W = \int_0^\delta P_1 d\delta_1 \quad (12-16)$$

The integral in this equation may be interpreted geometrically as the area below the load-deflection curve shown in Fig. 12-15c.

The **strain energy density** u (that is, the strain energy per unit volume of material) can be obtained by considering a differential volume element of unit dimensions subjected to a stress σ_1 and a strain ϵ_1 ; thus,

$$u = \int_0^\epsilon \sigma_1 d\epsilon_1 \quad (12-17)$$

where $\epsilon = \delta/L$ is the maximum strain. The integral in Eq. (12-17) represents the area below the stress-strain curve in Fig. 12-15b. This same expression for u can be obtained from the expression for the total strain energy (Eq. 12-16) by dividing by the volume V of the bar (equal to AL) and noting that $\sigma_1 = P_1/A$ and $d\epsilon_1 = d\delta_1/L$. Conversely, the total strain energy U can be obtained from the strain energy density by integrating as follows:

$$U = \int u dV \quad (12-18)$$

where dV is an element of volume and the integration is performed throughout the volume of the bar.

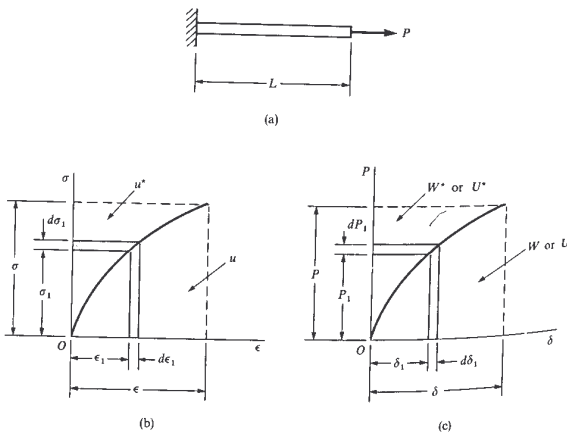
In the special case when the stress-strain curve follows Hooke's law, so that $\sigma_1 = E\epsilon_1$ (and hence $P_1 = EA\delta_1/L$), the expressions for U and u (Eqs. 12-16 and 12-17) yield

$$U = \frac{EA\delta^2}{2L} \quad (12-19)$$

$$u = \frac{E\epsilon^2}{2} \quad (12-20)$$

These expressions are the same as those derived in Section 2.8 (see Eqs. 2-39b and 2-41b).

Let us now define another type of work for the prismatic bar shown



y and

in Fig. 12-15. This new kind of work is called **complementary work**, W^* , and is defined as follows:

$$W^* = \int_0^P \delta_1 dP_1$$

The complementary work is represented by the area between the load-deflection curve and the load axis (Fig. 12-15c). It does not have a physical meaning as does the work W , but note that

$$W + W^* = P\delta \tag{12-21}$$

Thus, in a geometric sense, the work W^* is the complement of the work W because it completes the rectangle shown in Fig. 12-15c.

The **complementary energy** U^* of the bar is equal to the complementary work of the applied load, so that

$$U^* = W^* = \int_0^P \delta_1 dP_1 \tag{12-22}$$

The **complementary energy density** u^* (or the complementary energy per unit volume) is obtained by considering a volume element subjected to the stress σ_1 and strain ϵ_1 , in a manner analogous to that used in defining the strain energy density; thus,

$$u^* = \int_0^\sigma \epsilon_1 d\sigma_1 \tag{12-23}$$

The complementary energy density is equal to the area between the stress-strain curve and the stress axis (Fig. 12-15b). Also, the total complementary energy of the bar may be obtained from u^* by integration:

$$U^* = \int u^* dV \tag{12-24}$$

Sometimes the complementary energy is called **stress energy** in order to maintain the analogy with strain energy.

Again considering the special case of a material that follows Hooke's law ($\epsilon_1 = \sigma_1/E$ and $\delta_1 = P_1L/E A$), we substitute into Eqs. (12-22) and (12-23) to obtain the following expressions for U^* and u^* :

$$U^* = \frac{P^2L}{2EA} \tag{12-25}$$

$$u^* = \frac{\sigma^2}{2E} \tag{12-26}$$

Note that the complementary energy is expressed in terms of the load and that the strain energy (Eq. 12-19) is expressed in terms of the displacement. This distinction is inherent in the definitions of U and U^* (Eqs. 12-16 and 12-22, respectively). However, when Hooke's law holds, the strain and complementary energies are equal, and we obtain

$$U = U^* = \frac{EA\delta^2}{2L} = \frac{P^2L}{2EA} \tag{12-27}$$

$$u = u^* = \frac{E\epsilon^2}{2} = \frac{\sigma^2}{2E} \tag{12-28}$$

is larger than the total complementary energy U_m^* of the individual members. Thus, under these conditions, complementary energy is not conserved and some of it is "lost" during the loading process.

When more than one load acts on the structure, the total work done by the loads can be obtained by summation. The loads must be applied simultaneously and must be maintained in the same proportions to one another during the loading process. The work and the complementary work of the individual loads can be added to give the total work W and total complementary work W^* , as follows:

$$W = \sum_{i=1}^n \int_0^{\delta_i} P d\delta \quad W^* = \sum_{i=1}^n \int_0^{P_i} \delta dP \tag{12-29a, b}$$

In these equations, P_i and δ_i are the maximum values of the i th load and its corresponding displacement, respectively; P and δ represent intermediate values of those same quantities (between zero and the maximum values); and n is the total number of loads. The work W given by Eq. (12-29a) equals the strain energy U of the structure; it also equals the sum U_m of the strain energies of the individual members, regardless of whether the structure is materially and geometrically nonlinear. The complementary work W^* (Eq. 12-29b), which equals the complementary energy U^* of the structure, is equal to the sum U_m^* of the complementary energies of the members only if no geometric nonlinearities exist, as stated previously. Assuming that we can obtain the load-deflection relations, we can substitute into Eqs. (12-29) and evaluate both W and W^* . The former quantity will be expressed in terms of the displacements, and the latter will be in terms of the loads. However, since the relationships between the loads and their corresponding deflections usually are not known until the analysis of the structure is completed, the usual procedure is to evaluate the strain energy and complementary energy on a member-by-member basis (using Eqs. 12-16 and 12-22) and then to sum the energies to obtain U and U^* for the entire structure. This method for obtaining U is valid for structures with either kind of nonlinearity, but for U^* only material nonlinearities are permitted.

If the structure behaves linearly, the work W and the complementary work W^* of the loads are equal. Furthermore, each of these work terms is equal to the strain energy and the complementary energy of the structure ($W = W^* = U = U^*$). Since the work of the i th load is $P_i\delta_i/2$, we obtain the following equation for U and U^* :

$$U = U^* = \sum_{i=1}^n \frac{P_i\delta_i}{2} = \frac{P_1\delta_1}{2} + \frac{P_2\delta_2}{2} + \dots + \frac{P_n\delta_n}{2} \tag{12-30}$$

This equation expresses U and U^* in terms of the applied loads and their corresponding displacements.

We can also express U and U^* in terms of the displacements only or in terms of the loads only, simply by substituting for one quantity in terms of the other. Let us demonstrate this process symbolically in order

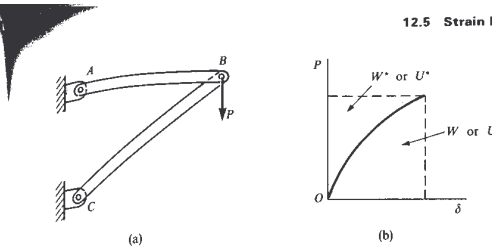


Fig. 12-16 Truss with material nonlinearity

Despite these equalities for the special case of a linear member, the conceptual distinctions between U and U^* must be maintained.

Although the preceding equations for strain energy and complementary energy were derived for a bar in tension, they can be extended readily to include other cases of loading of a bar, such as compression, torsion, and bending. Thus, we may consider the load-deflection curve shown in Fig. 12-15c to represent the relationship between a load and its corresponding displacement for any type of member. If the load is a couple M with a corresponding displacement θ , we merely replace P and δ with M and θ , respectively.

Next, consider an elastic structure composed of more than one member but supporting a single load P , such as the simple truss ABC shown in Fig. 12-16a. We assume that the material has the stress-strain curve shown in Fig. 12-15b. Consequently, the diagram of the load P versus the corresponding deflection δ (that is, the vertical deflection of joint B) will also be nonlinear (Fig. 12-16b). Shown on this load-deflection diagram are the work W and complementary work W^* of the load P . These quantities are equal, respectively, to the strain energy U and complementary energy U^* of the structure.

Now consider the individual members of the structure. Each member has both strain energy and complementary energy; these quantities can be found easily because we know the axial force in each member (from static equilibrium) and we know the stress-strain relationship. The sum U_m of the strain energies for the members equals the work W of the load P , by the principle of conservation of energy for an elastic structure (thus, $U_m = U$). This conclusion holds even when the structure is geometrically nonlinear; for instance, it holds when the deflections are large. However, the sum U_m^* of the complementary energies of the members equals the complementary work W^* of the load P only if the structure is geometrically linear (Ref. 12-14). Thus, complementary energy is conserved and $U_m^* = U^*$ when material nonlinearities are present but not when geometric nonlinearities exist. A necessary condition for geometric linearity is that the deflections be small, but this condition is not sufficient, as shown in Example 2 at the end of the section. If geometric nonlinearities are present, we define the complementary energy U^* of the structure as being equal to the complementary work W^* , but this energy

to show the nature of the resulting expressions. Because the structure behaves linearly, the loads may be expressed as linear combinations of the displacements, in the following general manner:

$$\begin{aligned} P_1 &= a_{11}\delta_1 + a_{12}\delta_2 + \dots + a_{1n}\delta_n \\ P_2 &= a_{21}\delta_1 + a_{22}\delta_2 + \dots + a_{2n}\delta_n \\ &\dots \\ P_n &= a_{n1}\delta_1 + a_{n2}\delta_2 + \dots + a_{nn}\delta_n \end{aligned} \tag{12-31}$$

where the coefficients $a_{11}, a_{12}, \dots, a_{nn}$ are constants that depend only upon the properties of the structure. If these relations are substituted into Eq. (12-30), the strain and complementary energies are expressed as a function of the displacements only. The general form of the resulting equation is as follows:

$$\begin{aligned} U = U^* &= b_{11}\delta_1^2 + b_{12}\delta_1\delta_2 + \dots + b_{1n}\delta_1\delta_n \\ &+ b_{21}\delta_2\delta_1 + b_{22}\delta_2^2 + \dots + b_{2n}\delta_2\delta_n \\ &\dots \\ &+ b_{n1}\delta_n\delta_1 + b_{n2}\delta_n\delta_2 + \dots + b_{nn}\delta_n^2 \end{aligned} \tag{12-32}$$

where the b 's are new constants obtained from the a 's. The expression on the right-hand side is called a **quadratic form**, which is a homogeneous polynomial of the second degree.

In addition to expressing the loads in terms of the displacements, we can also express the displacements as linear combinations of the loads:

$$\begin{aligned} \delta_1 &= c_{11}P_1 + c_{12}P_2 + \dots + c_{1n}P_n \\ \delta_2 &= c_{21}P_1 + c_{22}P_2 + \dots + c_{2n}P_n \\ &\dots \\ \delta_n &= c_{n1}P_1 + c_{n2}P_2 + \dots + c_{nn}P_n \end{aligned} \tag{12-33}$$

These equations can be obtained from Eqs. (12-31) by solving them simultaneously, hence the c 's also are constants that depend only upon the properties of the structure. When Eqs. (12-33) are substituted into Eq. (12-30), we get another quadratic form for U and U^* ; thus,

$$\begin{aligned} U = U^* &= d_{11}P_1^2 + d_{12}P_1P_2 + \dots + d_{1n}P_1P_n \\ &+ d_{21}P_2P_1 + d_{22}P_2^2 + \dots + d_{2n}P_2P_n \\ &\dots \\ &+ d_{n1}P_nP_1 + d_{n2}P_nP_2 + \dots + d_{nn}P_n^2 \end{aligned} \tag{12-34}$$

where the d 's are constants obtained from the c 's. These results show that, in the case of a linear elastic structure, the strain energy and the complementary energy may be expressed either as a quadratic function of the displacements or as a quadratic function of the loads. (Additional discussions of strain energy and complementary energy, with many examples, are given in Refs. 12-14 and 12-15.)

Example 1

Assume that a certain structure with material nonlinearities is acted on by a force P that produces a corresponding displacement δ given by the equation $\delta = CP^2$, where C is a constant (see Fig. 12-17). Determine the strain energy and complementary energy for this structure.

The strain energy is found from Eq. (12-16) by substituting $P_1 = \sqrt{\delta_1/C}$; thus,

$$U = \int_0^\delta \sqrt{\frac{\delta_1}{C}} d\delta_1 = \frac{2}{3} \sqrt{\frac{\delta^3}{C}} \quad (12-35)$$

The complementary energy, from Eq. (12-22), is

$$U^* = \int_0^P CP_1^2 dP_1 = \frac{CP^3}{3} \quad (12-36)$$

Note that the strain energy is expressed in terms of the displacement and the complementary energy is expressed in terms of the load. These forms for the energies are consistent with the nature of the definitions of U and U^* ; furthermore, we will see in subsequent sections that these forms are the most useful when finding deflections and analyzing structures. Of course, in some cases it is quite possible to express strain energy in terms of loads and complementary energy in terms of displacements. Such a result could be accomplished for this example by substituting from the original load-deflection relationship $\delta = CP^2$ into Eqs. (12-35) and (12-36). Also, note that U and U^* are not equal for this nonlinear structure (in this particular example, $U = 2U^*$).

Example 2

A structure consisting of two horizontal bars AC and CB , each of length L , is shown in Fig. 12-18a. The bars are pinned supports and are linked together at C . The material of the bars is linearly elastic, and each bar has constant axial rigidity EA . If a vertical load P is applied at C , the bars must rotate because they are incapable of supporting the load when they are horizontal. Thus, joint C deflects downward and tensile forces develop in the bars. When an equilibrium position is reached, the structure has a deflection δ at joint C (Fig. 12-18b). Determine the strain energy and complementary energy for this structure, assuming that the deflection δ remains small.

To determine the strain energy U , we will obtain the strain energy in one member and then multiply by 2. The strain energy of one member (since Hooke's law holds for the material) is obtained from the formula $EA\Delta^2/2L$ (see Eq. 12-19), in which Δ is the elongation and L' is the length of the member. To find the length L' , we note from Fig. 12-18b that

$$L' = \frac{L}{\cos \beta} \quad (a)$$

where β is the small angle shown in the figure. The series expression for $\cos \beta$ is

$$\cos \beta = 1 - \frac{\beta^2}{2!} + \frac{\beta^4}{4!} - \dots \quad (b)$$

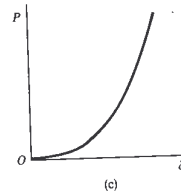
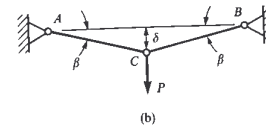
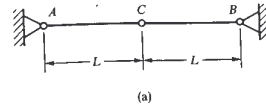


Fig. 12-18 Example 2. Struc geometric nonlinearity

Since β is a small quantity, we can disregard (in comparison to unity) all terms containing powers of β . Then we can take $\cos \beta$ equal to 1 and L' equal to L . To obtain the elongation Δ in terms of the deflection δ , we follow a similar procedure. First, we note that

$$L' = L + \Delta = \frac{L}{\cos \beta} = L \sec \beta \quad (c)$$

The series expression for $\sec \beta$ is

$$\sec \beta = 1 + \frac{\beta^2}{2!} + \frac{5\beta^4}{4!} + \dots \quad (d)$$

Substituting from this equation into Eq. (c), we get

$$L + \Delta = L \left(1 + \frac{\beta^2}{2!} + \frac{5\beta^4}{4!} + \dots \right)$$

or

$$\Delta = \frac{L\beta^2}{2} \left(1 + \frac{5\beta^2}{12} + \dots \right)$$

We can disregard all terms within the parentheses except the first, inasmuch as the angle β has a small value; therefore, we can assume that

$$\Delta = \frac{L\beta^2}{2} \quad (e)$$

Next, we observe from Fig. 12-18b that $\tan \beta = \delta/L$. However, for small angles we can replace $\tan \beta$ by β and obtain

$$\beta = \frac{\delta}{L} \quad (f)$$

Combining Eqs. (c) and (f), we get

$$\Delta = \frac{\delta^2}{2L} \quad (g)$$

Thus, the total strain energy of the members is

$$U_m = (2) \frac{EA\Delta^2}{2L'} = \frac{EA\delta^4}{4L^3} \quad (12-37)$$

This analysis is valid as long as δ remains small in comparison to the length L .

The complementary energy of the members is equal to the strain energy of the members because the material follows Hooke's law:

$$U_m^* = \frac{EA\delta^4}{4L^3} \quad (h)$$

However, this structure is geometrically nonlinear because the deflection of the structure alters the action of the forces; hence U_m^* does not represent the total complementary energy U^* . To show this fact, let us obtain the load-deflection equation for the structure and then evaluate both U and U^* from the work of the load P (see Eqs. 12-16 and 12-22). From static equilibrium at joint C (Fig. 12-18b), we obtain the tensile forces T in the members:

$$T = \frac{P}{2 \sin \beta}$$

Replacing $\sin \beta$ with β (because β is a small angle), and also using Eq. (f), we obtain

$$T = \frac{PL}{2\delta}$$

The elongation Δ of one bar is related to the axial force T as follows:

$$\Delta = \frac{TL}{EA} = \frac{PL}{2\delta} \left(\frac{L}{EA} \right) = \frac{PL^2}{2EA\delta} \quad (i)$$

Now we can eliminate Δ between Eqs. (g) and (i) and obtain the load-deflection relationship in either of the following forms:

$$P = \frac{EA\delta^3}{L^3} \quad \delta = \sqrt[3]{\frac{PL^3}{EA}} \quad (12-38a, b)$$

A graph of these equations is sketched in Fig. 12-18c. It is important to note that the structure is geometrically nonlinear, even though the material itself follows Hooke's law and the deflections are small.

Now we can calculate the strain energy of the structure from Eq. (12-16):

$$U = \int_0^\delta P_1 d\delta_1 = \int_0^\delta \frac{EA\delta_1^3}{L^3} d\delta_1 = \frac{EA\delta^4}{4L^3} \quad (12-39)$$

which agrees with Eq. (12-37). The complementary energy is found from Eq. (12-22):

$$U^* = \int_0^P \delta_1 dP_1 = \int_0^P \sqrt{\frac{P_1 L^3}{EA}} dP_1 = \frac{3P^{4/3} L}{4 \sqrt[3]{EA}} \quad (12-40)$$

Note again that the strain energy is expressed in terms of the displacement and the complementary energy is expressed in terms of the load.

In order to compare the complementary energy U^* with the complementary energy U_m^* of the members (Eq. h), we substitute from Eq. (12-38a) into Eq. (12-40), thus obtaining an alternate expression for the complementary energy:

$$U^* = \frac{3EA\delta^4}{4L^3} \quad (12-41)$$

This result is larger than U_m^* , which demonstrates that, when a structure has geometric nonlinearities, complementary energy is not conserved.

Example 3

A cantilever beam of length L and rectangular cross section (width b , height h) carries a concentrated load P at the free end (see Fig. 12-19). The stress-strain curve of the material in tension is represented by the equation $\sigma = B\sqrt{\epsilon}$, where B is a constant; the curve has the same shape in compression. Determine the strain energy and complementary energy for this beam.

In this example the stresses and strains vary throughout the volume of the beam, hence it is necessary to determine the strain energy density u and complementary energy density u^* and then integrate to obtain U and U^* . These quantities can be found if we know the stress σ , and the strain ϵ , at every point in the beam, which in turn requires that we know the curvature of the beam.

The curvature can be found by the techniques described in Section 10.7 for inelastic bending of beams. We begin by noting that the curvature is

$$\kappa = -\frac{\epsilon_1}{h} \quad (j)$$

where ϵ_1 is twice the strain at the bottom surface of the beam (see Eq. 10-22). Also, from Eq. (10-27), with $\epsilon_1 = \epsilon_2/2$, we get the following expression for the bending moment M at any cross section:

$$M = \frac{2bh^2}{\epsilon_1^2} \int_0^{\epsilon_1/2} \sigma \epsilon d\epsilon$$

Substituting $\sigma = B\sqrt{\epsilon}$ and then integrating, we find

$$M = \frac{Bbh^2 \sqrt{\epsilon_1}}{5\sqrt{2}}$$

$$\epsilon_1 = \frac{50M^2}{B^2 b^2 h^4}$$

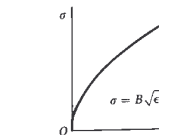
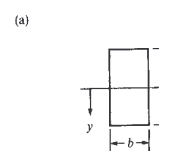
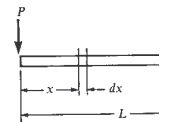


Fig. 12-19 Example 3 beam with material nonlin

The curvature can be found by eliminating ϵ_1 between Eqs. (j) and (k), substituting Px for the bending moment M , and using only absolute values:

$$\kappa = \frac{50P^2x^2}{B^2b^2h^5} \quad (l)$$

This equation gives the curvature as a function of the distance x measured along the axis of the beam (Fig. 12-19a).

The strain ϵ_1 at any point in any cross section of the beam is

$$\epsilon_1 = -\kappa y = -\frac{50P^2x^2y}{B^2b^2h^5} \quad (m)$$

as given by Eq. (10-1). The distance y is measured as shown in Fig. 12-19b. The stress can be found from the strain by using the stress-strain relationship:

$$\sigma_1 = B\sqrt{\epsilon_1} \quad (n)$$

Of course, the equation $\sigma = B\sqrt{\epsilon}$ is for the tension part of the stress-strain curve, which corresponds to the upper half of the beam in Fig. 12-19b (where y is negative). Therefore, we substitute Eq. (m) into Eq. (n) and again use only absolute values:

$$\sigma_1 = \frac{5\sqrt{2}Py^{1/2}x}{bh^{5/2}} \quad (o)$$

Thus, we now have expressions for the stress and strain at any point in the beam. The strain energy density (Eq. 12-17) is

$$u = \int_0^{\epsilon_1} \sigma_1 d\epsilon_1 = \int_0^{\epsilon_1} B\sqrt{\epsilon_1} d\epsilon_1 = \frac{2B\epsilon_1^{3/2}}{3}$$

Substituting for the strain ϵ (see Eq. m), and using only absolute values, we get

$$u = \frac{500\sqrt{2}P^3x^3y^{3/2}}{3B^2b^2h^{15/2}} \quad (p)$$

This expression gives the strain energy density as a function of the coordinates x and y . The strain energy U of the entire beam is found by integrating u throughout the volume of the beam. In setting up the integral, we will let x vary from 0 to L and y from 0 to $h/2$; then we will multiply by 2 to account for the two halves of the beam. Thus, the equation for the strain energy U is

$$U = \int u dV = 2 \int_0^L \int_0^{h/2} \left[\int_0^{h/2} u b dy \right] dx$$

Substituting from Eq. (p) for u , we get

$$U = \frac{1000\sqrt{2}P^3}{3B^2b^2h^{15/2}} \int_0^L \left[\int_0^{h/2} y^{3/2} dy \right] x^3 dx = \frac{25P^3L^4}{3B^2b^2h^5} \quad (12-42)$$

The work W done by the load P is given by this same expression: The complementary energy density (Eq. 12-23) is

$$u^* = \int_0^{\sigma_1} \epsilon_1 d\sigma_1 = \int_0^{\sigma_1} \frac{\sigma_1^2}{B^2} d\sigma_1 = \frac{\sigma_1^3}{3B^2}$$

where the partial derivative $\partial U/\partial \delta_i$ is the rate of change of the strain energy with respect to δ_i . We observe that, when the displacement δ_i is increased by the small amount $d\delta_i$, work is done by the corresponding force P_i but not by any of the other forces because the other displacements are not changed. This work, which is equal to $P_i d\delta_i$, is equal to the increase in strain energy stored in the structure:

$$dU = P_i d\delta_i$$

Equating the preceding expressions for dU gives

$$P_i = \frac{\partial U}{\partial \delta_i} \quad (12-44)$$

This equation states that the partial derivative of the strain energy with respect to any displacement δ_i is equal to the corresponding force P_i , provided that the strain energy is expressed as a function of the displacements. The equation is called **Castigliano's first theorem**, after the Italian engineer who derived and applied the theorem in his famous book, published in 1879 (see Refs. 12-16 through 12-20). The theorem can also be derived directly from the definition of strain energy (Eq. 12-16) by taking the derivatives of both sides of the equation.

As an illustration of Castigliano's first theorem, let us consider the nonlinear structure described in Example 1 of the preceding section. The strain energy of the structure is

$$U = \frac{2}{3} \sqrt{C\delta^3}$$

as given by Eq. (12-35). Note that this equation gives U as a function of the displacement δ corresponding to the load P . Applying Castigliano's first theorem, we get

$$P = \frac{dU}{d\delta} = \sqrt{C\delta}$$

from which $\delta = CP^2$, which is the correct relation between load and deflection.

In a similar manner, we can apply Castigliano's first theorem to the geometrically nonlinear structure shown in Fig. 12-18 and described in Example 2 of the preceding section. The strain energy of the structure (in terms of the displacement δ) is

$$U = \frac{EA\delta^4}{4L^3}$$

(see Eqs. 12-37 and 12-39). Thus, Castigliano's first theorem yields

$$P = \frac{dU}{d\delta} = \frac{EA\delta^3}{L^3}$$

This result agrees with the previous analysis (see Eq. 12-38a).

Substituting for the stress σ (see Eq. o), we get

$$u^* = \frac{250\sqrt{2}P^3x^3y^{3/2}}{3B^2b^2h^{15/2}} \quad (q)$$

which expresses the complementary energy density as a function of x and y . Now we can integrate throughout the volume of the beam, in the same manner as for strain energy:

$$U^* = \int u^* dV = 2 \int_0^L \left[\int_0^{h/2} u^* b dy \right] dx$$

Substitution of Eq. (q) for u^* gives

$$U^* = \frac{500\sqrt{2}P^3}{3B^2b^2h^{15/2}} \int_0^L \left[\int_0^{h/2} y^{3/2} dy \right] x^3 dx = \frac{25P^3L^4}{6B^2b^2h^5} \quad (12-43)$$

Thus, we have expressions for the strain energy and complementary energy of this beam. Note that the strain energy is twice the complementary energy, because the area below the stress-strain curve (Fig. 12-19c) is twice the area between the curve and the vertical axis.

12.6 STRAIN-ENERGY METHODS

We will now develop a strain-energy theorem that is important in structural analysis. Consider a structure subjected to n loads P_1, P_2, \dots, P_n that produce corresponding displacements $\delta_1, \delta_2, \dots, \delta_n$. As in previous discussions, it is understood that P and δ represent forces and corresponding displacements in a generalized sense, thereby including the possibility of a force and a translation, a couple and a rotation, a pair of forces and a relative displacement, or a pair of couples and a relative rotation. It is also understood that the structure may behave nonlinearly, which means that the relationship between any force P_i and the corresponding displacement δ_i is typified by the load-displacement diagram of Fig. 12-15c.

The strain energy U of the structure is equal to the work W done by the loads during their application, as discussed in the preceding section. Each force P_i theoretically can be expressed as a function of its corresponding displacement δ_i through the use of the appropriate load-displacement relationship. These expressions for the loads can be substituted into the expression for work (see Eq. 12-29a), thereby obtaining the strain energy U as a function of the displacements δ_i . With U expressed in terms of these displacements, we can evaluate the change in strain energy when one displacement δ_i is increased by a small amount $d\delta_i$, while all other displacements are held constant. This increase in strain energy, denoted by dU , is given by the expression

$$dU = \frac{\partial U}{\partial \delta_i} d\delta_i$$

Castigliano's first theorem is the basis for a method of structural analysis based upon strain energy. In order to explain the method, let us assume that we have a nonlinear structure with n unknown joint displacements D_1, D_2, \dots, D_n . We use the symbol D for these displacements to distinguish them from the displacements δ_i , which are more general quantities. Whereas δ_i and P_i may represent any displacement and corresponding force, the displacements D are joint displacements and represent the unknown quantities in the analysis. Furthermore, for practical purposes it is necessary that every joint displacement be included as one of the D 's. An additional restriction is that all loads on the structure must act at the joints. Thus, each load corresponds to a displacement. The loads will be denoted by P_1, P_2, \dots, P_n corresponding to D_1, D_2, \dots, D_n , respectively.

As already explained, it is theoretically possible to express the strain energy U of the structure in terms of the unknown joint displacements D_1, D_2, \dots, D_n . If U is expressed in this manner, we can apply Castigliano's first theorem with respect to each displacement and thereby obtain a set of n simultaneous equations:

$$P_1 = \frac{\partial U}{\partial D_1} \quad P_2 = \frac{\partial U}{\partial D_2} \quad \dots \quad P_n = \frac{\partial U}{\partial D_n} \quad (12-45)$$

If we examine a typical equation, say the i th equation, we find that it consists of terms on the right-hand side that contain the n joint displacements D_1, D_2, \dots, D_n as unknown quantities. Because these terms sum up to the load P_i itself, we conclude that the equation represents an equilibrium condition for forces corresponding to P_i . Thus, Eqs. (12-45) are a set of equilibrium equations that can be solved simultaneously for the joint displacements D_1, D_2, \dots, D_n in terms of the loads P_1, P_2, \dots, P_n . Knowing the joint displacements, we can calculate other quantities, such as reactions and stress resultants, from the displacements. Thus, the analysis of the structure is completed.

The strain-energy method described in the preceding paragraph utilizes joint displacements as unknowns and requires the solution of equilibrium equations. It is called the **displacement method** of analysis, and it may be used to analyze both linear and nonlinear structures. In the case of a linear structure, the method is called the **stiffness method**.

Let us consider in more detail the special case of a linear structure (that is, a structure for which the principle of superposition is valid). In this case the strain energy U is a quadratic function of the displacements, as explained in the preceding section. Therefore, when there are n unknown joint displacements D_1, D_2, \dots, D_n and n corresponding loads P_1, P_2, \dots, P_n , the general form for the strain energy U is

$$U = a_{11}D_1^2 + a_{12}D_1D_2 + \dots + a_{1n}D_1D_n + a_{21}D_2D_1 + a_{22}D_2^2 + \dots + a_{2n}D_2D_n + \dots$$

where the coefficients a_{11}, a_{12} , and so on, are new constants that depend only upon the properties of the structure. Applying Castigliano's first theorem (Eq. 12-44), we obtain the equations of equilibrium (Eqs. 12-45) in the following form:

$$\begin{aligned} P_1 &= \frac{\partial U}{\partial D_1} = S_{11}D_1 + S_{12}D_2 + \dots + S_{1n}D_n \\ P_2 &= \frac{\partial U}{\partial D_2} = S_{21}D_1 + S_{22}D_2 + \dots + S_{2n}D_n \\ &\dots \\ P_n &= \frac{\partial U}{\partial D_n} = S_{n1}D_1 + S_{n2}D_2 + \dots + S_{nn}D_n \end{aligned} \quad (12-46)$$

in which the coefficients S_{11}, S_{12} , and so on, are constants that depend upon the a 's (that is, upon the properties of the structure). These coefficients are known as **stiffness coefficients**, or **stiffnesses**, and Eqs. (12-46) are the **equilibrium equations** of the stiffness method of analysis.

An important relationship between the strain energy of the structure and the stiffnesses can be obtained by taking partial derivatives of Eqs. (12-46), as follows:

$$\begin{aligned} \frac{\partial P_1}{\partial D_1} &= S_{11} & \frac{\partial P_1}{\partial D_2} &= S_{12} & \dots & \frac{\partial P_1}{\partial D_n} &= S_{1n} & (a) \\ \frac{\partial P_2}{\partial D_1} &= S_{21} & \frac{\partial P_2}{\partial D_2} &= S_{22} & \dots & \frac{\partial P_2}{\partial D_n} &= S_{2n} & (b) \end{aligned}$$

and so forth for the remaining equations. Inasmuch as P_1 is equal to $\partial U / \partial D_1$, Eqs. (a) can be written as

$$S_{11} = \frac{\partial^2 U}{\partial D_1^2} \quad S_{12} = \frac{\partial^2 U}{\partial D_2 \partial D_1} \quad \dots \quad S_{1n} = \frac{\partial^2 U}{\partial D_n \partial D_1}$$

In a similar manner, Eqs. (b) become

$$S_{21} = \frac{\partial^2 U}{\partial D_1 \partial D_2} \quad S_{22} = \frac{\partial^2 U}{\partial D_2^2} \quad \dots \quad S_{2n} = \frac{\partial^2 U}{\partial D_n \partial D_2}$$

From the pattern of derivatives that emerges from these expressions, we conclude that the stiffness coefficients are related to the strain energy by the following general equation:

$$S_{ij} = \frac{\partial^2 U}{\partial D_j \partial D_i} \quad (12-47)$$

Thus, whenever the strain energy U is expressed as a quadratic function of the unknown displacements D_1, D_2, \dots, D_n , we can immediately get the stiffnesses for the structure by the process of differentiation. Further-

more, the order of differentiation of U is immaterial, and therefore we obtain the reciprocal theorem for stiffnesses:

$$S_{ij} = \frac{\partial^2 U}{\partial D_j \partial D_i} = \frac{\partial^2 U}{\partial D_i \partial D_j} = S_{ji} \quad (12-48)$$

Of course, the preceding discussion of stiffnesses is applicable only to linearly elastic structures. For a thorough discussion of the stiffness method, textbooks on structural analysis should be consulted (for example, see Ref. 12-22).

Example 1

The truss ABC shown in Fig. 12-20a supports a vertical load P at joint B . Bars AB and BC have constant cross-sectional area A . The stress-strain relationship for the material in tension is $\sigma = B\sqrt{\epsilon}$, where B is a constant (see Fig. 12-20b). The shape of the stress-strain curve is the same in both tension and compression. Analyze this materially nonlinear truss by the displacement method, using Castigliano's first theorem.

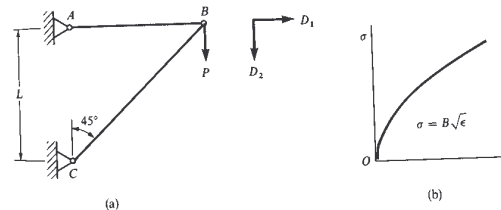


Fig. 12-20 Example 1. Truss of material with nonlinear stress-strain curve

Two unknown displacements may be identified at joint B of this structure, a horizontal displacement D_1 and a vertical displacement D_2 (Fig. 12-20). The strain energy of the structure must be expressed in terms of these displacements in order to obtain the equations of equilibrium by the use of Castigliano's first theorem. Thus, the strain energy is determined as follows. Considering only the displacement D_1 , we note that bar AB elongates by an amount equal to D_1 and bar BC elongates by an amount equal to $D_1/\sqrt{2}$. Also, due to the displacement D_2 alone, bar BC shortens by an amount equal to $D_2/\sqrt{2}$, and bar AB does not change in length. Thus, the total elongation of bar AB is D_1 and the total shortening of bar BC is $(D_2 - D_1)/\sqrt{2}$. Hence, the strains in the bars are

$$\epsilon_{ab} = \frac{D_1}{L} \quad (\text{elongation}) \quad (c)$$

$$\epsilon_{bc} = \frac{D_2 - D_1}{2L} \quad (\text{shortening}) \quad (d)$$

Next, the stresses are determined from the stress-strain law:

$$\sigma_{ab} = B\sqrt{\epsilon_{ab}} = \frac{P}{A} \quad (\text{tension})$$

$$\sigma_{bc} = B\sqrt{\epsilon_{bc}} = \frac{\sqrt{2}P}{A} \quad (\text{compression})$$

Finally, the axial forces N in the bars are

$$N_{ab} = \sigma_{ab}A = P \quad (\text{tension})$$

$$N_{bc} = \sigma_{bc}A = \sqrt{2}P \quad (\text{compression})$$

These results are readily verified by static equilibrium. In this example we have intentionally described all steps in the solution in order to illustrate the general concepts of the displacement method and the use of Castigliano's first theorem, even though the structure is very simple and could have been analyzed much more easily as a statically determinate structure. The use of the displacement method required the solution of two simultaneous equations because there are two unknown joint displacements. However, because the structure is statically determinate, it can also be analyzed as follows: (1) find the forces in the bars from static equilibrium, (2) find the stresses in the bars by dividing the forces by the cross-sectional areas, (3) obtain the strains in the bars from the stress-strain diagram, (4) determine the elongations of the bars from the strains, and (5) construct a Williot diagram (see Section 2.3) to obtain the displacements D_1 and D_2 of joint B .

Example 2

A truss consisting of four bars that meet at a common joint E is shown in Fig. 12-21a. All bars are constructed of the same linearly elastic material with modulus of elasticity E . Each bar has length L and cross-sectional area A , and the angle β equals 30° . Loads P_1 and P_2 act on the truss at joint E . Analyze this statically indeterminate truss by using Castigliano's first theorem and the stiffness method.

This truss has two unknown joint displacements, namely, the horizontal and vertical translations D_1 and D_2 at joint E (Fig. 12-21a). To express the strain

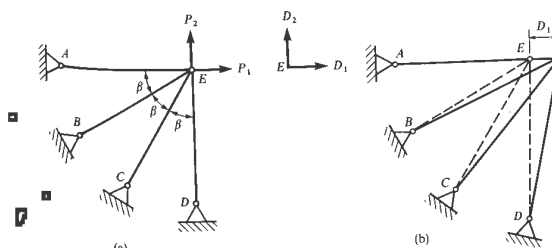


Fig. 12-21 Example 2. Truss of material that follows H

The strain energy density in each bar can be found from Eq. (12-17):

$$\begin{aligned} u_{ab} &= \int_0^{\epsilon_{ab}} \sigma_1 d\epsilon_1 = \int_0^{\epsilon_{ab}} B\sqrt{\epsilon_1} d\epsilon_1 = \frac{2B}{3} \left(\frac{D_1}{L} \right)^{3/2} \\ u_{bc} &= \int_0^{\epsilon_{bc}} \sigma_1 d\epsilon_1 = \int_0^{\epsilon_{bc}} B\sqrt{\epsilon_1} d\epsilon_1 = \frac{2B}{3} \left(\frac{D_2 - D_1}{2L} \right)^{3/2} \end{aligned}$$

Because the stress and strain are constant throughout the volume of each bar, we can get the total strain energy of each bar by multiplying the strain energy density by the volume of the bar. Then these strain energies can be added to give the total strain energy U of the structure:

$$U = U_{ab} + U_{bc} = u_{ab}AL + u_{bc}AL\sqrt{2}$$

from which

$$U = \frac{AB}{3\sqrt{L}} [2D_1^{3/2} + (D_2 - D_1)^{3/2}] \quad (12-49)$$

where A is the cross-sectional area of each bar. This equation gives the strain energy in terms of the unknown joint displacements D_1 and D_2 .

The equations of equilibrium can now be obtained by using Castigliano's first theorem (see Eqs. 12-44 and 12-45). The quantity P_1 in Eqs. (12-45) represents the load corresponding to D_1 and is equal to zero, while P_2 represents the load corresponding to D_2 and is equal to P . Thus, we get

$$P_1 = \frac{\partial U}{\partial D_1} = \frac{AB}{2\sqrt{L}} [2D_1^{1/2} - (D_2 - D_1)^{1/2}] = 0$$

$$P_2 = \frac{\partial U}{\partial D_2} = \frac{AB}{2\sqrt{L}} (D_2 - D_1)^{1/2} = P$$

Simplifying these two equations, we get

$$2D_1^{1/2} - (D_2 - D_1)^{1/2} = 0 \quad (c)$$

$$(D_2 - D_1)^{1/2} = \frac{2P\sqrt{L}}{AB} \quad (f)$$

Solving simultaneously the preceding equations, we obtain the joint displacements:

$$D_1 = \frac{P^2L}{A^2B^2} \quad D_2 = \frac{5P^2L}{A^2B^2} \quad (12-50a, b)$$

This step completes the essential part of the analysis by the displacement method, because, now that we know D_1 and D_2 , we can calculate all bar forces and reactions.

To illustrate these final calculations, let us determine the forces in the bars. The strains in the bars are obtained by substituting for D_1 and D_2 (Eqs. 12-50a and b) into Eqs. (c) and (d):

$$\epsilon_{ab} = \frac{D_1}{L} = \frac{P^2}{A^2B^2} \quad (\text{elongation})$$

$$\epsilon_{bc} = \frac{D_2 - D_1}{2L} = \frac{2P^2}{A^2B^2} \quad (\text{shortening})$$

energy U as a function of D_1 and D_2 , we begin by assuming that D_1 occurs alone (Fig. 12-21b). Under these conditions the elongations of the bars are as follows:

$$\Delta_{ac} = D_1 \quad \Delta_{bc} = \frac{\sqrt{3}D_1}{2} \quad \Delta_{ce} = \frac{D_1}{2} \quad \Delta_{de} = 0$$

as can be readily verified from the geometry of the figure. When the displacement D_2 occurs alone, the elongations of the members are

$$\Delta_{ac} = 0 \quad \Delta_{bc} = \frac{D_2}{2} \quad \Delta_{ce} = \frac{\sqrt{3}D_2}{2} \quad \Delta_{de} = D_2$$

Therefore, the elongations of the bars when both D_1 and D_2 occur simultaneously are as follows:

$$\Delta_{ac} = D_1 \quad \Delta_{bc} = \frac{\sqrt{3}D_1 + D_2}{2} \quad \Delta_{ce} = \frac{D_1 + \sqrt{3}D_2}{2} \quad \Delta_{de} = D_2 \quad (g)$$

The strain energy of each bar can be evaluated from its elongation (see Eq. 12-19), and then the total strain energy U of the truss can be obtained by summing the energies for all four bars:

$$U = \frac{EA}{2L} D_1^2 + \frac{EA}{2L} \left(\frac{\sqrt{3}D_1 + D_2}{2} \right)^2 + \frac{EA}{2L} \left(\frac{D_1 + \sqrt{3}D_2}{2} \right)^2 + \frac{EA}{2L} D_2^2$$

or

$$U = \frac{EA}{2L} (2D_1^2 + \sqrt{3}D_1D_2 + 2D_2^2) \quad (12-51)$$

Note that this expression gives the strain energy as a quadratic function of the displacements.

Applying Castigliano's first theorem, we get the following equations of equilibrium (see Eqs. 12-46):

$$P_1 = \frac{2EA}{L} D_1 + \frac{\sqrt{3}EA}{2L} D_2 \quad (h)$$

$$P_2 = \frac{\sqrt{3}EA}{2L} D_1 + \frac{2EA}{L} D_2 \quad (i)$$

These equations can be solved for the joint displacements; the results are

$$D_1 = \frac{2L}{13EA} (4P_1 - \sqrt{3}P_2) \quad D_2 = \frac{2L}{13EA} (-\sqrt{3}P_1 + 4P_2)$$

Finally, the axial forces N in the bars of the truss can be calculated. The procedure is to find the elongations Δ of the bars by substituting the joint displacements D_1 and D_2 into Eqs. (g), and then to find the bar forces from the elongations by using the equation $N = EA\Delta/L$. The results are

$$N_{ac} = \frac{8P_1}{13} - \frac{2\sqrt{3}P_2}{13} \quad N_{bc} = \frac{3\sqrt{3}P_1}{13} + \frac{P_2}{13}$$

$$N_{ce} = \frac{P_1}{13} + \frac{3\sqrt{3}P_2}{13} \quad N_{de} = -\frac{2\sqrt{3}P_1}{13} + \frac{8P_2}{13}$$

Thus, the complete analysis of the statically indeterminate truss has been performed by the stiffness method.

Example 3

The statically indeterminate frame shown in Fig. 12-22a has a fixed support at A and a pin support at C . The load on the structure is a couple M_0 acting at joint B . The material of the structure follows Hooke's law. Members AB and BC have length L and flexural rigidity EI . Determine the angles of rotation D_1 and D_2 at joints B and C , respectively (Fig. 12-22b).

The only unknown joint displacements for this frame are the angles of rotation D_1 and D_2 , inasmuch as we are disregarding the effects of axial deformations (and therefore the lengths of the members do not change). The strain energy of the frame must be expressed in terms of the unknown displacements D_1 and D_2 . To accomplish this step for a frame, it is helpful to imagine that the unknown joint displacements are imposed on the structure by the addition of restraints corresponding to those displacements (see Fig. 12-22c). Then each member of the frame is in the same condition as a fixed-end beam with rotations imposed at the ends. If we can obtain a formula for the strain energy stored in such a beam, we can use this formula to obtain the strain energy of the frame.

Consider the beam AB shown in Fig. 12-23. The ends A and B are assumed to be rotated through angles θ_1 and θ_2 , respectively. Our objective is to obtain a formula for the strain energy U of this beam in terms of θ_1 and θ_2 . One method is to derive the equation of the deflection curve by solving the fourth-order differential equation (Eq. 7-10c):

$$EIv'''' = q = 0$$

Four successive integrations of this equation yield

$$EIv = \frac{C_1x^3}{6} + \frac{C_2x^2}{2} + C_3x + C_4$$

The boundary conditions are as follows:

$$v(0) = -\theta_1 \quad v(L) = -\theta_2 \quad v'(0) = 0 \quad v'(L) = 0$$

Application of these conditions yields the following equation of the deflection curve:

$$v = -\frac{x^3}{L^2}(\theta_1 + \theta_2) + \frac{x^2}{L}(2\theta_1 + \theta_2) - \theta_1x$$

The strain energy of the beam can now be calculated (see Eq. 7-59b):

$$U = \frac{EI}{2} \int_0^L \left(\frac{d^2v}{dx^2} \right)^2 dx = \frac{2EI}{L} (\theta_1^2 + \theta_1\theta_2 + \theta_2^2) \quad (12-52)$$

Another way to find the strain energy of the beam is to determine the work done

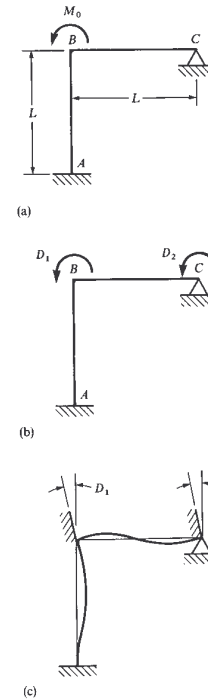
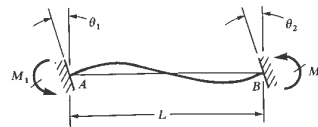


Fig. 12-22 Example 3. Frame material that follows Hooke's law

Fig. 12-23 Strain energy in a beam with rotations θ_1 and θ_2 at the ends

by the moments M_1 and M_2 acting at the ends of the beam (see Fig. 12-23). When these moments act on a simple beam, the angles at the ends are

$$\theta_1 = \frac{M_1L}{3EI} - \frac{M_2L}{6EI} \quad \theta_2 = -\frac{M_1L}{6EI} + \frac{M_2L}{3EI}$$

(see Case 7 of Table G-2 in Appendix G). These equations can be solved simultaneously for M_1 and M_2 :

$$M_1 = \frac{2EI}{L} (2\theta_1 + \theta_2) \quad M_2 = \frac{2EI}{L} (\theta_1 + 2\theta_2) \quad (12-53a,b)$$

The strain energy of the beam, from Eq. (12-30), is

$$U = \frac{M_1\theta_1}{2} + \frac{M_2\theta_2}{2}$$

Substituting from Eqs. (12-53), we obtain the same expression for U as before (see Eq. 12-52).

Now we are ready to determine the strain energy of the frame shown in Fig. 12-22 in terms of the displacements D_1 and D_2 . The procedure is to apply Eq. (12-52) to each member and then sum the results. For member AB we have $\theta_1 = 0$ and $\theta_2 = D_1$, and for member BC we have $\theta_1 = D_1$ and $\theta_2 = D_2$. Thus, the strain energy is

$$U = \frac{2EI}{L} (D_1^2) + \frac{2EI}{L} (D_1^2 + D_1D_2 + D_2^2) = \frac{2EI}{L} (2D_1^2 + D_1D_2 + D_2^2)$$

From Castigliano's first theorem we now get the following equations of equilibrium:

$$M_0 = \frac{\partial U}{\partial D_1} = \frac{2EI}{L} (4D_1 + D_2)$$

$$0 = \frac{\partial U}{\partial D_2} = \frac{2EI}{L} (D_1 + 2D_2)$$

These equations can be solved for the joint displacements D_1 and D_2 :

$$D_1 = \frac{M_0L}{7EI} \quad D_2 = -\frac{M_0L}{14EI}$$

Thus, the joint rotations have been found for the frame. As a final step in the solution, the moments at the ends of each member could be determined by using Eqs. (12-53).

This example is well suited to the use of strain energy and Castigliano's first theorem because the load M_0 corresponds to one of the unknown joint displacements. The only other possible load on the structure is a couple corresponding to D_2 , inasmuch as one of the requirements of this method of analysis is that each load must correspond to an unknown joint displacement. This fact raises the question of how to analyze a structure when there are loads at other locations, such as a concentrated load acting at the midpoint of a member. One possibility is to consider every point of loading to be a joint of the structure, thus introducing additional unknown joint displacements that correspond to the loads. The disadvantage of such an approach is that it greatly increases the number of equations of equilibrium to be solved. A method preferred by most

structural analysts is to replace any loads that act between the joints by a set of statically equivalent loads acting at the joints. Of course, the use of equivalent joint loads is possible only when the principle of superposition is valid. The technique for determining the equivalent loads is not difficult to use, however we will not explain it here. Instead, readers should consult books on structural analysis for further details (for example, see Ref. 12-22).

12.7 COMPLEMENTARY-ENERGY METHODS

In the preceding section we dealt with several important principles pertaining to strain energy. Now we turn to a consideration of some analogous principles relating to complementary energy. It was pointed out in earlier discussions that strain energy is usually expressed as a function of displacements, whereas complementary energy is usually expressed in terms of forces. Thus, it is quite natural that strain energy is related to the displacement and stiffness methods of analysis, whereas complementary energy is related to the force and flexibility methods, as explained in the following discussions.

To derive a basic theorem relating to complementary energy, let us consider again a nonlinear structure subjected to n loads P_1, P_2, \dots, P_n that produce corresponding displacements $\delta_1, \delta_2, \dots, \delta_n$. As in our earlier discussions, it is understood that P and δ represent forces and corresponding displacements in a generalized sense. The complementary energy U^* of the structure is defined as being equal to the complementary work W^* of the loads (see the discussion in the middle of Section 12.5). When evaluating this work, we express the displacements in terms of the loads and then integrate, as shown in Eq. (12-29b). The resulting expression for U^* is a function of the loads P_1, P_2, \dots, P_n . Then, if we imagine that one load, say P_i , is given a small increase dP_i while the other loads are unchanged, the complementary energy will be increased by a small amount dU^* , given by the following equation:

$$dU^* = \frac{\partial U^*}{\partial P_i} dP_i$$

This equation states that the increase in U^* is equal to the rate of change of U^* with respect to P_i multiplied by the increment in P_i .

Another way to obtain an expression for dU^* is to consider the complementary work of the loads when the force P_i is increased by the amount dP_i . This complementary work is the same as the increase dU^* in the complementary energy of the structure. The only load that does any complementary work is P_i itself, because the other forces are not changed. Therefore, the increase in complementary energy is the product of the displacement δ_i and the increment dP_i of the load:

$$dU^* = \delta_i dP_i$$

Equating the two preceding expressions for dU^* , we obtain

$$\delta_i = \frac{\partial U^*}{\partial P_i} \quad (12-54)$$

This equation states that the partial derivative of the complementary energy with respect to any load P_i is equal to the corresponding displacement δ_i , provided that the complementary energy is expressed as a function of the loads. The equation is called the **Crotti-Engesser theorem**, after the Italian engineer Francesco Crotti who derived it in 1878 (Refs. 12-23 and 12-24) and the German engineer Friedrich Engesser who independently obtained it in 1889 (Ref. 12-25). The theorem can also be obtained directly from the definition of complementary energy (see Eqs. 12-22 and 12-29b) by taking the derivatives of both sides of the equations.

The Crotti-Engesser theorem provides a remarkable analogy with Castigliano's first theorem (Eq. 12-44). In the case of the Crotti-Engesser theorem, we express the complementary energy as a function of the loads and then obtain the corresponding displacements by taking derivatives with respect to the loads, whereas, in the case of Castigliano's first theorem, we express the strain energy as a function of the displacements and then obtain the corresponding loads by taking derivatives with respect to the displacements. Both theorems are very general and apply to structures that behave nonlinearly. However, as explained in Section 12.5, the complementary energy U^* of the structure must be obtained from the complementary work of the loads. If no geometric nonlinearities exist, the complementary energy U^* is equal to the sum of the complementary energies of the members; hence, the member energies can be used to obtain U^* . If there are geometric nonlinearities, then the complementary energy of the members is less than the complementary energy U^* of the structure.*

To illustrate the Crotti-Engesser theorem, let us again consider the materially nonlinear structure described in Example 1 of Section 12.5. The complementary energy of the structure (from Eq. 12-36) is

$$U^* = \frac{CP^3}{3}$$

Note that this equation gives U^* as a function of the load P corresponding to the deflection δ . From the Crotti-Engesser theorem we get

$$\delta = \frac{dU^*}{dP} = CP^2$$

which is the correct relation between load and deflection.

* In the special case of a structure that behaves linearly, the complementary energy is equal to the strain energy and the Crotti-Engesser theorem reduces to Castigliano's second theorem (see Section 12.8).

where σ_{ab} and σ_{bc} are the stresses in the bars. Now we can obtain the total complementary energy of the truss from Eqs. (a) through (d); the result is

$$U^* = \frac{AL}{3B^2} (\sigma_{ab}^3 + \sqrt{2}\sigma_{bc}^3) \quad (e)$$

The load P acting on the truss (Fig. 12-20a) produces stresses in the bars that can be found from equilibrium:

$$\sigma_{ab} = \frac{P}{A} \quad \sigma_{bc} = \frac{\sqrt{2}P}{A} \quad (f)$$

in which we consider only the absolute values of the stresses. Therefore, the complementary energy of the truss (Eq. e) is

$$U^* = \frac{5P^3L}{3A^2B^2} \quad (12-56)$$

This equation expresses the complementary energy as a function of the load P . The next step is to apply the Crotti-Engesser theorem to obtain the displacement corresponding to P , as follows:

$$\delta_v = \frac{dU^*}{dP} = \frac{5P^2L}{A^2B^2} \quad (12-57)$$

This equation gives the vertical deflection δ_v of joint B of the truss. To find the horizontal deflection δ_h of joint B , it is necessary to add a horizontal load Q corresponding to that deflection. We can then repeat the procedure for finding the complementary energy U^* , the difference being that U^* is now a function of both P and Q . Then we obtain the horizontal deflection δ_h by applying the Crotti-Engesser theorem and taking the derivative with respect to Q . The resulting expression for δ_h contains both P and Q . Setting Q equal to zero gives the equation for the horizontal deflection due to P acting alone (see Problem 12.7-2).

Unit-load method. The direct use of the Crotti-Engesser theorem in finding displacements of structures, as illustrated in the preceding example, requires that the complementary energy of the structure be determined as a function of the loads. Then the derivatives of the complementary energy must be evaluated in order to obtain the desired displacements. This procedure is quite lengthy, but fortunately a more practical method is available, as will now be explained.

To derive the method in the simplest manner, we will discuss a truss structure in which the only stress resultants are the axial forces. Let us consider an individual member of the truss and assume that it has length L and cross-sectional area A and that it is subjected to an axial force N . Then the complementary energy U^* of this member is

$$U^* = \int_0^N \epsilon_1 L dN_1 \quad (g)$$

as obtained from Eq. (12-22) with $\delta_1 = \epsilon_1 L$, where ϵ_1 is the uniform strain in the bar due to the axial force N_1 . We may note that, as the

axial force N_1 increases from its initial value of zero to its maximum value N , the strain ϵ_1 increases from zero to a maximum value ϵ . Similarly, the stress σ_1 in the bar increases from zero to a maximum value σ . The relationship between the stress σ_1 and the strain ϵ_1 is assumed to be represented by a nonlinear stress-strain diagram such as that shown in Fig. 12-15b.

It is convenient to define a function F representing the complementary energy per unit length of the bar; thus, dividing Eq. (g) by the length L , we obtain

$$F = \int_0^N \epsilon_1 dN_1 \quad (h)$$

The quantity F , which is a function of the axial force N , can be evaluated with the aid of the stress-strain curve. (Note that the stress-strain curve gives the relationship between ϵ_1 and σ_1 , but, since $N_1 = \sigma_1 A$, we also know the relationship between ϵ_1 and N_1 . Thus, the integral in Eq. h can be evaluated.)

Now consider a truss composed of many members and subjected to loads P_1, P_2, \dots, P_n that produce corresponding displacements $\delta_1, \delta_2, \dots, \delta_n$. Also, let us consider a typical element of the truss between two cross sections a distance dx apart (Fig. 12-3a). The axial force acting on this element is N , and the corresponding elongation is $d\delta$ (equal to ϵdx). Therefore, the complementary energy of the element is $dU^* = F dx$, where F is given by Eq. (h). The complementary energy of the entire structure is

$$U^* = \int F dx \quad (i)$$

where it is understood that the integration extends along the axes of all members of the structure. Since we are obtaining U^* by summing the complementary energies of the members, we are restricted to structures with only material nonlinearities.

To obtain the displacement δ_i corresponding to the load P_i , we apply the Crotti-Engesser theorem to Eq. (i), thereby obtaining

$$\delta_i = \frac{\partial U^*}{\partial P_i} = \frac{\partial}{\partial P_i} \left[\int F dx \right]$$

Differentiating under the integral sign, we get

$$\delta_i = \int \frac{\partial F}{\partial P_i} dx$$

Now consider the derivative $\partial F / \partial P_i$. The quantity F is a function of the axial force N , as already explained in connection with Eq. (h). The axial force N is a function of the applied loads P_1, P_2, \dots, P_n . Therefore, F is a function of P_i through the intermediate variable N . Hence, we can rewrite the preceding equation in the form

$$\delta_i = \int \frac{\partial F}{\partial N} \frac{\partial N}{\partial P_i} dx \quad (j)$$

$$U^* = \frac{3P^{4/3}L}{4\sqrt{EA}}$$

(see Eq. 12-40). Thus, the Crotti-Engesser theorem yields

$$\delta = \frac{dU^*}{dP} = \sqrt[3]{\frac{PL^3}{EA}}$$

which agrees with the previous analysis (see Eq. 12-38b).

A third example is the materially nonlinear cantilever beam of Example 3 of Section 12.5, for which the complementary energy is

$$U^* = \frac{25P^3L^4}{6B^2b^2h^5}$$

(see Eq. 12-43). We can now determine the deflection δ at the end of the beam:

$$\delta = \frac{dU^*}{dP} = \frac{25P^2L^4}{2B^2b^2h^5} \quad (12-55)$$

Note that this deflection varies nonlinearly with the load P .

Example 1

The truss ABC shown in Fig. 12-20a supports a vertical load P at joint B . The material of the truss has a stress-strain relationship in both tension and compression that is given by the equation $\sigma = B\sqrt{\epsilon}$, where B is a constant. Determine the vertical deflection δ_v of joint B .

The first step in finding the deflection by means of the Crotti-Engesser theorem is to obtain the complementary energy of the structure in terms of the force P . Because the truss has no geometric nonlinearities, then the total complementary energy U^* by summing the energies of the two bars:

$$U^* = U_{ab}^* + U_{bc}^* \quad (a)$$

The complementary energy of an individual bar can be found by multiplying the complementary energy density by the volume of the bar, inasmuch as the stress and strain remain constant throughout the bar. Therefore, we have

$$U_{ab}^* = u_{ab}^* AL \quad U_{bc}^* = u_{bc}^* AL\sqrt{2} \quad (b)$$

where A is the cross-sectional area of each bar. The complementary energy density of each bar can be obtained from Eq. (12-23), as follows:

$$u_{ab}^* = \int_0^{\sigma_{ab}} \epsilon_1 d\sigma_1 = \int_0^{\sigma_{ab}} \frac{\sigma_1^2}{B^2} d\sigma_1 = \frac{\sigma_{ab}^3}{3B^2} \quad (c)$$

$$u_{bc}^* = \int_0^{\sigma_{bc}} \epsilon_1 d\sigma_1 = \int_0^{\sigma_{bc}} \frac{\sigma_1^2}{B^2} d\sigma_1 = \frac{\sigma_{bc}^3}{3B^2} \quad (d)$$

Each of the derivatives in this expression has a simple physical interpretation. The derivative $\partial F/\partial N$ is equal to ϵ (see Eq. h).^{*} The derivative $\partial N/\partial P_i$ represents the value of the axial force N caused by a unit value of the load P_i . Thus, in the notation of the unit-load method (Section 12.3), this derivative is equal to N_U , which is defined as the axial force due to a unit load corresponding to the displacement δ_i . Replacing the derivatives in Eq. (j) with ϵ and N_U , respectively, we obtain

$$\delta_i = \int \epsilon N_U dx = \int N_U d\delta \quad (k)$$

where $d\delta$, equal to ϵdx , is the elongation of an element (see Fig. 12-3a). The preceding equation is the fundamental equation of the unit-load method (Eq. 12-3) for the case in which only axial deformations are considered.

A similar derivation can be made if the structure is subjected to flexural deformations (see Fig. 12-3b), as in the case of a beam or frame. Let us begin by assuming that we have a beam of length L in pure bending under the action of couples M . These couples cause a relative rotation θ between the two ends of the beam. The complementary energy of the beam is obtained from Eq. (12-22) by replacing P and δ with M and θ , respectively; thus,

$$U^* = \int_0^M \theta_1 dM_1 \quad (l)$$

where M is the maximum value of the couples M_1 . The angle θ_1 between the ends of the beam increases from zero to a maximum value θ as the applied couples M_1 increase from zero to M . Also, the curvature κ of the beam varies from zero to a maximum value $\kappa = \theta/L$. Replacing the angle θ_1 in Eq. (l) by $\kappa_1 L$, we get

$$U^* = \int_0^M \kappa_1 L dM_1 \quad (m)$$

Now let us define a new function G representing the complementary energy per unit length of the beam:

$$G = \int_0^M \kappa_1 dM_1 \quad (n)$$

This quantity is a function of the bending moment M and can be evaluated for any particular beam with the aid of the stress-strain diagram.

Now consider a beam or plane frame subjected to loads P_1, P_2, \dots, P_n that produce corresponding displacements $\delta_1, \delta_2, \dots, \delta_n$. A typical element of this structure (see Fig. 12-3b) is subjected to a bending moment M and undergoes a flexural deformation $d\theta$ (equal to κdx). Based upon Eq. (m), we obtain the complementary energy of this element as

^{*} From calculus we know that

$$\frac{\partial}{\partial a} \int_0^a f(x) dx = f(a)$$

Applying this relationship to Eq. (h), we have $a = N$, $f(x) = \epsilon$, $dx = dN$, and $f(a) = \epsilon$.

$dU^* = G dx$; hence, the complementary energy of the entire structure is

$$U^* = \int G dx$$

where the integration includes all elements of the structure. Next we get the displacement δ_i of this structure from the Crotti-Engesser theorem:

$$\delta_i = \frac{\partial U^*}{\partial P_i} = \frac{\partial}{\partial P_i} \left[\int G dx \right] = \int \frac{\partial G}{\partial P_i} dx$$

Referring to the last derivative in this expression, we note that the quantity G is a function of the bending moment M (see Eq. m) and that M is a function of the loads. Therefore, the preceding equation can be rewritten in the form

$$\delta_i = \int \frac{\partial G}{\partial M} \frac{\partial M}{\partial P_i} dx \quad (n)$$

In this equation, the derivative $\partial G/\partial M$ is equal to the curvature κ (see Eq. m and the previous footnote), and the derivative $\partial M/\partial P_i$ is the bending moment in the beam due to a unit value of the load P_i . Thus, Eq. (n) becomes

$$\delta_i = \int \kappa M_U dx = \int M_U d\theta \quad (o)$$

in which we have used the relationship $d\theta = \kappa dx$. The quantity M_U is the bending moment in the structure due to a unit load corresponding to the displacement δ_i . Thus, Eq. (o) is the same as the fundamental equation of the unit-load method (Eq. 12-3) when only flexural deformations are taken into account.

Similar derivations can be made for structures in which the effects of shearing and torsional deformations are considered. Hence, we finally conclude that the use of complementary energy and the Crotti-Engesser theorem leads directly to the unit-load method as expressed by Eq. (12-3). The method is a very efficient means of determining displacements and is valid for structures that have material nonlinearities (but not geometric nonlinearities).^{*}

Example 2

A cantilever beam of length L and rectangular cross section carries a concentrated load P at the free end (see Fig. 12-19 and Example 3 of Section 12.5). The stress-strain relationship of the material is represented by the equation $\sigma = B\sqrt{\epsilon}$, where B is a constant. Determine the deflection δ at the free end of the beam by using the unit-load method.

Because only flexural deformations are important in this beam, we will use only the second term in the unit-load equation (Eq. 12-3). The bending

^{*} The case of linear structures is discussed in Section 12.8.

moment M_U is the moment caused by a unit load corresponding to the deflection δ ; therefore, the moment M_U is numerically equal to $1 \cdot x$, where x is the distance measured from the free end of the beam (Fig. 12-19a). The deformation $d\theta$ is numerically equal to κdx , where κ is the curvature. For the beam under discussion, the curvature is given by Eq. (l) of Section 12.5; hence, the deformation $d\theta$ is

$$d\theta = \frac{50P^2 x^2}{B^2 b^2 h^3} dx \quad (p)$$

Substituting into the unit-load equation, we obtain the following expression for the deflection:

$$\delta = \int M_U d\theta = \int_0^L 1(x) \left(\frac{50P^2 x^2}{B^2 b^2 h^3} \right) dx = \frac{25P^2 L^4}{2B^2 b^2 h^3} \quad (q)$$

This result agrees with the deflection found previously (see Eq. 12-55). However, the unit-load method provides an easier solution than the earlier example, because it is not necessary to go through the lengthy process of evaluating the complementary energy (see the derivation of Eq. 12-43).

Example 3

The truss ABC shown in Fig. 12-20a supports a vertical load P at joint B . The material of the truss has a stress-strain relationship given by the equation $\sigma = B\sqrt{\epsilon}$, where B is a constant. Determine the vertical deflection δ_c of joint B by using the unit-load method.

Since axial forces are the only stress resultants in the truss, we will use only the first term of Eq. (12-3). The unit load corresponding to the deflection δ_c is a vertical load at joint B . The corresponding axial forces N_U in the two members of the truss are as follows:

$$(N_U)_{ab} = 1 \quad (N_U)_{bc} = -\sqrt{2}$$

The strains in the bars are obtained from the stress-strain relationship:

$$\epsilon_{ab} = \frac{\sigma_{ab}^2}{B^2} \quad \epsilon_{bc} = \frac{\sigma_{bc}^2}{B^2}$$

The stresses are $\sigma_{ab} = P/A$ and $\sigma_{bc} = -\sqrt{2}P/A$, as obtained from equilibrium. Substituting these stresses into the expressions for the strains, we get

$$\epsilon_{ab} = \frac{P^2}{A^2 B^2} \quad \epsilon_{bc} = -\frac{2P^2}{A^2 B^2}$$

Finally, we can substitute the values for N_U and $d\delta$ (equal to ϵdx) into the unit-load equation and obtain the deflection:

$$\delta_c = \int N_U d\delta = \int_0^L 1 \left(\frac{P^2}{A^2 B^2} \right) dx + \int_0^{\sqrt{2}L} (-\sqrt{2}) \left(-\frac{2P^2}{A^2 B^2} \right) dx = \frac{5P^2 L}{A^2 B^2} \quad (r)$$

This deflection is the same as the deflection obtained earlier in Example 1 of this section (see Eq. 12-57). However, we again may observe the simplicity of the solution by the unit-load method. The advantage of the unit-load method is even more pronounced if the deflection to be calculated does not correspond to one of the actual loads on the structure (see Problem 12.7-2).

Force method. The use of complementary energy and the Crotti-Engesser theorem leads to another important method for analyzing structures. This method, called the *force method*, is based upon the concept of statical indeterminacy and utilizes statical redundants as the unknown quantities in the analysis. The fact that force quantities (stress resultants and reactions) are the unknowns is consistent with the requirement that the complementary energy must be expressed as a function of the forces in order to apply the Crotti-Engesser theorem.

Let us consider a materially nonlinear structure having n degrees of statical indeterminacy. After selecting the redundant quantities X_1, X_2, \dots, X_n , we then release these redundants by making suitable releases in the structure. For instance, a support may be removed if the redundant is a reaction, or a pin may be inserted if the redundant is a bending moment. The resulting released structure must be statically determinate and immovable. Next, we visualize the released structure as being subject not only to the actual loads but also to the redundants themselves. In other words, the redundant actions must be treated as loads acting on the released structure. Then the complementary energy U^* of the released structure can be evaluated in the usual manner. The only new feature lies in the fact that the complementary energy of the released structure is a function of both the loads and the redundants. According to the Crotti-Engesser theorem, we can obtain the displacements of the released structure corresponding to the redundants by taking partial derivatives of the complementary energy with respect to those redundants. Let us denote by the symbols D_1, D_2, \dots, D_n the displacements of the original structure corresponding to the redundants X_1, X_2, \dots, X_n , respectively. Then the Crotti-Engesser theorem (Eq. 12-54) yields n simultaneous equations, as follows:

$$D_1 = \frac{\partial U^*}{\partial X_1} \quad D_2 = \frac{\partial U^*}{\partial X_2} \quad \dots \quad D_n = \frac{\partial U^*}{\partial X_n} \quad (12-58)$$

Each of these equations has the same general form. If we examine the i th equation, we find that the right-hand side consists of terms containing both the statical redundants and the loads, with the redundants being the unknown quantities. These terms add up to the true displacement D_i of the original structure, which will be zero whenever the corresponding redundant X_i is a stress resultant or a support reaction that does not undergo any displacement. Thus, we see that Eqs. (12-58) actually represent compatibility conditions for displacements corresponding to the redundants. These equations can be solved simultaneously for the redundants in terms of the loads, and then the remaining reactions and stress resultants can be determined by static equilibrium.

The complementary-energy method of analysis described in the preceding paragraph utilizes statical redundants as the unknown quantities and requires the solution of compatibility equations. It is called the **force method** of analysis, and it applies to materially nonlinear struc-

tures. In the case of a linear structure, the method is known as the flexibility method.*

The force method, as represented by Eqs. (12-58), is analogous to the displacement method, represented by Eqs. (12-45). In the force method we express the complementary energy as a function of statical redundants, and then we use the Crotti-Engesser theorem to obtain equations of compatibility that can be solved for the redundant forces. In the displacement method we express the strain energy as a function of unknown joint displacements, and then we use Castigliano's first theorem to obtain equations of equilibrium that can be solved for the joint displacements.

Now let us consider the particular case of the force method in which there are no displacements in the original structure corresponding to the statical redundants. As already mentioned, this situation will exist if the redundants are stress resultants or reactions at supports that do not move. Under these conditions the displacements D_1, D_2, \dots, D_n in the compatibility equations (Eqs. 12-58) are zero. Then the equations simplify to the following:

$$\frac{\partial U^*}{\partial X_1} = 0 \quad \frac{\partial U^*}{\partial X_2} = 0 \quad \dots \quad \frac{\partial U^*}{\partial X_n} = 0 \quad (12-59)$$

These equations represent the conditions for a stationary value of the complementary energy. For a structure in stable equilibrium, the stationary value is actually a minimum value; hence, Eqs. (12-59) represent the principle of minimum complementary energy. This principle states that the statical redundants X_1, X_2, \dots, X_n for a stable structure have values such that the complementary energy is a minimum, provided that there are no displacements corresponding to the redundants in the original structure.**

Example 4

The truss shown in Fig. 12-24a is constructed of a material having a stress-strain relationship given by the equation $\sigma = B\sqrt{\epsilon}$, where B is a constant. Find the axial forces in all three bars by using complementary energy and the force method.

Assuming that the reactive force at joint B is the statical redundant X , we

* The flexibility method is discussed further in Section 12.8.
 ** The principle of minimum complementary energy was formulated first by Crotti (Refs. 12-23 and 12-24) and later by Engesser (Ref. 12-25). If the structure behaves linearly, the complementary energy and the strain energy are equal; then the principle of minimum complementary energy reduces to the principle of minimum strain energy (see Section 12.8). The complementary-energy methods have provided the basis for significant progress in structural mechanics. The reader who is interested in additional study of the methods should consult other sources, such as Refs. 12-14, 12-15, 12-26, and 12-27. The history of complementary-energy methods was traced by Oravos and McLean (Ref. 2-5); other historical comments are given in Refs. 12-15, 12-28, and 12-29.

obtain the released structure shown in Fig. 12-24b. The axial forces in the bars of the released structure, from equilibrium, are as follows:

$$N_{ad} = N_{cd} = \frac{P - X}{\sqrt{2}} \quad N_{bd} = X \quad (s)$$

The corresponding stresses are

$$\sigma_{ad} = \sigma_{cd} = \frac{P - X}{\sqrt{2}A} \quad \sigma_{bd} = \frac{X}{A}$$

in which A is the cross-sectional area of each bar.

The complementary energy density of bar BD is obtained as follows (see Eq. 12-23):

$$u_{bd}^* = \int_0^{\sigma_{bd}} \epsilon d\sigma = \int_0^{\sigma_{bd}} \frac{\sigma^2}{B^2} d\sigma = \frac{\sigma_{bd}^3}{3B^2} = \frac{1}{3B^2} \left(\frac{X}{A} \right)^3$$

The complementary energy density of bars AD and CD can be obtained in a similar manner; the results are

$$u_{ad}^* = u_{cd}^* = \frac{1}{3B^2} \left(\frac{P - X}{\sqrt{2}A} \right)^3$$

Finally, we can multiply the complementary energy density of each bar by the volume of the bar, and then we can sum the results to obtain the total complementary energy of the released structure:

$$U^* = \frac{L}{3A^2B^2} [(P - X)^3 + X^3]$$

This expression for U^* is a nonlinear function of both the load P and the redundant X .

The displacement in the original structure corresponding to the redundant X is zero because there is no displacement at support B . Therefore, the Crotti-Engesser theorem, when applied to the redundant X , gives the following equation (see Eqs. 12-58 and 12-59):

$$\frac{dU^*}{dX} = \frac{L}{3A^2B^2} [3(P - X)^2(-1) + 3X^2] = 0$$

from which we get $X = P/2$. Substituting this value for X into Eqs. (s) yields

$$N_{ad} = N_{cd} = \frac{P}{2\sqrt{2}} \quad N_{bd} = \frac{P}{2}$$

Thus, the axial forces in the bars of this statically indeterminate, nonlinear truss have been found by the force method.

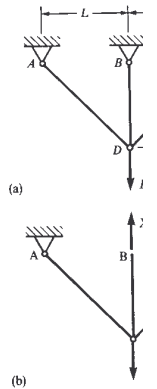


Fig. 12-24 Example

12.8 CASTIGLIANO'S SECOND THEOREM

In the preceding section we discussed the methods by which complementary energy may be used to find deflections and to analyze structures. We emphasized that the complementary-energy methods apply to

structures with nonlinear behavior. Let us now limit our discussion to structures that behave linearly and for which the principle of superposition applies. Under these conditions the complementary energy U^* and the strain energy U of the structure are equal.

Now assume that a linear structure is subjected to loads P_1, P_2, \dots, P_n and that these loads produce corresponding displacements $\delta_1, \delta_2, \dots, \delta_n$. Then both U and U^* may be expressed as quadratic functions of the loads (see Eq. 12-34). Also, we can replace U^* by U in the Crotti-Engesser theorem (Eq. 12-54) and obtain

$$\delta_i = \frac{\partial U}{\partial P_i} \quad (12-60)$$

This equation is known as Castigliano's second theorem, and it may be stated as follows: For a linear structure the partial derivative of the strain energy with respect to any load P_i is equal to the corresponding displacement δ_i , provided that the strain energy is expressed as a function of the loads. (For the history of this theorem, see Refs. 12-16 through 12-20.)

As an application of Castigliano's second theorem, let us consider a cantilever beam subjected to a load P and a couple M_0 acting at the free end (Fig. 12-25). The beam behaves linearly and has constant flexural rigidity EI . The strain energy of the beam can be found from Eq. (7-59a), which is repeated here:

$$U = \int \frac{M^2 dx}{2EI} \quad (12-61)$$

In this equation, M represents the bending moment at any cross section. For the beam shown in Fig. 12-25, the bending moment at distance x from the free end is $M = -Px - M_0$. Substituting this expression for M into Eq. (12-61), we get

$$U = \frac{1}{2EI} \int_0^L (-Px - M_0)^2 dx = \frac{P^2 L^3}{6EI} + \frac{PM_0 L^2}{2EI} + \frac{M_0^2 L}{2EI} \quad (a)$$

This equation expresses the strain energy U as a quadratic function of the loads P and M_0 .

In order to obtain the vertical deflection δ at the free end of the beam, we use Castigliano's second theorem and take the partial derivative of U with respect to P ; thus,

$$\delta = \frac{\partial U}{\partial P} = \frac{PL^2}{3EI} + \frac{M_0 L}{2EI}$$

In a similar manner, we can find the angle of rotation θ at the free end of the beam by taking the partial derivative of U with respect to M_0 :

$$\theta = \frac{\partial U}{\partial M_0} = \frac{PL}{2EI} + \frac{M_0}{EI}$$

The sign conventions for δ and θ are as follows. A positive sign for δ means that the deflection is in the same direction as the load P (that is, downward) and a positive sign for θ means that the angle of rotation has the same sense as the couple M_0 (that is, counterclockwise). As expected, both δ and θ are linear functions of the loads.

It is apparent that Castigliano's second theorem can be used only when finding displacements that correspond to loads acting on the structure, as is also the case for the Crotti-Engesser theorem. If the desired displacement does not correspond to a load, we must place a fictitious load on the structure corresponding to that displacement. Then we may calculate that displacement by using Castigliano's second theorem; the resulting expression for the displacement is in terms of both the actual loads and the fictitious load. By setting the fictitious load equal to zero, the displacement due to the actual loads is obtained.

Unit-load method. The process of finding displacements by a direct application of Castigliano's second theorem is cumbersome if more than two loads act on the structure. The reason is that the evaluation of the strain energy and its square is very lengthy. For instance, suppose that four loads act on the cantilever beam shown in Fig. 12-25 rather than two loads. Then the evaluation of the equation for the strain energy, analogous to Eq. (a), requires squaring a four-term expression, and the final result for U contains ten terms.

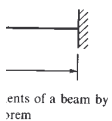
A considerable simplification in finding displacements is obtained if we apply Castigliano's second theorem before integrating the expression for the bending moment. To illustrate this point, consider a beam or frame in which only flexural deformations are important; then the strain energy U is given by Eq. (12-61). To obtain the deflection δ_i corresponding to the load P_i , we must take the partial derivative of U with respect to P_i . Thus, differentiating under the integral sign, we obtain

$$\delta_i = \frac{\partial U}{\partial P_i} = \frac{\partial}{\partial P_i} \int \frac{M^2 dx}{2EI} = \int \frac{M}{EI} \frac{\partial M}{\partial P_i} dx \quad (b)$$

The partial derivative $\partial M / \partial P_i$ represents the value of the bending moment M caused by a unit value of the load P_i . Thus, this derivative is equal to M_i , which is the bending moment in the structure due to a unit load corresponding to the desired displacement. The moment M appearing under the integral sign in Eq. (b) is the bending moment due to the actual loads on the structure; hence, this moment is equal to M_L . Using this notation, we see that Eq. (b) becomes

$$\delta_i = \int \frac{M_L M_i dx}{EI}$$

This equation is the unit-load equation (see Eq. 12-4) for the case when only flexural deformations are considered.



Similar derivations can be made for the effects of axial, shearing, and torsional deformations. We conclude, therefore, that the unit-load method as applied to linear structures (Eq. 12-4) can be derived directly from Castigliano's second theorem. This result is not surprising since we have already shown that the more general equation of the unit-load method (Eq. 12-3), which is applicable to nonlinear structures, can be derived from the Crotti-Engesser theorem. As already pointed out, the unit-load method is an efficient method for determining displacements of structures, and ordinarily it should be used instead of Castigliano's second theorem.

Flexibility method. In the preceding section we saw how complementary energy and the Crotti-Engesser theorem lead to the force method of structural analysis. A special case of the force method, called the **flexibility method**, occurs when the structure behaves linearly. Under such conditions the strain energy of the released structure, which is equal to the complementary energy, may be expressed as a quadratic function of both the loads and the statical redundants X_1, X_2, \dots, X_n . Then the application of Castigliano's second theorem leads to the following simultaneous equations:

$$D_1 = \frac{\partial U}{\partial X_1} \quad D_2 = \frac{\partial U}{\partial X_2} \quad \dots \quad D_n = \frac{\partial U}{\partial X_n} \quad (12-62)$$

in which D_1, D_2, \dots, D_n represent the displacements in the original structure corresponding to the redundants. The general form of each of these equations is the same. The right-hand sides consist of terms that represent displacements corresponding to the redundants; some of the displacements are due to the redundants themselves and others are due to the actual loads on the structure. These terms add up to the true displacements in the original structure, which are zero whenever the corresponding redundants are either stress resultants or reactions that do not undergo any displacements. Hence, we conclude that Eqs. (12-62) are equations of compatibility that can be solved simultaneously for the redundants in terms of the loads. Thus, Eqs. (12-62) are a special case of the compatibility equations for the force method (Eqs. 12-58), because we can use the strain energy U in place of the complementary energy U^* when a structure behaves linearly. Equations (12-62) are the equations of the flexibility method, which is the counterpart of the stiffness method.*

A special case arises whenever the redundants are either stress resultants or reactions that do not undergo any displacements. In such cases the displacements in the original structure corresponding to the

* The flexibility method was originated by J. C. Maxwell in 1864 and O. Mohr in 1874 (Refs. 12-1, 12-13, and 12-30), and it is often called the *Maxwell-Mohr method*. This commonly used method of structural analysis is discussed in detail in textbooks on structural analysis (for example, see Ref. 12-22).

redundants are zero; hence, the equations of the flexibility method (Eqs. 12-62) become

$$\frac{\partial U}{\partial X_1} = 0 \quad \frac{\partial U}{\partial X_2} = 0 \quad \dots \quad \frac{\partial U}{\partial X_n} = 0 \quad (12-63)$$

These equations represent the conditions for a stationary value of the strain energy. If the structure is in stable equilibrium, the stationary value is actually a minimum value. Therefore, Eqs. (12-63) represent the **principle of minimum strain energy**, which states that for a linear structure the redundant quantities X_1, X_2, \dots, X_n have values such that the strain energy is a minimum, provided that there are no displacements corresponding to the redundants in the original structure. The principle of minimum strain energy is a special case (for linear structures) of the more general principle of minimum complementary energy (Eqs. 12-59).*

In order to show in more detail the general form of the equations of the flexibility method (Eqs. 12-62), let us take a specific illustration. Assume that a certain structure is statically indeterminate to the second degree and that it supports two loads P_1 and P_2 . Then the strain energy of the released structure, which is a quadratic function of the two redundants X_1 and X_2 and the loads P_1 and P_2 , will have the following general form (see Eq. 12-34):

$$U = a_{11}X_1^2 + a_{12}X_1X_2 + a_{13}X_1P_1 + a_{14}X_1P_2 \\ + a_{21}X_2X_1 + a_{22}X_2^2 + a_{23}X_2P_1 + a_{24}X_2P_2 \\ + a_{31}P_1X_1 + a_{32}P_1X_2 + a_{33}P_1^2 + a_{34}P_1P_2 \\ + a_{41}P_2X_1 + a_{42}P_2X_2 + a_{43}P_2P_1 + a_{44}P_2^2$$

where the coefficients $a_{11}, a_{12}, \dots, a_{44}$ are constants that depend only upon the properties of the structure. The application of Castigliano's second theorem to the above expression for U gives the equations of compatibility (Eqs. 12-62):

$$D_1 = \frac{\partial U}{\partial X_1} = F_{11}X_1 + F_{12}X_2 + b_{11}P_1 + b_{12}P_2$$

$$D_2 = \frac{\partial U}{\partial X_2} = F_{21}X_1 + F_{22}X_2 + b_{21}P_1 + b_{22}P_2$$

in which the coefficients F and b are new constants that are obtained from the a 's and that depend only upon the properties of the structure. The constants $F_{11}, F_{12}, F_{21}, F_{22}$ are coefficients of the unknown redundants and are known as the **flexibility coefficients**, or **flexibilities**, of the released structure. The remaining terms depend only upon the loads P_1 and P_2 and the properties of the structure. These terms are the

* The principle of minimum strain energy is also known as the *principle of least work*. This name was used by L. F. Ménétreau, who first stated the principle in 1858 although without a satisfactory proof, and by Castigliano, who proved it in 1873 (see Refs. 12-16 through 12-20 and Ref. 12-31).

displacements of the released structure corresponding to the redundants and caused by the loads.

Suppose we now take additional partial derivatives of the preceding equations, as follows:

$$\frac{\partial D_1}{\partial X_1} = \frac{\partial^2 U}{\partial X_1^2} = F_{11} \quad \frac{\partial D_1}{\partial X_2} = \frac{\partial^2 U}{\partial X_2 \partial X_1} = F_{12} \\ \frac{\partial D_2}{\partial X_1} = \frac{\partial^2 U}{\partial X_1 \partial X_2} = F_{21} \quad \frac{\partial D_2}{\partial X_2} = \frac{\partial^2 U}{\partial X_2^2} = F_{22}$$

From these relationships we can readily discern the following general equation for the flexibilities:

$$F_{ij} = \frac{\partial^2 U}{\partial X_j \partial X_i} \quad (12-64)$$

This equation shows that the flexibilities for the released structure can be obtained from the strain energy U by the process of differentiation whenever the strain energy is expressed as a quadratic function of the statical redundants X_1, X_2, \dots, X_n . Also, because the order of differentiation of U is immaterial, we can write

$$F_{ij} = \frac{\partial^2 U}{\partial X_j \partial X_i} = \frac{\partial^2 U}{\partial X_i \partial X_j} = F_{ji} \quad (12-65)$$

Thus, the reciprocal theorem for flexibilities is established from strain-energy considerations.

Other methods of structural analysis. In addition to the flexibility method and the stiffness method, numerous other methods of structural analysis are of importance to engineers. For example, *matrix methods of structural analysis* are in common usage. The matrix methods consist of the flexibility and stiffness methods with the refinement that all equations are presented in matrix form and all derivations and calculations are performed with the aid of matrix algebra. The use of matrices makes the methods more systematic, provides compactness of presentation, and is ideally suited for computer programming.* The most general method for the numerical analysis of structures (including plates, shells, and solid continua) is the *finite-element method* (Ref. 12-32). These advanced methods of analysis require a thorough understanding of mechanics of materials, including the concepts of strain energy and complementary energy.

*12.9 SHEAR DEFLECTIONS OF BEAMS

Because the effects of shear deformations on the deflections of beams are usually relatively small compared to the effects of flexural

* Matrix methods of structural analysis are described in textbooks on structural theory (for example, see Ref. 12-22). A working knowledge of matrix algebra can be obtained from engineering mathematics books (for example, see Ref. 6-1).

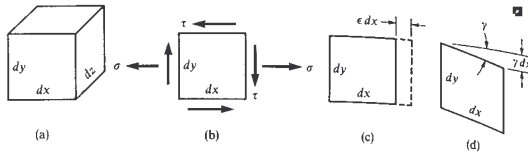
deformations, it is common practice to disregard them. However, if greater accuracy is required, the shear deflections can be determined and added to the bending deflections. This topic was discussed in Section 7.12, where we made a deflection analysis by using the differential equation of the deflection curve. The method consisted of adding a new term, containing the shear coefficient α_s , to the differential equation. The shear coefficient is the ratio of the shear stress at the neutral axis of the beam to the average shear stress (as an example, for a rectangular beam, $\alpha_s = 3/2$). The shear coefficient also appears in the equation of the unit-load method (Eq. 12-4).

Shear deflections obtained either by solving the differential equation or by using the unit-load method are approximate for at least two reasons: First, the deflections are based upon the shear strains at the neutral axis; hence, they do not take into account the variation in shear strains throughout the height of the beam. Second, the deflections are based upon a bending theory derived for the case of pure bending only. The latter defect can be remedied only by turning to the more exact methods of theory of elasticity, some results of which are given in Section 7.12, whereas the former defect can be removed by using the principle of virtual work (Eq. 12-1) and obtaining the internal work by integrating throughout the volume of the beam. This approach leads to a new shear factor in place of the shear coefficient α_s , as explained in the following paragraphs.

The unit-load method for obtaining beam deflections is based upon the principle of virtual work (see Sections 12.2 and 12.3). The method requires that expressions for both external and internal work be obtained. Because the unit load is the only load on the structure, the expression for the external work is $W_{\text{ext}} = 1 \cdot \Delta$, as given by Eq. (a) of Section 12.3. In that equation, Δ represents the desired deflection due to the actual loads on the beam and the 1 represents the unit load corresponding to that deflection.

The internal virtual work is the work performed by the stresses in the beam (the stresses are caused by the unit load) as those stresses move through the deformations caused by the actual loads. Previously, we considered four possible stress resultants: axial force, bending moment, shear force, and torque. Because we are now limiting our attention to shear deflections of beams, we will omit the effects of axial forces and torques. Also, in the previous derivation we obtained the internal virtual work by multiplying each stress resultant by the appropriate deformation quantity for a beam element; in this way we obtained Eq. (b) of Section 12.3. Now, however, we will deal directly with the stresses in the beam and integrate over the volume of the beam to obtain the internal virtual work.

Let us consider a differential element of dimensions dx, dy, dz (Fig. 12-26a) from the interior of a beam subjected to a unit load. Acting on the sides of this element are normal stresses σ and shear stresses τ (Fig. 12-26b) caused by the bending moment M_0 and the shear force V_0 pro-



m a beam

duced by the unit load. These stresses can be calculated from the flexure and shear formulas:

$$\sigma = \frac{M_U y}{I} \quad \tau = \frac{V_U Q}{Ib}$$

When using the unit-load method, the virtual deformations imparted to the element are chosen to be the same as the deformations caused by the actual loads. These loads produce bending moments M_L and shear forces V_L . The corresponding deformations consist of an extension (Fig. 12-26c) caused by the moment M_L and a shear distortion (Fig. 12-26d) caused by the shear force V_L . The extensional strain ϵ and the shear strain γ associated with these deformations are

$$\epsilon = \frac{M_L y}{EI} \quad \gamma = \frac{V_L Q}{GIb}$$

Therefore, the internal virtual work of the stresses σ and τ acting on the differential element is

$$dW_{int} = (\sigma dy dz)(\epsilon dx) + (\tau dy dz)(\gamma dx)$$

$$= \frac{M_U M_L y^2}{EI^2} dx dy dz + \frac{V_U V_L Q^2}{GI^2 b^2} dx dy dz$$

The total internal work is obtained by integrating the above expression throughout the volume of the beam; thus,

$$W_{int} = \int \frac{M_U M_L y^2}{EI^2} dx dy dz + \int \frac{V_U V_L Q^2}{GI^2 b^2} dx dy dz$$

This expression may be simplified by noting that, at a given cross section of the beam, the following quantities are constants: M_U , M_L , V_U , V_L , E , G , and I . Therefore, we can separate each of the preceding integrals into an integration over the cross-sectional area and an integration along the axis of the beam, as follows:

$$W_{int} = \int_L \frac{M_U M_L}{EI^2} \left[\int_A y^2 dy dz \right] dx + \int_L \frac{V_U V_L}{GI^2} \left[\int_A \frac{Q^2}{b^2} dy dz \right] dx \quad (a)$$

where the symbols L and A denote that the integration is to be carried out over the length L of the beam and over the cross-sectional area A , respectively.

The first term in brackets in Eq. (a) is the moment of inertia I , a property of the cross section. The second term in brackets is also dependent only upon the cross-sectional dimensions of the beam. Therefore, we define a new cross-sectional property f_s , called the **form factor for shear**, as follows:

$$f_s = \frac{A}{I^2} \int_A \frac{Q^2}{b^2} dA \quad (12-66)$$

where $dA = dy dz$ represents an element of area in the cross section of the beam. The form factor is a dimensionless quantity that can be evaluated for each particular shape of beam, as illustrated later.

Replacing the two terms in brackets in Eq. (a) with I and $f_s I^2/A$, respectively, we get the expression for internal virtual work:

$$W_{int} = \int \frac{M_U M_L dx}{EI} + \int \frac{f_s V_U V_L dx}{GA} \quad (b)$$

Finally, the **unit-load equation** for the deflection Δ is obtained by equating external work (equal to $1 \cdot \Delta$) with internal work (Eq. b):

$$\Delta = \int \frac{M_U M_L dx}{EI} + \int \frac{f_s V_U V_L dx}{GA} \quad (12-67)$$

Equation (12-67) may be used to find beam deflections when considering the effects of both bending moments and shear forces. The first term on the right-hand side of the equation is the same as the flexural term obtained previously (see Eq. 12-4). The second term differs slightly, however, from the previously obtained shear term; the difference lies in the replacement of the shear coefficient α_s by the form factor f_s . Thus, the **shearing rigidity** of a beam is now defined as GA/f_s instead of GA/α_s .

The form factor for shear must be evaluated for each particular shape of cross section. For example, if the cross section is rectangular with width b and height h , the expression for the first moment Q (see Fig. 5-24 and Eq. c of Section 5.5) is





$$Q = \frac{b}{2} (h^2 - y_1^2)$$

Also, for a rectangular beam the quantity A/I^2 equals $144/bh^5$. Therefore, the form factor is

$$f_s = \frac{144}{bh^5} \int_{-h/2}^{h/2} \frac{1}{4} (h^2 - y_1^2)^2 b dy_1 = \frac{6}{5}$$

In an analogous manner the form factors for other cross sections can be calculated. For instance, the form factor for a solid circular section equals 10/9 and for a thin tubular section equals 2. For an I-beam or box beam, we can assume that the shear stress is uniformly distributed over the height of the web and is approximately equal to the shear force divided by the area of the web (see Section 5.6 and Fig. 5-28). These

Table 12-4 Shear coefficient α_s and form factor f_s

Section	α_s	f_s
 Rectangle	$\frac{3}{2}$	$\frac{6}{5}$
 Circle	$\frac{4}{3}$	$\frac{10}{9}$
 Thin tube	2	2
 I-section or box section	$\frac{A}{A_{web}}$	$\frac{A}{A_{web}}$

assumptions lead to the conclusion that the form factor for such a beam is A/A_{web} , a ratio that typically is in the range of 2 to 5. A listing of values of the shear coefficient α_s and the form factor f_s is given in Table 12-4.

To illustrate the determination of shear deflections in a beam by using the unit-load method, let us obtain the deflection at the middle of a uniformly loaded beam with simple supports. With the coordinate distance x measured from the left-hand support of the beam, the expressions for the bending moment and shear force due to the actual load are

$$M_L = \frac{qLx}{2} - \frac{qx^2}{2} \quad V_L = \frac{qL}{2} - qx$$

where L is the length of the beam and q is the intensity of the uniform load. The unit load acting at the middle of the beam produces the following bending moments and shear forces:

$$M_U = \frac{1(x)}{2} \quad V_U = \frac{1}{2} \quad \left(0 \leq x \leq \frac{L}{2} \right)$$

Substitution of the above quantities into Eq. (12-67) yields the following expression for the deflection δ at the middle of the beam:

$$\delta = \frac{2}{EI} \int_0^{L/2} x \left(\frac{qLx}{2} - \frac{qx^2}{2} \right) dx + \frac{2f_s}{GA} \int_0^{L/2} \frac{1}{2} \left(\frac{qL}{2} - qx \right) dx$$

$$= \frac{5qL^4}{384EI} \left(1 + \frac{48f_s EI}{5GA L^2} \right) \quad (12-68)$$

This result agrees with the result obtained by solving the differential equation (see Eq. 7-76) except that the form factor f_s appears in place of the shear coefficient α_s . Similarly, if we use the unit-load method for the

case of a concentrated load P acting at the middle of a simple beam, we get for the deflection at the middle

$$\delta = \frac{PL^3}{48EI} \left(1 + \frac{12f_s EI}{GAL^2} \right) \quad (12-69)$$

which is the same as Eq. (7-80) if α_s is replaced by f_s .

For a cantilever beam with a concentrated load P at the free end, the unit-load method yields

$$\delta = \frac{PL^3}{3EI} + \frac{f_s PL}{GA} \quad (12-70)$$

as the deflection at the free end. Note that, in obtaining this result by the unit-load method, we did not make any assumptions about the support details at the fixed end. However, the second term on the right-hand side of Eq. (12-70) is consistent with the previous example of Section 7.12 for the particular case in which the boundary conditions at the fixed support are assumed to be such that warping occurs freely and the vertical side of an element located at the neutral axis remains vertical (see Eq. j, Section 7.12). For other conditions at the fixed support, the method of Section 7.12 gives different results (for instance, see Eq. k of Section 7.12). Thus, assumptions about the boundary conditions at a fixed support are implied when the unit-load method is used.

Strain energy of shear. The strain energy of shear in an element of a beam subjected to shear stresses τ (see Figs. 12-26b and d) is equal to $u dx dy dz$, where u is the strain energy of shear per unit volume. The strain energy per unit volume is $u = \tau^2/2G$, as given by Eq. (3-37a). Thus, we can express the strain energy of shear dU_s in terms of the shear stress τ as follows:

$$dU_s = \frac{\tau^2}{2G} dx dy dz$$

Since the shear stress τ is equal to VQ/Ib , the strain energy of shear becomes

$$dU_s = \frac{V^2 Q^2}{2GI^2 b^2} dx dy dz$$

Integrating this expression throughout the volume of the beam gives the total strain energy of shear:

$$U_s = \int_L \frac{V^2}{2GI^2} \left[\int_A \frac{Q^2}{b^2} dy dz \right] dx$$

where, as before, the symbols L and A indicate that the integrals are evaluated along the length of the beam and over the cross-sectional area, respectively. The term in brackets is equal to $f_s I^2/A$, as shown by

comparison with Eq. (12-66). Therefore, the expression for U_s simplifies to

$$U_s = \int \frac{f_s V^2 dx}{2GA} \quad (12-71)$$

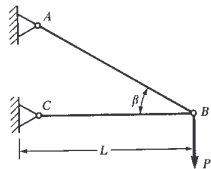
This equation gives the shear strain energy of a beam in terms of the shear force V . It is the same as the previously derived equation for shear strain energy (Eq. 7-84) except that α_s is replaced by f_s .

The form factor f_s has values that are very close to the values obtained by the more accurate methods of theory of elasticity (see Eqs. 7-83). Therefore, we recommend that the form factor f_s , instead of the shear coefficient α_s , be used when finding beam deflections and evaluating strain energy due to the effects of shear.

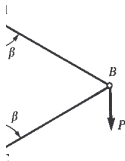
EMS / CHAPTER 12

for Section 12.3 are to be solved by the method.

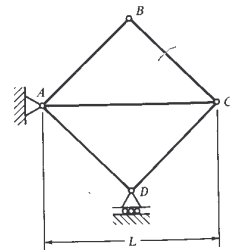
Truss ABC consisting of two members (see figure) supports a vertical load P at joint B. Each member has axial rigidity EA . Assuming $\beta = 60^\circ$, determine the following: (a) the vertical deflection δ_v of joint B, (b) the horizontal deflection δ_h of joint B, and (c) the rotation θ_{AB} of member AB.



Probs. 12.3-4 and 12.3-5



12.3-6 The four outside bars of the square truss shown in the figure have their temperatures lowered by an amount ΔT . What is the change in distance between joints B and D?



Prob. 12.3-6

1, 12.3-2, and 12.3-3

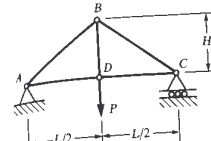
Solve the preceding problem assuming that members are subjected to a uniform temperature increase ΔT .

Solve Problem 12.3-1 for $\beta = 45^\circ$.

Determine the vertical deflection δ_v and horizontal deflection δ_h of joint B of the truss shown in the figure if members have axial rigidity EA and $\beta = 30^\circ$.

Solve the preceding problem for $\beta = 45^\circ$.

12.3-7 A symmetric truss ABCD has height $H = 3$ m and span length $L = 8$ m (see figure). A load $P = 100$ kN acts vertically at joint D. The cross-sectional area of each tension member is $A_t = 13$ cm² and of each compression member is $A_c = 32$ cm². The truss is made of steel with $E = 200$ GPa. Calculate the horizontal deflection δ_h of joint C and the vertical deflection δ_v of joint D.

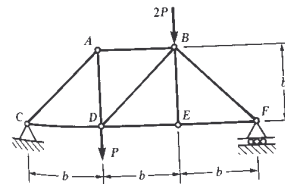


Probs. 12.3-7, 12.3-8, and 12.3-9

12.3-8 Solve the preceding problem for a truss with the following data: $H = 2$ m, $L = 4$ m, $P = 100$ kN, $A_t = 1200$ mm², $A_c = 2800$ mm², and $E = 210$ GPa.

12.3-9 Refer to the truss ABCD described in Problem 12.3-7 and assume $P = 0$. In order to eliminate the appearance of sagging under load, the truss will be constructed with an upward deflection, called *camber*, of joint D. By what amount ΔL should members AB and BC be increased in length (as compared to their theoretical lengths of 5 m) in order that the camber of joint D will be 12 mm?

12.3-10 The truss shown in the figure is constructed of nine bars, each having axial rigidity EA . Loads P and $2P$ act at joints D and B, respectively. Determine the following quantities: (a) the vertical deflection δ_v of joint A and (b) the increase δ_{AC} in the distance between joints A and E.

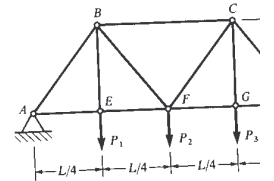


Prob. 12.3-10

12.3-11 A steel truss supports three loads as shown in the figure. The cross-sectional members are as follows:

- Members AB and CD: Area =
- Members AE, EF, FG, and GD: Area =
- Member BC: Area =
- Members BE, BF, CF, and CG: Area =

Calculate the vertical and horizontal deflection of joint F. Use the following data: $P_1 = P = 20$ kN, $A_1 = 40$ cm², $A_2 = 20$ cm², $A_3 = 14$ cm², $L = 12$ m, $H = 4$ m, and $E = 200$ GPa.

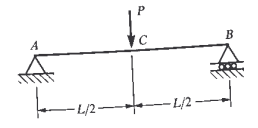


Probs. 12.3-11, 12.3-12, and 12.3-13

12.3-12 Refer to the truss described in the preceding problem and calculate the angle of rotation θ of member BC and the decrease δ_{BG} in the distance between joints B and G.

12.3-13 Solve Problem 12.3-11 using $P_1 = 30$ kN, $P_2 = 40$ kN, $P_3 = 20$ kN, $A_1 = 2000$ mm², $A_2 = 3000$ mm², $A_3 = 16$ mm², $H = 3$ m, and $E = 200$ GPa.

12.3-14 A simple beam AB of length l supports a concentrated load P (see figure). Determine the deflection δ and the angle of rotation θ_c at the left-hand end.



Prob. 12.3-14

APPENDIX

Centroids and Moments of Inertia of Plane Areas

C.1 CENTROIDS OF AREAS

The location of the **centroid** of a plane area is an important geometric property of the area.* To define the coordinates of the centroid, let us refer to the area A and the xy coordinate system shown in Fig. C-1. A differential element of area dA , with coordinates x and y , is shown in the figure. The total area A is defined as the following integral:

$$A = \int dA \quad (C-1)$$

In addition, the **first moments** of the area about the x and y axes, respectively, are

$$Q_x = \int y dA \quad Q_y = \int x dA \quad (C-2)$$

The coordinates \bar{x} and \bar{y} of the centroid C (Fig. C-1) are equal to the first moments divided by the area itself:

$$\bar{x} = \frac{\int x dA}{\int dA} = \frac{Q_y}{A} \quad \bar{y} = \frac{\int y dA}{\int dA} = \frac{Q_x}{A} \quad (C-3)$$

If the boundaries of the area are defined by simple mathematical expressions, we can evaluate the integrals appearing in Eqs. (C-3) in closed

* In accord with common terminology, we use the term "area" to mean *plane surface*. Strictly speaking, area is a measure of the size of a surface and is not the same thing as the surface itself.

form and thereby obtain formulas for \bar{x} and \bar{y} . A table of formulas obtained in this manner is given in Appendix D.

If an area is **symmetric about an axis**, the centroid must lie on that axis because the first moment about an axis of symmetry equals zero. For example, the centroid of the singly symmetric area shown in Fig. C-2 must lie on the x axis, which is the axis of symmetry; hence, only one distance must be calculated in order to locate C . If an area has two axes of symmetry, as in the case of the section shown in Fig. C-3, the position of the centroid can be determined by inspection because it lies at the intersection of the axes of symmetry. An area of the type shown in Fig. C-4 is **symmetric about a point**. It has no axes of symmetry, but there is a point (called the *center of symmetry*) such that every line in the area drawn through that point is symmetric about that point. Of course, the centroid coincides with the center of symmetry, and therefore the centroid can be located by inspection.

If the boundaries of the area are irregular curves not defined by mathematical expressions, then we can evaluate the integrals in Eqs. (C-3) by approximate numerical methods. The simplest procedure is to divide the area into small elements of area ΔA_i and replace the integrations with summations:

$$A = \sum_{i=1}^n \Delta A_i \quad Q_x = \sum_{i=1}^n y_i \Delta A_i \quad Q_y = \sum_{i=1}^n x_i \Delta A_i \quad (C-4)$$

in which n is the total number of elements of area, y_i is the y coordinate of the centroid of area ΔA_i , and x_i is the x coordinate of the centroid of area ΔA_i . The accuracy of the calculations for \bar{x} and \bar{y} depends upon how closely the selected elements fit the actual area.

Example

A parabolic semisegment OAB is bounded by the x axis, the y axis, and a parabolic curve (Fig. C-5). The equation of the curve is

$$y = f(x) = h \left(1 - \frac{x^2}{b^2} \right) \quad (a)$$

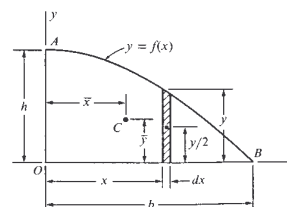


Fig. C-5 Example. C parabolic semisegment

C.1 Centroid

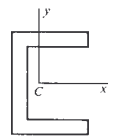


Fig. C-2 Area with symmetry

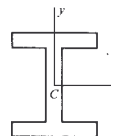


Fig. C-3 Area with symmetry

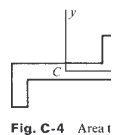


Fig. C-4 Area with a point

in which b is the base and h is the height of the semisegment. Locate the centroid C of the semisegment.

To carry out this analysis, we will select an element of area dA in the form of a thin strip of width dx and height y , as shown in the figure. The area of this element is

$$dA = y dx = h \left(1 - \frac{x^2}{b^2} \right) dx$$

and, therefore, the area of the segment is

$$A = \int dA = \int_0^b h \left(1 - \frac{x^2}{b^2} \right) dx = \frac{2bh}{3} \quad (b)$$

The first moment of the element of area about any axis can be obtained by multiplying the area of the element by the distance from its centroid to the axis. Since the x and y coordinates of the centroid of the element are x and $y/2$, respectively, the first moments are

$$Q_x = \int \frac{y}{2} dA = \int_0^b \frac{h^2}{2} \left(1 - \frac{x^2}{b^2} \right) dx = \frac{4bh^2}{15}$$

$$Q_y = \int x dA = \int_0^b hx \left(1 - \frac{x^2}{b^2} \right) dx = \frac{bh^2h}{4}$$

Now we can determine the coordinates of the centroid C as follows:

$$\bar{x} = \frac{Q_y}{A} = \frac{3b}{8} \quad \bar{y} = \frac{Q_x}{A} = \frac{2h}{5} \quad (c)$$

This problem may also be solved by taking the element of area dA as a horizontal strip of height dy and width

$$x = b \sqrt{1 - \frac{y}{h}}$$

which is obtained by solving Eq. (a) for x in terms of y . Yet another possibility is to take the element as a rectangle of width dx and height dy ; in this case, the expressions for A , Q_x , and Q_y are in the form of double integrals.

C.2 CENTROIDS OF COMPOSITE AREAS

In engineering work we frequently need to locate the centroid of an area composed of several parts, each part having a familiar geometric shape (such as a rectangle, a triangle, or a wide-flange section). Examples of such composite areas are the cross sections of beams, which often are composed of rectangular areas (for instance, see Figs. C-2, C-3, and C-4). The area and first moments of a composite area may be calculated by

summing the corresponding properties of its parts:

$$A = \sum_{i=1}^n A_i \quad Q_x = \sum_{i=1}^n y_i A_i \quad Q_y = \sum_{i=1}^n x_i A_i \quad (C-5)$$

in which A_i is the area of the i th part, x_i and y_i are the coordinates of the centroid of the i th part, and n is the number of parts. Note that it is possible to treat the absence of an area as a "negative area"; for instance, this concept is useful when a hole exists in an otherwise regular figure. Having found A , Q_x , and Q_y from Eqs. (C-5), we can determine the coordinates of the centroid from Eqs. (C-3).

To illustrate the procedure, let us consider the special case of a composite area that can be divided conveniently into two parts. The L-shaped area shown in Fig. C-6 is of this kind, because it can be divided into two rectangles of areas A_1 and A_2 . These rectangles have centroids C_1 and C_2 with known coordinates (x_1, y_1) and (x_2, y_2) , respectively. Thus, we obtain the following equations from Eqs. (C-5):

$$A = A_1 + A_2 \quad Q_x = y_1 A_1 + y_2 A_2 \quad Q_y = x_1 A_1 + x_2 A_2$$

Therefore, the coordinates of the centroid C are

$$\bar{x} = \frac{Q_y}{A} = \frac{x_1 A_1 + x_2 A_2}{A_1 + A_2} \quad \bar{y} = \frac{Q_x}{A} = \frac{y_1 A_1 + y_2 A_2}{A_1 + A_2} \quad (C-6)$$

(see Eqs. C-3). When an area is divided into only two parts, the centroid C of the entire area lies on the line joining the centroids C_1 and C_2 of the parts, as shown in the figure.

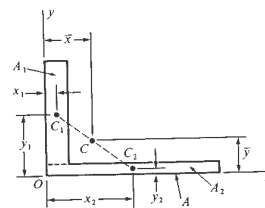


Fig. C-6 Centroid of a consisting of two parts

Example

The cross-section of a beam constructed of a $457 \times 191 \times 98$ kg UB section with a 150×12 mm cover plate welded to the top flange and a $254 \times 76 \times 28.3$ kg

channel section welded to the bottom flange is shown in Fig. C-7. Locate the centroid C of the cross-sectional area.

Let us denote the centroids of the cross-sectional areas of the cover plate, the UB section, and the channel section as C_1 , C_2 , and C_3 , respectively. Also, the corresponding areas are

$$A_1 = (150 \text{ mm})(12 \text{ mm}) = 18 \text{ cm}^2$$

$$A_2 = 125.2 \text{ cm}^2 \quad A_3 = 36 \text{ cm}^2$$

in which the areas A_2 and A_3 are obtained from Tables E-1 and E-4, Appendix E. If the x and y axes are taken with origin at C_2 , the centroidal distances for the three areas are

$$y_1 = \frac{467.4 \text{ mm}}{2} + \frac{12 \text{ mm}}{2} = 239.7 \text{ mm}$$

$$y_2 = 0 \quad y_3 = \frac{467.4 \text{ mm}}{2} + 18.6 \text{ mm} = 252.3 \text{ mm}$$

in which the pertinent dimensions of the sections also are obtained from Tables E-1 and E-4.

The area A and first moment Q_x of the entire cross section are

$$A = A_1 + A_2 + A_3 = 179.2 \text{ cm}^2$$

$$Q_x = y_1 A_1 + y_2 A_2 + y_3 A_3$$

$$= (239.7 \text{ mm})(1800 \text{ mm}^2) + 0 - (252.3 \text{ mm})(3600 \text{ mm}^2)$$

$$= -476,800 \text{ mm}^3$$

The coordinate \bar{y} to the centroid C is obtained from the following equation:

$$\bar{y} = \frac{Q_x}{A} = \frac{-476,800 \text{ mm}^3}{179,200 \text{ mm}^2} = -26.6 \text{ mm}$$

Since \bar{y} is positive in the same direction as the positive y axis, the minus sign means that the centroid C is located below the x axis (see figure). Thus, the distance \bar{c} between the x axis and the centroid C is

$$\bar{c} = -\bar{y} = 26.6 \text{ mm}$$

Note that the location selected for the x axis was arbitrary (but quite convenient).

C.3 MOMENTS OF INERTIA OF AREAS

The moments of inertia of a plane area (see Fig. C-1) with respect to the x and y axes, respectively, are defined by the integrals

$$I_x = \int y^2 dA \quad I_y = \int x^2 dA \quad (C-7)$$

in which x and y are the coordinates of the differential element of area

dA . Because dA is multiplied by the square of the distance, moments of inertia are also called **second moments of the area**.

To illustrate how moments of inertia are obtained by integration, let us consider the rectangle shown in Fig. C-8. The x and y axes have their origin at the centroid C . For convenience, we use an element of area in the form of a thin strip of width b and height dy , so that $dA = b dy$. Then the moment of inertia with respect to the x axis is

$$I_x = \int_{-h/2}^{h/2} y^2 b dy = \frac{bh^3}{12} \quad (a)$$

In a similar manner, we can use an element of area dA in the form of a vertical strip and obtain the moment of inertia with respect to the y axis:

$$I_y = \int_{-b/2}^{b/2} x^2 h dx = \frac{hb^3}{12} \quad (b)$$

If different axes are selected, then the moments of inertia will have different values. For instance, let us consider axis BB at the base of the rectangle. In that case, we define y as the distance from axis BB to the element of area dA . Then the calculations for the moment of inertia proceed as follows:

$$I_{BB} = \int y^2 dA = \int_0^h y^2 b dy = \frac{bh^3}{3} \quad (c)$$

Note that the moment of inertia is larger with respect to axis BB than with respect to the centroidal x axis. In general, the moment of inertia increases as the reference axis is moved parallel to itself farther from the centroid. Regardless of the axes that are selected, moments of inertia always are positive quantities because the coordinates x and y are squared (see Eqs. C-7).

The moment of inertia of a composite area with respect to a particular axis is the sum of the moments of inertia of its parts with respect to that same axis. An example is the hollow box section shown in Fig. C-9a. The x axis is an axis of symmetry through the centroid C . The moment of inertia with respect to the x axis is equal to the difference

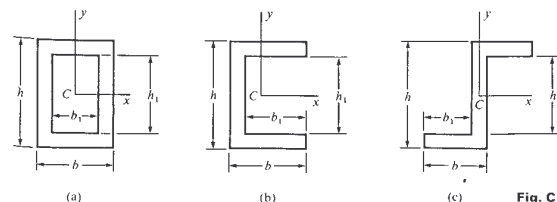


Fig. C-9

between the moments of inertia of the two rectangles:

$$I_x = \frac{bh^3}{12} - b_1h_1^3 \quad (d)$$

This same formula applies to the channel section and the Z-section shown in parts (b) and (c), respectively, of the figure. The same technique can be used to obtain the moment of inertia I_y for the hollow box section. However, in the case of the channel section and Z-section, I_y is most easily obtained by using the parallel-axis theorem, which is described in the next section.

Moments of inertia are tabulated in Appendix D for many common areas. The use of the formulas in the table in conjunction with the parallel-axis theorem (Section C.4) makes it possible to obtain moments of inertia for most other shapes that are encountered. However, if an area is of irregular shape, we can always obtain its moments of inertia by numerical methods. The procedure is to divide the area into small elements of area ΔA , multiply each such area by the square of its distance from the axis, and then sum the products.

Radius of gyration. A distance known as the **radius of gyration** of an area is used occasionally in mechanics. It is defined as the square root of the moment of inertia divided by the area itself; thus,

$$r_x = \sqrt{\frac{I_x}{A}} \quad r_y = \sqrt{\frac{I_y}{A}} \quad (C-8)$$

where r_x and r_y denote the radii of gyration with respect to the x and y axes, respectively. Since I has units of length to the fourth power and A has units of length to the second power, radius of gyration has units of length. We may consider the radius of gyration of an area to be the distance from the axis at which the entire area could be concentrated and still have the same moment of inertia as the original area.

Example

Determine the moments of inertia I_x and I_y for the parabolic semisegment OAB shown in Fig. C-5. The equation of the parabolic boundary is

$$y = f(x) = h \left(1 - \frac{x^2}{b^2} \right)$$

as given in the example of Section C.1.

Let us use the element of area dA shown as a vertical strip in Fig. C-5:

$$dA = y dx = h \left(1 - \frac{x^2}{b^2} \right) dx$$

Since every point in this element of area is at the same distance x from the y axis, the moment of inertia of the element with respect to the y axis is $x^2 dA$. Therefore, the moment of inertia of the entire area with respect to the y axis is determined as follows:

$$I_y = \int x^2 dA = \int_0^b x^2 h \left(1 - \frac{x^2}{b^2} \right) dx = \frac{2bh^3}{15} \quad (e)$$

To obtain the moment of inertia with respect to the x axis, we note that the element of area dA has a moment of inertia equal to

$$\frac{1}{3} (dx)y^3$$

with respect to the x axis (see Eq. c). Hence, the moment of inertia of the entire area is

$$I_x = \int_0^b \frac{y^3}{3} dx = \int_0^b \frac{h^3}{3} \left(1 - \frac{x^2}{b^2} \right)^3 dx = \frac{16bh^3}{105} \quad (f)$$

These same results can be obtained by using an element in the form of a horizontal strip or by using a rectangular element of area $dA = dx dy$ and performing a double integration.

C.4 PARALLEL-AXIS THEOREM FOR MOMENTS OF INERTIA

The moment of inertia of an area with respect to any axis in the plane of the area is related to the moment of inertia with respect to a parallel centroidal axis by the **parallel-axis theorem**. To derive this extremely useful theorem, we will consider the area shown in Fig. C-10. Assume that the x_c, y_c axes have their origin at the centroid C of the area. The xy axes are parallel to the x_c, y_c axes and have their origin at any point O . The distances between corresponding axes are d_1 and d_2 . From the definition of moment of inertia, we obtain the following equation for the moment of inertia I_x with respect to the x axis:

$$I_x = \int (y + d_1)^2 dA = \int y^2 dA + 2d_1 \int y dA + d_1^2 \int dA$$

The first integral on the right-hand side is the moment of inertia I_{x_c} with respect to the x_c axis; the second integral vanishes because the x_c axis passes through the centroid; and the third integral is the area A of the figure. Therefore, the preceding equation reduces to

$$I_x = I_{x_c} + Ad_1^2 \quad (C-9a)$$

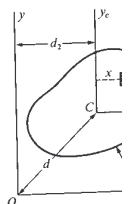


Fig. C-10 Derive theorems

Proceeding in the same manner for the y axis, we obtain

$$I_y = I_{y_c} + Ad_2^2 \quad (C-9b)$$

Equations (C-9) represent the parallel-axis theorem for moments of inertia: *The moment of inertia of an area with respect to any axis in its plane is equal to the moment of inertia with respect to a parallel centroidal axis plus the product of the area and the square of the distance between the two axes.*

From the parallel-axis theorem, we see that the moment of inertia increases as the axis is moved parallel to itself farther from the centroid. Hence, the moment of inertia about a centroidal axis is the least moment of inertia of the area (for a given direction of the axes).

The parallel-axis theorem is extremely useful for finding moments of inertia, especially for composite areas. When using the theorem, we must always keep in mind that one of the two parallel axes must be a centroidal axis. To illustrate this point, consider again the rectangle shown in Fig. C-8. Knowing that the moment of inertia about the x axis, which is through the centroid, is equal to $bh^3/12$ (see Eq. a of Section C.3), we can quickly determine the moment of inertia I_{BB} about the base of the rectangle:

$$I_{BB} = I_x + Ad^2 = \frac{bh^3}{12} + bh \left(\frac{h}{2} \right)^2 = \frac{bh^3}{3}$$

This result agrees with the result obtained previously by integration (Eq. c of Section C.3).

If it is necessary to find the moment of inertia I_1 about a noncentroidal axis when the moment of inertia I_2 about another noncentroidal (and parallel) axis is known, we must apply the parallel-axis theorem twice. First, we use the theorem to find the centroidal moment of inertia from the known moment of inertia I_2 . Then we use the theorem a second time to find I_1 from the centroidal moment of inertia.

In the case of a composite area, we can find the moment of inertia (with respect to a particular axis) of each part of the area and then add these moments of inertia to obtain I for the entire area. For instance, consider the Z-section shown in Fig. C-9c and assume that I_y is to be calculated. Then we can divide the area into three rectangles, each of which has a centroid that can be located by inspection. The moments of inertia of the rectangles, with respect to axes through their centroids parallel to the y axis, can be obtained from the general formula $I = bh^3/12$. Then we can use the parallel-axis theorem to calculate the moments of inertia with respect to the y axis. Adding these moments of inertia, we obtain I_y for the entire area.

Example 1

Determine the centroidal moments of inertia I_{x_c} and I_{y_c} for the parabolic semisegment OAB shown in Fig. C-11. The area of the semisegment is $2bh/3$, and the centroid C has coordinates $\bar{x} = 3b/8$ and $\bar{y} = 2h/5$; also, the moments of inertia with respect to the x and y axes are

$$I_x = \frac{16bh^3}{105} \quad I_y = \frac{2bh^3}{15}$$

(see Case 18, Appendix D).

To obtain the moment of inertia with respect to the x_c axis, we write the parallel-axis theorem as follows:

$$I_x = I_{x_c} + A\bar{y}^2$$

Therefore, the moment of inertia I_{x_c} is

$$I_{x_c} = I_x - A\bar{y}^2 = \frac{16bh^3}{105} - \frac{2bh}{3} \left(\frac{2h}{5} \right)^2 = \frac{8bh^3}{175}$$

In a similar manner, we obtain the moment of inertia with respect to the y_c axis:

$$I_{y_c} = I_y - A\bar{x}^2 = \frac{2bh^3}{15} - \frac{2bh}{3} \left(\frac{3b}{8} \right)^2 = \frac{19bh^3}{480}$$

Thus, the required centroidal moments of inertia have been found.

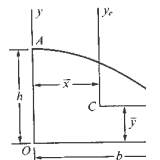


Fig. C-11 Example 1 theorem

Example 2

Determine the moment of inertia I_c with respect to a horizontal axis through the centroid C of the beam cross section described in the example of Section C.2 and shown in Fig. C-7. (This moment of inertia is required when calculating the stresses and deflections of the beam.)

To find the centroidal moment of inertia I_c of the composite area, we consider the area in three parts: (1) the cover plate, (2) the wide-flange section, and (3) the channel section. Also, we take the following properties and dimensions from the example of Section C.2:

$$A_1 = 18 \text{ cm}^2 \quad A_2 = 125.2 \text{ cm}^2 \quad A_3 = 36 \text{ cm}^2 \\ y_1 = 239.7 \text{ mm} \quad y_3 = 252.3 \text{ mm} \quad c = 26.6 \text{ mm}$$

The moments of inertia of the three parts with respect to their own centroids are as follows:

$$I_1 = \frac{bh^3}{12} = \frac{1}{12} (150 \text{ mm})(12 \text{ mm})^3 = 21,600 \text{ mm}^4 = 2.16 \text{ cm}^4 \\ I_2 = 45,650 \text{ cm}^4 \quad I_3 = 163 \text{ cm}^4$$

in which I_2 and I_3 are obtained from Tables E-1 and E-4, respectively.

Now we can use the parallel-axis theorem to calculate the moments of inertia about an axis through C for the three parts of the cross section:

$$\begin{aligned} I_{c1} &= I_1 + A_1(y_1 + \bar{c})^2 = 2.16 + 18(26.63)^2 = 12,770 \text{ cm}^4 \\ I_{c2} &= I_2 + A_2\bar{c}^2 = 45,650 + 125.2(2.66)^2 = 46,540 \text{ cm}^4 \\ I_{c3} &= I_3 + A_3(y_3 - \bar{c})^2 = 163 + 36(22.57)^2 = 18,500 \text{ cm}^4 \end{aligned}$$

The sum of these moments of inertia is

$$I_c = I_{c1} + I_{c2} + I_{c3} = 77,810 \text{ cm}^4$$

which is the centroidal moment of inertia of the entire cross section.

C.5 POLAR MOMENTS OF INERTIA

The moments of inertia discussed in the preceding sections are calculated with respect to axes lying in the plane of the area itself, such as the x and y axes in Fig. C-1. Now let us consider an axis perpendicular to the plane of the area and intersecting the plane at the origin O . The moment of inertia with respect to this axis is called the **polar moment of inertia** I_p ; it is defined as the integral

$$I_p = \int \rho^2 dA \tag{C-10}$$

in which ρ is the distance from point O to the element of area dA (see Fig. C-1). Inasmuch as $\rho^2 = x^2 + y^2$, where x and y are the rectangular coordinates of the element dA , we get the following expression for I_p :

$$I_p = \int \rho^2 dA = \int (x^2 + y^2) dA$$

Therefore, we obtain

$$I_p = I_x + I_y \tag{C-11}$$

This equation shows that the polar moment of inertia with respect to an axis perpendicular to the plane of the figure at point O is equal to the sum of the moments of inertia with respect to any two perpendicular axes x and y passing through that same point and lying in the plane of the figure. For simplicity, we usually will refer to I_p as the polar moment of inertia with respect to point O .

The calculation of polar moments of inertia with respect to various points is greatly facilitated by the **parallel-axis theorem for polar mo-**

ments of inertia. We can derive this theorem by referring again to Fig. C-10. Let us denote the polar moments of inertia about the origin O and the centroid C by I_{p_o} and I_{p_c} , respectively; then, we can write the following equations:

$$I_{p_o} = I_x + I_y \quad I_{p_c} = I_{x_c} + I_{y_c} \tag{a}$$

(see Eq. C-11). Next, let us introduce the parallel-axis theorems derived in Section C.4 (see Eqs. C-9):

$$I_{x_c} = I_x + Ad_1^2 \quad I_{y_c} = I_y + Ad_2^2 \tag{b}$$

Adding the last two equations, we get

$$I_{x_c} + I_{y_c} = I_x + I_y + A(d_1^2 + d_2^2)$$

Now substituting from Eqs. (a), and also noting that $d^2 = d_1^2 + d_2^2$ (see Fig. C-10), we obtain

$$I_{p_o} = I_{p_c} + Ad^2 \tag{C-12}$$

This equation represents the parallel-axis theorem for polar moments of inertia: *The polar moment of inertia of an area with respect to any point O in its plane is equal to the polar moment of inertia with respect to the centroid C plus the product of the area and the square of the distance between points O and C .*

To illustrate the determination of polar moments of inertia, consider a circle of radius r (Fig. C-12). Let us take an element of area dA in the form of a thin ring of radius ρ and thickness $d\rho$; thus, $dA = 2\pi\rho d\rho$. Since every point in this element is at the same distance ρ from the center C of the circle, the polar moment of inertia of the element with respect to C is $\rho^2 dA$, or $2\pi\rho^3 d\rho$. To obtain the polar moment of inertia for the entire circle, we integrate as follows:

$$I_p = \int \rho^2 dA = \int_0^r 2\pi\rho^3 d\rho = \frac{\pi r^4}{2} \tag{c}$$

The polar moment of inertia with respect to any point B on the circumference can be obtained from the parallel-axis theorem:

$$I_{p_b} = I_{p_c} + Ad^2 = \frac{\pi r^4}{2} + \pi r^2(r^2) = \frac{3\pi r^4}{2} \tag{d}$$

As an incidental matter, we can easily obtain the moment of inertia of a circle with respect to a diameter by using Eq. (C-11). For the circle in Fig. C-12, we get

$$I_x = I_y = \frac{I_p}{2} = \frac{\pi r^4}{4} \tag{e}$$

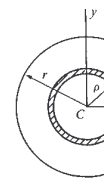


Fig. C-12 Pol a circle

A circle is obviously a special case in which the polar moment of inertia can easily be determined by integration. However, most of the shapes encountered in engineering work do not lend themselves to this technique. Instead, the polar moment of inertia is usually obtained by summing the moments of inertia about two perpendicular axes (Eq. C-11). The latter moments of inertia are found by the methods described in Sections C.3 and C.4.

C.6 PRODUCTS OF INERTIA

The product of inertia of a plane area is a property that is defined with respect to a set of perpendicular axes lying in the plane of the area. Thus, we refer again to the area A shown in Fig. C-1, and we define the **product of inertia** with respect to the x and y axes as follows:

$$I_{xy} = \int xy dA \tag{C-13}$$

From this definition we see that each element of area dA is multiplied by the product of its coordinates. As a consequence, products of inertia may be positive, negative, or zero, depending upon the position of the xy axes with respect to the area. If the area lies entirely in the first quadrant of the axes (as in Fig. C-1), then the product of inertia is positive because every element dA has positive coordinates x and y . If the area lies entirely in the second quadrant, the product of inertia is negative because every element has a positive y coordinate and a negative x coordinate. Similarly, areas entirely within the third and fourth quadrants have positive and negative products of inertia, respectively. When the area is located in more than one quadrant, the sign of the product of inertia depends upon the distribution of the area within the quadrants.

An important special case arises when one of the axes is an axis of symmetry of the area. For illustration, consider the area shown in Fig. C-13, which is symmetric about the y axis. For every element dA having coordinates x and y , there exists an equal and symmetrically located element dA having the same y coordinate but an x coordinate of opposite sign. Therefore, the products $xy dA$ cancel each other and the integral in Eq. (C-13) vanishes. Thus, *the product of inertia of an area is zero with respect to any pair of axes in which one axis is an axis of symmetry.* For instance, the product of inertia I_{xy} equals zero for the areas shown in Figs. C-7, C-8, C-9a, C-9b, and C-12. In contrast, the product of inertia has a positive nonzero value for the areas shown in Figs. C-6, C-9c, and C-11. These conclusions are valid for products of inertia with respect to the particular xy axes shown in the figures; of course, the product of inertia of an area is changed when the axes are shifted to another position.

The products of inertia of an area with respect to parallel sets of axes are related by a parallel-axis theorem that is analogous to the corresponding theorems for moments of inertia and polar moments of inertia. To obtain this theorem, let us consider again the area shown in Fig. C-10, and let us denote by $I_{x_c y_c}$ the product of inertia with respect to the centroidal $x_c y_c$ axes. The product of inertia I_{xy} with respect to any set of axes, parallel to the $x_c y_c$ axes, is

$$\begin{aligned} I_{xy} &= \int (x + d_1)(y + d_2) dA \\ &= \int xy dA + d_1 \int x dA + d_2 \int y dA + d_1 d_2 \int dA \end{aligned}$$

in which d_1 and d_2 are the coordinates of the centroid C with respect to the xy axes (thus, d_1 and d_2 may have positive or negative values). The first integral in the last expression is the product of inertia $I_{x_c y_c}$ with respect to the centroidal axes; the second and third integrals vanish because they are the first moments of the area with respect to the centroidal axes; and the last integral is the area A . Hence, the preceding equation reduces to

$$I_{xy} = I_{x_c y_c} + Ad_1 d_2 \tag{C-14}$$

This equation represents the **parallel-axis theorem** for products of inertia: *The product of inertia of an area with respect to any pair of axes in its plane is equal to the product of inertia with respect to parallel centroidal axes plus the product of the area and the coordinates of the centroid with respect to the pair of axes.*

To demonstrate the use of the parallel-axis theorem, let us determine the product of inertia of a rectangle with respect to xy axes with origin at a corner (Fig. C-14). The product of inertia with respect to the centroidal axes x_c and y_c is zero because they are axes of symmetry. Also, the coordinates of the centroid with respect to the xy axes are

$$d_1 = \frac{h}{2} \quad d_2 = \frac{b}{2}$$

Substituting into Eq. (C-14), we obtain

$$I_{xy} = I_{x_c y_c} + Ad_1 d_2 = 0 + bh \left(\frac{h}{2} \right) \left(\frac{b}{2} \right) = \frac{b^2 h^2}{4} \tag{a}$$

The product of inertia is positive because the entire area lies in the first quadrant. If the xy axes are translated horizontally so that the origin moves to point B at the lower right-hand corner of the rectangle (Fig. C-14), the entire area lies in the second quadrant and the product of inertia becomes $-b^2 h^2/4$.

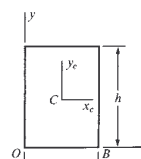


Fig. C-14 Parallel-axis theorem products of inertia

Example 1

Determine the product of inertia I_{xy} of a right triangle (Fig. C-15) with respect to xy axes with origin at the 90° vertex, and determine the product of inertia $I_{x_{xy}}$ with respect to parallel centroidal axes.

Let us consider an element of area dA in the form of a thin strip of height equal to dy and width equal to

$$\frac{(h-y)b}{h}$$

(see Fig. C-15). The product of inertia of this strip (which may be treated as a rectangle) with respect to axes through its own centroid and parallel to the xy axes is zero (from symmetry). Therefore, its product of inertia dI_{xy} with respect to the xy axes (from the parallel-axis theorem) is

$$dI_{xy} = dA d_1 d_2 = \left[\frac{(h-y)b dy}{h} \right] \left[y \right] \left[\frac{(h-y)b}{2h} \right] = \frac{b^2}{2h^2} (h-y)^2 y dy$$

The product of inertia I_{xy} of the triangle is obtained by integration:

$$I_{xy} = \int dI_{xy} = \frac{b^2}{2h^2} \int_0^h (h-y)^2 y dy = \frac{b^2 h^2}{24} \quad (b)$$

The product of inertia with respect to the parallel centroidal axes may now be determined from the parallel-axis theorem:

$$I_{x_{xy}} = I_{xy} - A d_1 d_2 = \frac{b^2 h^2}{24} - \frac{bh}{2} \left(\frac{h}{3} \right) \left(\frac{b}{3} \right) = -\frac{b^2 h^2}{72} \quad (c)$$

These results are given in Cases 6 and 7 of Appendix D.

Example 2

Determine the product of inertia I_{xy} of the Z-section shown in Fig. C-9c.

We divide the section into three rectangles, a web rectangle of width $b - b_1$ and height h and two flange rectangles of width b_1 and height $(h - h_1)/2$. The product of inertia of the web rectangle is zero (from symmetry). The product of inertia $(I_{xy})_1$ of the upper flange rectangle is determined by using the parallel-axis theorem:

$$(I_{xy})_1 = I_{x_{xy}} + A d_1 d_2 = 0 + b_1 \left(\frac{h - h_1}{2} \right) \left(\frac{h + h_1}{4} \right) \left(\frac{b}{2} \right) = \frac{bb_1}{16} (h^2 - h_1^2)$$

The product of inertia of the lower flange rectangle is the same; hence, the product of inertia of the entire Z-section is

$$I_{xy} = \frac{bb_1}{8} (h^2 - h_1^2) \quad (d)$$

Note that this product of inertia is positive because the flanges lie in the first and third quadrants.

C.7 ROTATION OF AXES

The moments of inertia of a plane area depend upon the position of the reference axes. Furthermore, for a given origin, the moments and product of inertia vary as the axes are rotated about the origin. The manner in which they vary, and the magnitudes of the maximum and minimum values, are discussed in this and the following sections.

Let us consider the plane area shown in Fig. C-16, and let us assume that the xy axes are a pair of arbitrarily located reference axes. The moments and products of inertia with respect to the xy axes are

$$I_x = \int y^2 dA \quad I_y = \int x^2 dA \quad I_{xy} = \int xy dA \quad (a)$$

in which x and y are the coordinates of an element of area dA . The $x_1 y_1$ axes have the same origin but are rotated through a counterclockwise angle θ with respect to the xy axes. The moments and product of inertia with respect to the $x_1 y_1$ axes are denoted by I_{x_1} , I_{y_1} , and $I_{x_1 y_1}$, respectively. To obtain these quantities, we need the coordinates x_1 and y_1 of the element dA ; these coordinates may be expressed in terms of the xy coordinates and the angle θ , as follows:

$$x_1 = x \cos \theta + y \sin \theta \quad y_1 = y \cos \theta - x \sin \theta \quad (b)$$

Then the moment of inertia with respect to the x_1 axis is

$$I_{x_1} = \int y_1^2 dA = \int (y \cos \theta - x \sin \theta)^2 dA \\ = \cos^2 \theta \int y^2 dA + \sin^2 \theta \int x^2 dA - 2 \sin \theta \cos \theta \int xy dA$$

or, by using Eqs. (a),

$$I_{x_1} = I_x \cos^2 \theta + I_y \sin^2 \theta - 2I_{xy} \sin \theta \cos \theta \quad (c)$$

Now we introduce the following trigonometric identities:

$$\cos^2 \theta = \frac{1}{2} (1 + \cos 2\theta) \quad \sin^2 \theta = \frac{1}{2} (1 - \cos 2\theta) \\ 2 \sin \theta \cos \theta = \sin 2\theta$$

Then Eq. (c) becomes

$$I_{x_1} = \frac{I_x + I_y}{2} + \frac{I_x - I_y}{2} \cos 2\theta - I_{xy} \sin 2\theta \quad (C-15a)$$

In a similar manner, we can obtain the product of inertia with respect to the $x_1 y_1$ axes:

$$I_{x_1 y_1} = \int x_1 y_1 dA = \int (x \cos \theta + y \sin \theta)(y \cos \theta - x \sin \theta) dA \\ = (I_x - I_y) \sin \theta \cos \theta + I_{xy} (\cos^2 \theta - \sin^2 \theta)$$

of the expression on the right-hand side of Eq. (C-15a) and set it equal to zero:

$$(I_x - I_y) \sin 2\theta + 2I_{xy} \cos 2\theta = 0 \quad (a)$$

Solving for θ from this equation, we get

$$\tan 2\theta_p = -\frac{2I_{xy}}{I_x - I_y} \quad (C-18)$$

in which θ_p denotes the angle defining a principal axis. This same result is obtained if we take the derivative of I_{x_1} (Eq. C-16). Two values of the angle $2\theta_p$ in the range from 0 to 360° are obtained from Eq. (C-18); these values differ by 180°. The corresponding two values of θ_p differ by 90° and define the two perpendicular principal axes, of which one corresponds to the maximum moment of inertia and the other corresponds to the minimum moment of inertia.

Now let us examine the variation in the product of inertia $I_{x_1 y_1}$ as θ varies (see Eq. C-15b). If $\theta = 0$, we get $I_{x_1 y_1} = I_{xy}$, as expected. If $\theta = 90^\circ$, we obtain $I_{x_1 y_1} = -I_{xy}$. Thus, during a 90° rotation the product of inertia changes sign, which means that, for some orientations of the axes, the product of inertia vanishes. To determine these orientations, we set $I_{x_1 y_1}$ (Eq. C-15b) equal to zero:

$$(I_x - I_y) \sin 2\theta + 2I_{xy} \cos 2\theta = 0$$

This equation is the same as Eq. (a), which defines the angle θ_p to the principal axes. Therefore, we conclude that the product of inertia is zero for the principal axes.

In Section C.6 we showed that the product of inertia of an area is zero with respect to any pair of axes in which one axis is an axis of symmetry. It follows that, if an area has an axis of symmetry, that axis and any axis perpendicular to it constitute a set of principal axes.

The preceding observations may be summarized as follows: (1) principal axes through an origin O are a pair of orthogonal axes for which the moments of inertia are a maximum and a minimum; (2) the orientation of the principal axes is given by the angle θ_p obtained from Eq. (C-18); (3) the product of inertia is zero for principal axes; and (4) an axis of symmetry is always a principal axis.

Now consider a pair of principal axes with origin at a given point O . If there exists a different pair of principal axes through that same point, then it follows that every pair of axes through that point is a set of principal axes. Furthermore, the moment of inertia must be constant as the angle θ is varied. These conclusions follow from the nature of the transformation equation for I_{x_1} (Eq. C-15a). Because this equation contains trigonometric functions of the angle 2θ , there is one maximum value and one minimum value of I_{x_1} as 2θ varies through a range of

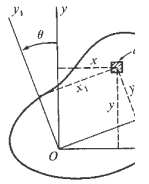


Fig. C-16 Rotation

C Centroids and Moments of Inertia of Plane Areas

Again using the trigonometric identities, we obtain

$$I_{x_1 y_1} = \frac{I_x - I_y}{2} \sin 2\theta + I_{xy} \cos 2\theta \quad (C-15b)$$

Thus, Eqs. (C-15) give the moment of inertia I_{x_1} and the product of inertia $I_{x_1 y_1}$ with respect to the rotated axes in terms of the moments and product of inertia for the original axes. These equations are called the **transformation equations for moments and products of inertia**. Note that they have the same form as the transformation equations for plane stress (Eqs. 6-4, Section 6.2), with I_{x_1} corresponding to σ_{x_1} , $I_{x_1 y_1}$ corresponding to $\tau_{x_1 y_1}$, I_x corresponding to σ_x , I_y corresponding to σ_y , and $-I_{xy}$ corresponding to τ_{xy} . Therefore, we can also analyze moments and products of inertia by the use of Mohr's circle (see Section 6.4).

The moment of inertia I_{y_1} is obtained by the same procedure that we used for I_{x_1} and $I_{x_1 y_1}$; thus,

$$I_{y_1} = \int x_1^2 dA = \int (x \cos \theta + y \sin \theta)^2 dA \\ = I_x \sin^2 \theta + I_y \cos^2 \theta + 2I_{xy} \sin \theta \cos \theta$$

Substituting the trigonometric identities, we get

$$I_{y_1} = \frac{I_x + I_y}{2} - \frac{I_x - I_y}{2} \cos 2\theta + I_{xy} \sin 2\theta \quad (C-16)$$

Taking the sum of I_{x_1} and I_{y_1} , we find

$$I_{x_1} + I_{y_1} = I_x + I_y \quad (C-17)$$

This equation shows that the sum of the moments of inertia with respect to a pair of axes remains constant as the axes are rotated about the origin. This sum is the polar moment of inertia of the area with respect to the origin.

C.8 PRINCIPAL AXES

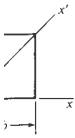
The transformation equations for moments and products of inertia of an area were derived in the preceding section (see Eqs. C-15). These equations show how the inertia quantities vary as the angle of rotation θ varies. Of special interest are the maximum and minimum values of the moment of inertia; such values are known as **principal moments of inertia**, and the corresponding axes are known as **principal axes**.

To find the values of the angle θ that make the moment of inertia I_{x_1} a maximum or a minimum, we take the derivative with respect to θ

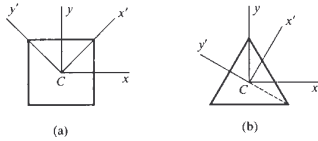
360°, or as θ varies through a range of 180°. If a second maximum exists, then the only possibility is that I_x remains constant, which means that every pair of axes is a set of principal axes and all moments of inertia are the same.

An illustration of this situation is the rectangle of width $2b$ and height b shown in Fig. C-17. The xy axes, with origin at point O , are principal axes of the rectangle because the y axis is an axis of symmetry. The $x'y'$ axes, with the same origin, are also principal axes because the product of inertia $I_{x'y'}$ equals zero (because the triangles are symmetrically located with respect to the x' and y' axes). Therefore, every pair of axes through O is a set of principal axes and every moment of inertia is the same (and equal to $2b^4/3$).

A useful corollary of the proposition described in the preceding two paragraphs applies to axes through the centroid C of an area. If an area has two different pairs of centroidal axes such that at least one axis in each pair is an axis of symmetry, then every centroidal axis is a principal axis and all moments of inertia are the same. Two examples, a square and an equilateral triangle, are shown in Fig. C-18. In each case, the xy axes are principal axes because at least one of the two axes is an axis of symmetry. Also, a second pair of axes (the $x'y'$ axes) has at least one axis of symmetry. It follows that both the xy and $x'y'$ axes are principal axes, and therefore every axis through C is a principal axis and has the same moment of inertia.



n in which every axis is a principal axis



Areas for which every axis is a principal axis: (a) and (b) an equilateral

If an area has three different axes of symmetry, the conditions described in the preceding paragraph are automatically fulfilled. (Note that the conditions are satisfied for two different axes of symmetry only if the axes are not perpendicular.) Hence, we conclude that, if an area has three or more axes of symmetry, all centroidal axes are principal axes and all moments of inertia are equal. These conditions are fulfilled for a circle and for regular polygons (equilateral triangle, square, regular pentagon, regular hexagon, and so on).

Let us now consider the determination of the principal moments of inertia, assuming that I_x , I_y , and I_{xy} are known. One method is to determine the two values of θ_p (differing by 90°) from Eq. (C-18) and then substitute these values into Eq. (C-15a) for $I_{x'y'}$. The resulting two values are the principal moments of inertia, denoted by I_1 and I_2 . The advantage of this method is that we know which of the two principal angles θ_p corresponds to each principal moment of inertia.

It is also possible to obtain general formulas for the principal moments of inertia. We note from Eq. (C-18) and Fig. C-19 that

$$\cos 2\theta_p = \frac{I_x - I_y}{2R} \quad \sin 2\theta_p = \frac{-I_{xy}}{R} \quad (C-19a, b)$$

in which

$$R = \sqrt{\left(\frac{I_x - I_y}{2}\right)^2 + I_{xy}^2} \quad (C-20)$$

When evaluating R , we always take the positive square root. Now we substitute the expressions for $\cos 2\theta_p$ and $\sin 2\theta_p$ into Eq. (C-15a) and obtain the algebraically larger of the two principal moments of inertia, denoted by I_1 :

$$I_1 = \frac{I_x + I_y}{2} + \sqrt{\left(\frac{I_x - I_y}{2}\right)^2 + I_{xy}^2} \quad (C-21a)$$

The smaller principal moment of inertia, denoted by I_2 , may be obtained from the equation

$$I_1 + I_2 = I_x + I_y$$

(see Eq. C-17). Substituting the expression for I_1 into this equation and solving for I_2 , we get

$$I_2 = \frac{I_x + I_y}{2} - \sqrt{\left(\frac{I_x - I_y}{2}\right)^2 + I_{xy}^2} \quad (C-21b)$$

Equations (C-21) provide a convenient way to calculate the principal moments of inertia.

Example

Determine the orientations of the principal centroidal axes and the magnitudes of the principal centroidal moments of inertia for the cross-sectional area of the Z-section shown in Fig. C-20. Use the following numerical data: $h = 400$ mm, $b = 175$ mm, and $t = 28$ mm.

Let us use the xy axes (Fig. C-20) as the reference axes through the centroid C . The moments and product of inertia with respect to these axes can be obtained by dividing the area into three rectangles and using the parallel-axis theorems. The results of such calculations are as follows:

$$I_x = 43,467 \text{ cm}^4 \quad I_y = 7858 \text{ cm}^4 \quad I_{xy} = -13,398 \text{ cm}^4$$

Substituting these values into the equation for the angle θ_p (Eq. C-18), we get

$$\tan 2\theta_p = \frac{-2I_{xy}}{I_x - I_y} = 0.7525 \quad 2\theta_p = 37.0^\circ \text{ and } 217.0^\circ$$

Thus, the two values of θ_p are

$$\theta_p = 18.5^\circ \text{ and } 108.5^\circ$$

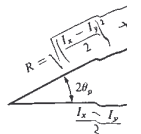


Fig. C-19

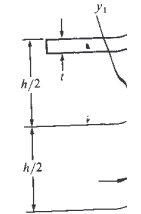


Fig. C-20 Example of a Z-section

APPENDIX D

Properties of Plane Areas

A = area
 \bar{x} , \bar{y} = distances to centroid C
 I_x , I_y = moments of inertia with respect to the x and y axes, respectively
 I_{xy} = product of inertia with respect to the x and y axes
 $I_x + I_y$ = polar moment of inertia
 I_{BB} = moment of inertia with respect to axis $B-B$

<p>Rectangle (Origin of axes at centroid.)</p> $A = bh \quad \bar{x} = \frac{b}{2} \quad \bar{y} = \frac{h}{2}$ $I_x = \frac{bh^3}{12} \quad I_y = \frac{hb^3}{12}$ $I_{xy} = 0 \quad I_p = \frac{bh}{12}(h^2 + b^2)$	<p>Rectangle (Origin of axes at corner.)</p> $I_x = \frac{bh^3}{3} \quad I_y = \frac{hb^3}{3}$ $I_{xy} = \frac{b^2h^2}{4} \quad I_p = \frac{bh}{3}(h^2 + b^2) \quad I_{BB} = \frac{b^3h^3}{6(b^2 + h^2)}$
--	--

<p>3</p>	<p>Triangle (Origin of axes at centroid.)</p> $A = \frac{bh}{2} \quad \bar{x} = \frac{b+c}{3} \quad \bar{y} = \frac{h}{3}$ $I_x = \frac{bh^3}{36} \quad I_y = \frac{bh}{36}(b^2 - bc + c^2)$ $I_{xy} = \frac{bh^2}{72}(b-2c) \quad I_p = \frac{bh}{36}(h^2 + b^2 - bc + c^2)$
<p>4</p>	<p>Triangle (Origin of axes at vertex.)</p> $I_x = \frac{bh^3}{12} \quad I_y = \frac{bh}{12}(3b^2 - 3bc + c^2)$ $I_{xy} = \frac{bh^2}{24}(3b-2c) \quad I_{BB} = \frac{bh^3}{4}$
<p>5</p>	<p>Isosceles triangle (Origin of axes at centroid.)</p> $A = \frac{bh}{2} \quad \bar{x} = \frac{b}{2} \quad \bar{y} = \frac{h}{3}$ $I_x = \frac{bh^3}{36} \quad I_y = \frac{hb^3}{48} \quad I_{xy} = 0$ $I_p = \frac{bh}{144}(4h^2 + 3b^2) \quad I_{BB} = \frac{bh^3}{12}$ <p>(Note: For an equilateral triangle, $h = \sqrt{3}b/2$.)</p>
<p>6</p>	<p>Right triangle (Origin of axes at centroid.)</p> $A = \frac{bh}{2} \quad \bar{x} = \frac{b}{3} \quad \bar{y} = \frac{h}{3}$ $I_x = \frac{bh^3}{36} \quad I_y = \frac{hb^3}{36} \quad I_{xy} = -\frac{b^2h^2}{72}$ $I_p = \frac{bh}{36}(h^2 + b^2) \quad I_{BB} = \frac{bh^3}{12}$
<p>7</p>	<p>Right triangle (Origin of axes at vertex.)</p> $I_x = \frac{bh^3}{12} \quad I_y = \frac{hb^3}{12} \quad I_{xy} = \frac{b^2h^2}{24}$ $I_p = \frac{bh}{12}(h^2 + b^2) \quad I_{BB} = \frac{bh^3}{4}$

Properties of Plane Areas

Trapezoid (Origin of axes at centroid.)

$$A = \frac{h(a+b)}{2} \quad \bar{y} = \frac{h(2a+b)}{3(a+b)}$$

$$I_x = \frac{h^3(a^2 + 4ab + b^2)}{36(a+b)} \quad I_{BB} = \frac{h^3(3a+b)}{12}$$

Circle (Origin of axes at center.)

$$A = \pi r^2 \quad I_x = I_y = \frac{\pi r^4}{4} = \frac{\pi d^4}{64}$$

$$I_{xy} = 0 \quad I_p = \frac{\pi r^4}{2} = \frac{\pi d^4}{32} \quad I_{BB} = \frac{5\pi r^4}{4} = \frac{5\pi d^4}{64}$$

Circular ring (Origin of axes at center.)
Approximate formulas for case when t is small.

$$A = 2\pi r t = \pi d t \quad I_x = I_y = \pi r^3 t = \frac{\pi d^3 t}{8}$$

$$I_{xy} = 0 \quad I_p = 2\pi r^3 t = \frac{\pi d^3 t}{4}$$

Semicircle (Origin of axes at centroid.)

$$A = \frac{\pi r^2}{2} \quad \bar{y} = \frac{4r}{3\pi}$$

$$I_x = \frac{(9\pi^2 - 64)r^4}{72\pi} \approx 0.1098r^4 \quad I_y = \frac{\pi r^4}{8}$$

$$I_{xy} = 0 \quad I_{BB} = \frac{\pi r^4}{8}$$

Quarter circle (Origin of axes at center of circle.)

$$A = \frac{\pi r^2}{4} \quad \bar{x} = \bar{y} = \frac{4r}{3\pi}$$

$$I_x = I_y = \frac{\pi r^4}{16} \quad I_{xy} = \frac{r^4}{8}$$

$$I_{BB} = \frac{(9\pi^2 - 64)r^4}{144\pi} \approx 0.05488r^4$$

Quarter-circular spandrel (Origin of axes at vertex.)

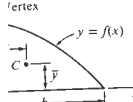
$$A = \left(1 - \frac{\pi}{4}\right)r^2$$

$$\bar{x} = \frac{2r}{3(4-\pi)} \approx 0.7766r \quad \bar{y} = \frac{(10-3\pi)r}{3(4-\pi)} \approx 0.2234r$$

$$I_x = \left(1 - \frac{5\pi}{16}\right)r^4 \approx 0.01825r^4 \quad I_y = I_{BB} = \left(\frac{1}{3} - \frac{\pi}{16}\right)r^4 \approx 0.1370r^4$$

Appendix D Properties of Plane Areas

Parabolic segment (Origin of axes at corner.)

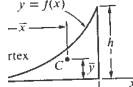


$$y = f(x) = h\left(1 - \frac{x^2}{b^2}\right)$$

$$A = \frac{2bh}{3} \quad \bar{x} = \frac{3b}{8} \quad \bar{y} = \frac{2h}{5}$$

$$I_x = \frac{16bh^3}{105} \quad I_y = \frac{2bh^3}{15} \quad I_{xy} = \frac{b^2h^2}{12}$$

Parabolic spandrel (Origin of axes at vertex.)

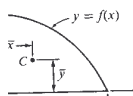


$$y = f(x) = \frac{hx^2}{b^2}$$

$$A = \frac{bh}{3} \quad \bar{x} = \frac{3b}{4} \quad \bar{y} = \frac{3h}{10}$$

$$I_x = \frac{bh^3}{21} \quad I_y = \frac{hb^3}{5} \quad I_{xy} = \frac{b^2h^2}{12}$$

Semisegment of nth degree (Origin of axes at corner.)



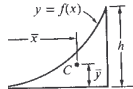
$$y = f(x) = h\left(1 - \frac{x^n}{b^n}\right) \quad n > 0$$

$$A = bh\left(\frac{n}{n+1}\right) \quad \bar{x} = \frac{b(n+1)}{2(n+2)} \quad \bar{y} = \frac{hn}{2n+1}$$

$$I_x = \frac{2bh^3n^3}{(n+1)(2n+1)(3n+1)}$$

$$I_y = \frac{hb^3n}{3(n+3)} \quad I_{xy} = \frac{b^2h^2n^2}{4(n+1)(n+2)}$$

Spandrel of nth degree (Origin of axes at vertex.)

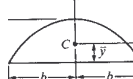


$$y = f(x) = \frac{hx^n}{b^n} \quad n > 0$$

$$A = \frac{bh}{n+1} \quad \bar{x} = \frac{b(n+1)}{n+2} \quad \bar{y} = \frac{h(n+1)}{2(2n+1)}$$

$$I_x = \frac{bh^3}{3(3n+1)} \quad I_y = \frac{hb^3}{n+3} \quad I_{xy} = \frac{b^2h^2}{4(n+1)}$$

Sine wave (Origin of axes at centroid.)

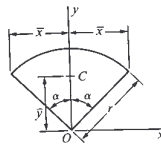


$$A = \frac{4bh}{\pi} \quad \bar{y} = \frac{\pi h}{8}$$

$$I_x = \left(\frac{8}{9\pi} - \frac{\pi}{16}\right)bh^3 \approx 0.08659bh^3 \quad I_y = \left(\frac{4}{\pi} - \frac{32}{\pi^3}\right)hb^3 \approx 0.2412hb^3$$

$$I_{xy} = 0 \quad I_{BB} = \frac{8bh^3}{9\pi}$$

14



Circular sector (Origin of axes at center of circle.)

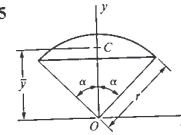
$$\alpha = \text{angle in radians} \quad \left(\alpha \leq \frac{\pi}{2}\right)$$

$$A = \alpha r^2 \quad \bar{x} = r \sin \alpha \quad \bar{y} = \frac{2r \sin \alpha}{3\alpha}$$

$$I_x = \frac{r^4}{4}(\alpha + \sin \alpha \cos \alpha) \quad I_y = \frac{r^4}{4}(\alpha - \sin \alpha \cos \alpha)$$

$$I_{xy} = 0 \quad I_p = \frac{\alpha r^4}{2}$$

15



Circular segment (Origin of axes at center of circle.)

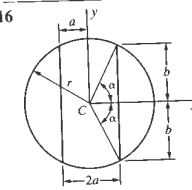
$$\alpha = \text{angle in radians} \quad \left(\alpha \leq \frac{\pi}{2}\right)$$

$$A = r^2(\alpha - \sin \alpha \cos \alpha) \quad \bar{y} = \frac{2r}{3} \left(\frac{\sin^3 \alpha}{\alpha - \sin \alpha \cos \alpha}\right)$$

$$I_x = \frac{r^4}{4}(\alpha - \sin \alpha \cos \alpha + 2 \sin^3 \alpha \cos \alpha) \quad I_{xy} = 0$$

$$I_y = \frac{r^4}{12}(3\alpha - 3 \sin \alpha \cos \alpha - 2 \sin^3 \alpha \cos \alpha)$$

16



Circle with core removed (Origin of axes at center of circle.)

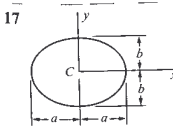
$$\alpha = \text{angle in radians} \quad \left(\alpha \leq \frac{\pi}{2}\right)$$

$$\alpha = \arccos \frac{a}{r} \quad b = \sqrt{r^2 - a^2}$$

$$A = 2r^2 \left(\alpha - \frac{ab}{r^2}\right) \quad I_{xy} = 0$$

$$I_x = \frac{r^4}{6} \left(3\alpha - \frac{3ab}{r^2} - \frac{2ab^3}{r^4}\right) \quad I_y = \frac{r^4}{2} \left(\alpha - \frac{ab}{r^2} + \frac{2ab^3}{r^4}\right)$$

17



Ellipse (Origin of axes at centroid.)

$$A = \pi ab \quad I_x = \frac{\pi ab^3}{4} \quad I_y = \frac{\pi ba^3}{4}$$

$$I_{xy} = 0 \quad I_p = \frac{\pi ab}{4}(b^2 + a^2)$$

Circumference $\approx \pi[1.5(a+b) - \sqrt{ab}]$

A P

Properties of Structural Steelwork

In the following tables, the properties of a few structural-steel shapes are presented as an aid to the reader in solving problems in the text. These tables were compiled from the extensive tables found in the *Structural Steelwork Handbook* published by the British Constructional Steelwork Association and Contrado, 1982 (Ref. 5-5). However the notation has been adapted to conform with that used in the text of this book.

Notation:
 I = moment of inertia
 S = section modulus
 $r = \sqrt{I/A}$ = radius of gyration

APPENDIX G

Deflections and Slopes of Beams

DEFLECTIONS AND SLOPES OF CANTILEVER BEAMS

v = deflection in y direction
 $v' = dv/dx$ = slope of deflection curve
 $\delta_b = v(L)$ = deflection at right end of beam
 $\theta_b = v'(L)$ = angle at right end of beam

$$v = \frac{qx^2}{24EI} (6L^2 - 4Lx + x^2)$$

$$v' = \frac{qx}{6EI} (3L^2 - 3Lx + x^2)$$

$$\delta_b = \frac{qL^4}{8EI} \quad \theta_b = \frac{qL^3}{6EI}$$

$$v = \frac{qx^2}{24EI} (6a^2 - 4ax + x^2) \quad 0 \leq x \leq a$$

$$v' = \frac{qx}{6EI} (3a^2 - 3ax + x^2) \quad 0 \leq x \leq a$$

$$v = \frac{qa^3}{24EI} (4x - a) \quad v' = \frac{qa^2}{6EI} \quad a \leq x \leq L$$

At $x = a$: $v = \frac{qa^4}{8EI} \quad v' = \frac{qa^3}{6EI}$

$$\delta_b = \frac{qa^3}{24EI} (4L - a) \quad \theta_b = \frac{qa^3}{6EI}$$

Deflections and Slopes of Beams

$$v = \frac{q_0x^2}{120LEI} (10L^3 - 10L^2x + 5Lx^2 - x^3)$$

$$v' = \frac{q_0x}{24LEI} (4L^3 - 6L^2x + 4Lx^2 - x^3)$$

$$\delta_b = \frac{q_0L^4}{30EI} \quad \theta_b = \frac{q_0L^3}{24EI}$$

$$v = \frac{q_0x^2}{120LEI} (20L^3 - 10L^2x + x^3)$$

$$v' = \frac{q_0x}{24LEI} (8L^3 - 6L^2x + x^3)$$

$$\delta_b = \frac{11q_0L^4}{120EI} \quad \theta_b = \frac{q_0L^3}{8EI}$$

$$v = \frac{qb^3x^2}{12EI} (3L + 3a - 2x) \quad 0 \leq x \leq a$$

$$v' = \frac{qb^3x}{2EI} (L + a - x) \quad 0 \leq x \leq a$$

$$v = \frac{q}{24EI} (x^4 - 4Lx^3 + 6L^2x^2 - 4a^3x + a^4) \quad a \leq x \leq L$$

$$v' = \frac{q}{6EI} (x^3 - 3Lx^2 + 3L^2x - a^3) \quad a \leq x \leq L$$

At $x = a$: $v = \frac{qa^2b}{12EI} (3L + a) \quad v' = \frac{qabL}{2EI}$

$$\delta_b = \frac{q}{24EI} (3L^4 - 4a^3L + a^4) \quad \theta_b = \frac{q}{6EI} (L^3 - a^3)$$

$$v = \frac{Px^2}{6EI} (3L - x) \quad v' = \frac{Px}{2EI} (2L - x)$$

$$\delta_b = \frac{PL^3}{3EI} \quad \theta_b = \frac{PL^2}{2EI}$$

$$v = \frac{Px^2}{6EI} (3a - x) \quad v' = \frac{Px}{2EI} (2a - x) \quad 0 \leq x \leq a$$

$$v = \frac{Pa^2}{6EI} (3x - a) \quad v' = \frac{Pa^2}{2EI} \quad a \leq x \leq L$$

At $x = a$: $v = \frac{Pa^3}{3EI} \quad v' = \frac{Pa^2}{2EI}$

$$\delta_b = \frac{Pa^2}{6EI} (3L - a) \quad \theta_b = \frac{Pa^2}{2EI}$$

$$v = \frac{M_0x^2}{2EI} \quad v' = \frac{M_0x}{EI}$$

$$\delta_b = \frac{M_0L^2}{2EI} \quad \theta_b = \frac{M_0L}{EI}$$

$$v = \frac{M_0x^2}{2EI} \quad v' = \frac{M_0x}{EI} \quad 0 \leq x \leq a$$

$$v = \frac{M_0a}{2EI} (2x - a) \quad v' = \frac{M_0a}{EI} \quad a \leq x \leq L$$

At $x = a$: $v = \frac{M_0a^2}{2EI} \quad v' = \frac{M_0a}{EI}$

$$\delta_b = \frac{M_0a}{2EI} (2L - a) \quad \theta_b = \frac{M_0a}{EI}$$

Appendix G Deflections and S

Table G-2 DEFLECTIONS AND SLOPES OF SIMPLE BEAMS

v = deflection in y direction
 $v' = dv/dx$ = slope of deflection curve
 $\delta_c = v(L/2)$ = deflection at center of beam
 x_1 = distance from A to point of maximum deflection
 $\delta_{max} = v_{max}$ = maximum deflection
 $\theta_a = v'(0)$ = angle at left end of beam
 $\theta_b = -v'(L)$ = angle at right end of beam

$$v = \frac{qx^2}{24EI} (L^3 - 2Lx^2 + x^3)$$

$$v' = \frac{q}{24EI} (L^3 - 6Lx^2 + 4x^3)$$

$$\delta_c = \delta_{max} = \frac{5qL^4}{384EI} \quad \theta_a = \theta_b = \frac{qL^3}{24EI}$$

$$v = \frac{qx^2}{384EI} (9L^3 - 24Lx^2 + 16x^3) \quad 0 \leq x \leq \frac{L}{2}$$

$$v' = \frac{q}{384EI} (9L^3 - 72Lx^2 + 64x^3) \quad 0 \leq x \leq \frac{L}{2}$$

$$v = \frac{qL}{384EI} (8x^3 - 24Lx^2 + 17L^2x - L^3) \quad \frac{L}{2} \leq x \leq L$$

$$v' = \frac{qL}{384EI} (24x^2 - 48Lx + 17L^2) \quad \frac{L}{2} \leq x \leq L$$

$$\delta_c = \frac{5qL^4}{768EI} \quad \theta_a = \frac{3qL^3}{128EI} \quad \theta_b = \frac{7qL^3}{384EI}$$

$$v = \frac{qx^2}{24LEI} (a^4 - 4a^3L + 4a^2L^2 + 2a^2x^2 - 4aLx^2 + Lx^3) \quad 0 \leq x \leq a$$

$$v' = \frac{q}{24LEI} (a^4 - 4a^3L + 4a^2L^2 + 6a^2x^2 - 12aLx^2 + 4Lx^3)$$

$$v = \frac{qa^2}{24LEI} (-a^2L + 4L^2x + a^2x - 6Lx^2 + 2x^3) \quad a \leq x \leq L$$

$$v' = \frac{qa^2}{24LEI} (4L^2 + a^2 - 12Lx + 6x^2) \quad a \leq x \leq L$$

$$\theta_a = \frac{qa^2}{24LEI} (2L - a)^2 \quad \theta_b = \frac{qa^2}{24LEI} (2L^2 - a^2)$$

$$v = \frac{Px}{48EI} (3L^2 - 4x^2) \quad 0 \leq x \leq \frac{L}{2}$$

$$v' = \frac{P}{16EI} (L^2 - 4x^2) \quad 0 \leq x \leq \frac{L}{2}$$

$$\delta_c = \delta_{max} = \frac{PL^3}{48EI} \quad \theta_a = \theta_b = \frac{PL^2}{16EI}$$

$$v = \frac{Pbx}{6LEI} (L^2 - b^2 - x^2) \quad 0 \leq x \leq a$$

$$v' = \frac{Pb}{6LEI} (L^2 - b^2 - 3x^2) \quad 0 \leq x \leq a$$

$$\theta_a = \frac{Pab(L+b)}{6LEI} \quad \theta_b = \frac{Pab(L+a)}{6LEI}$$

If $a \geq b$, $\delta_c = \frac{Pb(3L^2 - 4b^2)}{48EI}$

If $a \geq b$, $x_1 = \sqrt{\frac{L^2 - b^2}{3}}$ and $\delta_{max} = \frac{Pb(L^2 - b^2)^{3/2}}{9\sqrt{3}LEI}$

$$v = \frac{Px}{6EI} (3aL - 3a^2 - x^2) \quad 0 \leq x \leq a$$

$$v' = \frac{P}{2EI} (aL - a^2 - x^2) \quad 0 \leq x \leq a$$

$$v = \frac{Pa}{6EI} (3Lx - 3x^2 - a^2) \quad a \leq x \leq L - a$$

$$v' = \frac{Pa}{2EI} (L - 2x) \quad a \leq x \leq L - a$$

$$\theta_a = \theta_b = \frac{Pa(L-a)}{2EI} \quad \delta_c = \delta_{max} = \frac{Pa}{24EI} (3L^2 - 4a^2)$$

$$v = \frac{M_0x}{6LEI} (2L^2 - 3Lx + x^2)$$

$$v' = \frac{M_0}{6LEI} (2L^2 - 6Lx + 3x^2)$$

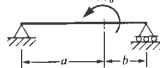
$$\delta_c = \frac{M_0L^2}{16EI} \quad \theta_a = \frac{M_0L}{3EI} \quad \theta_b = \frac{M_0L}{6EI}$$

$$x_1 = L \left(1 - \frac{\sqrt{3}}{3} \right) \text{ and } \delta_{max} = \frac{M_0L^2}{9\sqrt{3}EI}$$

$$v = \frac{M_0x}{24LEI} (L^2 - 4x^2) \quad 0 \leq x \leq \frac{L}{2}$$

$$v' = \frac{M_0}{24LEI} (L^2 - 12x^2) \quad 0 \leq x \leq \frac{L}{2}$$

$$\delta_c = 0 \quad \theta_a = \frac{M_0L}{24EI} \quad \theta_b = -\frac{M_0L}{24EI}$$

9 


$$v = \frac{M_0x}{6LEI} (6aL - 3a^2 - 2L^2 - x^2) \quad 0 \leq x \leq a$$

$$v' = \frac{M_0}{6LEI} (6aL - 3a^2 - 2L^2 - 3x^2) \quad 0 \leq x \leq a$$

At $x = a$: $v = \frac{M_0ab}{3LEI} (2a - L)$

At $x = a$: $v' = \frac{M_0}{3LEI} (3aL - 3a^2 - L^2)$

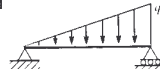
$$\theta_a = \frac{M_0}{6LEI} (6aL - 3a^2 - 2L^2) \quad \theta_b = \frac{M_0}{6LEI} (3a^2 - L^2)$$

10 

$$v = \frac{M_0x}{2EI} (L - x)$$

$$v' = \frac{M_0}{2EI} (L - 2x)$$

$$\delta_c = \delta_{max} = \frac{M_0L^2}{8EI} \quad \theta_a = \theta_b = \frac{M_0L}{2EI}$$

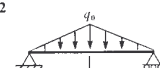
11 

$$v = \frac{q_0x}{360LEI} (7L^4 - 10L^2x^2 + 3x^4)$$

$$v' = \frac{q_0}{360LEI} (7L^4 - 30L^2x^2 + 15x^4)$$

$$\delta_c = \frac{5q_0L^4}{768EI} \quad \theta_a = \frac{7q_0L^3}{360EI} \quad \theta_b = \frac{q_0L^3}{45EI}$$

$$x_1 = 0.5193L \quad \delta_{max} = 0.00652 \frac{q_0L^4}{EI}$$

12 

$$v = \frac{q_0x}{960LEI} (5L^2 - 4x^2)^2 \quad 0 \leq x \leq \frac{L}{2}$$

$$v' = \frac{q_0}{192LEI} (5L^2 - 4x^2)(L^2 - 4x^2) \quad 0 \leq x \leq \frac{L}{2}$$

$$\delta_c = \delta_{max} = \frac{q_0L^4}{120EI} \quad \theta_a = \theta_b = \frac{5q_0L^3}{192EI}$$

$$v = \frac{Pbx}{6LEI} (L^2 - b^2 - x^2) \quad 0 \leq x \leq a$$

$$v' = \frac{Pb}{6LEI} (L^2 - b^2 - 3x^2) \quad 0 \leq x \leq a$$

$$\theta_a = \frac{Pab(L+b)}{6LEI} \quad \theta_b = \frac{Pab(L+a)}{6LEI}$$

If $a \geq b$, $\delta_c = \frac{Pb(3L^2 - 4b^2)}{48EI}$

If $a \geq b$, $x_1 = \sqrt{\frac{L^2 - b^2}{3}}$ and $\delta_{max} = \frac{Pb(L^2 - b^2)^{3/2}}{9\sqrt{3}LEI}$

$$v = \frac{Px}{6EI} (3aL - 3a^2 - x^2) \quad 0 \leq x \leq a$$

$$v' = \frac{P}{2EI} (aL - a^2 - x^2) \quad 0 \leq x \leq a$$

$$v = \frac{Pa}{6EI} (3Lx - 3x^2 - a^2) \quad a \leq x \leq L - a$$

$$v' = \frac{Pa}{2EI} (L - 2x) \quad a \leq x \leq L - a$$

$$\theta_a = \theta_b = \frac{Pa(L-a)}{2EI} \quad \delta_c = \delta_{max} = \frac{Pa}{24EI} (3L^2 - 4a^2)$$

$$v = \frac{M_0x}{6LEI} (2L^2 - 3Lx + x^2)$$

$$v' = \frac{M_0}{6LEI} (2L^2 - 6Lx + 3x^2)$$

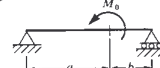
$$\delta_c = \frac{M_0L^2}{16EI} \quad \theta_a = \frac{M_0L}{3EI} \quad \theta_b = \frac{M_0L}{6EI}$$

$$x_1 = L \left(1 - \frac{\sqrt{3}}{3} \right) \text{ and } \delta_{max} = \frac{M_0L^2}{9\sqrt{3}EI}$$

$$v = \frac{M_0x}{24LEI} (L^2 - 4x^2) \quad 0 \leq x \leq \frac{L}{2}$$

$$v' = \frac{M_0}{24LEI} (L^2 - 12x^2) \quad 0 \leq x \leq \frac{L}{2}$$

$$\delta_c = 0 \quad \theta_a = \frac{M_0L}{24EI} \quad \theta_b = -\frac{M_0L}{24EI}$$

9 


$$v = \frac{M_0x}{6LEI} (6aL - 3a^2 - 2L^2 - x^2) \quad 0 \leq x \leq a$$

$$v' = \frac{M_0}{6LEI} (6aL - 3a^2 - 2L^2 - 3x^2) \quad 0 \leq x \leq a$$

At $x = a$: $v = \frac{M_0ab}{3LEI} (2a - L)$

At $x = a$: $v' = \frac{M_0}{3LEI} (3aL - 3a^2 - L^2)$

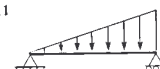
$$\theta_a = \frac{M_0}{6LEI} (6aL - 3a^2 - 2L^2) \quad \theta_b = \frac{M_0}{6LEI} (3a^2 - L^2)$$

10 

$$v = \frac{M_0x}{2EI} (L - x)$$

$$v' = \frac{M_0}{2EI} (L - 2x)$$

$$\delta_c = \delta_{max} = \frac{M_0L^2}{8EI} \quad \theta_a = \theta_b = \frac{M_0L}{2EI}$$

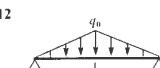
11 

$$v = \frac{q_0x}{360LEI} (7L^4 - 10L^2x^2 + 3x^4)$$

$$v' = \frac{q_0}{360LEI} (7L^4 - 30L^2x^2 + 15x^4)$$

$$\delta_c = \frac{5q_0L^4}{768EI} \quad \theta_a = \frac{7q_0L^3}{360EI} \quad \theta_b = \frac{q_0L^3}{45EI}$$

$$x_1 = 0.5193L \quad \delta_{max} = 0.00652 \frac{q_0L^4}{EI}$$

12 

$$v = \frac{q_0x}{960LEI} (5L^2 - 4x^2)^2 \quad 0 \leq x \leq \frac{L}{2}$$

$$v' = \frac{q_0}{192LEI} (5L^2 - 4x^2)(L^2 - 4x^2) \quad 0 \leq x \leq \frac{L}{2}$$

$$\delta_c = \delta_{max} = \frac{q_0L^4}{120EI} \quad \theta_a = \theta_b = \frac{5q_0L^3}{192EI}$$